DYNAMIC RETROVERSION OF STRABISMUS

CONSTANTINOS M. GLYNOS



Doctor of Philosophy (PhD) Thesis

National Centre of Computer Animation
Faculty of Media and Communication
Bournemouth University

May 2023

Submitted in part fulfilment of the requirements for the Thesis of Doctor of Philosophy at Bournemouth University, November 2019

Constantinos M. Glynos: *Dynamic Retroversion of Strabismus*, © May 2023

LOCATION: Bournemouth

DECLARATION

I hereby declare that this thesis and the work reported herein was composed by and originated entirely from me. Information derived from the published and unpublished work of others has been acknowledged in the text and references are given in the list of sources.

Constantinos M. Glynos (2023)

The copyright of this thesis rests with the author and is made available under a Creative Commons Attribution Non-Commercial No Derivatives licence. Researchers are free to copy, distribute or transmit the thesis on the condition that they attribute it, that they do not use it for commercial purposes and that they do not alter, transform or build upon it. For any reuse or redistribution, researchers must make clear to others the licence terms of this work.

ABSTRACT

Strabismus is a medical term used to define eye misalignment conditions that prevent both eyes from focusing on the same target simultaneously. Apart from having an aesthetic impact on the subject, strabismus is a disability that prohibits the correct perception of depth. The purpose of going through treatment is to realign the “bad" (strabismic) eye, so that it fixates on the same target as the “good" (dominant) eye. This research presents a novel system called Dynamic Eye Misalignment Retroversion System (DEMRS), that can dynamically adjust the light rays coming into each eye, such that both foveae are stimulated by the same target, simultaneously. To test the system, a simulated implementation was created using a set of strabismus cases for known targets. The simulated results show, that the system is able to re-align both light rays such that they intersect the target successfully. Furthermore, a research prototype was built to assess the efficacy of the DEMRS in the successful fusion of the stimuli coming into each eye, from the correct target, simultaneously. The clinical evaluation experiments were conducted under lab conditions, using subjects with normal vision and strabismus, between the ages of 8 and 98 years. Overall, 21 subjects underwent clinical evaluation and, in each experiment, the fusion success of both stimuli at near and far targets was recorded. The results indicate that the DEMRS is able to restore successfully the correct perception of depth, through binocular vision, for young children, adults and elders.

ACKNOWLEDGEMENTS

I would like to express my gratitude to Bournemouth University, Faculty of Media & Communication and the National Centre for Computer Animation (NCCA) for funding this research. I would also like to thank my two supervisors Hammadi Nait-Charif and Olusola Olumide Aina for their patience and helpful advice towards the progress and development of the system presented in this research. My deepest and sincerest gratitude to Prof. Alexandros Damanakis (M.D.) for his advice, training and guidance throughout the medical aspects of this research without whom it would not be possible to complete the work. Furthermore, I would like to thank Prof. Chris Hammond (M.D.), Dr. Stavros Giannikakis (M.D.), Gary Toms (Eng.), Vasilios Dedes (Eng.) and all other medical doctors and engineers who I have interviewed over the years, for their most valuable advice and consultation on the medical and technical aspects of this research. Special thanks to the participants who volunteered to take part in the clinical evaluation of the system. Almost last but not least, I would like to express my deepest love and appreciation to my father Dr. Michael Glynos, my mother Theodora Liakou-Glynou, my brother Anastasios Ilias Glynos, other family members and friends who stood by me throughout this journey. Finally, my warmest gratitude to Enrica Conrotto who, despite all odds, successfully handled the administration tasks of this PhD.

I would not have been able to fight this problem without you...

Thank you all

To children born with strabismus

PUBLICATIONS

Some of the work in this thesis has been presented in the following paper publications:

Glynos C. M., Aina O. O. and Nait-Charif H., Oct 2016. *"Dynamic Eye Misalignment Retroversion System (DEMRS)."*, In 2016 IEEE Applied Imagery Pattern Recognition Workshop (AIPR), Washington DC, USA. 1–7.
(Winner of the best paper and best poster award)

Glynos C. M., Glynos M. C., Aina O. O. and Nait-Charif H., Oct 2019. *"Assessing the Efficacy of the Dynamic Eye Misalignment Retroversion System (DEMRS) Prototype with Normal and Strabismus Subjects."* In ACM Proceedings of the 2019 4th International Conference on Biomedical Imaging, Signal Processing, ICBSP 2019, Nagoya, JPN. 1–8.

Glynos C. M., Aina O. O. and Nait-Charif H., 2019. *"Dynamic Eye Misalignment Retroversion System (DEMRS)."* (Submitted to Journal)

CONTENTS

Declaration iii
Abstract v
Acknowledgements vii
Dedication ix
Publications xi

List of Figures xviii
List of Tables xlv
List of Acronyms xlix
l

1 INTRODUCTION 1
1.1 Motivation . . . 2
1.2 Research Problem . . . 3
1.3 Hypothesis . . . 4
1.4 Objectives and Contributions . . . 4
1.5 Thesis Outline . . . 6
2 MECHANICS OF VISION, BINOCULARITY AND STEREOPSIS 9
2.1 Normal Human Vision in a Nutshell . . . 9
2.1.1 The Retina . . . 11
2.1.2 Central and Peripheral Vision . . . 14
2.2 Eye Movements . . . 16
2.2.1 Muscles of the Eye . . . 17
2.2.2 Oculomotor System . . . 19
2.3 Accommodation, Convergence and the AC/A Ratio . . . 23
2.4 Binocular Vision . . . 27
2.4.1 Normal Retinal Correspondence (NRC) . . . 29
2.4.2 Sensory vs Motor Fusion . . . 30
2.4.3 Retinal Rivalry . . . 31
2.4.4 The Horopter and Panum's Fusional Area . . . 31
2.5 Stereoscopic Vision . . . 33
2.5.1 Familiarity Cues . . . 34
2.5.2 Worth's Classification . . . 35
2.5.3 Milestones in Stereopsis Research . . . 36
2.6 Summary . . . 37

3 STRABISMUS 39
3.1 What, Who, When, How, Where, Which and Why (Six Ws and One H) of Strabismus . . . 40
3.1.1 What is strabismus? . . . 40
3.1.2 Who does strabismus affect? When does strabismus occur in life? How does strabismus develop? . . . 42
3.1.3 Where does strabismus originate from? . . . 44
3.1.4 Which parts of the world does strabismus affect? . . . 45
3.1.5 Why does strabismus exist? . . . 46
3.2 Binocular Disturbances and Adaptations . . . 46
3.2.1 Confusion and Diplopia . . . 47
3.2.2 Amblyopia . . . 48
3.2.3 Suppression . . . 49
3.2.4 Anomalous Retinal Correspondence (ARC) . . . 51
3.2.5 Compensatory Head Postures (CHP) . . . 56
3.2.6 Use of Familiarity Cues in Strabismus . . . 57
3.3 Classification of Strabismus . . . 58
3.3.1 Latency of Deviation: Phoria or Tropia . . . 59
3.3.2 Direction of Deviation . . . 62
3.3.3 Size of Deviation . . . 63
3.3.4 Comitancy of Deviation: Comitant or Incomitant . . . 64
3.3.5 Constancy of Deviation: Constant or Intermittent . . . 66
3.3.6 Involvement of Accommodation: Fully, Partially or None 68
3.3.7 State of Vergence: Excess/Insufficiency of Convergence or Divergence . . . 70
3.3.8 Laterality of Fixation: Unilateral, Alternate or Mono . 71
3.3.9 Time of Onset: Congenital or Acquired . . . 75
3.3.10 Other Properties: Dissociated, Paralytic, Mechanical-Restrictive, Orbital and Pseudo . . . 76
3.4 Diagnosis of Strabismus . . . 81
3.4.1 History and Observation . . . 81
3.4.2 Visual Acuity and Refractive Errors . . . 82
3.4.3 Cover Test . . . 84
3.4.4 Assessment of Ocular Motility . . . 86
3.4.5 Methods of Measuring Strabismic Deviations . . . 87
3.4.6 Assessment of Binocular Vision . . . 96
3.4.7 Assessment of Stereoscopic Vision . . . 100
3.5 Management and Treatment of Strabismus . . . 107
3.5.1 Non-Surgical . . . 108
3.5.2 Surgical . . . 118

3.6 A Case for Further Research . . . 121
3.7 Summary . . . 122
4 DYNAMIC RETROVERSION OF STRABISMUS 125
4.1 The DRS Principle . . . 125
4.2 Justification of DEMRS . . . 126
4.3 The DEMRS Simulator . . . 127
4.3.1 Coordinate System . . . 128
4.3.2 Eye Model . . . 129
4.3.3 Vision Vectors . . . 130
4.3.4 Fixation Target . . . 131
4.3.5 Mirrors and Prisms . . . 133
4.3.6 Lenses . . . 137
4.3.7 System Configuration . . . 138
4.4 DEMRS for horizontal and vertical strabismus (version HV-2.0) 143
4.4.1 Design and Description . . . 143
4.4.2 Retroversion Algorithm . . . 146
4.4.3 Simulations . . . 150
4.4.4 Visualizing Fusion . . . 165
4.4.5 Sensitivity Analysis . . . 170
4.4.6 Preliminary Evaluation Under Normal BSV . . . 176
4.4.7 Discussion . . . 178
4.5 DEMRS for horizontal, vertical and torsional strabismus (version HVT-2.5) . . . 179
4.5.1 Design and Description . . . 180
4.5.2 Retroversion Algorithm . . . 183
4.5.3 Simulations . . . 185
4.5.4 Discussion . . . 202
4.6 Summary . . . 203
5 A DEMRS PROOF OF CONCEPT DEVICE 205
5.1 Device Overview . . . 205
5.2 DEMRS Simulator - HCM . . . 209
5.3 Micro-Controller . . . 210
5.3.1 Arduino Uno . . . 211
5.3.2 Decoder-Latch Circuit Board . . . 213
5.4 Mirror Mounts . . . 220
5.4.1 Motors and Drivers . . . 221
5.4.2 The Mirrors . . . 224
5.4.3 3D Printed Mounts . . . 225
5.5 Base Board . . . 231

5.6 Testing the DEMRS POC Device using Lasers 233
5.6.1 Laser-Based Retroversion of Normal BSV 234
5.6.2 Laser-Based Retroversion of Strabismus 237
5.6.3 A Brief Critique 239
5.7 Summary 240
6 EVALUATION OF THE DEMRS POC DEVICE 241
6.1 Research Ethics 241
6.2 Demographic Data 242
6.2.1 Verifying Normal BSV 244
6.2.2 Verifying Strabismus 245
6.3 The Evaluation Process 247
6.3.1 Pin Test 248
6.3.2 Text Test 250
6.3.3 Anaglyph Test 251
6.3.4 Autostereogram Test 254
6.4 Results 258
6.4.1 Pin Test 258
6.4.2 Text Test 260
6.4.3 Anaglyph Test 261
6.4.4 Autostereogram Test 263
6.4.5 Discussion 266
6.5 Summary 267
7 DISCUSSION & CONCLUSION 269
7.1 Future Work 272
7.1.1 Improving the GUI of the DEMRS Simulator 272
7.1.2 Field of View Analysis 273
7.1.3 Eye Tracking 274
7.1.4 Target Deduction 278
7.1.5 Detect Alternate Strabismus 279
7.1.6 Improving the POC Device 280
A APPENDIX A 283
A.1 AC/A Formulae 283
A.1.1 Heterophoria Method 283
A.1.2 Gradient Method 284
B APPENDIX B 285
B.1 HV-2.0 Configuration 285
B.2 DEMRS for horizontal and vertical strabismus (version HV-1.0) 286
B.2.1 Design and Description 287
B.2.2 Retroversion 288

B.2.3 Simulations . . . 291
B.2.4 Evaluation . . . 294
B.2.5 Results . . . 296
B.2.6 Discussion . . . 297
B.3 Pivoted Mirror Rotation . . . 300
B.4 HVT-2.5 Configuration . . . 305
B.5 DEMRS for horizontal, vertical and torsional strabismus (version HVT-1.0) . . . 306
B.5.1 Design and Description . . . 307
B.5.2 Retroversion Algorithm . . . 310
B.5.3 Simulations . . . 312
B.5.4 Discussion . . . 319
B.6 DEMRS for horizontal, vertical and torsional strabismus (version HVT-2.0) . . . 321
B.6.1 Design and Description . . . 322
B.6.2 Retroversion Algorithm . . . 326
B.6.3 Simulations . . . 327
B.6.4 Discussion . . . 334
C APPENDIX C 335
C.1 Servo Motors in the DEMRS POC Device . . . 335
C.2 Rotation of a Mirror using an Arduino Uno and an 28byj48 Stepper Motor . . . 338
C.3 A Mirror Mount using Adapters . . . 339
C.4 DEMRS POC Configuration . . . 342
D APPENDIX D 345
D.1 Research Ethics Checklist . . . 345
D.2 Participant Information Sheets . . . 350
D.3 Participant Agreement Forms . . . 369
D.4 Certificate in Basic Diagnosis of Strabismus . . . 376
D.5 Sequence of Interactions during the Evaluation of the DEMRS Instance . . . 378
D.5.1 Pin Test . . . 378
D.5.2 Text Test . . . 380
D.5.3 Anaglyph Test . . . 382
D.5.4 Autostereogram Test . . . 384
E APPENDIX Z: A DAY WITH STRABISMUS 387
Bibliography 393

LIST OF FIGURES

Figure 1 *The eye: Basic illustration of the eye's anatomy. The dashed box on the right side of the figure shows the cell arrangement in the three retinal layers.* 11

Figure 2 *Visual pathway: Top-view illustration of the path that the impulses take until the reach the visual cortex of the brain.* 14

Figure 3 *Regions of the Macula (Yanoff and Duker, 2019): Shows the five concentric areas that compose the Macula. The central area, which includes the fovea, is responsible for one's crystal clear vision.* 15

Figure 4 *Ocular coordinate system: Axes of Fick, and Listing's plane going through the centre of the eye.* C *is the eye's centre of rotation,* X *is the horizontal (transverse) axis,* Z *is the vertical axis and* Y *is the normal (sagittal) axis. The* Y *axis passes through the anteroposterior poles of the eye and is perpendicular to* X *and* Z. 17

Figure 5 *Eye muscles: Illustration of the seven extraocular muscles. Six extraocular muscles rotate the eye horizontally, vertically and torsionally inside its socket. An additional (seventh) muscle, called levator palpebrae superioris, elevates the eye lid.* 18

Figure 6 *Eye Movements (Haines and Mihailoff, 2018): A summary of the seven eye movements and their characteristics, which include speed and latency times.* 23

Figure 7 *Accommodation & Convergence: Relation between accommodation, convergence and the fixation distance. The fixation distance varies* $(1 - 0.25\mathrm{m})$ *while the distance between the eyes is* 6cm. Dist *refers to the fixation distance measured in metres* (m), Acco *is the accommodation measured in lens dioptres* (D) *and* Conv *is the convergence which is measured in prismatic dioptres* (Δ). 25

Figure 8 *Inter-pupillary distances: An example of the horizontal (red) and vertical (blue) IPD between the eyes.* 28

Figure 9 *Normal binocular vision: The two principal visual directions (green), stimulating the foveae, originate from the house. The tree is perceived by peripheral visual directions (blue), stimulating other areas of the retina. Both eyes are visually stimulated by the house and tree at corresponding retinal areas.* 29

Figure 10 *Binocular vision with normal retinal correspondence (NRC): Both eyes, and their foveae* (F)*, fixate on the house at point* TF *(blue lines). The point of fixation determines the location of the horopter* (Hs*) which intersects all objects that satisfy normal retinal correspondence (dashed purple arc). The visual stimuli from the puppy (green lines) at point* TP_1 *and the tree (red lines) at* TP_2*, which also lie on the horopter, are received by corresponding retinal areas indicated by the peripheral retinal points* P_1 *and* P_2*. However, the visual stimuli from the beach ball (dashed grey lines) at point* TD *are received by disparate retinal areas* (D*) in each eye.* D *is located left from the fovea of the left eye, and right from the fovea of the right eye. The beach ball will appear double due to the physiological diplopia that occurs.* Ps *refers to Panum's fusional area which allows objects to be fused normally even if they do not lie directly on the horopter.* . 32

Figure 11 *Sir Charles Wheatstone's stereoscope: The two images (left and right) depict the same scene but from two slightly different angles, resembling the left and right eye views respectively. Each eye then focuses on the according image through a set of mirrors. When viewed binocularly, the brain fuses both images and constructs a 3D perception of the scene.* 36

Figure 12 *Strabismus: A simple illustration of strabismus where a subject, with IPD* $\approx 6\text{cm}$*, fixates on a target* $\approx 55\text{cm}$ *away from the centre of the eyes. The right eye (R) fixates on the target, as indicated by the green vertical line on the right eye, whereas the left eye (L) deviates outwards at a certain angle, indicated by the red vertical line on the left eye. The green vertical line next to the red vertical line indicates the correct position of the left eye that would have allowed it to converge on the same target as the right eye. Assuming that each eye has a radius of* $\approx 12\text{mm}$ *and that both eyes must rotate by* $\approx 3°$ *inwards in order to converge on the fixation target, it is estimated that the outwards deviation, of the right eye, is* $\approx 8-11°$ *(*$\approx 16-22\Delta$*).* 40

Figure 13 *Abnormalities with regards to retinal correspondence: The fovea (*F*) of the fixating eye receives visual stimuli deriving from the house, whereas, the fovea of the strabismic eye (*F*) receives visual stimuli deriving from the tree. However, a peripheral retinal element (*P*) of the strabismic eye also receives visual stimuli deriving from the house.* 47

Figure 14 *Partial-Occlusion test: The right eye, which is the dominant eye, fixates on PFT (grid), while the strabismic eye deviates outwards. The SFT (tree) is located behind the PFT, not visible to the dominant eye. Due to the pseudo-fovea of the deviated eye, the brain is not only able to perceive the SFT, but also position its projection, on the retina, behind the FPT.* 55

Figure 15 *CHP: Illustrates the aesthetic differences when CHP is adopted by a subject with medium to large deviation. By adopting a CHP (b), the angle of deviation has been considerably reduced, almost to the point of being unnoticeable.* 57

Figure 16 *Directions of deviation (Damanakis, 2005): Illustration of the six main heterotropic directions of deviation.* 63

Figure 17 *Incomitant strabismus: An example case of incomitant strabismus demonstrating primary and secondary angles of deviation. In this example the right eye is the normal ("good") eye and the left eye is the strabismic ("bad") eye.* 66

Figure 18 *Intermittent strabismus (Salmon, 2019): An example case of intermittent strabismus in which the left eye performs an exo deviation (exotropia) "under conditions of visual inattention".* 68

Figure 19 *Alternate Strabismus: (continued on next page)* 72
Figure 19 *Alternate Strabismus: An example of alternating strabismus in which the same subject can willingly fixate with the right eye (a), then with the left eye (b) and then using both eyes (c). Due to a hypermetropia on the left eye, in this figure, the right eye is the preferred fixating eye. Nevertheless, as the target moves to the far left dominance is swapped from the right eye to the left in order to comfortably fixate on the target.* 73
Figure 20 *Cover test of exotropia: An example case in which the left eye deviates outwards and strabismus is manifest. When the dominant eye (R) is covered and the strabismic eye (L) turns inwards, the covered eye (R) deviates at a secondary angle of deviation. Once the cover is removed, the right eye returns back to its primary position and the left eye deviates. For simplicity, this figure does not show the secondary compensatory movement performed by the covered eye.* . . 85
Figure 21 *Cover test of exophoria: An example case in which both eyes are straight, but when binocularity is interrupted the right eye deviates outwards.* 85
Figure 22 *Hirschberg's method: An example of corneal reflections observed in various amplitudes of esotropia.* 88
Figure 23 *Bruckner test (Dorhman, 2015): An example of unequal corneal and fundus reflections, indicating some form of amblyopia on the left eye.* 89
Figure 24 *Krimsky test: An example of left esotropia, where prisms are placed in front of the fixating (right) eye while observing the corneal reflection and position of the deviated eye.* . . . 90
Figure 25 *Prism cover test: An example of right esotropia, demonstrating the process of a prism cover test from steps 'a' to 'f'.* 91
Figure 26 *Synoptophore (Damanakis, 2005): An example of a child using a synoptophore with professional supervision.* 92
Figure 27 *Maddox rod: An example where the left eye is views a fixation target through a Maddox rod hand frame. The figure illustrates two cases in which the cylindrical strips are oriented vertically, therefore the line perceived is horizontal, and then horizontally, therefore the line perceived is vertical. The right part of the figure shows what is perceived in each case.* 93

Figure 28 *Maddox wing (MediSense, 2018): A hand held device consisting of a septum and two split apertures. The numbers, pointed to by the arrows of the device, represent the vertical and horizontal components of a deviation.* 94

Figure 29 *Lees' screen test (Ansons and Davis, 2014): A more optimal version of a Hess chart in which the right eye views a non-illuminated screen (B) and the left eye fixates on a dot (E) on the grid of the illuminated screen (A). Through the use of a plane mirror (C) and septum (D), the fixated dot from screen A is "projected" onto screen B, indicated by the position F. The examiner "illuminates screen B to note and record the position of the dot".* 95

Figure 30 *Red filter test: Examples of the red filter test with various case of strabismic deviations. The right part of the figure shows what is perceived in each case.* 96

Figure 31 *Bagolini striated glasses: A pair of spectacles in which each lens is rotated opposite to the other (45° and 135°). The right part of the figure shows a light central to a cross, which is perceived under normal BSV.* 97

Figure 32 *Worth's four lights: Consists of four lights (one white, one red and two green) that are viewed through red and green filtered glasses. Under normal BSV, four lights are perceived the white is perceived mixed coloured of red and green.* 98

Figure 33 *After-image: An example of the after-image effect showing the cross perceived under normal BSV, esotropia and exotropia. Each eye is stimulated separately by a different angled linear strobe light (horizontal or vertical), producing an after-image effect.* 98

Figure 34 *Lang's Two-Pencil (Damanakis, 2005): An example of the two pencil test. On the left part of the figure a subject fails to place the tip of a pencil on the tip of another pencil held by an examiner, as his one eye is covered. On the right part, with both eyes open, the subject successfully passes the test.* 101

Figure 35 *Autostereogram (contributors, 2021): An example in which a shark is revealed when the original image is perceived binocularly. The technique to view such images is to relax both eyes as if fixating on a far object, "through" the image. The right part of this figure shows the outline of a shark.* . 102

Figure 36 *TNO (Optician, 2017): A TNO test in which red and green filter glasses are used in order to perceive the red-green random dot stereogram.* 103
Figure 37 *Lang stereo image (Optician, 2017): The right part of the figure shows the structure of a lenticular stereo image and how each eye is able to view at different sides of the cylinders.* 104
Figure 38 *Frisby Near Stereo-test (FNS): An example of FNS where, under binocular vision, the central boids of the bottom left quadrant recede from the remaining boids.* 105
Figure 39 *Frisby Davis Distance (FD2): An example of FD2 in which the star shape, at the top right of the left part of the figure, is slightly pushed out. The right part of this figure shows a different case of an FD2 test from a side view, where the bottom left shape is pushed outwards.* 105
Figure 40 *Wirt and Titmus: The booklet consists of three stereoscopic tests employing polarised stereo images. The fly graphically demonstrates the presence of stereo vision, whereas the other two tests estimate the grade of stereoscopic vision.* 106
Figure 41 *Anaglyph: An example of a 3D anaglyph image depicting Mirto (the puppy). A pair of red/cyan 3D glasses are required in order to perceive the three dimensional illusion of this figure.* 107
Figure 42 *Occlusion: The sticky patch is placed in front of the normal eye forcing the subject to see with the strabismic eye.* . . . 109
Figure 43 *Corrective lenses: Types of lenses that are used to converge or diverge light. A convex lens (left part of the figure) is used to converge light, whereas, a concave lens (right part of the figure) is used to diverge light.* 110
Figure 44 *Bifocal lens: An example of a pair of bifocals where the bottom part of each lens is used for accommodating on near targets, whereas the top part on far targets.* 111
Figure 45 *Prism glasses: An example of Fresnel prism glasses.* 111
Figure 46 *Botox: Injection of Botox type A into the extraocular muscles of the strabismic eye. Part (a) of the figure shows an example of comitant strabismus and part (b) shows an example of paralytic strabismus.* 114

Figure 47 *Home and Office based vision therapy: The left part of the figure shows an example of HBVT using a computer program and red-blue filtered glasses. The right part of this figure shows an example of OBVT in which a subject undergoes treatment using a Hart chart (a matrix of letters on a piece of paper) and occlusion. Starting from a far distance and slowly moving closer, the subject is instructed to read the letters on the chart using either eye.* 115

Figure 48 *Pencil push-ups: A pencil is held directly in front of the subject's eyes, at reading distance, and is moved back and forth. The task for the subject is to maintain convergence on the tip of the pencil at various distances.* 116

Figure 49 *Stereo Pac-Man (Carvelho et al., 2008): The top part of the game consists of a random dot stereogram, whereas the bottom part a 3D stereoscopic view of the maze. A stereoscope is needed to go through this treatment.* 117

Figure 50 *Brock string: A subject who converges on the green, yellow and red beads. More coloured beads can be appended to the string.* 117

Figure 51 *Recession & Resection: An example of recession (a), in which the EOM is moved further back in order to relax its tension, and an example of resection (b), in which the muscle is stitched onto the same location it was detached after removing a small potion of muscular tissue from the EOM.* . 119

Figure 52 *Altering the functionality of an EOM: An example of the adjustment of an EOM, which is moved upwards.* 119

Figure 53 *DEMRS simulator: The basic structure of the DEMRS simulator, in which the retroversion engine is the main actor.* . 128

Figure 54 *Coordinate system: The DEMRS coordinate system whose origin is depicted by the yellow point. The gizmo is only used to illustrate the coordinate axes.* 129

Figure 55 *Visualization of an eye: Part (a) shows how an eye, located at the origin, is visualized by the DEMRS simulator. Part (b) illustrates the locators, which represent retinal points. The umbo is represented by a black locator. Peripheral points in the fovea are represented by the sky blue locators, and peripheral points outside the fovea are represented by the yellow locators.* 129

Figure 56 *Visualization of dominance and strabismic deviations: When strabismus occurs, the principal vision vector of the deviating eye is coloured in red, whereas the principal vision vector of the dominant eye is in green. (a) illustrates normal BSV as both eyes are dominant and their vision vectors are parallel. In (b) the right eye is dominant and the left eye performs an exo-hyper tropia of $< 6, 8, 0 >$, where the left eye rotates outwards by $8°$ and upwards by $6°$. (c) shows a right eso-tropia of $< 0, 10, 0 >$, where the right eye rotates inwards by $10°$.* 131

Figure 57 *Visualization of vision vectors: Both eyes along with the principal and peripheral vision vectors. The peripheral vision vectors originating from the fovea are coloured in sky-blue, whereas the peripheral vision vectors originating from outer parts of the retina are coloured in yellow. Lastly, the principal vision vectors of both eyes is coloured in green because both eyes are dominant, thereby simulating normal BSV.* 131

Figure 58 *Near and far fixation targets: Two examples of a left eso-tropia, in which both $VV_{F_{L/R}}$ are adjusted by the system in order to achieve retroversion. In (a) both $VV_{F_{L/R}}$ converge on a target T, located $< 6m$. In (b) both $VV_{F_{L/R}}$ are parallel to each other and pass through the corresponding targets Tp_L and Tp_R. E_L and E_R are the left and right eyes, and δ represents the IPD.* 132

Figure 59 *Mirror sections: The two faces and four edges of a mirror as visualized by the DEMRS simulator.* 133

Figure 60 *Mirror: The coordinate system of a mirror and the pivot of rotation. Also, the figure shows two examples of a mirror rotating about the y-axis (yaw rotation) of P. The gizmo is only used to illustrate the coordinate axes.* 134

Figure 61 *Mirror reflection: The reflection of a principal vision vector (red) by a mirror in the DEMRS simulator. The white cross on the centre-right of the mirror is the pivot of rotation, and the thin red line projecting from the centre of the mirror indicates the normal of the surface.* 135

Figure 62 *Delta/Dove prism effect: The rotation and inversion of the visual stimuli refracted by a prism. (a) illustrates the effect of inversion as a bottle is perceived upside down through each prism, oriented at 0°. (b) shows two images of a Rubik's cube and a toy viewed through a dove prism. On the left side of (b), the dove prism is not rotated therefore the image is only inverted. On the right side of (b), the dove prism is rotated by 90°, therefore the transmitted image is rotated and inverted. Consequently, although the orientation of the Rubik's cube and the toy is normal, the bottom of the Rubik's cube appears on the left and the bottom of the toy appears on the right.* 136

Figure 63 *Dove prism rotation: The path of the vision vectors when rotated and inverted by a dove prism. To clearly visualize the direction of the vision vectors when refracted by the prism, each polyline has been assigned a different colour. The principal vision vector is the green polyline.* 137

Figure 64 *Delta prism rotation: The path of the vision vectors when rotated and inverted by a delta prism. To clearly visualize the direction of the vision vectors when refracted by the prism, each polyline was assigned to a different colour. The principal vision vector is the green polyline.* 137

Figure 65 *Lenses: The effect of the convex and concave lenses in the direction of the peripheral vision vectors (sky-blue). The principal vision vectors are illustrated by the green polylines.* . 138

Figure 66 *Visualization output from listing 1: The output from the visualizer of the DEMRS simulator. This example is not a representation of DEMRS and, therefore, retroversion is not expected to be achieved. Although the resulting vision vectors are parallel, which is expected when the fixation target is at a distance of 6m from the DEMRS origin, the resulting pupillary distance is abnormal, i.e. does not match the original IPD, and retroversion fails. Therefore, the vision vectors are coloured in red.* 142

Figure 67 *DEMRS HV-2.0: A schematic of the system, where* $VV_{F_{L/R}}$ *are the left and right principal vision vectors,* $VV_{P_{L/R}}$ *are the peripheral vision vectors,* $CxL_{L/R}$ *and* $CvL_{L/R}$ *are the convex and concave lenses,* $M_{1,2,3,4_{L/R}}$ *are the left and right set of mirrors, and* $E_{L/R}$ *represent the left and right eyes.* 143

Figure 68 *Pivot of rotation: Comparison of two pivots of rotation. (a) the pivot of rotation (blue dot) located at the centre of the mirror, (b) the pivot of rotation on the right edge of the mirror.* 144

Figure 69 *Using lenses: The first two mirrors on either side of HV-2.0, with and without lenses. A convex lens is not installed on the left side of HV-2.0, therefore the peripheral vision vectors (VV_{P_L}) escape the system. However, because the principal vision vector (VV_{F_L}) is reflected towards the next mirror, and eventually the target, the retinal images would contain the target as well as arbitrary objects in the periphery. A convex lens is installed on the right side of HV-2.0, therefore the vision vectors are constrained within the system and reflected towards the next mirror, and eventually the target.* 145

Figure 70 *Auxiliary vision vector: Left auxiliary vision vector VV_{A_L} created from a left exotropic eye (E_L) and target T. Because E_R is the normal eye, VV_{A_R} overlaps with VV_{F_R} and, therefore, is not shown in this figure.* 146

Figure 71 *Offset created by chained retroversion: The orange/yellow point shows the LPR, whereas the red point shows where the principal vision vector (VV_{F_L}) is reflected by M_{4_L}. The purple points indicate the pivot of rotation of each mirror and the dashed blue line is the auxiliary vision vector, used to calculate the LPR. (a) before rotating M_{4_L}, the point where VV_{F_L} is reflected by M_{4_L} is the LPR. However, because VV_{F_L} does not direct towards the target T, M_{4_L} must rotate. The offset is shown in (b) where M_{4_L} has rotated and the LPR is no longer the point of reflection between VV_{F_L} and M_{4_L}.* 147

Figure 72 *Pivoted rotation problem: Two examples where a mirror is rotated by an angle ϕ. In (a), the mirror rotates about a pivot P whereas, in (b), the mirror rotates about a pivot P located on the edge of the mirror. B is the point that the reflected ray (green) passes through before the mirror rotates. G is the point that the reflected ray (blue) intends to pass through after the mirror has rotated. The incident ray (red) starts from A and has direction $\vec{I_A}$. The mirror is the black horizontal line with a pivot of rotation P and normal vector $\vec{N}$. Y is the point of reflection between $\vec{I_A}$ and the mirror.* 149

Figure 73 *(continued on next page)* 151
Figure 73 *Simulation with lenses and mirrors: (a) and (b) show the efficacy of the lenses in HV-2.0. (c) the lenses are added to the left side of the system only in order to compare the direction and arrangement of the vision vectors on both sides.* 152
Figure 74 *Showing the peripherals: Part (a) is cluttered with peripheral vision vectors, whereas in (b), the principal vision are clearly displayed.* 152
Figure 75 *DEMRS HV-2.0 retroversion where* $\mathsf{T} = \{0, 0, 600\}$*: Screenshots of simulations before (c) and after (d) retroversion of normal BSV, where* $\mathsf{T} = \{0, 0, 600\}$*. Because of the far distance of the target from the DEMRS origin, the target is not visible in (c) and (d). Therefore two additional screenshots were taken from a close up view of the target and principal vision vectors, where (a) is the extension of (c), and (b) is the extension of (d).* 153
Figure 76 *DEMRS HV-2.0 retroversion where* $\mathsf{T} = \{0, 0, 80\}$*: Screenshots of simulations before (a) and after (b) retroversion of normal BSV, where* $\mathsf{T} = \{0, 0, 80\}$*. Part (c) shows a different perspective view of the target.* 155
Figure 77 *DEMRS HV-2.0 retroversion where* $\mathsf{T} = \{0, 30, 200\}$*: Screenshots of simulations before (a) and after (b) retroversion of normal BSV, where* $\mathsf{T} = \{0, 30, 200\}$*. Part (c) shows a side view of the simulation and target.* 156
Figure 78 *DEMRS HV-2.0 retroversion where* $\mathsf{T} = \{45, 0, 700\}$*: Screenshots of simulations before (c) and after (d) retroversion of normal BSV, where* $\mathsf{T} = \{45, 0, 700\}$*. The target is not visible in (c) and (d),because of the far distance of the target from the DEMRS origin. Therefore two additional screenshots were taken from a close up view of the target and principal vision vectors, where (a) is the extension of (c), and (b) is the extension of (d).* 157
Figure 79 *DEMRS HV-2.0 retroversion where* $\mathsf{T} = \{0, 0, 100\}$*: (continued on next page)* 158
Figure 79 *DEMRS HV-2.0 retroversion where* $\mathsf{T} = \{0, 0, 100\}$*: Screenshots of simulations before (a) and after (b) retroversion for a left exo-tropia with large deviation* 25° *(*$\approx 50\Delta$*), where* $\mathsf{T} = \{0, 0, 100\}$*. (c) close up view of the strabismic deviation showing the original and auxiliary vision vectors. (d) the result from a perspective view of the target.* 159

Figure 80 *DEMRS HV-2.0 retroversion where* $T = \{-15, 0, 200\}$*: Screenshots of simulations before (a) and after (b) retroversion of a right hypo-tropia with moderate deviation of* 12° *(*$\approx 24\Delta$*), where* $T = \{-15, 0, 200\}$*. Because the hypo deviation is not clearly seen from a top views (a,b), two additional screenshots (c, d) were taken from a side view of the system in order to emphasize the direction of the original and retroverted vision vectors.* 160

Figure 81 *DEMRS HV-2.0 retroversion where* $T = \{0, -20, 300\}$*: (continued on next page)* 161

Figure 81 *DEMRS HV-2.0 retroversion where* $T = \{0, -20, 300\}$*: Screenshots of simulations before (a) and after (b) retroversion of a left hyper-tropia with a small deviation of* 8° *(*$\approx 16\Delta$*), where* $T = \{0, -20, 300\}$*. (c) and (d) side views of the simulations emphasizing the locations of the target, and original vision vectors.* 162

Figure 82 *DEMRS HV-2.0 retroversion where* $T = \{0, 0, 800\}$*: Screenshots of simulations before (a) and after (b) retroversion of a right eso-tropia with micro deviation of* 5° *(*$\approx 10\Delta$*), where* $T = \{0, 0, 800\}$*. Because of the far distance of the target from the DEMRS origin, the target is not visible in (c) and (d). Therefore two screenshots were taken from a close up view of the target and principal vision vectors, where (a) is the extension of (c), and (b) is the extension of (d).* 163

Figure 83 *DEMRS HV-2.0 retroversion where* $T = \{0, 0, 200\}$*: Screenshots of simulations before (a) and after (b) retroversion of a left exo-hyper-tropia with moderate deviation of* 12° *(*$\approx 24\Delta$*) exo and* 6° *(*12Δ*) hyper, where* $T = \{0, 0, 200\}$*. Because of the hyper deviation, which is not clearly seen from a top view (a,b), two additional screenshots were taken (c, d) from a front view of the system that show the direction of the original and retroverted vision vectors.* 164

Figure 84 *Simulating fusion without HV-2.0: (a) screenshot of the DEMRS simulator where both eyes fixate on the target. (b) screenshot of Maya containing a perspective camera at the position of each eye, and a planar surface textured with the autostereogram, placed at the position of the target. (c) render of the autostereogram from the left camera, whereas (d) render of the autostereogram from the right camera. (e) fusion of left and right camera renders.* 167

Figure 85 *Simulating fusion with HV-2.0: (a) screenshot of the DEMRS simulator post retroversion. (b) screenshot of the scene in Maya containing the cameras, the autostereogram texture, the eight planar surfaces representing the mirrors, and two polylines to illustrate the vision vectors. (c) and (d) are the renders of the autostereogram from the left and right cameras, respectively. Lastly, (e) fusion of left and right camera renders.* 169

Figure 86 *Fusional area: Part (a) shows the DEMRS after retroversion whereby both principal vision vectors (green polylines) pass through the target (deep pink point). Part (b) focuses on the target, including the two parallel targets (plum points), along with the fusional area, which is the white ellipse around the target.* 170

Figure 87 *Sensitivity analysis of* $M1_L$, $M2_L$, $M3_L$ *and* $M4_L$*: This graph presents the minimum and maximum tolerance of each mirror. The central line represents the correct retroversion angle (vr).* 172

Figure 88 *Sensitivity analysis of* $M3_L$ *and* $M4_L$*: The sensitivity of HV-2.0 when an error of* 10% *is introduced to* $M3_L$ *and* $M4_L$*. Part (a) and part (b) show the minimum and maximum tolerance of* $M4_L$ *when* $M3_L$ *is rotated by an error of* 10%*, whereas parts (c) and (d) show the minimum and maximum tolerance of* $M3_L$ *when* $M4_L$ *is rotated by an error of* 10%*.* 174

Figure 89 *Sensitivity analysis of all mirrors.* 175

Figure 90 *Preliminary evaluation: Photograph showing a subject undergoing testing using the DEMRS apparatus.* 178

Figure 91 *DEMRS HVT-2.5: A schematic of the system, where* $VV_{F_{L/R}}$ *are the left and right principal vision vectors,* $VV_{P_{L/R}}$ *are the peripheral vision vectors,* $CxL_{L/R}$ *and* $CvL_{L/R}$ *are the convex and concave lenses,* $M1,2,3,4_{L/R}$ *are the left and right set of mirrors,* $E_{L/R}$ *represent the left and right eyes, and* $P1,2_{L/R}$ *are the delta prisms.* 180

Figure 92 *Consecutive prisms: The transmitted image is perceived when viewed through two rotatory prisms, consecutively placed one in front of the other. Part (a) shows that when the bottle gets inverted by the first delta prism, the second delta prism corrects the inversion. Also, (a) shows two dove prisms in order to compare their length against two delta prisms. Part (b) is a photograph of two dove prisms, whereby the first prism is rotated by ≈ 20°. (b) shows that the transmitted image is rotated but not inverted.* 182

Figure 93 *Torsional retroversion: (a) View from behind the eyes emphasizing on the torsional deviation of* E_L *by* 40°. *The right eye (*E_R*) is dominant, which is why the peripheral point is at* 0° *from the umbo. (b) View of the delta prisms on the left side of the system, where the first prism performs a roll rotation of* 20° *to compensate for the torsional deviation. Before the refraction of the vision vectors by the prism, the peripheral vision vector is located higher than the principal vision vector, due to the torsional deviation. After the rotation of the first prism, the peripheral vision vector is located at the same height as the principal vision vector, similar to the normal eye. This can be seen in (c), which shows the torsional deviation of the left eye and resultant torsion of the vision vectors. (d) Retroversion shown from a top view emphasizing the equal resultant directions of the peripheral vision vectors of the strabismic and dominant eye.* 187

Figure 94 *DEMRS HVT-2.5 retroversion where* $T = \{0, 0, 600\}$*: Screenshots of simulations before (c) and after (d) retroversion of normal BSV, where* $T = \{0, 0, 600\}$. *Because of the far distance of the target from the DEMRS origin, the target is not visible in (c) and (d). Therefore two additional screenshots were taken from a close up view of the target, peripheral and principal vision vectors, where (a) is the extension of (c), and (b) is the extension of (d).* 188

Figure 95 *DEMRS HVT-2.5 retroversion where* $T = \{0, 0, 80\}$*: Screenshots of simulations before (a) and after (b) retroversion of normal BSV, where* $T = \{0, 0, 80\}$. 190

Figure 96 *DEMRS HVT-2.5 retroversion where* $T = \{0, 20, 200\}$*: Screenshots of simulations before (a) and after (b) retroversion of normal BSV, where* $T = \{0, 20, 200\}$. *(c) side view of the simulation test showing the height of the target.* 191

Figure 97 *DEMRS HVT-2.5 retroversion where* $T = \{45, 0, 700\}$*: Screenshots of simulations before (a) and after (b) retroversion of normal BSV, where* $T = \{45, 0, 700\}$*. Because of the far distance of the target from the DEMRS origin, the target is not visible in this figure. However, the green coloured vision vectors in (b) indicate that retroversion is successful.* 192

Figure 98 *DEMRS HVT-2.5 retroversion for near, mid, and far targets: (continued on next page)* 193

Figure 98 *DEMRS HVT-2.5 retroversion for near, mid, and far targets: Screenshots of simulations showing the results after retroversion of a left eso-hyper-excyclo-tropia, with* 7° *(*$\approx 14\Delta$*) eso,* 4° *(*$\approx 8\Delta$*) hyper, and* 5° *(*$\approx 10\Delta$*) incyclo deviations, from two different views, when: (a,d)* $T = \{0, 0, 100\}$*, (b,e)* $T = \{0, 0, 300\}$*, and (c,f)* $T = \{0, 0, 600\}$*. Parts (b), (c), (e) and (f) do not show the target, because it is positioned at a far distance from the DEMRS origin. However, the green coloured vision vectors indicate that retroversion is successful.* 194

Figure 99 *DEMRS HVT-2.5 retroversion where* $T = \{-25, 0, 400\}$*: Screenshots of simulations before (a) and after (b) retroversion of a left eso-incyclo-tropia with large deviations of* 25° *(*$\approx 50\Delta$*) and* 10° *(*$\approx 20\Delta$*), where* $T = \{-25, 0, 400\}$*. Because of the far distance of the target from the DEMRS origin, the target is not visible in this figure.* 196

Figure 100 *DEMRS HVT-2.5 retroversion where* $T = \{0, -35, 70\}$*: Screenshots of simulations before (a) and after (b) retroversion of a right hypo-tropia with moderate deviation of* 12° *(*$\approx 24\Delta$*), where* $T = \{0, -35, 70\}$. 197

Figure 101 *DEMRS HVT-2.5 retroversion where* $T = \{40, 0, 800\}$*: (continued on next page)* 198

Figure 101 *DEMRS HVT-2.5 retroversion where* $T = \{40, 0, 800\}$*: Screenshots of simulations before (a, c) and after (b, d) retroversion of a left hyper-incyclo-tropia with small deviations of* 8° *(*$\approx 16\Delta$*) and* 6° *(*$\approx 12\Delta$*), where* $T = \{40, 0, 800\}$*. Because of the far distance of the target from the DEMRS origin, the target is not visible in this figure.* 199

Figure 102 *DEMRS HVT-2.5 retroversion where* $T = \{0, 50, 200\}$*: Screenshots of simulations before (a) and after (b) retroversion of a right exo-excyclo-tropia with micro deviations of* 5° *(*$\approx 10\Delta$*) and* 2° *(*$\approx 4\Delta$*), where* $T = \{0, 50, 200\}$. 200

Figure 103 *DEMRS HVT-2.5 retroversion where* $\mathsf{T} = \{25, 40, 300\}$*: (continued on next page)* 201

Figure 103 *DEMRS HVT-2.5 retroversion where* $\mathsf{T} = \{25, 40, 300\}$*: Screenshots of simulations before (a), (b), (c) and after (d), (e), (f) retroversion of a left exo-hyper-excyclo-tropia with moderate deviations of* 16° *(*$\approx 32\Delta$*),* 10° *(*$\approx 20\Delta$*) and* 8° *(*$\approx 16\Delta$*), where* $\mathsf{T} = \{25, 40, 300\}$*. This simulation is shown from a various different angles in order to emphasize the location of the target, strabismic deviation, and torsional rotation of the prism.* 202

Figure 104 *DEMRS POC: An overview of the POC device based on HV-2.0, where* $\mathsf{VV}_{\mathsf{F}_{\mathsf{L/R}}}$ *are the left and right principal vision vectors,* $\mathsf{M}_{1,2,3,4_{\mathsf{L/R}}}$ *are the left and right set of mirrors, and* $\mathsf{E}_{\mathsf{L/R}}$ *represent the left and right eyes. Each orange coloured point represents the pivot of rotation of each mirror mount. The blue rectangle at the centre of the system represents a micro-controller* MC *that controls the orientation of the mirrors, whereas the* BB *represents the base board, which supports the mirror mounts.* 206

Figure 105 *Device schematics: Top and perspective views of the POC device, where* BB *is the base board,* $\mathsf{L}_{1,2,3,4}$ *are four adjustable support legs of the board,* MC *is the micro-controller, and* $\mathsf{M}_{1,2,3,4_{\mathsf{L/R}}}$ *are the left and right set of mirrors.* 208

Figure 106 *Device pipeline: (continued on next page)* 208

Figure 106 *Device pipeline: Diagrams illustrating the communication pipeline between the DEMRS simulator and the POC device.* 209

Figure 107 *Arduino Uno: An image of the Arduino Uno micro-controller board showing the* 14 *digital and* 6 *analog input/output pins (Arduino, 2019).* 211

Figure 108 *SN74LS138N: A 3 Line to 8 Line Decoder Demultiplexer device where* A, B *and* C *are the Input pins connected to the Arduino Uno,* G2A, G2B *and* G1 *are the Enable switches of the decoder device,* GND *is noted as the Ground,* Vcc *is the Power supply and* $\mathsf{Y}_{[0-7]}$ *are the Output pins.* 213

Figure 109 *M74HCT573B1R: Illustration of an Octal Tri-state Transparent Latch, where* OE *is the Output Enable switch,* $\mathsf{D}_{[0-7]}$ *are the Input Data pins,* GND *is the Ground,* Vcc *is the Power supply,* $\mathsf{Q}_{[0-7]}$ *are the Output Latch pins and* LE *is the Latch Enable switch.* 215

Figure 110 *Decoder-Latch path: This diagram shows the pathway of a retroversion angle, calculated by the simulator, that is transferred from the HCM to the Arduino Uno, and next to the decoder-latch, until it reaches the corresponding motor to rotate* M_{1_L} *by* 10°. 215

Figure 111 *Decoder-Latch circuitry: An example of the circuit on a simple breadboard to demonstrate the logic of the design. The Arduino Uno is located on the left side of the figure, whereas the decoder (top device) and latch (bottom device) are located on the right side of the figure. The steppers motors are not shown because the focus is the design of the decoder-latch circuit. Only four wires are connected to the latch, suggesting the use of one motor.* 216

Figure 112 *Decoder-Latch circuit board: The circuit in the form of a board, which is used to control eight mirrors. One 3 Line to 8 Line Decoder Demultiplexer (top left device) enables all the eight Octal Tri-state Transparent Latches.* 217

Figure 113 *Decoder-Latch circuit board: Designed to support eight mirrors, but can also support two prisms. The two small chips on the far left are the Decoder Demultiplexers that enable five Octal Tri-state Transparent Latches on both sides. The lighter red lane represents the* 5V *power supply connected to the chips, the darker red lane is the* 13.8V *power supply (see subsect. 5.4.1) that is connected to the motors and the black lane represents the common ground.* 218

Figure 114 *Testing each latch separately: The driver controlling the motors through the first latch on the left side (top row of chips) of the circuit board, which connects to* M_{1_L}*, is enabled (led lights are on) when a retroversion angle is sent from the DEMRS simulator to the Arduino Uno to rotate* M_{1_L}. . . 219

Figure 115 *28BYJ-48 and ULN2003: The 28BYJ-48 stepper motor (Components101, 2019) is shown on the left side of the figure, whereas the ULN2003 driver (Welten Holdings Ltd, 2019) is shown on the right side of the figure.* 222

Figure 116 *Testing the rotation of a mirror: The mirror is mounted on a base placed firmly on shaft of the 28BYJ-48* 5V *stepper motor. The motor is controlled by an ULN2003 driver, whereby two of the four LEDs are turned on when the mirror rotates indicating which coils are enabled. The input pins of the driver are connected into four digital I/O pins on the Arduino Uno, programmed to rotate the mirror by* 20°*. The driver and motor are powered by an external* 6V *battery pack, therefore a capacitor was used as precaution to regulate the current.* 223

Figure 117 *Connecting two* 12V *28BYJ-48 stepper motors to an Arduino Uno: Two 28BYJ-48 stepper motors connected onto an Arduino Uno micro-controller using two ULN2003 drivers. The left stepper is controlled by the* 9, 10, 11, 12 *digital pins, connected to the* IN1, IN2, IN3, IN4 *inputs of the ULN2003 driver on the left. The right stepper is controlled by the* 2, 3, 4, 5 *digital pins, connected to the* IN1, IN2, IN3, IN4 *inputs of the ULN2003 driver on the right. The black cables are connected to the common ground.* 224

Figure 118 *Abstract mirror rotations: Two types of mirror mounts, whereby two motors (dark grey shapes) are mounted such that a mirror (light blue rectangle) rotates in two dimensions.* $\mathfrak{m}_h$ *is the motor that rotates the mirror horizontally,* $\mathfrak{m}_v$ *is the motor that rotates the mirror vertically, and* P *(yellow point) is the pivot of rotation for the mirror. Part (a) shows a mirror that can rotate from its edge, whereas part (b) shows a mirror that rotates from the centre.* 225

Figure 119 *Mirror mounts: Designs of the mounts that allow a mirror to be rotated from the centre (part a) and side (part b). The stepper motors are coloured in red (Sm_H and Sm_V). The black coloured part, which is called SmH-holder (stepper motor for horizontal rotation), is used to keep the Sm_H firmly in place. The x-axis joint (green) is fitted either onto the shaft of the Sm_H to the support handle (yellow). The yellow part, which is called support handle, fits onto the edge of the x-axis joint and prevents the mirror from tilting. The y-axis joint (blue) is fitted onto the other edge of the x-axis joint and holds the Sm_V (stepper motor for horizontal rotation) firmly in place. At the bottom of the y-axis joint, the bearing case (light grey) holds a small ball bearing that reduces friction. The mirror case (purple) fits onto the shaft of the Sm_V and the support handle. Also, the case allows a mirror (light blue) to slide in.* 226

Figure 120 *Individual parts of a mirror mount: The Front / Back labels indicate the views of each part, whereas Centre / Side labels indicate to which type of mirror mount the part belongs to. If no Centre / Side labels are shown, the part can be used in both types of mirror mounts.* 227

Figure 121 *SmH-holder: (a) and (b) show the top and side views of the SmH-holder design. The length of the holder is measured to be $\approx 6cm$ and the height to be $\approx 2.1cm$. (c) and (d) show the final 3D printed SmH-holder matching the size of the holder in the design.* 229

Figure 122 *Testing the assembled component of M_1: This component is used in order to rotate M_{1_L}, from the side.* 230

Figure 123 *Wooden board: Drawing board used as the base of the DEMRS POC device. The board includes clear markings of the positions and default orientation of each mirror. The SL markings indicate the positions of the four support legs.* 232

Figure 124 *Plexi glass: Final base of the POC device, including a plexi glass placed between the wooden drawing board and the mirror components.* 232

Figure 125 *Evaluation using lasers: Illustrates the setup of the tests, where* $\mathrm{Lp}_{L/R}$ *are the two laser pointers located* $\approx$ 8cm *from the POC device,* δ *is the distance between the lasers,* $\mathrm{VV}_{F_{L/R}}$ *are the light beams emitted from the lasers that represent both principal vision vectors,* T *is the pin, and* D_{LT} *is the distance from the lasers to the target. (a) shows an example of normal BSV, whereas (b) shows an example of left exotropia.* 234

Figure 126 *Before retroversion: (a) shows the visualization output from the DEMRS simulator as reference. (b) is a picture of the POC device at its default state.* 235

Figure 127 *After retroversion: (a) the visualization output from the DEMRS simulator as reference. (b) picture of the POC device after the rotation of the mirror mounts. Both laser points overlap, but because the intensity of the green laser is much greater than the red laser, the light point from the red laser is not visible.* 236

Figure 128 *Before retroversion: (a) the visualization output from the DEMRS simulator as reference. (b) picture of the POC device at its default state.* 238

Figure 129 *After retroversion: (a) the visualization output from the DEMRS simulator as reference. (b) picture of the POC device after the rotation of the mirror mounts. Both laser points overlap, but because the intensity of the green laser is much greater than the red laser, the light point from the red laser is not visible.* 238

Figure 130 *Controlled study design: An overview of the study design in which all subjects undergo testing, initially without using the DEMRS instance and then using the DEMRS instance.* 247

Figure 131 *Anaglyph images: The two anaglyph images used to test successful retroversion of strabismus and crude stereopsis. The use of red/cyan filter glasses is necessary to perceive the 3D illusion from anaglyph images.* 252

Figure 132 *Autostereogram images: (continued on next page)* 255

Figure 132 *Autostereogram images: The seven autostereogram images (Magic Eye II (Smith, 1994)) along with their solutions. The technique, described in subsection 3.4.7, must be applied in order to perceive the illusion.* 256

Figure 133 *DEMRS HVT-2.5 as a head mounted wearable device.* . . 272

Figure 134 *Hypothetical design of HV-2.0 with a rail: This design includes a rail, illustrated by the blue dashed line, on which mirrors* $M_{3,4_{L/R}}$ *are mounted so that they can move and rotate during retroversion, thereby expanding the FOV of the system.* 274

Figure 135 *Extended design of DEMRS HV-2.0: A schematic of the system, where* $C_{L/R}$ *are the two infra-red cameras,* A *is the accelerometer/gyroscope sensor,* $VV_{F_{L/R}}$ *are the left and right principal vision vectors,* $VV_{P_{L/R}}$ *are the peripheral vision vectors,* $CxL_{L/R}$ *and* $CvL_{L/R}$ *are the convex and concave lenses,* $M_{1,2,3,4_{L/R}}$ *are the left and right set of mirrors, and* $E_{L/R}$ *are the left and right eyes.* 277

Figure 136 *Target deduction problem: In this figure,* $E_{L/R}$ *are both eyes, the blue line indicates the IPD, the purple dotted line represents the median plane* MP *of the face,* $VV_{F_{L/R}}$ *are the two principal vision vectors,* VV_{A_L} *is the auxiliary vision vector of the strabismic eye, and the black dots are the estimated fixation targets. (a) shows that if* T *is assumed to lie on* MP, VV_{A_L} *can be calculated using basic trigonometry, or by mirroring the direction of* VV_{F_R}. *However, (b) shows that if* T *is not assumed to lie on* MP, VV_{A_L} *cannot be calculated as the only known information are the direction of* VV_{F_R} *and the IPD.* 278

Figure 137 *DEMRS HV-1.0: A schematic of the system, where* $VV_{F_{L/R}}$ *are the left and right principal vision vectors,* $M_{1,2L/R}$ *are the left and right set of mirrors, and* $E_{L/R}$ *represent the left and right eyes.* 287

Figure 138 *Retroverse on* T*: An overview of retroversion, where* T *is the fixation target,* $VV_{F_{L/R}}$ *are the left and right principal vision vectors,* $M_{1,2_{L/R}}$ *are the left and right set of mirrors,* $E_{L/R}$ *are the left and right eyes, and* d *represents the distance between the eyes and the fixation target* T. 289

Figure 139 *From* B *to* G*: The upper part of the figure shows an example of strabismus in which the principal vision vector (red line) of a strabismic eye, deviates outwards towards* B. *The principal vision vector (green line) of the dominant eye is directed towards* G, *which is the fixation target. The lower part of this figure illustrates the objective of retroversion, which is to redirect the vision vector of the strabismic eye as if the eye was too fixating on* G. 289

Figure 140 *Law of reflection: The first part of this figure (a) shows a vector $\vec{I_A}$ reflect on a non-oriented mirror, whereas the second part (b) shows the vector $\vec{I_A}$ reflected on a mirror that has been rotated by an angle ϕ. The incidence ray (red line) starts from point A with direction $\vec{I_A}$, the mirror surface is the black horizontal line with P being the pivot of rotation and $\vec{N}$ being the normal vector of the mirror. Y is the point of intersection between the incidence ray and the mirror, θi is the angle of incidence and θr is the angle of reflection.* . 290

Figure 141 *3D scene: A perspective view of the 3D scene that was used to simulate retroversion. The fixation target is a 3D model of a house, located at a distance of $\approx 45cm$ from the centre of both eyes ($E_{L/R}$). $M1_{L/R}$ and $M2_{L/R}$ are the four mirrors in the system used to redirect both principal vision vectors. Two cameras are placed inside the eyes, and one cyclopean camera placed further behind the eyes.* 291

Figure 142 *DEMRS HV-1.0 with BSV: This figure shows the default and retroverted states of HV-1.0 in the presence of BSV, where $E_{L/R}$ are the left and right eyes, $M1_{L/R}$ and $M2_{L/R}$ are the four mirrors in the system and $VV_{F_{L/R}}$ are the two principal vision vectors. When HV-1.0 is at default state, the vision vectors do not intersect the target and the rendered images appear empty. When the mirrors of HV-1.0 are rotated so that both VV_{F_L} and VV_{F_R} intersect the target, the rendered images show how each eye views the target through the system.* 292

Figure 143 *DEMRS HV-1.0 with strabismus: This figure shows the default and retroverted states of HV-1.0 in the presence of exotropia of $\approx 10°$, or $\approx 20\Delta$, where $E_{L/R}$ are the left and right eyes, $M1_{L/R}$ and $M2_{L/R}$ are the four mirrors in the system and $VV_{F_{L/R}}$ are the two principal vision vectors. When HV-1.0 is at default state, the vision vectors do not intersect the target and the rendered images appear empty. When the mirrors of HV-1.0 are rotated so that both VV_{F_L} and VV_{F_R} intersect the target, the rendered images show how each eye views the target through the system.* 293

Figure 144 *Autostereogram test: (a) shows the original autostereogram, and (b) shows the illusion perceived when the required technique is applied to view the autostereogram.* 294

Figure 145 *Convergence test: This figure shows a subject with exotropia using the apparatus. A MacBook (laptop) was used to simulate the test in order to assist in the orientation of the mirrors.* 296

Figure 146 *Problem 1: This figure illustrates the excessive binocular disparity created by the large distance between* M_{2_L} *and* M_{2_R}. *(a) shows that both principal vision vectors* VV_{F_L} *and* VV_{F_R} *converge on target* T, *whereas (b) shows* VV_{F_L} *and* VV_{F_R} *in parallel when* T *is at far distance. In this figure,* δ_1 *represents the IPD,* δ_2 *represents the resultant IPD,* $\theta_{L/R}$ *is the normal binocular disparity angle, and* $\phi_{L/R}$ *is the resultant binocular disparity.* 298

Figure 147 *Problem 3: Illustration of the two central mirrors colliding when rotating inwards.* 298

Figure 148 *Problem 2: Illustration of the peripheral vision vectors,* VV_{P_L} *and* VV_{P_R}, *that escape the system after being reflected by* $M_{1_{L/R}}$. *These peripheral vision vectors pass through arbitrary objects in the environment, causing the visual stimuli received by the eyes* $E_{L/R}$ *to contain arbitrary objects from the environment.* 299

Figure 149 *Pivoted rotation problem: The incidence vision vector is defined by point* A *and direction* $\vec{I_A}$. M *is the mirror with normal vector* $\vec{N_y}$ *and pivot of rotation* P. *When* M *has not rotated,* Y *is the point of reflection and* $\vec{R_{YB}}$ *is the reflection vector that intersects point* B. *When* M *is rotated by an angle* ϕ, *which creates the normal* $\vec{N_q}$, $\vec{I_A}$ *is reflected at point* Q *and the reflection vector* $\vec{R_{QG}}$ *intersects point* G. *Parts (b) and (c) are examples of the pivoted mirror rotation problem in 3D, where* G *is elevated and* P *is at the bottom side of* M. 300

Figure 150 *Step 1* 301

Figure 151 *Step 2* 302

Figure 152 *Step 3* 303

Figure 153 *Step 4* 304

Figure 154 *DEMRS HVT-1.0: A schematic of the system, where* $VV_{F_{L/R}}$ *are the left and right principal vision vectors,* $VV_{P_{L/R}}$ *are the peripheral vision vectors,* $CxL_{L/R}$ *and* $CvL_{L/R}$ *are the convex and concave lenses,* $M_{1,2,3,4_{L/R}}$ *are the left and right set of mirrors,* $E_{L/R}$ *represent the left and right eyes, and* $P_{L/R}$ *are dove prisms.* 307

Figure 155 *DEMRS HVT-1.0 retroversion for* $\mathsf{T} = \{0, 0, 800\}$*: Simulation tests before (c) and after (d) retroversion of normal BSV, where* $\mathsf{T} = \{0, 0, 800\}$*. Because of the far distance of the target from the DEMRS origin, the target is not visible in (c) and (d). Therefore two additional screenshots were taken from a close up view of the target, peripheral and principal vision vectors, before (a) and after (b) retroversion. In this figure, (a) is the extension of (c), and (b) is the extension of (d).* 313

Figure 156 *DEMRS HVT-1.0 retroversion for* $\mathsf{T} = \{0, 0, 150\}$*: Simulation tests before (a) and after (b) retroversion of normal BSV, where* $\mathsf{T} = \{0, 0, 150\}$. 314

Figure 157 *DEMRS HVT-1.0 retroversion for* $\mathsf{T} = \{0, 0, 100\}$*, and* $\mathsf{T} = \{0, 0, 700\}$*: Simulation tests showing the attempted retroversion of a left exo-hyper-incyclo-tropia, with horizontal, vertical and torsional deviations of* $8°$*,* $4°$ *and* $10°$*. (a) and (c) show the results of the retroversion when* $\mathsf{T} = \{0, 0, 100\}$*, whereas (b) and (d) show the results of the retroversion when* $\mathsf{T} = \{0, 0, 700\}$. 316

Figure 158 *DEMRS HVT-1.0 retroversion for* $\mathsf{T} = \{10, 0, 170\}, \{0, 0, 170\}, \{-10, 0, 170\}$*: Simulation tests showing the attempted retroversion of a left exo-incyclo-tropia, with horizontal, and torsional deviations of* $6°$*, and* $5°$*. (a), (b), and (c) show the results of the retroversion when* T *is left, centre, and right.* 317

Figure 159 *DEMRS HVT-1.0 retroversion for* $\mathsf{T} = \{45, 0, 600\}, \{0, 0, 600\}, \{-45, 0, 600\}$*: Simulation tests showing the attempted retroversion of a left eso-excyclo-tropia, with horizontal, and torsional deviations of* $9°$*, and* $7°$*. (a), (b), and (c) show the results of the retroversion when* T *is left, centre, and right.* 317

Figure 160 *DEMRS HVT-1.0 retroversion for* $\mathsf{T} = \{0, 25, 200\}, \{0, 0, 200\}, \{0, -25, 200\}$*: Simulation tests showing the attempted retroversion of a right hypo-incyclo-tropia, with vertical, and torsional deviations of* $12°$*, and* $8°$*. (a), (b), and (c) show the results of the retroversion when* T *is up, centre, and down.* 318

Figure 161 *DEMRS HVT-1.0 retroversion for* $\mathsf{T} = \{0, 35, 400\}, \{0, 0, 400\}, \{0, -35, 400\}$*: Simulation tests showing the attempted retroversion of a left hyper-excyclo-tropia, with vertical, and torsional deviations of* $10°$*, and* $6°$*. (a), (b), and (c) show the results of the retroversion when* T *is up, centre, and down.* 318

Figure 162 *Pivot of rotation of prisms on* LPR*: Illustrates the ideal configuration of the system in order to retroverse strabismus when: a) the target* T *is central at near distance, b) the target* T *is right at near distance, and c) the target* T *is right at far distance. This figure shows that when each mirror rotates about the* LPR *(blue point) on* $M4_{L/R}$*, both vision vectors pass through the same target.* 319

Figure 163 *Pivot of rotation of prisms central to* $M4_{L/R}$*: Illustrates examples of retroversion when the pivots of rotation of the prisms are the centres of* $M4_{L/R}$*. The same targets are used as in the previous figure. When the prisms rotate about* $M4_{L/R}$*, the vision vectors are not centrally refracted by* $P_{L/R}$*, causing* $VV_{F_{L/R}}$ *to deviate.* 320

Figure 164 *Collision problem: Illustrates that, even if the pivot of rotation of each prism is located at the last point of reflection on* $M4_{L/R}$*, when both dove prisms* $P_{L/R}$ *converge, i.e. rotate inwards, they collide with each other.* 321

Figure 165 *DEMRS HVT-2.0: A schematic of the system, where* $VV_{F_{L/R}}$ *are the left and right principal vision vectors,* $VV_{P_{L/R}}$ *are the peripheral vision vectors,* $CxL_{L/R}$ *and* $CvL_{L/R}$ *are the convex and concave lenses,* $M1,2,3,4_{L/R}$ *are the left and right set of mirrors,* $E_{L/R}$ *represent the left and right eyes, and* $P1,2_{L/R}$ *are two dove prisms.* 322

Figure 166 *Consecutive dove prisms: Illustration of two dove prisms placed one in front of the other, where the bottle is inverted by the first prism but re-inverted by the second prism so that it is perceived normally.* 325

Figure 167 *DEMRS HVT-2.0 retroversion for* $T = \{0, 0, 800\}$*: Simulation tests before (c) and after (d) retroversion of normal BSV, where* $T = \{0, 0, 800\}$*. Because of the far distance of the target from the DEMRS origin, the target is not visible in (c) and (d). Therefore two additional screenshots were taken from a close up view of the target, peripheral and principal vision vectors, where (a) is the extension of (c), and (b) is the extension of (d).* 328

Figure 168 *DEMRS HVT-2.0 retroversion for* $T = \{0, 0, 150\}$*: Simulation tests before (a) and after (b) retroversion of normal BSV, where* $T = \{0, 0, 150\}$. 330

Figure 169 *DEMRS HVT-2.0 retroversion for* $\mathsf{T} = \{0, 0, 100\}$, *and* $\mathsf{T} = \{0, 0, 700\}$: *Simulation tests showing retroversion of a left exo-hypo-incyclo-tropia, with horizontal, vertical and torsional deviations of* $8°$, $4°$ *and* $15°$. *(a) and (c) show the results of the retroversion when* $\mathsf{T} = \{0, 0, 100\}$, *whereas (b) and (d) show the results of the retroversion when* $\mathsf{T} = \{0, 0, 700\}$. *(e) and (f) correspond to the tests shown in (a,c) and (b,d) respectively, and show close up views of the prisms emphasizing the torsional rotation of* P_{1_R}. 332

Figure 170 *DEMRS HVT-2.0 retroversion for* $\mathsf{T} = \{10, 0, 170\}, \{0, 0, 170\}, \{-10, 0, 170\}$: *Simulation tests showing retroversion of a right eso-incyclo-tropia, with horizontal, and torsional deviations of* $12°$, *and* $5°$. *(a), (b), and (c) show the results of the retroversion when* T *is left, centre, and right.* 332

Figure 171 *DEMRS HVT-2.0 retroversion for* $\mathsf{T} = \{45, 0, 600\}, \{0, 0, 600\}, \{-45, 0, 600\}$: *Simulation tests showing retroversion of a right exo-excyclo-tropia, with horizontal, and torsional deviations of* $9°$, *and* $7°$. *(a), (b), and (c) show the results of the retroversion when* T *is left, centre, and right.* 333

Figure 172 *DEMRS HVT-2.0 retroversion for* $\mathsf{T} = \{0, 25, 200\}, \{0, 0, 200\}, \{0, -25, 200\}$: *Simulation tests showing retroversion of a left hypo-incyclo-tropia, with vertical, and torsional deviations of* $12°$, *and* $8°$. *(a), (b), and (c) show the results of the retroversion when* T *is up, centre, and down.* 333

Figure 173 *DEMRS HVT-2.0 retroversion for* $\mathsf{T} = \{0, 35, 400\}, \{0, 0, 400\}, \{0, -35, 400\}$: *Simulation tests showing retroversion of a right hyper-excyclo-tropia, with vertical, and torsional deviations of* $10°$, *and* $6°$. *(a), (b), and (c) show the results of the retroversion when* T *is up, centre, and down.* 334

Figure 174 *SpringRC SM-S4303R: The white cylindrical part at the top of the motor is the shaft, the black wire is connected to the ground, the red wire is for the power supply and the white wire is the control signal (Pololu, 2019).* 335

Figure 175 *Testing two SpringRC SM-S4303R servos using a paper card: The base servo performs a yaw rotation of the blue coloured card, whereas the other servo that is mounted on the L bracket, performs a pitch rotation of the card.* 336

Figure 176 *Tower Pro MG995 Digi Hi Speed servo motor: The metallic cylindrical part at the top of the motor, is the shaft of the motor that rotates. In this motor, the brown wire is connected to the ground, the red wire is for the power supply and the orange (yellow-ish) wire is the control signal.* 337
Figure 177 *Basic mount: Tilting under the weight of the cold mirror.* . . 337
Figure 178 *Mirror mount using adapters: This mount consists of two 28BYJ-48 stepper motors, which are used to rotate the mirror.* B_{Mirror} *is the base of the mirror,* A_{sb} *is the 3D printed adapter that connects the motor with the base,* Sm_V *is the stepper motor responsible for the vertical rotation,* FW_{sl} *is the 3D printed flat wheel that connects the motor with the L bracket, and* Sm_H *is the stepper motor fitted inside the glashier bush responsible for the horizontal rotation. Lastly,* P *indicates the pivot of rotation of this mirror mount.* . . . 339
Figure 179 *Flat wheel: This is the design of the flat wheel, which has a rectangular shaped hole at the bottom that matches the shape and size of shaft of the motor.* 340
Figure 180 *Illustration of the adapter screw that connects the 28BYJ-48 stepper motor with the metallic base. The figure shows both sides of the same adapter. The left part of the image shows the side of the adapter that fits into the motors' shaft and the right part of the image shows the side connecting to the provided base.* 341
Figure 181 *Problem caused by the size of a mirror mount: Illustration of the problem that would be caused if two mirror mounts are placed further apart from each other. In this figure* E_L *and* E_R *are the left and right eyes with pupillary distance* d_E, d_{M1} *is the distance between the* $M1_L$ *and* $M1_R$, *and* d_{M4} *is the distance between the* $M4_L$ *and* $M4_R$. 342
Figure 182 *View from the normal eye: ARC is noticeable in the first picture because the cone is perceived even when it is occluded by the wall of the airplane. As the airplane moves, the cone appears within the visual field of the normal eye.* 389
Figure 183 *View from the normal eye: ARC is noticeable in the first picture because the pedestrian is perceived even when they are occluded by the sidebar of the windscreen. The pedestrian becomes visible when crossing the street.* 389

LIST OF TABLES

Table 1 *Tests to assess binocular vision and determine the existence of ARC.* 52

Table 2 *Advantages and disadvantages of the partial occlusion test with respect to the time of execution, cost of equipment used, complexity of setting-up the test and amount of cooperation required by a subject.* 55

Table 3 *The complete list of valid fields of a JSON configuration file, split into two categories. The "general" category lists the fields that are not exclusive to any component, whereas the "components" category lists the fields that are associated with each component. In the "general" category, the* `symmetrical` *field determines whether the system is symmetrical, i.e. the components on the left side are mirrored to the right and vice versa. The* `component` *field indicates which component is currently described in the element of the JSON configuration file, ex. prism, whereas the* `type` *field indicates the type of the component being described, ex. dove or delta. In the "components" category,* `side` *determines whether the component is associated with the left or right eye,* `id` *is the number id of a component that belongs to an array of similar components,* `rfidx` *is the refractive index of each prism and lens,* `oppangle` *is the opposite angle theta used to model the prisms,* `centret` *is the centre thickness of each lens,* `rad` *is the radius of the curvature of a lens that is used to refract vision vectors, and* `edget` *is the edge thickness of a concave lens.* 140

Table 4 *Configuration of components in HV-2.0.* 150

Table 5 *DEMRS HV-2.0 retroversion angles for normal BSV, where* $T = \{0, 0, 600\}$. 154

Table 6 *DEMRS HV-2.0 retroversion angles for normal BSV, where* $T = \{0, 0, 80\}$. 155

Table 7 *DEMRS HV-2.0 retroversion angles for normal BSV, where* $T = \{0, 30, 200\}$. 156

Table 8 *DEMRS HV-2.0 retroversion angles for normal BSV, where* $T = \{45, 0, 700\}$. 157

Table 9 *DEMRS HV-2.0 retroversion angles for left exo-tropia with large deviation of* 25° (≈ 50Δ), *where* T = {0, 0, 100}. . . 159
Table 10 *DEMRS HV-2.0 retroversion angles for right hypo-tropia with moderate deviation of* 12° (≈ 24Δ), *where* T = {−15, 0, 200}. 161
Table 11 *DEMRS HV-2.0 retroversion angles for left hyper-tropia with a small deviation of* 8° (≈ 16Δ), *where* T = {0, −20, 300}. 162
Table 12 *DEMRS HV-2.0 retroversion angles for right eso-tropia with micro deviation of* 5° (≈ 10Δ), *where* T = {0, 0, 800}. 163
Table 13 *DEMRS HV-2.0 retroversion angles for left exo-hyper-tropia with moderate deviation of* 12° (≈ 24Δ) *exo and* 6° (12Δ) *hyper, where* T = {0, 0, 200}. 165
Table 14 *Sensitivity test of each mirror, rounded up to one decimal place.* 171
Table 15 *Sensitivity test of* M_{3_L} *and* M_{4_L}, *rounded up to one decimal place.* 173
Table 16 *Sensitivity test of all mirrors, rounded up to one decimal place.* 175
Table 17 *Demographic data of subjects in the preliminary evaluation of DEMRS* 177
Table 18 *Configuration of components in HVT-2.5.* 185
Table 19 *DEMRS HVT-2.5 retroversion angles for normal BSV, where* T = {0, 0, 600}. 189
Table 20 *DEMRS HVT-2.5 retroversion angles for normal BSV, where* T = {0, 0, 80}. 190
Table 21 *DEMRS HVT-2.5 retroversion angles for normal BSV, where* T = {0, 20, 200}. 192
Table 22 *DEMRS HVT-2.5 retroversion angles where* T = {45, 0, 700}. 193
Table 23 *DEMRS HVT-2.5 retroversion angles for left eso-hyper-excyclo-tropia with* 7° (≈ 14Δ) *eso,* 4° (≈ 8Δ) *hyper, and* 5° (≈ 10Δ) *incyclo deviations, where* T = {0, 0, 100}. . . . 194
Table 24 *DEMRS HVT-2.5 retroversion angles for left eso-hyper-excyclo-tropia with* 7° (≈ 14Δ) *eso,* 4° (≈ 8Δ) *hyper, and* 5° (≈ 10Δ) *incyclo deviations, where* T = {0, 0, 300}. . . . 195
Table 25 *DEMRS HVT-2.5 retroversion angles for left eso-hyper-excyclo-tropia with* 7° (≈ 14Δ) *eso,* 4° (≈ 8Δ) *hyper, and* 5° (≈ 10Δ) *incyclo deviations, where* T = {0, 0, 600}. . . . 195
Table 26 *DEMRS HVT-2.5 retroversion angles for left eso-incyclo-tropia with large deviations of* 25° (≈ 50Δ) *and* 10° (≈ 20Δ), *where* T = {−25, 0, 400}. 197

Table 27 *DEMRS HVT-2.5 retroversion angles for right hypo-tropia with moderate deviation of* 12° *(*$\approx 24\Delta$*), where* $\mathsf{T} = \{0, -35, 70\}$. 198
Table 28 *DEMRS HVT-2.5 retroversion angles for left hyper-incyclotropia with small deviations of* 8° *(*$\approx 16\Delta$*) and* 6° *(*$\approx 12\Delta$*), where* $\mathsf{T} = \{40, 0, 800\}$. 199
Table 29 *DEMRS HVT-2.5 retroversion angles for right exo-excyclotropia with micro deviations of* 5° *(*$\approx 10\Delta$*) and* 2° *(*$\approx 4\Delta$*), where* $\mathsf{T} = \{0, 50, 200\}$. 201
Table 30 *DEMRS HVT-2.5 retroversion angles for left exo-hyper-excyclo-tropia with moderate deviations of* 16° *(*$\approx 32\Delta$*),* 10° *(*$\approx 20\Delta$*) and* 8° *(*$\approx 16\Delta$*), where* $\mathsf{T} = \{25, 40, 300\}$. . . 202
Table 31 Process of the HCM shown by the pseudocode (left) and flowchart (right). 210
Table 32 Process of the Arduino Uno shown by the pseudocode (left) and a flowchart (right). 212
Table 33 *Binary input combinations that enable one of the eight logical outputs on the 3 Line to 8 Line Decoder Demultiplexer device, where* $\mathsf{A}, \mathsf{B}, \mathsf{C}$ *are the Input pins,* $\mathsf{Y}_{[0-7]}$ *are the Output pins,* 1 *represents a True/On value and* 0 *represents a False/Off value.* 214
Table 34 *Arduino Uno usage of pins.* 218
Table 35 *Retroversion angles of the mirrors.* 236
Table 36 *Retroversion angles of the mirrors.* 239
Table 37 *Demographic data.* 243
Table 38 *Questions asked during and on completion of the pin test.* 249
Table 39 *Questions asked during and on completion of the text test.* . 251
Table 40 *Questions asked during and on completion of the stereoscopic image test.* 253
Table 41 *Questions asked during and on completion of the autostereogram test.* 257
Table 42 *Results from the pin test indicating the number of subjects who passed the test. The two pie charts illustrate the percentage rate of success prior to using the DEMRS instance (left), and while using the DEMRS instance (right).* . . . 259
Table 43 *Results from the text test indicating the number of subjects who passed the test. The two pie charts illustrate the percentage rate of success prior to using the DEMRS instance (left), and while using the DEMRS instance (right).* 261

Table 44 *Results from the anaglyph test indicating the number of subjects who passed the test. The two pie charts illustrate the percentage rate of success prior to using the DEMRS instance (left), and while using the DEMRS instance (right).* 262
Table 45 *Results from the autostereogram test indicating the number of subjects who passed the test. The two pie charts illustrate the percentage rate of success prior to using the DEMRS instance (left), and while using the DEMRS instance (right).* 264
Table 46 *Pie charts illustrating the percentage rate of success of the total test cases prior to DRS (left), and during DRS (right).* 266
Table 47 *Retroversion yaw angles of mirrors in HV-1.0.* 293
Table 48 *Demographic data used in the basic evaluation of the DEMRS HV-1.0* 295
Table 49 *DEMRS HVT-1.0 retroversion angles for normal BSV, where* $T = \{0, 0, 800\}$. 314
Table 50 *DEMRS HVT-1.0 retroversion angles for normal BSV, where* $T = \{0, 0, 150\}$. 315
Table 51 *Summary of strabismus and targets used in the simulations of DEMRS HVT-1.0.* 315
Table 52 *DEMRS HVT-2.0 retroversion angles for normal BSV, where* $T = \{0, 0, 800\}$. 329
Table 53 *DEMRS HVT-2.0 retroversion angles for normal BSV, where* $T = \{0, 0, 150\}$. 330
Table 54 *Summary of strabismus and targets used in the simulations of DEMRS HVT-2.0.* 331

LIST OF ACRONYMS

2D Two Dimensions

3D Three Dimensions

ABS Acrylonitrile Butadiene Styrene

AI Artificial Intelligence

API Application Programming Interface

Botox Botulinum Toxin

BSV Binocular Single Vision

BW Black and White

cm centimetre

CV Computer Vision

DEMRS Dynamic Eye Misalignment Retroversion System

DRS Dynamic Retroversion of Strabismus

EOG Electro Oculography

FOV Field Of View

FPA Far Point Accommodation

GUI Graphical User Interface

HBVT Home Based Vision Therapy

HCM Hardware Communication Module

HV Horizontal Vertical

HVT Horizontal Vertical and Torsional

IOG Infrared Oculography

IR Infrared

IPD Inter-Pupillary Distance

JSON JavaScript Object Notation

m metre

mm millimetre

NPA Near Point Accommodation

OBVT Office Based Vision Therapy

PLA Polylactic Acid

POC Proof of Concept

PWM Pulse-Width Modulation

RGB Red Green Blue

RPE Retinal Pigment Epithelium

SSC Scleral Search Coils

USB Universal Serial Bus

USD Universal Scene Descriptor

VOG Video Oculography

1

INTRODUCTION

> "... τὸ ὁρᾶν αἱρούμεθα ἀντὶ πάντων ὡς εἰπεῖν τῶν ἄλλων. αἴτιον δ' ὅτι μάλιστα ποιεῖ γνωρίζειν ἡμᾶς αὕτη τῶν αἰσθήσεων καὶ πολλὰς δηλοῖ διαφοράς."
>
> — Αριστοτέλης Μετ.[980α][21]

> *"... we favour our vision, above all other senses, because it lets us gain knowledge and reveals many differences."*
>
> — Aristotle Met.[980a][21]

Vision is a luxury we take for granted everyday without considering the consequences should it be lost. This thesis presents a novel approach to compensate for strabismus by adjusting the direction of the visual stimuli, received by the strabismic and fixating eye, so that the retinal images contain the same object. The thesis investigates an ophthalmological condition known as strabismus and explores alternative ways to assist in its diagnosis and treatment. Briefly, each eye converts the visual stimuli it receives, from light, into a two-dimensional (2D) projection of the environment, also known as a monocular retinal image (Barlow *et al.*, 1967). In normal vision, due to the distance between both eyes on a face, each retinal image depicts a slightly different angled projection of the same environment (Lambert and Lyons, 2017). When the brain receives both retinal images from the eyes, it fuses them into a single three dimensional (3D) perception of the environment (Stidwill and Fletcher, 2010). The ability to fixate on an object using both eyes simultaneously (binocularly) and in a coordinated manner, results in one's stereopsis (stereoscopic vision) and correct perception of depth (Benjamin and Borish, 2006). Strabismus is a condition in which the eyes are unable to fixate on the same object simultaneously (Rowe, 2012). Other than the aesthetic, psychological and social impact it has on a subject, strabismus prevents the correct perception of depth (Lipton, 1970). Amongst the ophthalmology community, a strabismic eye is referred to as the "deviating" or "bad" eye and the normal eye is referred to as the "fixating" or "good" eye (Haines and Mihailoff, 2018) (Yanoff and Duker, 2019). As explained in chapter 3, due to the inability of the eyes to fixate on the same object simultaneously, the visual stimuli forming both retinal images are different (Billson,

2003). Consequently, the brain is unable to fuse the two retinal images it receives (Damanakis, 2005).

This thesis presents a novel principle referred to as Dynamic Retroversion of Strabismus (DRS), which is the basis for a class of novel systems called Dynamic Eye Misalignment Retroversion Systems (DEMRS). DRS compliant systems, i.e. DEMRS, are designed and developed to compensate for strabismus by adjusting the direction of the visual stimuli, received by the strabismic and fixating eye, so that the retinal images contain the same object. As explained in chapter 4, the aim of a DEMRS is to dynamically retroverse strabismus, i.e restore normal vision, so that both eyes can form fusible retinal images. It should be noted that DRS compliant systems are not invasive, therefore they do not alter the position and orientation of the eyes. A proof of concept (POC) device of a DEMRS was built, and a software application has been developed to simulate DEMRS and control the device. Additionally, the software application provides a front-end interface to DEMRS. The efficacy of a DEMRS in the successful fusion of both visual stimuli was assessed via a series of simulated and physical tests. These tests indicate that the DRS compliant systems, presented in this thesis, are able to re-align the visual stimuli received by both eyes such that they “fixate" on the same object simultaneously. Consequently, the eyes form retinal images which the brain is able to fuse successfully, and thereby restore the correct perception of depth through binocular vision.

1.1 MOTIVATION

Chapter 2 describes how each normal human eye translates the received light into a two dimensional (2D) retinal image through a series of biological processes. In normal vision, where both eyes simultaneously fixate on the same object, the visual stimuli received by the eyes are translated into retinal images that the brain can fuse, in order to perceive depth (Noorden and Campos, 2002). The ability to binocularly perceive depth is crucial when performing tasks that require precise vision.

Unfortunately, not everyone can perceive depth binocularly, thereby, lacking the ability to appreciate an environment in three dimensions. Strabismus, discussed in Chapter 3, is a neuromuscular disorder in which the eyes are not properly aligned and, therefore, do not fixate on the same object (Wilson *et al.*, 2009). Consequently, the retinal images, formed by both eyes, are different and cannot be fused by the brain (Ansons and Davis, 2014). Most strabismus subjects are known to have monocular vision and are therefore

considered to be stereo-blind, which means that they cannot perceive depth using both eyes (Richards, 1970). Some subjects suffering from strabismus are able to use alternative ways to estimate depth and measure distances (Agrawal, 2019). The ability to estimate depth, however, is not sufficient enough to carry out tasks that require precise vision (Helveston, 2010).

The objective of undergoing strabismus treatment is to allow the brain fuse both retinal images, develop normal binocular vision and depth perception (Lueder, 2011). Currently, strabismus is treated using non-surgical methods, which include occlusion and vision therapy, and surgical methods, which include a technique referred to as adjustable sutures (Momeni Moghaddam *et al.*, 2015) (Gawęcki, 2020). Ophthalmologists agree that strabismus is most effectively managed when diagnosed in the early stages of its development (Damanakis, 2013) (Hammond, 2014). Unfortunately, the success rate of binocular fusion from current treatments is extremely low (Cooper, 2007) (Nihalani and Hunter, 2011).

One of the reasons that could explain the low success rate of treatments is the lack of diagnostic information (Shen *et al.*, 2013) (Hammond, 2014). Generally, strabismus is diagnosed by an ophthalmologist, orthoptist, or another trained specialist, in an office at a pre-scheduled date and time, which, unfortunately, does not represent or reveal the actual variability of a deviation (Damanakis, 2013) (Lambert and Lyons, 2017). Current diagnostic and treatment methods are limited (Carvelho *et al.*, 2008) (Rowe, 2012) (Ansons and Davis, 2014) by the: (a) type of strabismus, (b) age of a subject, (c) variability, size and direction of a deviation, (d) time and day, on which the diagnosis or treatment is conducted, (e) experience of an examiner, or surgeon, and (f) cooperation and motivation of a subject.

1.2 RESEARCH PROBLEM

Currently, there is no system available that can, or has the potential to, compensate for strabismus in such a way that the visual stimuli, received by both eyes, dynamically derive from the same fixation target simultaneously, located at various distances and directions. This thesis investigates the development of such a system, with the following attributes:

- compensate for all types of strabismus.
- be suitable for various age groups, including young children, adults and the elderly.
- motivate a subject to undergo and complete therapy.

- gather diagnostic information, such as the orientation of both eyes.
- be appropriate for use in home and office.

According to specialists in the field of strabismus, including Damanakis (2013) and Hammond (2014), such a system will have a tremendous impact on the diagnosis and treatment of strabismus and potential to be used in other areas of ophthalmology.

1.3 HYPOTHESIS

This research tests the hypothesis that: (a) it is possible for the normal and strabismic eyes to dynamically receive matching visual stimuli of the same fixation target using non-invasive methods, and (b) the correct perception of depth through binocular vision can be restored, without altering the position and orientation of a strabismic eye.

1.4 OBJECTIVES AND CONTRIBUTIONS

This thesis presents a novel principle referred to as Dynamic Retroversion of Strabismus (DRS) on which Dynamic Eye Misalignment Retroversion Systems (DEMRS) are based. Therefore, a DEMRS is a DRS compliant system. A DEMRS is designed to dynamically redirect the visual stimuli received by both eyes, in order to compensate for strabismus, at various distances and directions. This is so that the retinal images formed, by the strabismic and fixating eye, derive from the same target simultaneously. The objective of a DEMRS is to allow the brain fuse the two retinal images it receives. Unlike other diagnostic and treatment methods that use a set of static images as targets, a DEMRS is a system that redirects light. As such, a DEMRS is not limited to any pre-determined target, thus making it suitable for various types of strabismus. In its final product form, a DEMRS would be a head mounted wearable device suitable to be used by young children, adults and the elderly, allowing them to perform personal tasks, in order to promote their motivation to complete treatment.

The novel research contributions made in this thesis are the:

1. Description of the Partial-Occlusion test used to determine the existence of Anomalous Retinal Correspondence (ARC) (see subsect. 3.2.4).
2. Introduction to the principle of Dynamic Retroversion of Strabismus (DRS).

3. Development of a software that simulates DEMRS and controls a proof of concept device. The software provides an assistive visual representation of the system's operation (simulation).

4. Designs of Dynamic Eye Misalignment Retroversion Systems (DEMRS).

5. Construction of a DEMRS POC device.

6. Evaluating the efficacy of the DEMRS POC device in the successful fusion of the visual stimuli received by both eyes.

This thesis describes the development of DEMRS in four stages beginning with the concept of DRS, and ending with the evaluation process of the DEMRS POC device.

The first stage explains the principle of DRS and justifies the development of DEMRS. Furthermore, it describes the software application that was developed in order to simulate DRS compliant systems. The software application consists of the configuration of a DEMRS variant, the engine/module that calculates retroversion, a set of inputs, such as the inter-pupillary distance and strabismic deviation, and two outputs as front-ends to the system. The visualization output is a 3D representation of a DEMRS that is evaluated through a series of simulated tests, whereas, the hardware output connects the DEMRS simulator with the proof of concept (POC) device. This application was originally developed on a Mac OS High Sierra, but has been tested on Linux RedHat 7 and Windows 10.

In the second stage, two designs of systems compliant with the DRS principle are proposed, one compensating for horizontal and vertical deviations, and the other for horizontal, vertical and torsional deviations. Each DEMRS relies on a deterministic geometric algorithm, which redirects the light rays such that they derive from the same target simultaneously. Also, this stage presents the simulation of each design and evaluates its efficacy in the retroversion of strabismus through a series of simulated tests.

The third stage outlines the construction of the DEMRS POC device. The purpose of constructing a DEMRS POC device is to determine the efficacy of a DEMRS in the restoration of normal BSV on human subjects with strabismus. This stage describes the individual components of the POC device, and discusses the methods that were adopted to overcome certain difficulties encountered during its development.

The final stage presents the efficacy of the DEMRS POC device in the achievement of retroversion. The POC device is evaluated, primarily, in the retroversion of normal BSV and strabismus, and secondly, in the fusibility of the visual stimuli received by both eyes, which would determine the grade

of binocularity achieved during DRS. For the purposes of this study, ethical approval was obtained from Bournemouth University Ethics committee in order to enrol a group of human volunteer subjects to take part in the evaluation of DRS.

1.5 THESIS OUTLINE

This thesis consists of the following seven chapters, chapter 1 being the current chapter:

Chapter 2 reviews the visual process, in stages, from when light enters a normal human eye until it reaches the primary visual cortex of the brain. This chapter also describes the six extraocular muscles that control the position and rotation of an eye, and analyses the oculomotor system, which contributes to steady vision. The principles of accommodation and convergence are explained along with the two main methods of calculating the AC/A ratio. Finally, this chapter delves into the concepts of binocular vision and stereopsis (stereoscopic vision) explaining their importance in the normal perception of depth.

Chapter 3 explores strabismus, a medical term used to define the ophthalmological condition in which the eyes are not properly aligned and, therefore, do not fixate on the same object. Apart from delving into the medical aspects of strabismus, this chapter investigates the origin of strabismus and reviews its physiological, psychological and social impact in a person's life. Furthermore, the chapter discusses current diagnostic and treatment methods, which intend to identify the type of strabismus and restore normal vision. Finally, this chapter identifies the limitations with current diagnostic and treatment methods, and makes a case for further research in the topic of strabismus.

Chapter 4 presents a novel principle referred to as Dynamic Retroversion of Strabismus (DRS), which is the basis for a class of novel systems called Dynamic Eye Misalignment Retroversion Systems (DEMRS). The first section of this chapter discusses the term "retroversion of strabismus", and introduces the principle of DRS, which establishes a set of criteria to achieve retroversion of strabismus. The second section explains the rationale of DRS, and briefly compares it to other therapeutic methods. The third section describes the DEMRS simulator, which is a software application that was developed in order to simulate DRS compliant systems. The final two sections of this chapter propose two

designs of systems, compliant with the DRS principle, one compensating for horizontal and vertical deviations, and the other for horizontal, vertical and torsional deviations.

Chapter 5 describes the construction history of a DEMRS proof of concept (POC) device, which can be used to determine the efficacy of a DEMRS in the restoration of normal BSV on human subjects with strabismus. This chapter outlines the individual components of the POC device, and discusses the methods that were adopted to overcome certain difficulties encountered during its development. Finally, a series of tests were designed, using two laser pointers to represent both eyes, in order to assess the functionality of the DEMRS POC device.

Chapter 6 evaluates the efficacy of the DEMRS POC device, primarily, in the achievement of retroversion of normal BSV and strabismus, and secondly, in the fusibility of the visual stimuli received by both eyes. The evaluation process, described in this chapter, comprised of a number of experiments that were conducted under laboratory conditions. Finally, this chapter discusses the results of the evaluation experiments, and presents few of the feedback provided by the subjects while using the DEMRS POC device.

Chapter 7 critiques the research contributions, of this thesis, based on the initial objectives and hypothesis. The chapter summarizes the principle of DRS, along with the development of DEMRS, and outlines the perks of DRS using the POC device. The concept of DRS, and DEMRS, were presented to strabismologists, through personal interviews, who provided valuable feedback towards the development of the system. Finally, this chapter identifies current limitations with DEMRS and suggests remedial actions that can be further investigated, or developed, in the future.

2

MECHANICS OF VISION, BINOCULARITY AND STEREOPSIS

"Ουκ ένι ιατρικήν είδέναι, όστις μη οίδεν ό τι εστίν άνθρωπος."

— Ιπποκράτης, 460-370 π.Χ.

"It is impossible for one to know medicine when one does not understand what a human is."

— Hippocrates, 460-370 BC

This chapter reviews the visual process, in stages, from when light enters a normal human eye until it reaches the primary visual cortex, the part of a human brain responsible for the visual perception of an object. The anatomical parts of the eye, encountered in each stage of the visual process, are briefly described with particular emphasis on the conformation and functionality of the retina. Due to the importance of the retina in the development of central and peripheral vision, this chapter goes into considerable detail when discussing the structure of the retina. However, this chapter is not intended to provide in-depth information about the anatomy of the eye nor the underlying neuroscience of the visual process, as several related medical books have already been published on these subjects, e.g. (Standring, 2008), (Hubel, 1998), (Yanoff and Duker, 2019), (Haines and Mihailoff, 2018), (Remington, 2012), (Kolb *et al.*, 2020) and (Salmon, 2019).

Furthermore, this chapter outlines the muscles that control the position and orientation of the eyes and provides a detailed description of the oculomotor system, which is responsible for maintaining a clear and stable visual projection of the environment on each retina. Lastly, the phenomena of binocular vision and stereopsis are reviewed in detail, including how the brain is able to unify the retinal images it receives, from both eyes, into a single three dimensional perception.

2.1 NORMAL HUMAN VISION IN A NUTSHELL

A human eye is a complex organ that has the ability to convert light, from the environment, into visual perception through a series of biological

processes (Remington, 2012) (Snell and Lemp, 2013). Even though the shape of an eye is considered to be spherical, "its approximate diameters are 24mm anteroposterior, 23mm vertical, and 23.5mm horizontal" (Remington, 2012). The outermost opaque white shell of an eye is called Sclera, which maintains the shape of the eye and protects it from internal and external forces (fig. 1a) (Standring, 2008) (Giannikakis, 2008). As light enters the eye it encounters the following anatomical parts of the eye, in list order, before reaching the retina (fig. 1a):

- **Cornea:** The transparent anterior section of an eye, an extension of the sclera, that not only protects the iris and pupil but, is also responsible for "about two-thirds of the eye's refractive power" (Yanoff and Duker, 2019). The purpose of the cornea is to refract light and allow it to enter the eye[1] (Giannikakis, 2008). The border separating the cornea from the sclera is known as Corneal Limbus (fig. 1a) (Kolb *et al.*, 2020).

- **Aqueous Humor:** A liquid that nourishes the inner parts of the eye, including the lens, removes waste and supports the shape (lump) of the cornea (Remington, 2012).

- **Iris and Pupil:** The iris is a coloured thin layer that regulates the amount of light entering the pupil (Standring, 2008). The pupil is the circular gap at the centre of the iris, which in the early stages of life is attached to a membrane that later on degenerates (Snell and Lemp, 2013). Two muscles, known as the sphincter and dilator, control the diameter of the pupil by contracting and expanding the iris (Wilson *et al.*, 2009).

- **Lens:** The crystalline lens of the eye is "a transparent, biconvex, avascular mass of uniquely differentiated epithelial cells" (Lambert and Lyons, 2017) covered by a membrane that retains the shape of the lens (Giannikakis, 2008). The refractive power of the lens depends on its curvature, which is controlled by a set of muscles known as ciliary muscles (Remington, 2012). Furthermore, the "metabolic needs of the lens are met by the aqueous and the vitreous humor" (Yanoff and Duker, 2019).

- **Vitreous Humor:** A transparent gel-like substance, enveloped in a membrane, that nourishes the lens and other parts of the eye (Snell and Lemp, 2013). The vitreous humor comprises about 2/3 of the eye's volume (Standring, 2008).

1 A human eye scatters around 10% of the incident light whereas the eye of an eagle is fully transparent, partially explaining why the resolution of the eagle eye is far better than in humans (Yanoff and Duker, 2019).

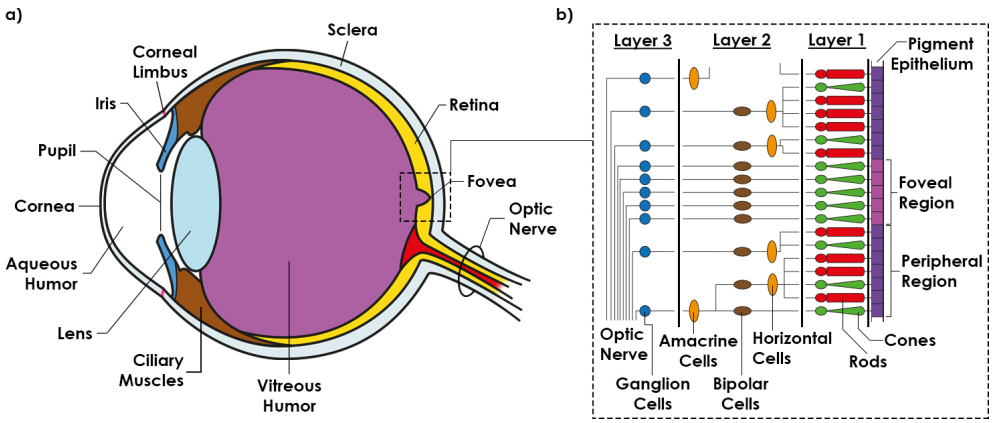

Figure 1: *The eye: Basic illustration of the eye's anatomy. The dashed box on the right side of the figure shows the cell arrangement in the three retinal layers.*

2.1.1 *The Retina*

The retina is a light sensitive "thin sheet of cells" (Standring, 2008) which converts the gathered light into electrical impulses (Brodsky, 2016). According to Yanoff and Duker (2019), "the retina is derived embryologically from the optic vesicle, an outpouching of the embryonic forebrain". Anatomically, the retina consists of ten layers of nerve cells (Standring, 2008) (Snell and Lemp, 2013), but for simplicity, it is usually described as though it consists of only three layers (Rowe, 2012) (Yanoff and Duker, 2019). Figure 1b illustrates the three layers of nerve cells interconnected by synapses[2] (Lambert and Lyons, 2017) (Snell and Lemp, 2013). The first layer contains photoreceptor cells and is located closest to the choroid, a layer of connective tissues that lies between the retina and the sclera (fig. 1b) (Haines and Mihailoff, 2018). The third layer lies at the surface of the retina closest to the vitreous humor, and the second layer sits between the first and third layers (fig. 1b) (Snell and Lemp, 2013). When light reaches the retina it passes through the third and second layers, which become active when they receive impulses from the first layer (Snell and Lemp, 2013). When it reaches the photoreceptors in the first layer, the impulses generated by the photoreceptors are transmitted to the third layer via the second layer (Standring, 2008) (Kolb *et al.*, 2020).

2 A nerve cell (neuron) consists of the nucleus, dendrites and axons, and it is covered by the cell membrane (Standring, 2008). The dendrites, which are protoplasmic extensions of the nerve cell, and the nucleus, which is the body of the cell, receive stimuli from other neurons (Yanoff and Duker, 2019). The axons, which are longer protoplasmic extensions than the dendrites, transmit stimuli to other nerve cells through terminals (Haines and Mihailoff, 2018). The chemical reaction that allows the stimuli to be transmitted from one cell to another is called a synapse (Hendrickson, 2009) (Hubel, 1998).

RETINAL PIGMENT EPITHELIUM: Behind the photoreceptors of the first layer, exists a layer of cuboidal pigment cells called Retinal Pigment Epithelium (RPE) (fig. 1b) (Sparrrow *et al.*, 2010). The RPE cells are tightly packed and "their cytoplasm contains numerous melanosomes" (melanin) (Standring, 2008). The RPE has several functions such as the ability to absorb light that has failed to stimulate a photoreceptor cell and, would otherwise, scatter inside the eye degrading the quality of the retinal image (Hubel, 1998) (Snell and Lemp, 2013) (Sparrrow *et al.*, 2010). The ability of the RPE to absorb light, helps to relieve the stress that may be caused from excessive light (Haines and Mihailoff, 2018).

LAYER 1: The first layer of the retina (fig. 1b) contains two types of photoreceptor nerve cells, known as Rods and Cones (Kolb *et al.*, 2020). Rods are cells that are stimulated under dim lighting conditions, whereas cones are cells that establish the colours and details of the perceived environment (Haines and Mihailoff, 2018) (Snell and Lemp, 2013). Yanoff and Duker (2019) claim that the human retina contains approximately 120 million rods and about 6 million cones totalling in 126 million photoreceptors[3]. Although the total number of photoreceptor cells may vary from one human eye to another, their purpose is to convert the light received into electrical impulses and transmit them to the second layer of cells (Remington, 2012). Depending on their position on the retina, photoreceptor cells transmit their impulses, to the second layer, in two different ways (fig. 1b) (Standring, 2008) (Lambert and Lyons, 2017). Photoreceptors that are central to the retina synapse their impulses directly to the cells in the second layer (Wilson *et al.*, 2009) (Hendrickson, 2009). Moving outwardly, from the centre of the retina, some photoreceptors collectively transmit their impulses, in groups, into a single cell of the second layer (Hubel, 1998) (Remington, 2012).

LAYER 2: The second layer contains three types of transmitting nerve cells, known as Horizontal, Bipolar and Amacrine cells (Haines and Mihailoff, 2018). Similar to photoreceptors, these cells transmit the received impulses, to the third layer, in two different ways (fig. 1b) (Snell and Lemp, 2013). Central to the retina, photoreceptors from the first layer transmit their impulses directly to bipolar cells which, in turn, transmit these impulses directly to the third layer of nerve cells (Remington, 2012) (Hendrickson, 2009). Moving outwardly, from the centre of the retina, some photoreceptor cells

3 Hubel (1998) suggested that the first layer of cells contains approximately 125 million photoreceptors but Rowe (2012) argued that it contains 105 million photoreceptors. However, Haines and Mihailoff (2018) and Yanoff and Duker (2019) confirmed Hubel (1998) suggestion that there are $\approx$ 125 million photoreceptors in the retina.

(rods and cones) would collectively, as groups, transmit their impulses into a single horizontal cell which, in turn, transmits that merged impulse to a single bipolar cell (Hubel, 1998) (Yanoff and Duker, 2019). Additionally, some bipolar cells would transmit their impulses collectively, as groups, to the third layer of cells through a single amacrine cell (Haines and Mihailoff, 2018).

LAYER 3: The third layer consists of photosensitive cells known as the Retinal Ganglion Cells (RGC), also referred to as Ganglion cells (fig. 1) (Hendrickson, 2009). Standring (2008) identifies 15 types of ganglion cells with distinct functionalities. Haines and Mihailoff (2018) narrow the count of ganglion cell types to two. The first type of cells are involved in the final quality of the retinal image and the second are sensitive to blue light (Yanoff and Duker, 2019). The latter type consists of melanopsin-containing ganglion cells that occupy only 1% of the third layer, whereas the remaining 99% of the the third layer is occupied by the first type of ganglion cells (Haines and Mihailoff, 2018). Ansons and Davis (2014) explain that, amongst other functions, "melanopsin-containing cells are not used for seeing images; instead, they monitor light levels to adjust the body's clock and control constriction of the pupil in the eye". Like in previous layers, depending on their position on the retina, ganglion cells receive impulses, from the second layer, in two different ways. Central to the retina, bipolar cells from the second layer synapse their impulses directly to ganglion cells (Wilson *et al.*, 2009) (Hendrickson, 2009). Moving outwardly, from the centre of the retina, bipolar cells would collectively, as groups, transmit their impulses into a single amacrine cell which, in turn, transmits that merged impulse to a single ganglion cell (Standring, 2008) (Remington, 2012). This behaviour of collectively transmitting impulses, from one layer to the next, occurs more frequently further away from the centre of the retina reducing the quality of the retinal image (Yanoff and Duker, 2019) (Hendrickson, 2009).

The ganglion cells extend and converge on the optic disc to form a bundle of long nerve streams, known as the optic nerve (Hubel, 1998) (Snell and Lemp, 2013). Noorden and Campos (2002) explain that "the ganglion cells are the cells of origin of the optic nerve fibers". The optic nerve transmits the impulses through the optic chiasm and lateral geniculate bodies before reaching the corpus callosum and primary visual cortex of the brain (fig. 2) (Hendrickson, 2009) (Stidwill and Fletcher, 2010).

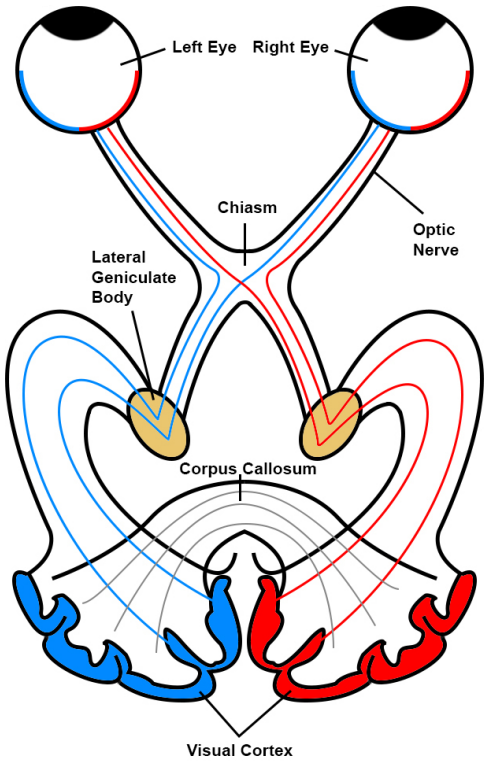

Figure 2: *Visual pathway: Top-view illustration of the path that the impulses take until the reach the visual cortex of the brain.*

2.1.2 *Central and Peripheral Vision*

As mentioned earlier, the collective transmission of retinal impulses, from a group of cells on one layer to a single cell on the next layer, degrades the quality of the retinal image. This happens because "there are in the region of $1.2 - 1.5$ million retinal ganglion cells ... with an average ratio of 1 retinal ganglion cell to 100 photoreceptors" (Rowe, 2012). It should be noted that the smaller the ratio of photoreceptors to ganglion cells, the higher the resolution of the retinal image (Standring, 2008). Moving towards the central area of the retina this ratio becomes progressively smaller until it reaches $1 : 1$ (Remington, 2012). This area is known as Macula and is composed of several sub-regions that contribute to crystal clear vision (Yanoff and Duker, 2019) (Hendrickson, 2009). Further from the centre of the retina, the ratio of photoreceptors to ganglion cells increases and, as a result, vision gets progressively blurrier (Hubel, 1998) (Haines and Mihailoff, 2018). The area around the macula is responsible for blurry peripheral vision (Snell and Lemp, 2013) (Kolb *et al.*, 2020).

At the edge of the macula and towards its centre, cones, as opposed to rods, increase in number and become more compact (Yanoff and Duker,

2019) (Hendrickson, 2009). Cones are responsible for colour vision and the ability to observe detail (Remington, 2012). There are three types of cones, namely the L-Cone which is sensitive to long wavelengths (red colour), M-Cone which is sensitive to medium wavelengths (green colour) and S-Cone which is sensitive to short wavelengths (blue colour) (Haines and Mihailoff, 2018). Because of their contribution to clear vision (detail and colour), the central regions of the macula include only cone photoreceptors and no rods (Standring, 2008) (Snell and Lemp, 2013).

The macula is composed of five concentric regions which are the perifovea, parafovea, fovea, foveola, and umbo (fig. 3) (Yanoff and Duker, 2019) (Hendrickson, 2009).

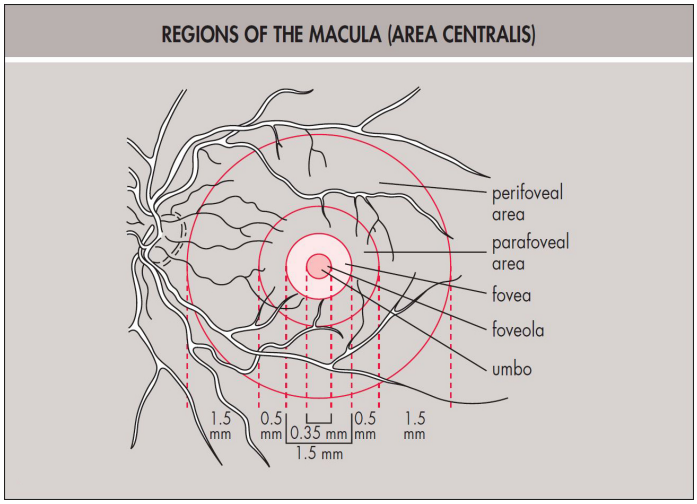

Figure 3: *Regions of the Macula (Yanoff and Duker, 2019): Shows the five concentric areas that compose the Macula. The central area, which includes the fovea, is responsible for one's crystal clear vision.*

Perifovea: This is the outermost region of the macula which measures to be $5-6$mm wide (Standring, 2008). Within this region, the flow of impulses, between retinal layers, is almost similar to the flow found in peripheral regions, i.e. collective synapses but from smaller groups (Hendrickson, 2009).

Parafovea: This region is surrounded by the perifovea and measures to be 2.5mm wide (Kolb *et al.*, 2020). The flow of impulses, between the retinal layers in this region, is similar to the perifovea with the exception that the parafovea consists of more bipolar cells and fewer ganglion cells (Yanoff and Duker, 2019).

Fovea: The fovea is the region with the "highest resolving power" (Noorden and Campos, 2002) and measures to be 1.5mm wide (Standring, 2008). The fovea forms a cavity (pit) at the centre of the macula

that is caused by the thinning of the inner retinal layers allowing "a maximum amount of light to reach the photoreceptors with optimal fidelity" (Wilson *et al.*, 2009). This region has the highest concentration of cone cell types, and the ratio of photoreceptors to ganglion cells approaches 1 : 1 (Remington, 2012) (Snell and Lemp, 2013).

Foveola: Yanoff and Duker (2019) describe the foveola as "the bouquet of central cones". This region measures to be 0.35mm wide and consists of densely packed cone cells (Standring, 2008) (Hendrickson, 2009).

Umbo: The umbo is not measured in width (Hendrickson, 2009) because it "represents the precise centre of the macula, ... that results in the highest visual acuity" (Haines and Mihailoff, 2018).

The peripheral area around the macula is also divided into four concentric regions: near, middle, far and extreme (Yanoff and Duker, 2019).

Central and peripheral vision play an important role in the perception of the environment. When the eye fixates on an object of interest, that object is projected at the centre of each retina (fovea) where vision (central vision) is more acute (Hendrickson, 2009) (Stidwill and Fletcher, 2010). Peripheral vision clears potential confusion caused by surrounding objects in the same environment (Hubel, 1998) (Damanakis, 2013). If peripheral vision was as clear as central vision, then the retinal image formed by the eye would lack focus, thereby, causing the brain to overwork in order to make sense of the excessively detailed retinal image.

2.2 EYE MOVEMENTS

A human eye has the ability to perform translatory and rotatory movements that are described with respect to the primary position of the eye (de Lahunta and Glass, 2009) (Haslwanter, 1995). In ophthalmology, an eye is at primary position, or at rest, when an individual is "looking straight ahead with body and head erect" (Noorden and Campos, 2002). Eye rotations are performed around a point, central to the eye, called centre of rotation (Damanakis, 2005) (Snell and Lemp, 2013). Depending on the eye movement, each centre of rotation undergoes minor translation offsets, but for practical purposes, the centre of rotation is considered to be located at the centre of the eye (Salmon, 2019) (Wright *et al.*, 2006). All rotatory movements of an eye are performed around the eye's centre of rotation which is also considered to be the origin of three theoretical axes, perpendicular to each other (Agrawal, 2019) (Remington, 2012). These axes, known as axes of

Fick, define the horizontal (transverse), vertical and normal (sagittal) axes denoted by the letters 'X', 'Z' and 'Y', respectively (fig. 4) (Ramey *et al.*, 2008) (Ansons and Davis, 2014). Furthermore, Fick's axes intersect an "imaginary coronal plane passing through the centre of rotation" (Salmon, 2019), known as Listing's plane (fig. 4) (Hansard and Horaud, 2010).

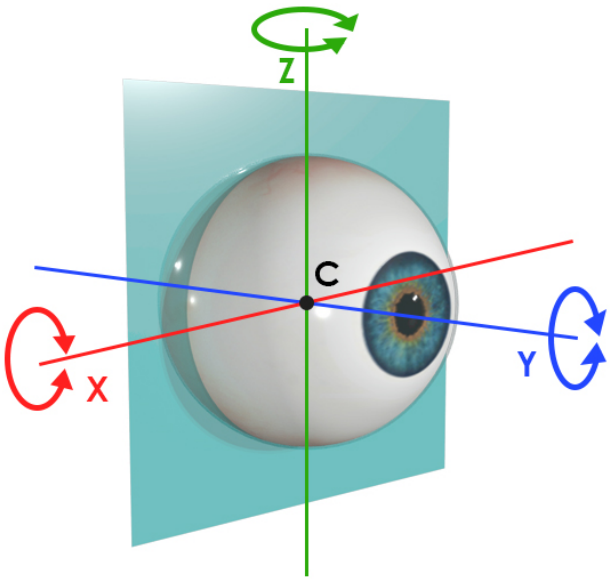

Figure 4: *Ocular coordinate system: Axes of Fick, and Listing's plane going through the centre of the eye. C is the eye's centre of rotation, X is the horizontal (transverse) axis, Z is the vertical axis and Y is the normal (sagittal) axis. The Y axis passes through the anteroposterior poles of the eye and is perpendicular to X and Z.*

Other coordinate systems have also been used to describe eye movements, such as Helmholtz's coordinates, which consider 'X' to be the normal axis, and Cartesian coordinates, which assume 'Z' to be the normal axis (Haslwanter, 1995) (Remington, 2012). Even though rotations of an eye can be described using Euler angles (Haslwanter, 1995), the terms 'pitch' (horizonal rotation), 'yaw' (vertical rotation) and 'roll' (torsional rotation) are rarely used in ophthalmology.

2.2.1 *Muscles of the Eye*

The eye is able to translate and rotate horizontally, vertically and torsionally due to six extraocular muscles that control the movement of the eye inside its socket, or orbit (fig. 5) (Haines and Mihailoff, 2018) (Haslwanter, 1995). These six muscles are divided into four rectus muscles (superior, medial, lateral and inferior) and two oblique muscles (superior and inferior) (Shumway *et al.*, 2019) (Salmon, 2019). A seventh muscle, called levator

palpebrae superioris, is responsible for the elevation of the eyelid (fig. 5) (Remington, 2012).

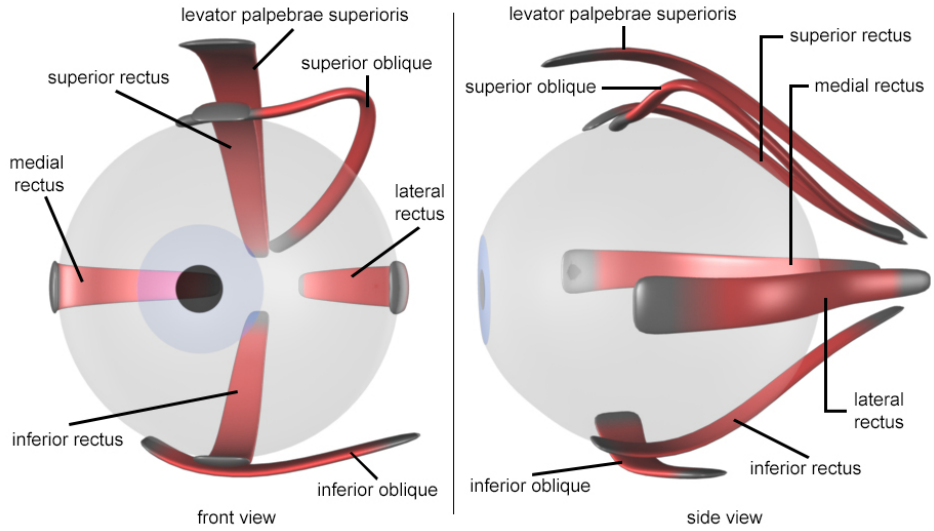

Figure 5: *Eye muscles: Illustration of the seven extraocular muscles. Six extraocular muscles rotate the eye horizontally, vertically and torsionally inside its socket. An additional (seventh) muscle, called levator palpebrae superioris, elevates the eye lid.*

Snell and Lemp (2013) explain that the rotation of an eye (horizontal, vertical and torsional) is accomplished through contraction and relaxation of the following muscles:

- **Superior Rectus:** Rotates the eye upwards and inwards
- **Medial Rectus:** Rotates the eye inwards
- **Lateral Rectus:** Rotates the eye outwards
- **Inferior Rectus:** Rotates the eye downwards and inwards
- **Superior Oblique:** Rotates the eye downwards and outwards
- **Inferior Oblique:** Rotates the eye upwards and outwards

It is estimated that, on average, the eye is able to rotate upwards by 25°, downwards by 30°, left and right by $35-45°$, and torsionally by 15° (Van Cott and Kinkade, 1972) (Hammond, 2014).

The extraocular muscles act collaboratively, in groups, as agonists, antagonists, synergists or yoke (Remington, 2012) (Wright *et al.*, 2006). An agonist is the “primary muscle moving the eye in a given direction" (Salmon, 2019). For example, the contraction of an agonist muscle, which rotates the eye, causes another extraocular muscle, known as antagonist, to act upon the

same eye but in opposite direction (Haines and Mihailoff, 2018) (Agrawal, 2019). Synergists are a group of extraocular muscles that move the eye in the same direction (Standring, 2008) (Lambert and Lyons, 2017). Any two muscles, one in either eye, that perform synergistic actions in order to rotate both eyes in the same direction, are called yoke muscles (Damanakis, 2005) (Barry and Denniston, 2017).

There are four laws that describe ocular translatory and rotatory movements:

- **Donder's law:** Every direction of gaze corresponds to a definite horizontal, vertical and torsional orientation of the eye (Rowe, 2012) (Hore *et al.*, 1992).
- **Listing's law:** Every eye movement is achieved by a single rotation about an axis lying on Listing's plane (Stidwill and Fletcher, 2010) (Wong, 2004).
- **Sherrington's law:** When an extraocular muscle contracts (agonist), in response to an impulse from the brain, its direct antagonist relaxes, in response to an equivalent inhibitory impulse (Salmon, 2019) (Wright *et al.*, 2006).
- **Hering's law:** When an extraocular muscle, of one eye, contracts (agonist), in response to an impulse from the brain, an equivalent impulse is received by the corresponding yoke muscle, of the other eye, that causes a similar contraction (Westheimer, 2014) (Agrawal, 2019).

Sherringon's law describes the relationships between agonist and antagonist muscles, of the same eye, which are responsible for the smooth movement of the eye (Remington, 2012). Hering's law[4] explains the relationships of yoke muscles that are responsible for the coordinated eye movements in normal binocular vision (Rowe, 2012).

2.2.2 *Oculomotor System*

A normal human eye is able to perform conjugate and disconjugate rotations using its six extraocular muscles (Remington, 2012). A conjugate movement, known as a version, is characterized by the simultaneous rotation of both eyes towards the same direction (Ansons and Davis, 2014). Versions occur when both eyes fixate on an object that is located far away ($\gtrapprox$ 6m)

4 In 1764, Thomas Reid "advanced exactly the same view as Hering, using almost identical arguments" (Westheimer, 2014).

(Damanakis, 2005). At such fixation distances, both eyes are considered to be parallel (Salmon, 2019). The version movements, which an eye can perform, are (Yanoff and Duker, 2019):

- **Dextroversion:** Both eyes turn right
- **Levoversion:** Both eyes turn left
- **Supraversion:** Both eyes turn upwards
- **Infraversion:** Both eyes turn downwards
- **Dextrocycloversion:** Both eyes turn right (torsionally)
- **Levocycloversion:** Both eyes turn left (torsionally)

A disconjugate or disjugate movement, known as a vergence, is defined by the simultaneous rotation of both eyes on opposite directions (Rowe, 2012) (Remington, 2012). Vergence movements occur when both eyes fixate on a target that is less than 6m away, but become more apparent at reading distances ($\approx 40\text{cm}$) (Ramey *et al.*, 2008). The vergence movements, which an eye can perform, are (Damanakis, 2005) (Yanoff and Duker, 2019):

- **Convergence:** Both eyes turn inwards
- **Divergence:** Both eyes turn outwards
- **Positive Vertical Divergence:** When the right eye turns upwards, the left eye turns downwards
- **Negative Vertical Divergence:** When the right eye turns downwards, the left eye turns upwards
- **Incyclovergence:** Both eyes turn inwards (torsionally)
- **Excyclovergence:** Both eyes turn outwards (torsionally)

The objective of the oculomotor system is to perform adjustment movements, also referred to as targeting movements, on both eyes so that the visual stimuli received by both retinas can be translated into steady and clear retinal images (Kolb *et al.*, 2020) (Remington, 2012). There are seven types of targeting movements, also referred to as functions, systems or responses, whose speed is measured in degrees per second ($^\circ/\text{s}$) (Ansons and Davis, 2014) (Haines and Mihailoff, 2018):

- **Foveation:** This is, both, a conjugate and a disconjugate movement where both eyes perform three actions in order to maintain a clear projection of the fixation target onto both foveae (Haines and Mihailoff,

2018). The thee actions, which are also referred to as the near-triad or accommodation reflex (Kolb *et al.*, 2020), are the: (a) simultaneous convergence or divergence of both eyes on the target (Damanakis, 2005), (b) constriction or dilation of the pupil, which prevents peripheral light from obstructing the clarity of the retinal image (Ansons and Davis, 2014), and (c) adjustment of the len's curvature, which improves its focus on the target (lens accommodation) (Yanoff and Duker, 2019). Furthermore, foveation is a movement that can occur monocularly (Haines and Mihailoff, 2018).

- **Saccade:** This is a rapid conjugate movement where the eye changes its fixation from one target to another (Salmon, 2019). When a peripheral object enters the visual field of view, it attracts attention which forces the eye to perform a rapid movement in order to briefly fixate the fovea on the new object before returning to its original position (Kolb *et al.*, 2020). Generally, a saccadic movement goes unnoticed because its speed is so fast, approximately $200 - 700°/s$, that the brain suppresses the corresponding visual stimuli (Billson, 2003). A saccadic response can be voluntary or involuntary (Yanoff and Duker, 2019). Voluntary saccades "include willed refixations, those in response to command and memory-guided saccades" (Rowe, 2012), whereas, involuntary (reflex) saccades can occur due to a new object entering the visual field or even a sound that attracts attention (Ansons and Davis, 2014).

- **Smooth Pursuit:** This is a slow conjugate movement which allows both eyes to track a fixation target that is in motion (Salmon, 2019). The objective of smooth pursuit is to stabilize the projected image of a moving target on both foveae by matching the velocity of the target (Billson, 2003). Smooth pursuit also occurs when the target is stationary and the subject is in motion (Noorden and Campos, 2002). If a target is moving too fast the eyes may perform a quick saccade to compensate for the high speed (Kolb *et al.*, 2020). Generally, smooth pursuit involves a slow paced tracking movement, around $30 - 40°/s$ (Ansons and Davis, 2014). However, it has been noticed that the eye is able to follow a target up to $70 - 100°/s$ (Haines and Mihailoff, 2018).

- **Vergence:** This is a disconjugate movement where both eyes rotate towards a fixation target so that the visual stimuli is received by both foveae simultaneously (Remington, 2012). Convergence of the eyes occurs when the fixation target moves towards observer and vice versa, thereby, shortening the distance between them (Billson, 2003). Diver-

gence of the eyes occurs when the distance between the eyes and the fixation target increases (Kolb *et al.*, 2020). Vergence functions trigger the accommodation reflex (near-triad) in order to improve the clarity of the retinal image (Haines and Mihailoff, 2018). During vergence, the eyes rotate at a maximum velocity of $15 - 20°/s$ (Rowe, 2012).

- **Vestibular & Optokinetic:** These are conjugate eye responses that compensate for slow and fast head movements (Noorden and Campos, 2002). During any head movement, for instance a left turn, the environment appears to be moving in the opposite direction at a certain speed. This effect, in which the projected environment appears to be moving on the retina, is known as a retinal slip (Billson, 2003). The objective of this compensatory eye movement is to maintain a steady projection of the environment on the retina, more precisely on the fovea, by counteracting the direction of the head movement with matching velocity (Salmon, 2019). At the beginning of a head movement i.e., during acceleration, the vestibular function gets activated in order to compensate for the slow-phased retinal slips and maintain the fixation on the target (Yanoff and Duker, 2019). This vestibular function causes each eye to move/rotate opposite to the direction of the head motion at the same speed (Haines and Mihailoff, 2018) (Billson, 2003). If a head movement turns into a constant motion i.e. continuously moving for $\approx 2secs$ reaching a constant velocity, the effect of the vestibular function decreases (Haines and Mihailoff, 2018). At the same time, both optokinetic and smooth pursuit functions get activated when performing fast-phased compensatory movements in order to form a steady retinal image (Stidwill and Fletcher, 2010). Yanoff and Duker (2019) explain that the "optokinetic system complements the vestibulo–ocular system when it becomes inadequate". When the head motion is too fast for the optikinetic function to compensate, a quick saccade may occur in order to re-fixate the fovea on the target (Ansons and Davis, 2014). Both, vestibular and optokinetic movements, have a compensatory speed of less than $500°/sec$ (Haines and Mihailoff, 2018).

- **Physiological Nystagmus (fast phase):** Nystagmus is a term that describes all involuntary oscillatory movements of the eyes (Damanakis, 2005) that are defined by the: (a) direction of the oscillation (horizontal, vertical, torsional) (Billson, 2003), (b) speed (slow-phased, fast-phased) and range (small, big) of the oscillatory movement (Remington, 2012), and (c) waveform of the oscillation (pendular, jerky) (Furman, 2014). In normal human vision, nystagmus is associated with vestibular move-

ments that alternate between smooth pursuit and saccades (Noorden and Campos, 2002). Physiological nystagmus has three variations: (a) End–Point, which is a fast-phased jerky oscillation that occurs when the eyes fixate on a target for longer than a few seconds (Stidwill and Fletcher, 2010), (b) Optokinetic, which combines slow-phased (compensatory) and fast-phased (saccades) jerky oscillations (Furman, 2014) "to achieve fixation of consecutive target stimulus" (Remington, 2012), and (c) Postrotatory, which refers to a jerky oscillation that occurs when the environment spins around the eyes (Yanoff and Duker, 2019). Fast phased nystagmic movements are conjugate functions ($500°/sec$) whose objective is to recentre both foveae during continuous vestibular and optokinetic movements (Haines and Mihailoff, 2018).

Figure 6 summarizes the seven eye movements described above including speed and latency times.

Table 28.1 Summary of Eye Movement Characteristics

CLASS	FUNCTION	CONJUGATE	SPEED	LATENCY	CLINICAL POINTS
Foveation	Hold fovea on target	NA	None		Look for drifts, especially holding eccentric gaze
			Only very small oscillations	NA	
Saccade	Acquisition of new target	Yes	100-700 degrees/s	200 ms	Sedative sensitive Test: look between points
			Amplitude dependent		
Smooth pursuit	Follow a moving target	Yes	Variable <100 degrees/s	100 ms	Test: follow a slow-moving target
			Target speed dependent		
Vergence	Direct fovea at targets of different distances	No	≈15 degrees/s	150 ms	Test: move target toward and away from nose
			Disconjugate saccades faster		
Vestibular (VOR)	Compensate for initial head movement	Yes	Variable <500 degrees/s	<15 ms	Dizziness and nausea Test: caloric (irrigate ear)
			Head acceleration dependent	Lasts 45 s	
Optokinetic (OKR)	Compensate for continued head movement	Yes	Variable <100 degrees/s	50-100 ms	Test: steady movement of a striped drum or cloth
			Retinal slip dependent		
Nystagmic fast phase	Recenter eye during continuous VOR or OKR	Yes	500 degrees/s	NA	Nystagmus: alternating fast- and slow-phase movements

NA, not applicable; OKR, optokinetic reflex; VOR, vestibuloocular reflex.

Figure 6: *Eye Movements (Haines and Mihailoff, 2018): A summary of the seven eye movements and their characteristics, which include speed and latency times.*

2.3 ACCOMMODATION, CONVERGENCE AND THE AC/A RATIO

In ophthalmology, a target is termed to be at a near distance when it is located $\approx 33cm$ away from the eyes and at a far distance when it is located $\approx 6m$ away from the eyes.

Lens accommodation, also known as accommodation, is a function (mechanism) that allows an eye to focus on a target at near distance i.e., less than $6m$, to form a clear and precise retinal image (Wright *et al.*, 2006) (Hainline *et al.*, 1992). It is associated with the accommodative reflex which includes vergence and adjustment of the pupil (Noorden and Campos, 2002). During accommodation, the muscles regulating the shape of the lens, known as cil-

iary muscles, contract the lens of the eye in order to increase its curvature (convexity) (Giannikakis, 2008) and, thereby, increase its refractive power, which improves focus of the lens on the fixation target (Lambert and Lyons, 2017). When a fixation target is located more than 6m away from the subject, the eyes do not need to accommodate (Ansons and Davis, 2014).

Accommodation is distinguished by: near-point accommodation (NPA), far-point accommodation (FPA), range and amplitude (Yanoff and Duker, 2019). NPA refers to the nearest target that an eye can focus on using its maximum power of accommodation (Nelson, 2019). FPA, being the opposite of NPA, refers to the farthest target that requires an eye to accommodate (Cooper and Duckman, 1978). This range is depicted by the distance between NPA and FPA points (Remington, 2012). The amplitude "is the difference in the focus power of the eye whilst fixating for near distance and fixating for far distance" (Rowe, 2012).

In ophthalmology, accommodation is expressed in lens dioptres (D), a reciprocal (multiplicative inverse) of focal length ($1D = 1m^{-1}$), where 1D is the accommodative power required by an eye to focus on a target at 1m (Hainline *et al.*, 1992) (Stidwill and Fletcher, 2010). As the distance between the fixation target and the eye shortens the accommodative power, required for a clear focus, increases (Noorden and Campos, 2002) (Wright *et al.*, 2006). For example, an eye needs to accommodate by 2D when it fixates on a target at 50cm (Hainline *et al.*, 1992). Accommodation (A) is calculated using equation 1 (Damanakis, 2005).

$$A_{(D)} = \frac{1}{FD_{(m)}} \tag{1}$$

where:

A = accommodation

FD = fixation distance

Convergence (C) (see subsect. 2.2.2) occurs when both eyes simultaneously turn inwards in order to fixate on the same target. The objective of convergence is to allow the visual stimuli, derived from that target, to be received by both foveae simultaneously (Yanoff and Duker, 2019). The light received by the fovea is referred to as the central line of sight (Wright *et al.*, 2006). When both central lines of sight intersect a target, at a distance less that 6m, they form an angle known as the convergence angle which increases as the target moves closer to the eyes (Lambert and Lyons, 2017). Convergence (C) is expressed in dioptres (Δ), where $1^\circ = 1.75\Delta \approx 2\Delta$, and is calculated using equation 2 (Rowe, 2012).

$$C_{(\Delta)} = \frac{1}{FD_{(m)}} \times \delta_{(cm)} \tag{2}$$

where:

C = convergence

FD = fixation distance

δ = distance between the eyes

Figure 7 illustrates the relationship between accommodation and convergence at various fixation distances.

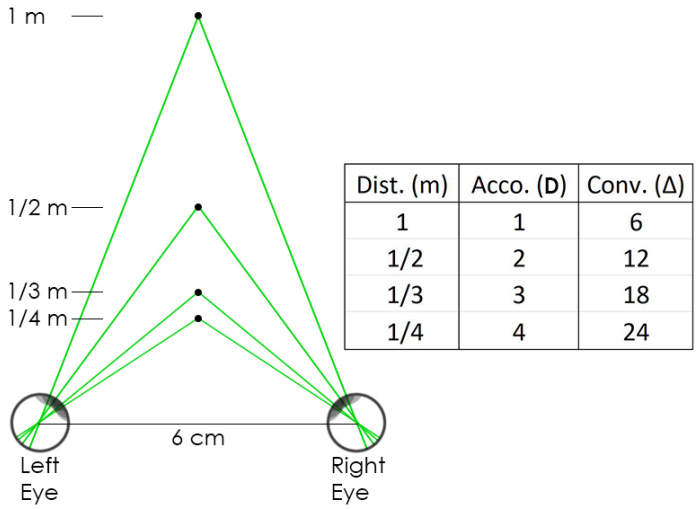

Dist. (m)	Acco. (D)	Conv. (Δ)
1	1	6
1/2	2	12
1/3	3	18
1/4	4	24

Figure 7: *Accommodation & Convergence: Relation between accommodation, convergence and the fixation distance. The fixation distance varies* $(1 - 0.25\text{m})$ *while the distance between the eyes is* 6cm. Dist *refers to the fixation distance measured in metres* (m), Acco *is the accommodation measured in lens dioptres* (D) *and* Conv *is the convergence which is measured in prismatic dioptres* (Δ).

Placing a negative lens of 3D, which blurs vision, in front of one eye while the other eye is covered, the uncovered eye is forced to accommodate by 3D in order to see the target clearly (Yanoff and Duker, 2019). During accommodation, the covered eye will converge by a certain amount (Lambert and Lyons, 2017). This phenomenon, whereby convergence is elicited from accommodation, is known as Accommodative Convergence (AC) (Hainline *et al.*, 1992) (Wright *et al.*, 2006). The amount of accommodative convergence produced by each unit of accommodation is determined by the ratio of Accommodative Convergence to Accommodation, i.e. AC/A (Yanoff and Duker, 2019) (Nelson, 2019). For example, when a subject accommodates by 3D and both eyes converge, in response to the accommodation, by 12Δ then the AC/A ratio is $12 : 3 = 4(\Delta/D)$ (Damanakis, 2005). A ratio of $2 - 6\Delta : 1D$ is considered normal (Ansons and Davis, 2014) (Wybar, 1974). Ansons and

Davis (2014) suggest that an "individual's AC/A ratio, which may be genetically determined, has been shown to remain virtually unchanged from childhood to at least presbyopic age".

The AC/A ratio is used to diagnose convergence irregularities caused by various conditions such as strabismus (Nelson, 2019) (Rowe, 2012), an eye misalignment condition that is discussed in the next chapter. In such conditions, a high AC/A ratio suggests greater convergence (eso-deviation) per unit of accommodation, whereas, a low AC/A ratio determines lower convergence (exo-deviation) per unit of accommodation (Wybar, 1974). In all, there are five different methods used to calculate the AC/A ratio, namely, the: (a) heterophoria method, (b) gradient method, (c) oculographic method, (d) fixation disparity method, and (e) haploscopic method (Noorden and Campos, 2002). Of these five methods, only two are considered to be accurate, quick to calculate and require little cooperation from the subjects (Salmon, 2019). These are:

- **Heterophoria Method:** Initially, the distance between both eyes is measured in cm and refractive lenses are used to resolve any pre-existing conditions that would affect a subject's ability to accommodate (Yanoff and Duker, 2019) (Nelson, 2019). Next, the ocular deviations are measured for near ($33cm$) and far ($6m$) distances using prisms (Wybar, 1974). The AC/A ratio is calculated using the following equation (eq. 3) (Noorden and Campos, 2002):

$$AC/A_{(\Delta/D)} = \delta_{(cm)} + \frac{N_{\Delta} - F_{\Delta}}{A_{(D)}} \tag{3}$$

  where:

  AC/A = accommodative convergence to accommodation

  δ = distance between the eyes

  N = deviation at near

  F = deviation at far

  A = accommodation at near

  According to Rowe (2012), a "positive sign is used for eso-deviations and a negative sign is used for exo-deviations".

- **Gradient Method:** This method uses spherical lenses while covering either eye to measure accommodation at a pre-determined fixation distance, near or far (Damanakis, 2005). At near distances ($\approx 33cm$), a subject's accommodation is measured using convex lenses because they

can decrease the accommodative power of the eyes, whereas at far distances ($\approx$ 6m), accommodation is measured using concave lenses as they can increase the accommodative power of the eyes (Wright *et al.*, 2006) (Ansons and Davis, 2014). In order to calculate the AC/A ratio, the eye angles are measured twice (Wybar, 1974). First, without using lenses and, again, while using both convex and concave lenses (Yanoff and Duker, 2019). The AC/A ratio is determined by the angular difference between the two measurements, with and without a lens, divided by the power of the lens (Yanoff and Duker, 2019). The AC/A ratio is calculated using the following equation (eq. 4) (Stidwill and Fletcher, 2010):

$$AC/A_{(\Delta/D)} = \frac{Q1_{\Delta} - Q0_{\Delta}}{Lp_{(D)}} \tag{4}$$

where:

AC/A = accommodative convergence to accommodation

$Q0$ = deviation of the eye without using a lens

$Q1$ = deviation of the eye using a lens

Lp = accommodative power of the lens

Similarly to the heterophoria method, a high (positive) AC/A ratio indicates eso-deviation and a low (negative) ratio indicates exo-deviation (Ansons and Davis, 2014).

Worked examples of calculating the AC/A ratio using the aforementioned methods, heterophoria and gradient, are included in appendix A.1.

In ophthalmological conditions where convergence is irregular (abnormal), the calculations of accommodation, convergence and AC/A ratio can be used to deduce, with relative accuracy, the fixation distance of the eyes (Damanakis, 2013) (Wybar, 1974).

2.4 BINOCULAR VISION

The visual stimuli, received by a normal human eye, is converted by the retina into a two dimensional (2D) array of stimuli, a projection of the environment, known as a monocular retinal image (Barlow *et al.*, 1967) (Stidwill and Fletcher, 2010). The retinal cells stimulated by light are commonly referred to as stimulated retinal points, retinal elements or retinal areas (Yanoff and Duker, 2019) (Haines and Mihailoff, 2018) (Rowe, 2012). Additionally, the light from the surface of an object to a retinal point forms a virtual line

which is referred to as a line of direction or a direction ray or visual direction (Billson, 2003) (Lambert and Lyons, 2017). When a retinal area is stimulated by light, it "localizes the stimulus as a visual percept in a specific direction, a visual direction" (Noorden and Campos, 2002), which is relative to the visual direction of the fovea (Damanakis, 2005). There are two types of visual directions, namely, the principal visual direction, which refers to the light that stimulates the foveal (macula) area, and the peripheral visual direction, which refers to the light that stimulates a peripheral retinal area (Billson, 2003) (Kolb *et al.*, 2020). Once a retinal image is formed, by the ganglion cells of an eye, it is transmitted to the visual cortex of the brain, through the lateral geniculate bodies, in such a way that all information gathered from the visual stimuli i.e., shape, colour, size, brightness and visual direction, match the positions of the ganglion cells in the retina (Yanoff and Duker, 2019) (Stidwill and Fletcher, 2010). There are two lateral geniculate bodies, also referred to as lateral geniculate nuclei (LGN), each receiving impulses from both eyes and transmitting them to the visual cortex of the brain (Hubel, 1998). In addition to providing a relay station (gateway) for the retinal ganglion cells, the LGN receives feedback from the brain that could affect the processing of the impulses received from both retinae (Covington and Al Khalili, 2020). Haines and Mihailoff (2018) explain that "the map of visual space on the retina is maintained in the lateral geniculate nucleus and ultimately in the visual cortex".

In normal human vision, the location of both eyes, being at the front of a face, and the distance between their pupils, referred to as inter-pupillary distance (IPD) (fig. 8), causes the visual field of views from both eyes to overlap (Richards, 1970). The brain receives and superimposes both retinal images both of which depict a slightly different angled projection of the same environment (Lambert and Lyons, 2017) (Damanakis, 2013) (Vishwanath and Hibbard, 2013). Rowe (2012) defines the phenomenon of superimposition as "the simultaneous perception of the two images formed on corresponding areas, with the projection of these images to the same position in space".

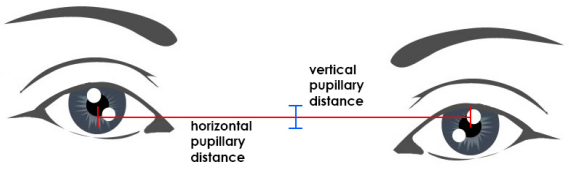

Figure 8: *Inter-pupillary distances: An example of the horizontal (red) and vertical (blue) IPD between the eyes.*

The ability of the brain to simultaneously receive both (bi-, Latin word *bis* = 'two') retinal images from the eyes (oculi, plural of the Latin word *ocu-*

lus = 'eye') is called Binocular vision (fig. 9) (Barlow *et al.*, 1967). In ophthalmology, normal binocular vision is defined as the cerebral process in which the retinal images, from both eyes, contribute to a common single perception (binocular single vision, BSV) (Lambert and Lyons, 2017) (Ansons and Davis, 2014). In 1942, Hering suggested that, in normal binocular vision, the environment is "seen" by an imaginary third eye located centrally between the two eyes (Erkelens and van Ee, 2002). In 1962, Von Helmholtz termed Hering's concept as the Cyclopean eye (fig. 9) (Damanakis, 2005) (Kolb *et al.*, 2020). However, current research has shown that "binocular perception is incompatible with vision from a single vantage point" (Erkelens and van Ee, 2002), suggesting that Hering's concept "is sometimes inappropriate and always irrelevant as far as vision is concerned" (Erkelens and van Ee, 2002).

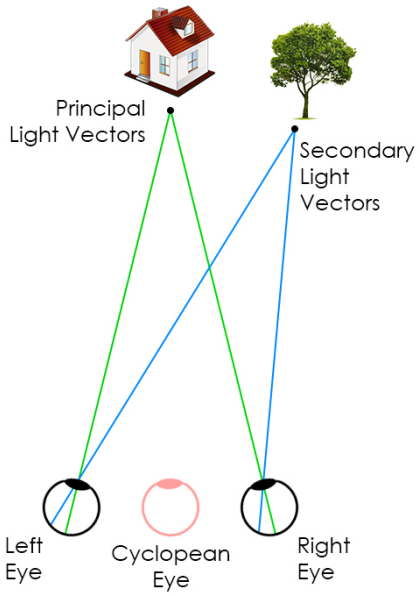

Figure 9: *Normal binocular vision: The two principal visual directions (green), stimulating the foveae, originate from the house. The tree is perceived by peripheral visual directions (blue), stimulating other areas of the retina. Both eyes are visually stimulated by the house and tree at corresponding retinal areas.*

2.4.1 *Normal Retinal Correspondence (NRC)*

Normal Retinal Correspondence (NRC) is characterized by the simultaneous stimulation of corresponding retinal areas with matching visual directions (fig. 9) (Cooper and Record, 1986) (Wright *et al.*, 2006). Rowe (2012) defines normal NRC as "a binocular condition in which the fovea and areas on the nasal and temporal side of one retina correspond to and have, respectively, common visual directional sensitivity with the fovea and temporal

and nasal areas of the retina of the other eye". In normal binocular vision, the visual stimuli projected on corresponding retinal areas are fused, by the brain, into a single three dimensional perception (Tychsen, 2005) (Parker, 2009). The visual stimuli projected on non-corresponding (disparate) retinal areas, cannot be fused by the brain and, therefore, are perceived as double (Ansons and Davis, 2014) (Billson, 2003). Binocular single vision occurs when the visual stimuli, received by both eyes, are projected on corresponding retinal areas, whereas, double binocular vision occurs when the visual stimuli is received by non-corresponding (disparate) retinal areas (Parker, 2009).

2.4.2 *Sensory vs Motor Fusion*

Fusion is a cerebral process that takes place in the visual cortex of a human brain in which the retinal images, from both eyes, are merged (unified) into a single perception, subject to, normal retinal correspondence (Hughes and Townsend, 1998). In order to develop a meaningful perception of an environment the brain, amongst other functionalities, compares, contrasts and superimposes both retinal images (Brodsky, 2016). There are two types of fusion:

- **Sensory:** Refers to the ability of the brain to merge both retinal images into a single unified perception (Kang *et al.*, 2018) (Parker, 2009). Noorden and Campos (2002) define sensory fusion as "the unification of visual excitations from corresponding retinal images into a single visual percept, a single visual image".

- **Motor:** Refers to the ability of the eyes to simultaneously verge on an object, satisfying normal retinal correspondence, in order to maintain sensory fusion (Pratt-Johnson and Tillson, 1984) (Billson, 2003). Ansons and Davis (2014) describe motor fusion as "the ability to maintain a single fused image during vergence movements".

In order for the brain to fuse both retinal images, the visual stimuli from the same object must be received by both foveae simultaneously (Hughes and Townsend, 1998). Fusion is not possible if the two retinal images do not match one another, i.e. are majorly disparate (Kolb *et al.*, 2020) (Hammond, 2014). Further details about on fusional ranges amongst horizontal, vertical and torsional retinal images are described in subsection 2.4.4.

2.4.3 *Retinal Rivalry*

In normal binocular vision, retinal rivalry is a physiological phenomenon that occurs when each retina is stimulated by visual stimuli deriving from different objects (Stidwill and Fletcher, 2010). Consequently, the retinal images produced by each eye are majorly different, or dissimilar, preventing sensory fusion (Lambert and Lyons, 2017). When retinal rivalry occurs, the subject "will see one target, then the other, or a mosaic of contours, but not both simultaneously" (Rowe, 2012), resulting in alternating perception (Pratt-Johnson and Tillson, 1984) (Kolb *et al.*, 2020). van Dam and van Ee (2006) refers to retinal rivalry as a "perceptual bistability phenomenon ... because it can dissociate the visual input from the perceptual output".

2.4.4 *The Horopter and Panum's Fusional Area*

The Horopter is a virtual arc intersecting all points in the environment that are projected on corresponding retinal areas (fig. 10) (Stidwill and Fletcher, 2010) (Yanoff and Duker, 2019). The centre of the horopter is the midpoint of the eyes and its apex is the point of bifoveal fixation (Damanakis, 2005). An object that is located on the horopter is projected on corresponding retinal areas and perceived as a single object in the environment (fig. 10) (Billson, 2003). If an object is located outside the horopter, then it is projected on different retinal areas and perceived as double (fig. 10) (Hubel, 1998) (Kolb *et al.*, 2020). This phenomenon is known as physiological (natural) diplopia (Agrawal, 2019) (Kang *et al.*, 2018). Even though physiological diplopia is present in normal binocular vision it is unnoticed, as most of the time there will be other objects located closer or farther away to the fixation object (Lambert and Lyons, 2017). The most important part of vision is formed by the foveae that contribute to central vision (Snell and Lemp, 2013) (Fray, 2017).

In 1858, Panum remarked that every retinal point on one eye corresponds to a small region that includes and surrounds the matching retinal point of the other eye (Stidwill and Fletcher, 2010) (Kolb *et al.*, 2020). Before Panum's discovery it was suggested that "singleness in vision with two eyes was explained by the theory of corresponding retinal points" (Qin *et al.*, 2004). Panum demonstrated that retinal correspondence is a binocular condition that occurs not just between retinal points, but also, between retinal areas (Damanakis, 2005). This means that binocular vision is maintained, through normal fusion of both retinal images, even if the fixation object is not positioned directly on the horopter but, within an area that surrounds the

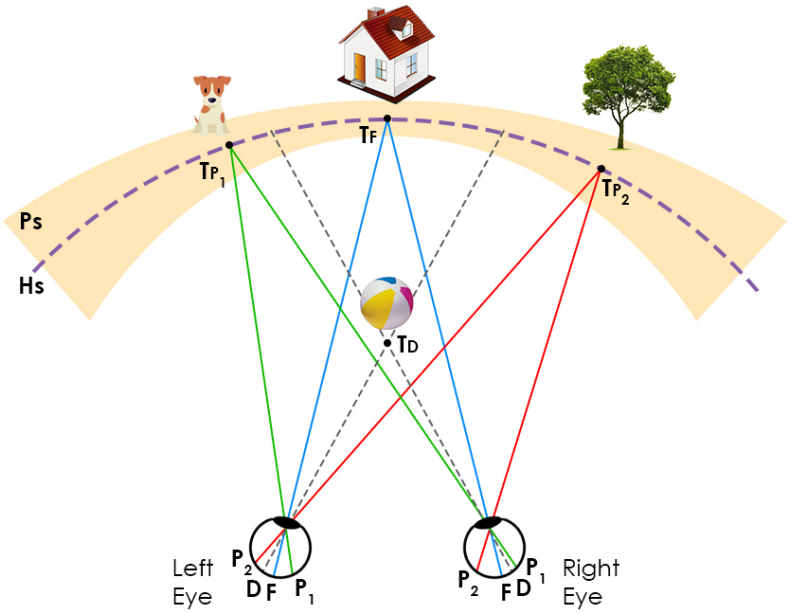

Figure 10: *Binocular vision with normal retinal correspondence (NRC): Both eyes, and their foveae (*F*), fixate on the house at point* TF *(blue lines). The point of fixation determines the location of the horopter (*Hs*) which intersects all objects that satisfy normal retinal correspondence (dashed purple arc). The visual stimuli from the puppy (green lines) at point* TP_1 *and the tree (red lines) at* TP_2*, which also lie on the horopter, are received by corresponding retinal areas indicated by the peripheral retinal points* P_1 *and* P_2*. However, the visual stimuli from the beach ball (dashed grey lines) at point* TD *are received by disparate retinal areas (*D*) in each eye.* D *is located left from the fovea of the left eye, and right from the fovea of the right eye. The beach ball will appear double due to the physiological diplopia that occurs.* Ps *refers to Panum's fusional area which allows objects to be fused normally even if they do not lie directly on the horopter.*

horopter (fig. 10) (Lambert and Lyons, 2017). This area, known as Panum's fusional area, "is narrow at the fixation point and widens towards the periphery" (Rowe, 2012) (fig. 10). It is worth noting that the size of Panum's area is not standard, but depends on the characteristics of the visual stimuli i.e., the area becomes smaller for small objects and larger for large objects that can be fused even at wider disparities (Ansons and Davis, 2014) (Lambert and Lyons, 2017). Additionally, this area is not in physical space, but subjective to a specific visual stimulus (Agrawal, 2019). This phenomenon is also referred to as binocular fixation disparity, which is the ability of the brain to fuse both retinal images despite the fact that the fixation target is projected on different retinal points within Panum's area (Richards, 1970) (Agrawal, 2019).

It was believed that Panum's fusional area was very small, around $6-12$ arc minutes near the fovea and approximately $30-41$ in the periphery (Noorden and Campos, 2002). Qin *et al.* (2006) discovered that "the disparity limit in the horizontal meridian (0 and 180), about 32–40 min of arc, is evidently

larger than the limit in the vertical meridian (90 and 270), about 19.2–25.6 arcmin". However, recent research has shown that Panum's fusional area is considerably larger and fusion can occur at $2^\circ - 3^\circ$ of disparities between the foveae (Noorden and Campos, 2002) (Stidwill and Fletcher, 2010). Although measurements of fusional amplitudes tend to be similar amongst individuals, "there is no agreed standard" (Fray, 2017) within the ophthalmic community. Nevertheless, it is considered that mean fusional amplitudes include:

- **Horizontal:** $\approx 4 - 6\Delta$ ($2^\circ - 3^\circ$) (Georgievski *et al.*, 2007)
- **Vertical:** $\approx 3\Delta$ (1.5°) (Stidwill and Fletcher, 2010)
- **Torsional:** $\approx 3\Delta$ (1.5°) (Traboulsi and Utz, 2016)

Although the differences between horizontal and vertical fusional limits suggest that Panum's fusional area is formed as an ellipse, Qin *et al.* (2004) have demonstrated that "the nasalward limits are obviously larger than the temporalward limits". Furthermore, Georgievski *et al.* (2007) observed that horizontal fusion breaks when torsional disparity exceeds $\geqslant 4^\circ$. Ansons and Davis (2014) suggests that "stimulation of disparate retinal elements within the area allows fusion of the images" and that "not only is single vision possible in Panum's area but visual objects are seen stereoscopically" (Noorden and Campos, 2002).

2.5 STEREOSCOPIC VISION

Stereopsis or stereoscopic vision comes from the Greek words 'στερεό' (stereo = solid) and 'όψη' (opsi = view). In its literal meaning, it refers to the perception of three dimensional solid objects that are viewed in the environment. The terms binocular vision and stereopsis are sometimes used interchangeably implying that stereopsis is a derivative of binocular vision (Hibbard *et al.*, 2017) (Giaschi *et al.*, 2013). However, it is argued that stereopsis can be accomplished using either one or both eyes and that it should not be mistaken for what is known as binocular depth perception (Barlow *et al.*, 1967) (Parker, 2019). Vishwanath and Hibbard (2013) draw a clear distinction between "binocular depth perception, which is the capacity to perceive quantitative depth relations using the visual information from two eyes, and stereopsis, the qualitative vividness of depth that often obtains as a result of this capacity". In ophthalmology, stereopsis refers to the ability of a human brain to perceive depth, by forming the third dimension from both retinal images, when normal binocular vision is present (Richards, 1970) (Parker,

2019) (Helveston, 2010). Ansons and Davis (2014) suggest that stereopsis "is not present at birth but has been demonstrated at $3-4$ months of age".

Due to a horizontal disparity, caused by the horizontal IPD, each eye views the same object from a different angle and forms a slightly disparate retinal image compared to the other eye (Parker, 2019) (Richards, 1970) (Hibbard *et al.*, 2017). Normal retinal correspondence and Panum's area, which includes the horopter, are key factors in the brain's ability to fuse both retinal images into a single three dimensional perception (Lambert and Lyons, 2017) (Ancona *et al.*, 2014). Stereopsis is not possible when vertical disparities are present (Parker, 2009) (Hubel, 1998). The importance of stereopsis is explained by Barlow *et al.* (1967) who suggest that animals with overlapping visual fields are advantaged when perceiving depth compared to other animals, because the retinal images formed, by both eyes, contain far more direct clues which the brain uses to measure distance.

2.5.1 *Familiarity Cues*

When the brain fuses both retinal images, it uses memorable clues, like shapes, sizes and colours, familiar to each individual, in order to assist in the analysis and comprehension of the perceived environment (Parker, 2019) (Vishwanath and Hibbard, 2013). These clues, also known as familiarity cues, are not associated with binocular vision, which is why they can be used when viewing the environment monocularly (Agrawal, 2019).

The most notable familiarity cues are:

- **Motion Parallax:** When an individual looks at two objects in the environment, one located closer to the individual than the other, and moves from side to side the "movement of the objects becomes apparent" (Noorden and Campos, 2002). The farthest object from the individual appears to move in the same direction as the individual whilst the near object appears to move in the opposite direction (de la Malla *et al.*, 2016).

- **Linear Perspective:** In this cue, objects that are parallel to each other and also extend into the distance appear to diverge at near and converge at far (Hubel, 1998) (Damanakis, 2005). Examples of linear perspective include roads and railroad tracks that appear to shrink and converge at far distances (Stidwill and Fletcher, 2010). A large building from a perspective angle would also reveal this cue as the farthest sections of the top and bottom edges of the building would appear to converge (Kolb *et al.*, 2020).

- **Overlay of Contours:** The relative position of two objects is perceived when the contour of one object covers part of the contour of another object (Lambert and Lyons, 2017). In this cue, the “overlapped object is considered further away" (Kolb *et al.*, 2020).
- **Relative Size of Known Objects:** When the size of an object in the environment is already known from experience then, its distance from a viewer is estimated by its apparent size (Damanakis, 2005). For example, a car that initially appears to be small in size but gradually becomes bigger and bigger, suggests that the car is moving towards the viewer.
- **Distribution of Highlights and Shadows:** The shapes and positions of shadows are used to estimate an object’s shape, size and depth (Hubel, 1998). The visual system is able to recognize shadows that have been formed by sunlight coming from above (Stidwill and Fletcher, 2010), and when light comes from below, it results in “a totally different perception" (Kolb *et al.*, 2020).
- **Aerial Perspective:** This cue represents information about an object’s colour, contrast and texture that has been influenced by the atmosphere (Rowe, 2012) (Noorden and Campos, 2002). Due to the blue light in the atmosphere, “distance objects appear more blue" (Kolb *et al.*, 2020). Furthermore, due to the atmospheric density, objects at a far distance are perceived blurry compared to objects at a near distance that are perceived with fine contours (Hubel, 1998) (Kolb *et al.*, 2020). According to Noorden and Campos (2002), “Chinese painters are masters at creating extraordinary depth in landscapes by using subtle variations of shading".

The importance of these cues in the estimation of depth by subjects suffering from binocular vision disorders is discussed in the next chapter.

2.5.2 *Worth’s Classification*

Worth classifies binocular vision into three grades which indicate the degree of binocularity (Ansons and Davis, 2014):

- Simultaneous perception
- Fusion (sensory and motor)
- Stereoscopic vision

This classification indicates that an individual may lack stereoscopic vision, but could possess binocular vision (Ansons and Davis, 2014) (Damanakis,

2013). However, in order for a person to accurately perceive depth, stereopsis must be present and the visual stimuli from the fixation object must be simultaneously received by both foveae (Rowe, 2012) (Damanakis, 2005).

2.5.3 *Milestones in Stereopsis Research*

In 1838, Sir Charles Wheatstone invented the stereoscope, a device which allowed both eyes to look at two slightly different images, through a set of oriented mirrors (fig. 11) (Bowers, 2001) (Carvelho *et al.*, 2008). The objective of the stereoscope was to allow the brain fuse the corresponding retinal images and perceive depth (Bowers, 2001) (Parker, 2009). Using this invention, Wheatstone was able to discover that "stereopsis occurs when horizontally disparate retinal elements are stimulated simultaneously" (Noorden and Campos, 2002).

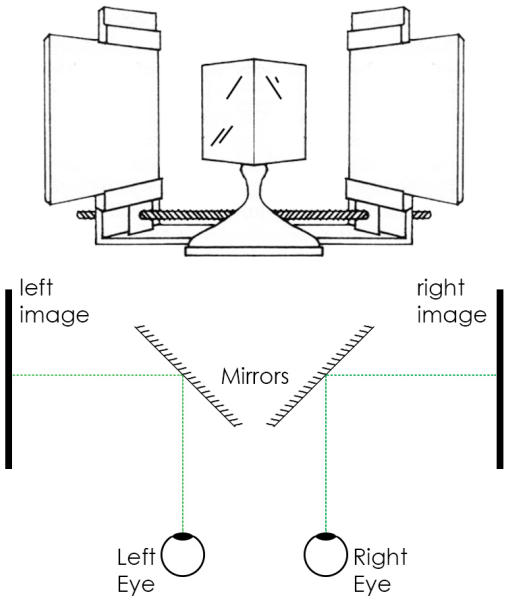

Figure 11: *Sir Charles Wheatstone's stereoscope: The two images (left and right) depict the same scene but from two slightly different angles, resembling the left and right eye views respectively. Each eye then focuses on the according image through a set of mirrors. When viewed binocularly, the brain fuses both images and constructs a 3D perception of the scene.*

Wheatstone acknowledged that the first person to nearly come close discovering stereopsis was Leonardo da Vinci (Parker, 2009) (Bowers, 2001). Unfortunately, da Vinci used a spherical object as his fixation target – "ironically the one object whose shape stays the same when viewed from different directions" (Hubel, 1998), and was unable to determine the disparate views from each eye (Bowers, 2001).

The stereoscope underscored the importance of binocular disparity in sensory fusion, creating opportunities for further research in stereopsis. Ortony (1971) introduced a stereo-viewing system in which a pair of images were shown on a CRT (Cathode Ray Tubes) monitor, one on top of the other, by splitting the screen horizontally. Ortony's system used a transmitting/reflecting (T/R) surface (a type of mirror) that allowed the lower image to be transmitted through and the upper image to be reflected off the T/R surface (Ortony, 1971). Unlike Wheatstone's stereoscope, which was usable by only one viewer, Ortony's system allowed several viewers to simultaneously perceive a 3D image stereoscopically (Ortony, 1971).

In his research about binocular depth perception, Julesz (1964) discovered that stereopsis could be achieved through binocular disparity, without processing any familiarity cues. The core of Julesz's technique was to camouflage an object such that it could only be perceived when viewed stereoscopically (Julesz, 1964) (Ansons and Davis, 2014). This was accomplished by creating random-dot (randot) stereo images, a technique to devoid all familiarity cues (Kolb *et al.*, 2020) (Vishwanath and Hibbard, 2013). When the random-dot stereogram is viewed monocularly, no recognizable features are perceived. However, when viewed stereoscopically the brain is able to fuse both retinal images allowing the viewer to successfully perceive a three dimensional illusion of a hidden object (Julesz, 1964) (Yanoff and Duker, 2019). Randot stereograms are discussed further in subsection 3.4.7.

Many modern education and entertainment systems employ, or rely on, binocular depth perception, through stereoscopic vision, in order to improve user engagement. Lambert and Lyons (2017) suggest that the visualization "of structures can aid understanding, highlighted by the implementation of 3D technology in the classroom in subjects such as astronomy and biology".

2.6 SUMMARY

A human eye is a complex organ that has the ability to convert light, from the environment, into a two dimensional retinal image. The anatomical structure of a retina, including its concentric regions, explains why vision is at its most optimal fidelity centrally to the retina and why vision becomes progressively more crude and blurry peripherally to the retina. This chapter reviewed the mechanics of vision, including the various movements of the eyes and functionality of the oculomotor system, which maintains a clear and stable retinal image on each eye. It was also described how convergence

is elicited from the act of accommodation, a concept defined as accommodative convergence.

Once the brain receives both retinal images, it fuses them into a single three dimensional perception of the environment. It was mentioned that animals with overlapping visual fields are advantageous when perceiving depth compared to other animals, because the retinal images formed, by both eyes, contain far more direct clues which the brain uses to measure distance. This chapter discussed the conditions under which stereopsis is enabled emphasizing on its contribution to binocular depth perception. In order for an individual to accurately perceive depth, using both eyes, stereopsis must be present and the visual stimuli, derived from the object of fixation, must be received by both foveae simultaneously. The individual should also be able to use familiarity cues in order to assist in the better understanding of the perceived environment. Furthermore, when an object is located on the horopter and projected on corresponding retinal areas, it is perceived as a single object. Theoretically, objects that do not fall on the horopter are perceived as double. However, Panum's area determines that the brain is still able to fuse both retinal images into a single perception even when the fixation object does not fall exactly on the horopter.

This chapter underscores the importance of stereopsis, through binocular vision, as it enables the perception of depth and allows an individual to judge distances accurately. Unfortunately, not everyone can perceive depth binocularly. The next chapter delves into the ophthalmological condition known as Strabismus, a neuromuscular disorder that disturbs the proper alignment of the eyes and prevents the binocular perception of depth.

3

STRABISMUS

> "Οι άνθρωποι συνηθίζουν να κρίνουν περισσότερο απ΄ τις σκιές παρά απ΄ την πραγματικότητα, γιατί η όραση ανήκει σε πολλούς, ενώ η αντίληψη σε λίγους..."
>
> — Πλάτων Πολ.[514α–517α]

> *"People tend to form judgements based on shadows rather than reality, as vision belongs to many whilst perception to few..."*
>
> — Plato Pol.[514a–517a]

This chapter explores an ocular condition known as strabismus, in which the eyes are not aligned and, therefore, do not fixate on the same object. Apart from delving into the medical aspects of strabismus, including the binocular disturbances caused by an ocular misalignment and the adaptations enforced by the brain, this chapter investigates the origin of strabismus and reviews its physiological, psychological and social impact in a person's life. Although, this chapter discusses strabismus into considerable detail, it is not intended to be an exhaustive description of the condition, as several books on the subject have already been published e.g. (Noorden and Campos, 2002), (Damanakis, 2005), (Wilson *et al.*, 2009), (Rowe, 2012), (Ansons and Davis, 2014), (Traboulsi and Utz, 2016) and (Agrawal, 2019).

Furthermore, this chapter describes the process of diagnosing strabismus and outlines the most up to date diagnostic methods that are used to measure the amplitude of strabismus and assess the presence of binocular vision and stereopsis. Current management and treatment methods are also discussed in detail, with emphasis on the suitability of each treatment in various types of strabismus. Lastly, this chapter identifies the limitations with current diagnostic and treatment methods, and makes a case for further research in the topic of strabismus.

3.1 WHAT, WHO, WHEN, HOW, WHERE, WHICH AND WHY (SIX WS AND ONE H) OF STRABISMUS

This section analyses an ocular condition referred to as strabismus, using six elements of investigation, also known as elements of circumstances[1].

3.1.1 *What is strabismus?*

Ocular motility disturbances include conditions that are characterized, either, by difficulties in controlling eye movements or by an abnormal alignment of the eyes (Lambert and Lyons, 2017). Strabismus, coming from the Greek word 'στραβό' (strabo = bent, not straight) and the suffix '-ισμός' (-ismos = -ismus), is defined as a neuromuscular disorder in which the principal (foveal) visual directions, of both eyes, are not simultaneously directed towards the same object (fig. 12) (Damanakis, 2013) (Oystreck and Lyons, 2012) (Stidwill and Fletcher, 2010). In loose terms, strabismus is a condition in which both eyes are unable to have matching visual directions whilst fixating on the same object. As one eye fixates on an object, with its principal visual direction directed towards that object, the other eye deviates with its foveal visual direction directed somewhere else (fig. 12).



Figure 12: *Strabismus: A simple illustration of strabismus where a subject, with IPD* $\approx$ 6cm*, fixates on a target* $\approx$ 55cm *away from the centre of the eyes. The right eye (R) fixates on the target, as indicated by the green vertical line on the right eye, whereas the left eye (L) deviates outwards at a certain angle, indicated by the red vertical line on the left eye. The green vertical line next to the red vertical line indicates the correct position of the left eye that would have allowed it to converge on the same target as the right eye. Assuming that each eye has a radius of* $\approx$ 12mm *and that both eyes must rotate by* $\approx 3°$ *inwards in order to converge on the fixation target, it is estimated that the outwards deviation, of the right eye, is* $\approx 8-11°$ *(*$\approx 16-22\Delta$*).*

1 In 350 BC, Aristotle suggested that in order to compile a complete investigation, distinguishing between voluntary and involuntary actions, the questions of 'what', 'who', 'when', 'where', 'why' and the occasional 'how' must be answered (Sloan, 2010). Aristotle also believed that ignorance of one of these questions (elements of circumstances), not only implies involuntary action, but also a shallow understanding of the problem, underscoring that the most important question which needs to be answered, is 'why'.

A strabismic deviation is characterized by an abnormal angle formed between the visual directions of both foveae (Beauchamp *et al.*, 2003) (Helveston, 2010). Strabismus is considered to be a polymorphic neuromuscular anomaly (Rutstein *et al.*, 2011) because "it may display characteristics which vary greatly from one subject to the next" (Bui Quoc and Milleret, 2014). Also, the deviation of a strabismic eye may vary depending on the physical or mental state of the person suffering from strabismus, i.e. bored, tired, sleepy, ill, anxious, happy, stressed (Hammond, 2014) (Weinstock *et al.*, 1998) (Lipton, 1970). As such, the behaviour and functionality of the oculomotor system, controlling the strabismic eye, is unpredictable (Damanakis, 2013) (Salmon, 2019) (Agrawal, 2019). Furthermore, some types of strabismus are periodic (Stidwill and Fletcher, 2010).

When the eyes are not properly aligned, the two retinal images formed by both eyes are majorly different (Hammond, 2014). The displacement of these two retinal images is either larger or smaller than the fusible range determined by Panum's area (Nelson and Olitsky, 2014) (Billson, 2003). Consequently, a subject with strabismus cannot perceive depth binocularly, because the brain is unable to fuse both retinal images and develop BSV (Helveston, 2010) (Rowe, 2012). A common characteristic of strabismus is that, of the two eyes, only one eye would deviate (Wright *et al.*, 2006) (Cooper and Record, 1986). The dominant eye is the eye that has "a strong preference to take up fixation" (Agrawal, 2019). Strabismologists refer to the strabismic eye as "deviating" or "bad" eye and the normal eye as "fixating", "dominant" or "good" eye (Baker *et al.*, 2008) (Damanakis, 2005) (Rowe, 2012) (Yanoff and Duker, 2019) (Haines and Mihailoff, 2018).

In addition to preventing binocular depth perception, strabismus often has adverse psychological and social effects on a person's quality of life (Helveston, 2010) (Bui Quoc and Milleret, 2014). Children with strabismus who are unable to participate in friendly activities, such as ballgames, are at risk of "isolation at school, poor self-esteem, and social dysfunction ... often endure the teasing of classmates and the misguided frustration of teachers ('Why don't you look at me when you are speaking?')" (Weinstock *et al.*, 1998). The significance of binocular vision and stereopsis is highlighted when considering that education and entertainment products increasingly incorporate three dimensional technology (Michaelides and Moore, 2004). Lambert and Lyons (2017) suggest that "not being able to engage with the immersive, interactive 3D virtual worlds that children enter via games, children with abnormal binocular vision are not able to interact with their peers in this context". Additionally, Lambert and Lyons (2017) explain how "impaired binocular vision can result in debilitating symptoms, such as headaches, eye

strain, and diplopia, impacting on quality of life, with lifelong consequences related to a child's future occupation choices". Furthermore, adults with strabismus can have difficulty securing employment, maintaining relationships, participating in sports and performing well at work or in education (Lipton, 1970). Studies have shown that, in general, individuals with normal binocular vision perform better at completing some tasks than subjects suffering from strabismus (Agrawal, 2019). For example, "a buzz-wire task in which subjects had to guide a wire hoop around a 3D track without bringing the hoop into contact with the track" (Read *et al.*, 2013). The inefficient performance by strabismic subjects is partially attributed to the deficit of binocular motility (Cooper and Jamal, 2012) (Wright *et al.*, 2006). Weinstock *et al.* (1998) state that "abnormal binocular vision can interfere with visual motion processing and with reading".

3.1.2 *Who does strabismus affect? When does strabismus occur in life? How does strabismus develop?*

Depth perception, through binocular vision and stereopsis, primarily requires normal development of the: (a) oculomotor system, (b) eye structure, and (c) visual cortex of the brain, including all central processes and pathways that contribute into visual perception (Billson, 2003) (Bui Quoc and Milleret, 2014).

The development of binocular single vision takes place during a particular time-frame in life known as critical period, also referred to as sensitive period, in which the brain is at its maximum plasticity (Hammond, 2014) (Bui Quoc and Milleret, 2014). The critical period occurs at an early postnatal stage, typically between the ages of 5 and 8 (Lambert and Lyons, 2017) (Voss, 2013). However, it has been noted that visual maturation can continue up to 9 or 10 years of age (Awadein *et al.*, 2008) (Beauchamp *et al.*, 2003) (Billson, 2003).

During the critical period, both lateral geniculate bodies, which receive retinal images from the corresponding left and right eyes (Snell and Lemp, 2013), "compete for synaptic space on cortical cells" (Haines and Mihailoff, 2018). In normal binocular single vision (BSV) the nerve cells from each lateral geniculate body are able to evenly transmit impulses to the cells in the primary visual cortex (Yanoff and Duker, 2019) (Billson, 2003). At the end of the critical period "the synaptic connections made during the competition phase become permanent" (Haines and Mihailoff, 2018) and a disruption of binocular vision at a later time does not affect the efficiency and equal dis-

tribution of the synapses from both lateral geniculate bodies to the primary visual cortex (Salmon, 2019) (Snell and Lemp, 2013). In strabismus however the nerve cells in the lateral geniculate body, corresponding to the strabismic eye, cannot transmit impulses as effectively as the nerve cells in the lateral geniculate body that receives retinal images from the normal eye (Noorden and Campos, 2002). Consequently, stereopsis and, thereby binocular depth perception, is not developed (Agrawal, 2019) because the cells in the primary visual cortex receive impulses primarily from the nerve cells, in the lateral geniculate bodies, that have been stimulated by the ganglion cells of the normal eye (Lambert and Lyons, 2017) (Remington, 2012). Stereopsis, however, can be restored if strabismus is successfully treated during the critical period in which the brain is at its maximum plasticity (Agrawal, 2019) (Hammond, 2014). Failing to do so can result in loss of binocularity, as the "lateral geniculate neurons that lost the competition are permanently shut out, and binocular vision cannot be regained" (Haines and Mihailoff, 2018).

According to Bui Quoc and Milleret (2014), an "alteration of postnatal visual experience and/or of eye movements during the critical period ... leads to the abnormal development of various structures in the brain, both anatomically and functionally". Strabismus is a condition that may occur at any age (Lipton, 1970). When strabismus occurs at birth, or infancy around 6 months of age, it is referred to as congenital strabismus and it is noted as a consequence of such abnormal cerebral developments (Billson, 2003) (Rutstein *et al.*, 2011) (Remington, 2012). When strabismus occurs after the fist 6 months of age it is referred to as acquired strabismus (Stidwill and Fletcher, 2010) (Nelson and Olitsky, 2014) and could be the result of "refractive error (high hyperopia), tumors (eg, retinoblastoma), head trauma, neurologic conditions (eg, cerebral palsy; spina bifida; palsy of the 3rd cranial nerve, 4th cranial nerve, or 6th cranial nerve), viral infections (eg, encephalitis, meningitis), and acquired eye defects" (Bui Quoc and Milleret, 2014). Some cases of acquired strabismus have been reported after cataract surgery or an accident that caused brain injury (Kapoor *et al.*, 2004) (Capo *et al.*, 1996). It should be noted that, in some types of strabismus, the precise age which separates congenital and acquired strabismus, varies between $6-12$ months of age (Lambert and Lyons, 2017). Strabismus may affect both genders and all ages, including young children, adults and the elderly (Billson, 2003) (Lipton, 1970). In general, however, strabismus usually appears at infancy, around 6 months of age, or at a really young age (Damanakis, 2005) (Richard and Parks, 1983). Congenital strabismus may be a result of "an abnormal development of both the geniculo-cortical pathway and inter-hemispheric connections through the corpus callosum" (Bui Quoc and Milleret, 2014). However,

it may also originate from an abnormal development of the visual pathway, starting from an abnormal innervation of the extraocular muscles and ending with an abnormal neural activity of the visual cortex in the brain (Remington, 2012) (Bateman and Isenberg, 2013). Hippocrates ($460 - 375$BC) was the first to suggest that strabismus may run in families, as an inherited condition (Richards, 1970) (Rutstein *et al.*, 2011) (Noorden and Campos, 2002).

3.1.3 *Where does strabismus originate from?*

Unfortunately, the origins of strabismus are still unknown (Michaelides and Moore, 2004) (Lipton, 1970). The "pathophysiological basis(es) of most cases are poorly understood" (Bateman and Isenberg, 2013) and "the important question of the origins of strabismus remains poorly understood" (Bui Quoc and Milleret, 2014). Additionally, Bateman and Isenberg (2013) state that the "causes of strabismus are poorly understood and the natural history differs in children compared to adults". Currently, two competing theories have been proposed to explain the aetiology of strabismus:

- **Sensory vs. Motor:** This theory assumes that strabismus occurs either due to oculomotor deficiencies or due to abnormalities in the functions of the visual cortex, such as the lack of binocular fixation, lack of stereopsis and abnormal fusion mechanisms (Billson, 2003) (Bateman and Isenberg, 2013).

- **Peripheral vs. Central:** This theory opposes the "sensory vs motor" theory and suggests that strabismus occurs due to genetic abnormalities in the development of the neuronal system (Wright *et al.*, 2006) (Salmon, 2019) such as the innervation of the six extraocular muscles including "muscular dystrophies and the palsy of the 3rd, 4th, or 6th cranial nerves" (Bui Quoc and Milleret, 2014).

Of these two theories, the "sensory vs motor" theory has wider acceptance by the strabismology community (Bui Quoc and Milleret, 2014) (Michaelides and Moore, 2004). de Lahunta and Glass (2009) support the "sensory vs motor" theory by suggesting that strabismus is "an abnormal position of the eye relative to the orbit or palpebral fissure that is a clinical sign of loss of innervation to the extraocular muscles". In most cases of strabismus, the extraocular muscles are structurally normal and the deviation of either one eye is caused by "aberrant signals from the brain that cause excessive movement of the muscles in a certain direction" (Lueder, 2015). Damanakis (2013) and Tychsen (2005) agree that strabismus is a disorder originating from the

brain, thereby suggesting, that the brain must be repaired in order to treat strabismus effectively.

3.1.4 *Which parts of the world does strabismus affect?*

Although the precise number of people, worldwide, who suffer from strabismus is currently unknown, several estimates have been made from the general number of cases that have been reported around the world. Onua (2019) explains that strabismus "is a relatively common condition worldwide especially among newborns". Scheiman *et al.* (2005) and Lavrich (2010) noted that between $2.25 - 8.3\%$ of the human population in the United States suffers from Convergence Insufficiency (CI), which is only one type of strabismus (Scheiman *et al.*, 2005) (Lavrich, 2010), discussed later in this chapter. Beauchamp *et al.* (2003) suggested that the "prevalence of strabismus in adults in the United States is believed to be approximately 4%". In 2012 however, Cooper and Jamal (2012) estimated that approximately 5% of the population in the United States suffers only from CI. In Nigeria, it is estimated that the prevalence of strabismus is approximately 2.4% of the population (Onua, 2019). Rowe (2012) and Damanakis (2013) agree that between $5 - 8\%$ of the human population worldwide suffers from strabismus. Their estimation however, barely overlaps with Rutstein *et al.* (2011), who suggest that strabismus occurrences vary between $2 - 5\%$ worldwide. Bui Quoc and Milleret (2014) seem to partially agree with Rutstein *et al.* (2011) by noting that strabismus affects only 2% of the general human population. This estimation however contradicts Lambert and Lyons (2017) who state that strabismus "occurs in 1.3–5.7% of all children" without considering any adult cases. Friedman *et al.* (2009) observed that, within a limited age group, a "recent study from Sydney, Australia found a prevalence rate of manifest strabismus of 2.8% from a population-based sample of six-year old school children". In Russia, Ukraine and Kazakhstan the prevalence of strabismus in children is as high as 12.1% (Olivan Gonzalvo, 2018).

The conclusion that can be drawn, from the aforementioned statements, is that even the estimated percentage of strabismus occurrences is not very accurate, as it varies mostly between $2 - 8\%$ of the human population worldwide. It should be noted that the samples, from which the estimates were made, consider mostly children, with few mentions of adults, and do not include cases from every country in each continent of the world. Most strabismus cases have been recorded in Western Europe and North America (Oystreck and Lyons, 2012) which, combined together, gather less than 15%

of the entire human population. Unfortunately, the statistics gathered by the remaining continents are very poor, as very little research has been conducted into finding strabismus occurrences in other continents, including the rest of America, Africa, Asia and Australia. In order to estimate the prevalence of strabismus worldwide, to a higher accuracy, more extensive research needs to be conducted that would gather statistics from every country around the world considering all types of strabismus in children and adults.

3.1.5 *Why does strabismus exist?*

Unfortunately, in spite of much research the aetiology of strabismus remains unknown, as stated by multiple authors and specialists including (Noorden and Campos, 2002) (Michaelides and Moore, 2004) (Engle, 2006) (Thomas and Guha, 2010) (Oystreck and Lyons, 2012) (Damanakis, 2013) (Bateman and Isenberg, 2013) (Bui Quoc and Milleret, 2014) (Lambert and Lyons, 2017) (Yanoff and Duker, 2019) (Nelson, 2019).

3.2 BINOCULAR DISTURBANCES AND ADAPTATIONS

Previously, it was mentioned that normal retinal correspondence (NRC) is the basis of BSV, because sensory fusion is only possible when corresponding retinal elements, and more importantly both foveae, receive visual stimuli derived from the same fixation object. A strabismic deviation disturbs the normal development and maintenance of BSV by phenomena (symptoms) known as Confusion and Diplopia (Agrawal, 2019) (Stidwill and Fletcher, 2010). Consequently, the brain develops sensory and motor mechanisms (adaptations), which include Amblyopia, Suppression, Anomalous Retinal Correspondence (ARC) and Compensatory Head Postures (CHP), in order to counter such sensory disturbances[2] (Wright *et al.*, 2006) (Billson, 2003) (Sung *et al.*, 2020).

2 Interestingly, Noorden and Campos (2002) states that these sensory disturbances "may be present at birth, heritable, and indeed the cause of a deviation". Nevertheless, Noorden and Campos (2002) acknowledges the fact that evidence to support the aforementioned statement is very poor.

3.2.1 *Confusion and Diplopia*

In strabismus, the visual stimuli from a fixation target are received by different (non-corresponding) retinal elements of both eyes leading to the following aberrations (fig. 13) (Agrawal, 2019) (Stidwill and Fletcher, 2010):

- Each fovea receives visual stimuli from different objects in the environment.
- Non-corresponding retinal elements, i.e. the fovea of the fixating eye and a peripheral element of the strabismic eye, receive visual stimuli from the same fixation object.

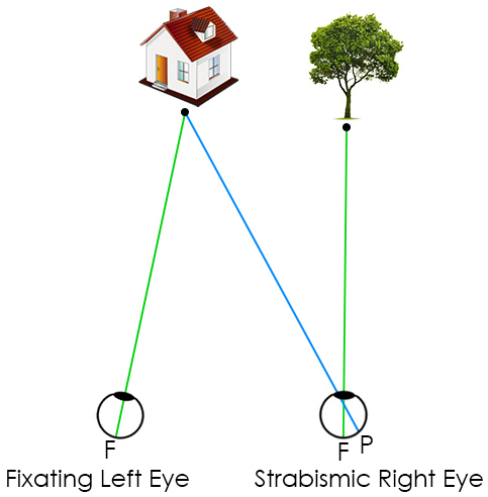

Figure 13: *Abnormalities with regards to retinal correspondence: The fovea (F) of the fixating eye receives visual stimuli deriving from the house, whereas, the fovea of the strabismic eye (F) receives visual stimuli deriving from the tree. However, a peripheral retinal element (P) of the strabismic eye also receives visual stimuli deriving from the house.*

The first aberration, in which both foveae simultaneously receive visual stimuli deriving from different objects, is responsible for the misperception that these different objects occupy the same space in the environment, i.e. share the same position (Wright *et al.*, 2006). This aberration is known as confusion and appears in the form of retinal rivalry or superimposition (Pratt-Johnson and Tillson, 1984) (Lambert and Lyons, 2017).

The second aberration, in which the fixation object is projected onto two non-corresponding retinal areas, results in the simultaneous perception of the fixation object at two different positions in the same environment (Ansons and Davis, 2014) (Duane, 1932). This aberration is known as binocular pathological diplopia (double vision) (Danchaivijitr and Kennard, 2004). De-

pending on the type of deviation, a pathological diplopia can be characterized as:

- **Homonymous/Uncrossed:** The visual stimuli, deriving from the fixation object, are received by the nasal aspect of the retina of the strabismic eye (Kolb *et al.*, 2020).
- **Heteronymous/Crossed:** The visual stimuli, deriving from the fixation object, are received by the temporal aspect of the retina of the strabismic eye (Duane, 1932). Figure 13 illustrates an example of heteronymous, or crossed, diplopia.

Confusion and diplopia are considered to be very problematic symptoms, because they may be impossible to resolve (Noorden and Campos, 2002). However, in some cases of strabismus the brain develops sensory and motor defence mechanisms, including suppression (see subsect. 3.2.3), ARC (see subsect. 3.2.4) and CHP (see subsect. 3.2.5), that intend to alleviate the stress caused by these aberrations (Danchaivijitr and Kennard, 2004). However, such defensive mechanisms are typically developed during the critical period, therefore adults and the elderly remain at risk of constant and persistent double vision (Stidwill and Fletcher, 2010).

3.2.2 *Amblyopia*

Amblyopia is an ophthalmological term used to characterize conditions that reduce visual acuity, of one or both eyes, regardless of whether or not prescription glasses are used, which intend to correct refractive conditions such as hypermetropia[3] and myopia[4] (Campos, 1995) (Lembo *et al.*, 2019). Rowe (2012) defines amblyopia as a condition which is not "a result of any clinically demonstrable anomaly of the visual pathway and ... not relieved by the elimination of any defect that constitutes a dioptric obstacle to the formation of the foveal image".

Amblyopia is a developmental problem, occurring during the critical period, (Nelson and Olitsky, 2014) caused by "lack of use of one or both eyes or a result of a long-standing defocused image" (Yanoff and Duker, 2019). Haines and Mihailoff (2018) explain that if "the input from one eye is dysfunctional during the critical period for visual system development ...,

3 Hypermetropia, or hyperopia, is a term used to describe long-sightedness (Remington, 2012). It is a condition where light is focused far behind the retina causing near objects to appear blurred and far objects to appear clear (Snell and Lemp, 2013).

4 Myopia is a term used to describe short-sightedness (Remington, 2012). Contrary to hyperopia, light is focused far forward from the retina causing near objects to appear clear and far objects to appear blurred (Haines and Mihailoff, 2018).

the axon terminals carrying information from that eye are at a disadvantage ... the 'good' eye has exclusive access to the visual cortex, and input from the 'bad' eye is ignored". An amblyopic eye, also referred to as a 'lazy eye', produces a blurred retinal image that can permanently damage the visual cortex of the brain if it is left untreated (Wright *et al.*, 2006).

The classification of amblyopia includes several types, one of which is known as strabismic (Maurer and McKee, 2018). Strabismic amblyopia is a consequence of strabismus and is always present on the deviating eye due to dominance of the fixating eye (Lambert and Lyons, 2017) (Billson, 2003). It is developed in early childhood and is the result of cortical suppression (Agrawal, 2019) (Campos, 1995), a sensory adaption of strabismus explained later in this chapter. Other classified types of amblyopia include anisometric, ametropic, stimulus-deprivation, meridional and idiopathic (Ansons and Davis, 2014) (Yanoff and Duker, 2019).

3.2.3 *Suppression*

Suppression is a sensory mechanism developed by the brain in order to eliminate confusion and diplopia (Sengpiel *et al.*, 2006). In normal binocular vision, suppression occurs physiologically (physiological suppression) when objects outside Panum's fusional area appear double or blurred (Stidwill and Fletcher, 2010). In strabismus, suppression is a pathological phenomenon (pathological suppression) described as an "active central inhibition of disparate and confusing images originating from the retina of the deviated eye" (Noorden and Campos, 2002). During pathological suppression, the brain selectively projects scotomata (black dots) at the particular retinal areas of the deviated eye that cause confusion and diplopia (Pratt-Johnson and Tillson, 1984) (Cooper and Record, 1986). The area and size of a suppressive scotoma depends on the type of strabismus and the angle of deviation (Ansons and Davis, 2014). For the remainder of this thesis, the term 'suppression' will refer to pathological suppression.

A suppression may be characterized as:

- **Central:** The fovea, of the deviating eye, is suppressed because it is not visually stimulated by the fixation object (Damanakis, 2005). Suppression of the fovea alleviates confusion.
- **Peripheral:** The peripheral area, of the deviating eye, is suppressed because it is visually stimulated by the fixation object (Wright *et al.*, 2006). Suppression of this area alleviates diplopia.

- **Monocular:** Defined by a constant suppression of the retinal image of the deviated eye, which leads to strabismic amblyopia (Hochberg, 1964). This is due to the constant predominance of the retinal image of the normal eye, over the retinal image of the deviating eye (Pratt-Johnson and Tillson, 1984).

- **Alternating:** When dominance of the fixating eye is alternated, i.e. switched from one eye to the other, suppression alternates, which reduces the chances of developing strabismic amblyopia (Daum, 1984) (Economides *et al.*, 2014).

- **Facultative:** In periodic strabismus, the retinal image of the strabismic eye is suppressed only when the deviation occurs (Agrawal, 2019).

- **Obligatory:** The retinal image of the strabismic eye is constantly suppressed "irrespective of whether the eyes are deviated or straight" (Salmon, 2019). Obligatory suppression always leads to amblyopia of the deviated eye.

The primary visual cortex of the brain uses suppression, not only to defend against confusion and diplopia but also, in order to develop Abnormal Binocular Vision (ABV) (Olitsky *et al.*, 1999). In ABV, the entire retinal image from the fixating eye and some parts of the retinal image from the strabismic eye are used, by the brain, in order to perceive the environment (Hiles *et al.*, 1968). However, fusion, and thereby depth perception via normal binocular vision, is not possible (Olitsky *et al.*, 1999). According to Billson (2003), suppression "develops in the immature visual cortex as a response to differing inputs from each eye and is a barrier to the development of fusion". There are some cases where suppression is permanent and the "individual is unable to see the object" (Rowe, 2012).

Suppression is a developmental phenomenon that is formed during infancy or early childhood (Wright *et al.*, 2006) (Salmon, 2019). Although Billson (2003) suggests that suppression "may also occur in the adult as a result of an adaptation to visual confusion", he (Billson, 2003) warns that when strabismus is not treated properly and the new retinal images are ill-formed, an adult may suffer from permanent (constant) and persistent diplopia. In the critical period, where the brain is at its maximum plasticity, a child's brain will adapt by suppressing the newly ill-formed retinal images without any risk of constant and persistent diplopia (Bateman and Isenberg, 2013). Rowe (2012) raises the question "as to whether adults can truly develop suppression" because, although related, "inattention to diplopia and true suppression are different" (Rowe, 2012).

3.2.4 *Anomalous Retinal Correspondence (ARC)*

Anomalous, or abnormal, Retinal Correspondence (ARC) is another sensory mechanism, developed by the brain, in order to neutralize confusion and diplopia (Pickwell, 1980) (Nelson and Olitsky, 2014). In ARC, the brain adjusts the sensitivity of a peripheral area in the retina of the deviating eye, such that it develops similar sensitivity to the fovea of the fixating eye (Campos, 1986) (Stidwill and Fletcher, 2010). Consequently, the brain alters the correspondence between the retinal elements of both eyes (Wong *et al.*, 2000) and "establishes a new functional fovea called the pseudo-fovea that corresponds to the true fovea of the dominant fellow eye" (Wright *et al.*, 2006). The offset between the pseudo-fovea, of the deviating eye, and the fovea, of the fixating eye, is known as angle of anomaly (Nelson and Olitsky, 2014).

There are two types of ARC:

- **Harmonious:** Occurs when the angle of anomaly is equal to the amount of strabismic deviation. In harmonious ARC, the pseudo-fovea receives the visual stimuli deriving from the fixation object and, therefore, has developed similar sensory properties to the fovea of the fixating eye (Zivotofsky and Schrader, 2004).

- **Unharmonious:** Occurs when the angle of anomaly is not equal to the amount of strabismic deviation. In unharmonious ARC, the pseudo-fovea does not receive the visual stimuli deriving from the fixation object and, therefore, has not developed similar sensory properties to the fovea of the fixating eye (Noorden and Campos, 2002).

Unlike suppression, which inhibits the retinal elements of the deviating eye that cause confusion, ARC restores, at some level, binocular vision (Wong *et al.*, 2000) as it allows the brain to superimpose both retinal images and develop very "limited fusion and stereoscopic capabilities" (Yanoff and Duker, 2019). However, the quality of binocular vision varies from one subject to another and depends heavily on the angle of deviation (Zivotofsky and Schrader, 2004). According to Rowe (2012), ARC is present when the angle of deviation is $\leqslant 20\Delta$. In most cases of strabismus, suppression and ARC co-exist in order to eliminate confusion and diplopia that occur in central and peripheral vision (Damanakis, 2005).

The most commonly performed tests that are used to determine the presence of ARC are the: after-image test, Bagolini striated glasses test, Worth's four lights test and major amblyoscope/synoptophore test (Noorden and Campos, 2002) (Rowe, 2012) (Nelson and Olitsky, 2014). Table 1 summarizes

the aforementioned tests and lists the advantages and disadvantages of each test with respect to time of execution, cost of equipment used, complexity of setting-up the test, and amount of cooperation required by a subject.

Table 1: *Tests to assess binocular vision and determine the existence of ARC.*

Name of Test & Author	Description
After-image (Wright *et al.*, 2006)	Each eye is stimulated separately by a different angled linear strobe light (horizontal or vertical), producing an after-image effect. Under normal BSV, a cross is perceived. If ARC is present, due to the deviation of the eye, the after-image cross is perceived displaced. **Equipment:** electronic flash gun, camera with flash or synoptophore. **Pros:** low subject cooperation. **Cons:** slow to perform, complex to set-up, relatively expensive.
Bagolini striated glasses (Stidwill and Fletcher, 2010)	A pair of spectacles that have no refractive power and "allow a small spot of light to appear as a streak but without obscuring the view of surrounding objects". Each lens is rotated opposite to the other (45° and 135°). Under normal BSV, a cross is perceived with one point light appearing at the centre of the cross. In strabismus, a displaced cross is perceived with one or two point lights appearing on the sides of each line. ARC is determined when a deviation is present and the cross is perceived normally or with a gap. **Equipment:** Bagolini glasses, pen torch. **Pros:** fast to perform, simple to set-up. **Cons:** medium subject cooperation, relatively expensive.

Worth's four lights (Nelson and Olitsky, 2014)	Consists of four lights (one white, one red and two green) that are viewed through red and green filtered glasses. The number of lights seen indicates if a subject possess normal or abnormal binocular vision. Under normal BSV, four lights are perceived (one red, two green and one mixed). Depending on the type of strabismus, the number of lights and colours perceived varies. ARC is detected when a deviation is present, but a subject is able to perceive all four lights. **Equipment:** red and green filtered glasses, device that contains four lights. **Pros:** fast to perform, relatively cheap equipment. **Cons:** relatively complex set-up, medium-high subject cooperation.
Synoptophore (Major amblyoscope) (Ansons and Davis, 2014)	A haploscopic device, discussed in detail later in this chapter, requires a subject to manually adjust (move and rotate) a pair of dissimilar images, using handles one on each side, so that they can be fused as one. Under normal BSV, both images are simultaneously perceived. Depending on the type of strabismus, the images may appear superimposed, separated or perceived by either eye. ARC is detected when the two images, from the synoptophore, are perceived simultaneously but displaced. **Equipment:** haploscopic device. **Pros:** fast to perform, low-medium subject cooperation. **Cons:** expensive, complex set-up requiring supervision.

The aforementioned tests are either complex to set up or require the use of expensive and delicate equipment. This thesis introduces a simple and cost-free test, referred to as partial-occlusion test, the purpose of which is

to determine the existence of ARC on subjects with strabismus. The partial-occlusion test has been clinically validated by Damanakis (2014b).

PARTIAL-OCCLUSION TEST In this test, the primary fixation target (PFT) refers to an object upon which the dominant eye fixates. The secondary fixation target (SFT) refers to an object that is occluded by PFT, intended to be perceived by the strabismic eye through ARC. The only condition that needs to be satisfied when performing this test is to ensure that the SFT is completely occluded by the PFT, and therefore, not visible by the dominant eye. The partial-occlusion test reveals the existence and type of ARC when the subject is able to: (a) perceive the SFT, via the deviated eye and without alternating dominance, and (b) verify that the location of the perceived SFT is central to PFT.

If there are enough objects in the environment that can be used as secondary fixation targets, and light is sufficient for the subject to see clearly, there are no other essential prerequisites to performing the partial-occlusion test. However, it would be preferable to use a small piece of paper (eg. $45.0 \times 45.0\text{cm}$), depicting a simple 2D grid, as PFT because it can further be used to estimate the type of ARC. Otherwise, a subject's palm would suffice as PFT.

The partial-occlusion test is performed as follows:

- **Step 1:** The subject is instructed to place the PFT, at reading distance, in front of the dominant eye (fig. 14). The PFT should completely occlude the SFT, located further behind the PFT.
- **Step 2:** The subject is instructed to fixate on the PFT, using the dominant eye, and verify if the occluded SFT is perceived.
- **Step 3:** If the occluded SFT is perceived, the subject is instructed to describe the location of the SFT with respect to PFT.

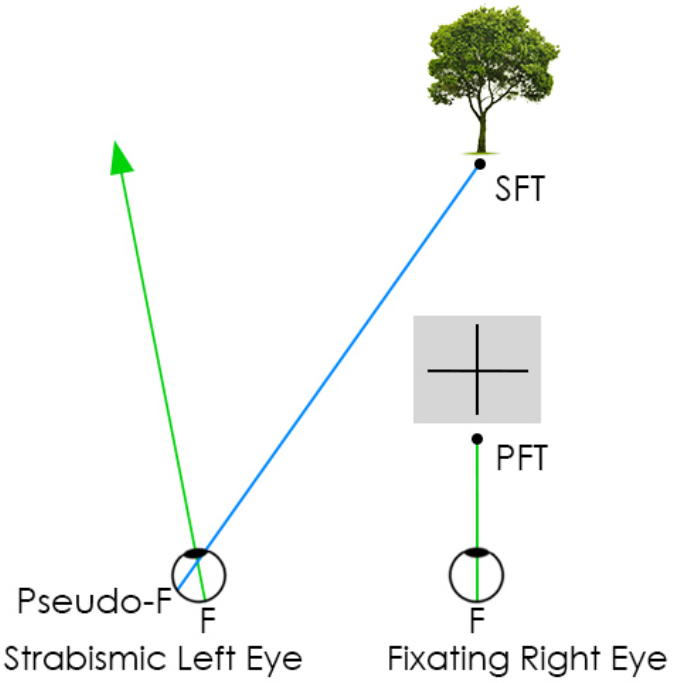

Figure 14: *Partial-Occlusion test: The right eye, which is the dominant eye, fixates on PFT (grid), while the strabismic eye deviates outwards. The SFT (tree) is located behind the PFT, not visible to the dominant eye. Due to the pseudo-fovea of the deviated eye, the brain is not only able to perceive the SFT, but also position its projection, on the retina, behind the FPT.*

Possible results, of the partial-occlusion test, include the following:

- The SFT is not perceived, which indicates suppression and no ARC.
- The SFT is perceived, which indicates ARC. The position of SFT relative to the centre of the grid can be used to indicate the type of ARC (harmonious or unharmonious). If SFT is central to PFT, then ARC is harmonious.

Table 2 summarizes the advantages and disadvantages of the partial-occlusion test.

Table 2: *Advantages and disadvantages of the partial occlusion test with respect to the time of execution, cost of equipment used, complexity of setting-up the test and amount of cooperation required by a subject.*

Pros	Cons
Fast to perform Cost-free Simple set-up	Quality of feedback depends heavily on subject cooperation

The partial-occlusion test was repeatedly performed on an adult subject with exotropia, an outwards strabismic deviation explained later in this

chapter, who verified the existence of ARC without it being previously diagnosed through other tests. The subject reported that the SFT was perceived centrally to PFT. However, the projections of PFT and SFT were neither superimposed or simultaneously fused. The subject was able to fixate on PFT while describing the presence of SFT as "annoying" in the overall perception of the environment.

3.2.5 *Compensatory Head Postures (CHP)*

Compensatory head posture (CHP), otherwise referred to as anomalous or abnormal head posture (AHP), is a motor adaptation in strabismus that, similarly to sensory adaptions, eliminates confusion and diplopia (Morris *et al.*, 2009) (Rowe, 2012). In some types of strabismus, where the angle of deviation is relatively small, a subject may adopt a CHP in order to align both eyes and maintain binocular vision (Wright *et al.*, 2006). According to Salmon (2019), a subject with strabismus "will turn the head into the direction of the field of action of the weak muscle, so that the eyes are then automatically turned the opposite direction and as far as possible away from its field of action (i.e. the head will turn where the eye cannot)". There are three components to CHP: (a) face turn (b) head tilt (c) chin elevation or depression (Ansons and Davis, 2014) (Kraft *et al.*, 1992).

A combination of these postures may be adopted in order to minimize the angle of deviation, thereby, allowing the brain to fuse both retinal images and achieve binocular single vision (Agrawal, 2019). CHP is most commonly observed in children, as a consequence of congenital strabismus (Mohamad Fadzil *et al.*, 2019). However, adults may also adopt CHP in order to compensate for acquired strabismus that causes constant and persistent diplopia (Nelson and Olitsky, 2014). Sometimes, CHP is not detected early in life and adults, with congenital strabismus, may not be aware of CHP until they experience symptoms of decompensation (Salmon, 2019). When CHP is responsible for maintaining BSV, loss of CHP results into a disruption of fusion and, therefore, binocular vision (Billson, 2003). Unfortunately, when the angle of deviation is relatively large, a change to the head posture does not compensate strabismus and, therefore, subjects with a large angle of deviation do not adopt CHP (Morris *et al.*, 2009) (Ansons and Davis, 2014).

Most authors, including (Noorden and Campos, 2002), (Rowe, 2012), (Nelson and Olitsky, 2014), (Ansons and Davis, 2014), (Lambert and Lyons, 2017), (Agrawal, 2019), (Salmon, 2019), have attributed CHP to the development and maintenance of BSV, but only when the angle of deviation is small.

Nevertheless, people who suffer from larger strabismic deviations may also adopt CHP, not to develop and maintain BSV but, purely for aesthetic purposes. As shown in figure 15, a person with strabismus may prefer to adopt an abnormal head posture in order to hide the deviation.



(a) *No CHP is adopted and the deviation of the left eye is obvious.*

(b) *CHP is adopted and the deviation of the left eye is almost hidden.*

Figure 15: *CHP: Illustrates the aesthetic differences when CHP is adopted by a subject with medium to large deviation. By adopting a CHP (b), the angle of deviation has been considerably reduced, almost to the point of being unnoticeable.*

3.2.6 *Use of Familiarity Cues in Strabismus*

As previously discussed, the perception of depth is accomplished only through normal binocular single vision. Nevertheless, the three dimensional perception of objects, including their environment, can be achieved using other complementary criteria, or clues, referred to as familiarity cues (see subsect. 2.5.1). These cues are gained mostly through experience and do not depend on the mechanisms of normal binocular vision, which is why they are also referred to as monocular cues (Stidwill and Fletcher, 2010). Noorden and Campos (2002) explain that "the monocular or experiential clues, are important in our estimation of the relative distance of visual objects and are active in monocular as well as binocular vision".

Strabismus subjects, who cannot maintain BSV, rely on familiarity cues in order to estimate depth (Damanakis, 2013). When the environment is surrounded by several objects, which can contribute to a more accurate estimation of depth, familiarity cues are often sufficient to carry out tasks that re-

quire keen depth perception, e.g. driving a car (Kolb *et al.*, 2020) (Nuzzi and Cantù, 2003). Wright *et al.* (2006) confirm that "athletes, microsurgeons, even ophthalmologists have been successful using monocular depth perception". However, people suffering from strabismus are at a disadvantage compared to people who are able to perceive depth stereoscopically (Hammond, 2014) (Lambert and Lyons, 2017). Strabismus not only forces the brain to perform "complex image processing" (Barlow *et al.*, 1967) but since familiarity cues are based on experience "false judgments are possible" (Noorden and Campos, 2002). For example, when playing football or driving a car, the cues found on the football pitch or on the road, including the pitch itself and other players or the buildings and other cars, contribute towards a more accurate estimation of distance and depth. Playing tennis, however, can be troublesome because when a tennis ball falls down nearly at a perpendicular angle, after being hit very high in the air, there are no cues available to help the player estimate how far the tennis ball is. Additionally, because the tennis ball is small in size, the gradual increase in its relative size, as it falls down, is too small to contribute in any useful information about its distance from the player.

When familiarity cues are not sufficient enough to contribute in the estimation of depth, a subject with strabismus would not be able to judge distances and, therefore, perceive the environment in two dimensions. Nuzzi and Cantù (2003) deduced that "experience does not seem to play any role in spatial orientation, and subjects presenting anomalous binocular vision and suppression areas in the binocular visual field do not appear to be able to perceive space".

3.3 CLASSIFICATION OF STRABISMUS

This polymorphic nature of strabismus complicates an accurate diagnosis primarily because the oculomotor system of the strabismic eye is unpredictable (Hammond, 2014) (Noorden and Campos, 2002). Nevertheless, all ocular deviations exhibit properties and characteristics that assist in the classification of strabismus (Ansons and Davis, 2014). In ophthalmology, strabismus is classified according to the following properties of a deviation (Rowe, 2012) (Nelson and Olitsky, 2014) (Rutstein *et al.*, 2011):

- **Latency** – phoria or tropia (latent or manifest)
- **Direction** – eso, exo, hyper, hypo, incyclo, excyclo
- **Size** – micro, small, moderate or large

- **Comitancy** – comitant or incomitant
- **Frequency** – constant or intermittent
- **Involvement of Accommodation** – accommodative or non-accommodative
- **State of Vergence** – excess/insufficiency of convergence or divergence
- **Laterality of Fixation** – unilateral, alternate, bilateral or mono
- **Time of Onset** – congenital or acquired
- **Other Properties** – dissociated, paralytic, mechanical-restrictive, orbital or pseudo

3.3.1 *Latency of Deviation: Phoria or Tropia*

The term 'phoria', derived from the Greek word '-φορία → φέρω' (phoria = carry), is used to define latent deviations that occur only when binocularity is disrupted (Lavrich, 2010) (Bateman and Isenberg, 2013). In contrast, 'tropia', derived from the Greek word '-τροπία → τροπή' (tropia = turn, direction), is an ophthalmological term used to define manifest deviations that are present regardless of whether binocularity is disrupted (Yanoff and Duker, 2019) (Weinstock *et al.*, 1998).

3.3.1.1 *Orthophoria vs Orthotropia*

The terms orthophoria and orthotropia are used to identify deviations that occur in normal binocular vision (physiological) or to indicate the optimum results from treating strabismus (Ansons and Davis, 2014) (Awadein *et al.*, 2008). Orthophoria, derived from the Greek words 'ορθό' (ortho = correct) and 'phoria', is an ophthalmological term used to define the ideal behaviour and condition of the oculomotor system where the visual axes, of both eyes, perfectly match one another even when binocular vision is disrupted (Damanakis, 2005) (Noorden and Campos, 2002). In orthophoric vision, both eyes are parallel when fixating at far distance and converge properly when fixating at near distance, regardless of whether ro not binocularity is interrupted (Salmon, 2019). According to Rowe (2012), orthophoria occurs when "both visual axes are directed towards the fixation point and do not deviate on dissociation". Orthophoria is extremely rare to non existent because if normal binocular vision is disrupted, by covering one eye, the covered eye will perform a small drift (Yanoff and Duker, 2019) (Stidwill and Fletcher,

2010). Usually this drift is characterized by an inwards rotation, of the covered eye, so small that it cannot be detected by ordinary clinical methods (Nelson and Olitsky, 2014). Wright *et al.* (2006) explain that "virtually all normally sighted people, with normal bifoveal fusion, have a small phoria but maintain alignment through motor fusion".

Because most people, with normal binocular vision, are unable to maintain orthophoria when binocularity is interrupted, ophthalmologists consider a small amount of ocular deviation to be normal (Noorden and Campos, 2002). Therefore, a new term was introduced to describe the behaviour of the oculomotor system, under normal binocular vision, in the presence of small phorias (Chen and Aziz, 2003) (Rutstein *et al.*, 2011). Orthotropia, coming from the Greek words 'ortho' and 'tropia', is an ophthalmological term used to define the absence of obvious (manifest) ocular deviations (Damanakis, 2005) (Stidwill and Fletcher, 2010). Orthotropia is considered to be the "optimum outcome to facilitate the development of BSV" (Ansons and Davis, 2014) and a more suitable term used to describe normal binocular vision "implying a negative cover test (on covering either eye) in the absence of amblyopia" (see subsect. 3.4.3) (Agrawal, 2019).

Noorden and Campos (2002) suggest that, for far fixation distances, the following phorias, measured in prismatic dioptres (Δ), should be considered physiologic: (a) inwards of $1-2\Delta$, (b) outwards of $1-4\Delta$, (c) upper of 0.5Δ, and (d) lower of 0.5Δ. However, in order to facilitate BSV, the eyes must be aligned within the range of 10Δ, either side (Awadein *et al.*, 2008) (Yanoff and Duker, 2019) (Lambert and Lyons, 2017). Additionally, Sharma *et al.* (2017) and Ansons and Davis (2014) claim that an inwards deviation of 15Δ is still acceptable as it is compatible with stereopsis, whereas, outward deviation of more than $8-10\Delta$ would be problematic as it could result in a permanent deviation. It should be noted that these optimal alignment angles are relative to the direction of deviation. Even though an alignment of both eyes to within 10Δ horizontally can facilitate BSV, this is not the case for vertical or torsional deviations, which need to be almost perfectly aligned (Goldchmit *et al.*, 2003) (Woo *et al.*, 2005).

3.3.1.2 *Heterophoria vs Heterotropia*

The terms heterophoria and heterotropia are used to identify different types of deviations that occur in strabismus (Weinstock *et al.*, 1998). Heterophoria, derived from the Greek words 'ἕτερο' (hetero = other) and 'phoria', is an ophthalmological term used to define latent deviations (Damanakis, 2005) (Babinsky *et al.*, 2015). In heterophoria, a strabismic deviation occurs

only on dissociation of the eyes, i.e. when binocularity is disrupted (Bateman and Isenberg, 2013) (Wright *et al.*, 2006). When binocular vision is not disrupted, sensory and motor fusion mechanisms are responsible for maintaining the proper alignment of both eyes, allowing them to simultaneously fixate on the same target (Chen and Aziz, 2003) (Agrawal, 2019). However, compared to the effort required by a human brain to sustain normal binocular vision, in heterophoria, the brain spends significantly more energy in order to maintain bifoveal fixation on a target, by controlling the extraocular muscles of both eyes (Wybar, 1974) (Salmon, 2019). By covering either eye and disrupting binocularity, the influence of fusion is removed and the covered eye performs a relative deviation (Chen and Aziz, 2003). Heterophoria is "variably present when fusion is broken" (Yanoff and Duker, 2019) because when "sensory fusion is artificially suspended by excluding one eye from participating in vision, motor fusion is frustrated" (Noorden and Campos, 2002). However, when binocularity is restored, by uncovering both eyes, the brain resumes its excessive control of the extraocular muscles in order to reposition both eyes such that they fixate on the same target (Babinsky *et al.*, 2015) (Rowe, 2012). Due to the tendency of both eyes to deviate only on dissociation of binocularity, heterophorias "may be defined as deviations kept latent by the fusion mechanism" (Noorden and Campos, 2002).

An individual's binocularity could be disrupted by fatigue, stress or illness which would cause a heterophoric deviation to become apparent (Weinstock *et al.*, 1998). Heterophoria can also "cause central nervous system depression and diminish motor fusion" (Wright *et al.*, 2006). Common symptoms of heterophoria include headaches, eye strain (asthenopia), extreme sensitivity to light (photophobia), loss of concentration, defective focus between near and far objects, blurry vision, loss of depth perception and diplopia (Adler, 2002) (Agrawal, 2019). If heterophoria is left untreated it could turn into a permanent deviation (Babinsky *et al.*, 2015). Wright *et al.* (2006) state that a "phoria that is difficult to control may spontaneously become manifest".

Heterotropia, derived from the Greek words 'hetero' and 'tropia', is an ophthalmological term used to define manifest (obvious) deviations (Ansons and Davis, 2014) (Damanakis, 2005). In heterotropia, both eyes are unable to have matching visual directions while fixating on the same object, regardless of whether binocularity is disrupted (Rowe, 2012) (Helveston, 2010). Heterotropic strabismus is mainly characterized by a relatively wide angle of deviation between the visual directions of both eyes (Beauchamp *et al.*, 2003) (Hiles *et al.*, 1968). According to Salmon (2019), heterotropia is "a manifest deviation in which the visual axes do not intersect at the point of fixation".

In contrast to heterophoria, where fusion occurs normally but breaks only when binocularity is interrupted, heterotropia prevents fusion and, thereby binocular depth perception, because the brain does not have the same control over the muscles of both eyes (Babinsky *et al.*, 2015) (Lipton, 1970). Noorden and Campos (2002) assert that such deviations "are manifest deviations not kept in check by fusion".

Symptoms of heterotropia vary depending on the time of onset (Lambert and Lyons, 2017) (Hammond, 2014). When acquired after the critical period, it causes permanent and persistent diplopia (double vision) (Wright *et al.*, 2006) (Haines and Mihailoff, 2018). In congenital cases, or these acquired during the pre-critical period, the brain uses sensory and motor adaptations in order to avoid confusion and diplopia (Billson, 2003) (Pratt-Johnson and Tillson, 1984). If strabismus is left untreated, an individual suffering from heterotropia could "develop amblyopia and impaired stereopsis (binocular depth perception)" (Rutstein *et al.*, 2011).

3.3.2 *Direction of Deviation*

Depending on the type of strabismus, a deviating eye can rotate in any direction (Kim *et al.*, 2012a). Nevertheless, strabismus is classified based on the following six directions of deviation (Economides *et al.*, 2016) (Billson, 2003):

- **Eso:** Esophoria or esotropia describes latent or manifest strabismus in which both principal visual directions converge. During an eso deviation, the strabismic eye rotates towards the nasal area (Havertape *et al.*, 2001).
- **Exo:** Exophoria or exotropia describes latent or manifest strabismus in which both principal visual directions diverge. During an exo deviation, the strabismic eye rotates towards the temporal area (Bateman and Isenberg, 2013).
- **Hyper:** Hyperphoria or hypertropia describes latent or manifest strabismus in which the principal visual direction of the deviating eye is displaced higher in relation to the principal visual direction of the fixating eye (Agrawal, 2019).
- **Hypo:** Hypophoria or hypotropia describes latent or manifest strabismus in which the principal visual direction of the deviating eye is displaced lower in relation to the principal visual direction of the fixating eye (Rowe, 2012).

- **Incyclo:** Incyclophoria or incyclotropia describes latent or manifest strabismus in which the strabismic eye rotates torsionally about the visual axis (sagittal axis or Y axis of Fick) towards the nasal area (Hansard and Horaud, 2010).

- **Excyclo:** Excyclophoria or excyclotropia describes latent or manifest strabismus in which the strabismic eye rotates torsionally about the visual axis (sagittal axis or Y axis of Fick) towards the temporal area (Helveston, 1973).

It should be noted that cyclodeviations "are mostly manifest; hence, differentiation between cyclophoria and cyclotropia is difficult to justify on clinical grounds" (Noorden and Campos, 2002). Figure 16 illustrates the six directions of deviation.

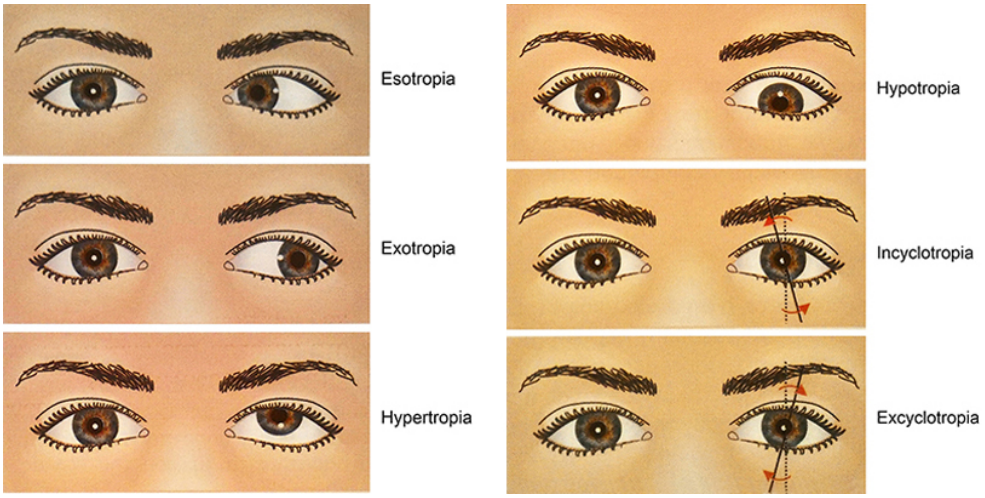

Figure 16: *Directions of deviation (Damanakis, 2005): Illustration of the six main heterotropic directions of deviation.*

Some subjects may display a combination of the aforementioned deviations which complicates the precise identification and classification of strabismus (Engle, 2006) (Damanakis, 2013) (Hammond, 2014).

3.3.3 *Size of Deviation*

Strabismic deviations are measured in prism dioptres (Δ) and categorized into the following sizes:

- **Micro:** A micro deviation angle is measured less than 5° or 10Δ (Houston *et al.*, 1998).

- **Small:** A small deviation angle is considered to be 5° – 10° or 10Δ – 20Δ (Sung *et al.*, 2020).

- **Moderate:** A moderate deviation angle is measured $10° - 25°$ or $20\Delta - 50\Delta$ (Rutstein, 2008).
- **Large:** A large deviation angle is measured greater than $25°$ or 50Δ (Thomas and Guha, 2010).

The angles used in the list above, indicating the range or limit of each size category, are related to eso and exo deviations, which are the most common types of strabismus (Ansons and Davis, 2014) (Thomas and Guha, 2010). In general, the categorization of the size of strabismus to micro, small, moderate or large, is relative to the direction of the deviation. For example, Goldchmit *et al.* (2003) considers a mean value of 20.2Δ ($10.1°$), in hypertropias, to be large. Furthermore, Hammond (2014) suggests that, on average, large scale cyclo deviations can measure up to $\approx 15\Delta$ ($7.5°$) whereas, Woo *et al.* (2005) suggests that cyclo deviations can reach a mean value of $9.68°$ ($\approx 19.36\Delta$) in the primary position of gaze. However, such angles of deviation are considered small or moderate when describing exo or eso deviations. According to Noorden and Campos (2002), a large esotropia is considered to be $\geqslant 30\Delta$.

The size of strabismus is a crucial factor when deciding the appropriate method of treatment (Damanakis, 2013) (Ansons and Davis, 2014). This is because some types of treatments such as corrective surgery, discussed later in this chapter, can cause additional complications if performed on micro or small angles of deviation (Sung *et al.*, 2020) (Shen *et al.*, 2013).

3.3.4 *Comitancy of Deviation: Comitant or Incomitant*

There are two major forms of strabismus, known as comitant and incomitant (Agrawal, 2019). The term comitant or concomitant, which derives from the Latin prefix '*con*' (with, together) and the word '*comitor*' (accompany, attend, follow) (Billson, 2003), is used to describe strabismus "in which the angle of deviation remains the same in all directions of gaze, whichever eye is fixing" (Rowe, 2012). In fact, the angle of deviation is not always the same but variable within 5Δ, but for practical reasons it is considered the same (Oystreck and Lyons, 2012) (Salmon, 2019). Comitant strabismus can occur at any age (congenital or acquired) and it is considered to be derived by the combination of various factors (Thomas and Guha, 2010). However, Oystreck and Lyons (2012) state that in "the absence of obvious structural anomalies of the eye and brain, the aetiology remains unclear". The maintenance of comitant movement is explained by Hering's law of equal innervation (Snell and Lemp, 2013), described in the previous chapter (see subsect. 2.2.1).

When comitant eye movements are disrupted they become incomitant. The term incomitant or non-comitant is used to describe strabismus in which the angle of deviation varies depending on: (a) the direction of gaze, and (b) which eye assumes dominance (Oystreck and Lyons, 2012).

Incomitant strabismus usually occurs due to an extraocular muscle palsy (paralysis), overactivity or underactivity of an extraocular muscle, or restrictions caused by the oculomotor system (mechanical-restrictive) (Billson, 2003) (Kushner, 2010). According to Agrawal (2019), "incomitance can be related to abnormalities of the extraocular muscles, orbit, neuromuscular junction, cranial nerves or their nuclei, supranuclear control, or combined mechanisms". Even though incomitant strabismus can occur at any age, Remington (2012) has shown that "horizontal rectus muscles are displaced inferiorly with age", and could possibly cause acquired incomitant strabismus in the elderly (Yanoff and Duker, 2019). Because the angles of deviation vary in their amplitude depending on the eye that fixates on a target or the direction of gaze, two deviations, termed primary and secondary, are considered when classifying incomitant strabismus (Nelson and Olitsky, 2014). A primary angle of deviation is identified when a subject fixates on a target using the normal ("good") eye (fig. 17a), whereas, a secondary angle of deviation is determined by the deviation produced when a subject fixates using the strabismic ("bad") eye (fig. 17b) (Kushner, 2010) (Benjamin and Borish, 2006). Figure 17 illustrates an example of incomitant strabismus along with the primary and secondary angles of deviation.

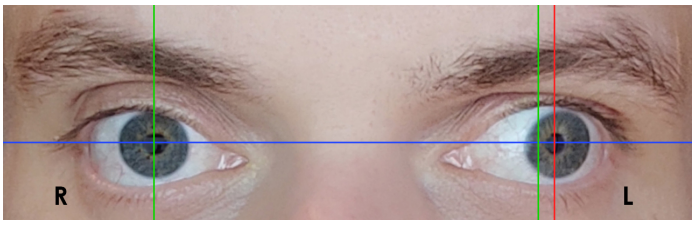

(a) *Primary angle of deviation: As the right eye fixates on a target at* $\approx$ 55cm*, the left eye displays an exo deviation. Since both eyes are uncovered, this type of strabismus is determined to be a left exotropia.*

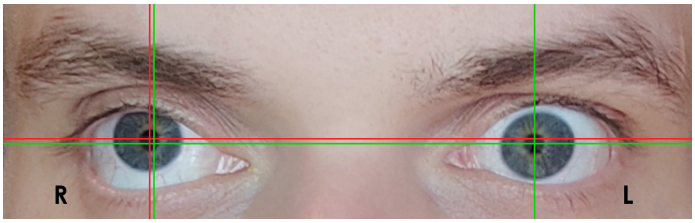

(b) *Secondary angle of deviation: As the left eye fixates on a target at* $\approx$ 55cm*, the right eye displays a exo-hyper deviation. Since both eyes are uncovered, this type of strabismus is determined to be a right exohypertropia.*

Figure 17: *Incomitant strabismus: An example case of incomitant strabismus demonstrating primary and secondary angles of deviation. In this example the right eye is the normal ("good") eye and the left eye is the strabismic ("bad") eye.*

In subjects with incomitant strabismus, the secondary deviation is generally more complex than the primary deviation (Wright *et al.*, 2006). Incomitant strabismus should be identified during the early stages of its development, because over "time strabismus becomes less incomitant and it is harder to assess whether it is congenital or long standing" (Rowe, 2012).

3.3.5 *Constancy of Deviation: Constant or Intermittent*

The terms constant and intermittent are used in order to describe the frequency of occurrence of manifest deviations (Yanoff and Duker, 2019) (Rutstein *et al.*, 2011). Constant strabismus is defined as a manifest ocular deviation that is always present regardless of any circumstances, including emotional or physical state of the subject, time during the day and direction or distance of gaze (Damanakis, 2005) (Lambert and Lyons, 2017). The amplitude of the deviation may be affected by the aforementioned circumstances, but the deviation will always be present (Billson, 2003). In constant strabismus, the fusion mechanism of the brain is unable to properly align both eyes which results in a permanent and persistent deviation (Bui Quoc and Milleret, 2014) (Agrawal, 2019). Generally, constant deviations are present at birth or early in the critical period and are characterized by a relatively

large angle of deviation (Weinstock *et al.*, 1998) (Bateman and Isenberg, 2013). Nevertheless, constant strabismus can be acquired in later ages by various causes such as head injuries, strokes and brain tumours (Kapoor *et al.*, 2004) (Hepworth *et al.*, 2015). Because of the constant angle of deviation the brain receives two different retinal images that, not only cannot be fused but also, cause confusion of the perceived environment (Ansons and Davis, 2014) (Economides *et al.*, 2012). Sensory and motor adaptations, including suppression and ARC, not only protect the brain from confusion and diplopia but, at some level, restore binocular vision (Damanakis, 2013) (Pickwell, 1980).

A “manifest deviation need not be present at all times" (Noorden and Campos, 2002). When the brain is able to align both eyes but fails to do so under certain conditions, the deviation is considered to be intermittent (Wright *et al.*, 2006) (Billson, 2003). These conditions include emotional or physical state of the subject, time during the day and direction or distance of gaze (Richard and Parks, 1983) (Issaho *et al.*, 2017). Subjects with intermittent strabismus have normal depth perception (Holmes *et al.*, 2011), through binocular vision and stereopsis, but when strabismus occurs their brain suppresses the retinal image of the deviating eye (Cooper and Record, 1986) (Sung *et al.*, 2020). It has been noted that an intermittent deviation is mostly presented as an esotropia or exotropia and can be congenital or acquired (Thomas and Guha, 2010). Although uncommon, if intermittent strabismus goes undetected or left untreated, it could turn into constant strabismus (Rutstein *et al.*, 2011) (Mohney *et al.*, 2019). According to Rowe (2012), a “deviation may have been intermittent first and then became constant; older children and adults may present like this". However, this degradation, from intermittent to constant strabismus, varies from one subject to another as some individuals are able to maintain intermittency for longer periods of time than others whose strabismus becomes constant much sooner (Yanoff and Duker, 2019) (Mohney *et al.*, 2019). Figure 18 illustrates an example of intermittent strabismus where the deviation, a left exotropia, occurs “under conditions of visual inattention or fatigue" (Salmon, 2019).



(a) *Normal: Both eyes fixate on a target.*



(b) *Strabismus: The right eye maintains the correct position, but the left eye deviates outwards (exotropia).*

Figure 18: *Intermittent strabismus (Salmon, 2019): An example case of intermittent strabismus in which the left eye performs an exo deviation (exotropia) "under conditions of visual inattention".*

Variable strabismus is identified when the direction and size of a deviation varies greatly (Kim *et al.*, 2012a) (Economides *et al.*, 2016). Congenital strabismus is initially considered variable because the deviation does not stabilize until the first few moths of life (Agrawal, 2019). However, when strabismus is related to conditions, such as cerebral palsy, that affect a subject's movement and co-ordination the deviation does not just remain variable, but also unpredictable (Erkkilä *et al.*, 1996) (Agrawal, 2019). Compared to normal binocular vision where both eyes are able to steadily fixate on a target, variable strabismus "impairs the ability to fixate targets steadily" (Economides *et al.*, 2016).

3.3.6 *Involvement of Accommodation: Fully, Partially or None*

Section 2.3 discussed the phenomenon of Accommodative Convergence (AC), whereby convergence is elicited from accommodation. In strabismus, the angle of deviation can be significantly influenced by accommodation because an excessive amount of accommodation produces an equally excessive amount of AC causing one of the eyes to over-converge (Lambert and Lyons, 2017) (Rutstein, 2008). This type of strabismus is known as fully accommodative convergent strabismus and it is related to eso-deviations (Kushner, 2010).

When the fusion mechanism of the brain is able to compensate (counterbalance or "correct") the increased eso-deviation, strabismus remains latent and it is referred to as accommodative esophoria (Benjamin and Borish, 2006) (Babinsky *et al.*, 2015). On the contrary, when fusion is unable to compensate for the increased eso-deviation, strabismus becomes manifest and is referred to as accommodative esotropia (Lembo *et al.*, 2019). According to Noorden and Campos (2002), the "vast majority of people have adequate motor fusion and therefore are not heterotropic; but if the fusional amplitudes are inadequate or if the fusion mechanism is impaired by some sensory obstacle, ... heterotropia is established". In some types of strabismus, such as intermittent exotropia, an excessive AC "may be used to maintain ocular alignment as fusional convergence becomes insufficient" (Ahn *et al.*, 2012).

The two main reasons for fully accommodative strabismus are a high AC/A ratio and an abnormal amount of accommodation caused by conditions with regards to refractive errors, e.g. hypermetropia (Rutstein, 2008) (Lembo *et al.*, 2019). When the refractive error of the underlying hypermetropia is corrected, using corrective lenses (see subsubsect. 3.5.1.1), strabismus is eliminated resulting in orthotropia (Rowe, 2012) (Oystreck and Lyons, 2012). Non-refractive accommodative esotropia is explained by a high AC/A ratio in which the amount of accommodation produced, when fixating on a near target, results in an excessive amount of convergence (Esposito Veneruso *et al.*, 2018) (Kim *et al.*, 2012b). Non-refractive accommodative strabismus is unrelated to any refractive errors of the eye's lens (von Noorden and Avilla, 1990) and is characterized by "minimal or no esotropia at distance fixation and larger esotropia at near fixation" (Rutstein, 2008). Bifocal glasses (see subsubsect. 3.5.1.1) are used by subjects who are capable of binocular single vision and stereopsis, but only when their eyes are nearly aligned when fixating on a far target and present a residual esotropia when fixating on a near target (Salmon, 2019) (Lembo *et al.*, 2019).

When accommodation, refractive or non-refractive, is only partially responsible for an eso-deviation, the type of strabismus is referred to as partially accommodative (Damanakis, 2005) (Agrawal, 2019). In partially accommodative esotropia, correcting the underlying hypermetropia reduces strabismus but does not completely eliminate it (Salmon, 2019) (von Noorden and Avilla, 1990). Non-accommodative strabismus is identified when the use of optical lenses, which correct refractive errors, does not change the angle of eso-deviation (Mulvihill *et al.*, 2000). It has been reported that subjects with partially accommodative esotropia "have a nonaccommodative element to the esotropia that results in a manifest deviation for near and distance when the accommodative component is corrected" (Ansons and Davis, 2014).

3.3.7 *State of Vergence: Excess/Insufficiency of Convergence or Divergence*

Vergence, defined in the previous chapter as a disconjugate movement of the eyes, can be impaired by strabismus and lead to diplopia (Kang *et al.*, 2018). In 1896, Duane (Thomas, 2000) stated that divergence "is an active process rather than relaxation of convergence with a return of the eyes to parallelism" (Noorden and Campos, 2002) and that divergent strabismus "develops either from insufficiency of convergence or from excess of divergence or from a combination of the two" (Bielschowsky, 1934). However, Bielschowsky (1934) argued that Duane had not considered "the anomalous position of rest dependent on purely mechanical conditions, which vary within wide limits in different cases". Currently, both theories from Duane and Bielschowsky are considered when classifying exodeviations. Esodeviations, namely convergence excess and convergence insufficiency, have been described by Donders in 1864 (Vivian *et al.*, 2002), von Graefe in 1855 (Cooper and Jamal, 2012) and Duane in 1896 (Arnoldi, 1999) who all suspected the impact of accommodation on convergence.

Eso and exo deviations, related to vergence, are classified as follows:

- **Convergence Excess (CE):** An eso-deviation characterized by an angle of deviation that is larger when fixating on a near target rather than on a far distant target (von Noorden and Avilla, 1986). The most common causes of CE include a "high AC/A ratio (accommodative convergence excess), abnormally high proximal convergence (non-accommodative convergence excess), or decreased accommodative amplitudes (hypoaccommodative convergence excess)" (Arnoldi, 1999). Eso-deviations in CE are measured to be greater than 8Δ when any underlying refractive-error condition, such as hypermetropia and myopia, has been fully corrected (Vivian *et al.*, 2002).

- **Convergence Insufficiency (CI):** An exodeviation characterized by an angle of deviation that is greater when fixating on a near target (Near Point Convergence, NPC) rather than on a far distant target (Lavrich, 2010). Due to the ineffective functionality of the extraocular muscles, the eyes are unable to maintain a convergent position and cannot smoothly converge on an object that is moving from a far distance to near (Adler, 2002). The symptoms of CI may vary from mild to severe including headaches, diplopia, loss of concentration and blurred vision (Cooper, 1988) (Lavrich, 2010). Additionally, CI may cause a subject to read slowly, have pulling sensations (eye strains), heavy eyelids, dull orbital pains, nausea, panoramic headaches and poor depth perception

(Cooper and Duckman, 1978). Poor "accommodation has been implicated as a possible cause of CI" (Cooper and Jamal, 2012) which can affect children, adults and the elderly including people with presbyopia[5] (Cooper and Duckman, 1978). Scheiman *et al.* (2005) and Cooper and Jamal (2012) stated that a mean exodeviation in CI is measured to be 9.3Δ, whereas Noorden and Campos (2002) suggest that the exodeviation produced when fixating on a near target should be, at least, 15Δ greater than the exodeviation measured when fixating on a far target.

- **Divergence Excess (DE):** An exodeviation characterized by an angle of deviation that is greater when fixating on a far target rather than on a near target (Bielschowsky, 1934). Compared to other types of exodeviations, where the angles of deviation are similar when fixating on far and near targets (Daum, 1984), in DE fixating on a far target results in an exodeviation that is, at least, 10Δ greater than the deviation observed when fixating on a near target (Lim *et al.*, 2011). There are two types of DE, referred to as 'true' and 'simulated' (Pickwell, 1979). Unlike 'true' DE, 'simulated' DE lacks a manifest deviation when fixating on a near target, which is attributed to high AC/A ratio (Cooper *et al.*, 1982). (Goldrich, 1980) observed that subjects with DE retain their binocularity by aligning "their eyes spontaneously when it was functionally advantageous for them ... during sports or during other interesting, strongly motivating activities".

- **Divergence Insufficiency (DI):** An eso-deviation characterized by an angle of deviation that is greater when fixating on a far distant target than on a near target (Jacobson, 2000). In subjects with DI, the type of strabismus is defined by a comitant esotropia and constant diplopia when fixating on a far target and binocular single vision when fixating on a near target (Thomas, 2000). Kohmoto *et al.* (2010) noted several cases in which divergence insufficiency was associated with high myopia identified by "a nasal shift of the superior rectus and an inferior shift of the lateral rectus".

3.3.8 *Laterality of Fixation: Unilateral, Alternate or Mono*

Two main types of ocular fixations, termed unilateral and alternating are associated with strabismus (Ansons and Davis, 2014). When a strabis-

5 Presbyopia is a term used to describe the inability of the eyes "to focus (accommodate) due to hardening of the crystalline lens with age" (Yanoff and Duker, 2019).

mic deviation is always presented by the same eye, it is referred to as unilateral or non-alternating strabismus (Goodman *et al.*, 2011). In unilateral heterotropias, subjects always use the same “good" (dominant) eye to fixate on a target while the “bad" (strabismic) eye deviates (Damanakis, 2005). Sireteanu (1982) highlights that subjects with unilateral strabismus use “exclusively one eye for fixation, while the visual capacity of the other eye is severely impaired". Mazur *et al.* (2018) agree that, in non-alternating strabismus, “the affected eye has profoundly reduced visual function compared to the non-affected fellow eye".

Alternate strabismus is defined by the ability of a subject to switch, or swap, dominance from one eye to the other causing the deviation to occur in the opposite eye to the one that is fixating (fig. 19) (Goodman *et al.*, 2011) (Williams *et al.*, 1984).

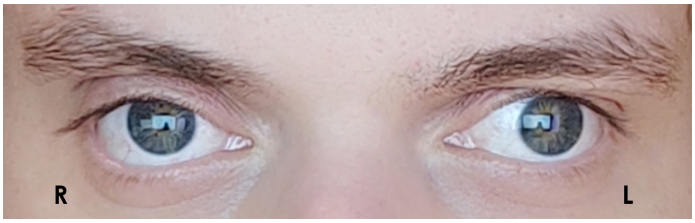

(a) *Right eye is fixating.*

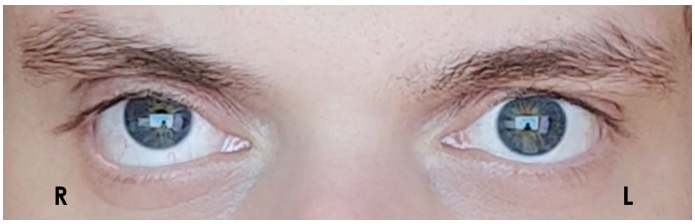

(b) *Left eye is fixating.*

Figure 19: *Alternate Strabismus: (continued on next page)*



(c) *Both eyes are pseudo-fixating. In this particular case, the subject is able to willingly align both eyes in order to aim at the same target. Unfortunately, even though the brain is trying to fuse both retinal images it receives into a single perception, the target is not perceived binocularly but perceived separately by either eye, indicating retinal rivalry. Peripherally however, the environment is perceived as a single perception. Due to a hypermetropia on the left eye, the overall perception of the environment is blurry and out of focus. The willingful alignment of both eyes is a result of repetitive training whereby the subject was alternating fixation between both eyes in a very fast pace until he was able to control the orientation of the deviating eye separately to the fixating eye.*

Figure 19: *Alternate Strabismus: An example of alternating strabismus in which the same subject can willingly fixate with the right eye (a), then with the left eye (b) and then using both eyes (c). Due to a hypermetropia on the left eye, in this figure, the right eye is the preferred fixating eye. Nevertheless, as the target moves to the far left dominance is swapped from the right eye to the left in order to comfortably fixate on the target.*

Economides *et al.* (2014) explain that it "is common for a person with alternating exotropia to view a target with one eye and make an accurate saccade to fixate a new target with the other eye". Subjects with alternating strabismus tend to favour one eye over the other, and the preference of which eye becomes dominant depends on the visual acuity of each eye and the direction of gaze (van Leeuwen *et al.*, 2001). True alternators are subjects "who have no preferences for fixation" (Schlossman and Shier, 1955). Generally, alternate strabismus is more prevalent than unilateral strabismus (Mazur *et al.*, 2018) and a "whole spectrum of fixation habits exists, ranging from extreme unilaterality to free random alternation" (Noorden and Campos, 2002).

Bilateral strabismus is a term used to describe rare cases in which "both eyes are deviated from the primary position" (Noorden and Campos, 2002). In skew deviations, for instance, "the eyes are deviated vertically and often exhibit cyclotorsional disturbance" (Salmon, 2019). Bilateral conditions are also related to Dissociated Strabismus Complex (DSC), discussed later in this chapter, as they do not obey the fundamental laws of ocular motility (Nelson and Olitsky, 2014).

Mono-fixation syndrome, or monofixational phoria, is a term introduced by Parks, in 1961, to describe unilateral strabismus with "harmonious anomalous correspondence with partial stereopsis and usually slight amblyopia in the non fixing eye" (Lang, 1966). Additionally, Parks (1969) mentioned that

mono-fixation strabismus is distinguished from other types of strabismus due to an ultra small angle of deviation ($8-10\Delta$). Lang (1966) argued that the use of the term 'phoria', coined by Parks, was not compatible with this type of strabismus because all diagnosed cases, of mono-fixation, presented a tropia, not a phoria (Lang, 1966). For several years, Lang (1966) used the term "spurious strabismus" to describe this type of strabismus before proposing the term microtropia or microstrabismus.

Regardless of Parks' concerns about the term introduced by Lang the term microtropia, or microstrabismus, is currently used to define manifest strabismus in which an abnormal form of BSV exists and the angle of deviation is smaller than $8-10\Delta$ horizontally and $2-3\Delta$ vertically (Houston *et al.*, 1998) (Wright *et al.*, 2006). Microtropia has been described as subnormal binocular vision because subjects with microtropia may exhibit: (a) orthotropia or heterophoria, (b) normal visual acuity on both eyes, (c) normal or near-normal fusional amplitudes, (d) normal retinal correspondence, (e) foveal suppression of the deviated eye, and (f) reduced or absent stereopsis (Noorden and Campos, 2002) (Ibironke, 2011). However, the most common features of microstrabismus include foveal suppression, eccentric (non-foveal) retinal fixation, ARC, normal peripheral fusion, amblyopia on the deviated eye and reduced stereopsis from abnormal BSV (Agrawal, 2019) (Stidwill and Fletcher, 2010). According to Rowe (2012), microtropia is also associated with "normal retinal correspondence with an expanded Panum's fusional area", which permits fusion in spite of the small deviation (Fray, 2017) (Yanoff and Duker, 2019).

Microtropia is divided into two main categories:

- **With Identity:** A microstrabismus with eccentric fixation and harmonious ARC, where the angle of anomaly is equal to the angle of eccentricity (Houston *et al.*, 1998). This means that the fixation target is projected on a peripheral retinal point of the deviated eye, which is also the retinal point of eccentricity (Ansons and Davis, 2014).

- **Without Identity:** A microstrabismus with eccentric or central fixation and ARC, where the angle of anomaly is greater than the angle of eccentricity (Tomaç *et al.*, 2002). This means that the fixation target is projected on the fovea of the normal eye and a peripheral retinal point of the deviated eye, which is different to the retinal point of eccentricity (Damanakis, 2005).

Depending on the time of onset, a microtropia is classified into primary or secondary (Ibironke, 2011). A primary microtropia occurs "when

microtropia is the initial defect and there is no history of a larger angle of strabismus" (Ansons and Davis, 2014). Secondary, or residual, microtropia occurs after treatment of a larger angle of deviation (Tomaç *et al.*, 2002). Rowe (2012) discusses a possible third classification, known as primary decompensating, in which "the deviation has decompensated into a larger angle".

Rutstein *et al.* (2011) states that microtropia "is usually diagnosed later than the more obvious types of strabismus". Due to the ultra small angle of deviation, most people suffering from microtropia are not able to detect any manifest strabismus through simple observation (Lambert and Lyons, 2017). According to Damanakis (2013) and Hammond (2014), people with microstrabismus complain of reduced visual acuity that cannot be resolved by wearing glasses. This is because microstrabismus is usually accompanied by anisometropia[6], hypermetropia and amblyopia (Ibironke, 2011). Several tests, including Worth's four lights test (see subsect. 3.2.4 and 3.4.6), cover test (see subsect. 3.4.3), 4Δ prism test (see subsect. 3.4.6) and Bagolini striated glasses test (see subsect. 3.2.4 and 3.4.6), are used to diagnose microstrabismus (Tomaç *et al.*, 2002). However, microtropia is not easily diagnosed, as the selection of an appropriate diagnostic examination depends on the amplitude and characteristic of the deviation (Ansons and Davis, 2014).

3.3.9 *Time of Onset: Congenital or Acquired*

Previously, in subsection 3.1.2, it was established that strabismus can affect both genders and may occur at any age. The time of onset of strabismus is distinguished into two categories:

- **Congenital:** Strabismus occurs at birth or infancy, around 6 months of age, and it is noted as a consequence of abnormal cerebral developments (Bateman and Isenberg, 2013). The terms congenital and infantile have been used interchangeably (Stidwill and Fletcher, 2010). However, Rutstein *et al.* (2011) notes that "infantile esotropia is not congenital and most likely develops between 2 and 4 months of age, a period during which most infants are becoming orthotropic".

- **Acquired:** Strabismus occurs after the fist 6 months of age and could be attributed to various reasons, including high hyperopia, tumor or head trauma (Nelson, 2019) (Fawcett *et al.*, 2004). In acquired cases, normal BSV existed prior to the occurrence of strabismus (Zakher *et al.*, 2019).

6 A condition in which the lenses of both eyes have varying, uneven, refractive powers (Billson, 2003).

The age basis for classifying strabismus as congenital or acquired may vary between $6-12$ months of age, as it depends upon the type of strabismus and the maturity of the visual system (Lambert and Lyons, 2017) (Nelson and Olitsky, 2014) (Kapoor *et al.*, 2004).

3.3.10 *Other Properties: Dissociated, Paralytic, Mechanical-Restrictive, Orbital and Pseudo*

Other types of strabismus, with less common properties, include dissociated deviations, paralytic, mechanical-restrictive, orbital and pseudo strabismus.

3.3.10.1 *Dissociated Strabismus Complex (DSC)*

Dissociated deviations are one of the most obscure and atypical oculomotor disturbances observed in strabismus, as they do not obey the laws of ocular motility (Agrawal, 2019). Additionally, dissociated deviations can be bilateral or strictly unilateral, symmetric or asymmetric (Brodsky *et al.*, 2005). The following types of dissociated deviations form what is currently known as Dissociated Strabismus Complex (DSC) (Ansons and Davis, 2014):

- **Dissociated Vertical Deviation (DVD):** Defined by a progressive vertical deviation of the strabismic eye when it is covered, or when the subject with strabismus is under emotional or physical exhaustion or stress (Hatt *et al.*, 2015). DVD can be accompanied by other forms of strabismus, but the most common deviation associated with DVD is an excyclo deviation (Kolb *et al.*, 2020) (Salmon, 2019). In this case, when uncovered, the strabismic eye returns to its primary position by performing a hypo-incyclo deviation (Traboulsi and Utz, 2016). DVD is differentiated from other vertical deviations because the deviation occurs whilst the normal eye remains still, thereby disobeying Hering's law of yoke muscles (see subsect. 2.2.1) (Wright *et al.*, 2006). Brodsky (1999) explains that during "the period of vertical misalignment, visual input from the hyperdeviated eye is usually suppressed by the brain so that the affected individuals do not experience diplopia". However, in some cases, the subject would suffer from diplopia and eye strains (Hatt *et al.*, 2015). The aetiology behind the development of DVD remains poorly understood and, although several reports suggest that DVD is associated with congenital esotropia, it is considered to be an acquired strabismus, developed around $2-3$ years of age (Nelson and Olitsky, 2014) (Benjamin and Borish, 2006).

- **Dissociated Horizontal Deviation (DHD):** Defined by a progressive horizontal deviation of the strabismic eye, unrelated to accommodation, when it is covered, or when the subject with strabismus is under emotional or physical exhaustion or stress (Brodsky, 2007). DHD is far less common than DVD and is frequently observed as a side-effect of previous treatment, usually surgery (Brodsky and Fray, 2007). DHD may be unilateral or bilateral but rarely symmetric, and the strabismus is usually determined by a slow exo deviation (Ansons and Davis, 2014) (Brodsky *et al.*, 2005). Lambert and Lyons (2017) explains that, sometimes, DVD is mistaken for DHD and "DHD may merely be a DVD with a large horizontal component". When the strabismic eye is uncovered, it returns to its primary position by performing a horizontal deviation, similar to the behaviour of an esophoria or exophoria (Billson, 2003). Similarly to DVD, other forms of strabismus may coexist alongside DHD (Nelson and Olitsky, 2014).

- **Dissociated Torsional Deviation (DTD):** Defined by a progressive torsional deviation of the strabismic eye when it is covered, or when the subject with strabismus is under emotional or physical exhaustion or stress (Brodsky, 1999) (Damanakis, 2005). Although DTD usually occurs alongside DVD or DHD, it can also be the dominant deviation that occurs prior to any other signs of dissociated strabismus (Ansons and Davis, 2014) (Traboulsi and Utz, 2016).

3.3.10.2 *Paralytic*

In ophthalmology, the term 'palsy', or 'paralysis', suggests a complete lack of muscular function, whereas the term 'paresis' indicates partial (weak) muscular function (Noorden and Campos, 2002) (Wright *et al.*, 2006). Paralytic strabismus is defined as an incomitant variable deviation that is caused by a palsy or paresis of one, or more, extraocular muscles (Snell and Lemp, 2013) (Prasad and Volpe, 2010). According to Nelson and Olitsky (2014), paralytic strabismus is "characterized by a deviation that varies according to the direction of gaze and fixation with the involved or uninvolved eye". In paralytic strabismus, the motility of the deviated eye becomes restricted as it moves towards the field of action of the paralytic extraocular muscles (Yanoff and Duker, 2019) (Piña-Garza, 2013). Consequently, the strabismic deviation becomes larger (Lueder, 2015).

When the normal eye is dominant, the deviation of the strabismic eye is called primary (Rowe, 2012). A secondary deviation occurs when dominance is assumed by the strabismic eye, which results to a larger angle of deviation

(Benjamin and Borish, 2006). This is because during secondary deviations, in which the strabismic eye is dominant, the paralytic extraocular muscles are highly innervated by the brain, which forces the muscles to apply extra effort in order to retain fixation of the strabismic eye (Lambert and Lyons, 2017) (Agrawal, 2019). According to Hering's law (see subsect. 2.2.1), the yoke muscles of the normal eye receive equal innervation to the yoke muscles of the strabismic eye, but because the yoke muscles of the normal eye are non-paralytic they overact in response to the larger impulses from the brain, thereby causing a large angle of deviation (Lee, 1996) (Kushner, 2010).

Paralytic strabismus is caused by a palsy or paresis of the following cranial nerves:

- **Third:** The oculomotor nerve that innervates "the medial rectus, inferior rectus, superior rectus, and inferior oblique muscles, as well as the levator palpebrae" (Prasad and Volpe, 2010).
- **Fourth:** The trochlear nerve that innervates the superior oblique muscle (Nelson and Olitsky, 2014).
- **Sixth:** The abducens nerve that innervates the lateral rectus muscle (Piña-Garza, 2013).

If paralytic strabismus is acquired after binocular vision has been developed diplopia is very likely to occur (Oystreck and Lyons, 2012). In congenital cases, however, diplopia and confusion are suppressed and the subject may develop amblyopia (Traboulsi and Utz, 2016). Regardless of the time of onset, CHP is often adopted by a subject with paralytic strabismus in order to develop and maintain binocular vision (Ansons and Davis, 2014).

3.3.10.3 *Mechanical-Restrictive*

The ability of an eye to perform translatory and rotatory movements, in order to fixate on a target, can be restricted by structural alterations of: (a) an agonist extraocular muscle, (b) an antagonist extraocular muscle, or (c) the tissue that surrounds the extraocular muscles (Noorden and Campos, 2002) (Damanakis, 2005). According to Wright *et al.* (2006), ocular restrictions are caused by two mechanisms, "a mechanical tether on eye movements or misdirected muscle forces that work against the normal agonist muscle function".

Because a deviation occurs from non-innervational conditions, this type of strabismus is known as mechanical-restrictive (Agrawal, 2019). Similar to paralytic deviations, a subject with mechanical-restrictive strabismus may

adopt CHP in order to develop and maintain BSV (Ansons and Davis, 2014). Mechanical-restrictive conditions include thyroid Graves disease, congenital fibrosis syndrome, congenital Brown's syndrome and fat adherence to extraocular muscle (Damanakis, 2005) (Lambert and Lyons, 2017).

The most effective methods to distinguish between mechanical-restrictive and innervational strabismus, are the:

- **Measurement of Saccadic Velocity:** Observation of fast saccadic movements (Stidwill and Fletcher, 2010). In paralytic strabismus, the extraocular muscles are not able to generate saccadic movements causing the strabismic eye to slowly drift towards the saccadic direction (Metz, 1983). Mechanical-restrictive strabismus "is associated with normal, but shortened, saccadic movements as the eye stops abruptly when the restriction is met" (Wright *et al.*, 2006).

- **Forced Ductions Test:** Determines "the tone of the muscle by attempting to move the eye with forceps in different directions" (Rowe, 2012), particularly, in the direction of the restrictive field (Jivraj and Patel, 2015). In mechanical-restrictive strabismus, the eye resists movement, whereas in paralytic strabismus the eye rotates without resistance (Metz, 1976) (Oei *et al.*, 1983).

- **Active Force Generation Test:** Assesses the generated forces of extraocular muscles, which allow an eye to perform translatory and rotatory movements (Ansons and Davis, 2014). In this test, the strabismic eye is "grasped with forceps after instilling the area with anaesthetic on a cotton bud tip" (Billson, 2003) and the subject is asked to rotate the eye in the direction of the restrictive field (Metz, 1976). In paralytic strabismus, the subject does not feel any eye strain, or tug, while attempting to rotate the eye (Jivraj and Patel, 2015). In mechanical-restrictive strabismus a tug is felt by the subject, which means that an attempt has been made to rotate the eye normally but, due to a restrictive element of the extraocular muscles, the eye cannot rotate (Kushner, 2010) (Karthiga, 2020).

3.3.10.4 *Orbital*

Craniosynostosis is a medical term used to define conditions responsible for an undergrowth or overgrowth of the anatomical structures of the face and head (Traboulsi and Utz, 2016). In craniosynostosis, the premature joining of the different bones in a skull, including the closure of one

or more cranial sutures[7], limits (restricts) the growth of the brain (Kimonis *et al.*, 2007) (Nelson and Olitsky, 2014). Orbital strabismus may occur due to the abnormal development of the brain and skull (shape and size) (Nelson, 2019) (Yanoff and Duker, 2019). Noorden and Campos (2002) defines orbital strabismus as any "ocular misalignment caused by anomalies of the orbit or of the face (craniofacial dysostosis, plagiocephaly, hydrocephalus, heterotopia of muscle pulleys, and so forth)".

In orbital strabismus, the structure of an eye's socket and functionality of the extraocular muscles are affected by anatomical deformities (Kabbani and Raghuveer, 2004) (Rowe, 2012). According to Lueder (2015), "the abnormal orbital anatomy affects the function of the extraocular muscles, usually by either changing the position of the muscle insertion or by an alteration of the muscle pathway". For instance, plagiocephaly, which is a condition that deforms the shape and symmetry of the skull, is caused either by an asymmetrical unification (joining) of the bones in the skull or a large compression of the skull (Laughlin *et al.*, 2011). Consequently, in one side, the socket of the eye is located higher, or lower, than the other (De Bock *et al.*, 2017) (Damanakis, 2005). Similar to mechanical-restrictive strabismus, subjects with orbital strabismus may adopt CHP in order to develop and maintain BSV (Traboulsi and Utz, 2016).

Other conditions that develop orbital strabismus include craniofacial anomalies, orbital masses, orbital trauma and anomalous orbital structures (Snell and Lemp, 2013) (Lueder, 2015).

3.3.10.5 *Pseudo*

Some conditions, including facial anomalies, are responsible for a false impression of strabismus (Pritchard and Jr., 2007). Pseudo strabismus is an ophthalmological term used to describe conditions where the eyes appear to deviate, but without the occurrence of an actual deviation (Sefi-Yurdakul and Tuğcu, 2016). A relatively large distance between the inner canthi of the eyes, accompanied with an epicanthus[8], gives the false impression of an esotropia (Lambert and Lyons, 2017). An epicanthus is quite common in newborns, but gradually recedes as the child grows (Xu *et al.*, 2020).

7 The skull of an infant is not fully constructed until the brain has been fully formed (Lueder, 2015). The gaps between an infants skull are called sutures, and allow the skull to grow depending on the size of the brain (Kabbani and Raghuveer, 2004). Around the age of 2 years, the sections of the skull join together and the sutures turn into bone (Wright *et al.*, 2006).

8 An epicantus is defined by a folding of the skin on the upper eyelid, covering the inner corner of the eye (Standring, 2008).

Anatomical deformities that cause orbital strabismus, including craniosynostosis and an abnormal structure of the eye socket, may also be responsible for pseudo strabismus (Sefi-Yurdakul and Tuğcu, 2016). A relatively small distance between the eye sockets, and thereby the distance between both eyes, may give the false impression of an esotropia (Rutstein *et al.*, 2011). In contrast, a relatively large distance between the eyes may give the false impression of an exotropia (Xu *et al.*, 2020).

3.4 DIAGNOSIS OF STRABISMUS

The diagnosis of strabismus is a challenging task, not only because it requires relatively high cooperation by the subject undergoing examination (Hammond, 2014) but also because, strabismus is a "dynamic condition" (Traboulsi and Utz, 2016) that may unexpectedly change states, thereby, rendering a diagnosis inaccurate (Damanakis, 2013). The process of compiling a complete diagnosis of strabismus includes the collation of a detailed history of the deviation and an assessment of the visual acuity, ocular motility, strabismic deviation, binocular vision and stereopsis (Ansons and Davis, 2014).

3.4.1 *History and Observation*

In order to diagnose strabismus a detailed history of the condition, in the form of an oral or written questionnaire, must be obtained prior to any diagnostic examination (Traboulsi and Utz, 2016). This is because the information gathered from a historical questionnaire would assist in the diagnosis, treatment and prognosis of strabismus (Damanakis, 2005). If a subject is young and unable to provide detailed information about the condition, the historical questionnaire is presented to the subject's guardians (Hammond, 2014). The origin of a strabismic condition can be identified from a family history, including distant relatives, as it can relate to an inherited condition (Billson, 2003). Furthermore, it is important to gather information about: (a) the time of onset of strabismus, including the possibility that a deviation occurred after the treatment of another ocular condition, (b) any current symptoms caused from strabismus, such as double vision or headaches, (c) birth history of the subject, (d) other ocular conditions of a subject, including amblyopia, myopia or hypermetropia, and (e) the general health of a subject, e.g. cerebral palsy, diabetes, stress (Salmon, 2019) (Ansons and Davis, 2014). The history should also include detailed information about the characteristics of a deviation because some features of strabismus, including constancy and

variability, may not be deduced during the diagnostic examination (Noorden and Campos, 2002) (Benjamin and Borish, 2006).

Apart from obtaining a history with regards to the deviation, a major part in the diagnosis of strabismus is a keen observation of the head and eyes (Damanakis, 2013). An abnormal head posture could indicate CHP, suggesting an adaptation to an underlying strabismus. CHP could also be adopted by a subject in order to convert a manifest deviation into latent, which would allow the subject to maintain binocularity (Wright *et al.*, 2006). A keen observation of the eyes is essential in the detection of small to large angles of manifest strabismus and could help identify cases of paralytic, mechanical-restrictive, orbital or pseudo strabismus (Nelson and Olitsky, 2014). Latent deviations, in which the proper alignment of both eyes is maintained by fusion, or microtropias cannot be detected by simple observation (Cooper, 1988) (Ibironke, 2011).

3.4.2 *Visual Acuity and Refractive Errors*

Visual acuity (VA) is an extremely complex "function of the dioptric apparatus of the eye and also of the retina, the nervous pathways and central nervous mechanisms" (Rowe, 2012). VA is comprised of four senses:

- **Light:** The ability to determine whether objects are lit or dark (Kniestedt and Stamper, 2003).
- **Form:** The ability to "distinguish between spatially separate visual stimuli and to discern the size and shape of objects from the position and orientation of their edges" (Ansons and Davis, 2014).
- **Colour:** The ability to analyse and perceive colours of the visual spectrum (Clarkson, 2008).
- **Motion:** The ability to detect motion by inferring the speed and direction of elements in a scene (Westheimer and McKee, 1975).

The first examination, in a diagnostic process, is the assessment of visual acuity for far (6m) and near ($0.3\text{m} - 0.6\text{m}$) fixation targets (Benjamin and Borish, 2006). Initially, VA of each eye is tested separately, i.e. monocularly, and further, binocularly (Salmon, 2019). Each test is repeated with and without the use of prescription glasses in order to determine the presence of amblyopia or other refractive error conditions, including myopia or hypermetropia (Thomas and Guha, 2010). Binocular VA (BVA) must be thoroughly assessed on subjects who display poor VA under monocular fixation, on either eye, as

other conditions, including pathological nystagmus[9], may be responsible for normal VA when tested binocularly and poor VA when tested monocularly (Esposito Veneruso *et al.*, 2018) (Serra and Leigh, 2002).

VA thresholds are classified into the following categories:

- **Minimum Visible:** Determine the presence or absence of a target using light discrimination features, including brightness and colours, i.e. by comparing the brightness of a target against its background (Noorden and Campos, 2002) (Kniestedt and Stamper, 2003).
- **Minimum Separable/Resolvable:** Discriminate between two or more spatially separated targets (Rowe, 2012).
- **Minimum Discriminable:** Detect a difference in the relative positions of two or more targets, with respect to one another (Kniestedt and Stamper, 2003) (Clarkson, 2008).
- **Minimum Legible:** Recognize target that become progressively smaller (Bailey and Lovie, 1976).

The age of a subject, refractive errors or progression of a disease (Westheimer, 1979), determine which examination method is to be used in order to assess VA, as cooperation levels differ in preverbal children ($<$ 2 years of age) and verbal children ($\geqslant$ 2 years of age) (Lambert and Lyons, 2017) (Salmon, 2019). The "E chart", which is a chart of optotypes displaying the letter E at various orientations and sizes, is used to assess VA in children around the age of 2 years (Agrawal, 2019). The child is given a plastic E toy and is asked to match its orientation to a designated E on the chart (Nelson and Olitsky, 2014). Moreover, depending on the mental state of a subject, adults and the elderly, are tested using similar methods to preverbal and verbal children.

Part of VA testing is the examination of refractive errors. It is imperative that the presence of any potential refractive errors is assessed, as it would reveal other ocular conditions, including cycloplegia[10] (Esposito Veneruso *et al.*, 2018). Cycloplegic conditions cause lack of accommodation, which may contribute in the development of strabismus (Charman, 2008) (Lembo *et al.*, 2019). According to Ansons and Davis (2014), "refractive errors may

9 Pathological nystagmus is an ophthalmological term used to define various types of manifest nystagmus (see subsect. 2.2.2) that occur during birth or in the first few weeks of age (Serra and Leigh, 2002). One of the most common types of nystagmus observed in strabismus is known as latent nystagmus, which occurs during the occlusion of either eye (Brodsky and Tusa, 2004).

10 Cycloplegia is defined by a paralysis of the ciliary muscles, which are responsible for contracting and relaxing the lens of an eye.

indicate the nature of the deviation rather than the binocular potential". Conditions related to refractive errors include: (a) hypermetropia, in which light focuses behind the retina (Yanoff and Duker, 2019), (b) myopia, where light focuses in front of the retina (Haines and Mihailoff, 2018), (c) astigmatism, where light is not focused evenly on the retina (Grosvenor, 1978), (d) anisometropia, in which the lens has varying refractive powers and focus is uneven (Noorden and Campos, 2002), (e) antimetropia, where one eye is myopic and the other hyperopic (Vincent and Read, 2014), (f) emmetropisation, "the mechanism in which refractive error dissipates during early visual development of infants" (Rowe, 2012), but differs when accompanied by strabismus, (g) monovision, in which one eye is used to fixate on a far target and the other eye to fixate on a near target, e.g. presbyopia (Charman, 2008) (Evans, 2007), and (h) aniseikonia, where the retinal images of both eyes differ in size or shape (Kolb *et al.*, 2020).

3.4.3 *Cover Test*

A cover test is a diagnostic examination, in which either eye is covered by an opaque cover paddle (Traboulsi and Utz, 2016). It is the simplest, but most accurate, examination method used to determine the: (a) presence of strabismus, (b) type of strabismus, e.g. latent or manifest, comitant or incomitant, constant or intermittent, and (c) size and direction of the strabismic deviation (Damanakis, 2005) (Rowe, 2012).

During a cover test, the subject is required to fixate on near and far targets, at various directions (Scheiman *et al.*, 2005) (Benjamin and Borish, 2006). Noorden and Campos (2002) explain that the "test should always be done for distance and near fixation to establish any differences". Furthermore, the cover test is repeated with and without prescription glasses, in order to determine if strabismus is caused by refractive error conditions (Lembo *et al.*, 2019) (von Noorden and Avilla, 1990). The fixation target can be any object, e.g. a small toy when testing young children, or a pen torch, which can be used to detect strabismus from corneal reflections (Nelson, 2019) (Richard and Parks, 1983).

Manifest strabismus (tropia) is identified when covering the dominant eye causes the uncovered eye to assume dominance and perform a compensatory movement in order to fixate on the target (fig. 20a, 20b) (Damanakis, 2014a) (Yehezkel *et al.*, 2020). Once the cover is removed, the previously covered eye reassumes dominance, causing the other eye to deviate (fig. 20c) (Brodsky *et al.*, 2005).



(a) *The right eye is dominant and the left eye is strabismic.*

(b) *A cover paddle is placed in front of the dominant eye (R) which forces the strabismic eye (L) to assume dominance and turn inwards.*

(c) *When the cover paddle is removed, the right eye reassumes dominance and the left eye returns to its previous deviation.*

Figure 20: *Cover test of exotropia: An example case in which the left eye deviates outwards and strabismus is manifest. When the dominant eye (R) is covered and the strabismic eye (L) turns inwards, the covered eye (R) deviates at a secondary angle of deviation. Once the cover is removed, the right eye returns back to its primary position and the left eye deviates. For simplicity, this figure does not show the secondary compensatory movement performed by the covered eye.*

Contrary to tropia, in latent strabismus (phoria) the uncovered eye does not perform a compensatory movement when the dominant eye is covered (fig. 21a, 21b) (Damanakis, 2014a) (Babinsky *et al.*, 2015). Instead, the covered eye performs a compensatory movement and, as the cover is removed, it returns to its primary position (fig. 21c) (Lim *et al.*, 2011).



(a) *Both eyes are straight.*

(b) *A cover paddle is placed in front of the right eye and the left eye remains straight.*

(c) *As the cover paddle is removed, the right eye moves inwards betraying its previous deviation when the cover was on.*

Figure 21: *Cover test of exophoria: An example case in which both eyes are straight, but when binocularity is interrupted the right eye deviates outwards.*

There are two types of cover tests:

- **Cover-Uncover:** Each eye is covered using a cover paddle in order to observe a compensatory movement by the uncovered eye (Ansons and Davis, 2014) (Zheng *et al.*, 2019). A tropia is diagnosed if either eye performs a compensatory movement, whereas, if neither uncovered eye performs a compensatory movement, tropia does not occur (Yehezkel *et al.*, 2020). In a phoria the deviation is not obvious because the alignment of both eyes is maintained by fusion. However, when a cover paddle is placed in front of either eye, fusion is disrupted and the covered eye deviates (Issaho *et al.*, 2017). The deviation is not visible as it occurs behind the cover paddle, but when the cover is removed and fusion is restored, the eye moves towards its primary position, reassuming fixa-

tion (Nelson and Olitsky, 2014). In cover-uncover testing enough time is given in order to allow the eyes perform compensatory movements (Babinsky *et al.*, 2015). The amount of a compensatory movement is an indication of the size of strabismus and the reversed direction of a compensatory movement is the direction of the strabismic deviation (Rowe, 2012).

- **Alternate Cover:** Each eye is alternately covered using a cover paddle, which is moved from side to side at a relatively fast pace, such that both eyes are not left uncovered long enough for fusion to take effect (Hrynchak *et al.*, 2010) (Stidwill and Fletcher, 2010). If neither eye performs a compensatory movement, no form of strabismus (tropia or phoria) occurs. If a compensatory movement is observed, strabismus is present and conducting a cover-uncover test would reveal which form of strabismus exists (Babinsky *et al.*, 2015). Because both eyes are almost always covered, the alternating cover test ensures a complete dissociation of the eyes (Hrynchak *et al.*, 2010), which not only makes this test reliable when diagnosing heterophorias but also assists in the diagnosis of variable strabismus (Economides *et al.*, 2016). Additionally, an alternate cover test reveals the maximum angle of deviation that may occur in the presence of strabismus.

Damanakis (2005) explains that a cover test does not return accurate results when a subject has very poor visual acuity. Furthermore, some cases of micro strabismus and pure cyclo deviations are not detectable by cover testing, because the angle of deviation or movement of the strabismic eye is either too small or cannot be observed (Noorden and Campos, 2002) (Yanoff and Duker, 2019). Apart from identifying the characteristics of a deviation, it is important to observe and analyse the compensatory movements that occur, including speed and jerkiness, as they would reveal more details about the nature of strabismus (Stidwill and Fletcher, 2010). For instance, in paralytic or mechanical-restrictive conditions, covering the dominant eye will be followed by a very limited or no compensatory movement of the strabismic eye (Murray, 2015).

3.4.4 *Assessment of Ocular Motility*

Traboulsi and Utz (2016) states that every ophthalmic “exam should include a thorough evaluation of ocular motility in all directions of gaze, noting horizontal limitation of movement and the presence of accompanying vertical deviations or paradoxical eye movements". A target, which can be

any small object or a pen torch, is positioned at a distance of $\approx$ 50cm and moved in all directions of gaze (Agrawal, 2019). According to Ansons and Davis (2014) and Damanakis (2014a), the directions, or positions, of gaze are: (a) centre, which is primary, (b) left, (c) right, (d) top, (e) bottom, (f) top left, (g) top right, (h) bottom left, and (i) bottom right.

The directions of gaze are defined by six cardinal directions, which do not include a top gaze and a bottom gaze (Benjamin and Borish, 2006). Nevertheless, an assessment of ocular motility includes testing top and bottom directions of gaze in order to identify hyper and hypo deviations (Deepa *et al.*, 2019). The purpose of performing an ocular motility test is to reveal the following:

1. Limited motility of the strabismic eye in a particular direction, which could be due to an extraocular muscular paresis or anatomical anomalies that restrict the natural turn of the eye (Prasad and Volpe, 2010).

2. Excessive motility of either eye in a particular direction, which could be due to overactivity of the corresponding extraocular muscles (Kushner, 2010) (Vivian *et al.*, 2002).

3. Variability of the strabismic deviation at different directions of gaze, i.e. incomitant strabismus (Rutstein *et al.*, 2011).

4. Presence of pathological nystagmus (Mohamad Fadzil *et al.*, 2019).

5. Dissociated conditions and other syndromes, including Duane[11], Möbius[12] and Brown[13] syndromes (Nelson, 2019).

3.4.5 *Methods of Measuring Strabismic Deviations*

Strabismic deviations are measured in degrees (°) or dioptres (Δ) (Traboulsi and Utz, 2016), where the relationship between degrees and dioptres is expressed by equation 5.

$$P_{(\Delta)} = 100 \times \tan(\theta^{(\circ)}) \tag{5}$$

11 Duane Syndrome (DS), also referred to as Duane Retraction Syndrome (DRS), "is a congenital eye movement disorder characterized by a limitation of abduction and/or adduction, narrowing of the palpebral fissure, and retraction of the globe on adduction" (Kalevar *et al.*, 2015).

12 Möbius syndrome "is a complex, rare developmental anomaly of the hindbrain that has been described historically as the combination of congenital palsies of the abducens and facial nerves, frequently with additional features, including orofacial malformations, limb defects, and musculoskeletal, behavioral, and cognitive abnormalities" (MacKinnon *et al.*, 2014).

13 Brown syndrome "is an ocular motility disorder characterized by limited active and passive elevation of the eye in adduction" (Coussens and Ellis, 2015).

The precise conversion of 1° to prismatic dioptres (Δ) is $1° = 1.74551\Delta \approxeq 1.75\Delta$, but in clinical practice it is rounded to $1° \approxeq 2\Delta$ (Benjamin and Borish, 2006). For angles $\leqslant 45°$, the small rounding error is not considered to be clinically important, but for larger angles "this approximation of 2Δ per degree is no longer valid; as one approaches 90°, the number of prism dioptres per degree rises to infinity" (Irsch, 2015).

The deviation of strabismus is measured by objective and subjective methods, which differ only in the method of gathering information (Noorden and Campos, 2002). Objective tests are based on observations drawn by a strabismologist, whereas subjective tests depend heavily on the feedback provided by the subject (Wilson *et al.*, 2009). Objective and subjective methods, used to determine and measure strabismus, include:

- **Hirschberg:** This method is not very accurate and only yields an estimate of the angle of deviation (Eskridge *et al.*, 1988). Nevertheless, it is considered to be helpful when the subject is uncooperative or the subject's visual acuity is very poor (Nelson and Olitsky, 2014). In Hirschberg's method the position of the corneal reflection, of the strabismic eye, is measured with respect to the pupil and iris of the eye, in which every 1mm of eccentricity of corneal reflection corresponds to a deviation of 7° or 15Δ (fig. 22) (Stidwill and Fletcher, 2010) (Eskridge *et al.*, 1988). Eso-deviations occur when the corneal reflection is located towards the temporal area, whereas exodeviations occur when the corneal reflection is located towards the nasal area (Billson, 2003).

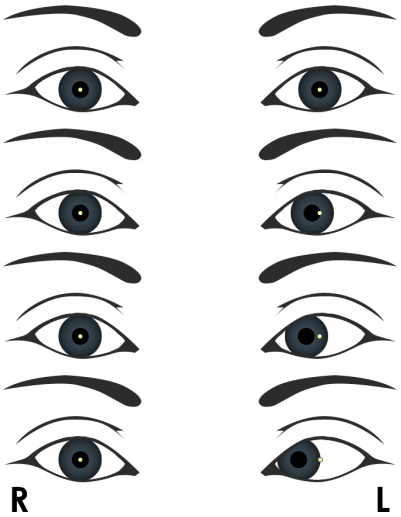

Figure 22: *Hirschberg's method: An example of corneal reflections observed in various amplitudes of esotropia.*

- **Brückner:** Similar to Hirschberg's method, the Brückner test compares the corneal reflection with the fundus[14] reflection in order to detect the presence of ocular conditions, including amblyopia, anisometropia, cataract and strabismus (fig. 23) (Miller *et al.*, 1995). In this test, both eyes are illuminated using an ophthalmoscope[15] from a distance of $\approx$ 1m, which allows the reflections to be compared (Agrawal, 2019). A strabismic deviation is identified when one of the reflections is brighter than the other (Lambert and Lyons, 2017).



Figure 23: *Bruckner test (Dorhman, 2015): An example of unequal corneal and fundus reflections, indicating some form of amblyopia on the left eye.*

- **Krimsky:** Although this method uses corneal reflections to determine strabismus, the angle of deviation is measured by placing a prism in front of and along the primary gaze of the fixating eye (Aouchiche and Dankner, 1988) (Benjamin and Borish, 2006). The prism causes the fixating eye to deviate, forcing the eye to return to the primary position of gaze (Rutstein *et al.*, 2011). Consequently, the deviating eye also moves by the same amount as the fixating eye. As shown in figure 24, for every increase in the prismatic strength the angle of deviation decreases until both eyes are aligned. When the strabismic eye reaches the primary position of gaze the corneal reflections are central to the pupil (Aouchiche and Dankner, 1988). The strength of the prism used to align both eyes, indicates the angle of deviation (Nelson, 2019).

14 The fundus of an eye includes the interior parts of the eye including the retina, optic disc, macula and posterior pole (Standring, 2008) (Snell and Lemp, 2013).

15 An ophthalmoscope, also known as a funduscope, is a diagnostic instrument that allows the user to examine the interior parts of an eye by projecting a bright light (Remington, 2012).

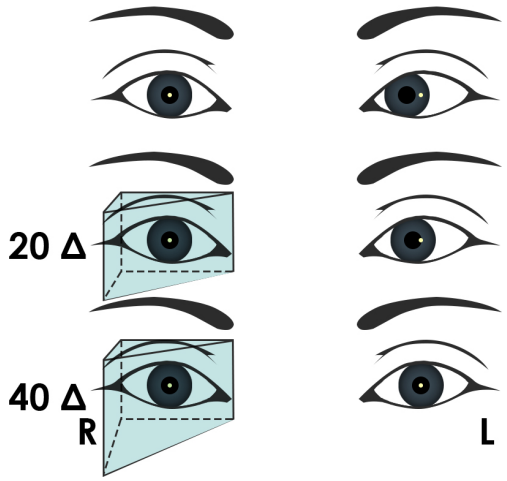

Figure 24: *Krimsky test: An example of left esotropia, where prisms are placed in front of the fixating (right) eye while observing the corneal reflection and position of the deviated eye.*

- **Prism Reflection:** A very similar test to Krimsky test, where corneal reflections and prisms are used to detect strabismus and measure the angle of deviation (Ansons and Davis, 2014). In contrast to a Krimsky test, the prism is placed in front of the deviating eye, instead of the fixating eye (Salmon, 2019). During a prism reflection test, the "examiner observes the position of the corneal reflections and the prism strength is gradually increased until the corneal reflections appear symmetrical" (Rowe, 2012). Compared to a Krimsky test, a disadvantage, of the prism reflection test, is that the corneal reflection is not easily observed through the prism, therefore its position could be misjudged (Agrawal, 2019). An advantage of this test, compared to a Krimsky test, is that the direction of gaze of the fixating eye does not change, which improves the realism of the test (Damanakis, 2005). The prism reflection test is preferred to a Krimsky test in the presence of paralytic or mechanical-restrictive deviations (Wright *et al.*, 2006).

- **Prism Cover:** This test is one of the most reliable methods of measuring strabismic deviations ($\pm 2\Delta$), as it can be applied for near and far targets, at all directions of gaze (Damanakis, 2014a). In this test, a prism is positioned in front of the strabismic eye, which reduces the deviation, while an alternate cover test is performed, with the purpose of revealing the largest possible angle of deviation that could occur (Wilson *et al.*, 2009). The prismatic strength is adjusted until, under the alternate cover test, both eyes remain steady at the primary direction of gaze (fig. 25) (Economides *et al.*, 2014) (Goodman *et al.*, 2011). The prismatic strength is "further increased until a reversal movement is

seen to confirm that the maximum angle has been elicited" (Ansons and Davis, 2014), and reduced until no movement is observed. The prism cover test cannot be used in the presence of large amblyopia or eccentric fixation (Traboulsi and Utz, 2016).

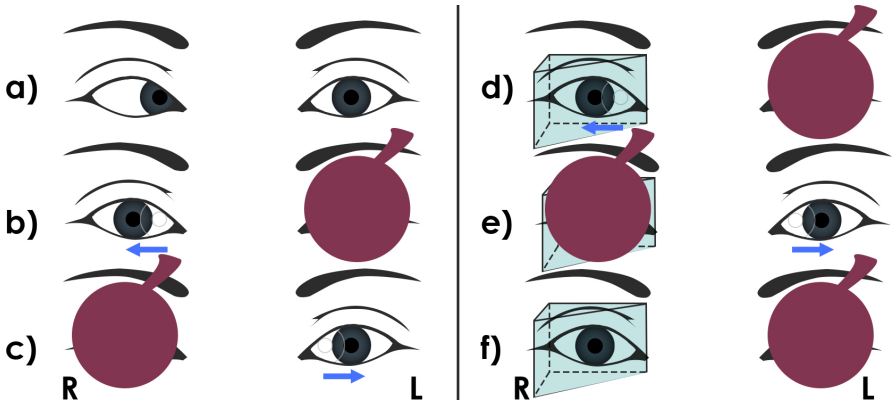

Figure 25: *Prism cover test: An example of right esotropia, demonstrating the process of a prism cover test from steps 'a' to 'f'.*

- **Simultaneous Prism Cover:** Preferred when the angle of manifest deviation is very small and accompanied by a latent deviation, e.g. microstrabismus (Lueder, 2011). Due to the additional latent strabismus, a prism cover test cannot be used to measure the manifest angle of deviation, because the alternate cover test will return the accumulation of the manifest and latent angles of deviation (Benjamin and Borish, 2006). Instead, a prism is placed in front of the deviating eye and a cover-uncover test is performed on the fixating eye (Nelson and Olitsky, 2014). The prismatic strength is gradually increased until the strabismic eye rests at the primary position (Lambert and Lyons, 2017). However, Holmes *et al.* (2008) underscored "the difficulty of determining the magnitude of small tropias and the difficulty of determining whether a small deviation even exists".

- **Synoptophore:** A synoptophore (fig. 26) is a haploscopic[16] device that measures strabismus angles by allowing the user to adjust the position and orientation of two images, e.g. of a lion on the left side and of a cage on the right side, until they are perceived binocularly (Georgievski, 1995) (Damanakis, 2005). The task for the subject is to "place" the lion inside the cage by manually adjusting the position of each handle on the synoptophore, in order to alter the orientation and

16 A haploscope, derived from the Greek words 'απλό' (haplo = simple) and '-σκόπιο → σκοπέω' (scope = target), is an optical instrument that presents a different image to each eye, so that the brain can fuse both images in a single perception (Phillips *et al.*, 2019). A stereoscope, for example, is a type of haploscope.

position of the corresponding image (Stidwill and Fletcher, 2010). The adjusted handles of the synoptophore indicate the angle of deviation (Sekeroğlu *et al.*, 2013) (Georgievski, 1995). In normal BSV, the lion appears to be in the cage. In strabismus, the two images are either not perceived simultaneously or the lion is position outside of its cage. A synoptophore is used to accurately measure horizontal, vertical and torsional strabismic deviations (Woo *et al.*, 2005) (A.B. Somani *et al.*, 1998). Ramey *et al.* (2008) describe the use of a haploscopic apparatus to measure the movement and position of the eyes under specified conditions of vergence, cover testing and head tilting. The apparatus consists of two cameras and an eye tracking software that adjusts the haploscope in all three axis of eye rotations. Irsch *et al.* (2008) increased the accuracy of the eye tracking method by attaching black dots with a white border to the inner canthi of the subject. More recent haploscopes are designed and built to utilize augmented reality, "which allows the viewing of virtual objects superimposed against the real world" (Phillips *et al.*, 2019).

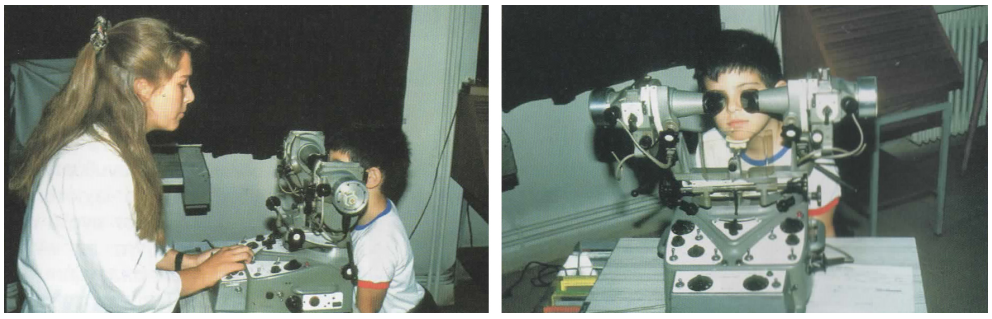

Figure 26: *Synoptophore (Damanakis, 2005): An example of a child using a synoptophore with professional supervision.*

- **Maddox Rod:** This test relies on a specially designed lens, called a Maddox lens, composed of "a series of parallel high power plano-convex cylinders that convert a point source of light into a line seen perpendicular to the axis of the cylinders" (Rowe, 2012). Due to the lens's composure, a Maddox lens is also referred to as Maddox rod. As shown in figure 27, a Maddox rod can be mounted on test-frame glasses or a hand frame (Yanoff and Duker, 2019). As the subject fixates on the light emitted by a pen torch, the Maddox rod is placed in front of either eye (Dolman, 1919). In normal binocular vision, the red line from the Maddox lens is perceived as going through the light; however in strabismus the line, from the Maddox lens, does not pass through the light (Benjamin and Borish, 2006). Horizontal deviations

are measured when the cylinders, in a Maddox lens, are oriented horizontally, thereby, forming a vertical line, and vertical deviations are measured when the cylinders are oriented vertically, forming a horizontal line (Nelson and Olitsky, 2014). Similar to the Prism Cover test, prisms are used to measure the angle of deviation and the Maddox rod test is repeated (Agrawal, 2019). The Maddox rod test can also be used to diagnose torsional strabismus by using two Maddox lenses, also referred to as Double Maddox Rod test, one red and one white with parallel cylinders (Brodsky, 2016). If torsional strabismus is present, the red and white lines will not be perceived in parallel (Kowal and Georgievski, 1996).

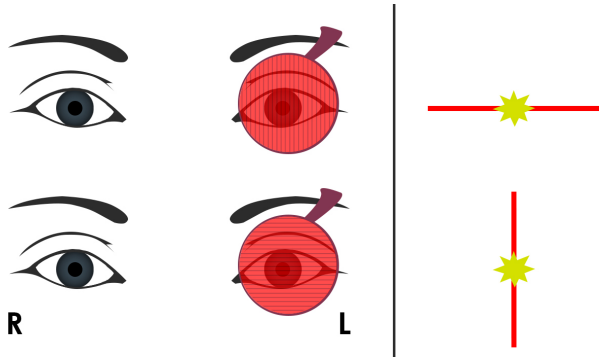

Figure 27: *Maddox rod: An example where the left eye is views a fixation target through a Maddox rod hand frame. The figure illustrates two cases in which the cylindrical strips are oriented vertically, therefore the line perceived is horizontal, and then horizontally, therefore the line perceived is vertical. The right part of the figure shows what is perceived in each case.*

- **Maddox Wing:** A device used to measure heterophorias and small heterotropias at near that consists of two slit apertures, one for each eye (fig. 28) (Pointer, 2005). The Maddox wing device has a split view, in which one eye views a horizontal and vertical graph of numbers that represent prism dioptres, and the other eye views two arrows, a white arrow pointing upwards and a red arrow pointing to left (fig. 28) (Salmon, 2019). When a person uses the Maddox wing device, the two retinal images formed are different, indicating the absence of fusion and the complete dissociation of both eyes (Kowal and Georgievski, 1996). The arrows seen by one eye point to the numbers seen by the other eye, which represent the horizontal and vertical components of the deviation (Ansons and Davis, 2014). Similar to a Maddox rod test, a Maddox wing test is used to determine horizontal, vertical and torsional strabismic deviations (Pointer, 2005). Torsional strabismus is identified when the arrow pointing upwards, viewed in one side, is

not parallel to the vertical scale, viewed on the other side (Kowal and Georgievski, 1996).

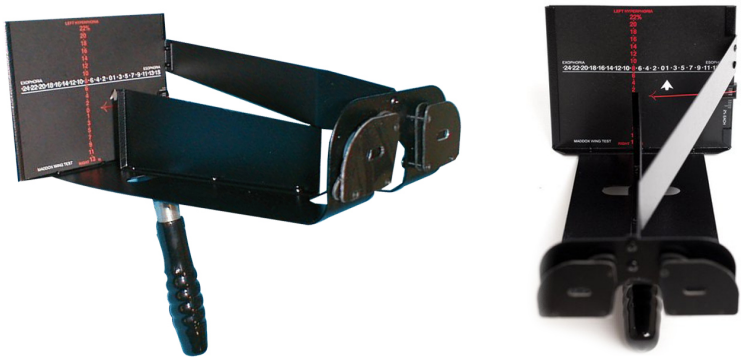

Figure 28: *Maddox wing (MediSense, 2018): A hand held device consisting of a septum and two split apertures. The numbers, pointed to by the arrows of the device, represent the vertical and horizontal components of a deviation.*

- **Hess and Lees' Charts:** A Hess chart is one of the most accurate methods of diagnosing diplopia, incomitant strabismus and torsional deviations (Sekeroğlu *et al.*, 2013) (Hammond, 2014). This method, not only assists in the identification of the paretic muscle but also, estimates the magnitude of the paresis (Thorisdottir *et al.*, 2018). During a Hess chart (Hess screen) test, a subject is required to wear a pair of dichromatic glasses (red and green), which dissociate the eyes, and fixate on a screen containing a pattern of red dots used as targets (Roper-Hall, 2006). The subject uses a pen torch that projects a green light and tries to aim the green light at the red lit targets (Traboulsi and Utz, 2016). In cases of strabismus, the subject is not able to accurately aim the green pen torch on the red target (Agrawal, 2019). Contrary to a Hess chart, a Lees' chart (Lees' screen, fig. 29) "consists of two opalescent screens placed at 90° to each other and a two-sided mirror septum at 45° to the screens, which dissociates the visual fields" (Rowe, 2012). A Lees screen test is preferred in practise, as opposed to a Hess chart (Watts *et al.*, 2011), because it offers several advantages, including the lack of dichromatic glasses, thereby allowing the examiner to view the subject's eyes during the test (Timms, 2006).



Figure 29: *Lees' screen test (Ansons and Davis, 2014): A more optimal version of a Hess chart in which the right eye views a non-illuminated screen (B) and the left eye fixates on a dot (E) on the grid of the illuminated screen (A). Through the use of a plane mirror (C) and septum (D), the fixated dot from screen A is "projected" onto screen B, indicated by the position F. The examiner "illuminates screen B to note and record the position of the dot".*

- **Red Filter:** Like the Maddox rod, a red filter test is a diplopia type test that requires relatively high cooperation from a subject (Damanakis, 2005). According to Noorden and Campos (2002), "one determines the subjective localization of a single object point imaged on the fovea of the fixating eye and an extrafoveal retinal area in the other eye". As a subject fixates on a small light source (pen torch), a red filter is placed in front of the deviating eye (Yoo *et al.*, 2017). As illustrated in figure 30, a subject with strabismus views two coloured lights, red and white, and the position of the red light, in relation to the white light, determines the direction of the deviation (Wilson *et al.*, 2009). A red filter test is also used to test single vision due to fusion or suppression, as it is possible for a subject to perceive one light monocularly (Benjamin and Borish, 2006). Suppression is detected when the red filter is placed in front of the deviating eye but only a white light is perceived (Yoo *et al.*, 2017). Transferring the red filter in front of the fixating eye may work as an occluder, which would remove suppression (Cooper and Record, 1986). Additionally, prisms can be used to bring both lights one on top of the other and measure the angle of deviation (Goodman *et al.*, 2011). A red filter test is used to determine horizontal and vertical strabismic deviations, however this method cannot be used to measure torsion (Wilson *et al.*, 2009).

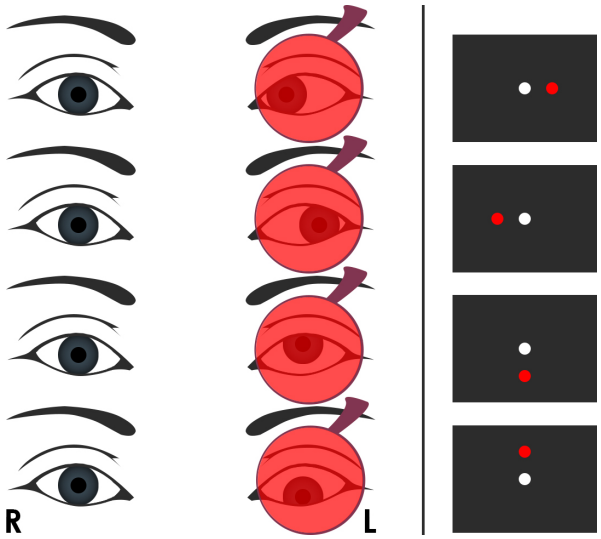

Figure 30: *Red filter test: Examples of the red filter test with various case of strabismic deviations. The right part of the figure shows what is perceived in each case.*

- **Sbisa Bar:** This test measures the grade of suppression by using a row of ($\approx$ 17) red filters, mounted on a bar at increasing density order, ranging from pale red to dark red (Crawford and Griffiths, 2015). The bar, referred to as sbisa bar, is placed in front of the dominant eye, which fixates on the light of a pen torch used as the fixation target (Ansons and Davis, 2014). The sbisa bar is moved vertically, by the ophthalmologist, until the normal eye is unable to see the target, and the deviated eye is forced to assume dominance (Stidwill and Fletcher, 2010). When dominance is assumed by the strabismic eye and the subject perceives a white light, the grade of the filter is noted as it represents the density of suppression (Crawford and Griffiths, 2015).

3.4.6 *Assessment of Binocular Vision*

A clinical investigation of BSV includes the assessment of the: (a) presence or absence of binocular vision, (b) grade of binocularity, (c) range of fusion, and (d) retinal correspondence (Brodsky, 2016) (Lueder, 2011).

The following methods are used to investigate binocular vision and differentiate between single vision due to fusion and single vision due to fusion suppression.

- **Bagolini Striated Glasses:** The Bagolini glasses, which are also used to detect ARC (see subsect. 3.2.4), consist of a pair of striated lenses that have no refractive power and only cause slight blurriness in vision (Schultinga *et al.*, 2013). In this test, a subject fixates on the light of a pen

torch, which is used as the fixation target, and a bright line is perceived, perpendicular to the striates of each lens (Stidwill and Fletcher, 2010). The biggest advantage of this method is that it doesn't dissociate the eyes, and therefore allows the position of either eye to be monitored by a cover test (Benjamin and Borish, 2006). Normal binocular vision, with central and peripheral fusion, is found to be present when the subject is able to perceive two lines that intersect the fixation light but a cover test does not reveal any deviation (fig. 31) (Nelson and Olitsky, 2014). A central scotoma along with peripheral fusion is found to exist when one line is seen to intersect the fixation light but the other is perceived with a central gap (Schultinga *et al.*, 2013). If only one line is perceived, central and peripheral fusion does not occur.

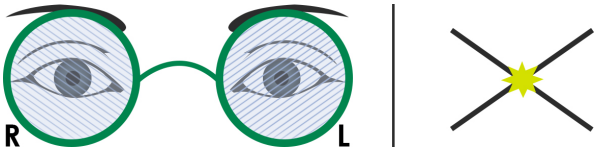

Figure 31: *Bagolini striated glasses: A pair of spectacles in which each lens is rotated opposite to the other (45° and 135°). The right part of the figure shows a light central to a cross, which is perceived under normal BSV.*

- **Worth's Four Lights:** This method is used to determine the presence of fusion, suppression and ARC (see subsect. 3.2.4). It consists of four coloured lights (one red, two green and one white) viewed through red and green filtered glasses that allow a person, with normal BSV, perceive four colours (one red, two green and one mixed of red and green) (fig. 32) (Roper-Hall, 2004). The size of the area of each retinal image that contain the visual stimuli from the four lights, depends on the distance of a subject from the lights (Frank *et al.*, 1981). If the subject is located near the four lights, the area, visually stimulated by the four lights, on both retinae increases (Traboulsi and Utz, 2016). In the presence of a central scotoma the subject is unable to perceive the four lights, therefore, the subject is placed closer to the four lights so that the lights can be perceived by the peripheral vision (Roper-Hall, 2004). Normal binocular vision, with central and peripheral fusion, is noted to exist when the subject is able to perceive the four lights and a cover test does not reveal any deviation (Salmon, 2019). Suppression is detected when two red or three green lights are perceived (Frank *et al.*, 1981). However, peripheral fusion occurs when the subject is able to perceive all four colours when moving closer to the lights. Diplopia is diagnosed when five lights are perceived (Roper-Hall, 2004).

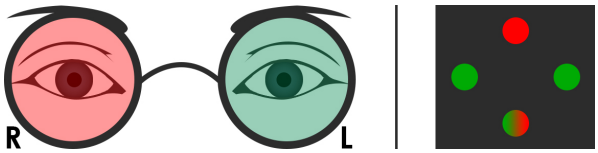

Figure 32: *Worth's four lights: Consists of four lights (one white, one red and two green) that are viewed through red and green filtered glasses. Under normal BSV, four lights are perceived the white is perceived mixed coloured of red and green.*

- **Polaroid Four-Dot:** This test is very similar to Worth's four lights test with the only difference being that polarising glasses are worn in order to view four polarised lights. Also, the polaroid four-dot test is only used to assess central, i.e. bifoveal, fusion by placing the four polarized lights ≈ 6m away from a subject (Ansons and Davis, 2014). Consequently, the area of each retinal image, visually stimulated by the lights, decreases and the visual stimuli is focused on the fovea.

- **After-image:** In this test one of both eyes is exposed to a linear light filament that has been oriented horizontally, whilst the other eye is covered (Porter, 1979). Next, the other eye is exposed to the light filament, oriented vertically, whilst the first eye is covered (Billson, 2003). Each eye is exposed for approximately ten seconds, thereby imprinting an after-image across both eyes (Porter, 1979). Primarily used for the assessment of retinal correspondence (see subsect. 3.2.4) in which, under normal BSV, the brain fuses both retinal images and forms the after-image perception of a cross (fig. 33) (Hansen, 1954). In strabismus, however, due to a deviation of the eye, the after-image cross is perceived as displaced (Wright *et al.*, 2006). The amount of displacement depends on the angle and direction of a deviation (Noorden and Campos, 2002).



Figure 33: *After-image: An example of the after-image effect showing the cross perceived under normal BSV, esotropia and exotropia. Each eye is stimulated separately by a different angled linear strobe light (horizontal or vertical), producing an after-image effect.*

- **Prism Adaptation:** In addition to assessing binocular vision, this test measures the true angle of a deviation in types of strabismus where the

deviation is not always present or regulated by fusion (Ohtsuki *et al.*, 2001). This test is also used to determine whether ARC is present. In this test, the "angle of deviation is overcorrected by $5-10$ prism dioptres with fresnel prisms ... observed after a period of at least 24 hours" (Rowe, 2012). Binocular vision is confirmed if the eyes are found to have maintained a straight position (Kiyak Yilmaz *et al.*, 2015). However, if both eyes remain in the over-corrected position, normal BSV is absent (Matsuo *et al.*, 2010). The prism adaptation test is performed prior to surgical treatment, as "preoperative prism correction allows a more accurate determination of the amount of surgery, prevents the risk of undue overcorrection and promotes the development of binocularity" (Kiyak Yilmaz *et al.*, 2015).

- **Prism Reflex:** This is essentially Krimsky's diagnostic test (see subsect. 3.4.5), which is also used to "determine the presence of motor fusion and to prove the presence of BSV" (Ansons and Davis, 2014). Whist a subject fixates on a target, a 20Δ or 15Δ base-out prism is placed in front of either eye, which causes the visual stimuli derived from the target to shift away from the fovea and, therefore, stimulate a peripheral point on the retina (Noorden and Campos, 2002). In normal BSV, the eye behind the prism performs a compensatory movement in order to bring the fovea to the point where the visual stimuli, derived from the desired target, stimulates the retina (Salmon, 2019). However, due to Hering's law, the other eye will perform a conjugate rotation causing diplopia (Westheimer, 2014). Diplopia is eliminated and normal BSV is restored when the eye that performed the conjugate rotation moves back to its original position, thereby, allowing the visual stimuli, derived from the target, to stimulate the fovea (Wright *et al.*, 2006). When the prism is placed in front of the fixating eye, the deviated eye does not return to its original position, as the diplopia elicited from the conjugate movement is eliminated by suppression (Cooper and Record, 1986). Furthermore, if the prism is placed in front of the deviated eye, no compensatory movement will take place, because the eye is not dominant and the shifted visual stimuli is suppressed.

- **The 4Δ Prism:** The principle of this test is very similar to a prism reflex test with the only difference being that a 4Δ prism is used because it "keeps the image within the central retinal area and elicits the smallest movement" (Ansons and Davis, 2014). Due to the low refractive power of the prism, base-out, base-up and base-down prisms can also be used (Yekta *et al.*, 1989). The side of a prism's base determines the

direction of the shift applied to the visual stimuli deriving from the target (Damanakis, 2011).

- **Prism Fusion Amplitude:** A prism fusion amplitude test relies on the normal function of motor fusion, described in a prism reflex test, in order to assess the maximum ranges of fusion (Lambooij *et al.*, 2010). Horizontal fusional ranges are tested using base-out and base-in prisms, whereas vertical fusional ranges are tested using base-up and base-down prisms (Aziz *et al.*, 2006). For instance, the "strongest base-out prism through which binocular single vision can be maintained marks the limit of ... convergent fusion range" (Rowe, 2012).

- **Synoptophore:** This is the most reliable and accurate method of determining BSV or the presence of strabismus and ARC (see subsect. 3.4.5) by presenting two images to the subject, one on either side of the synoptophore (Damanakis, 2005). In normal BSV, the brain is able to superimpose and fuse both images into a single perception. Furthermore, the synoptophore is able to determine whether motion fusion and fusional amplitudes are achieved, including horizontal, vertical and torsional ranges (A.B. Somani *et al.*, 1998).

- **Controlled Binocular Acuity (CBA):** A CBA test, which was previously referred to as Binocular Visual Acuity (BVA) test, assesses the maximum visual acuity measured while maintaining BSV (Ansons and Davis, 2014). CBA is tested similarly to a monocular visual acuity test, i.e. using a chart of optotypes that displays rows of letters or numbers in decreasing size order (Agrawal, 2019) (Walsh *et al.*, 2000). A subject is required to read each line, whilst maintaining BSV. The test is repeated for near and far distances in order to detect any latent deviations (Ahn *et al.*, 2012). Other CBA tests, such as a bar reading test, are able to determine binocular visual acuity and provide further measurements for shorter reading distances (Lambert and Lyons, 2017).

3.4.7 *Assessment of Stereoscopic Vision*

Previously it was mentioned that, in normal BSV, visual stimuli derived from objects located inside Panum's fusional area, including the horopter, stimulate corresponding retinal areas in both eyes. The smallest binocular disparity that allows both retinal images to be fused, into a three dimensional perception, determines a person's stereoscopic visual acuity, also referred to as stereoacuity (Deepa *et al.*, 2019) (Stidwill and Fletcher, 2010).

Stereoacuity is measured in seconds of arc (sec/arc), where, as the grade of stereoacuity increases as the sec/arc value decreases (McKee, 1983) (Ancona *et al.*, 2014). In ophthalmology, a stereoacuity value of $\leqslant 40 sec/arc$ suggests normal bifoveal vision (Rowe, 2012). Stereoacuity is divided into two categories (Giaschi *et al.*, 2013):

- **Coarse:** Also referred to as gross stereopsis, determines the ability to perceive depth in peripheral vision.
- **Fine:** Determines the ability to perceive depth in central vision.

The following methods assess stereoscopic vision at various grades:

- **Lang's Two-Pencil:** A very simple, yet satisfactory, method used to crudely detect stereopsis (Sharma *et al.*, 2017). In Lang's two-pencil test, the examiner holds a pencil directed straight upward, and the subject holds another pencil directed straight downward (Nongpiur and Sharma, 2010). As shown in figure 34, the subject is asked to place the tip of the pencil onto the tip of the pencil held by the examiner (Mojon, 2009). If the subject is able to pass the test, stereopsis is present (Pugesgaard *et al.*, 1987). This test is repeated until a verdict can be reached about the presence and grade of stereopsis (Lambert and Lyons, 2017). Strabismus subjects may also undergo this test, or a cover two pencil test (CTPT), in order to determine the presence of ARC (Mojon, 2009). The test is repeated, first, with both eyes open and, further, with the deviating eye occluded (fig. 34) (Damanakis, 2005). ARC is present when the subject is able to place the tip of the pencil on the tip of the pencil held by the examiner, suggesting that the deviating eye contributes towards binocular vision (Pugesgaard *et al.*, 1987) (Nongpiur and Sharma, 2010). The integrity of this test depends on the environment at which it is performed, because monocular cues may assist a subject, with strabismus, to pass the test.



Figure 34: *Lang's Two-Pencil (Damanakis, 2005): An example of the two pencil test. On the left part of the figure a subject fails to place the tip of a pencil on the tip of another pencil held by an examiner, as his one eye is covered. On the right part, with both eyes open, the subject successfully passes the test.*

- **Synoptophore:** A synoptophore (see subsect. 3.4.6) can be used to assess stereopsis using stereoscopic images. A stereoscopic image consists of a pair of superimposed two-dimensional images depicting the same object from slightly different angled views, thereby, imitating normal binocular disparity (Jones *et al.*, 2001). When viewed stereoscopically, a three dimensional illusion of the embedded object is perceived. The perception of a three dimensional illusion, using a synoptophore, is accomplished by the dissociation of both eyes (Godts *et al.*, 2006), such that each eye is presented with either part of the stereoscopic image (A.B. Somani *et al.*, 1998).

- **Autostereogram:** This is a type of stereoscopic image that does not require the dissociation of both eyes, in order to perceive an underlying three-dimensional illusion (fig. 35) (Kolb *et al.*, 2020) (McKee *et al.*, 2007). Autostereograms portray patterns that embed arbitrary shapes, which allow the perception of a three dimensional illusion when viewed stereoscopically and by applying the correct amount of vergence between both eyes (Kimmel, 2002) (Noorden and Campos, 2002). The simplest form of an autostereogram, known as wallpaper effect, was developed by David Brewster in 1844 (McKee *et al.*, 2007). In a wallpaper effect, any "horizontally repeating pattern ... may be viewed with the eyes converged (or diverged, if the repetition angle is sufficiently small) so that a given repetition cycle in one eye is in correspondence with the adjacent repetition cycle in the other eye" (Tyler and Clarke, 1990). One of the methods used to perceive the illusion hidden within an autostereogram is by relaxing both eyes until they are parallel, as if looking far into distance through the image, and slowly moving back from the image until the illusion is perceived.

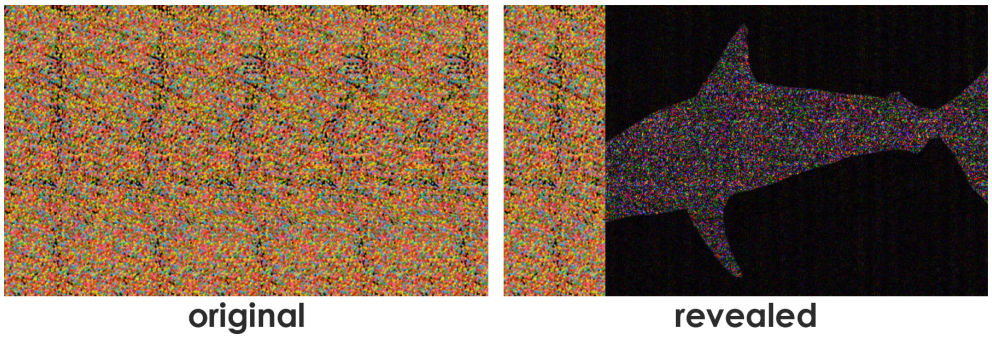

Figure 35: *Autostereogram (contributors, 2021): An example in which a shark is revealed when the original image is perceived binocularly. The technique to view such images is to relax both eyes as if fixating on a far object, "through" the image. The right part of this figure shows the outline of a shark.*

- **Randot:** Similar to an autostereogram, a random dot (randot) stereogram (see subsect. 2.5.3) is composed of a pair of stereo-images that allow stereopsis to be achieved, without relying on familiarity cues (Julesz, 1964) (Cooper, 2007). A randot stereogram embeds randomly placed dots, or other small shapes, that are similar in the areas, of the image, that correspond to the "hidden" illusion (Carvelho *et al.*, 2008) (Parker, 2009). Stereopsis is achieved when the three dimensional illusion of the "hidden" shape is perceived (Wong, 2004) (Georgievski *et al.*, 2007). This test can only be passed by subjects who possess BSV, because the random dots prevent the perception of the "hidden" shape through monocular vision (Ancona *et al.*, 2014) (Nelson and Olitsky, 2014). Strabismus subjects may also undergo this test in order to determine the presence of ARC (Wong *et al.*, 2000).

- **TNO:** TNO stands for Toegepast Natuurwetenschappelijk Onderzoek, which is the Netherlands organisation for applied scientific research (Walraven, 1975). A TNO image is a type of randot that portrays randomly placed red and green dots (Ancona *et al.*, 2014), "devoid of any monocular clues, and the stereoscopic figures of the test can be visible only in depth" (Walraven, 1975) (fig. 36). In this test, a TNO image is placed $\approx$ 40cm from a subject, wearing a pair of coloured (red and green) glasses, that allow the three dimensional illusion to be perceived (Zhao and Wu, 2019). According to Damanakis (2005) and Ansons and Davis (2014), this type of test measures stereoacuities of $1980 - 15 sec/arc$ with finer grades in the range of $480 - 15 sec/arc$.



Figure 36: *TNO (Optician, 2017): A TNO test in which red and green filter glasses are used in order to perceive the red-green random dot stereogram.*

- **Lang Stereo-image:** This test applies to young children and adults and is designed to detect early problems in stereoscopic vision (Huynh *et al.*, 2005). A Lang stereo test is another type of randot autostere-

ogram in which a lenticular image, composed of a series of cylindrical strips vertically parallel to one another, is used to separate two images, each consisting of random dots (fig. 37) (Brown *et al.*, 2001). When viewed stereoscopically from a distance of 40cm, such that each eye views one side of the lenticular image, the "hidden" shape is perceived (Rechichi *et al.*, 2017). An advantage of this test, compared to a TNO test, is that a subject does not need to wear special glasses, because the IPD between both eyes constrains the view of each eye to the corresponding side of the lenticular image (Huynh *et al.*, 2005). There are two types of Lang stereo tests designed to deduce different grades of stereoacuity. The first test, called Lang I, measures stereoacuity between $1200 - 600 sec/arc$, which represents very crude stereopsis, whereas the second test, called Lang II, measures stereoacuity between $600 - 200 sec/arc$, which represents finer stereopsis (Salmon, 2019) (Rechichi *et al.*, 2017).



Figure 37: *Lang stereo image (Optician, 2017): The right part of the figure shows the structure of a lenticular stereo image and how each eye is able to view at different sides of the cylinders.*

- **Frisby Near Stereo-test (FNS):** The FNS test requires three transparent plates of different thicknesses (6mm, 3mm, 1.5mm), where each plate consists of four quadrants and each quadrant portrays a cluster of randomly arranged arrowheads, or boids, of various sizes (fig. 38) (Benjamin and Borish, 2006). The central boids, in one of the four quadrants, are printed on one side of the plate, whereas the peripheral boids of the quadrant, including the boids in the remaining quadrants, are printed on both sides of the plate (Zhao and Wu, 2019). A subject with normal BSV is able to identify which quadrant contains the central boids that are printed on one side, as they appear to stand out or recede from the remaining boids (fig. 38) (Garnham and Sloper, 2006). A disadvantage of this test is that familiarity cues, including motion parallax, can reveal the correct quadrant and a subject with strabismus may pass the test. The FNS test measures stereoacuity between $600 - 5 sec/arc$,

which represents ranges of medium to high quality of stereopsis (Bohr and Read, 2013).

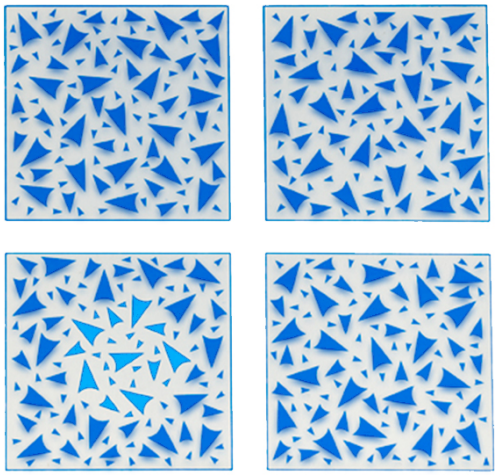

Figure 38: *Frisby Near Stereo-test (FNS): An example of FNS where, under binocular vision, the central boids of the bottom left quadrant recede from the remaining boids.*

- **Frisby Davis Distance (FD2):** A very similar test to FNS, but designed to assess stereoacuity from a relatively far distance (Nongpiur and Sharma, 2010) (Agrawal, 2019). As shown in figure 39, four shapes "are mounted on rods that can be set to protrude from the background" (Ansons and Davis, 2014). One shape is randomly selected and moved slightly forward from the remaining shapes (fig. 39) (Garnham and Sloper, 2006). A subject is asked to identify which of the four shapes is protruded from the others (Bohr and Read, 2013). The FD2 test measures stereoacuity between $50 - 5sec/arc$, "with normal adults reaching an average of 10 seconds of arc" (Ansons and Davis, 2014).

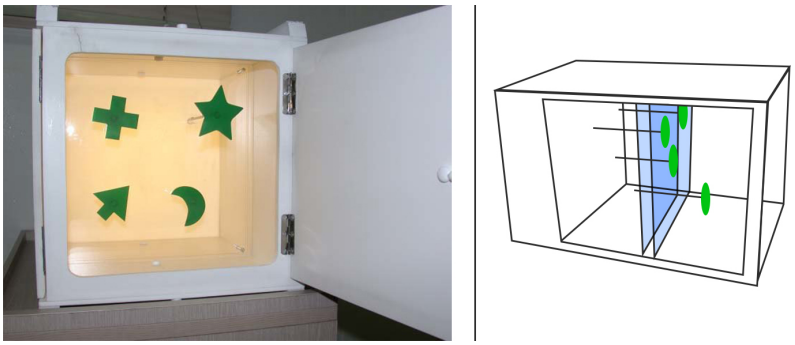

Figure 39: *Frisby Davis Distance (FD2): An example of FD2 in which the star shape, at the top right of the left part of the figure, is slightly pushed out. The right part of this figure shows a different case of an FD2 test from a side view, where the bottom left shape is pushed outwards.*

- **Wirt and Titmus:** In these tests polarising filter glasses are worn in order to view a set of stereoscopic images (Ancona *et al.*, 2014). According to Garnham and Sloper (2006), a Titmus/Wirt test "uses black, contoured stimuli, with polaroid glasses to separate the stimuli presented to each eye". Each anaglyph is composed of two superimposed polarising images, which create the illusion of depth when viewed through polarizing glasses (Guo *et al.*, 2016). As shown in figure 40, a Wirt and Titmus stereo test includes: (a) an image of a fly, which represents stereoacuity of 3000sec/arc (Wong *et al.*, 2000) (Wong *et al.*, 2000) (Tomaç *et al.*, 2002), (b) three rows of animal images, which represent stereoacuities of 400, 200 and 100sec/arc (Traboulsi and Utz, 2016) (Noorden and Campos, 2002), and (c) nine diamond shapes containing four circles each, which represent stereoacuities of $400 - 40$sec/arc (Zhao and Wu, 2019). A subject is instructed to wear the polarizing glasses, while viewing each stereo image, and report the perception of depth formed by the three dimensional illusions (Ancona *et al.*, 2014). For instance, gross "stereopsis is demonstrated if the wings of the fly are perceived as standing out from the body of the fly" (Rowe, 2012). However, Wilson *et al.* (2009) warn that isolating pure disparity sensitivity is a very difficult task and, most tests including a Frisby test, may return false-positive results due to monocular familiarity cues revealing depth. Also, Wilson *et al.* (2009) noted that the "Titmus stereotest is probably the most well-known example of a stereotest flawed by these artefacts. A stereoblind patient may demonstrate deceptively good stereoacuity due to the nonstereoscopic, image displacement cues".



Figure 40: *Wirt and Titmus: The booklet consists of three stereoscopic tests employing polarised stereo images. The fly graphically demonstrates the presence of stereo vision, whereas the other two tests estimate the grade of stereoscopic vision.*

- **Anaglyph:** A type of stereogram that portrays a scene using a pair of superimposed images (Wright *et al.*, 2006). The images are composed

of polarizing or opposite coloured (red-blue) filters (fig. 41) (Benjamin and Borish, 2006). The three dimensional illusion is perceived by viewing the stereo image through appropriate filter glasses.

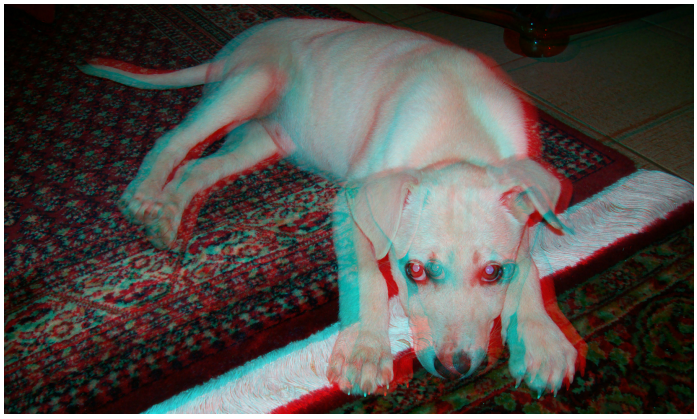

Figure 41: *Anaglyph: An example of a 3D anaglyph image depicting Mirto (the puppy). A pair of red/cyan 3D glasses are required in order to perceive the three dimensional illusion of this figure.*

- **Randot Distance:** This test combines the use of polarising filter glasses and randot autostereograms in order to assess stereoacuity for distance ($\approx$ 3m) (Ahn *et al.*, 2012). Similarly to a randot test, a subject is required to identify the three dimensional illusion of a "hidden" shape (Wang *et al.*, 2010). A randot distance stereo test measures stereoacuity between $480 - 60 \text{sec/arc}$. Other similar methods, including a randot preschool test, are used to determine stereoacuity of $800 - 40 \text{sec/arc}$ in children (Holmes *et al.*, 2011) (Wang *et al.*, 2010).

3.5 MANAGEMENT AND TREATMENT OF STRABISMUS

The appropriate management and treatment of strabismus depends upon the classification, time of onset, aetiology and unique features of a deviation (Traboulsi and Utz, 2016). Of particular importance is the age of an individual undergoing therapy, as some therapeutic methods have been shown to cause more complications to adults than children (Bui Quoc and Milleret, 2014) (Beauchamp *et al.*, 2003) (Rowe, 2012). For instance, in strabismic conditions where binocular vision is present, e.g. convergence insufficiency (CI), treatment can take place at any age without the risk of permanent and persistent diplopia. However, where suppression is present, e.g. constant exotropia, subjects can undergo therapy until the end of the critical period. This is because, in the event of diplopia, the brain of a child is capable of suppressing the confusing retinal image, whereas, the brain of an adult can-

not suppress, causing permanent and persistent diplopia. Ophthalmologists agree that, whether congenital or acquired, strabismus is most effectively managed when diagnosed in the early stages of its development (Damanakis, 2013) (Hammond, 2014) (Nelson and Olitsky, 2014). Depending on the type of strabismus and age of a subject, current treatments aim to (Ansons and Davis, 2014) (Lueder, 2011):

- overcome suppression
- extend fusion amplitudes
- restore BSV, with prospects of stereopsis
- improve aesthetic appearance
- relieve symptoms, including CHP, diplopia, headaches and nausea
- improve visual acuity
- reduce a deviation to within 10Δ, especially in primary gaze
- accomplish orthotropia

Some forms of strabismus may disappear with time or when the source, causing a deviation, is treated, e.g. restricted eye movement and double vision from injury (Noorden and Campos, 2002) (Kapoor *et al.*, 2004). All other forms must be managed, with care, by a professional strabismologist (Rutstein *et al.*, 2011). Management and treatment methods are divided into two categories, namely, non-surgical and surgical. Non-surgical treatment methods include the prescription of corrective lenses or other types of glasses, use of pharmacological substances and orthoptic exercises (Agrawal, 2019). Surgery, followed by other forms of non-surgical treatment, is required when the angle of deviation is $\geqslant 20\Delta$ (Ansons and Davis, 2014).

3.5.1 *Non-Surgical*

Non-surgical methods are categorized into: (a) optical treatments, (b) pharmacological treatments, and (c) orthoptic exercises (vision therapy) (Wilson *et al.*, 2009) (Billson, 2003).

3.5.1.1 *Optical Treatment*

Optical treatments, including the occlusion of the normal eye using a patch, wearing prismatic glasses, bifocals or corrective lenses, are used in order to improve visual acuity, alignment and coordination of both eyes without the need to intervene at the muscles of the strabismic eye.

OCCLUSION Occluding the normal eye forces the strabismic eye to assume dominance and resume fixation (Cooper and Jamal, 2012). During the critical period, the purpose of occlusion is to convert unilateral strabismus into alternating strabismus, thereby training a subject to fixate using either eye. In older ages, occlusion is used to improve visual acuity of the deviating eye (Tychsen, 2005). This is one of the oldest, but most effective, methods of treating amblyopia (Sharma *et al.*, 2017). There are two grades to occlusion, full and partial, and depending on the length of time the normal eye is occluded, occlusion is also categorized as either full-time or part-time (Nelson, 2019). Full occlusion prevents light from entering the normal eye, whereas, partial occlusion reduces visual acuity whilst light enters the eye (Damanakis, 2005). A sticky eye patch (opticlude) placed over the dominant ("good") eye is considered full occlusion as it forces a subject to fixate using the strabismic ("bad") eye (fig. 42) (Helveston, 2010). The administration of Atropine drops is considered partial occlusion, because it blurs vision of the normal eye (Rashad, 2012) (Osborne *et al.*, 2018).

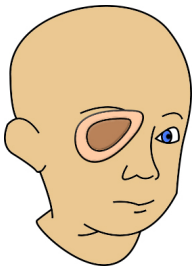

Figure 42: *Occlusion: The sticky patch is placed in front of the normal eye forcing the subject to see with the strabismic eye.*

Previously, it was mentioned that an adaptation to strabismus is suppression (see subsect. 3.2.3), which reduces visual acuity. Noorden and Campos (2002) and Bui Quoc and Milleret (2014) note that extreme cases of reduced VA may result in blindness and that the use of occlusion is recommended to children, adults and the elderly, in order to improve visual acuity and eliminate suppression. Other conditions that are managed by occlusion include:

- **Microtropia:** A subject may also benefit from occlusion because it not only improves the visual acuity of the deviating eye but also improves stereoscopic vision (Ibironke, 2011).
- **Intermittent Strabismus:** Occlusion of the normal eye assists in the prevention of suppression by the strabismic eye, which aids in strengthening of fusion and, therefore, proper alignment of the eyes (Nelson and Olitsky, 2014).

- **Paralytic Strabismus:** When prismatic glasses are not able to alleviate diplopia, occlusion is considered to be the next best option to alleviate diplopia until managed by a pharmacological treatment or surgery (Prasad and Volpe, 2010).

CORRECTIVE AND BIFOCAL LENSES Conditions caused by refractive errors, including hypermetropia and myopia, are primarily treated with corrective glasses or contact lenses (Issaho *et al.*, 2017) (Godts *et al.*, 2006). Depending on the condition, plus (convex) or minus (concave) lenses are prescribed, which either converge or diverge light (fig. 43) (Malacara-Hernandez and Malacara-Hernandez, 2017) (Damanakis, 2011).

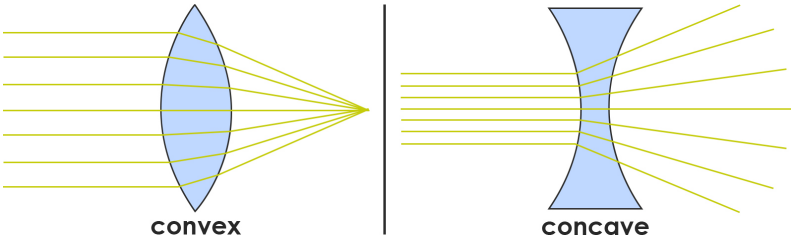

Figure 43: *Corrective lenses: Types of lenses that are used to converge or diverge light. A convex lens (left part of the figure) is used to converge light, whereas, a concave lens (right part of the figure) is used to diverge light.*

Refractive errors affect accommodation and may elicit accommodative strabismus. Fully accommodative strabismus, with normal AC/A ratio, suggests the presence of hypermetropia. When the appropriate lenses are used, which treat hypermetropia, the deviation is reduced (Rutstein, 2008). Partially accommodative strabismus, with normal AC/A ratio, is only partially treated with corrective lenses, because the deviating eye continues to suppress the visual stimuli it receives (Mulvihill *et al.*, 2000). Therefore, further treatment with prismatic glasses, occlusion and surgery is required (Vivian *et al.*, 2002). Contrary to normal AC/A ratio, in fully or partially accommodative strabismus with high AC/A ratio, a deviation can be majorly affected by even the slightest amount of hypermetropia (Benjamin and Borish, 2006). However, even when the underlying refractive error is treated using corrective lenses, the deviation continues to persist (Lambert and Lyons, 2017). Treatments of accommodative strabismus with high AC/A ratio include the use of bifocals or surgery.

A bifocal lens (fig. 44) consists of two segments with two different prescriptions, such as the accommodation of far and near vision (Snell and Lemp, 2013). The segments are laid out such that the top part is used for far vision and the bottom part for near vision (Yanoff and Duker, 2019). The bottom segments are also used to eliminate excessive accommodation,

consequently reducing the previously elicited strabismic deviation (Rutstein, 2008). Unfortunately, bifocals are required to be worn constantly, which is not only aesthetically displeasing but may also cause other problems including the adoption of CHP, due to the preference of using the top segments of the bifocal glasses (Traboulsi and Utz, 2016) (Lembo *et al.*, 2019).

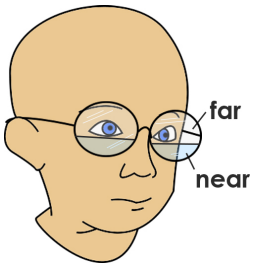

Figure 44: *Bifocal lens: An example of a pair of bifocals where the bottom part of each lens is used for accommodating on near targets, whereas the top part on far targets.*

Similar to hypermetropia or myopia, conditions such as anisometropia and astigmatism, which are also treated using corrective or bifocal lenses, affect a subject's VA and prevent the development of normal BSV (Rowe, 2012). In other conditions, including micro strabismus and pathological nystagmus, corrective lenses are used to eliminate any underlying refractive error in order to improve visual acuity and reduce the angle of deviation (Houston *et al.*, 1998) (J., 2017).

PRISMATIC GLASSES A prismatic lens, which is composed of one or more layers of prisms (fig. 45), is used to refract light in order to compensate for strabismic deviations of small amplitude (Traboulsi and Utz, 2016). The angle of deviation is used to prescribe the appropriate amount of prism refraction required so that both eyes could receive visual stimuli from the same fixation target (Agrawal, 2019). Prismatic glasses are mostly used in cases of Diplopia and are considered to be "a passive, compensatory treatment rather than an active treatment approach designed to remediate the condition" (Scheiman *et al.*, 2005).

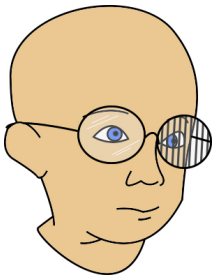

Figure 45: *Prism glasses: An example of Fresnel prism glasses.*

Depending on the direction of a strabismic deviation, prisms can be fitted horizontally, vertically or diagonally (Nelson, 2019). However, prismatic glasses are not viable for most types of strabismus, because it is not possible to compensate for large angles of deviation or variable strabismus (Damanakis, 2005). Rutstein *et al.* (2011) explains that prisms "are generally prescribed for patients with strabismic deviations of less than 20 PD who are capable of fusion". Furthermore, prism prescriptions are not stable and may change depending on the state of a deviation (Ansons and Davis, 2014). Lavrich (2010) and Cooper and Duckman (1978) assert that the effectiveness of prism glasses is no greater than common training or placebo reading glasses. Nevertheless, conditions that are commonly managed with prismatic glasses include:

- **Partially Accommodative Strabismus:** With normal AC/A ratio, corrective lenses are used to treat the underlying hypermetropia and base-out prisms are used to manage the remaining eso deviation. For this purpose, Fresnel stick-on prisms are fitted to the prescribed corrective glasses, which should be worn constantly (Benjamin and Borish, 2006).

- **Phoria:** Generally, phoria is treated by orthoptic exercises but if symptoms such as double vision, nausea, headaches and confusion persist, prism glasses can be used to alleviate these symptoms (Danchaivijitr and Kennard, 2004). In the elderly where symptoms of double vision occur alongside presbyopia, prisms can be fitted in their presbyopic glasses to eliminate diplopia (Charman, 2008) (Cooper and Jamal, 2012).

- **Comitant Strabismus:** Because the angle of deviation is equal in all directions of gaze, regardless of which eye assumes dominance, Fresnel prisms can be used to reduce the deviation (Oystreck and Lyons, 2012).

- **Convergence Insufficiency (CI):** Although orthoptic exercises are recommended for CI, occasionally they are insufficient. In such cases, base-in prismatic glasses are used to assist with convergence (Lavrich, 2010).

- **Paralytic Strabismus:** Occasionally, prisms are used to manage paralytic deviations in order to alleviate symptoms to diplopia (Jivraj and Patel, 2015). However, prisms cannot compensate for the variability of a paralytic deviation or the cyclo deviation if present.

3.5.1.2 *Pharmacological Treatment*

Pharmacological treatments, such as the administration of Levodopa and the use of Botulinum A toxin (Botox), have been employed in order to improve VA and reduce the amplitude of a deviation.

LEVODOPA The administration of Levodopa – "a catecholamine precursor used to treat adults with Parkinson's disease and children with dopamine-responsive dystonia" (Rashad, 2012), has shown to significantly improve visual acuity of subjects with amblyopia (Sharma *et al.*, 2017). According to Yanoff and Duker (2019), studies "have shown that low doses of levodopa, alone or together with carbidopa, have been shown to augment the effect of occlusion therapy, even in children over age 12 years". However, the use of occlusion in tandem to the administration of Levodopa does not further improve visual acuity or the increase the chances of eliminating amblyopia (Wright *et al.*, 2006). Kang *et al.* (2018) and Cooper and Jamal (2012) note that the administration of levodopa to subjects with CI and Parkinson's decease can reduce the symptoms of strabismus.

BOTULINUM TOXIN (BOTOX) Botox is a polypeptide of high toxicity, derived from the bacterium Clostridium botulinum, which can cause food poisoning and fatal paralysis of the muscles of the lungs (Brodsky, 2016). Yanoff and Duker (2019) explain that Botox "blocks the release of acetylcholine from motor neurons at the neuromuscular junction, producing temporary chemodenervation of muscles lasting upward of 3 months". Scott (1981), a pioneer in the treatment of strabismus using Botox, explained that injecting Botox type A into the extraocular muscles, of a subject with strabismus, causes temporary paralysis of the muscles, thereby, allowing the realignment of the deviated eye. When Botox is injected into the muscular tissue (fig. 46), it is instantly absorbed by the local nerve fibers, preventing the release of the toxin into the blood stream (Brodsky, 2016). However, long term use of Botox "does invariably cause atrophy of the muscle" (Scott, 1981).

Among other conditions, including "treatment of eyelid retraction in Graves' disease" (Traboulsi and Utz, 2016), Botox is currently used as alternative to muscle surgery in order to manage comitant and paralytic strabismus (Lueder, 2011). In comitant strabismus, the temporary paralysis of an extraocular muscle, of the strabismic eye, causes the injected muscle to relax, and stretch, whilst its antagonist contracts, and shrinks, resulting into an overcorrection in the orientation of the eye (fig. 46a) (Nelson and Olitsky, 2014). Due to the alteration in length of the extraocular muscles, when Botox

diffuses and the eye recovers from the toxin, it remains aligned (orthotropic) for some time before reassuming its deviation (fig. 46a) (Salmon, 2019). In paralytic deviations, injecting the antagonist of a paralytic muscle does not cause an overcorrection of the eye, but rather causes the eye to rest in the primary position (fig. 46b) (Damanakis, 2005). When Botox diffuses and the eye recovers from the toxin, the eye returns to its previous deviation (fig. 46b) (Ansons and Davis, 2014).

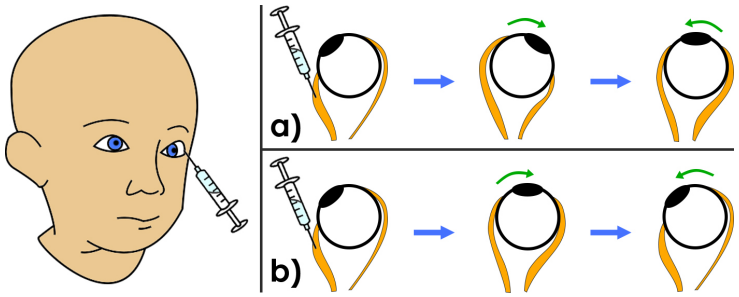

Figure 46: *Botox: Injection of Botox type A into the extraocular muscles of the strabismic eye. Part (a) of the figure shows an example of comitant strabismus and part (b) shows an example of paralytic strabismus.*

In practice, this treatment is primarily used for aesthetic reasons, as the small dosage of toxin does not last for long and the injection of Botox must be repeated (Hammond, 2014). Although several concerns have been expressed with regards to injecting Botox into children (Speeg-Schatz *et al.*, 2017), Botox has been used to treat infantile esotropia (Sharma *et al.*, 2017). Furthermore, regardless of the health risks and limitations of this treatment, Botox may ensure normal BSV when both eyes are in primary position, i.e. looking straight ahead, until a more permanent treatment is performed (Piña-Garza, 2013). Other conditions that are managed by Botox include:

- **Microtropia:** Microtropia and other small angle deviations may benefit from Botox as it has proven to achieve sufficient long term alignment of both eyes (Speeg-Schatz *et al.*, 2017).
- **Pathological Nystagmus:** Botox may be used to temporarily alleviate symptoms caused by nystagmus, including dizziness and reduced vision (Carruthers, 1995).

3.5.1.3 *Orthoptic Exercises*

Vision Therapy (VT) is a term used to describe a series of supervised orthoptic exercises that aim to overcome binocular vision disorders by: (a) improving coordination of both eyes, (b) enhancing stereopsis, and (c) reducing suppression (Rowe, 2012) (Wilson *et al.*, 2009). There are two categories

of VT, namely Home Based Vision Therapy (HBVT) and Office Based Vision Therapy (OBVT) (fig. 47) (Cooper, 2007). HBVT includes orthoptic exercises such as pencil push-ups and computer games that can be performed at home with minimal or no supervision (Scheiman *et al.*, 2005) (Carvelho *et al.*, 2008). OBVT includes orthoptic exercises such as the Brock string and stereo images that require supervision by orthoptists, or specially-trained technicians, and incorporate specialist equipment (Lavrich, 2010) (Cooper and Jamal, 2012). Generally, VT exercises are customized for each subject depending on factors such as the type of strabismus and the age of the subject (Rutstein, 2008).

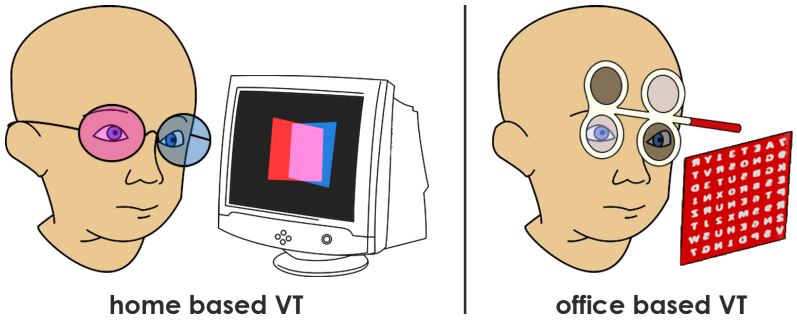

Figure 47: *Home and Office based vision therapy: The left part of the figure shows an example of HBVT using a computer program and red-blue filtered glasses. The right part of this figure shows an example of OBVT in which a subject undergoes treatment using a Hart chart (a matrix of letters on a piece of paper) and occlusion. Starting from a far distance and slowly moving closer, the subject is instructed to read the letters on the chart using either eye.*

Orthoptic exercises are a complementary rehabilitation treatment of strabismus most commonly used for intermittent deviations and phorias, which cause various symptoms, e.g. headaches, eye strains, fatigue and double vision (Aziz *et al.*, 2006) (Stidwill and Fletcher, 2010). Types of strabismus that can be managed by VT include:

- **Amblyopia:** VT complements the use of corrective lenses in order to improve visual acuity. Also, VT reduces the need for occlusion, hence improving a subject's appearance (Wright *et al.*, 2006).
- **Microtropia:** Often accompanied by anisometropia, which can be treated by corrective lenses or occlusion. VT can improve stereopsis, peripheral fusion and reduce suppression (Ibironke, 2011).
- **Convergence Insufficiency:** VT can help restore the ability of both eyes to converge on a target, usually at near (Near Point Convergence, NPC), and eliminates symptoms including diplopia (Lavrich, 2010). It has been reported that, for convergence insufficiency (CI), "VT is an effective form of therapy" (Adler, 2002).

- **Pathological Nystagmus:** Because nystagmus is an involuntary movement of the eyes, VT can be used to enhance visual acuity, reduced CHP and improve tracking of targets (J., 2017).

PENCIL PUSH-UPS This orthoptic exercise, also referred to as Near Point Convergence exercise, is one of the simplest exercises used to improve the coordination of both eyes (Momeni Moghaddam *et al.*, 2015). In pencil push-ups a subject is instructed to follow the tip of a pencil which is repeatedly moved close and then far (fig. 48) (Traboulsi and Utz, 2016).

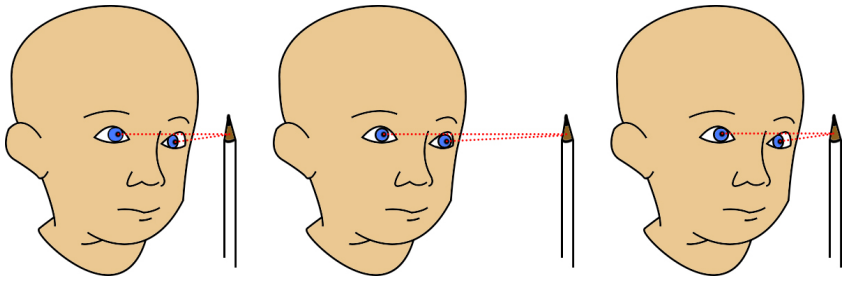

Figure 48: *Pencil push-ups: A pencil is held directly in front of the subject's eyes, at reading distance, and is moved back and forth. The task for the subject is to maintain convergence on the tip of the pencil at various distances.*

A common misconception is that pencil push-ups are intended to strengthen the muscles of a strabismic eye, so that it can align with the normal eye (Damanakis, 2013) (Hammond, 2014). Pencil push-ups, however, are intended to improve the communication between the brain and eyes, in order to improve the coordination of both eyes and develop normal BSV (Momeni Moghaddam *et al.*, 2015).

COMPUTERIZED VISION THERAPY Computerized Vision Therapy (CVT) uses a series of computer programs, typically computer games, to train the coordination of the eyes (Cooper, 2007). Carvelho *et al.* (2008) introduced a three dimensional version of the classic Pac-Man computer game, called Stereo Pac-Man, in which the main window of the game is split into two smaller windows (left and right, fig. 49) that are to be viewed via a customized stereoscope. The game was designed so that the top portion, of each sub-window, "consists of a random dot stereogram that contains a top-down view of the current maze", whereas the bottom portion "contains a three dimensional stereoscopic representation of the current maze" (fig. 49).

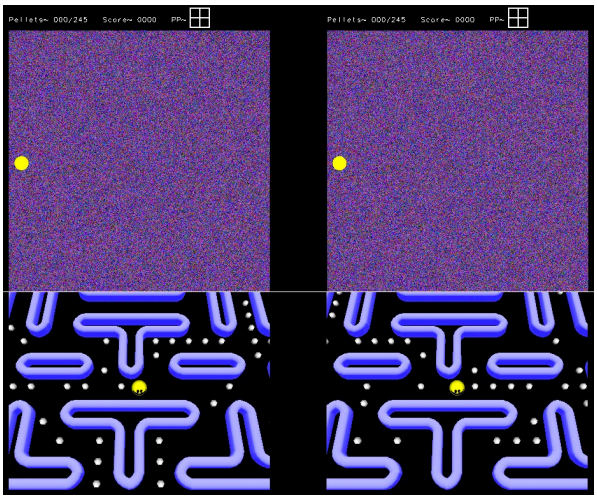

Figure 49: *Stereo Pac-Man (Carvelho et al., 2008): The top part of the game consists of a random dot stereogram, whereas the bottom part a 3D stereoscopic view of the maze. A stereoscope is needed to go through this treatment.*

Lavrich (2010) and Cooper (1988) assert that, compared to other HBVT and OBVT exercises, CVT improves the effectiveness and reliability of treatment because it enhances the motivation of a subject to undergo therapy. According to Cooper (2007), computerization "improves ... motivation, eliminates experimental bias, simplifies therapy goals, provides immediate reinforcement to encourage correct responding, and provides meaningful data to evaluate progress".

BROCK STRING A Brock string is an orthoptic exercise used to improve coordination of both eyes during convergence (Wilson *et al.*, 2009). In this exercise, three or more coloured beads are evenly spaced at various lengths on a ($\approx 3-5$m) string (fig. 50) (Scheiman *et al.*, 2005). A subject is instructed to fixate on each bead separately, whilst holding one end of the string near the nose (Nehad *et al.*, 2018). The other end of the string is placed further away from the subject so that the beads form a straight line.

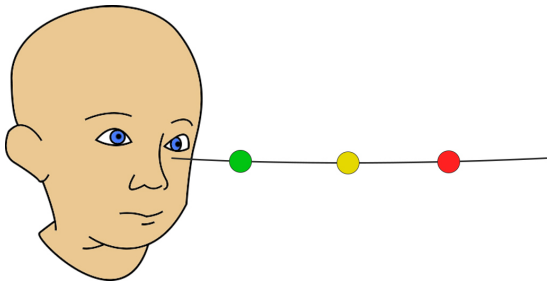

Figure 50: *Brock string: A subject who converges on the green, yellow and red beads. More coloured beads can be appended to the string.*

The level of difficulty of a Brock string exercise can be adjusted by changing the distance between the beads and nose (Singman *et al.*, 2014). Compared to pencil push-ups, a Brock string exercise offers longer ranges of fixation targets and can also be used to diagnose CI, CE and suppression (Berryman *et al.*, 2020).

3.5.2 *Surgical*

For some types of strabismus surgery is considered to be the most advisable course of action (Damanakis, 2013) (Hammond, 2014). The aim of every surgical treatment of strabismus is to achieve orthophoria within 10Δ, at primary gaze, and to establish normal ocular motility (Ansons and Davis, 2014) (Schutte *et al.*, 2008). Other than to restore normal BSV and develop fusion, surgery is recommended in order to improve the aesthetic appearance of a subject (Nihalani and Hunter, 2011) (Rowe, 2012). Strabismus surgery is divided into three categories:

- Surgery that weakens or strengthens EOM by recession and resection or plication (Lueder, 2011). Recession is performed to weaken an EOM by detaching the muscle from its original insertion on the eye and reattaching it further back, thereby relaxing the tension of the muscle (fig. 51a) (Billson, 2003). Resection is performed to strengthen an EOM either by detaching and reattaching the muscle forward from its original insertion, or, by detaching the muscle from the eye, removing a portion of the muscle and reattaching the shortened muscle at its original insertion position on the eye (fig. 51b) (Christiansen *et al.*, 2010). In plication, instead of removing a section of the muscle, the muscle is folded and stitched together (Agrawal, 2019). Recession and resection or plication techniques are employed in order to balance the forces applied to a strabismic eye, by its EOM, and achieve proper alignment of both eyes (Oya *et al.*, 2009).

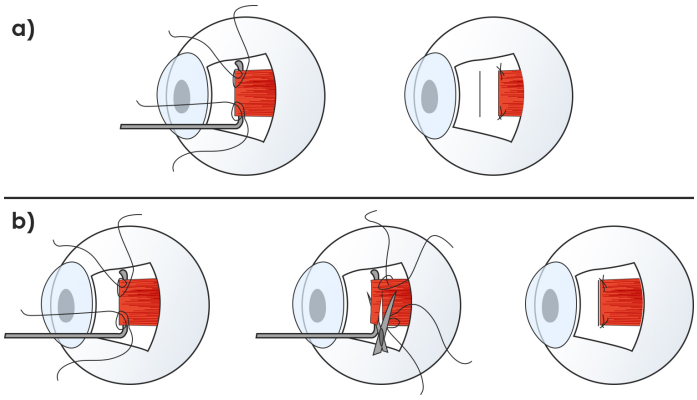

Figure 51: *Recession & Resection: An example of recession (a), in which the EOM is moved further back in order to relax its tension, and an example of resection (b), in which the muscle is stitched onto the same location it was detached after removing a small potion of muscular tissue from the EOM.*

- Surgery that alters the functionality of EOM. The functionality of a muscle, i.e. the way a muscle affects the orientation of an eye, can be adjusted either by changing the position of an EOM on the eye, e.g. vertical offset of the horizontal rectus muscles, (Oya *et al.*, 2009) or by an intervention at particular sections of an EOM, e.g. tenotomy of the superior oblique muscle (Sekeroğlu *et al.*, 2013).

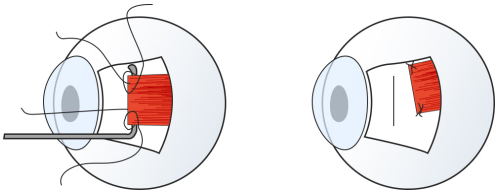

Figure 52: *Altering the functionality of an EOM: An example of the adjustment of an EOM, which is moved upwards.*

- Surgery that removes anatomical deformities that restrict the motility of EOM of the strabismic eye (Jivraj and Patel, 2015) (Lueder, 2015).

Regardless of the type of surgery, the most important factors that need to be considered are the selection of EOM to be operated on and the amount of adjustment or offset, measured in mm, that should be applied to the selected EOM during surgery (Wilson *et al.*, 2009) (Damanakis, 2005). Nihalani and Hunter (2011) explain that despite “accurate measurements ..., the outcome of strabismus surgery can be unpredictable, even in the short term". Furthermore, Nihalani and Hunter (2011) observed that “the same amount of surgery for the same angle of deviation will yield different results in different" subjects. For this reason, strabismus surgery is considered to be a two stage process, in which a second surgery is a post-operative adjustment of

an initial surgery (Morris and Luff, 1992). A technique, known as adjustable sutures, is employed, usually in post-operative surgery, because it allows the operated eye to be adjusted after surgery, when anaesthesia has receded and the 'true' deviation of the eye is revealed (Gawęcki, 2020). Adjustable sutures are recommended in cases of strabismus where the post-operative result of the first surgery is unpredictable . According to Awadein *et al.* (2008), the success rate of surgery is "notably greater in the adjustable group ... versus the non-adjustable group".

Although surgical techniques have been advanced and show "improvements of central and peripheral binocular visual function" (Beauchamp *et al.*, 2003), the success rate of surgery is extremely low (Oystreck and Lyons, 2012) (Traboulsi and Utz, 2016). In practice, strabismus surgery occasionally restores BSV in children and improves binocular vision but, in adults, surgery is performed mostly for cosmetic purposes (Schutte *et al.*, 2008). Complications of surgery, including diplopia, post-operative pain, rash and abnormal position of the eye lid (Kushner, 2002) (Shumway *et al.*, 2019), prevent the restoration of normal BSV because, even after surgery, a deviation is very likely to reoccur, at non primary directions of gaze or at various distances of gaze (Rutstein *et al.*, 2011) (Hatt *et al.*, 2015) (Sekeroğlu *et al.*, 2013). Sung *et al.* (2020) suggest that, considering the risk of surgical complications, if "cosmetic problems are not significant, surgical intervention could be delayed without concern of permanent loss of binocular function".

One possible explanation for the low success rate of surgery is the lack of accurate diagnostic information (Shen *et al.*, 2013) (Hammond, 2014). Generally, strabismus is diagnosed by an ophthalmologist, orthoptist, or another trained specialist, at an office at a pre-scheduled date and time, which the variability of the deviation may not reveal itself, thus rendering the diagnosis imprecise (Damanakis, 2013) (Lambert and Lyons, 2017).

Depending on the type of strabismus, surgery is planned to accomplish different results (Schutte *et al.*, 2008). For instance, in partially accommodative strabismus, with normal AC/A ratio, surgery is not used to treat the refraction error or the deviation, but to convert the partial accommodative strabismus into fully accommodative strabismus (Godts *et al.*, 2006) (Lembo *et al.*, 2019). In other types of strabismus, surgery is avoided in order to avoid causing further damage. In types of strabismus where the angle of deviation is very small and abnormal BSV or diplopia are present, including microtropia and CI, a surgical treatment may result in diplopia, a larger deviation and suppression (Ansons and Davis, 2014) (Ibironke, 2011).

3.6 A CASE FOR FURTHER RESEARCH

Strabismus is a very complex ocular misalignment condition that is not properly understood by practitioners and researchers. The lack of knowledge about strabismus complicates an accurate diagnosis and effective treatment. Christiansen *et al.* (2010) states that one "of the complexities in treating strabismus is that its aetiology is not understood".

Apart from cover testing, which cannot be used to measure torsional deviations, the most reliable tool to diagnose strabismus is a synoptophore (see subsect. 3.4.6). Unfortunately, a synoptophore constrains the eyes to a primary direction of gaze, requires relatively high cooperation from a subject and can only be performed in an office environment under professional supervision. Strabismologists have reported that one of the issues that degrades the accuracy of a diagnosis is the lack of information about the position of a strabismic eye, outside office-based diagnostic condition (Damanakis, 2013) (Hammond, 2014).

Compared to other treatments, surgery actively intends to resolve strabismus by adjusting the orientation of a deviating eye, whereas most non-surgical treatments aim to alleviate symptoms caused by amblyopia and diplopia. Unfortunately, the most effective non-surgical treatments can only be performed in office with supervision and restricted freedom of movement, therefore subjects tend to lose their motivation to complete their therapy (Carvelho *et al.*, 2008). Cooper (2007) states that "VT is often slow, arduous and unreliable", and (Sharma *et al.*, 2017) notes that the "conventional form of patching has been associated with low compliance".

Furthermore some types of strabismus characterized by variable deviations, are complex to diagnose and treat. This is because size and direction of a deviation may vary, sometimes by a considerable amount, during a day. Economides *et al.* (2016) noted that the "variability in the position of the deviated eye, ... wandered over a range of 12° horizontally and 6° vertically". None of the aforementioned treatments is able of compensating for such deviations. Prismatic glasses, for example, cannot change their refractive strength or the angle of refraction while being worn by a subject, thereby failing to compensate for incomitant, intermittent and other variations.

Regardless of the advancements made in diagnosis and treatment methods, the aforementioned techniques are still limited by the: (a) type of strabismus, (b) age of a subject, (c) variability, size and direction of a deviation, (d) time and day, on which the diagnosis or treatment is conducted, (e) experience of an examiner, or surgeon, and (f) cooperation and motivation of a subject to undergo diagnosis and complete therapy.

Currently, there is no system available capable of compensating strabismus in such a way that the visual stimuli, received by both eyes, dynamically derive from the same fixation target, located in various distances and directions. Such a system should:

- compensate for all types of strabismus, including variable strabismus, in order to reduce a deviation to within 10Δ in all directions of gaze.
- be suitable for various age groups, including young children, adults and the elderly.
- motivate a subject to undergo and complete therapy, by not using predetermined fixation targets in office based set-ups.
- gather diagnostic information, such as the orientation of both eyes.
- be appropriate for HBVT and OBVT.

The present work investigates this research challenge. According to Damanakis (2013) and Hammond (2014), such a system would have a tremendous impact on the diagnosis and treatment of strabismus and could potentially be used in other areas of ophthalmology.

3.7 SUMMARY

Strabismus is a polymorphic ocular misalignment condition in which, due to unmatched visual directions, one eye does not receive visual stimuli deriving from a fixation object. This condition prevents the subject from perceiving an environment in three dimensions, because the retinal images, formed by both eyes and received by the brain, are not fusible. Unfortunately, the aetiology of strabismus remains an enigma.

This chapter discussed several aspects of strabismus, including two theories surrounding its potential origins. Most strabismologists support the 'sensory vs motor' theory, which assumes that strabismus originates from the brain, and it is the brain that needs treatment. Throughout this chapter, it was established that normal BSV can be restored if strabismus is treated during the critical period. Particular emphasis was given to the physiological, physchological and social effects of strabismus on a person's life.

Strabismus prevents normal BSV by causing confusion and diplopia, and is associated with symptoms such as headaches, nausea and an inability to focus. Consequently, the brain develops certain adaptations, including suppression and ARC, in order to counter these disturbances and symptoms. However, depending on the type of strabismus, the adaptations developed

by the brain cause monocular vision or abnormal BSV. In some cases, the brain does not develop any adaptations and the individual suffers from permanent and persistent diplopia.

Because not enough is currently known about strabismus, current diagnosis and treatment methods are limited by the type of the deviation. Furthermore, the cooperation and motivation of a subject are key elements towards an accurate diagnosis and successful treatment of strabismus. However, the most effective non-surgical therapies can only be performed in office with supervision and restricted freedom of movement, therefore subjects tend to lose their motivation to undergo and complete their therapy. Surgery remains the most advisable treatment for strabismus, even though the rate of success is low.

This chapter identified a number of limitations with current diagnostic and treatment methods, and made a case for further research in the development of a system that would be able to dynamically compensate strabismus when the fixation target is located at various distances and directions.

4

DYNAMIC RETROVERSION OF STRABISMUS

> *"The reasonable man adapts himself to the world; the unreasonable man persists in trying to adapt the world to himself. Therefore all progress depends on the unreasonable man."*
>
> — George Bernard Shaw, Man and Superman

This chapter presents a novel principle referred to as Dynamic Retroversion of Strabismus (DRS), which is the basis for a class of systems called Dynamic Eye Misalignment Retroversion Systems (DEMRS). Therefore, a DEMRS is a DRS compliant system. The first section of this chapter discusses the term "retroversion of strabismus", which is the objective of a system designed to assist in the development of normal BSV. Furthermore, the first section introduces the principle of DRS, which establishes a set of criteria required to achieve retroversion of strabismus. The next section explains the rationale of DRS, and briefly compares it to other therapeutic methods discussed in the previous chapter. Next, the DEMRS simulator is presented, which is a software application that was developed in order to simulate the functionality of DEMRS. The final two sections of this chapter propose two systems, compliant with the DRS principle, one compensating for horizontal and vertical deviations (HV-2.0), and the other compensating for horizontal, vertical and torsional deviations (HVT-2.5).

4.1 THE DRS PRINCIPLE

In medical terms, retroversion refers to the abnormal backwards rotation of an organ or other body part. For example, femoral retroversion refers to an abnormal rotation of the femur (thigh-bone) in relation to the knee (Standring, 2008). However, retroversion is also defined as the process of returning to a former state (Dictionary, 2021). This thesis adopts the later definition to indicate that the effects of strabismus are reversed, or retroverted, when binocular single vision and depth perception are restored.

Although there are two types of visual directions, namely principal and peripheral, emphasis is given on principal visual directions because they are responsible for central vision (see sect. 2.4). Also, because in some types of

strabismus the brain primarily suppresses the fovea (see subsect. 3.2.3), emphasis is given on principal visual directions with the purpose of eliminating foveal suppression. Because there are infinite number of visual directions emanating from a fixation target, it is impossible to determine which visual direction should be retroverted in order to be received by the fovea of an eye. Therefore, in order to trace the visual direction that originates from the fixation target but, also, received by the fovea, the principal visual direction of the eye is inverted. In this thesis, an inverted principal visual direction is termed principal vision vector, and is defined by: (a) an origin, which is the fovea, and (b) a direction, indicated by the rotation of the eye. The benefit of using vision vectors is that performing analysis on projections of visual directions to the retina, in order to assert that the visual stimuli originating from a target are received by both foveae, is no longer necessary. In order to aid consistency, peripheral visual directions are also inverted, and therefore referred to as peripheral vision vectors. In the description of DEMRS, vision vectors that originate from the fovea and are directed towards the fixation target are termed principal vision vectors. Vision vectors that originate from peripheral areas of the retina and intersect arbitrary objects in the environment are termed peripheral vision vectors. Lastly, vision vectors that originate from the fovea but are directed towards the surrounding area near the fixation target are also termed peripheral vision vectors.

The DRS principle states that:

> Retroversion of strabismus is achieved through the dynamic redirection of the principal vision vectors such that they simultaneously intersect the same fixation target, while maintaining normal resultant inter-pupillary distance, normal binocular disparity, and normal orientation of the visual stimuli.

The aforementioned principle establishes four criteria required in order to achieve retroversion of strabismus, namely the: (a) simultaneous intersection of both principal vision vectors on the same fixation target, (b) maintenance of normal resultant inter-pupillary distance (IPD), (c) maintenance of normal binocular disparity, and (d) maintenance of normal orientation of the visual stimuli received by both eyes. A system (e.g. DEMRS) is DRS compliant when it meets these four criteria.

4.2 JUSTIFICATION OF DEMRS

The DRS principle was developed to assist in the diagnosis and treatment of strabismus, due to the inability of other treatments to dynamically adjust

the visual stimuli that derive from a fixation target. Unlike haploscopic devices (see subsect. 3.4.7), which constrain both eyes to primary gaze whilst viewing a pair of images, or surgery (see subsect. 3.5.2), in which the muscles of a strabismic eye are operated to achieve orthotropia within 10Δ (≈ 5°) at primary gaze, DEMRS describes a class of systems that can dynamically redirect light.

A DEMRS:

1. Is a non-surgical compensatory method of treating strabismus, as it does not actively change the orientation of a strabismic eye.
2. Achieves retroversion of strabismus for any stable or moving object in the environment, located at various distances and directions.
3. Compensates for all classifications of strabismus, including deviations that arise as a result from an abnormal structure of the skull.
4. Compensates for any variable change in strabismic deviations, and is not restricted by latency, comitancy or frequency of strabismus.
5. Can be used as HBVT and OBVT by various age groups including young children, adults and elderly.
6. Is designed to motivate a subject to undergo and complete therapy, by not using pre-determined fixation targets in office based set-ups, but allowing the subject to perform various personal tasks e.g. watching a film or reading a book.
7. Assists in the diagnosis of strabismus by allowing the dissociation of both eyes to fixate on different targets.

4.3 THE DEMRS SIMULATOR

A software application was developed that simulates the DRS compliant systems, discussed later in this thesis. This application was originally developed on a Mac OS High Sierra (version 10.13.6, 2.4 GHz Intel Core i7, 8 GB DDR3 RAM and Intel HD Graphics 3000 GPU), but has been tested on Linux RedHat 7 and Windows 10, using QtCreator[1], C++[2] and OpenGL[3]. The latest

1 Qt Creator is a cross platform integrated development environment, which simplifies the development of GUI applications.
2 C++ is a general purpose programming language that supports several features, including object-oriented and generic programming.
3 OpenGL is a cross platform and cross language API used for rendering 2D and 3D graphics.

version of the software application, hereafter referred to as DEMRS simulator, is available at https://bitbucket.org/cglynos/demrs/src/master/HVT_25/.

As shown by the diagram in figure 53, the DEMRS simulator consists of the configuration of a DEMRS variant, the engine/module that calculates retroversion, a set of inputs, such as the IPD and strabismic deviation, and provides two outputs as front-ends to the system. The visualization output is a 3D representation of a DEMRS, including its sub-components, and the path that the principal and peripheral vision vectors assume when retroverted by the DEMRS. The functionality of DEMRS is evaluated through a series of simulated tests, whereas, the hardware communication module (HCM) output connects the DEMRS simulator with a proof of concept (POC) device, discussed in the next chapter.

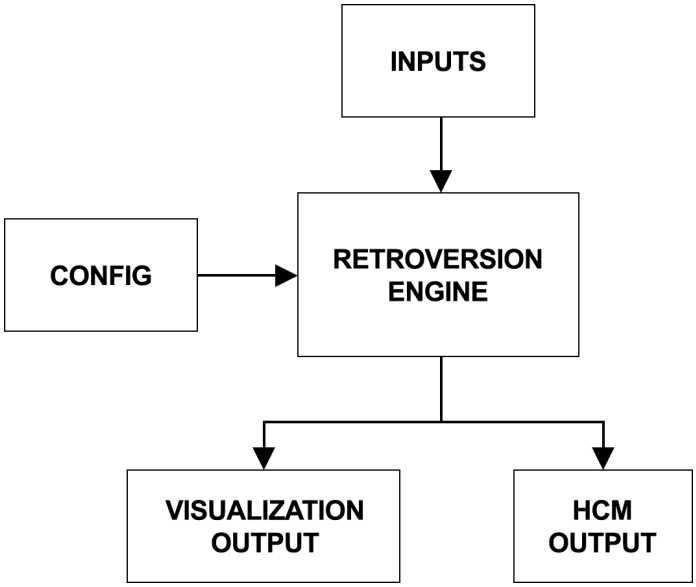

Figure 53: *DEMRS simulator: The basic structure of the DEMRS simulator, in which the retroversion engine is the main actor.*

4.3.1 *Coordinate System*

The DEMRS simulator utilizes a Cartesian coordinate system in which the three axes, perpendicular to each other, are called abscissa (x-axis), ordinate (y-axis) and applicate (z-axis) (fig. 54). Right is defined by the positive x-axis, up is defined by the positive y-axis and front is defined as the positive z-axis. Furthermore, the x, y, and z axes correspond to pitch (ϕ), yaw (θ), and roll (ψ) rotations, respectively (fig. 54). For example, a vertical rotation of an object is a pitch rotation of the object about the x-axis. These axes meet

at the origin, which is at $< x : 0, y : 0, z : 0 >$ (fig. 54). Objects created by the DEMRS simulator, can translate and rotate within this coordinate system.

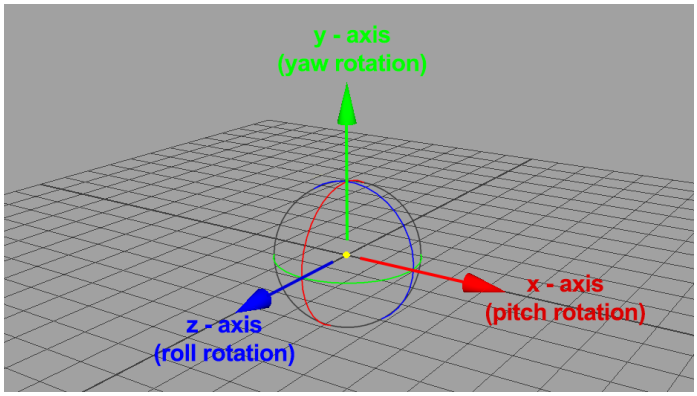

Figure 54: *Coordinate system: The DEMRS coordinate system whose origin is depicted by the yellow point. The gizmo is only used to illustrate the coordinate axes.*

4.3.2 *Eye Model*

In order to simulate strabismic deviations, the DEMRS simulator requires the model of two eyes each of which is defined as a sphere with default diameter set to 24mm (see sect. 2.1). The central point of the fovea (umbo), which is at the back of the eye, is represented by a locator object (see subsect. 2.1.2). Also, each eye model can be configured so that additional locators can track peripheral points on the retina. Figure 55 shows how an eye is visualized within the DEMRS simulator, along with the locators used to represent points on the retina.

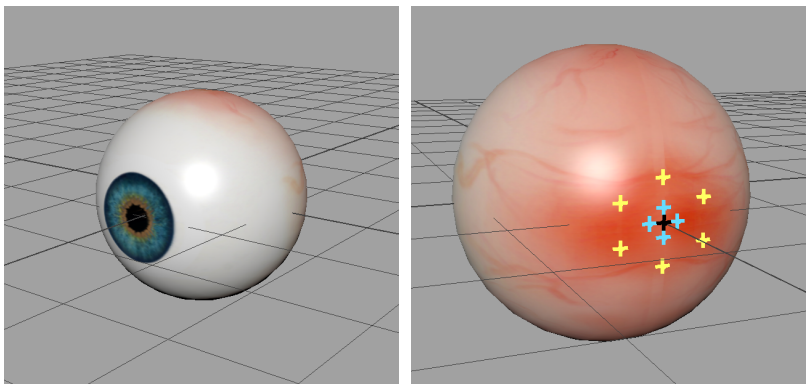

(a) *perspective view of an eye* (b) *view from behind*

Figure 55: *Visualization of an eye: Part (a) shows how an eye, located at the origin, is visualized by the DEMRS simulator. Part (b) illustrates the locators, which represent retinal points. The umbo is represented by a black locator. Peripheral points in the fovea are represented by the sky blue locators, and peripheral points outside the fovea are represented by the yellow locators.*

The first input to the DEMRS simulator is an IPD, which is used to determine the position of the eyes at the appropriate distance from each other. The origin of the DEMRS simulator is at $< 0, 0, 0 >$, whereas the origin of a DRS compliant system is the centre of the eyes, hereafter referred to as DEMRS origin. By default, the origin of the DEMRS simulator and the DEMRS origin are identical, i.e. the DEMRS origin is also at $< 0, 0, 0 >$. For example, if the IPD is set to $6cm$, the left eye would be positioned at $< 3, 0, 0 >$ and the right eye at $< -3, 0, 0 >$.

The second input to the DEMRS simulator specifies the dominant eye, and the third input is a set of rotation angles that indicate a strabismic deviation, relative to the orientation of the dominant eye. There are three options for specifying dominance: left, right, and both. When the left eye is declared dominant, the right eye deviates by the strabismus angles. When the right eye is dominant, the left eye deviates by the strabismus angles. Normal BSV is simulated when both eyes are declared dominant, in which case the strabismus angles are ignored.

4.3.3 *Vision Vectors*

The DEMRS simulator requires the concept of a vision vector, which is simulated as a polyline consisting of one line segment. The start point of the line segment, i.e. the origin of the vision vector, is a retinal point on the eye, whereas the end point of the line segment is calculated using a default distance of $> 6m$ and the visual direction of the eye, as shown by equation 6. For example, the principal vision vector (VV_F) of an eye that "looks" straight ahead, i.e. along the positive z-axis, originates from the umbo of the eye and has a direction of $< 0, 0, 1 >$.

$$vv_end = vv_start + (600 \times vv_dir) \tag{6}$$

where:

vv_end = end point of the vision vector

vv_start = start point of the vision vector, i.e. umbo

vv_dir = direction of the vision vector

Vision vectors have been modelled with polylines so that the number of points in a polyline can increase or decrease, thus making it visually possible to trace the path of a vision vector from the umbo to a fixation target. Figure 56 shows three cases of dominance including the principal vision vec-

tors ($VV_{F_{L/R}}$) emanating from both foveae. Figure 57 shows an example of principal and peripheral vision vectors ($VV_{P_{L/R}}$) originating from the fovea and from the outer parts of the retina of each eye.

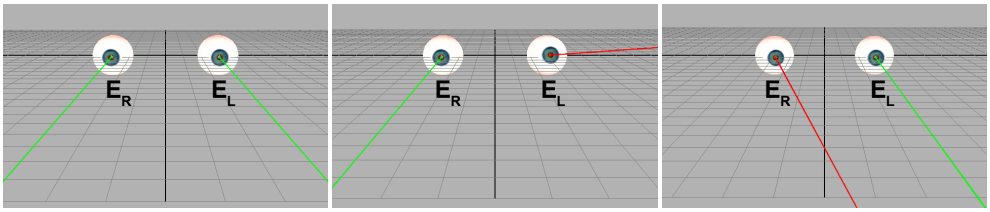

(a) *normal bsv* (b) *left exo-hyper-tropia* (c) *right eso-tropia*

Figure 56: *Visualization of dominance and strabismic deviations: When strabismus occurs, the principal vision vector of the deviating eye is coloured in red, whereas the principal vision vector of the dominant eye is in green. (a) illustrates normal BSV as both eyes are dominant and their vision vectors are parallel. In (b) the right eye is dominant and the left eye performs an exo-hyper tropia of* $< 6, 8, 0 >$*, where the left eye rotates outwards by* $8°$ *and upwards by* $6°$*. (c) shows a right eso-tropia of* $< 0, 10, 0 >$*, where the right eye rotates inwards by* $10°$*.*

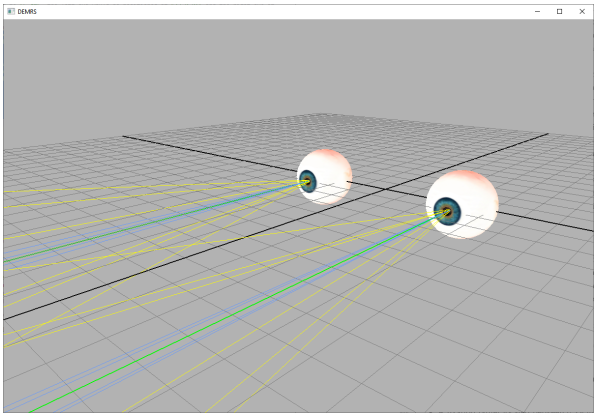

Figure 57: *Visualization of vision vectors: Both eyes along with the principal and peripheral vision vectors. The peripheral vision vectors originating from the fovea are coloured in sky-blue, whereas the peripheral vision vectors originating from outer parts of the retina are coloured in yellow. Lastly, the principal vision vectors of both eyes is coloured in green because both eyes are dominant, thereby simulating normal BSV.*

4.3.4 *Fixation Target*

In addition to the eyes and vision vectors, the DEMRS simulator requires a fixation target (T) as a single point, in a three dimensional space, at which the principal vision vector of the dominant eye is directed. The fixation target is the fourth input to the DEMRS simulator. As previously mentioned in subsection 2.2.2, the orientation of the eyes depends on the distance of the target from the eyes. Depending on the distance of the fixation target from

the origin, a DEMRS is designed to converge or parallelize both principal vision vectors on the fixation target. If T is located $< 6m$ from the origin, both principal vision vectors ($VV_{F_{L/R}}$) converge on T (fig. 58a), whereas if T is located $\geqslant 6m$ from the origin, both principal vision vectors are aligned parallel to each other. As shown in figure 58b, this is achieved by creating two additional targets (Tp_L and Tp_R) on either side of T, where the distance between Tp_L and Tp_R is the IPD (δ).

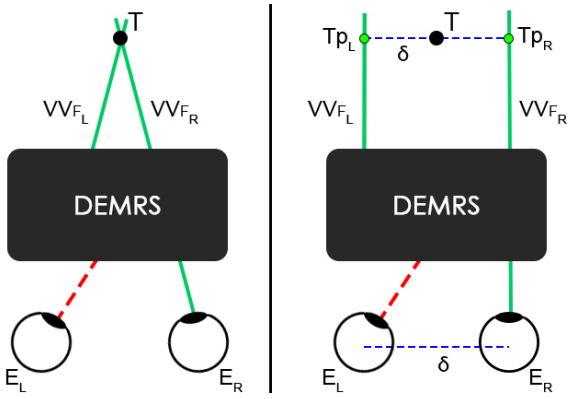

(a) *retroversion of left eso-tropia for* T

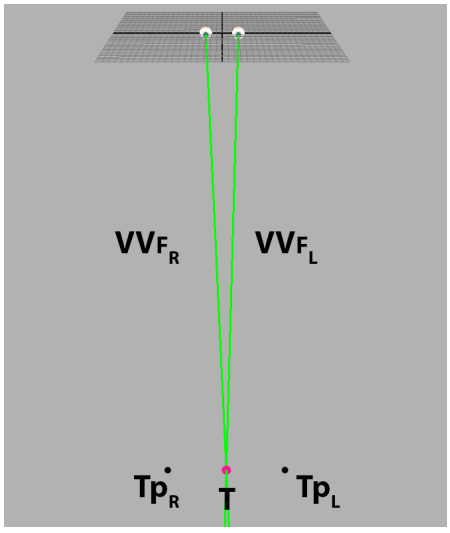

(b) *converge on* T, *when* $\mathrm{Dist}(T) = 1m$

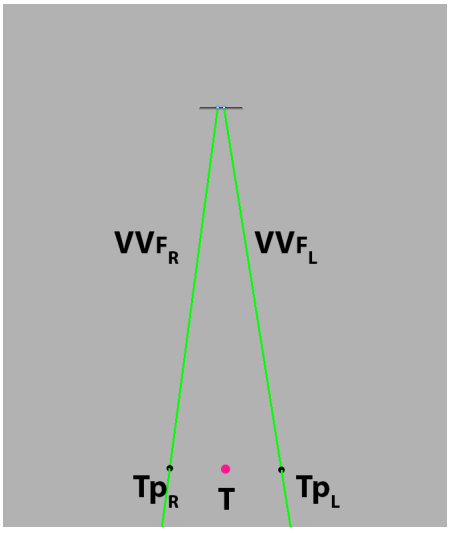

(c) *parallel on* $Tp_{L/R}$, *when* $\mathrm{Dist}(T) = 6m$

Figure 58: *Near and far fixation targets: Two examples of a left eso-tropia, in which both* $VV_{F_{L/R}}$ *are adjusted by the system in order to achieve retroversion. In (a) both* $VV_{F_{L/R}}$ *converge on a target* T, *located* $< 6m$. *In (b) both* $VV_{F_{L/R}}$ *are parallel to each other and pass through the corresponding targets* Tp_L *and* Tp_R. E_L *and* E_R *are the left and right eyes, and* δ *represents the IPD.*

The DEMRS simulator achieves retroversion for any fixation target (T):

- positioned at various distances and directions from the DEMRS origin.
- that lies in the direction of the principal vision vector (VV_F) of the dominant eye, constrained to a predefined distance.

- deduced, or inferred, from the orientation of both eyes. For instance, the position of T could be calculated from the intersection between VV_F of the dominant eye and the median plane of the face. If the distance between T and the DEMRS origin is $\geqslant 6m$, the additional targets Tp_L and Tp_R could be used to parallelize both principal vision vectors.

Furthermore, for the purpose of diagnosing strabismus, the DEMRS simulator can retrovert both principal vision vectors towards two dissociated fixation targets (T_L and T_R) that are positioned at various distances and directions unrelated to each other, i.e. the left eye fixates on T_L while the right eye fixates on T_R.

4.3.5 *Mirrors and Prisms*

The DRS compliant systems, introduced in this thesis, are designed to redirect principal and peripheral vision vectors by orienting a set of mirrors and prisms, in order to achieve retroversion of strabismus. Although the design of each system depends on the type of strabismus, for example prisms are only used when torsional deviations are present, the DEMRS simulator is used to calculate the orientation of these components (mirrors and prisms) for various configurations of DEMRS. Consequently, the DEMRS simulator must model a mirror and a prism. A mirror is modelled as a rectangular object, of default size $w \times h \times d = 12.70 \times 10.16 \times 0.30cm$, that can reflect vision vectors. A mirror is modelled based on the specifications of commercially available cold mirrors provided by Edmund Optics (2019a). As shown in figure 59, a mirror has two faces (front, back) and four edges (left, right, top, bottom). The edge of a mirror is identified with respect to the front face of the mirror, and only the front face can reflect vision vectors.

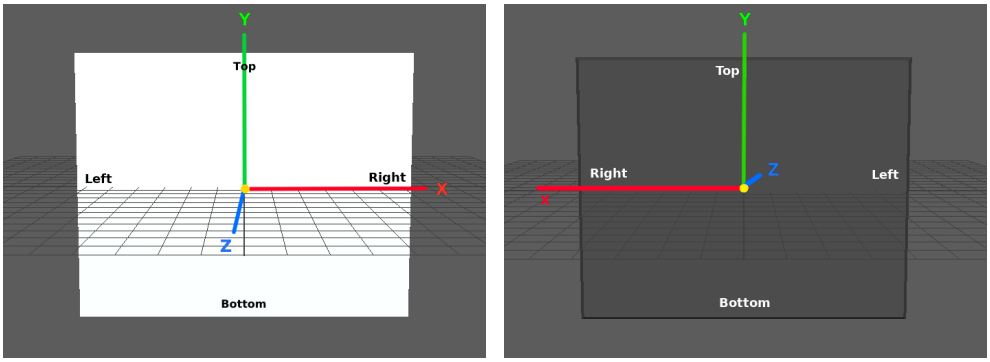

(a) *front face* (b) *back face*

Figure 59: *Mirror sections: The two faces and four edges of a mirror as visualized by the DEMRS simulator.*

A mirror can rotate horizontally (yaw), vertically (pitch) and torsionally (roll) about a pivot (P) (fig. 60), which is the origin of the local coordinate system of a mirror. The pivot of rotation (P) can be central to the mirror or on the edge of the mirror, as shown in fig. 60 respectively. Also, figure 60 shows two examples of a mirror rotating horizontally, i.e. yaw rotation, about P. In the first example P is central to the mirror, whereas in the second example P is on the centre-right edge of the mirror. Lastly, figure 61 shows the reflection of a principal vision vector by a mirror, in the DEMRS simulator. Due to the reflection by the mirror, an additional point is added to the polyline in order to simulate the reflected vision vector.

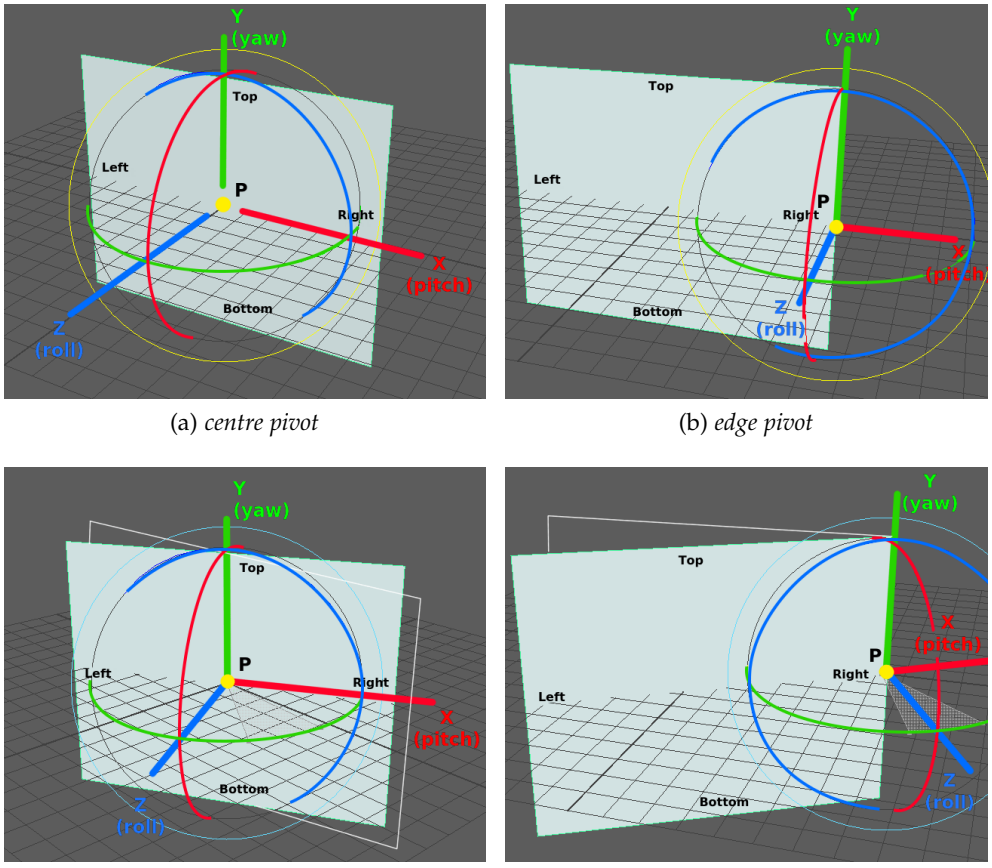

(a) *centre pivot*

(b) *edge pivot*

(c) *yaw about the centre*

(d) *yaw about the edge*

Figure 60: *Mirror: The coordinate system of a mirror and the pivot of rotation. Also, the figure shows two examples of a mirror rotating about the y-axis (yaw rotation) of* P. *The gizmo is only used to illustrate the coordinate axes.*

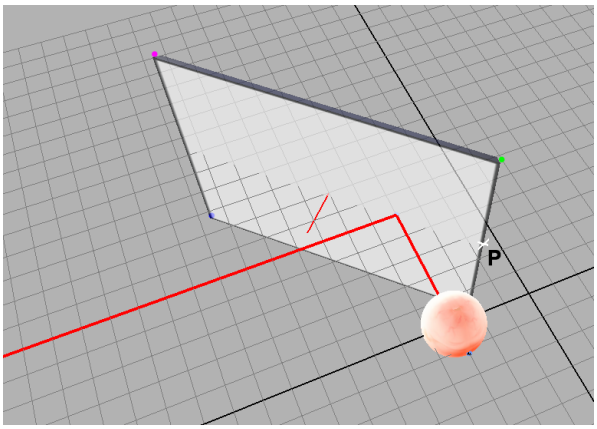

Figure 61: *Mirror reflection: The reflection of a principal vision vector (red) by a mirror in the DEMRS simulator. The white cross on the centre-right of the mirror is the pivot of rotation, and the thin red line projecting from the centre of the mirror indicates the normal of the surface.*

In order to retroverse torsional strabismus, some of the DRS compliant systems described in this thesis incorporate two types of rotatory prisms, namely a dove prim and a delta prism. These prisms were modelled based on the specifications of commercially available prisms provided by Thorlabs (2021). A dove prism (fig. 62a) is a trapezoid prism that torsionally rotates the transmitted image (refracted visual stimuli) by twice the angle of prism rotation (Swift, 1972) (Yoder and Vukobratovich, 2015). Additionally, a dove prism inverts the transmitted image (Padgett and Paul Lesso, 1999) (Malacara-Hernandez and Malacara-Hernandez, 2017). A delta prism (fig. 62a) is a triangular prism that has the same effect as a dove prism but is more compact in size (Murty, 1973). As shown in figure 62b, when the dove prism is oriented at 0° the visual stimuli are inverted, and the transmitted image of the environment is perceived as upside down. However, when the dove prism is rotated by 90° (roll rotation) the visual stimuli are inverted and a transmitted image is rotated by 180°. Therefore, although the environment is inverted it is perceived with normal orientation (fig. 62b).

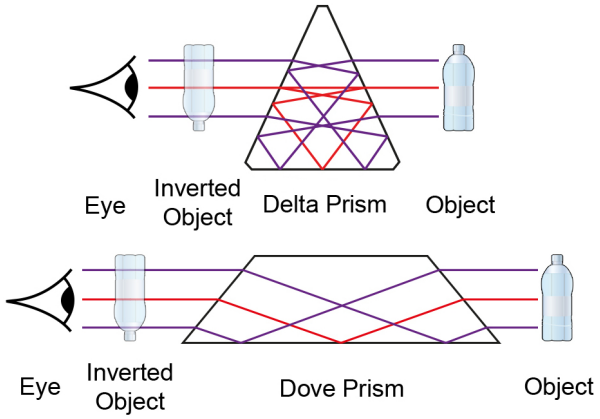

(a) *Inversion of visual stimuli.*

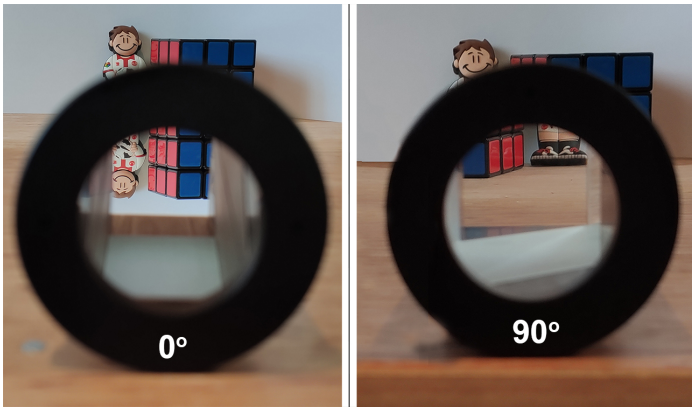

(b) *Rotation and inversion of visual stimuli by a dove prism.*

Figure 62: *Delta/Dove prism effect: The rotation and inversion of the visual stimuli refracted by a prism. (a) illustrates the effect of inversion as a bottle is perceived upside down through each prism, oriented at 0°. (b) shows two images of a Rubik's cube and a toy viewed through a dove prism. On the left side of (b), the dove prism is not rotated therefore the image is only inverted. On the right side of (b), the dove prism is rotated by 90°, therefore the transmitted image is rotated and inverted. Consequently, although the orientation of the Rubik's cube and the toy is normal, the bottom of the Rubik's cube appears on the left and the bottom of the toy appears on the right.*

A dove prism is modelled as an isosceles trapezoid, of default size $w \times h \times l = 3 \times 3 \times 12.6\text{cm}$ and 45° opposite angles. Figure 63 shows the effect of a dove prism when rotated by 0° and, next 45°. To aid clarity, the peripheral vision vectors have the same direction as the principal vision vector. In the first example, the dove prism is not rotated and, therefore, the vision vectors are only inverted. In the second example, where the prism is rotated by 45°, the resultant vision vectors are inverted and rotated by 90°, i.e. twice the roll rotation of the prism.

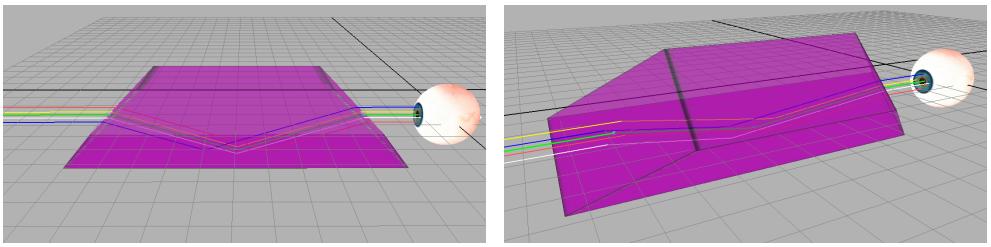

(a) *rotated by* 0° (b) *rotated by* 45°

Figure 63: *Dove prism rotation: The path of the vision vectors when rotated and inverted by a dove prism. To clearly visualize the direction of the vision vectors when refracted by the prism, each polyline has been assigned a different colour. The principal vision vector is the green polyline.*

A delta prism is modelled as an isosceles triangular prism of default size $w \times h \times l = 3 \times 3 \times 3.7\text{cm}$ and 66.58° opposite angles. Figure 64 shows the effect of a delta prism rotated by 0° and, 45°. In the first example, the delta prism is not rotated and, therefore, the vision vectors are only inverted. In the second example, where the prism is rotated by 45°, the resultant vision vectors are inverted and rotated by 90°, i.e. twice the roll rotation of the prism.

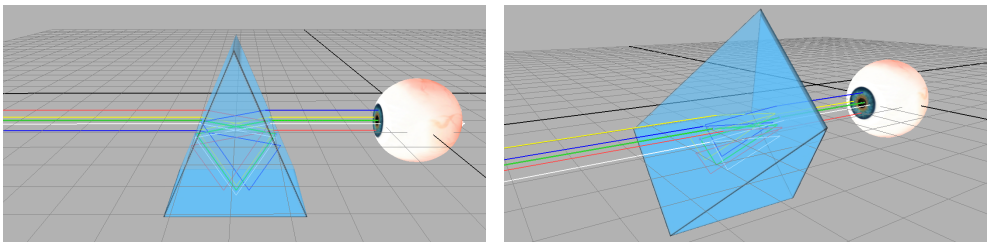

(a) *rotated by* 0° (b) *rotated by* 45°

Figure 64: *Delta prism rotation: The path of the vision vectors when rotated and inverted by a delta prism. To clearly visualize the direction of the vision vectors when refracted by the prism, each polyline was assigned to a different colour. The principal vision vector is the green polyline.*

4.3.6 *Lenses*

The DEMRS simulator supports two types of lenses, namely a convex and a concave lens. As previously described in subsection 3.5.1.1, a convex lens converges light, and a concave lens diverges light. Therefore, these lenses are added to the designs of DEMRS in order to constrain the direction of the peripheral vision vectors so that they don't escape the system when reflected by a mirror. More details about the advantages of using lenses are discussed later in this chapter. The lenses were modelled based on the speci-

fications of commercially available lenses manufactured by Edmund Optics (2021b) and Edmund Optics (2021a). A convex lens is modelled as an ellipsoid with a default radius of 6.085cm, 0.850cm centre thickness and effective focal length (EFL) of 3.37cm. A concave lens is modelled as a cylinder, with both of its caps curved towards the centre of the cylinder. The default radius of each cap 16.672cm, the centre thickness is 0.8, the edge thickness is 1.029 and the effective focal length (EFL) is 4.13cm. Figure 65 shows the effect of the convex and concave lenses on the direction of the peripheral vision vectors. Also, the figure shows that the direction of the peripheral vision vectors is unchanged after refraction.

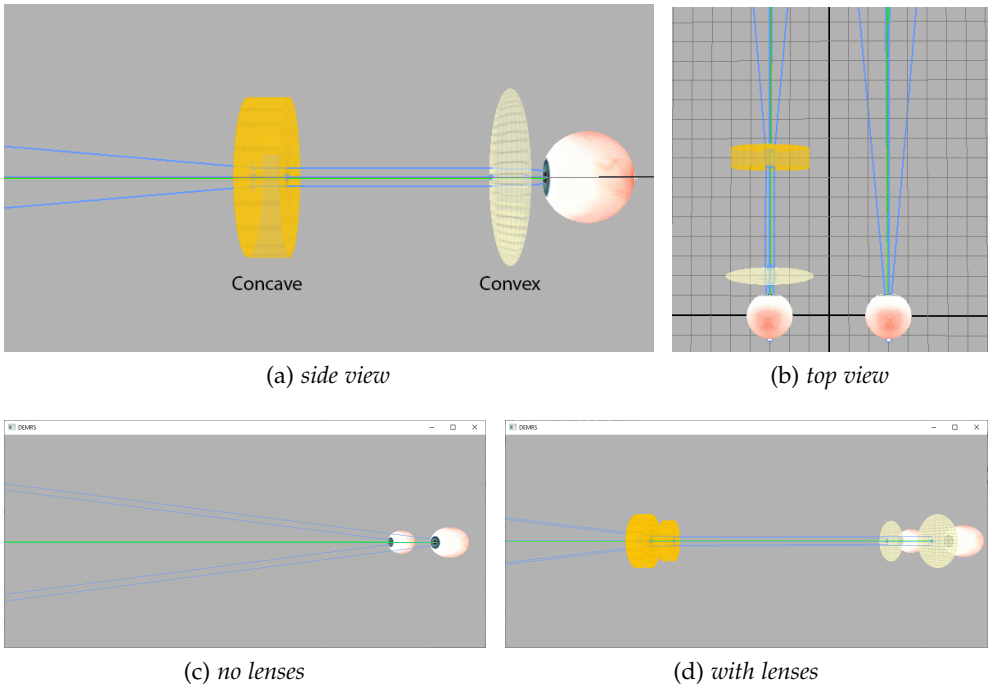

(a) *side view* (b) *top view*

(c) *no lenses* (d) *with lenses*

Figure 65: *Lenses: The effect of the convex and concave lenses in the direction of the peripheral vision vectors (sky-blue). The principal vision vectors are illustrated by the green polylines.*

4.3.7 *System Configuration*

The DEMRS simulator describes a unique system by parsing a JSON[4] configuration file that defines the initial position and rotation of the components, unique to the design of the system. The configuration file may also include additional fields that would allow the user of the DEMRS simulator

4 JavaScript Object Notation (JSON) is a lightweight data-interchange format, which is parsed by a program in order to generate a JSON object. This object is an unordered set of name/-value pairs.

to override the values of the default parameters of a component. For example, the configuration of a DRS compliant system that can achieve retroversion of horizontal, vertical and torsional strabismus, would include the initial position and orientation of each mirror, prism and lens used by the system. Additionally, the configuration may include the size of a mirror and the refractive power (refractive index) of the prisms.

Table 3 presents the complete list of valid fields per component of the JSON configuration file of a DEMRS. The default values of the parameters of each component can also be found in the source code of the DEMRS simulator. Listing 1 presents an example of a JSON configuration file, which declares and initializes the position and orientation of one convex lens, two mirrors and one delta prism. The configuration file also includes a field for the refractive index (`rfidx`) of the delta prism (list. 1). Figure 66 shows the output from the visualizer of the DEMRS simulator after parsing the configuration file.

It should be noted that in the current version of the DEMRS simulator, the order in which the components of a DEMRS system are listed in a JSON configuration file indicate the order by which a principal vision vector must be reflected, or refracted, by these components. If a principal vision vector does not intersect one, or more, of the components, the DEMRS simulator will reject retroversion even if the DRS principle is satisfied. For example, if the delta prism in listing 1 did not refract the principal vision vector, the DEMRS simulator would reject retroversion even if the vision vectors did pass through the same target, with normal resultant IPD, binocular disparity and orientation.

Table 3: *The complete list of valid fields of a JSON configuration file, split into two categories. The "general" category lists the fields that are not exclusive to any component, whereas the "components" category lists the fields that are associated with each component. In the "general" category, the* `symmetrical` *field determines whether the system is symmetrical, i.e. the components on the left side are mirrored to the right and vice versa. The* `component` *field indicates which component is currently described in the element of the JSON configuration file, ex. prism, whereas the* `type` *field indicates the type of the component being described, ex. dove or delta. In the "components" category,* `side` *determines whether the component is associated with the left or right eye,* `id` *is the number id of a component that belongs to an array of similar components,* `rfidx` *is the refractive index of each prism and lens,* `oppangle` *is the opposite angle theta used to model the prisms,* `centret` *is the centre thickness of each lens,* `rad` *is the radius of the curvature of a lens that is used to refract vision vectors, and* `edget` *is the edge thickness of a concave lens.*

			general				
fields		symmetrical	true / false				
		component	mirror	prism		lens	
		type		dove / delta		convex / concave	
			components				
			mirror	dove	delta	convex	concave
fields	translate	x	✓	✓	✓	✓	✓
		y	✓	✓	✓	✓	✓
		z	✓	✓	✓	✓	✓
	rotate	ϕ	✓	✓	✓	✓	✓
		θ	✓	✓	✓	✓	✓
		ψ	✓	✓	✓	✓	✓
	scale	w	✓	✓	✓		✓
		h	✓				✓
		d	✓				
	pivot	x	✓	✓	✓	✓	✓
		y	✓	✓	✓	✓	✓
		z	✓	✓	✓	✓	✓
	side		✓	✓	✓	✓	✓
	id		✓	✓	✓		
	rfidx			✓	✓		
	oppangle			✓	✓		
	centret					✓	✓
	rad					✓	✓
	edget						✓

Listing 1: Example of a JSON configuration file

```
{
	"example" :
	[
	{
		"symmetrical" : "false"
	},
	{
		"component" : "lens",
		"type" : "convex",
		"side" : "left",
		"translate" : [3.0, 0.0, 3.0]
	},
	{
		"component" : "mirror",
		"side" : "left",
		"id" : 0,
		"pivot" : [6.35, 0.0, 0.0],
		"translate" : [0.0, 0.0, 6.0],
		"rotate" : [0.0, 225.0, 0.0]
	},
	{
		"component" : "mirror",
		"side" : "left",
		"id" : 1,
		"translate" : [18.0, 0.0, 9.0],
		"rotate" : [0.0, 45.0, 0.0]
	},
	{
		"component" : "prism",
		"side" : "left",
		"type" : "delta",
		"rfidx" : 1.85,
		"translate" : [18.0, 0.0, 18.0],
		"rotate" : [0.0, 0.0, 90.0]
	}
	]
}
```

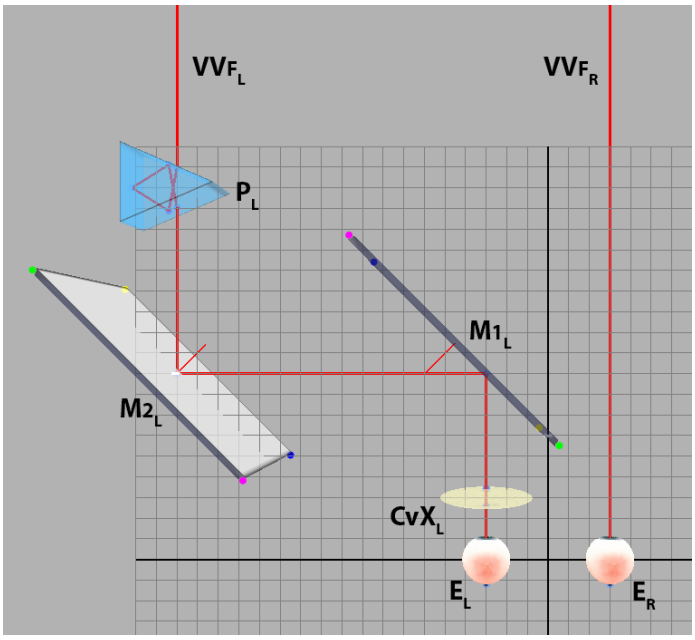

Figure 66: *Visualization output from listing 1: The output from the visualizer of the DEMRS simulator. This example is not a representation of DEMRS and, therefore, retroversion is not expected to be achieved. Although the resulting vision vectors are parallel, which is expected when the fixation target is at a distance of 6m from the DEMRS origin, the resulting pupillary distance is abnormal, i.e. does not match the original IPD, and retroversion fails. Therefore, the vision vectors are coloured in red.*

Lastly, the DEMRS simulator accepts the following inputs: 1. IPD, 2. dominant eye, 3. strabismic deviation, 4. target, 5. system configuration file These inputs are passed into the DEMRS simulator as command line arguments. For example:

```
DEMRS_Simulator.exe -ipd 6.0 -dom "right" -strabdev 8.0
    -12.0 4.0 -trgt 0.0 0.0 600.0 -sysconfig
    hv20_config.json


where:
      -ipd = inter-pupillary distance
      -dom = dominant eye
      -strabdev = strabismic deviation (pitch, yaw, roll)
      -trgt = position of fixation target
      -sysconfig = system configuration file
```

4.4 DEMRS FOR HORIZONTAL AND VERTICAL STRABISMUS (VERSION HV-2.0)

DEMRS HV-2.0 is a conceptual DRS compliant system designed to retroverse horizontal and vertical strabismus. This system is designed to redirect principal and peripheral vision vectors by orienting a set of mirrors, horizontally about the local y-axis (yaw rotation) and vertically about the local x-axis (pitch rotation), in order to achieve retroversion. This system does not retroverse torsional deviations, because the orientation of the visual stimuli is assumed to be normal.

4.4.1 *Design and Description*

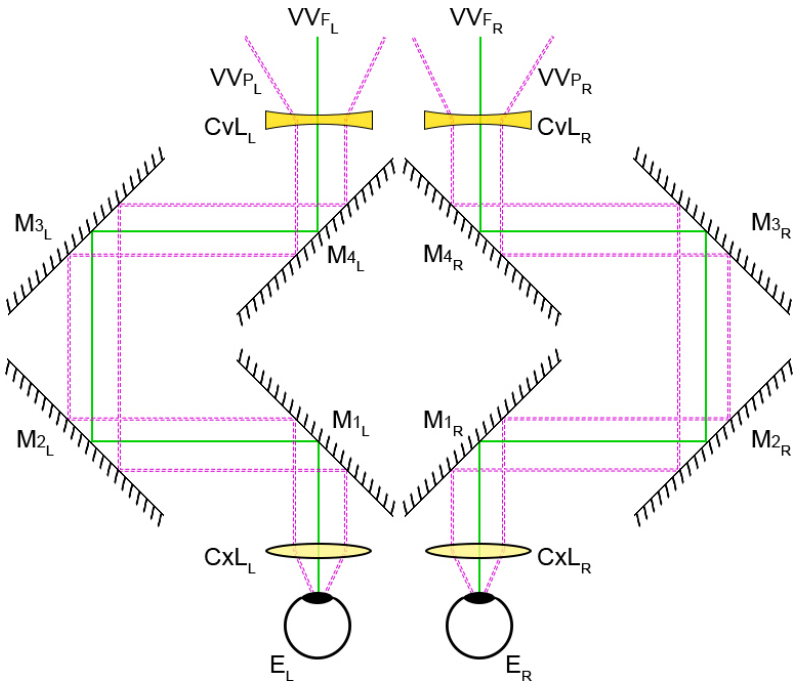

Figure 67: *DEMRS HV-2.0: A schematic of the system, where* $VV_{F_{L/R}}$ *are the left and right principal vision vectors,* $VV_{P_{L/R}}$ *are the peripheral vision vectors,* $CxL_{L/R}$ *and* $CvL_{L/R}$ *are the convex and concave lenses,* $M_{1,2,3,4_{L/R}}$ *are the left and right set of mirrors, and* $E_{L/R}$ *represent the left and right eyes.*

HV-2.0 (fig. 67) consists of eight mirrors, four on each side ($M_{1_{L/R}}$, $M_{2_{L/R}}$, $M_{3_{L/R}}$ and $M_{4_{L/R}}$), for the purpose of redirecting the principal vision vectors ($VV_{F_{L/R}}$) towards the fixation target. Additionally, HV-2.0 uses two convex ($CxL_{L/R}$) and two concave ($CvL_{L/R}$) lenses, in order to constrain the peripheral vision vectors ($VV_{P_{L/R}}$). The JSON configuration of HV-2.0 is shown in appendix B.1.

Mirrors $M1_{L/R}$ and $M4_{L/R}$ are located centrally to the eyes so that the system can provide a larger visual field, when achieving retroversion for: (a) various angles of strabismic deviations, and (b) various directions of a fixation target. Also, the pivots of rotation of $M1_{L/R}$ and $M4_{L/R}$ are located on the following edges, as described in subsection 4.3.5:

- $M1_L$: centre-right
- $M1_R$: centre-left
- $M4_L$: centre-left
- $M4_R$: centre-right

Because $M1_{L/R}$ and $M4_{L/R}$ are very close to each other, if their pivots of rotation were centred, the mirrors would be at risk of colliding with each other when rotating in opposite directions. The pivots of rotation of $M2_{L/R}$ and $M3_{L/R}$ remain central to the mirrors, as there is no risk of collisions. Figure 68 compares the rotation of a mirror when the pivot of rotation is located at the centre and on the right edge of the mirror.

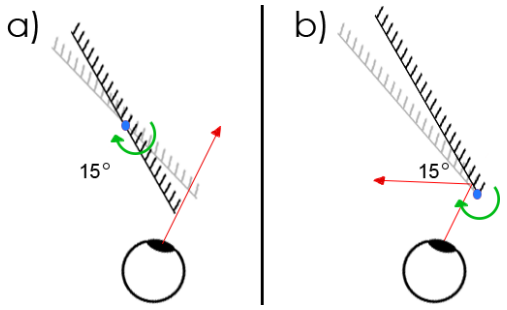

Figure 68: *Pivot of rotation: Comparison of two pivots of rotation. (a) the pivot of rotation (blue dot) located at the centre of the mirror, (b) the pivot of rotation on the right edge of the mirror.*

The default state of HV-2.0, as shown in figure 67, is based on the assumption that the fixation target is located centrally to both eyes at a distance $\geqslant$ 6m from the DEMRS origin. This is because at and beyond 6m the eyes assume their primary position of gaze (see sect. 2.2). Therefore, by default, each mirror is oriented horizontally about the y-axis (yaw rotation) by 45°. Also, the distance between the points of reflection of VV_{F_L} on $M4_L$ and VV_{F_R} on $M4_R$, respectively, is termed the resultant IPD.

HV-2.0 is designed such that $M3{,}4_L$ and $M3{,}4_R$ maintain normal IPD. Furthermore, $M4_L$ and $M4_R$ maintain normal binocular disparity. When HV-2.0 achieves retroversion, a process described in the next subsection, $M3_L$ and $M3_R$ reflect the vision vectors towards $M4_L$ and $M4_R$, which are rotated such that the distance between the point of reflection of VV_{F_L} on $M4_L$ and the

point of reflection of VV_{F_R} on M_{4_R}, i.e. resultant IPD, remains normal. Also, after the rotation of M_{4_L} and M_{4_R}, the angles from which the resultant vision vectors intersect the fixation target maintain normal binocular disparity. The sequence in which a vision vector is reflected by the mirrors, as it travels from the eye to a target (T), is as follows[5]:

$$E \rightarrow M_1 \rightarrow M_2 \rightarrow M_3 \rightarrow M_4 \rightarrow T$$

The lenses were added to the design of the system in order to constrain the direction of the peripheral vision vectors so that they are not reflected by the mirrors in arbitrary directions, and thus escape the system. As shown in figure 69, when lenses are not used (left side only), the peripheral vision vectors are reflected in arbitrary directions, although the principal vision vector is reflected in the direction of the target. This causes confusion in the fused perception of the environment, because the retinal image of the left eye would consist of visual stimuli derived from the target, as well as arbitrary objects from the peripheral environment. However, when lenses are used (fig. 69, right side only) the principal and peripheral vision vectors are directed towards the next mirror, and eventually the target. Therefore, the retinal images would be formed by visual stimuli deriving from the fixation target, and the fused perception of the environment would be normal.

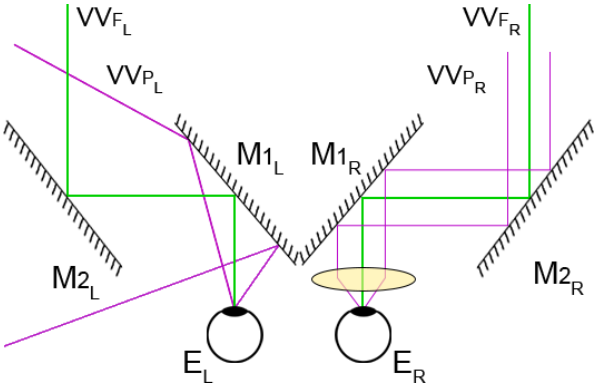

Figure 69: *Using lenses: The first two mirrors on either side of HV-2.0, with and without lenses. A convex lens is not installed on the left side of HV-2.0, therefore the peripheral vision vectors (VV_{P_L}) escape the system. However, because the principal vision vector (VV_{F_L}) is reflected towards the next mirror, and eventually the target, the retinal images would contain the target as well as arbitrary objects in the periphery. A convex lens is installed on the right side of HV-2.0, therefore the vision vectors are constrained within the system and reflected towards the next mirror, and eventually the target.*

5 Naturally, visual stimuli are light rays emanating from a light source, such as the sun, that are reflected by the fixation target before entering the eyes. Consequently, the sequence in which a light ray would be reflected by the mirrors, is: $T \rightarrow M_{4_{L/R}} \rightarrow M_{3_{L/R}} \rightarrow M_{2_{L/R}} \rightarrow M_{1_{L/R}} \rightarrow E_{L/R}$

The design of HV-2.0 satisfies three criteria defined by the principle of retroversion, as follows:

1. The rotations of the mirrors enable the convergence of both principal vision vectors on the same fixation target at near, or parallel vision vectors on fixation targets at far.
2. $M3_{L/R}$ and $M4_{L/R}$ maintain normal IPD.
3. $M4_{L/R}$ maintain normal binocular disparity.

Because HV-2.0 is not designed to retroverse torsional strabismus it is not necessary for this system to maintain normal orientation of the visual stimuli, which is the fourth criterion of the principle of retroversion.

4.4.2 *Retroversion Algorithm*

In order to maintain normal resultant IPD and normal resultant binocular disparity, it is imperative to determine the point of reflection of $VV_{F_{L/R}}$ on $M4_{L/R}$. These points are referred to as last points of reflection (LPR), where each LPR determines the point on the surface of $M4_{L/R}$ that $VV_{F_{L/R}}$ must be reflected so that normal binocular disparity is maintained. Additionally, the distance between both LPR is used to maintain normal resultant IPD. However, because the visual direction of a strabismic eye deviates from the fixation target, HV-2.0 uses two auxiliary vision vectors (VV_{A_L} and VV_{A_R}), which represent both principal vision vectors under normal BSV (fig. 70). Therefore, both LPR are determined by the points of intersection between $VV_{A_{L/R}}$ and $M4_{L/R}$.

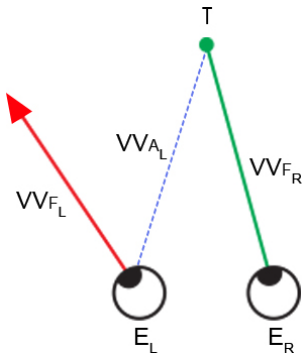

Figure 70: *Auxiliary vision vector: Left auxiliary vision vector* VV_{A_L} *created from a left exotropic eye* (E_L) *and target* T. *Because* E_R *is the normal eye,* VV_{A_R} *overlaps with* VV_{F_R} *and, therefore, is not shown in this figure.*

CHAINED RETROVERSION Initially, DEMRS HV-2.0 was based on an algorithm called chained retroversion, which sequentially calculates the orientation of the mirrors in an orderly fashion starting from $M1_{L/R}$ to $M4_{L/R}$. More specifically, the chained retroversion algorithm calculates the angles of each mirror such that $VV_{F_{L/R}}$ is, firstly, reflected by $M1_{L/R}$ to the centre of $M2_{L/R}$. Secondly, the reflected $VV_{F_{L/R}}$ is reflected by $M2_{L/R}$ to the centre of $M3_{L/R}$, and thirdly, by $M3_{L/R}$ to the LPR of $M4_{L/R}$. Lastly, the reflected $VV_{F_{L/R}}$ is reflected by $M4_{L/R}$ to the fixation target. The order in which the mirrors rotate in chained retroversion is: $M1_{L/R} \rightarrow M2_{L/R} \rightarrow M3_{L/R} \rightarrow M4_{L/R}$.

Because of the orderly rotation of the mirrors and the pivot of rotation of $M4_{L/R}$, when $VV_{F_{L/R}}$ is reflected by $M4_{L/R}$, an offset is generated during the rotation of $M4_{L/R}$ (fig. 71). Therefore, the point where $VV_{F_{L/R}}$ is reflected by $M4_{L/R}$ is not the LPR (fig. 71). The offset is the distance between the LPR on $M4_{L/R}$ and the point where $VV_{F_{L/R}}$ is reflected by $M4_{L/R}$ (fig. 71).

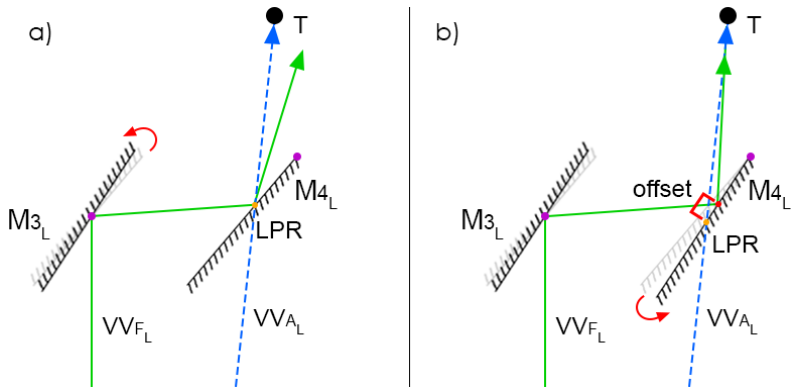

Figure 71: *Offset created by chained retroversion: The orange/yellow point shows the* LPR, *whereas the red point shows where the principal vision vector (VV_{F_L}) is reflected by $M4_L$. The purple points indicate the pivot of rotation of each mirror and the dashed blue line is the auxiliary vision vector, used to calculate the* LPR. *(a) before rotating $M4_L$, the point where VV_{F_L} is reflected by $M4_L$ is the* LPR. *However, because VV_{F_L} does not direct towards the target* T, *$M4_L$ must rotate. The offset is shown in (b) where $M4_L$ has rotated and the* LPR *is no longer the point of reflection between VV_{F_L} and $M4_L$.*

For example, in figure 71, $M3_L$ has been rotated so that VV_{F_L} can be reflected by $M3_L$ to the LPR on $M4_L$. But when $M4_L$ rotates, in order to direct VV_{F_L} towards the target, the LPR changes and the offset is generated. Theoretically, if the pivot of rotation of $M4_L$ was also the LPR, the offset would not be generated because the LPR would remain constant, even after the rotation of $M4_L$. But the LPR cannot be constant because it is calculated based on the location of the target[6]. Unfortunately, this offset may increase or decrease the resultant IPD and binocular disparity, thereby invalidating

6 The pivot of rotation could be dynamic, i.e. assume the position of the LPR, but it is not a practical solution to this problem.

two of the criteria of the principle of retroversion. As explained later in this chapter, small offsets are insignificant to the retroversion of strabismus but larger offsets can cause problems in the fusibility of the visual stimuli.

BIDIRECTIONAL RETROVERSION In order to address the offset problem with chained retroversion, another algorithm was developed called bidirectional retroversion. Compared to chained retroversion, bidirectional retroversion calculates the precise orientation of the mirrors such that no offset is generated when $M4_{L/R}$ rotates. In addition, the algorithm can be split into the following two concurrent tasks:

1. The first task calculates the orientation of $M1_{L/R}$ so that $VV_{F_{L/R}}$ can be reflected by $M1_{L/R}$ to the centre of $M2_{L/R}$. Next, the orientation of $M2_{L/R}$ is calculated so that the reflected $VV_{F_{L/R}}$ can be reflected by $M2_{L/R}$ to the centre of $M3_{L/R}$.
2. The second task uses an inverted $VV_{F_{L/R}}$, noted by $INV_V V_{F_{L/R}}$, that originates from the target and directs to the fovea. In this task the orientation of $M4_{L/R}$ is calculated so that the $INV_V V_{F_{L/R}}$ can be reflected by the LPR, on $M4_{L/R}$, to the centre of $M3_{L/R}$. Next, the orientation of $M3_{L/R}$ is calculated so that the reflected $INV_V V_{F_{L/R}}$ can be reflected by $M3_{L/R}$ to the centre of $M2_{L/R}$.

The following pseudocode presents the bidirectional retroversion algorithm:

Algorithm 1: Bidirectional Retroversion of HV-2.0

```
Begin
    vv_f ← principal vision vector;
    inv_vv_f ← inverse principal vision vector;
    vv_a ← auxiliary vision vector;
    lpr = intersection(vv_a, M4);
    // ----- Task 1 -----
    for m in [M1, M2] do
        poi = intersection(vv_f, m);
        updated_vv = reflection(vv_f, m);
        next_poi = intersection(updated_vv, m + 1);
        if next_poi not central to m + 1 then
            rotate m so that updated_vv is reflected centrally to m + 1;
        end
        update(vv_f);
    end
```

continue on next page...

(continue begin)

```
// ----- Task 2 -----
for m in [M4, M3] do
    poi = intersection(inv_vvf, m);
    updated_vv = reflection(inv_vvf, m);
    next_poi = intersection(updated_vv, m + 1);
    if next_poi not central to m + 1 then
        rotate m so that updated_vv is reflected centrally to m + 1;
    end
    update(inv_vvf);
end
end
```

PIVOTED ROTATIONS According to the law of reflection, discussed in appendix B.2.2, when a mirror rotates by an angle ϕ, the reflected vision vector will rotate by an angle of 2ϕ. Therefore, as shown in figure 72a, in order to change the direction of an incident ray ($\vec{I_A}$) such that the reflected ray can pass through point G, instead of point B, the mirror must rotate by half of the angle between $\angle$BYG, where Y is the point that $\vec{I_A}$ intersects the mirror. Also, Y is the pivot of rotation (P) of the mirror (fig. 72a). However, as shown in figure 72b, when $Y \neq P$, and a mirror rotates by half of the angle between $\angle$BYG, the reflected ray does not pass through point G.

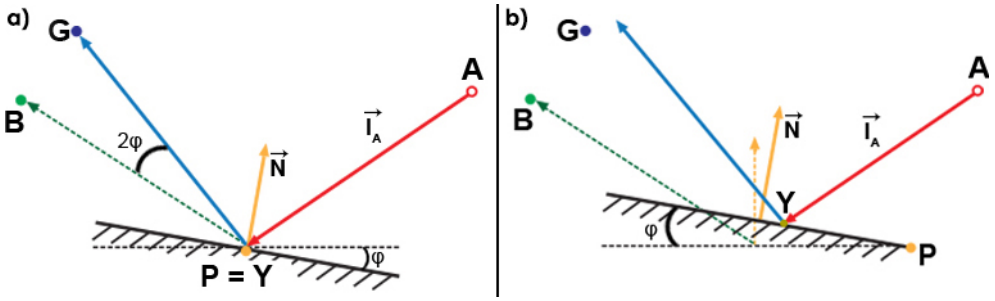

Figure 72: *Pivoted rotation problem: Two examples where a mirror is rotated by an angle ϕ. In (a), the mirror rotates about a pivot P whereas, in (b), the mirror rotates about a pivot P located on the edge of the mirror. B is the point that the reflected ray (green) passes through before the mirror rotates. G is the point that the reflected ray (blue) intends to pass through after the mirror has rotated. The incident ray (red) starts from A and has direction $\vec{I_A}$. The mirror is the black horizontal line with a pivot of rotation P and normal vector $\vec{N}$. Y is the point of reflection between $\vec{I_A}$ and the mirror.*

Appendix B.3 describes a deterministic geometric solution to this problem, such that when a mirror rotates about an arbitrary pivot P, where $P \neq Y$, the resultant reflection vector passes through point G.

4.4.3 *Simulations*

A series of simulations were performed in order to evaluate the effectiveness of HV-2.0 in the retroversion of normal BSV and strabismus at near ($\leqslant$ 1m), mid ($\approx$ 3m) and far ($\geqslant$ 6m) fixation targets, and at various directions from the DEMRS origin. As previously discussed in subsection 3.3.1 latent deviations (phorias), occur only when binocularity is voluntarily or involuntarily disrupted. Until then, normal BSV is present. Consequently, although normal BSV does not require retroversion, a DRS compliant system must be able to retroverse normal BSV, in order to compensate for a phoria. In the following simulations, the eyes are assigned an IPD of 6cm, and the DEMRS simulator is configured via the JSON configuration file of HV-2.0 (see appendix B.1). Table 4 presents the default positions and rotations of each convex lens (Cx), concave lens (Cv) and mirror (M) of HV-2.0 in the DEMRS simulator.

Table 4: *Configuration of components in HV-2.0.*

Default	Translation (cm)			Rotation (°)		
	x	y	z	x (pitch)	y (yaw)	z (roll)
Cx_L	3.000	0.000	2.000	−180.000	0.000	−180.000
$M1_L$	0.510	0.000	2.500	−180.000	−45.000	−180.000
$M2_L$	17.000	0.000	6.990	0.000	45.000	0.000
$M3_L$	17.000	0.000	18.010	−180.000	45.000	180.000
$M4_L$	0.510	0.000	22.500	0.000	−45.000	0.000
Cv_L	3.000	0.000	23.500	−180.000	0.000	0.000
Cx_R	−3.000	0.000	2.000	−180.000	0.000	180.000
$M1_R$	−0.510	0.000	2.500	−180.000	45.000	180.000
$M2_R$	−17.000	0.000	6.990	0.000	−45.000	0.000
$M3_R$	−17.000	0.000	18.010	−180.000	−45.000	−180.000
$M4_R$	−0.510	0.000	22.500	0.000	45.000	0.000
Cv_R	−3.000	0.000	23.500	−180.000	0.000	0.000

In the following simulations, when the fixation target (T) is located at a distance of $<$ 6m from the DEMRS origin, retroversion is successful when both principal vision vectors pass through T. When T is located at a distance $\geqslant$ 6m from the DEMRS origin, retroversion is successful if each principal vision vector passes through the corresponding parallel target Tp_L and Tp_R. Additionally, the resultant binocular disparity must be within the range of $horizontal : 3°, vertical : 1.5°, torsional : 1.5°$, which represents Panum's fusible binocular disparity (see subsect. 2.4.4).

To aid clarity in the visualization of the simulations:

- The eyes are illustrated as two textured 3D models.
- The principal vision vectors are drawn in green when retroversion succeeds, and red when retroversion fails. The peripheral vision vectors are drawn in sky blue, whereas the auxiliary vision vector of the deviating eye is depicted as a white dashed line. The original principal vision vectors of the eyes are the light blue lines unaffected by the system.
- The mirrors are illustrated as light grey flat surfaces.
- The convex and concave lenses are depicted as light yellow and dark yellow meshes at each end of the system.
- The fixation target T is illustrated as a deep pink point circle, whereas Tp_L and Tp_R are illustrated as two smaller purple circles.

Initially, HV-2.0 was simulated with and without lenses, in order to compare the efficacy of the lenses in constraining peripheral vision vectors during retroversion. In this test normal vision is simulated where both eyes fixate on the target, located centrally at a distance of 6m from the DEMRS origin. As shown in figure 73a, if the lenses are not used some of the peripheral vision vectors are reflected in arbitrary directions, away from the target. When lenses are used (fig 73b), the peripheral vision vectors are reflected in the direction of the target. Figure 73 shows that both principal vision vectors are coloured in green because they successfully pass through $Tp_{L/R}$. However, without lenses the peripheral vision vectors scatter, and escape the system (right of fig. 73c). With lenses, the vision vectors are parallel, and contained within the system (left of fig. 73c).

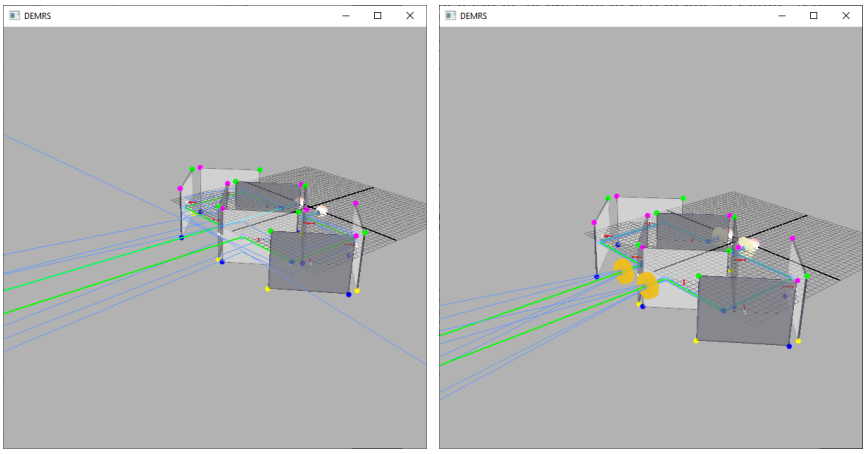

(a) *HV-2.0 without lenses.* (b) *HV-2.0 with lenses.*

Figure 73: *(continued on next page)*

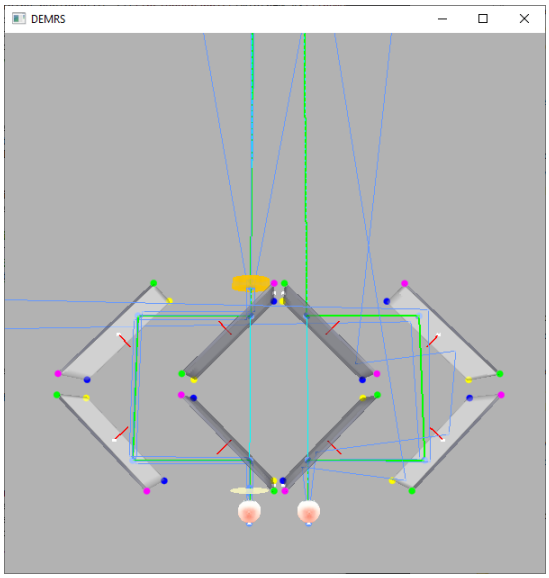

(c) *comparison with and without lenses.*

Figure 73: *Simulation with lenses and mirrors: (a) and (b) show the efficacy of the lenses in HV-2.0. (c) the lenses are added to the left side of the system only in order to compare the direction and arrangement of the vision vectors on both sides.*

Figure 74a shows that displaying peripheral vision vectors, in simulation, reduces the clarity of the results and, compared to figure 74b, the visibility of the principal vision vectors is obscured. Therefore, the following screenshots of the simulation do not show peripheral vision vectors and lenses.

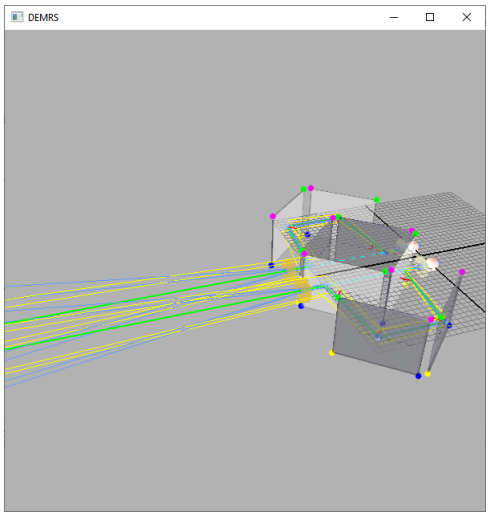

(a) *visible peripherals.*

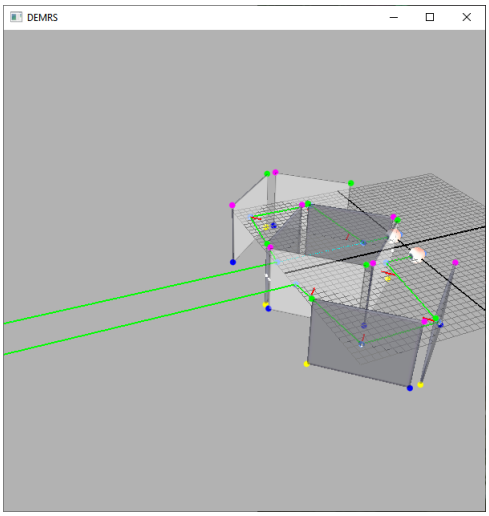

(b) *hidden peripherals.*

Figure 74: *Showing the peripherals: Part (a) is cluttered with peripheral vision vectors, whereas in (b), the principal vision are clearly displayed.*

Four simulations were performed, assuming normal BSV, whereby both eyes fixate on a target located: (a) centrally, at far distance of 6m, (b) centrally, at near distance of 80cm, (c) up, i.e. on the positive y-axis, at mid distance of 2m, and (d) left, i.e. on the positive x-axis, at far distance of 7m. In the following simulations, the distance of the target from the DEMRS origin is given in cm, such that a target located centrally at a distance of 6m would be presented as $T = \{0, 0, 600\}$. Figures 75, 76, 77 and 78 show screenshots before and after retroversion. Tables 5, 6, 7 and 8 present the angles of the mirrors required to achieve retroversion.

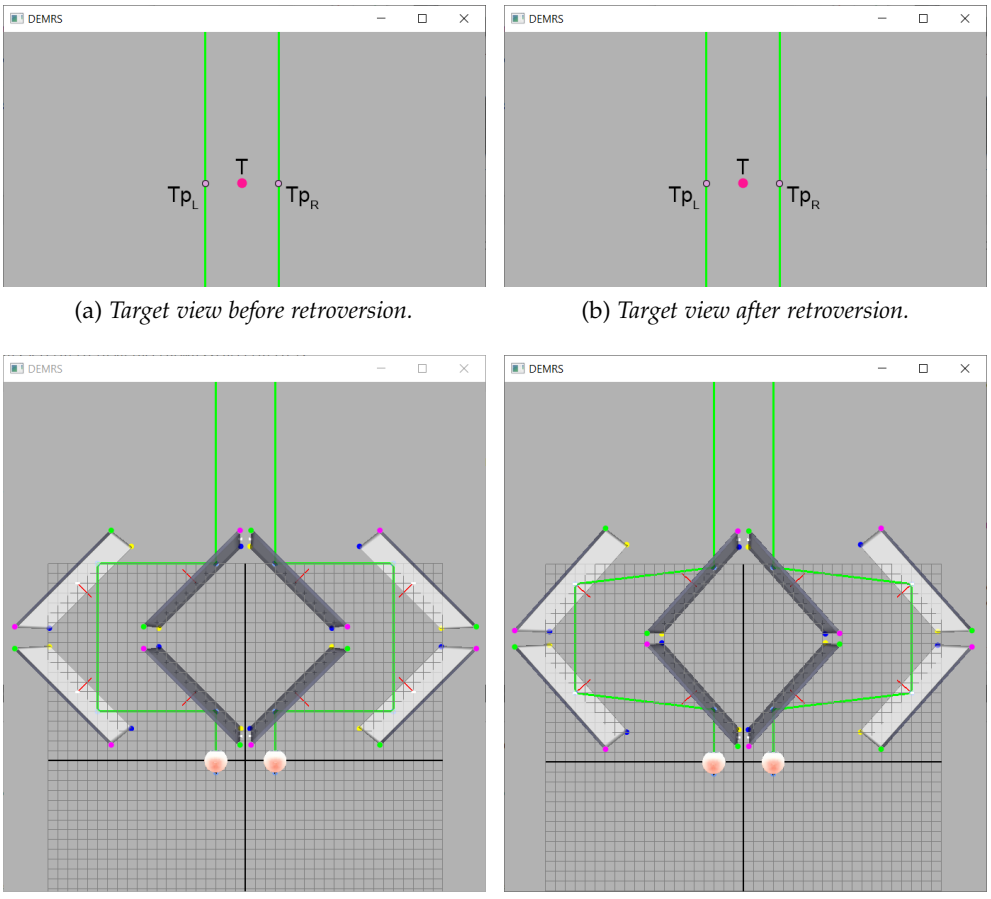

(a) *Target view before retroversion.* (b) *Target view after retroversion.*

(c) *Before retroversion.* (d) *After retroversion.*

Figure 75: *DEMRS HV-2.0 retroversion where* $T = \{0, 0, 600\}$*: Screenshots of simulations before (c) and after (d) retroversion of normal BSV, where* $T = \{0, 0, 600\}$*. Because of the far distance of the target from the DEMRS origin, the target is not visible in (c) and (d). Therefore two additional screenshots were taken from a close up view of the target and principal vision vectors, where (a) is the extension of (c), and (b) is the extension of (d).*

Table 5: *DEMRS HV-2.0 retroversion angles for normal BSV, where* $T = \{0, 0, 600\}$.

Components	Retroversion (°)		
	x (pitch)	y (yaw)	z (roll)
$M1_L$	0.000	3.427	0.000
$M2_L$	0.000	3.427	0.000
$M3_L$	0.000	−3.427	0.000
$M4_L$	0.000	−3.427	0.000
$M1_R$	0.000	−3.427	0.000
$M2_R$	0.000	−3.427	0.000
$M3_R$	0.000	3.427	0.000
$M4_R$	0.000	3.427	0.000

In figure 75 prior to retroversion, both principal vision vectors ($VV_{F_{L/R}}$) were shown in green, which means that they pass through Tp_L and Tp_R even when the mirrors remain at default orientation. Consequently, no retroversion is required by HV-2.0 when the target is located centrally at a distance of 6m or more. This is because, when both eyes are at rest, the $VV_{F_{L/R}}$ have directions of $< 0, 0, 1 >$, and since T is located centrally at a distance of 6m each parallel target $Tp_{L/R}$ is located straight ahead of each eye $E_{L/R}$, respectively. However, prior to retroversion, the $VV_{F_{L/R}}$ were not reflected by the centres of $M2_{L/R}$ and $M3_{L/R}$, whereas after retroversion, the $VV_{F_{L/R}}$ were reflected by the centres of $M2_{L/R}$ and $M3_{L/R}$. The benefit of $VV_{F_{L/R}}$ being centrally reflected by $M2_{L/R}$ and $M3_{L/R}$ is that the peripheral vision vectors do not escape the system.

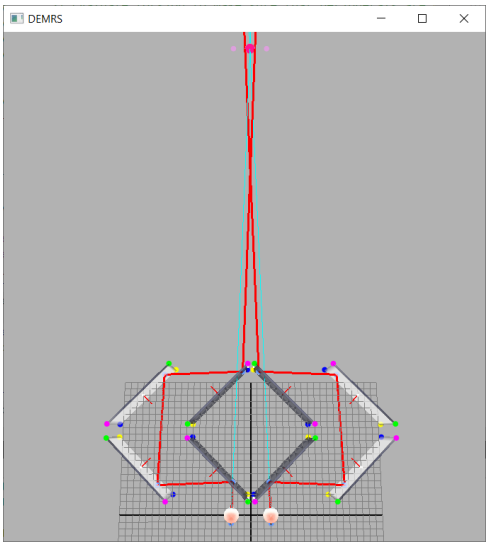

(a) *Before retroversion.*

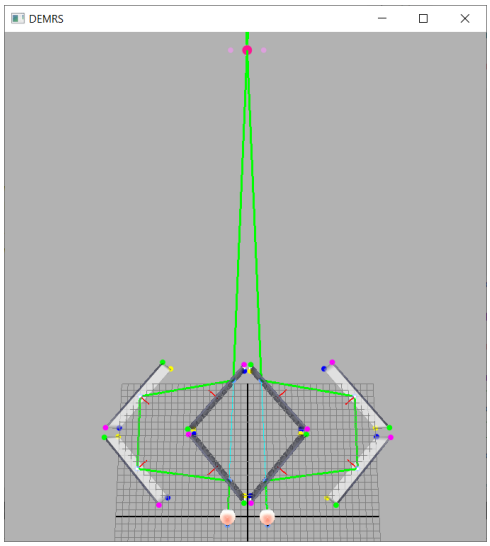

(b) *After retroversion.*

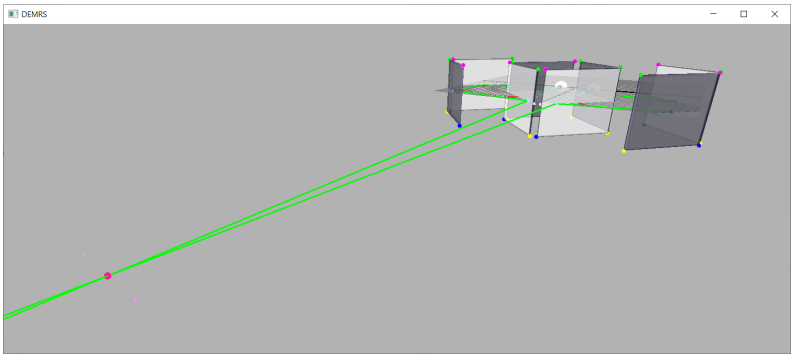

(c) *After retroversion.*

Figure 76: *DEMRS HV-2.0 retroversion where* $\mathsf{T} = \{0, 0, 80\}$*: Screenshots of simulations before (a) and after (b) retroversion of normal BSV, where* $\mathsf{T} = \{0, 0, 80\}$*. Part (c) shows a different perspective view of the target.*

Table 6: *DEMRS HV-2.0 retroversion angles for normal BSV, where* $\mathsf{T} = \{0, 0, 80\}$.

Components	Retroversion (°)		
	x (pitch)	y (yaw)	z (roll)
$M1_L$	0.000	4.663	0.000
$M2_L$	0.000	3.589	0.000
$M3_L$	0.000	−4.854	0.000
$M4_L$	0.000	−3.780	0.000
$M1_R$	0.000	−4.663	0.000
$M2_R$	0.000	−3.589	0.000
$M3_R$	0.000	4.854	0.000
$M4_R$	0.000	3.780	0.000

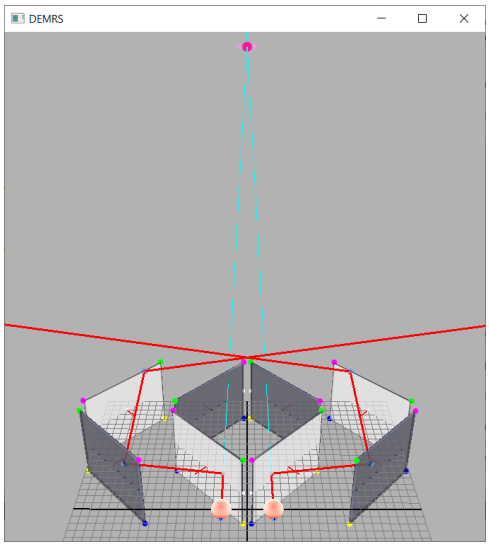

(a) *Before retroversion.*

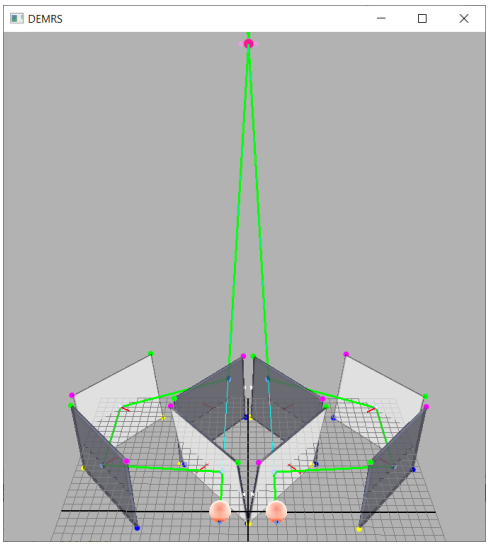

(b) *After retroversion.*

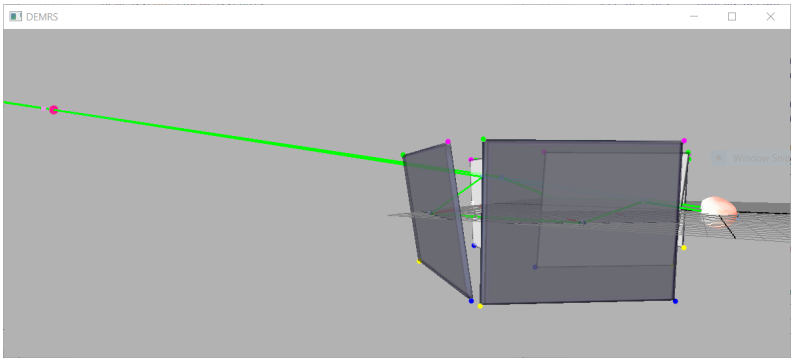

(c) *After retroversion.*

Figure 77: *DEMRS HV-2.0 retroversion where* $\mathsf{T} = \{0, 30, 200\}$*: Screenshots of simulations before (a) and after (b) retroversion of normal BSV, where* $\mathsf{T} = \{0, 30, 200\}$*. Part (c) shows a side view of the simulation and target.*

Table 7: *DEMRS HV-2.0 retroversion angles for normal BSV, where* $\mathsf{T} = \{0, 30, 200\}$.

Components	Retroversion (°)		
	x (pitch)	y (yaw)	z (roll)
$M1_L$	−6.480	4.284	0.000
$M2_L$	1.760	3.610	0.000
$M3_L$	6.717	−3.888	0.000
$M4_L$	−1.894	−3.611	0.000
$M1_R$	−6.480	−4.284	0.000
$M2_R$	1.760	−3.610	0.000
$M3_R$	6.717	3.888	0.000
$M4_R$	−1.894	3.611	0.000

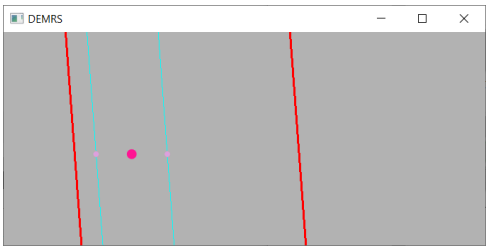

(a) *Target view before retroversion.*

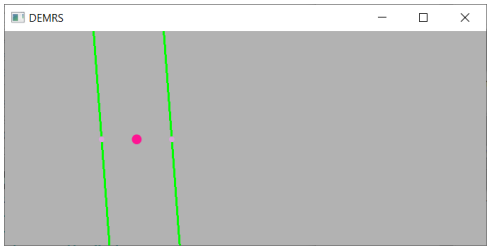

(b) *Target view after retroversion.*

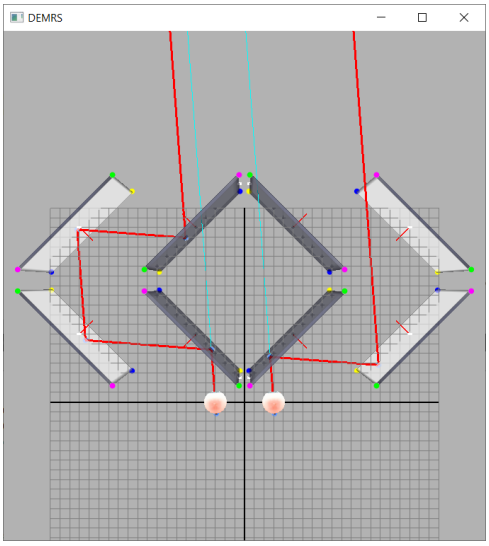

(c) *Before retroversion.*

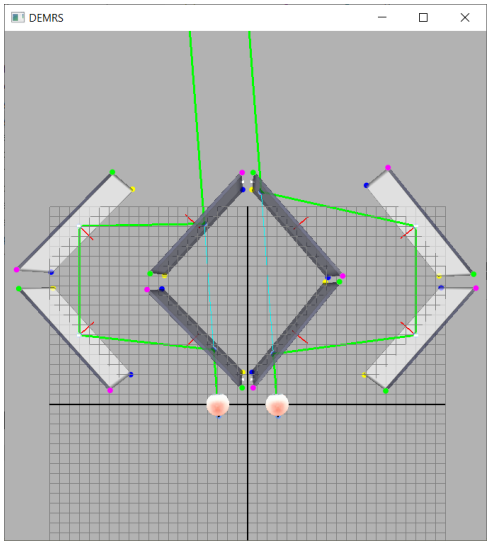

(d) *After retroversion.*

Figure 78: *DEMRS HV-2.0 retroversion where* $\mathsf{T} = \{45, 0, 700\}$*: Screenshots of simulations before (c) and after (d) retroversion of normal BSV, where* $\mathsf{T} = \{45, 0, 700\}$*. The target is not visible in (c) and (d),because of the far distance of the target from the DEMRS origin. Therefore two additional screenshots were taken from a close up view of the target and principal vision vectors, where (a) is the extension of (c), and (b) is the extension of (d).*

Table 8: *DEMRS HV-2.0 retroversion angles for normal BSV, where* $\mathsf{T} = \{45, 0, 700\}$.

Components	Retroversion (°)		
	x (pitch)	y (yaw)	z (roll)
$M1_L$	0.000	1.790	0.000
$M2_L$	0.000	3.221	0.000
$M3_L$	0.000	−1.518	0.000
$M4_L$	0.000	−2.949	0.000
$M1_R$	0.000	−5.075	0.000
$M2_R$	0.000	−3.644	0.000
$M3_R$	0.000	5.328	0.000
$M4_R$	0.000	3.897	0.000

Five more tests were performed under the assumption that strabismus is present. In the following tests, the target T was located: (a) centrally, at near distance of 1m, (b) right, i.e. on the negative x-axis, at mid distance of 2m, (c) down, i.e. on the negative y-axis, at mid distance of 3m, (d) centrally, at far distance of 8m, and (e) centrally, at mid distance of 2m. In order to determine that retroversion is achieved for various types of strabismus, a different type of artificial strabismus was assumed in each test, namely: (a) left exo-tropia with large deviation of 25° (≈ 50Δ), (b) right hypo-tropia with moderate deviation of 12° (≈ 24Δ), (c) left hyper-tropia with small deviation of 8° (≈ 16Δ), (d) right eso-tropia with micro deviation of 5° (≈ 10Δ), and (e) left exo-hyper-tropia with moderate deviation of 12° (≈ 24Δ) exo and 6° (12Δ) hyper. Figures 79, 80, 81, 82 and 83 show the results before and after retroversion. Tables 9, 10, 11, 12 and 13 present the retroversion angles of the mirrors required to achieve retroversion.

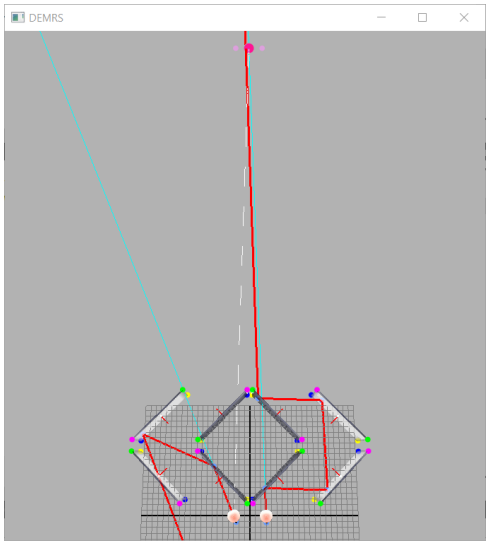

(a) *Before retroversion.*

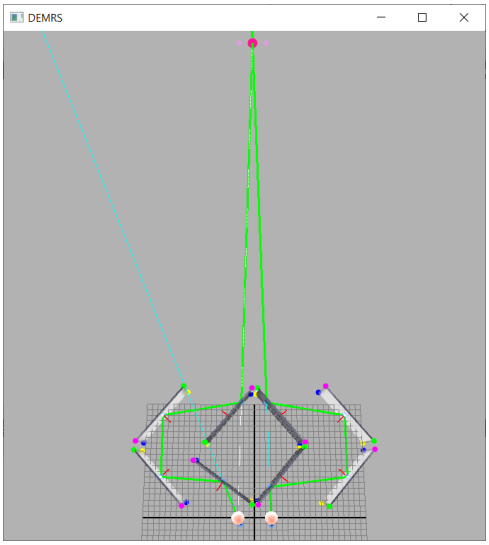

(b) *After retroversion.*

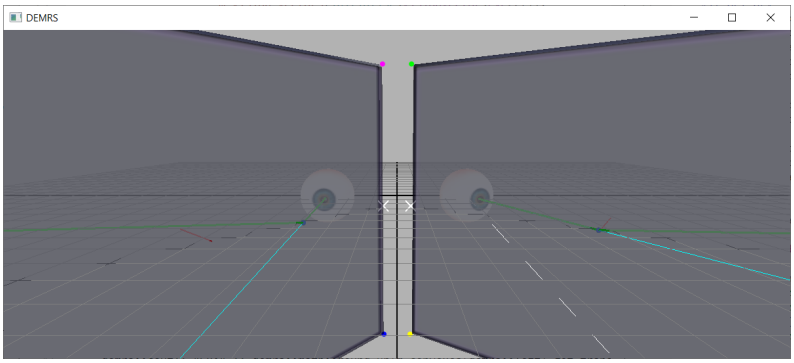

(c) *After retroversion.*

Figure 79: *DEMRS HV-2.0 retroversion where* $T = \{0, 0, 100\}$*: (continued on next page)*

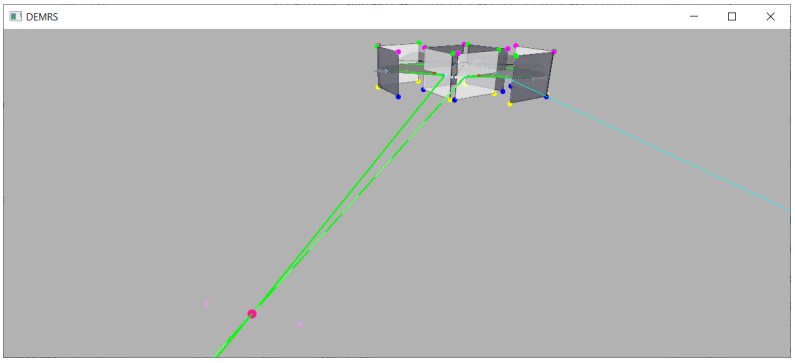

(d) *After retroversion.*

Figure 79: *DEMRS HV-2.0 retroversion where* $T = \{0, 0, 100\}$*: Screenshots of simulations before (a) and after (b) retroversion for a left exo-tropia with large deviation* 25° *(*$\approx 50\Delta$*), where* $T = \{0, 0, 100\}$*. (c) close up view of the strabismic deviation showing the original and auxiliary vision vectors. (d) the result from a perspective view of the target.*

Table 9: *DEMRS HV-2.0 retroversion angles for left exo-tropia with large deviation of* 25° *(*$\approx 50\Delta$*), where* $T = \{0, 0, 100\}$*.*

Components	Retroversion (°)		
	x (pitch)	y (yaw)	z (roll)
$M1_L$	0.000	9.229	0.000
$M2_L$	0.000	−2.412	0.000
$M3_L$	0.000	4.525	0.000
$M4_L$	0.000	3.665	0.000
$M1_R$	0.000	4.371	0.000
$M2_R$	0.000	3.512	0.000
$M3_R$	0.000	−4.525	0.000
$M4_R$	0.000	−3.665	0.000

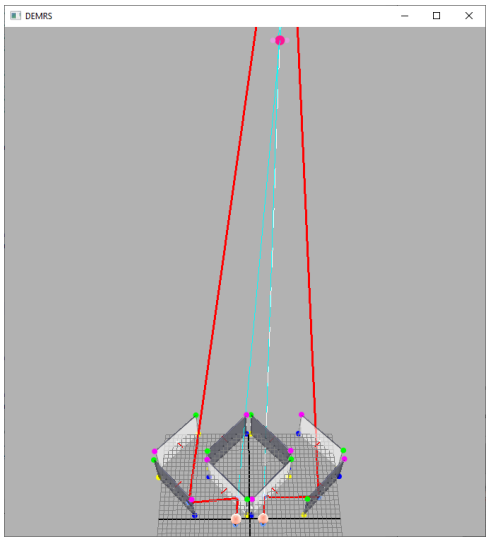

(a) *Before retroversion.*

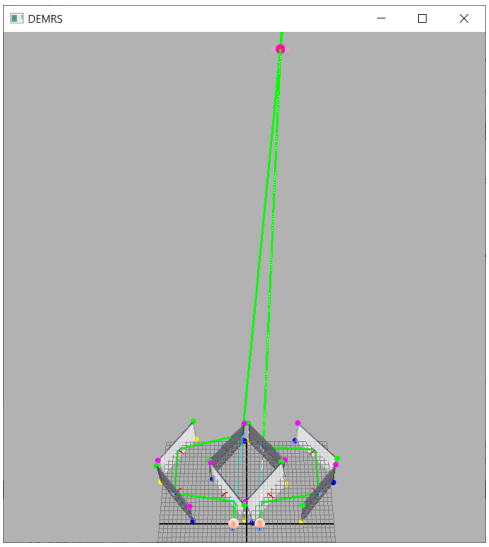

(b) *After retroversion.*

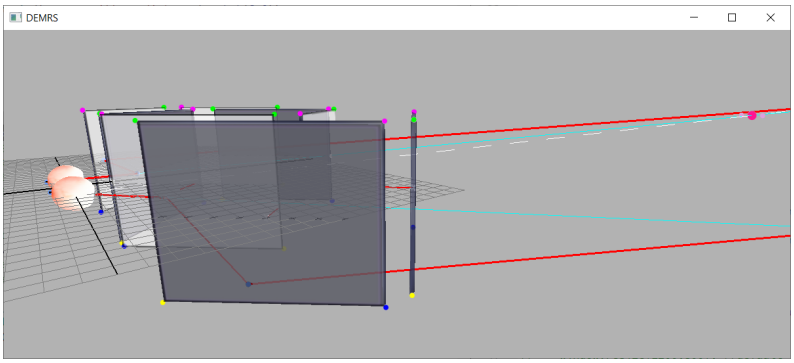

(c) *After retroversion.*

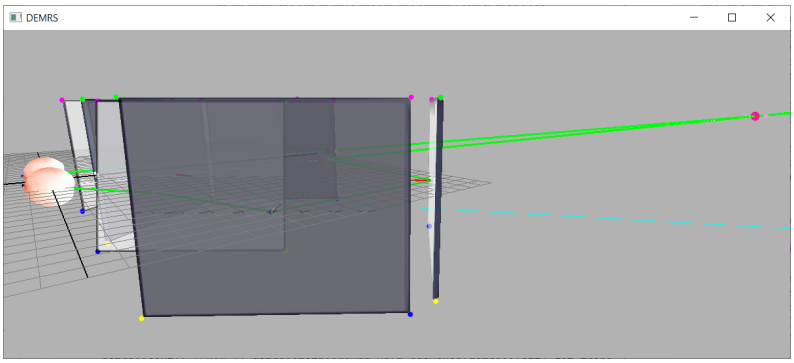

(d) *After retroversion.*

Figure 80: *DEMRS HV-2.0 retroversion where* $\mathsf{T} = \{-15, 0, 200\}$*: Screenshots of simulations before (a) and after (b) retroversion of a right hypo-tropia with moderate deviation of* 12° *(*$\approx 24\Delta$*), where* $\mathsf{T} = \{-15, 0, 200\}$*. Because the hypo deviation is not clearly seen from a top views (a,b), two additional screenshots (c, d) were taken from a side view of the system in order to emphasize the direction of the original and retroverted vision vectors.*

Table 10: *DEMRS HV-2.0 retroversion angles for right hypo-tropia with moderate deviation of* 12° *(*$\approx 24\Delta$*), where* $\mathsf{T} = \{-15, 0, 200\}$.

Components	Retroversion (°)		
	x (pitch)	y (yaw)	z (roll)
$M1_L$	0.000	−7.103	0.000
$M2_L$	0.000	−3.823	0.000
$M3_L$	0.000	5.643	0.000
$M4_L$	0.000	2.170	0.000
$M1_R$	12.759	1.808	0.000
$M2_R$	−3.200	3.521	0.000
$M3_R$	0.000	−0.236	0.000
$M4_R$	0.000	−2.665	0.000

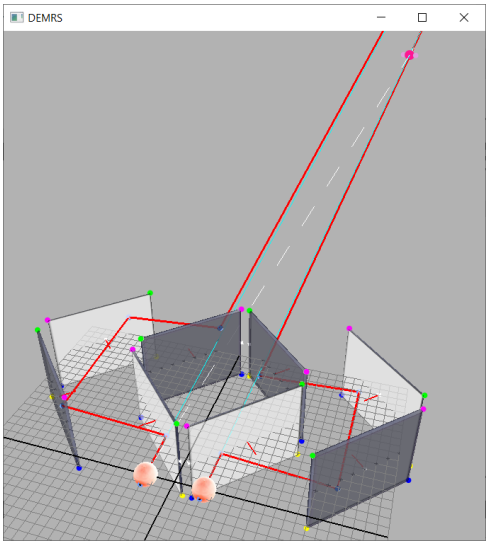

(a) *Before retroversion.*

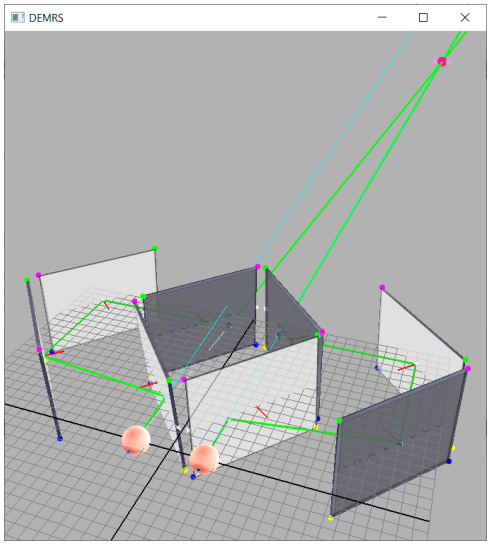

(b) *After retroversion.*

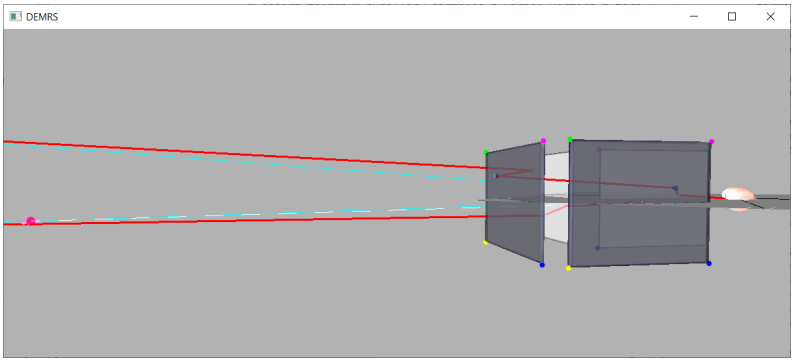

(c) *Before retroversion.*

Figure 81: *DEMRS HV-2.0 retroversion where* $\mathsf{T} = \{0, -20, 300\}$*:* *(continued on next page)*

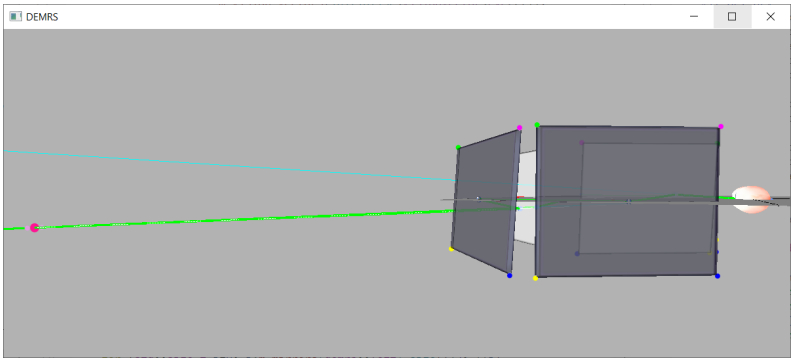

(d) *After retroversion.*

Figure 81: *DEMRS HV-2.0 retroversion where* $\mathsf{T} = \{0, -20, 300\}$*: Screenshots of simulations before (a) and after (b) retroversion of a left hyper-tropia with a small deviation of* 8° *(*$\approx 16\Delta$*), where* $\mathsf{T} = \{0, -20, 300\}$*. (c) and (d) side views of the simulations emphasizing the locations of the target, and original vision vectors.*

Table 11: *DEMRS HV-2.0 retroversion angles for left hyper-tropia with a small deviation of* 8° *(*$\approx 16\Delta$*), where* $\mathsf{T} = \{0, -20, 300\}$*.*

Components	Retroversion (°)		
	x (pitch)	y (yaw)	z (roll)
$M1_L$	−2.297	−3.766	0.000
$M2_L$	0.584	−3.455	0.000
$M3_L$	−5.879	3.636	0.000
$M4_L$	1.553	3.512	0.000
$M1_R$	5.719	3.968	0.000
$M2_R$	−1.450	3.521	0.000
$M3_R$	−5.879	−3.636	0.000
$M4_R$	1.553	−3.512	0.000

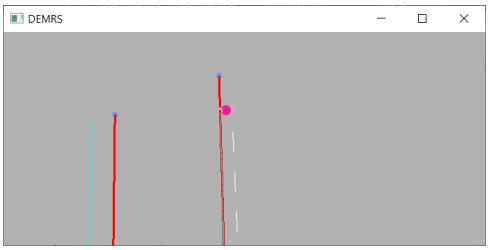

(a) *Before retroversion.*

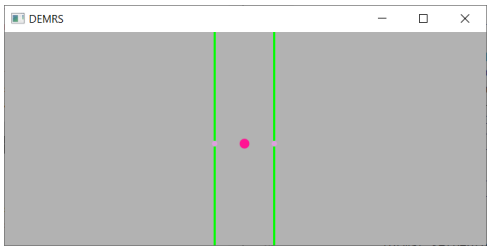

(b) *After retroversion.*

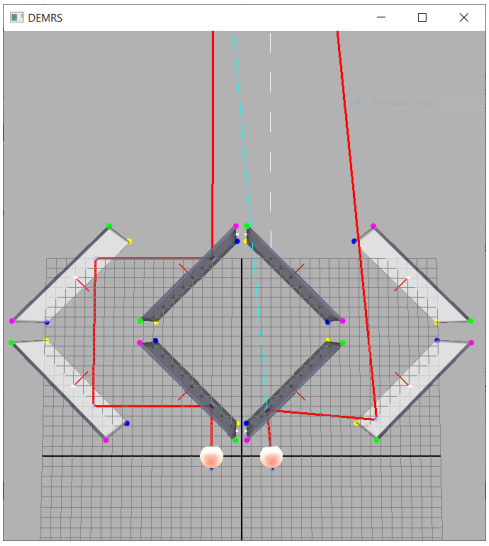

(c) *Before retroversion.*

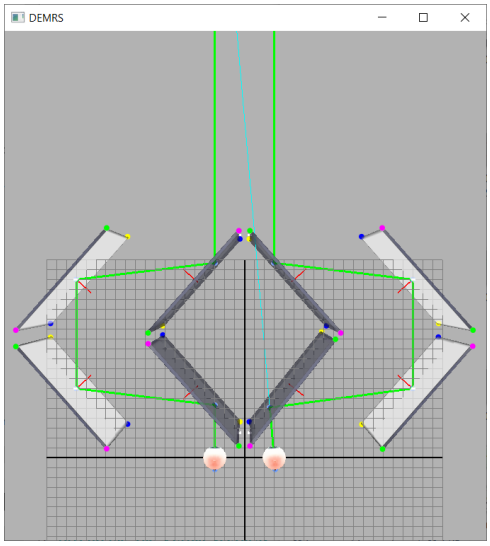

(d) *After retroversion.*

Figure 82: *DEMRS HV-2.0 retroversion where* $\mathsf{T} = \{0, 0, 800\}$*: Screenshots of simulations before (a) and after (b) retroversion of a right eso-tropia with micro deviation of* 5° *(*$\approx 10\Delta$*), where* $\mathsf{T} = \{0, 0, 800\}$*. Because of the far distance of the target from the DEMRS origin, the target is not visible in (c) and (d). Therefore two screenshots were taken from a close up view of the target and principal vision vectors, where (a) is the extension of (c), and (b) is the extension of (d).*

Table 12: *DEMRS HV-2.0 retroversion angles for right eso-tropia with micro deviation of* 5° *(*$\approx 10\Delta$*), where* $\mathsf{T} = \{0, 0, 800\}$*.*

Components	Retroversion (°)		
	x (pitch)	y (yaw)	z (roll)
$M1_L$	0.000	−3.408	0.000
$M2_L$	0.000	−3.408	0.000
$M3_L$	0.000	3.408	0.000
$M4_L$	0.000	3.408	0.000
$M1_R$	0.000	6.219	0.000
$M2_R$	0.000	3.719	0.000
$M3_R$	0.000	−3.408	0.000
$M4_R$	0.000	−3.408	0.000

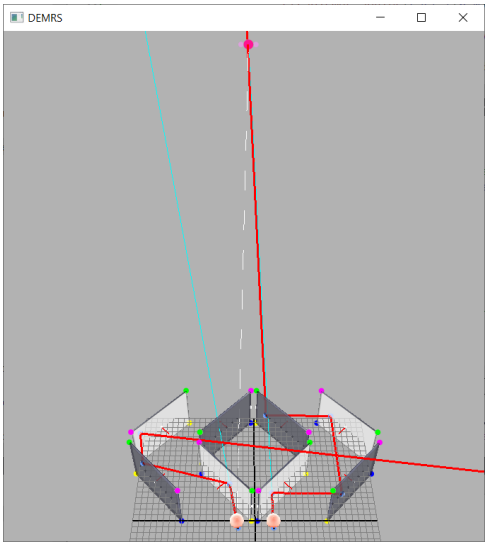

(a) *Before retroversion.*

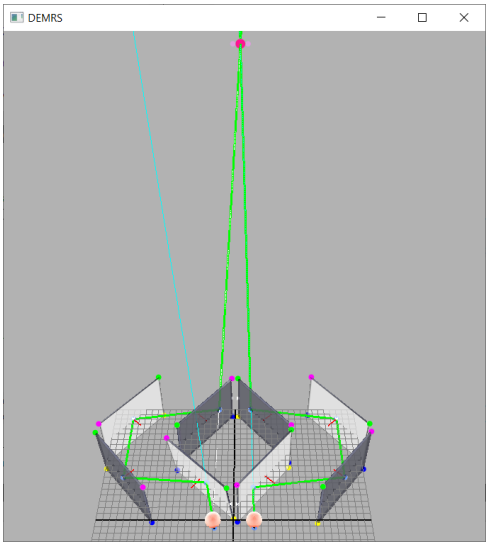

(b) *After retroversion.*

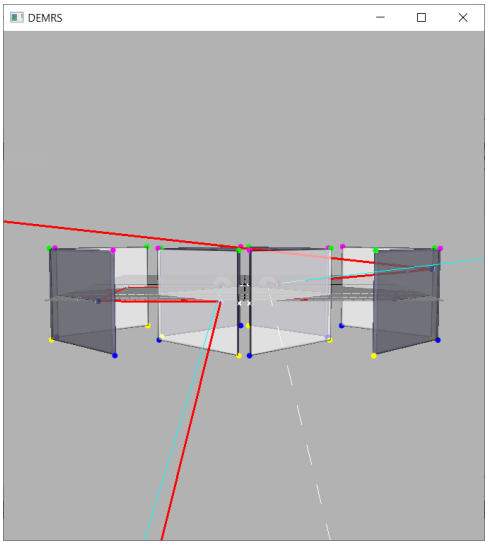

(c) *Before retroversion.*

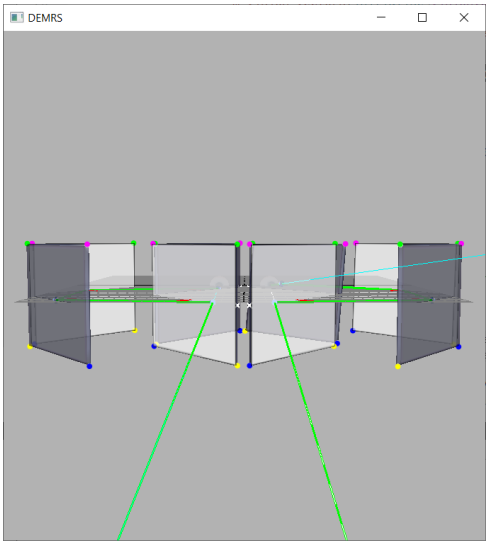

(d) *After retroversion.*

Figure 83: *DEMRS HV-2.0 retroversion where* $T = \{0, 0, 200\}$*: Screenshots of simulations before (a) and after (b) retroversion of a left exo-hyper-tropia with moderate deviation of* 12° *(*$\approx 24\Delta$*) exo and* 6° *(*12Δ*) hyper, where* $T = \{0, 0, 200\}$*. Because of the hyper deviation, which is not clearly seen from a top view (a,b), two additional screenshots were taken (c, d) from a front view of the system that show the direction of the original and retroverted vision vectors.*

Table 13: *DEMRS HV-2.0 retroversion angles for left exo-hyper-tropia with moderate deviation of* 12° (≈ 24Δ) *exo and* 6° (12Δ) *hyper, where* $T = \{0, 0, 200\}$.

Components	Retroversion (°)		
	x (pitch)	y (yaw)	z (roll)
$M1_L$	−7.055	2.411	0.000
$M2_L$	1.801	−2.951	0.000
$M3_L$	0.000	3.967	0.000
$M4_L$	0.000	3.537	0.000
$M1_R$	0.000	3.889	0.000
$M2_R$	0.000	3.460	0.000
$M3_R$	0.000	−3.967	0.000
$M4_R$	0.000	−3.537	0.000

4.4.4 *Visualizing Fusion*

Although the simulations show that HV-2.0 can successfully retroverse strabismus, it is not yet possible to visualize a fused binocular image, or perception, of the target. Therefore, the following simulation was designed to complement the efficacy of HV-2.0 in the perception of depth by rendering, overlapping and blending together the views from the left and right eyes in order to visualize a single “fused" image.

As previously discussed in chapter 2, fusion is a highly complex cerebral process, where superimposition and blending are two functions performed by the brain in order to fuse both images. In order to synthesize the views from the eyes, representing both retinal images, the DEMRS simulator exports the transformations (position, rotation, and scale) of the eyes, mirrors, and target to a file, which is parsed by a custom Python[7] application (access: https://bitbucket.org/cglynos/demrs/src/master/HVT_25/fusion_visualization/HV_20/). This application creates an Autodesk Maya[8] 3D scene identical to the visualizer of the DEMRS simulator. It should be noted that Maya was used for rendering purposes only.

The simulation is performed in two phases. The IPD is set to 6cm, and the target is placed centrally at a distance of 80cm from the DEMRS origin. Normal BSV is assumed so that both eyes fixate on the same target. In the first phase, HV-2.0 is disabled and hidden by the DEMRS simulator such that only the eyes and fixation target are visible (fig. 84a). This is done so that the

7 Python is an interpreted high-level programming language.
8 Autodesk Maya is a 3D computer graphics software that is used to create assets for interactive 3D applications, including video games, animated films, and visual effects.

“fused" image can be created uninfluenced by HV-2.0, and compared later with the “fused" image created when HV-2.0 is used. The transformations of the eyes and fixation target are exported to a Maya scene, in which a camera is placed at the position of each eye and a textured image of an autostereogram, depicting a bolt, is placed at the position of the target (fig. 84b). Two renders are generated, one from each camera, representing the views from the left and right eyes (fig. 84c, fig. 84d). The two rendered images are overlapped and blended in Adobe Photoshop using the difference blend mode[9], in order to approximate a “fused" image (fig. 84e). Figure 84e shows that when both eyes fixate on the target, the illusion from the autostereogram is not perceived.

9 According to (Adobe, 2021), the difference blend mode retrieves and subtracts the colour information from the RGB channels of two images.

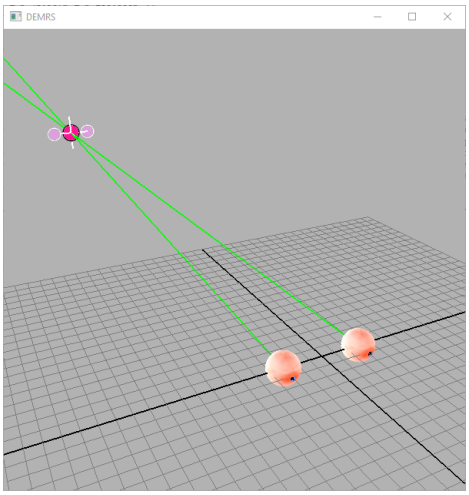

(a) *DEMRS simulator with HV-2.0 hidden.*

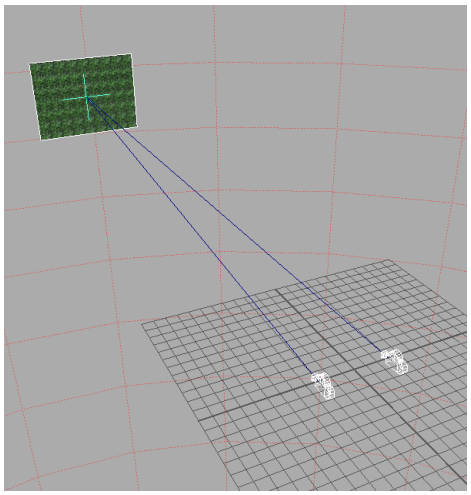

(b) *Maya scene with HV-2.0 hidden.*

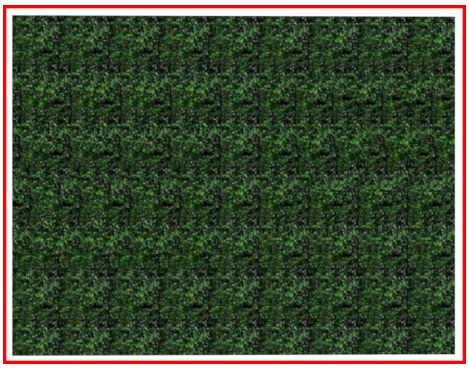

(c) *Render from left camera/eye.*

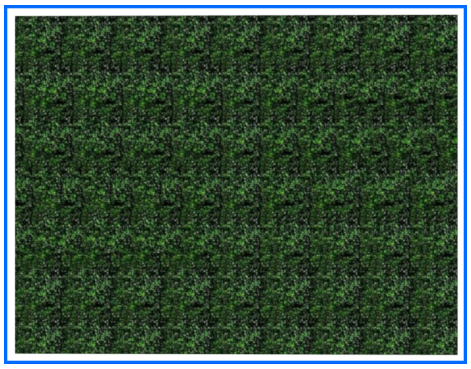

(d) *Render from right camera/eye.*

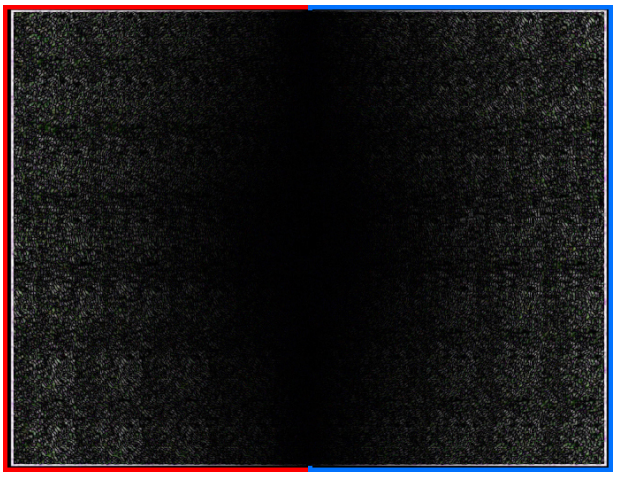

(e) *Fusion of left and right renders.*

Figure 84: *Simulating fusion without HV-2.0: (a) screenshot of the DEMRS simulator where both eyes fixate on the target. (b) screenshot of Maya containing a perspective camera at the position of each eye, and a planar surface textured with the autostereogram, placed at the position of the target. (c) render of the autostereogram from the left camera, whereas (d) render of the autostereogram from the right camera. (e) fusion of left and right camera renders.*

In the second phase of the simulation, HV-2.0 is re-enabled by the DEMRS simulator. As discussed in subsection 3.4.7, in order to perceive the 3D illusion from an autostereogram both eyes must fixate at a point beyond the plane of the image. Therefore, in the DEMRS simulator, a locator is placed centrally at distance of 80cm from the DEMRS origin to indicate the position of the autostereogram, whereas the fixation target is placed further behind the locator at a distance of 106.5cm (fig 85a). The transformations of the eyes, mirrors, target and locator are exported to a Maya scene, where in addition to the cameras and autostereogram, contains eight planar surfaces with reflective shaders (fig. 85b). Furthermore, two linear control vertex curves representing the principal vision vectors were created, and used to verify that the vision vectors from the DEMRS simulator and Maya are identical (fig. 85b). Figure 85c and figure 85d show the two renders from the left and right cameras, whereas figure 85e shows the “fused" image of the two renders.

As the fixation target, in the DEMRS simulator, is moved further from the autostereogram (fig. 85b), the illusion of the bolt starts to appear in the “fused" image. However, the illusion is lost if the target is moved beyond a certain point. In this simulation, the illusion of the bolt appeared when the locator was placed in the region of $\approx 102 - 108$cm from the DEMRS origin, but clearest when placed at a distance of 106.5cm.

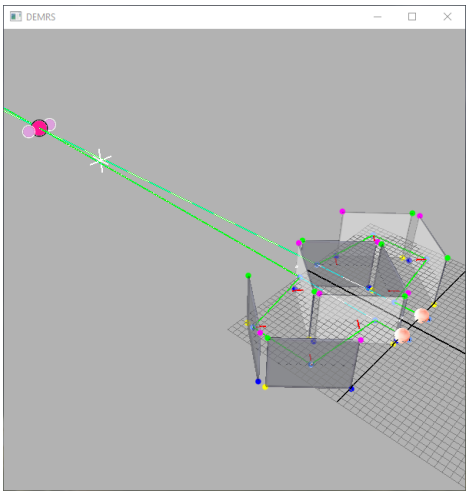

(a) *DEMRS simulator with HV-2.0.*

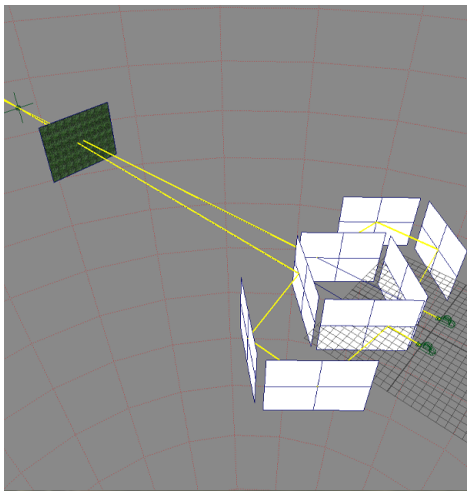

(b) *Maya scene with HV-2.0.*

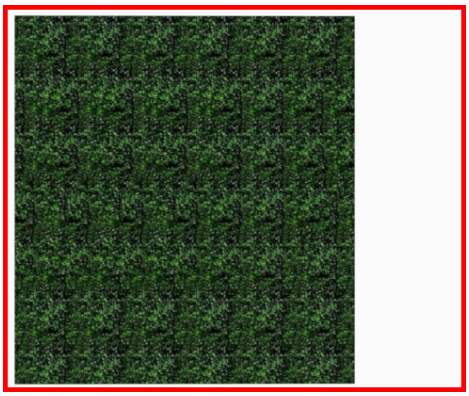

(c) *Render of left camera/eye.*

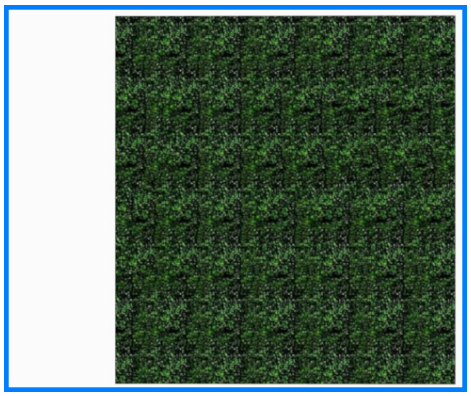

(d) *Render of right camera/eye.*

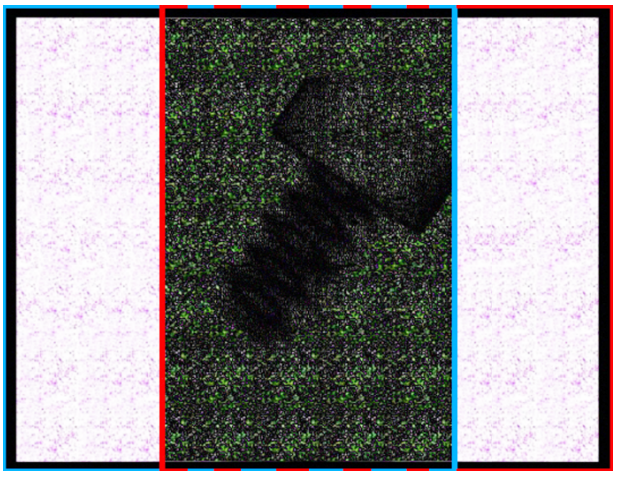

(e) *Fusion of left and right renders.*

Figure 85: *Simulating fusion with HV-2.0: (a) screenshot of the DEMRS simulator post retroversion. (b) screenshot of the scene in Maya containing the cameras, the autostereogram texture, the eight planar surfaces representing the mirrors, and two polylines to illustrate the vision vectors. (c) and (d) are the renders of the autostereogram from the left and right cameras, respectively. Lastly, (e) fusion of left and right camera renders.*

4.4.5 *Sensitivity Analysis*

A sensitivity analysis of HV-2.0 mirror orientations was conducted to determine the relative significance of errors in the rotations performed by different mirrors. In addition, the sensitivity analysis quantified the maximal permissible error in the orientation of each mirror.

In this analysis the fixation target was placed in the DEMRS simulator, centrally, at a distance of $\approx$ 4m from the DEMRS origin. The retroversion algorithm (see subsect. 4.4.2) was executed in order to calculate the correct orientation of each mirror. The distance from the DEMRS origin to the fixation target, and the mean fusional amplitudes, discussed in chapter 2, are used to calculate the area around the target where fusion can occur. This fusional area (see subsect. 2.4.4) is shown in figure 86, depicted by an ellipse.

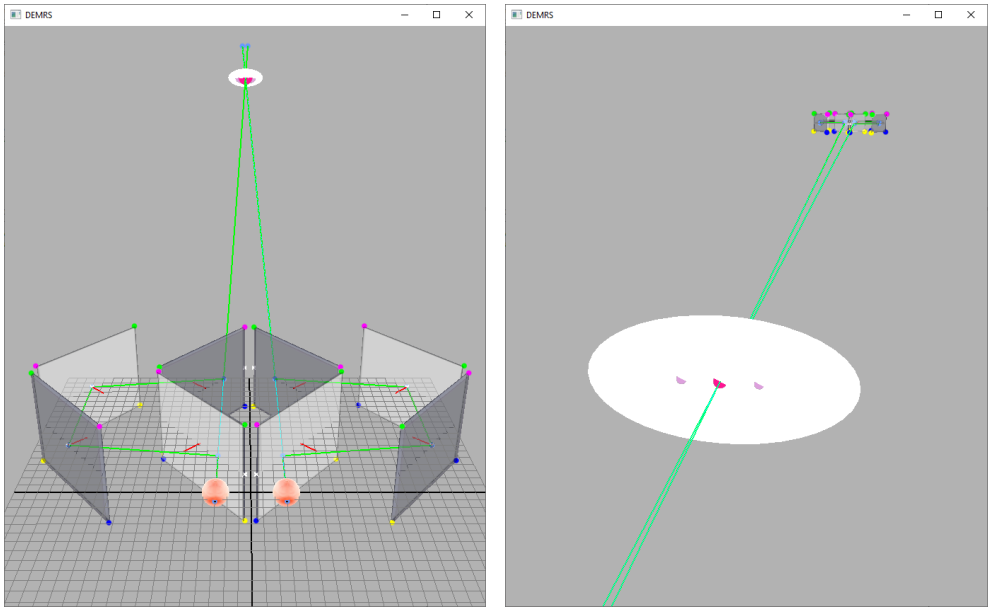

(a) *DEMRS and principal vision vectors.* (b) *Fusion area.*

Figure 86: *Fusional area: Part (a) shows the DEMRS after retroversion whereby both principal vision vectors (green polylines) pass through the target (deep pink point). Part (b) focuses on the target, including the two parallel targets (plum points), along with the fusional area, which is the white ellipse around the target.*

Because DEMRS HV-2.0 is symmetrical, only the mirrors on the left side are considered in the sensitivity analysis. Normally, the retroversion algorithm calculates the precise orientations of all mirrors in the system so that the principal vision vectors pass through the target. In order to test the rotation sensitivity of a particular mirror in the system, an error was created in the rotation of the mirror. The process of testing the sensitivity of a particular mirror is as follows:

1. Normal retroversion is executed, which calculates the rotations (vr) for all mirrors.

2. One or more mirrors are selected to be tested for sensitivity in their rotations.

3. The retroversion rotations (vr) of the selected mirror(s) are replaced by error rotations (vr_ϵ), calculated by the following equation:

$$vr_\epsilon = vr \times \left(\frac{100 \pm \delta}{100}\right) \tag{7}$$

where:

vr = retroversion rotations

vr_ϵ = error rotations

δ = percentage error

4. The system determines whether or not the resultant principal vision vectors intersect the fusional area around the target.

The sensitivity analysis of HV-2.0 consists of three tests. In the first test, a sensitivity analysis was performed on each mirror on the left side of the system using positive and negative rotation errors. Due to the target located centrally, at eye level, only the y-axis (yaw rotation) is used to orient each mirror. Table 14 presents the yaw rotations of M_{1_L}, M_{2_L}, M_{3_L} and M_{4_L} and the minimum and maximum deviation angles that are tolerable by the system in order to retroverse both principal vision vectors towards the fusible area around the target.

Table 14: *Sensitivity test of each mirror, rounded up to one decimal place.*

Mirror		$vr(^\circ)$	$\delta(\%)$	$vr_\epsilon(^\circ)$
M_{1_L}	min	3.7	−19.3	3.0
	max	3.7	19.4	4.4
M_{2_L}	min	3.5	−21.4	2.7
	max	3.5	21.4	4.2
M_{3_L}	min	−3.7	−20.5	−3.0
	max	−3.7	20.5	−4.5
M_{4_L}	min	−3.5	−22.7	−2.7
	max	−3.5	22.7	−4.3

Figure 87 presents a graph that illustrates the sensitivity analysis of the system to the rotations of each mirror.

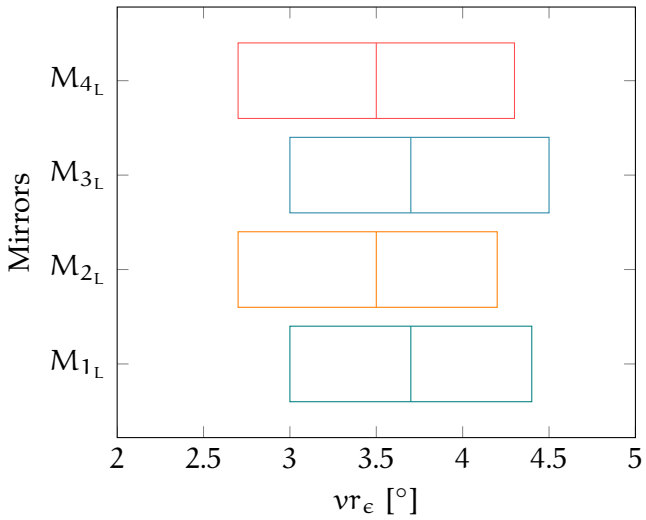

Figure 87: *Sensitivity analysis of $M1_L$, $M2_L$, $M3_L$ and $M4_L$: This graph presents the minimum and maximum tolerance of each mirror. The central line represents the correct retroversion angle (vr).*

The first test shows that, when the target is located centrally at a distance of $\approx$ 4m, all mirrors in the system have relatively similar sensitivity. However, the system is slightly more sensitive to the rotations of $M1_L$ and $M3_L$, compared to the rotations of $M2_L$ and $M4_L$, as the ranges between the minimum and maximum error deviations (vr_ϵ) of $M1_L$ and $M3_L$ are smaller than the ranges of $M2_L$ and $M4_L$ (fig. 87). The sensitivity analysis shows that the least sensitive mirror is $M4_{L/R}$, and the most sensitive mirror is $M1_{L/R}$. This is because $M4_{L/R}$ is the mirror located closest to the target, whereas $M1_{L/R}$ is located furthest away from the target. Because a principal vision vector is reflected by the mirrors in an orderly fashion, starting from $M1_{L/R}$ and ending at $M4_{L/R}$, implies that a deviation error caused by $M1_{L/R}$ results into an accumulated deviation of the direction of the principal vision vector at $M4_{L/R}$.

In the second sensitivity analysis, two mirrors on the left side of the system are randomly selected to test the sensitivity of the system. Similar to the first test, the retroversion rotations (vr) of both randomly selected mirrors are replaced by error rotations (vr_ϵ) according to equation 7. The first mirror is given an error rotation of a random percentage, which is retained throughout testing in order to determine the minimum and maximum ranges of sensitivity of the second mirror. For example, if $M2_L$ and $M3_L$ are the two selected mirrors for testing, $M2_L$ is rotated using 5% error in order to determine the minimum and maximum sensitivity of $M3_L$. Next, $M3_L$ is rotated

using 5% in order to determine the minimum and maximum sensitivity of M_{2_L}. This method of testing the sensitivity of two mirrors is applied to a group of any number of mirrors in the system. Table 15 presents the sensitivity analysis of the system with errors in the rotations of M_{3_L} and M_{4_L}. Additionally, the table presents deviations considering yaw rotations as the target is located, centrally, at a distance of $\approx 4m$ away from the eyes.

Table 15: *Sensitivity test of* M_{3_L} *and* M_{4_L}*, rounded up to one decimal place.*

Mirror		$vr(^\circ)$	$\delta(\%)$	$vr_\epsilon(^\circ)$
M_{3_L}	min	−3.7	−10.0	−3.3
M_{4_L}	min	−3.5	−33.8	−2.3
	max	−3.5	11.7	−3.9
M_{3_L}	max	−3.7	10.0	−4.1
M_{4_L}	min	−3.5	−11.6	−3.1
	max	−3.5	33.8	−4.7
M_{4_L}	min	−3.5	−10.0	−3.1
M_{3_L}	min	−3.7	−29.5	−2.6
	max	−3.7	11.5	−4.1
M_{4_L}	max	−3.5	10.0	−3.8
M_{3_L}	min	−3.7	−11.5	−3.3
	max	−3.7	29.5	−4.8

Figure 88 illustrates the sensitivity of HV-2.0 to errors in the rotations of M_{3_L} and M_{4_L}. Graph 88a and graph 88b show the sensitivity of M_{4_L} when an error of 10% is introduced to the rotation of M_{3_L}, whereas graph 88c and graph 88d show the sensitivity of M_{3_L} when an error of 10% is introduced to the rotation of M_{4_L}.

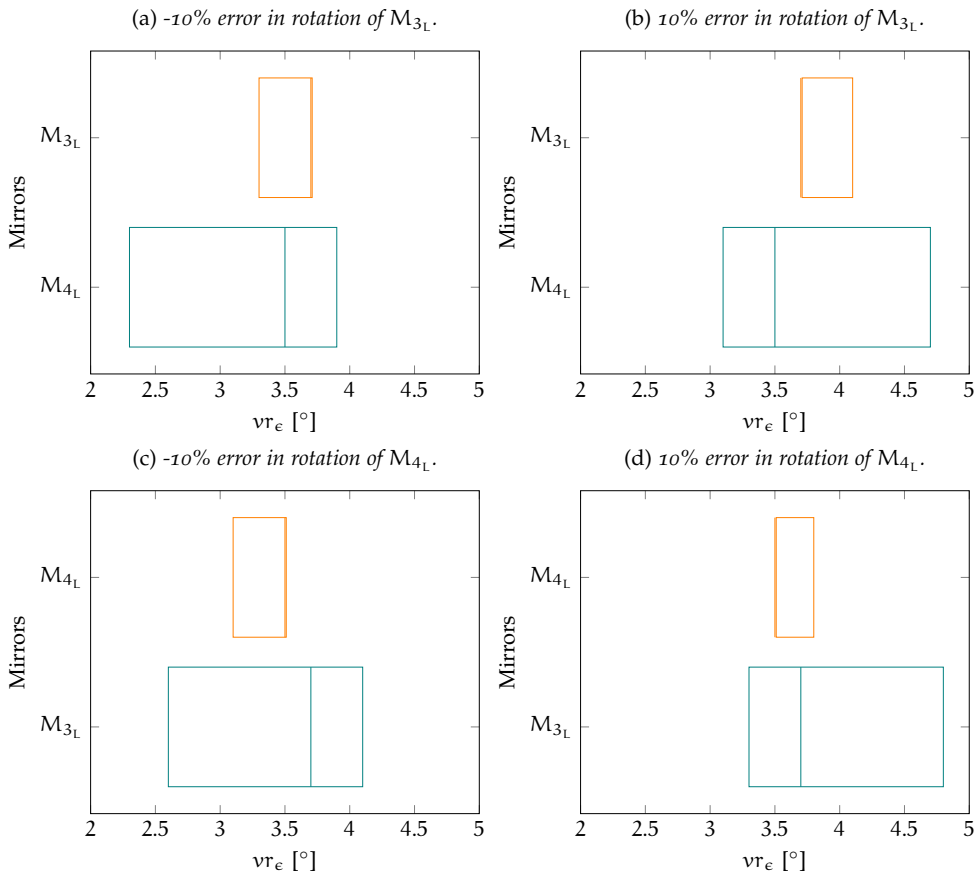

Figure 88: *Sensitivity analysis of M_{3_L} and M_{4_L}: The sensitivity of HV-2.0 when an error of 10% is introduced to M_{3_L} and M_{4_L}. Part (a) and part (b) show the minimum and maximum tolerance of M_{4_L} when M_{3_L} is rotated by an error of 10%, whereas parts (c) and (d) show the minimum and maximum tolerance of M_{3_L} when M_{4_L} is rotated by an error of 10%.*

The results from the second test show that the tolerance of HV-2.0 is 11.5%, when an error is induced in the rotations of M_{3_L} and M_{4_L}. Furthermore, the maximum tolerance of deviation of $M_{4_{L/R}}$ is less than its minimum tolerance, when there is a -10% error in the rotation of $M_{3_{L/R}}$ (fig. 88a). Conversely, the maximum deviation tolerance of $M_{4_{L/R}}$ is greater than its minimum tolerance, when there is a 10% error in the rotation of $M_{3_{L/R}}$ (fig. 88b). This difference in sensitivity is attributed to clockwise versus counter-clockwise mirror rotations, performed by some mirrors in the system, that cancel out the errors induced by each other. During retroversion $M_{3_{L/R}}$ performs a clockwise yaw rotation whereas $M_{4_{L/R}}$ performs a counter-clockwise yaw rotation. As such, when $M_{3_{L/R}}$ rotates clockwise by a 10% error, the tolerance of $M_{4_{L/R}}$ is lesser when rotating clockwise than when rotating counter-clockwise. This is because when $M_{4_{L/R}}$ rotates counter-clockwise it corrects the rotation error induced by $M_{3_{L/R}}$ and, therefore, the tolerance on counter-clockwise rotations is greater. Similar reasoning applies to the mini-

mum and maximum tolerances of $M3_{L/R}$, when an error of $\pm 10\%$ is induced to the rotation of $M4_{L/R}$ (fig. 88c, fig. 88d).

In the third and final sensitivity analysis, rotation errors are introduced to all four mirrors on the left side of HV-2.0 in order to determine the tolerance of the system. Similar to the previous tests, the retroversion rotations (vr) of all mirrors are replaced by rotation errors (vr_ϵ) according to equation 7. Because some mirrors rotate clockwise and other mirrors rotate counterclockwise, the rotation errors in this test have been rotated so that no mirror would cancel out (correct) the rotation error induced by another mirror. Table 16 presents the minimum and maximum deviation angles that are tolerable by the system in order to retroverse both principal vision vectors towards the fusible area around the target.

Table 16: *Sensitivity test of all mirrors, rounded up to one decimal place.*

Mirror		$vr(°)$	$\delta(\%)$	$vr_\epsilon(°)$
$M1_L$	min	3.7	−5.2	3.5
	max	3.7	5.2	3.9
$M2_L$	min	3.5	−5.2	3.3
	max	3.5	5.2	3.6
$M3_L$	min	−3.7	−5.2	−3.5
	max	−3.7	5.2	−3.9
$M4_L$	min	−3.5	−5.2	−3.3
	max	−3.5	5.2	−3.7

Figure 89 illustrates the sensitivity analysis of HV-2.0 to the rotations of all mirrors.

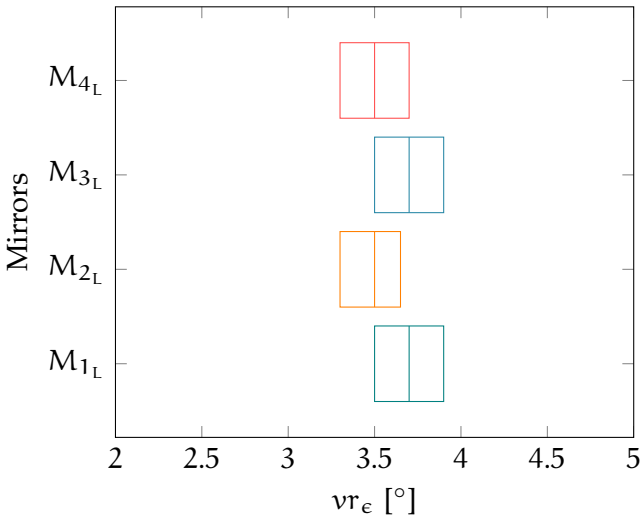

Figure 89: *Sensitivity analysis of all mirrors.*

The third sensitivity test shows that the minimum/maximum amount of error the system can tolerate is $\pm 5.2\%$ in the rotations of all the mirrors. Due to the position of the left eye and the positions of the mirrors on the left side, HV-2.0 is less sensitive to the rotations of the mirrors that cause the principal vision vector to be reflected on the right side of the target, and more sensitive to the rotations of the mirrors that cause the principal vision vector to be reflected on the left side of the target. However, this difference in the sensitivity of the system is noticeable when the deviation (νr_ϵ) is measured in three or more decimal places.

This sensitivity analysis shows that HV-2.0 is less sensitive to large errors in rotation of one or two mirrors but more sensitive to small errors in the rotations of all four mirrors.

4.4.6 *Preliminary Evaluation Under Normal BSV*

One of the concerns in the design of HV-2.0 was the effects of such a system on people with normal binocular vision. A DEMRS cannot be considered a viable method for the diagnosis and treatment of strabismus if it has negative effects on people with normal vision. Therefore, a series of physical tests were designed to evaluate the efficacy of a DEMRS in the perception of depth, under normal BSV. These tests would verify whether or not a DEMRS has adverse effects on subjects with normal BSV.

The tests were conducted under laboratory conditions, in a relatively large office room with ambient lighting located at Bournemouth University. A basic apparatus was assembled based on the design of HV-2.0, which was composed of eight mirrors and eight bases, provided by Edmund Optics (2019b), that held the mirrors in an upright position. The mirrors were placed on a desk, located near the wall, and rotated according to the default state of HV-2.0, i.e. at a 45° angle. The fixation target was an autostereogram, depicting a bunny when viewed stereoscopically, placed centrally on the wall at a distance of $\approx 80\text{cm}$ from the subject's eyes. Compared to other methods used for the assessment of stereopsis, including FNS and FD2 that are prone to errors due to familiarity cues (see subsect. 3.4.7), an autostereogram test is low cost, simple to setup and provides accurate results, as an individual will not be able to perceive the three dimensional illusion without possessing binocular depth perception. A height adjustable chair was used by the subject in order to level their head with the mirrors, and comfortably view the fixation target through the DEMRS apparatus that was placed $\approx 2-5\text{cm}$

from the subject. Also, the DEMRS simulator was used to calculate the retroversion angles of the mirrors, of the DEMRS apparatus.

In order to determine the effect of the DEMRS apparatus, only subjects who were unable to perceive the illusion from an autostereogram were selected to take part in the preliminary evaluation. Therefore, each subject was asked to view the autostereogram and report whether or not the illusion was perceived. Three adult volunteers were enrolled in this study, aged between 30 and 55 years (mean 39.3 years), possessing normal BSV but unable to perceive the illusion from the autostereogram. The IPD of the subjects range between $\approx$ 5.9cm and $\approx$ 6.2cm, with mean IPD $\approx$ 6.05cm. Table 17 lists the demographic data of the subjects who participated in the preliminary evaluation of the HV-2.0 based apparatus.

Table 17: *Demographic data of subjects in the preliminary evaluation of DEMRS*

Characteristics	No. Studied	Percent %
Gender		
Male	3	100.0%
Female	0	0.0%
Age range $[30-55]$ (years)		
$\leqslant 39.3$	2	66.6%
> 39.3	1	33.3%
Vision		
Normal BSV	3	100.0%
Strabismus	0	0.0%
Total	**3**	**100%**

Initially, the IPD of each subject, and position of the fixation target were passed into the DEMRS simulator so that the correct retroversion angles of the mirrors could be calculated by the retroversion engine. After the computation of retroversion, each physical mirror was manually rotated to match the orientation angles calculated by the DEMRS simulator. The subject was asked whether or not the autostereogram could be properly viewed, without perceiving the illusion. This step is necessary because, although the target is located 80cm from the subject, the default state of a DEMRS assumes that the target is located at a distance of 6m. Consequently, the default state of the DEMRS apparatus would not allow the subject to view properly view the autostereogram.

Next, because of the technique required to perceive the illusion from an autostereogram, the fixation target in the DERMS simulator was moved further from the position of the autostereogram. When the target was moved, and retroversion was calculated, the physical mirrors were manually rotated to match the retroversion angles calculated by the DEMRS simulator. Also, the subject was asked to report whether or not the illusion was perceived. This step was repeated until the subject was able to perceive and describe the illusion. Figure 90 shows a photograph of a subject undergoing testing using the DEMRS apparatus.

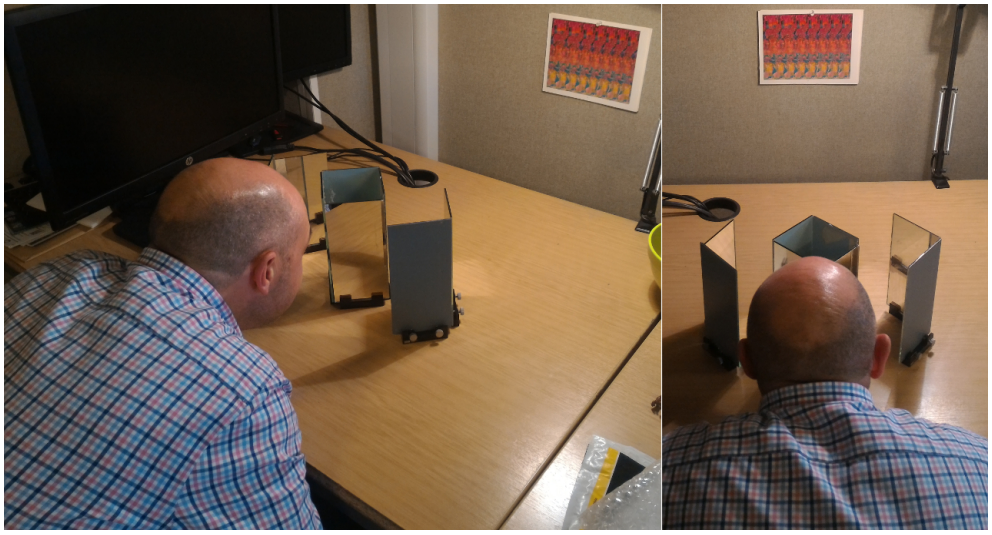

Figure 90: *Preliminary evaluation: Photograph showing a subject undergoing testing using the DEMRS apparatus.*

All 3 subjects underwent the autostereogram test once. Prior to using the DEMRS apparatus, none (0%) of the subjects were able to pass the test by describing the illusion from the autostereogram. When the DEMRS apparatus was used, all (100%) subjects were able to describe the illusion.

The preliminary evaluation showed that a DRS compliant system: (a) does not negatively affect normal BSV, and (b) promotes the perception of depth.

4.4.7 *Discussion*

DEMRS HV-2.0 is a DRS compliant system designed to achieve retroversion of strabismus. The simulations show that the retroversion engine can correctly calculate the rotations of the mirrors, such that both principal vision vectors pass through the same fixation target. Also, the retroversion engine takes into consideration mirrors $M_{3_{L/R}}$ and $M_{4_{L/R}}$, which are used to maintain normal binocular disparity and resultant IPD. Moreover, the simulations show that HV-2.0 is able to achieve retroversion for various clas-

sifications of strabismus, including micro-deviations. The efficacy of HV-2.0 in the normal binocular perception of depth was complemented by the visualization of the “fused" image, of the left and right rendered views of an autostereogram, using third-party software. This test showed that redirecting both principal vision vectors further “through" the autostereogram, causes the illusion to appear.

A sensitivity analysis of HV-2.0 mirror orientations was conducted to determine the relative significance of errors in the rotations performed by different mirrors. In addition, the sensitivity analysis quantified the maximal permissible error in the orientation of each mirror.

Although the experiments performed with the DEMRS simulator and visualization of fusion showed promising results, they were not sufficient to suggest the efficacy of HV-2.0 in the binocular perception of depth by human subjects. Also, the simulation experiments could not verify whether or not a DRS compliant system has adverse effects on subjects with normal BSV. Therefore, a basic apparatus was built, based on the design of HV-2.0, in order to conduct a series of preliminary physical tests on human subjects with normal BSV and an autostereogram as fixation target. These tests determined that: (a) HV-2.0 is applicable to human subjects, and (b) subjects with normal BSV can perceive the illusion from an autostereogram, when viewing through the HV-2.0 apparatus. The results from the preliminary evaluation showed that HV-2.0 allows a subject to binocularly perceive depth.

A limitation of the DEMRS HV-2.0 is that it is not designed to retroverse torsional strabismus. This is addressed by the another DRS complaint system presented in the next section.

The predecessor of HV-2.0, which is called HV-1.0 presented in appendix B.2, did not meet the criteria of the DRS principle, and therefore could not achieve retroversion of strabismus. Briefly, the inability of HV-1.0 to achieve retroversion was attributed to estimated orientations of the mirrors, excessive binocular disparity, large resultant IPD and collisions between some mirrors in the system.

4.5 DEMRS FOR HORIZONTAL, VERTICAL AND TORSIONAL STRABISMUS (VERSION HVT-2.5)

DEMRS HVT-2.5 is a conceptual DRS compliant system designed to retroverse horizontal, vertical and torsional strabismus, using a set of mirrors and rotatory prisms. Similar to HV-2.0, this system is designed to redirect principal and peripheral vision vectors by orienting a set of mirrors, horizontally

and vertically, in order to achieve retroversion. The prisms are designed to rotate torsionally about the z-axis (roll rotation) so that the vision vectors of the left and right eyes can have matching orientations.

4.5.1 *Design and Description*

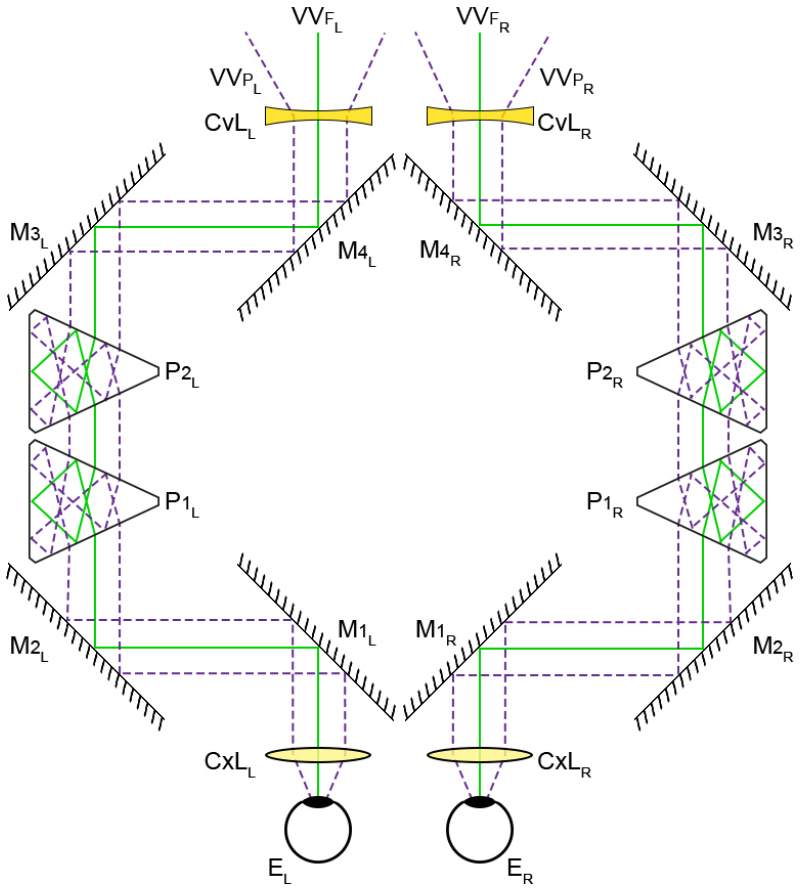

Figure 91: *DEMRS HVT-2.5: A schematic of the system, where* $VV_{F_{L/R}}$ *are the left and right principal vision vectors,* $VV_{P_{L/R}}$ *are the peripheral vision vectors,* $CxL_{L/R}$ *and* $CvL_{L/R}$ *are the convex and concave lenses,* $M_{1,2,3,4_{L/R}}$ *are the left and right set of mirrors,* $E_{L/R}$ *represent the left and right eyes, and* $P_{1,2_{L/R}}$ *are the delta prisms.*

The design of HVT-2.5 (fig. 91) consists of eight mirrors, four on each side ($M_{1_{L/R}}$, $M_{2_{L/R}}$, $M_{3_{L/R}}$ and $M_{4_{L/R}}$), for the purpose of redirecting the principal vision vectors ($VV_{F_{L/R}}$) towards the fixation target, whereas the two convex ($CxL_{L/R}$) and two concave ($CvL_{L/R}$) lenses are used to constrain the peripheral vision vectors ($VV_{P_{L/R}}$). Additionally, HVT-2.5 uses four delta prisms, two on each side ($P_{1_{L/R}}$, $P_{2_{L/R}}$), in order to retroverse torsional deviations. In order to reduce the overall size of the system, delta prisms were se-

lected instead of dove prisms. The JSON configuration of HVT-2.5 is shown in appendix B.4.

Similar to HV-2.0, HVT-2.5 is designed with four mirrors on each side so that $M_{3,4_L}$ and $M_{3,4_R}$ can be used to maintain normal resultant IPD and normal binocular disparity. $M_{1_{L/R}}$ and $M_{4_{L/R}}$ are located centrally to the eyes so that the system can provide a larger visual field, when achieving retroversion for: (a) various angles of strabismic deviations, and (b) various directions of a fixation target. Also, the pivots of rotation of $M_{2_{L/R}}$ and $M_{3_{L/R}}$ remain central to the mirrors, whereas the pivots of rotation of $M_{1_{L/R}}$ and $M_{4_{L/R}}$ are located on the following edges:

- M_{1_L}: centre-right
- M_{1_R}: centre-left
- M_{4_L}: centre-left
- M_{4_R}: centre-right

The default state of HVT-2.5, as shown in figure 91, is based on the assumption that the fixation target is located centrally to both eyes at a distance of $\geqslant 6m$ from the DEMRS origin. Therefore, by default, each mirror is oriented horizontally about the y-axis (yaw rotation) by 45°.

As previously explained in subsection 4.3.5, a rotatory prism, such as a dove or delta, inverts and rotates the transmitted image (refracted visual stimuli) by twice the angle of prism rotation. Therefore, if HVT-2.5 was designed with only one prism, the vision vectors would be rotated, and inverted. Consequently, HVT-2.5 is designed with two delta prisms ($P_{1,2_{L/R}}$), one in front of the other on each side, so that the second prism ($P_{2_{L/R}}$) would only invert the vision vectors that were previously inverted by $P_{1_{L/R}}$. As shown in figure 166, when two delta, or dove, prisms are consecutively placed one in front of the other the visual stimuli is rotated and inverted by the fist prism but the inversion is corrected by the second prism, thereby allowing the transmitted image to be rotated without inversion.

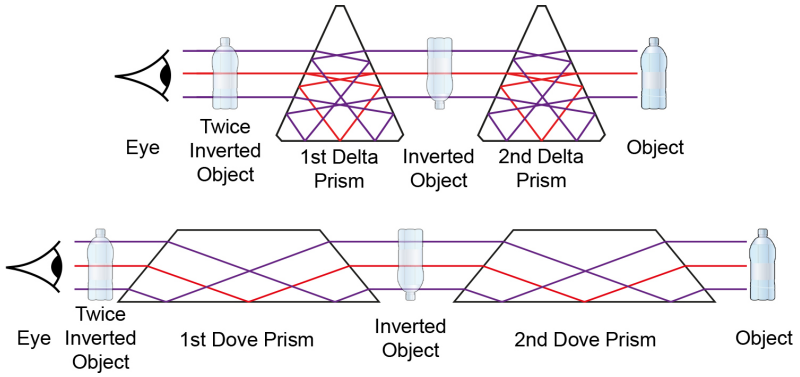

(a) *Correcting the inversion problem*

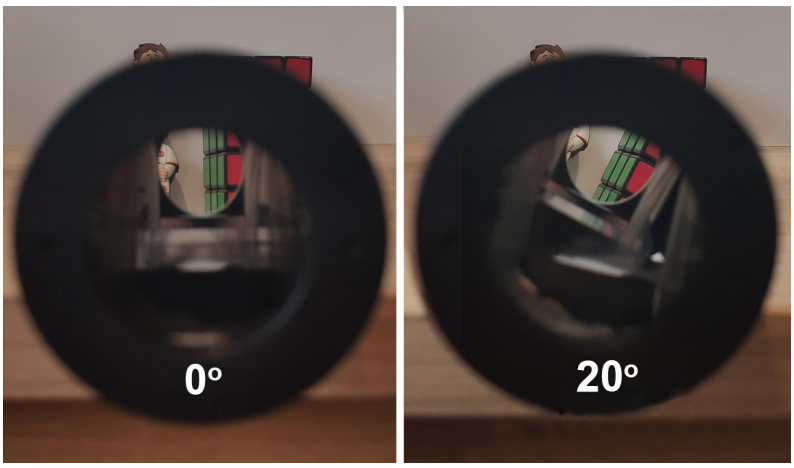

(b) *Rotation of first prism*

Figure 92: *Consecutive prisms: The transmitted image is perceived when viewed through two rotatory prisms, consecutively placed one in front of the other. Part (a) shows that when the bottle gets inverted by the first delta prism, the second delta prism corrects the inversion. Also, (a) shows two dove prisms in order to compare their length against two delta prisms. Part (b) is a photograph of two dove prisms, whereby the first prism is rotated by* $\approx 20°$*. (b) shows that the transmitted image is rotated but not inverted.*

The delta prisms have been placed between $M2_{L/R}$ and $M3_{L/R}$ (fig. 91) so that they only rotate about the z-axis. This is because the retroversion algorithm, previously described in subsection 4.4.2, ensures that the principal vision vectors are centrally reflected by $M2_{L/R}$ and $M3_{L/R}$, thereby directed only along the z-axis. Of the two prisms, $P1_{L/R}$ rotates by half of the angular difference between the normal eye and the strabismic eye, whereas $P2_{L/R}$ is fixed at a 90° angle. Initially, the vision vectors are reflected by $M1_{L/R}$ to the centre of $M2_{L/R}$ and, next, by $M2_{L/R}$ to the centre of $P1_{L/R}$, which rotates and inverts the vision vectors. Subsequently, the vision vectors are refracted by $P2_{L/R}$, which does not rotate but inverts the rotated vision vectors. Finally, the vision vectors are reflected by $M3_{L/R}$ to the LPR on $M4_{L/R}$. The sequence in which a vision vector is reflected by the mirrors and refracted by the prisms as it travels from the eye to a target (T), is as follows:

$$E \rightarrow M_1 \rightarrow M_2 \rightarrow P_1 \rightarrow P_2 \rightarrow M_3 \rightarrow M_4 \rightarrow T$$

Similar to HV-2.0, the lenses were added to the design of the system in order to constrain the direction of the peripheral vision vectors so that they are not reflected by the mirrors towards arbitrary directions, escaping the system. The design of HVT-2.5 satisfies all the criteria of the principle of retroversion, as follows:

1. The rotation of the mirrors enables the simultaneous intersection of both principal vision vectors on the same fixation target.
2. $M3_{L/R}$ and $M4_{L/R}$ are used to maintain normal resultant IPD.
3. $M4_{L/R}$ are used to maintain normal binocular disparity.
4. $P1_{L/R}$ and $P2_{L/R}$ are used to maintain normal orientation of the visual stimuli.

4.5.2 *Retroversion Algorithm*

The retroversion algorithm used in HVT-2.5 is based on the bidirectional retroversion algorithm of HV-2.0 (see subsect. 4.4.2) with modifications that incorporate the rotation of delta prisms, following the rotation of $M2_{L/R}$. Similar to HV-2.0, in order to maintain normal resultant IPD and normal resultant binocular disparity, it is imperative to determine the last points of reflection (LPR) on $M4_{L/R}$. Consequently, HVT-2.5 uses the auxiliary vision vectors VV_{A_L} and VV_{A_R}, which represent both principal vision vectors under normal BSV, in order to calculate both LPR.

Because the rotation of the prisms does not depend on the rotation of the mirrors, the bidirectional retroversion algorithm can be split into the following three concurrent tasks:

1. The first task calculates the orientation of $M1_{L/R}$ so that $VV_{F_{L/R}}$ can be reflected by $M1_{L/R}$ to the centre of $M2_{L/R}$. Next, the orientation of $M2_{L/R}$ is calculated so that the reflected $VV_{F_{L/R}}$ can be reflected by $M2_{L/R}$ to the centre of $M3_{L/R}$.
2. The second task calculates the orientation of $P1_{L/R}$ from the angular difference between the normal eye and the strabismic eye.
3. The third task uses an inverted $VV_{F_{L/R}}$, noted by $INV_V V_{F_{L/R}}$, that originates from the target and directs to the fovea. In this task the orientation of $M4_{L/R}$ is calculated so that the $INV_V V_{F_{L/R}}$ can be reflected

by the LPR, on $M4_{L/R}$, to the centre of $M3_{L/R}$. Next, the orientation of $M3_{L/R}$ is calculated so that the reflected $INV_V V_{F_{L/R}}$ can be reflected by $M3_{L/R}$ to the centre of $M2_{L/R}$.

The following pseudocode presents the bidirectional retroversion algorithm, modified for HVT-2.5:

Algorithm 2: Bidirectional Retroversion of HVT-2.5

```
Begin
    vv_f ← principal vision vector;
    inv_vv_f ← inverse principal vision vector;
    vv_a ← auxiliary vision vector;

    // ----- Task 1 -----
    for m in [M1, M2] do
        poi = intersection(vv_f, m);
        updated_vv = reflection(vv_f, m);
        next_poi = intersection(updated_vv, m + 1);
        if next_poi not central to m + 1 then
            rotate m so that updated_vv is reflected centrally to
              m + 1;
        end
        update(vv_f);
    end

    // ----- Task 2 -----
    ψ = torsion(normal_eye, strabismic_eye)/2;
    rotate(prism, ψ);

    // ----- Task 3 -----
    lpr = intersection(vv_a, M4);

    for m in [M4, M3] do
        poi = intersection(inv_vv_f, m);
        updated_vv = reflection(inv_vv_f, m);
        next_poi = intersection(updated_vv, m + 1);
        if next_poi not central to m + 1 then
            rotate m so that updated_vv is reflected centrally to
              m + 1;
        end
        update(inv_vv_f);
    end
```

The bidirectional algorithm above uses the same method to calculate pivoted rotations as HV-2.0 (see appendix B.3).

4.5.3 *Simulations*

A series of simulations were performed to evaluate the effectiveness of HVT-2.5 in achieving retroversion for near ($\leqslant$ 1m), mid ($\approx$ 3m) and far ($\geqslant$ 6m) fixation targets, at various directions from the DEMRS origin. Because a DEMRS must be able to compensate for various types of strabismus, including phorias, HVT-2.5 is tested with normal BSV and strabismus. In the following simulations, the IPD is set to 6cm, whereas the DEMRS simulator was configured based on the JSON configuration file of HVT-2.5 (see appendix B.4). Table 18 presents the default positions and rotations of each convex lens (Cx), concave lens (Cv), mirror (M) and prism (P) of HVT-2.5 in the DEMRS simulator.

Table 18: *Configuration of components in HVT-2.5.*

Default	Translation (cm)			Rotation (°)		
	x	y	z	x (pitch)	y (yaw)	z (roll)
Cx_L	3.000	0.000	2.000	−180.000	0.000	180.000
$M1_L$	0.510	0.000	2.500	−180.000	−45.000	−180.000
$M2_L$	17.000	0.000	6.990	0.000	45.000	0.000
$P1_L$	17.000	0.000	13.876	−180.000	0.000	90.000
$P2_L$	17.000	0.000	18.647	−180.000	0.000	90.000
$M3_L$	17.000	0.000	25.533	−180.000	45.000	180.000
$M4_L$	0.510	0.000	30.023	0.000	−45.000	0.000
Cv_L	3.000	0.000	31.023	−180.000	0.000	180.000
Cx_L	−3.000	0.000	2.000	−180.000	0.000	180.000
$M1_L$	−0.510	0.000	2.500	−180.000	45.000	180.000
$M2_L$	−17.000	0.000	6.990	0.000	−45.000	0.000
$P1_L$	−17.000	0.000	13.876	180.000	0.000	−90.000
$P2_L$	−17.000	0.000	18.647	180.000	0.000	−90.000
$M3_L$	−17.000	0.000	25.533	−180.000	−45.000	−180.000
$M4_L$	−0.510	0.000	30.023	0.000	45.000	0.000
Cv_L	−3.000	0.000	31.023	−180.000	0.000	180.000

In the following simulations, when the fixation target (T) is located at a distance of $<$ 6m from the DEMRS origin, retroversion is successful when both principal vision vectors pass through T. When T is located at a distance $\geqslant$ 6m from the DEMRS origin, retroversion is successful if each principal vision vector passes through the corresponding parallel target Tp_L and Tp_R.

To aid clarity in the visualization of the simulations:

- The eyes are illustrated by the two textured 3D models.
- The principal vision vectors are drawn in green when retroversion is successful, and red when retroversion has failed. The peripheral vision vectors are drawn in sky blue, whereas the auxiliary vision vector of the deviating eye is depicted by a white dashed line. The original principal vision vectors of the eyes are the light blue lines that are not reflected or refracted by the components of the system.
- The mirrors are illustrated by the light grey flat surfaces.
- The delta prisms are illustrated by the light blue triangular prismatic meshes located between $M_{2_{L/R}}$ and $M_{3_{L/R}}$.
- The convex and concave lenses are depicted by the light yellow and dark yellow meshes on each end of the system.
- The fixation target T is illustrated by a deep pink point circle, whereas Tp_L and Tp_R are illustrated by two smaller plum coloured point circles.

Initially, a simple experiment was conducted to determine whether HVT-2.5 can retroverse torsional strabismus, without considering horizontal and vertical deviations. An abnormally large torsional deviation of 40° was assigned to the left eye (fig. 93a) causing the first prism, on the left side of HVT-2.5, to significantly rotate in order to achieve retroversion (fig. 93b). Prior to the rotation of the vision vectors by the prisms, the peripheral vision vector of the left eye is located higher than the principal vision vector of the left eye (fig. 93b). When the vision vectors are rotated by the prisms, the peripheral vision vector of the left eye is located at the same height as the principal vision vector of the left eye (fig. 93b). The orientation of the vision vectors of the left eye is similar to the orientation of the vision vectors of the normal eye, indicating successful torsional retroversion (fig. 93c). Emphasis is given to the rotation of the delta prism, which causes the resultant vision vectors to have matching orientations and directions (fig. 93d). To aid clarity of the results, the grid and mirrors are hidden in the DEMRS simulator, and only one peripheral vision vector is shown per eye.

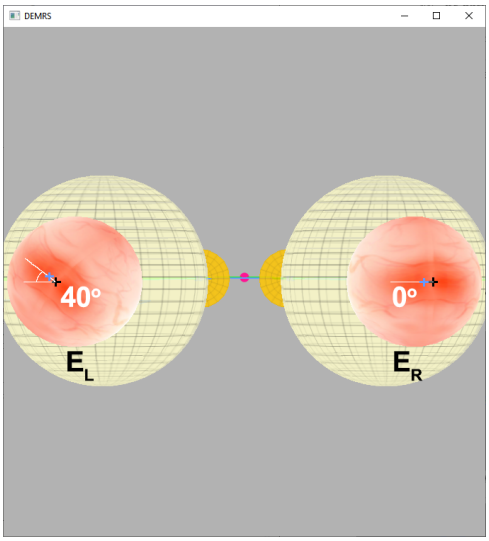

(a) *Behind the eyes, where the left eye deviates torsionally by 40°.*

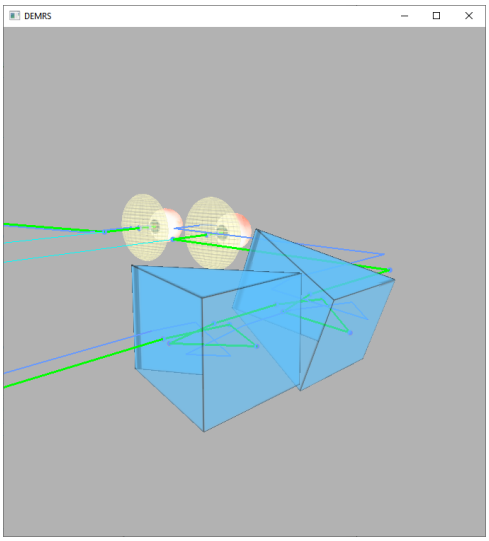

(b) *Prism rotation by 20°. Before refraction, the peripheral vision vector is higher than the principal vision vector. After refraction, both vision vectors are level.*

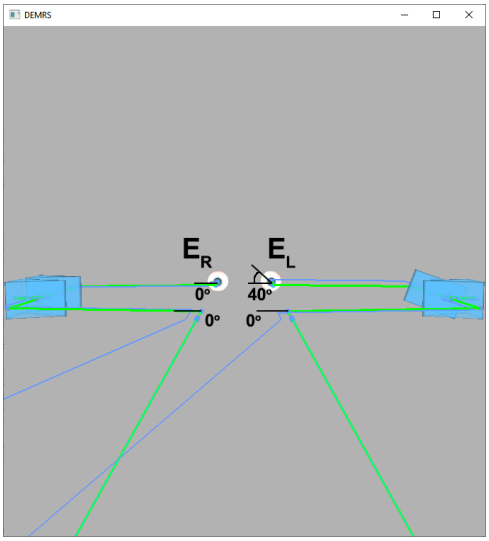

(c) *Front view of resultant vision vectors with similar orientations.*

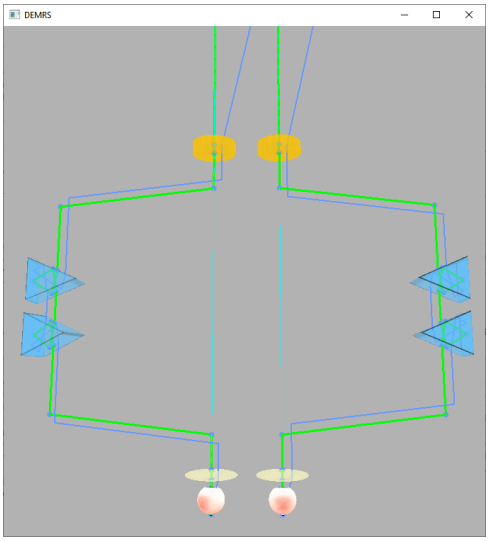

(d) *Top view of resultant vision vectors with similar directions.*

Figure 93: *Torsional retroversion: (a) View from behind the eyes emphasizing on the torsional deviation of* E_L *by 40°. The right eye (*E_R*) is dominant, which is why the peripheral point is at 0° from the umbo. (b) View of the delta prisms on the left side of the system, where the first prism performs a roll rotation of 20° to compensate for the torsional deviation. Before the refraction of the vision vectors by the prism, the peripheral vision vector is located higher than the principal vision vector, due to the torsional deviation. After the rotation of the first prism, the peripheral vision vector is located at the same height as the principal vision vector, similar to the normal eye. This can be seen in (c), which shows the torsional deviation of the left eye and resultant torsion of the vision vectors. (d) Retroversion shown from a top view emphasizing the equal resultant directions of the peripheral vision vectors of the strabismic and dominant eye.*

Four tests were performed, under the assumption that normal BSV is present, whereby both eyes simultaneously fixate on a target located: (a) centrally, at far distance of 6m, (b) centrally, at near distance of 80cm, (c) up, i.e. on the positive y-axis, at mid distance of 2m, and (d) left, i.e. on the positive x-axis, at far distance of 7m. Similar to HV-2.0, the distance of the target from the DEMRS origin is described in cm, such that a target located centrally at a distance of 6m would be presented as $T = \{0, 0, 600\}$. Figures 94, 95, 96 and 97 show screenshots before and after retroversion. Furthermore, tables 19, 20, 21 and 22 present the retroversion angles of the mirrors and prisms required to achieve retroversion.

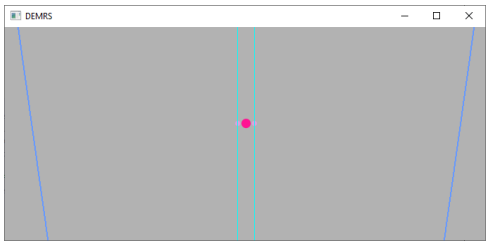

(a) *Target view before retroversion.*

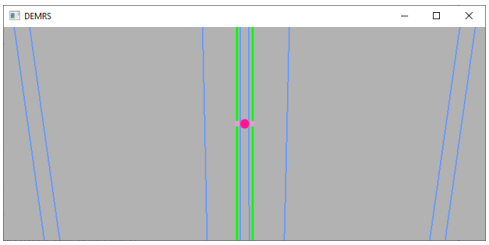

(b) *Target view after retroversion.*

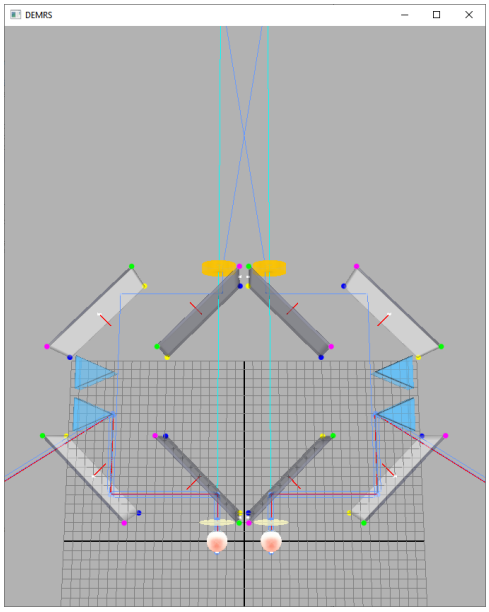

(c) *Before retroversion.*

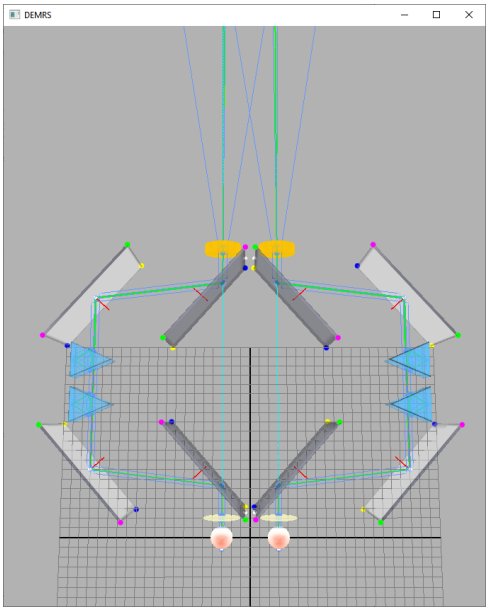

(d) *After retroversion.*

Figure 94: *DEMRS HVT-2.5 retroversion where* $T = \{0, 0, 600\}$*: Screenshots of simulations before (c) and after (d) retroversion of normal BSV, where* $T = \{0, 0, 600\}$*. Because of the far distance of the target from the DEMRS origin, the target is not visible in (c) and (d). Therefore two additional screenshots were taken from a close up view of the target, peripheral and principal vision vectors, where (a) is the extension of (c), and (b) is the extension of (d).*

Table 19: *DEMRS HVT-2.5 retroversion angles for normal BSV, where* $T = \{0, 0, 600\}$.

Components	Retroversion (°)		
	x (pitch)	y (yaw)	z (roll)
Cx_L	0.000	0.000	0.000
$M1_L$	0.000	3.427	0.000
$M2_L$	0.000	3.427	0.000
$P1_L$	0.000	0.000	0.000
$P2_L$	0.000	0.000	0.000
$M3_L$	0.000	−3.427	0.000
$M4_L$	0.000	−3.427	0.000
Cv_L	0.000	0.000	0.000
Cx_R	0.000	0.000	0.000
$M1_R$	0.000	−3.427	0.000
$M2_R$	0.000	−3.427	0.000
$P1_L$	0.000	0.000	0.000
$P2_L$	0.000	0.000	0.000
$M3_R$	0.000	3.427	0.000
$M4_R$	0.000	3.427	0.000
Cv_R	0.000	0.000	0.000

In figure 94, each eye has five vision vectors, four peripheral and one principal. Prior to retroversion, both principal vision vectors are shown in red, because they do not pass through $Tp_{L/R}$. Also, because the principal vision vectors are not properly refracted by the delta prisms, they are directed arbitrarily (fig. 94c). This is because the vision vectors are not centrally reflected by $M2_{L/R}$ and $M3_{L/R}$, which would allow the vision vectors to be centrally refracted by $P1_{L/R}$. After retroversion, the principal and peripheral vision vectors of both eyes are centrally reflected by $M2_{L/R}$ and $M3_{L/R}$, and therefore properly refracted by the delta prisms (fig. 94d). Consequently, retroversion is successful because both principal vision vectors pass through $Tp_{L/R}$, with normal binocular disparity and normal resultant IPD. Additionally, the peripheral vision vectors have resumed their original direction after refraction by the lenses, as the original direction of one of the peripheral vision vectors from the left eye was $\{-0.14, 0.00, 0.99\}$, and after refraction by the concave lenses the direction of the same peripheral vision vectors remains $\{-0.14, 0.00, 0.99\}$[10].

10 Due to floating point representations/inaccuracies, in the simulation, the original direction is $\{-0.140249, 0.000000, 0.990116\}$, whereas the resultant direction is $\{-0.140221, 0.000000, 0.990120\}$. However, such floating point errors are insignificant to the calculation of retroversion.

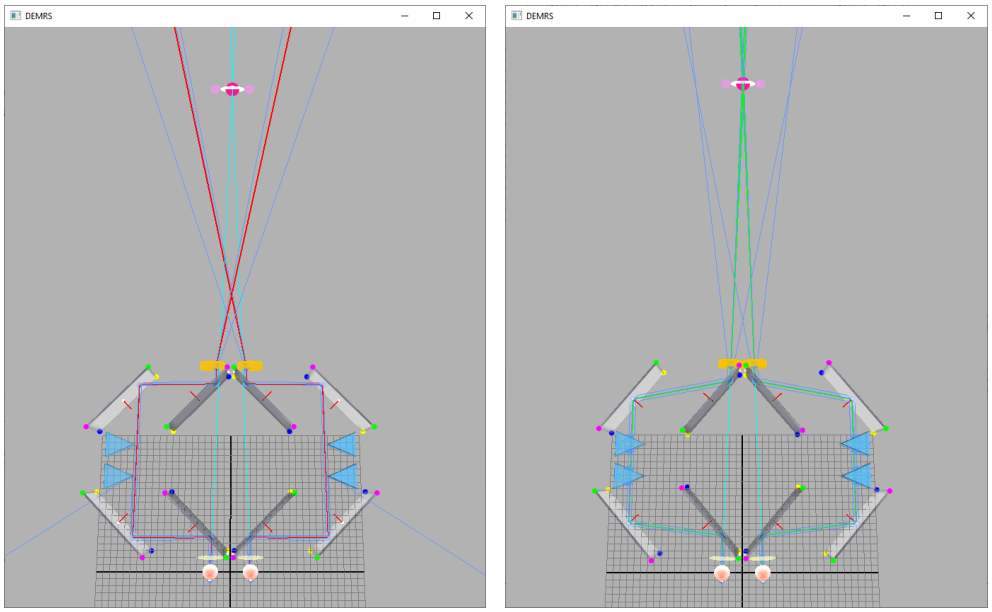

(a) *Before retroversion.* (b) *After retroversion.*

Figure 95: *DEMRS HVT-2.5 retroversion where* $T = \{0, 0, 80\}$*: Screenshots of simulations before (a) and after (b) retroversion of normal BSV, where* $T = \{0, 0, 80\}$*.*

Table 20: *DEMRS HVT-2.5 retroversion angles for normal BSV, where* $T = \{0, 0, 80\}$*.*

Components	Retroversion (°)		
	x (pitch)	y (yaw)	z (roll)
Cx_L	0.000	−2.148	0.000
$M1_L$	0.000	4.663	0.000
$M2_L$	0.000	3.589	0.000
$P1_L$	0.000	0.000	0.000
$P2_L$	0.000	0.000	0.000
$M3_L$	0.000	−5.329	0.000
$M4_L$	0.000	−4.255	0.000
Cv_L	0.000	2.148	0.000
Cx_R	0.000	2.148	0.000
$M1_R$	0.000	−4.663	0.000
$M2_R$	0.000	−3.589	0.000
$P1_L$	0.000	0.000	0.000
$P2_L$	0.000	0.000	0.000
$M3_R$	0.000	5.329	0.000
$M4_R$	0.000	4.255	0.000
Cv_R	0.000	−2.148	0.000

In the previous two simulations, each eye was configured with four peripheral vision vectors, in addition to the principal vision vector. However, in the interest of clarity and in order to emphasize the direction of the principal vision vectors, the following simulations do not display the peripheral vision vectors or the lenses.

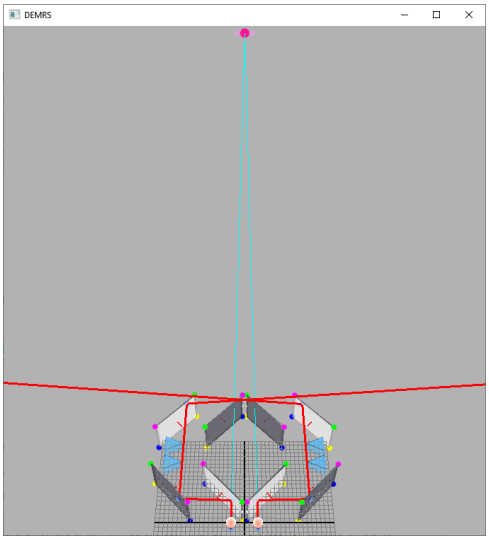

(a) *Before retroversion.*

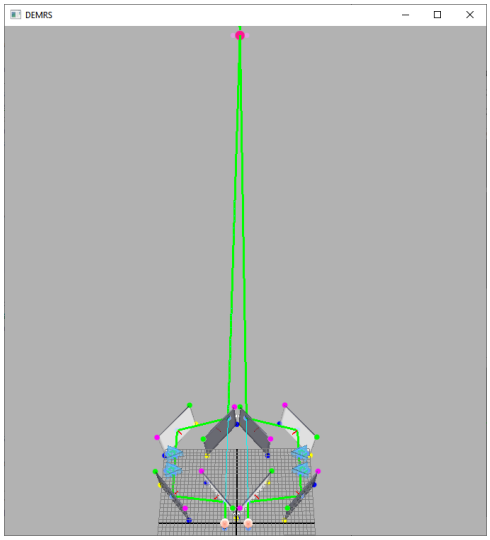

(b) *After retroversion.*

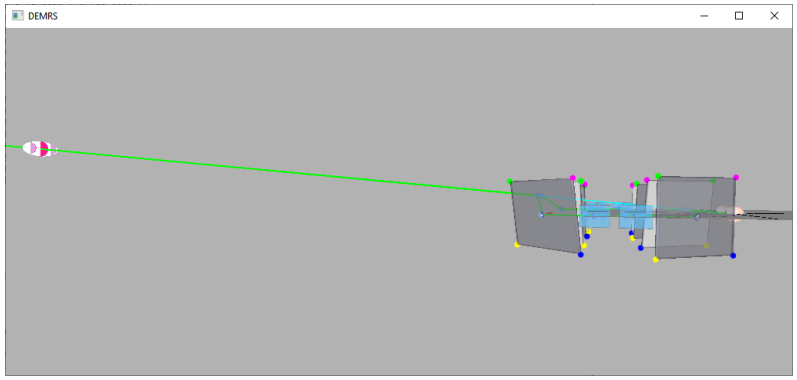

(c) *After retroversion.*

Figure 96: *DEMRS HVT-2.5 retroversion where* $\mathsf{T} = \{0, 20, 200\}$*: Screenshots of simulations before (a) and after (b) retroversion of normal BSV, where* $\mathsf{T} = \{0, 20, 200\}$*. (c) side view of the simulation test showing the height of the target.*

Table 21: *DEMRS HVT-2.5 retroversion angles for normal BSV, where* $\mathsf{T} = \{0, 20, 200\}$.

Components	Retroversion (°)		
	x (pitch)	y (yaw)	z (roll)
$M1_L$	−5.846	4.171	0.000
$M2_L$	1.590	3.582	0.000
$P1_L$	0.000	0.000	0.000
$P2_L$	0.000	0.000	0.000
$M3_L$	8.340	−4.146	0.000
$M4_L$	−3.988	−3.878	0.000
$M1_R$	−5.846	−4.171	0.000
$M2_R$	1.590	−3.582	0.000
$P1_L$	0.000	0.000	0.000
$P2_L$	0.000	0.000	0.000
$M3_R$	8.340	4.146	0.000
$M4_R$	−3.988	3.878	0.000

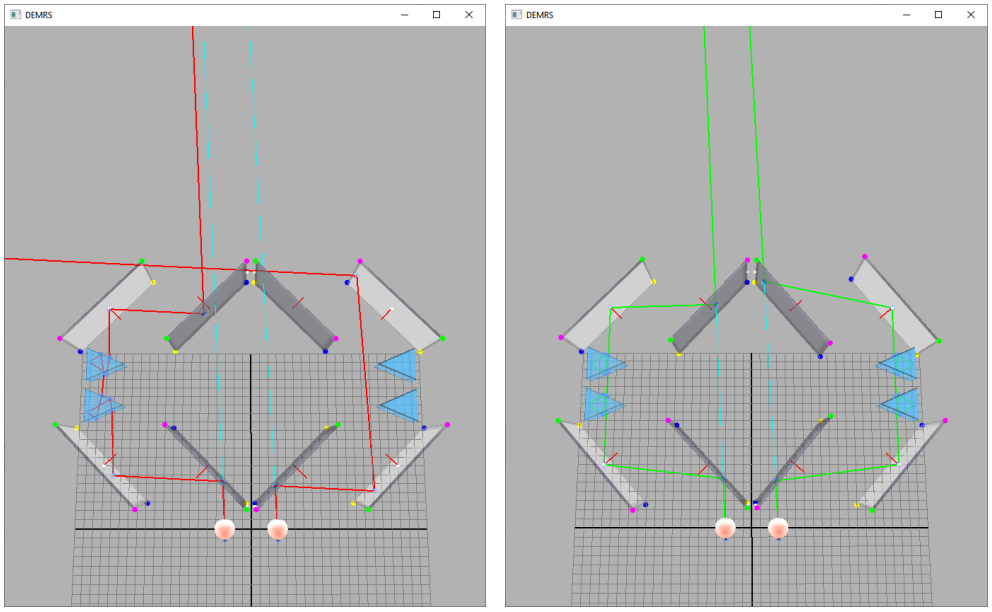

(a) *Before retroversion.* (b) *After retroversion.*

Figure 97: *DEMRS HVT-2.5 retroversion where* $\mathsf{T} = \{45, 0, 700\}$*: Screenshots of simulations before (a) and after (b) retroversion of normal BSV, where* $\mathsf{T} = \{45, 0, 700\}$*. Because of the far distance of the target from the DEMRS origin, the target is not visible in this figure. However, the green coloured vision vectors in (b) indicate that retroversion is successful.*

Table 22: *DEMRS HVT-2.5 retroversion angles where* $T = \{45, 0, 700\}$.

Components	Retroversion (°)		
	x (pitch)	y (yaw)	z (roll)
$M1_L$	0.000	2.334	0.000
$M2_L$	0.000	3.288	0.000
$P1_L$	0.000	0.000	0.000
$P2_L$	0.000	0.000	0.000
$M3_L$	0.000	−1.726	0.000
$M4_L$	0.000	−2.681	0.000
$M1_R$	0.000	−4.525	0.000
$M2_R$	0.000	−3.571	0.000
$P1_L$	0.000	0.000	0.000
$P2_L$	0.000	0.000	0.000
$M3_R$	0.000	5.118	0.000
$M4_R$	0.000	4.163	0.000

The following simulations show the effectiveness of HVT-2.5 in the retroversion of a left eso-hyper-excyclo-tropia, with 7° (≈ 14Δ) eso, 4° (≈ 8Δ) hyper, and 5° (≈ 10Δ) incyclo deviations. The distance of the target from the DEMRS origin ranges at: (a) near distance of 1m, (b) mid distance of 3m, and (c) far distance of 6m. In order to emphasize the strabismic deviation and direction of both principal vision vectors, figure 98 is split into two rows, where the first row shows screenshots of the retroversion from a top view, and the bottom row shows screenshots of the same retroversion from a front view. Tables 23, 24 and 25 present the retroversion angles of the mirrors and prisms required to achieve retroversion at near, mid, and far, respectively.

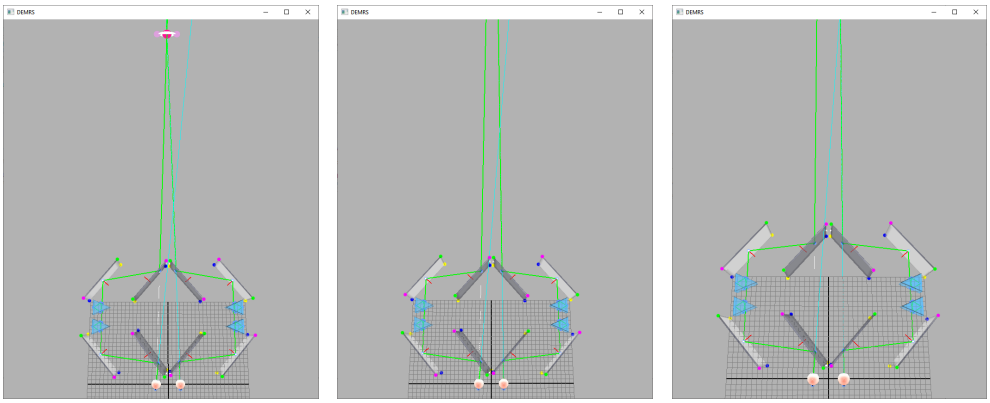

(a) *Convergence of vision vectors where* $T = \{0, 0, 100\}$.

(b) *Convergence of vision vectors where* $T = \{0, 0, 300\}$.

(c) *Parallel vision vectors where* $T = \{0, 0, 600\}$.

Figure 98: *DEMRS HVT-2.5 retroversion for near, mid, and far targets:* *(continued on next page)*

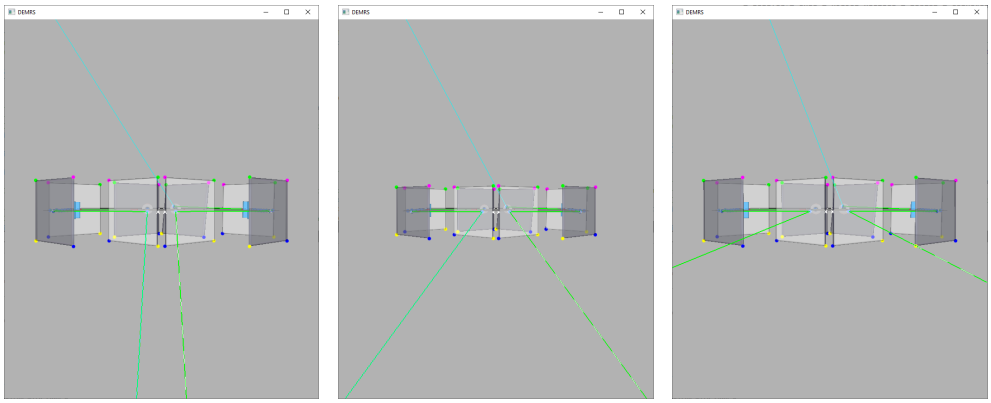

(d) *Convergence of vision vectors where* $T = \{0, 0, 100\}$.

(e) *Convergence of vision vectors where* $T = \{0, 0, 300\}$.

(f) *Parallel vision vectors where* $T = \{0, 0, 600\}$.

Figure 98: *DEMRS HVT-2.5 retroversion for near, mid, and far targets: Screenshots of simulations showing the results after retroversion of a left eso-hyper-excyclo-tropia, with 7° (≈ 14Δ) eso, 4° (≈ 8Δ) hyper, and 5° (≈ 10Δ) incyclo deviations, from two different views, when: (a,d)* $T = \{0, 0, 100\}$, *(b,e)* $T = \{0, 0, 300\}$, *and (c,f)* $T = \{0, 0, 600\}$. *Parts (b), (c), (e) and (f) do not show the target, because it is positioned at a far distance from the DEMRS origin. However, the green coloured vision vectors indicate that retroversion is successful.*

Table 23: *DEMRS HVT-2.5 retroversion angles for left eso-hyper-excyclo-tropia with 7° (≈ 14Δ) eso, 4° (≈ 8Δ) hyper, and 5° (≈ 10Δ) incyclo deviations, where* $T = \{0, 0, 100\}$.

Components	Retroversion (°)		
	x (pitch)	y (yaw)	z (roll)
$M1_L$	−6.759	7.076	0.000
$M2_L$	1.819	3.991	0.000
$P1_L$	0.000	0.000	2.500
$P2_L$	0.000	0.000	0.000
$M3_L$	0.000	−4.949	0.000
$M4_L$	0.000	−4.090	0.000
$M1_R$	0.000	−4.415	0.000
$M2_R$	0.000	−3.556	0.000
$P1_L$	0.000	0.000	0.000
$P2_L$	0.000	0.000	0.000
$M3_R$	0.000	4.949	0.000
$M4_R$	0.000	4.090	0.000

Table 24: *DEMRS HVT-2.5 retroversion angles for left eso-hyper-excyclo-tropia with 7° (≈ 14Δ) eso, 4° (≈ 8Δ) hyper, and 5° (≈ 10Δ) incyclo deviations, where* $\mathsf{T} = \{0, 0, 300\}$.

Components	Retroversion (°)		
	x (pitch)	y (yaw)	z (roll)
$M1_L$	−6.848	6.418	0.000
$M2_L$	1.846	3.903	0.000
$P1_L$	0.000	0.000	2.500
$P2_L$	0.000	0.000	0.000
$M3_L$	0.000	−3.935	0.000
$M4_L$	0.000	−3.649	0.000
$M1_R$	0.000	−3.756	0.000
$M2_R$	0.000	−3.470	0.000
$P1_L$	0.000	0.000	0.000
$P2_L$	0.000	0.000	0.000
$M3_R$	0.000	3.935	0.000
$M4_R$	0.000	3.649	0.000

Table 25: *DEMRS HVT-2.5 retroversion angles for left eso-hyper-excyclo-tropia with 7° (≈ 14Δ) eso, 4° (≈ 8Δ) hyper, and 5° (≈ 10Δ) incyclo deviations, where* $\mathsf{T} = \{0, 0, 600\}$.

Components	Retroversion (°)		
	x (pitch)	y (yaw)	z (roll)
$M1_L$	−6.894	6.090	0.000
$M2_L$	1.861	3.859	0.000
$P1_L$	0.000	0.000	2.500
$P2_L$	0.000	0.000	0.000
$M3_L$	0.000	−3.427	0.000
$M4_L$	0.000	−3.427	0.000
$M1_R$	0.000	−3.427	0.000
$M2_R$	0.000	−3.427	0.000
$P1_L$	0.000	0.000	0.000
$P2_L$	0.000	0.000	0.000
$M3_R$	0.000	3.427	0.000
$M4_R$	0.000	3.427	0.000

Four more tests were conducted with strabismus. In the following simulations, the target T is located: (a) right, i.e. on the negative x-axis, at mid distance of 4m, (b) down, i.e. on the negative y-axis, at near distance of 70cm, (c) left, i.e. on the positive x-axis, at far distance of 8m, and (d) up, i.e. on the positive y-axis, at mid distance of 2m. Also, in order to determine that retroversion is achieved for various types of strabismus, a different type of artificial strabismus was assumed in each simulation, namely: (a) left eso-incyclo-tropia with large deviations of 25° (≈ 50Δ) and 10° (≈ 20Δ), (b) right hypo-tropia with moderate deviation of 12° (≈ 24Δ), (c) left hyper-incyclo-tropia with small deviations of 8° (≈ 16Δ) and 6° (≈ 12Δ), and (d) right exo-excyclo-tropia with micro deviations of 5° (≈ 10Δ) and 2° (≈ 4Δ) Figures 99, 100, 101, and 102 show screenshots of the results before and after retroversion. Tables 26, 27, 28, and 29 present the retroversion angles of the mirrors and prisms required to achieve retroversion.

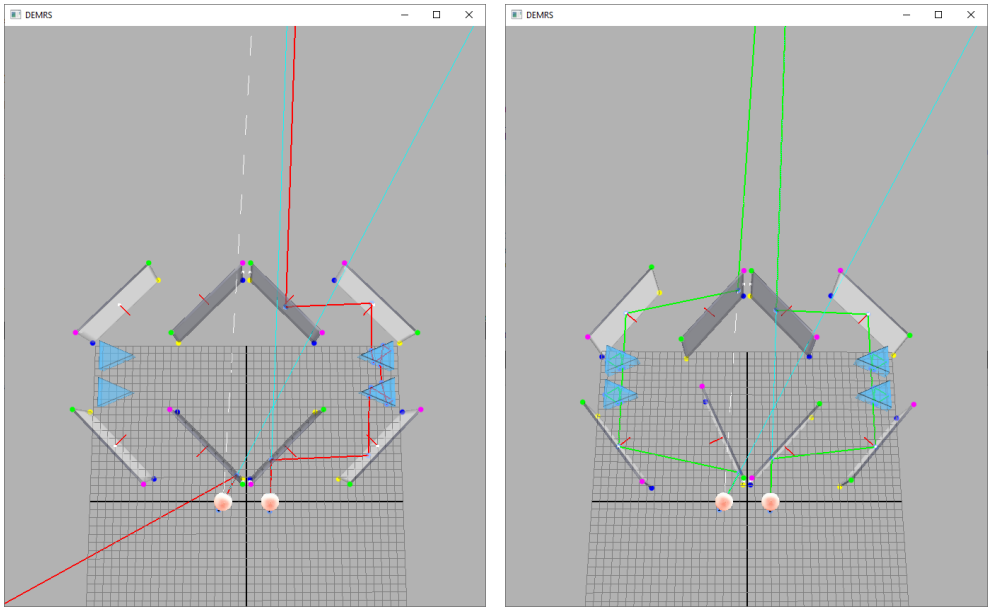

(a) *Before retroversion.* (b) *After retroversion.*

Figure 99: *DEMRS HVT-2.5 retroversion where* $\mathsf{T} = \{-25, 0, 400\}$*: Screenshots of simulations before (a) and after (b) retroversion of a left eso-incyclo-tropia with large deviations of* 25° (≈ 50Δ) *and* 10° (≈ 20Δ)*, where* $\mathsf{T} = \{-25, 0, 400\}$*. Because of the far distance of the target from the DEMRS origin, the target is not visible in this figure.*

Table 26: *DEMRS HVT-2.5 retroversion angles for left eso-incyclo-tropia with large deviations of* 25° *(*$\approx 50\Delta$*) and* 10° *(*$\approx 20\Delta$*), where* $\mathsf{T} = \{-25, 0, 400\}$.

Components	Retroversion (°)		
	x (pitch)	y (yaw)	z (roll)
$M1_L$	0.000	20.071	0.000
$M2_L$	0.000	5.926	0.000
$P1_L$	0.000	0.000	−5.000
$P2_L$	0.000	0.000	0.000
$M3_L$	0.000	−6.338	0.000
$M4_L$	0.000	−4.692	0.000
$M1_R$	0.000	−2.034	0.000
$M2_R$	0.000	−3.251	0.000
$P1_L$	0.000	0.000	0.000
$P2_L$	0.000	0.000	0.000
$M3_R$	0.000	1.257	0.000
$M4_R$	0.000	2.474	0.000

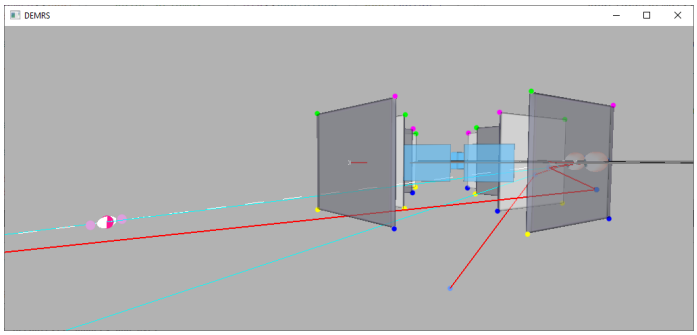

(a) *Before retroversion.*

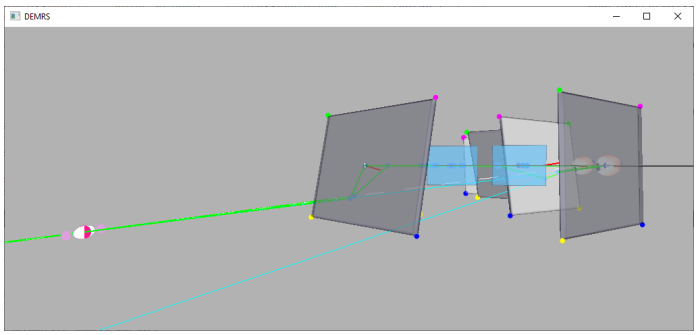

(b) *After retroversion.*

Figure 100: *DEMRS HVT-2.5 retroversion where* $\mathsf{T} = \{0, -35, 70\}$*: Screenshots of simulations before (a) and after (b) retroversion of a right hypo-tropia with moderate deviation of* 12° *(*$\approx 24\Delta$*), where* $\mathsf{T} = \{0, -35, 70\}$.

Table 27: *DEMRS HVT-2.5 retroversion angles for right hypo-tropia with moderate deviation of* 12° *(≈ 24Δ), where* $\mathsf{T} = \{0, -35, 70\}$.

Components	Retroversion (°)		
	x (pitch)	y (yaw)	z (roll)
$M1_L$	8.140	5.334	0.000
$M2_L$	−2.198	3.788	0.000
$P1_L$	0.000	0.000	0.000
$P2_L$	0.000	0.000	0.000
$M3_L$	−11.920	−5.517	0.000
$M4_L$	5.610	−4.617	0.000
$M1_R$	19.770	−7.946	0.000
$M2_R$	−5.115	−4.660	0.000
$P1_L$	0.000	0.000	0.000
$P2_L$	0.000	0.000	0.000
$M3_R$	−11.920	5.517	0.000
$M4_R$	5.610	4.617	0.000

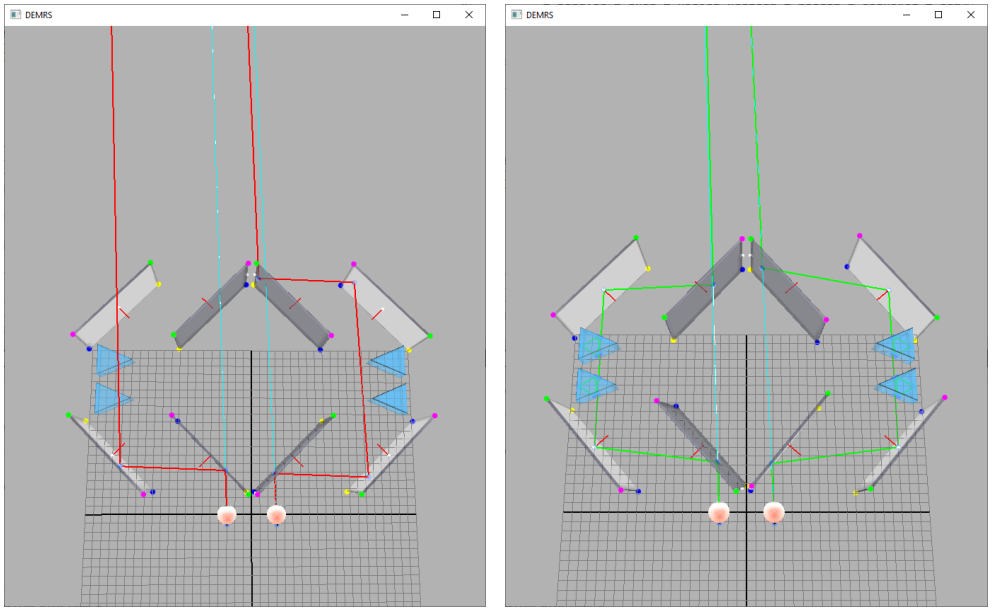

(a) *Before retroversion.* (b) *After retroversion.*

Figure 101: *DEMRS HVT-2.5 retroversion where* $\mathsf{T} = \{40, 0, 800\}$*:* *(continued on next page)*

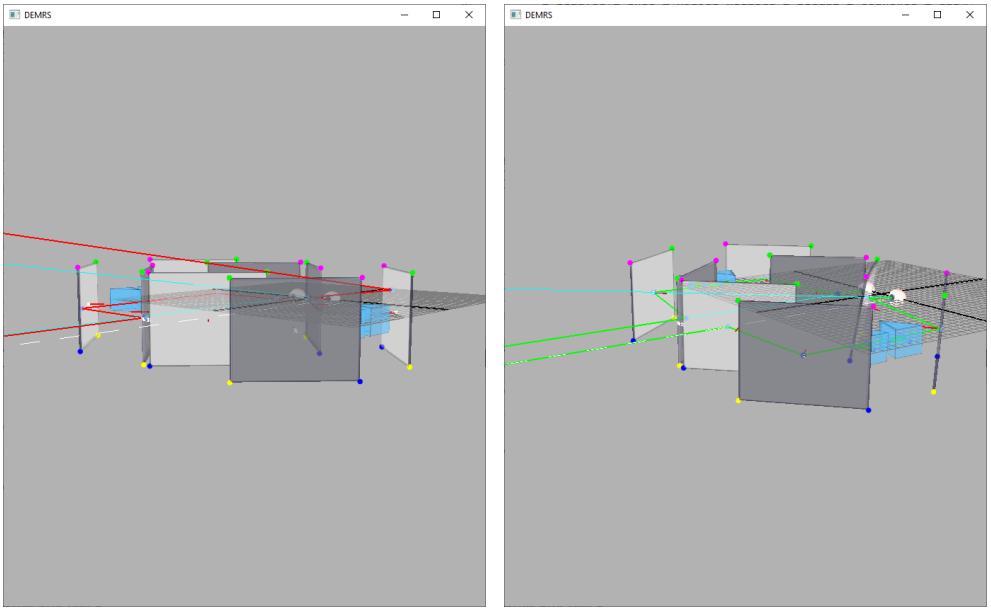

(c) *Before retroversion.* (d) *After retroversion.*

Figure 101: *DEMRS HVT-2.5 retroversion where* $T = \{40, 0, 800\}$*: Screenshots of simulations before (a, c) and after (b, d) retroversion of a left hyper-incyclo-tropia with small deviations of* 8° *(*$\approx 16\Delta$*) and* 6° *(*$\approx 12\Delta$*), where* $T = \{40, 0, 800\}$*. Because of the far distance of the target from the DEMRS origin, the target is not visible in this figure.*

Table 28: *DEMRS HVT-2.5 retroversion angles for left hyper-incyclo-tropia with small deviations of* 8° *(*$\approx 16\Delta$*) and* 6° *(*$\approx 12\Delta$*), where* $T = \{40, 0, 800\}$*.*

Components	Retroversion (°)		
	x (pitch)	y (yaw)	z (roll)
$M1_L$	−8.495	2.716	0.000
$M2_L$	2.311	3.463	0.000
$P1_L$	0.000	0.000	−3.000
$P2_L$	0.000	0.000	0.000
$M3_L$	0.000	−1.513	0.000
$M4_L$	0.000	−2.587	0.000
$M1_R$	0.000	−4.663	0.000
$M2_R$	0.000	−3.589	0.000
$P1_L$	0.000	0.000	0.000
$P2_L$	0.000	0.000	0.000
$M3_R$	0.000	5.329	0.000
$M4_R$	0.000	4.255	0.000

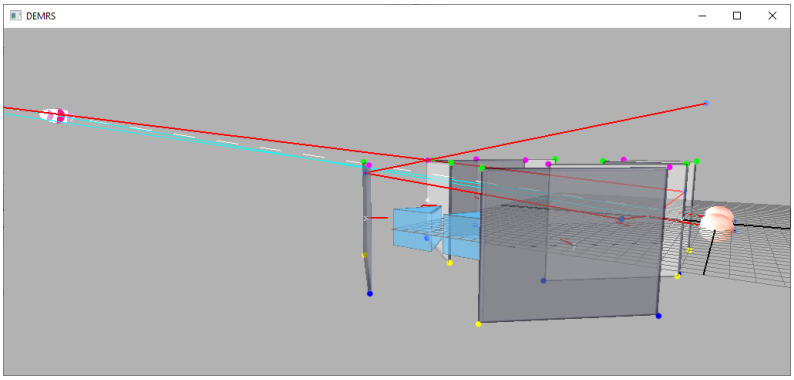

(a) *Before retroversion.*

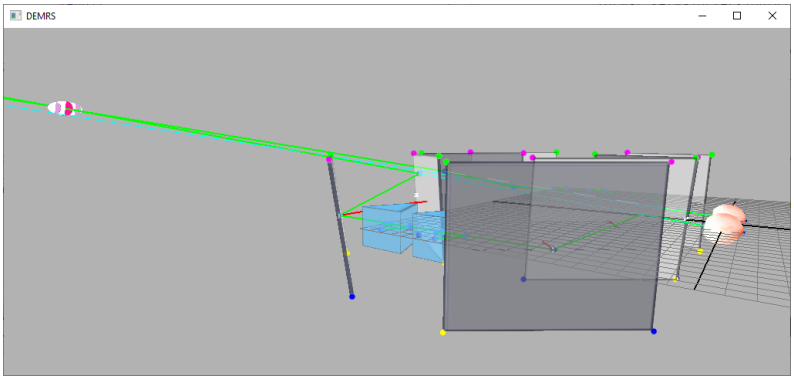

(b) *After retroversion.*

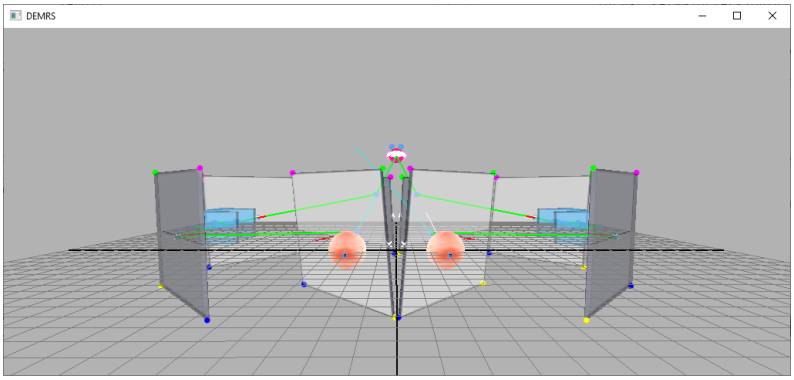

(c) *After retroversion.*

Figure 102: *DEMRS HVT-2.5 retroversion where* $\mathsf{T} = \{0, 50, 200\}$*: Screenshots of simulations before (a) and after (b) retroversion of a right exo-excyclo-tropia with micro deviations of* $5°$ *(*$\approx 10\Delta$*) and* $2°$ *(*$\approx 4\Delta$*), where* $\mathsf{T} = \{0, 50, 200\}$*.*

Table 29: *DEMRS HVT-2.5 retroversion angles for right exo-excyclo-tropia with micro deviations of* 5° (≈ 10Δ) *and* 2° (≈ 4Δ), *where* $T = \{0, 50, 200\}$.

Components	Retroversion (°)		
	x (pitch)	y (yaw)	z (roll)
$M1_L$	−5.846	4.171	0.000
$M2_L$	1.590	3.582	0.000
$P1_L$	0.000	0.000	0.000
$P2_L$	0.000	0.000	0.000
$M3_L$	8.340	−4.146	0.000
$M4_L$	−3.988	−3.878	0.000
$M1_R$	−5.487	−7.054	0.000
$M2_R$	1.479	−3.963	0.000
$P1_L$	0.000	0.000	1.000
$P2_L$	0.000	0.000	0.000
$M3_R$	8.340	4.146	0.000
$M4_R$	−3.988	3.878	0.000

The final HVT-2.5 simulation assesses the effectiveness of HVT-2.5 in retroversing strabismus on the left eye with horizontal, vertical and torsional deviations of 16° (≈ 32Δ), 10° (≈ 20Δ) and 8° (≈ 16Δ), respectively. The target is located upwards and to the left at mid distance of 3m, $T = \{25, 40, 300\}$. Figure 103 shows screenshots of the DEMRS HVT-2.5, before and after retroversion, and table 30 presents the retroversion angles of the mirrors and prisms required to achieve retroversion.

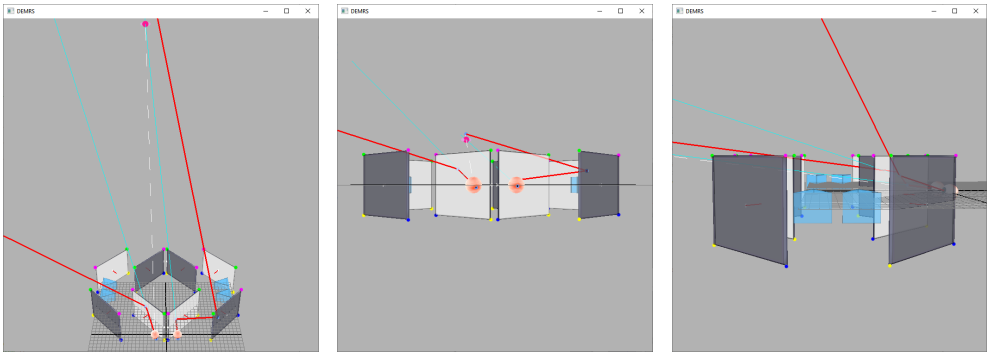

(a) *Before retroversion.* (b) *Before retroversion.* (c) *Before retroversion.*

Figure 103: *DEMRS HVT-2.5 retroversion where* $T = \{25, 40, 300\}$: *(continued on next page)*

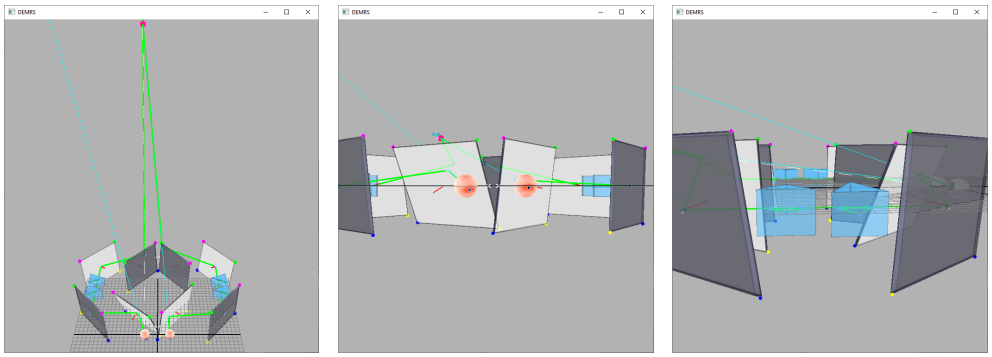

(d) *After retroversion.* (e) *After retroversion.* (f) *After retroversion.*

Figure 103: *DEMRS HVT-2.5 retroversion where* $T = \{25, 40, 300\}$*: Screenshots of simulations before (a), (b), (c) and after (d), (e), (f) retroversion of a left exo-hyper-excyclo-tropia with moderate deviations of* 16° *(≈* 32Δ*),* 10° *(≈* 20Δ*) and* 8° *(≈* 16Δ*), where* $T = \{25, 40, 300\}$*. This simulation is shown from a various different angles in order to emphasize the location of the target, strabismic deviation, and torsional rotation of the prism.*

Table 30: *DEMRS HVT-2.5 retroversion angles for left exo-hyper-excyclo-tropia with moderate deviations of* 16° *(≈* 32Δ*),* 10° *(≈* 20Δ*) and* 8° *(≈* 16Δ*), where* $T = \{25, 40, 300\}$*.*

Components	Retroversion (°)		
	x (pitch)	y (yaw)	z (roll)
$M1_L$	−19.496	−6.282	0.000
$M2_L$	5.248	3.146	0.000
$P1_L$	0.000	0.000	4.000
$P2_L$	0.000	0.000	0.000
$M3_L$	5.645	1.218	0.000
$M4_L$	−2.887	−1.433	0.000
$M1_R$	−3.644	−7.154	0.000
$M2_R$	0.984	−3.950	0.000
$P1_L$	0.000	0.000	0.000
$P2_L$	0.000	0.000	0.000
$M3_R$	1.464	3.191	0.000
$M4_R$	1.704	−0.217	0.000

4.5.4 *Discussion*

DEMRS HVT-2.5 is a DRS compliant system designed to achieve retroversion of strabismus, including torsional deviations. The simulations show that the retroversion engine can correctly calculate the rotations of the mirrors and delta prisms, such that the vision vectors pass through the same fixation target with normal orientation. Also, similar to HV-2.0, the retrover-

sion engine takes into consideration mirrors $M_{3_{L/R}}$ and $M_{4_{L/R}}$, which are used to maintain normal binocular disparity and resultant IPD. Moreover, the simulations show that HVT-2.5 is able to achieve retroversion for various classifications of strabismus, including deviations that combine torsion with other directions.

Although the predecessors of HVT-2.5, which were HVT-1.0 presented in appendix B.5 and HVT-2.0 presented in appendix B.6, satisfied the principle of DRS their designs had significant limitations that complicated, and sometimes prevented, the achievement of retroversion. Briefly, HVT-1.0 was designed to use one dove prism on each side, positioned in front of $M_{4_{L/R}}$. The simulations of HVT-1.0 showed that: (a) each dove prism required to be rotated and translated, in order for the principal vision vectors to be properly refracted by the prisms, (b) the length of a dove caused the prisms on both sides to collide with each other when rotating in opposite directions, and (c) the vision vectors were rotated, but inverted. The design of HVT-2.0 addressed the issues of HVT-1.0 by using an additional dove prism on each side, in order to invert the vision vectors that were previously inverted by the original prism. Also, the prisms were positioned between $M_{2_{L/R}}$ and $M_{3_{L/R}}$, so that they would only have to rotate about the z-axis in order to retroverse torsional deviations. However, the simulations of HVT-2.0 showed that the overall size of the system did not allow the retroversion of strabismus for near fixation targets of distance $\leqslant 1m$ from the DEMRS origin. Consequently, HVT-2.5 consists of delta prisms that significantly reduce the overall size of the system, thereby, achieving retroversion of strabismus for targets located less than $1m$ from the DEMRS origin.

4.6 SUMMARY

The DRS is a novel principle that was developed to assist in the diagnosis and treatment of strabismus, by establishing a set of criteria to achieve retroversion. A DEMRS, which is a DRS compliant system, must: (a) redirect both principal vision vectors so that they simultaneously pass through the same fixation target, (b) maintain normal resultant inter-pupillary distance, (c) maintain normal binocular disparity, and (d) maintain normal orientation of the vision vectors. Regardless of the classification of a strabismus, a DEMRS should achieve retroversion so that the brain can receive fusible visual stimuli deriving from the same fixation target. The objective of DRS is to enable binocular depth perception.

The DEMRS simulator is a software application that was developed in order to simulate DRS compliant systems. The simulator accepts a set of inputs to the retroversion engine, including the configuration of a DEMRS, and provides two outputs, visualization and hardware, as front-ends to a system. The visualization output is a 3D representation of a DEMRS that is evaluated through a series of simulations, whereas the hardware output connects the DEMRS simulator with a proof of concept device, presented in the next chapter.

This chapter described two DRS compliant systems, DEMRS HV-2.0 and DEMRS HVT-2.5, where HV-2.0 compensates for horizontal and vertical strabismus, and HVT-2.5 compensates for horizontal, vertical, and torsional strabismus. The simulations of HV-2.0 show that the retroversion engine can correctly calculate the rotations of the mirrors, such that both principal vision vectors pass through the same fixation target, while maintaining normal binocular disparity and resultant IPD. Furthermore, a visualization of the “fused" image of an autostereogram showed that by using HV-2.0 to redirect both principal vision vectors further “through" the autostereogram, the illusion appears. Finally, a basic apparatus was built and tested with human subjects who possessed normal BSV, in order to determine the fusibility of the visual stimuli received through DEMRS. Tests showed that this basic apparatus of HV-2.0 allowed subjects to binocularly perceive depth. Because HV-2.0 was not designed to retroverse torsional strabismus, HVT-2.5 was developed that consists of a set of rotatory delta prisms in order to compensate torsional deviations. The simulations show that the retroversion engine can calculate the rotations of the mirrors and prisms, such that the vision vectors pass through the fixation target with normal orientation, while maintaining normal binocular disparity and IPD. Lastly, as the scope of this thesis is the retroversion of strabismus with regards to principal vision vectors, a field of view analysis was not performed for either system.

The previous chapter mentioned that the majority of strabismic deviations are horizontal and vertical, with lesser occurrences of torsional strabismus. Hence, the next chapter presents a DEMRS proof of concept (POC) device that was built based on the design of HV-2.0, so that it can be used to test DRS involving human subjects with normal BSV and strabismus.

5

A DEMRS PROOF OF CONCEPT DEVICE

"Μη μου τους κύκλους τάραττε."
— Αρχιμήδης, 287-212 π.Χ.

"Do not ruin my circles."
— Archimedes, 287-212 BC

The principle of Dynamic Retroversion of Strabismus (DRS), presented in the previous chapter, defines a set of criteria in order to achieve retroversion, and provides overarching guidelines for developing a class of novel systems (DEMRS) that are designed to assist in the diagnosis and treatment of strabismus. The simulation studies indicate that such systems are viable. Therefore, this chapter presents the design and assembly of a DEMRS proof of concept (POC) device, which is intended to be used under laboratory conditions in order to demonstrate the efficacy of a DEMRS in the restoration of normal BSV on human subjects with strabismus (see chap. 6). It is vital to note that this POC device is not a working prototype of a DEMRS, and therefore it is not required to be compact or manufactured with high precision components and processes.

Because the majority of strabismic deviations are horizontal and vertical, the design of the POC device is based on the schematic of HV-2.0 (see sect. 4.4), which does not compensate for torsional deviations. This chapter outlines the individual components of the POC device, and discusses the methods that were adopted to overcome certain difficulties encountered during its development. Lastly, a series of tests have been designed in order to determine whether or not the principal vision vectors, deriving from a fixation target, can be simultaneously received by both eyes.

5.1 DEVICE OVERVIEW

The DEMRS POC device must meet the following requirements, in order to qualify as proof of concept. This device:

- is based on the design of HV-2.0, described in section 4.4.
- receives retroversion angles as input from the DEMRS simulator.

- dynamically rotates the mirrors in two dimension, as per the coordinate system defined in subsection 4.3.1.
- rotates each mirror within the error margin of ±5.2%, as per the sensitivity analysis in subsection 4.4.5.
- provides basic feedback about the rotation of each mirror.

Figure 104 shows the design of the DEMRS POC device, which compared to the layout of HV-2.0 (fig. 67) excludes the two sets of convex and concave lenses. This is because the evaluation of the DEMRS POC device, discussed in the next chapter, is focused in the retroversion of strabismus with regards to principal vision vectors, which are responsible for central vision, and the use of mirrors suffices for the clear view of the fixation target. Although lenses would produce a clear view of the surrounding environment without confusion from arbitrary peripheral visual stimuli (see appendix B.2.6), constraining the direction of peripheral vision vectors is not necessary for the development of a proof of concept device.

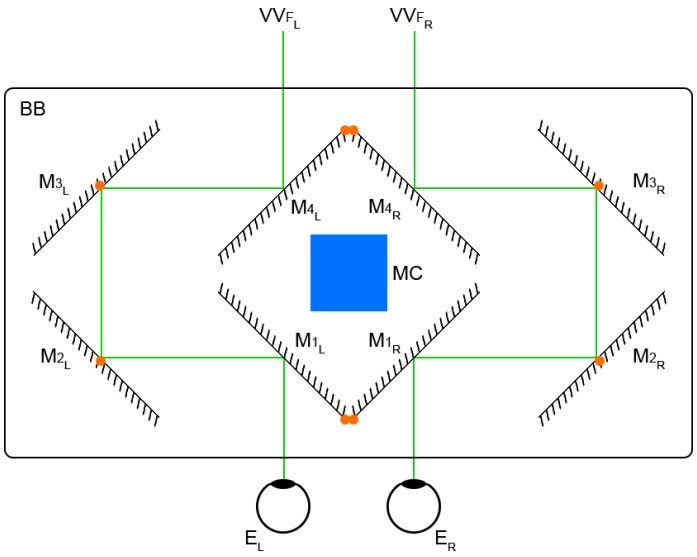

Figure 104: *DEMRS POC: An overview of the POC device based on HV-2.0, where* $VV_{F_{L/R}}$ *are the left and right principal vision vectors,* $M_{1,2,3,4_{L/R}}$ *are the left and right set of mirrors, and* $E_{L/R}$ *represent the left and right eyes. Each orange coloured point represents the pivot of rotation of each mirror mount. The blue rectangle at the centre of the system represents a micro-controller* MC *that controls the orientation of the mirrors, whereas the* BB *represents the base board, which supports the mirror mounts.*

The DEMRS POC device is divided into the following four clusters / groups, where each cluster / group consists of one or more components:

- **DEMRS Simulator:** As mentioned in the previous chapter, the simulator provides two outputs as front-ends to a DEMRS, visualization

and hardware communication module (HCM). The HCM output is responsible for the communication of the DEMRS simulator (software) with the POC device (hardware). The HCM was developed in order to transfer the retroversion angles calculated by the simulator to a micro-controller[1], in order to control the rotation of the physical mirrors.

- **Micro-controller:** The POC device requires the use of an Arduino Uno micro-controller in order to dynamically control the rotation of the mirror mounts, holding the physical mirrors. The micro-controller converts the retroversion angles to signals, in order to be received by a set of motors in each mirror mount. Due to the limited number of output pins, provided by an Arduino Uno, this cluster contains a custom decoder-latch circuit that enables a larger number of motors to be controlled by an Arduino Uno.

- **Mirror Mounts:** This cluster consists of four components: stepper motors and their drivers, 3D printed parts, and mirrors. The POC device is designed to use eight mirrors, four on each side ($M1_{L/R}$, $M2_{L/R}$, $M3_{L/R}$, and $M4_{L/R}$), where $M1_{L/R}$ and $M4_{L/R}$ can rotate about their edge, and $M2_{L/R}$ and $M3_{L/R}$ can rotate about their centre (fig. 104). Consequently, two types of mirror mounts are designed, one for each pivot of rotation. A mirror mount is composed of 3D printed parts, where some parts are designed to accommodate two stepper motors in order to rotate the mirror in two dimensions, i.e. horizontally about the y-axis (yaw) and vertically about the x-axis (pitch).

- **Base Board:** Consists of three components: a wooden board, a plexi glass, and four adjustable legs. The default position and orientation of each mirror mount was marked on the wooden board, so that each mirror could be placed on the board according to the design in figure 104. Also, the markings on the board are used as points of reference, in order to provide basic feedback about the rotation of each mirror. A plexi glass minimizes the friction between a mirror mount and the surface of the wooden board, whereas the four adjustable legs balance the mirrors and level the POC device. Additionally, the base board allows the micro-controller cluster to be placed underneath the mirrors.

Figure 105 shows two blueprints of the POC device illustrating its structure. The blueprints, including all measurements, can be accessed at `https://bitbucket.org/cglynos/demrs/src/master/POC_Device/`.

1 A micro-controller is an inexpensive compact computer that contains one or more CPUs, integrated memory and peripheral interfaces (Horowitz and Hill, 2015).

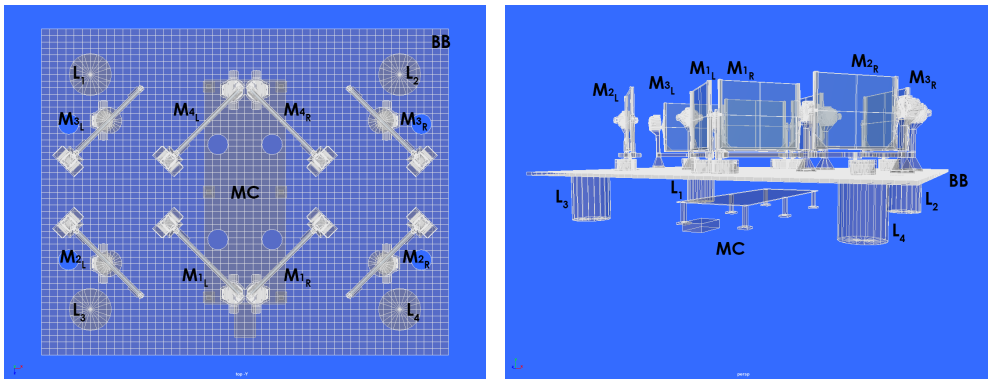

(a) *Top view* (b) *Perspective view*

Figure 105: *Device schematics: Top and perspective views of the POC device, where* BB *is the base board,* $L_{1,2,3,4}$ *are four adjustable support legs of the board,* MC *is the micro-controller, and* $M_{1,2,3,4_{L/R}}$ *are the left and right set of mirrors.*

As illustrated by the diagram in figure 106, the communication pipeline between the DEMRS simulator, running on a laptop, and the POC device is the outlined as follows:

1. The operator of the DEMRS provides a set of inputs to the simulator in order to calculate the retroversion angles of the mirrors (see sect. 4.3). The Hardware Communication Module (HCM) transfers the calculated retroversion angles to the micro-controller.

2. The Arduino Uno receives the retroversion angles from the HCM, converts them into signals, and transfers them to the decoder-latch (DL) circuit, which functions as a hub that enables the control of a larger number of stepper motors using an Arduino Uno.

3. Each output from the decoder-latch circuit is associated with a mirror mount. The decoder-latch circuit transfers the signals to the corresponding drivers, which control the motors that rotate the mirror.

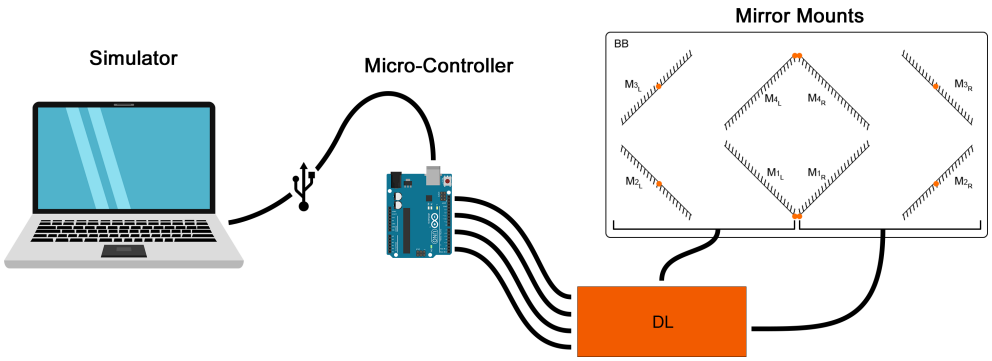

(a) *General view of pipeline.*

Figure 106: *Device pipeline: (continued on next page)*

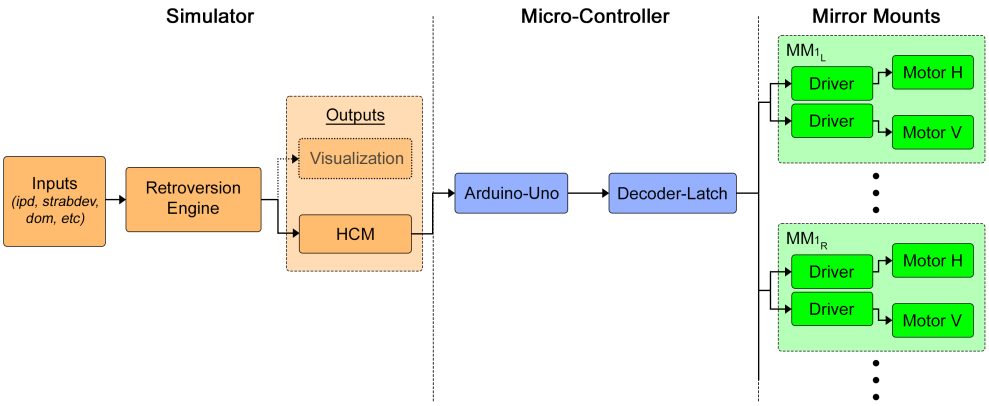

(b) *Component based view of pipeline.*

Figure 106: *Device pipeline: Diagrams illustrating the communication pipeline between the DEMRS simulator and the POC device.*

The following sections of this chapter describe each cluster, along with their underlying components.

5.2 DEMRS SIMULATOR - HCM

The computer running the DEMRS simulator is connected to the Arduino Uno micro-controller via a USB 2.0 cable, so that the Hardware Communication Module (HCM) can transfer the calculated retroversion angles to the micro-controller. Although the DEMRS simulator was tested under Windows, Mac and Linux, it was primarily executed on the MacBook Pro laptop, described in the previous chapter (see specifications in sect. 4.3), as the laptop could be placed near the POC device.

Initially, the HCM searches the available ports of the laptop, using the product identifier number and vendor identifier number of the Arduino Uno, in order to establish a connection with the micro-controller. If the micro-controller is not connected to the laptop the HCM fails to establish the connection, and does not proceed with the transfer of the retroversion angles. If the micro-controller is found the HCM connects with the Arduino Uno, and does not stop the connection until the DEMRS simulator is closed, or the USB cable removed.

The HCM stores the retroversion angles in a map[2], where the first element (key) is the id of a mirror, and the second element (value) is the retroversion angles associated with the mirror. In order to transfer the retroversion angles across, the HCM converts the retroversion angles into a string stream so that it can be sent to the micro-controller as an array of bytes. Table

2 In C++, a map is an associative container that stores elements in key-value pairs.

31 presents the process of HCM in which the retroversion angles are sent to the micro-controller.

Table 31: Process of the HCM shown by the pseudocode (left) and flowchart (right).

```
Begin
    for p in ports do
        if Arduino is connected then
            initialise(p)
        end
    end

    if Arduino is not connected then
        return
    end

    for i in retroversion_angles_map
    do
        stringify(i)
        send_data_to_arduino(i)
    end
```

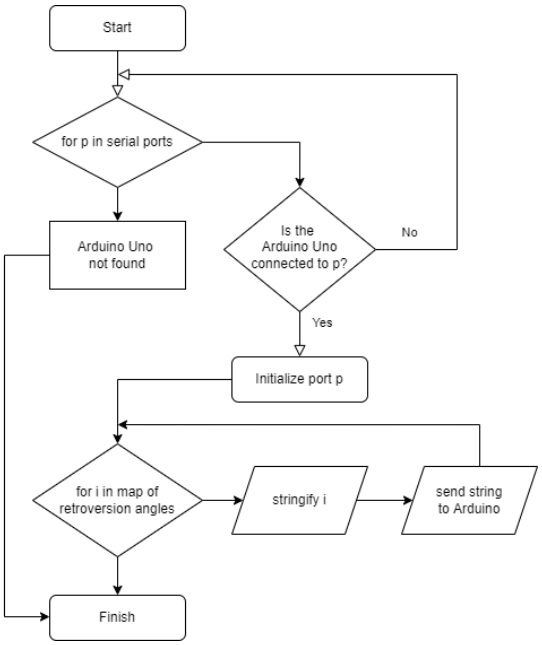

The complete code of the HCM can be accessed at https://bitbucket.org/cglynos/demrs/src/master/HVT_25/.

5.3 MICRO-CONTROLLER

This cluster is responsible for receiving the retroversion angles, from the HCM, and convert them into signals to control the rotation of the motors, residing in the mirror mounts. The micro-controller cluster consists of an Arduino Uno and a decoder-latch circuit board.
The Arduino Uno:

- receives retroversion angles as string streams, from the HCM.
- parses the string streams, and stores the angles.
- converts the angles into signals, to control the motors.
- sends the signals to the decoder-latch circuit board.

The decoder-latch:

- receives signals from the Arduino Uno via two input lines, such that each line delivers signals to the motors on either side of the DEMRS POC device.

- splits the input lines to eight output lines, arranged according to the position of each mirror mount.
- regulates voltage and current flow, so that the motors receive 12V but decoders and latches receive 5V.
- provides female pin headers, in order to send the signals to the driver of each motor.

5.3.1 *Arduino Uno*

The Arduino Uno (fig. 107) is a programmable micro-controller with 14 I/O digital pins and 6 I/O analog pins (Arduino, 2019). This micro-controller can be supplied with 5V power via the USB 2.0 connector, and with $7-12$V DC power using a power jack or through the Vin (voltage input) pin. If the Arduino Uno is supplied with more than 12V, the voltage regulator can overheat and damage the board. Regardless of the input voltage supplied to the Arduino Uno, the output pins of the board output $3.3-5$V DC.

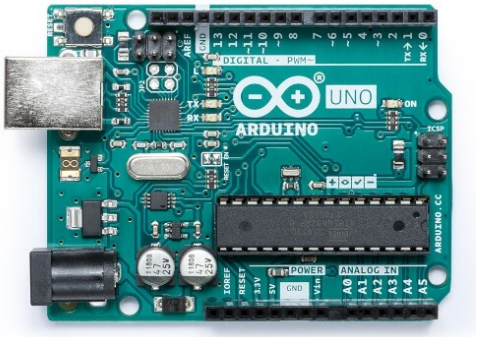

Figure 107: *Arduino Uno: An image of the Arduino Uno micro-controller board showing the 14 digital and 6 analog input/output pins (Arduino, 2019).*

The Arduino Uno micro-controller, used in the DEMRS POC device, is powered with 5V by the USB 2.0 cable that is also used to transfer retroversion angles from the DEMRS simulator. Furthermore, a custom application was developed to initialize the pins of the micro-controller, convert the retroversion angles into signals, and control the rotation of the motors. Initially, the Arduino Uno checks the connection to the serial port of the laptop. Next, the Arduino Uno parses the received string stream, and stores the retroversion angles of each mirror in a contiguous array, sorted such that the mirrors are rotated in following order: $M1_L$ -> $M2_L$ -> $M3_L$ -> $M4_L$ -> $M1_R$ -> $M2_R$ -> $M3_R$ -> $M4_R$. When the array is traversed, each angle is converted into signals (steps) using equation 8.

$$steps = \theta^{\circ} \times \frac{spr}{360} \tag{8}$$

where:

θ is the retroversion angle in degrees, and

spr are the steps per revolution of the motor.

Lastly, the signals are transferred to the decoder-latch using the digital and analog pins of the Arduino Uno, identified in the next subsection. Table 32 shows the process of the Arduino Uno, receiving the retroversion angles from the simulator in order to rotate the motors.

Table 32: Process of the Arduino Uno shown by the pseudocode (left) and a flowchart (right).

```
Begin
    if Arduino is not connected then
        return
    end
    initialise_pins()
    read_string()
    parse_retroversion_angles()
    for m in motors do
        convert_angle_to_signal()
        rotate(m)
    end
```

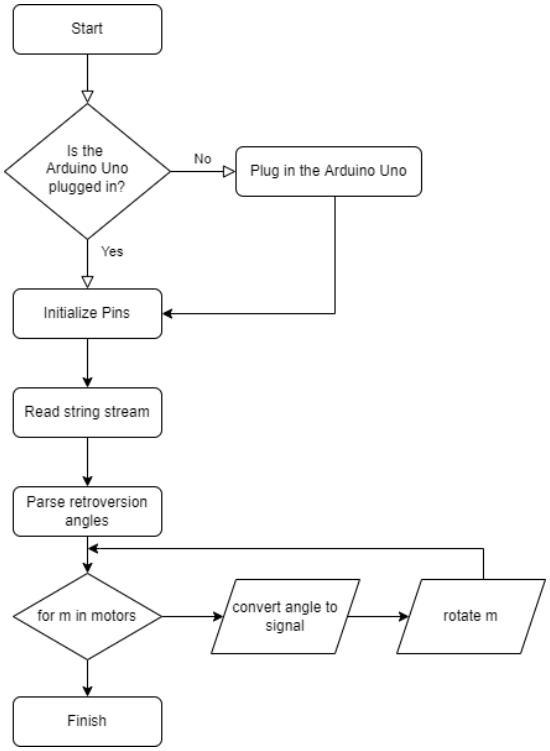

The latest version of the micro-controller program can be accessed at https://bitbucket.org/cglynos/demrs/src/master/HVT_25/include/Device/. The DEMRS POC device is designed to use sixteen motors in order to rotate eight mirrors, horizontally and vertically. Each motor is controlled by a driver, which connects into four digital pins on the Arduino Uno. Therefore, in order to control all motors in the DEMRS POC device, the micro-controller must supply 64 I/O digital pins. Unfortunately, the Arduino Uno board is limited to fourteen digital and six analog pins, which are not enough to control all the motors in the POC device. Consequently, the decoder-latch

circuit was developed, in order to enable the control of sixteen motors using the limited number of I/O pins provided by the Arduino Uno.

5.3.2 *Decoder-Latch Circuit Board*

The decoder-latch circuitry consists of two types of devices, a decoder/demultiplexer and a tri state latch. A 3 Line to 8 Line Decoder Demultiplexer (SN74LS138N) (Texas Instruments, 1988) accepts three binary inputs (A, B, C) through which eight possible outputs (Y_0...Y_7) are enabled (fig. 108) (Kreith and Goswami, 2005). Each input is connected to an I/O pin on the Arduino Uno, so that the combination of the binary inputs is programmed via the Arduino device.

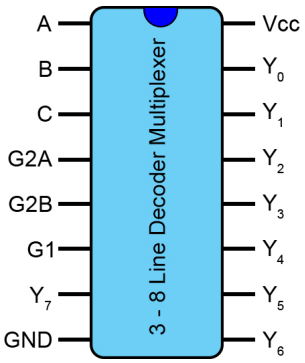

Figure 108: *SN74LS138N: A 3 Line to 8 Line Decoder Demultiplexer device where* A, B *and* C *are the Input pins connected to the Arduino Uno,* G2A, G2B *and* G1 *are the Enable switches of the decoder device,* GND *is noted as the Ground,* Vcc *is the Power supply and* $Y_{[0-7]}$ *are the Output pins.*

Apart from the three binary inputs (A, B, C), the decoder device (SN74LS138N) has three enable inputs (G1, G2A, G2B) that allow parallel expansion of the decoder device to a 1 of 32 (5 lines to 32 lines) decoder (Texas Instruments, 1988). For example, when G1 is enabled and both G2A and G2B are disabled, all outputs of the decoder device will be enabled. But if G1 is disabled, or either of G2A or G2B is enabled, then all outputs will be disabled. Assuming that G1 is the data input from the Arduino Uno and G2A, G2B are grounded, table 33 shows the truth table of the binary input combinations that enable each individual output of the decoder device.

Table 33: *Binary input combinations that enable one of the eight logical outputs on the 3 Line to 8 Line Decoder Demultiplexer device, where* A, B, C *are the Input pins,* $Y_{[0-7]}$ *are the Output pins,* 1 *represents a True/On value and* 0 *represents a False/Off value.*

INPUTS			OUTPUTS							
A	B	C	Y_0	Y_1	Y_2	Y_3	Y_4	Y_5	Y_6	Y_7
0	0	0	1	0	0	0	0	0	0	0
0	0	1	0	0	0	0	1	0	0	0
0	1	0	0	0	1	0	0	0	0	0
0	1	1	0	0	0	0	0	0	1	0
1	0	0	0	1	0	0	0	0	0	0
1	0	1	0	0	0	0	0	1	0	0
1	1	0	0	0	0	1	0	0	0	0
1	1	1	0	0	0	0	0	0	0	1

In the design of this decoder-latch circuitry, both G2A and G2B enable switches are connected to ground whereas G1 is connected to the power supply, which effectively keeps the decoder constantly enabled. Furthermore, the eight outputs of the decoder are used to control each pair of motors within a mirror mount. For example, enabling the Y_0 output enables the pair of motors that rotate $M1_L$. The combinations of the binary inputs are stored within an array whose order matches the order of the retroversion angles.

Each output from the decoder device is connected to the output enable pin (OE) of an Octal Tri-state Transparent Latch (M74HCT573B1R) (SGS Thomson, 1993), a device whose output changes when there is a change in the input signal (Horowitz and Hill, 2015). An Octal Tri-state Transparent Latch (fig. 109) has eight input pins (D_0...D_7), which are connected to eight digital pins on the Arduino Uno micro-controller, and eight output pins (Q_0...Q_7), which are connected to the drivers of the motors. The decoder-latch circuitry is designed to use eight latches, one for each pair of motors. The latch enable pin (LE) is also connected to a digital pin on the Arduino Uno, but it is constantly enabled.

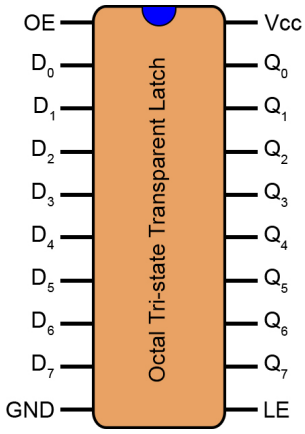

Figure 109: *M74HCT573B1R: Illustration of an Octal Tri-state Transparent Latch, where* OE *is the Output Enable switch,* $D_{[0-7]}$ *are the Input Data pins,* GND *is the Ground,* Vcc *is the Power supply,* $Q_{[0-7]}$ *are the Output Latch pins and* LE *is the Latch Enable switch.*

When the Arduino Uno sends the signals to the decoder latch, in order to rotate a mirror mount, it firstly enables the output of the decoder device that corresponds to the id of the mirror, ex. enable Y_0 to rotate $M1_L$, and next, sends the signals. The decoder receives the binary combination as input, and enables the corresponding output, while the remaining outputs of the decoder are disabled. Next, the output from the decoder enables the corresponding latch, in order to allow the drivers, connected to the latch, receive the signals. Lastly, the drivers control the orientation of the motors, in order to rotate the mirror mount. Through the decoder-latch circuitry, all motors receive the same signal from the Arduino Uno, but because their latch is disabled from the decoder, the motors do not rotate. Figure 110 shows a diagram of how a retroversion angle of 10° reaches the corresponding motors of the $M1_L$ mirror mount, through the decoder-latch circuitry.

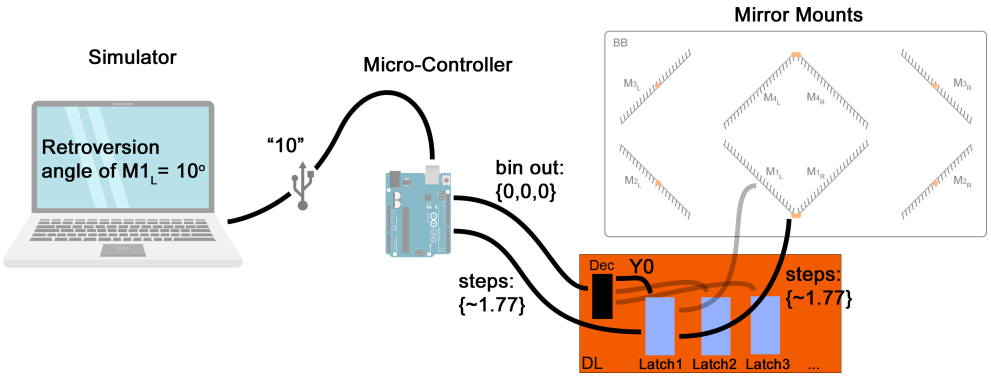

Figure 110: *Decoder-Latch path: This diagram shows the pathway of a retroversion angle, calculated by the simulator, that is transferred from the HCM to the Arduino Uno, and next to the decoder-latch, until it reaches the corresponding motor to rotate* $M1_L$ *by* 10°.

Figure 111 shows an example of the decoder-latch circuitry on a small breadboard. In this example, the A, B and C inputs of the decoder (top device) are connected to the digital pins of the Arduino Uno micro-controller numbered 11, 12 and 13. The G2A and G2B pins of the decoder are both connected to the common ground, whereas G1 is connected to the power supply, thus keeping the decoder device enabled perpetually. The output Y_0 of the decoder is connected to the OE pin of a latch (bottom device) so that, when Y_0 is enabled, the motors connected to outputs $Q_0 ... Q_3$, of the latch, rotate. The $D_0 ... D_3$ input pins 6, 5, 4, 3 of the latch are connected to the digital pins of the Arduino Uno micro-controller. Additionally, the latch enable switch (LE) is connected to the digital pin number 2, which allows the latch to be enabled or disabled from the Arduino Uno.

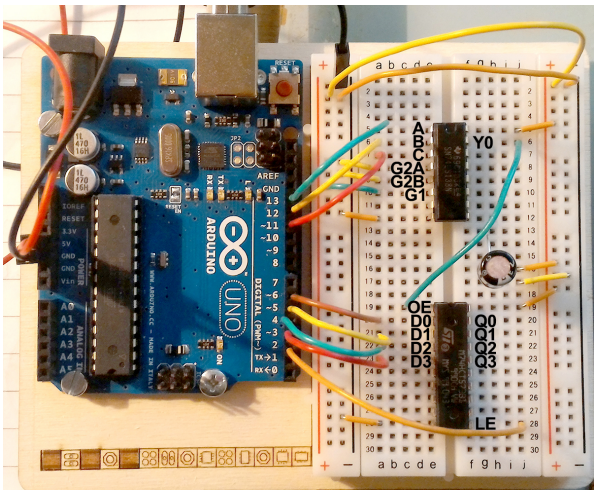

Figure 111: *Decoder-Latch circuitry: An example of the circuit on a simple breadboard to demonstrate the logic of the design. The Arduino Uno is located on the left side of the figure, whereas the decoder (top device) and latch (bottom device) are located on the right side of the figure. The steppers motors are not shown because the focus is the design of the decoder-latch circuit. Only four wires are connected to the latch, suggesting the use of one motor.*

The design of the decoder-latch circuitry as a complete board is shown in figure 112, illustrating how the outputs from one decoder device (top left device) connects to the eight latches.

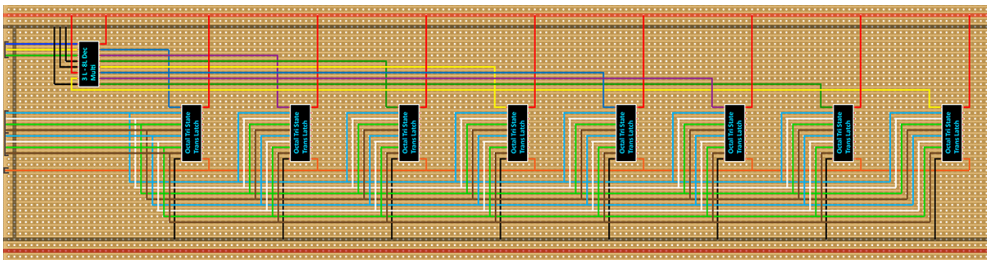

Figure 112: *Decoder-Latch circuit board: The circuit in the form of a board, which is used to control eight mirrors. One 3 Line to 8 Line Decoder Demultiplexer (top left device) enables all the eight Octal Tri-state Transparent Latches.*

Toms (2017) suggested that one probable issue with this design is that the length of the board is relatively long and, at 5V, which is the output Volts of an Arduino Uno, the current may have difficulties flowing through to the last latch. Also, although the DEMRS POC device is based on HV-2.0, which does not retroverse torsional strabismus, other variants of DEMRS such as HVT-2.5 (see sect. 4.5) use prisms to retroverse torsional deviations. Consequently, if a POC device was to be constructed that included prisms the decoder-latch circuit would require two more latches, in order to control the prisms. However, the problem is that the decoder used in this design has eight outputs and, therefore, cannot support additional latches.

In order to address these issues, the design of the decoder-latch circuit board was modified such that it uses two decoder devices, one for each side of the DEMRS POC device, and includes two additional latches for the potential use of prisms at a later stage (fig. 113). This design is much shorter in length, and can be used to potentially develop a POC device for other variants of DEMRS. Moreover, using two decoders instead of one means that two mirrors, one on each side, can be rotated simultaneously.

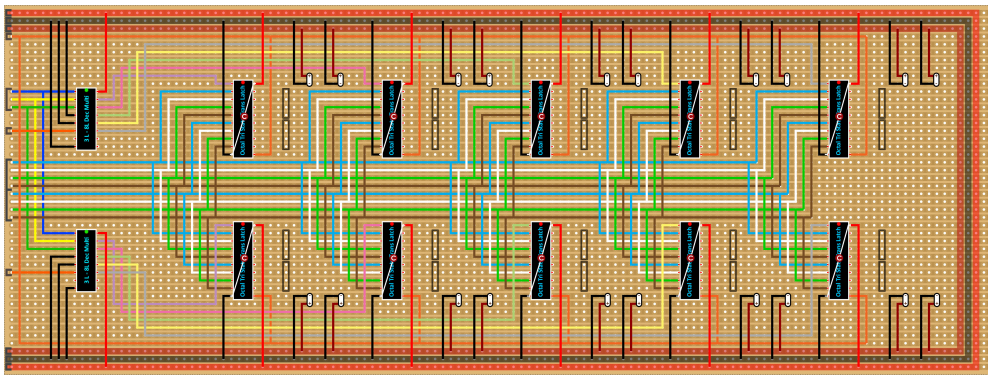

Figure 113: *Decoder-Latch circuit board: Designed to support eight mirrors, but can also support two prisms. The two small chips on the far left are the Decoder Demultiplexers that enable five Octal Tri-state Transparent Latches on both sides. The lighter red lane represents the* 5V *power supply connected to the chips, the darker red lane is the* 13.8V *power supply (see subsect. 5.4.1) that is connected to the motors and the black lane represents the common ground.*

Table 34 lists the I/O pins on the Arduino Uno that are connected to the decoder-latch circuit.

Table 34: *Arduino Uno usage of pins.*

Operations	Pin(s)
common ground	GND
DC output for decoders and latches	5V
latch clock	A0
enable DC flow on left side	A1
enable DC flow on right side	A2
enable all latches	0
right decoder switch	1
signal transfer to first motor	2, 3, 4, 5
left decoder switch	6
signal transfer to second motor	7, 8, 9, 10
decoder input controls	11, 12, 13

TESTING THE DECODER-LATCH CIRCUIT BOARD The decoder-latch circuit board was tested by:

1. individually connecting each latch to a pair of drivers, in order to check if the correct driver is enabled from the decoder.

2. connecting all drivers, and motors, to the circuit board, in order to check if a driver, other than the one enabled by the decoder, receives signals from the Arduino Uno.

Pre-requisites for the tests are:

- Computer running the DEMRS simulator.
- Arduino Uno.
- Decoder-latch circuit board.
- Sixteen drivers, and stepper motors.

In the first part of testing, a driver, attached to a motor, was connected to the first latch, which corresponds to the first mirror on the left side of the POC device. A retroversion angle of 20° was sent from the HCM to the Arduino Uno, in order to rotate the motor by 20°. This test is illustrated by figure 114 in which the LEDs on the driver are turned on when receiving the signal from the Arduino Uno. The angle by which the stepper motor rotated was verified using a 360° protractor. This part of the test was repeated for each latch individually.

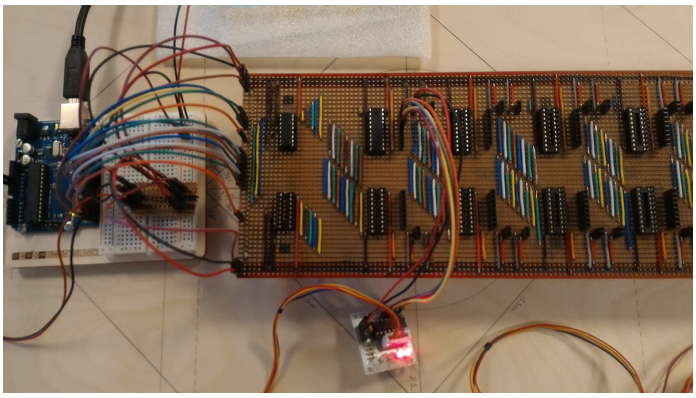

Figure 114: *Testing each latch separately: The driver controlling the motors through the first latch on the left side (top row of chips) of the circuit board, which connects to M_{1_L}, is enabled (led lights are on) when a retroversion angle is sent from the DEMRS simulator to the Arduino Uno to rotate M_{1_L}.*

In the second part of testing, sixteen drivers, each attached to a motor, were connected to the latches of the circuit board. A retroversion angle of 20° was sent from the HCM to the Arduino Uno, in order to rotate each motor by 20° with a delay of 30sec between each rotation. The delay time was added in order to review that no other driver was enabled, or motor rotated. Because this circuitry was built on an empty strip-board some connections may had not been severed properly, causing the DC current to flow into other latches and rotate the motors. In the occurrence of such event, the strip line was examined, the connection was severed, and the test was repeated.

The results from the first part of testing showed that the decoder enabled the latch, corresponding to the binary input provided in the Arduino Uno.

Also, each motor rotated by the correct retroversion angle. The results from the second part of testing showed that no other latch was unintentionally enabled alongside the selected latch.

5.4 MIRROR MOUNTS

This cluster is responsible for: (a) controlling the rotation of the mirrors in two dimensions, and (b) securely mounting the mirrors. The mirror mounts cluster consists of the stepper motors and drivers, the mirrors, and the custom designed mounts.
The drivers:

- receive signals from the decoder-latch.
- indicate which coils, within the motor, are triggered.
- able to supply 12V DC power to the motors.

The stepper motors:

- receive signals from the drivers.
- rotate by the retroversion angle, specified by the micro-controller.

The mirrors:

- are cleaned and flat.
- reflect $\geqslant$ 95% of the visible light.

The mounts of the mirrors:

- are level and stable.
- securely accommodate the stepper motors.
- securely mount the mirrors.
- allow motors to rotate while restraining their movement, potentially caused by the vibrations during a rotation.
- enable the rotation of the mirrors in two dimensions, horizontally (yaw) and vertically (pitch).

5.4.1 *Motors and Drivers*

Originally, each mirror mount was designed with two servo motors. However, the servo motors were replaced by stepper motors, mainly due to the inability to control the rotation of a servo motor from the Arduino Uno (see appendix C.1).

According to Dedes (2016) and Toms (2017) a stepper motor is recommended for applications that require high precision. For example, stepper motors are used in medical, aerospace and defence applications as they require a motor to operate accurately, reliably, safely and efficiently under extreme conditions and environments (Dedes, 2016) (Kreith and Goswami, 2005). A stepper motor is a type of motor that uses equal steps to perform one full revolution (360°). Unlike a servo motor, a stepper does not require a sensor for position feedback (see appendix C.1) in order to rotate its shaft by the correct angle (Horowitz and Hill, 2015). Nevertheless, because the rotation of a stepper motor can be affected by various forces, such as angular momentum or weight of the load, a position feedback device is recommended in order to correct the jumped steps. A step angle, also known as stride angle, is the angle, measured in degrees, by which the shaft of a motor rotates after one full step (Sandler, 1999). A step angle varies from one stepper to another as it is dependant upon the quality of the motor. Specifically, cheaper stepper motors usually have large step angles, whereas expensive stepper motors usually have small step angles, thus providing higher angular resolution (Toms, 2017). For instance, a NEMA MS23HAAL4500 is an expensive two phase bipolar stepper motor that offers high torque, low vibrations, and a high angular resolution of 0.9° per step, i.e. 400 steps per revolution (MOONS, 2021). Stepper motors are connected to drivers that allow the motors to be programmed such that the original step angle is divided into smaller steps. This is a technique that is referred to as half stepping, and it is used to acquire higher angular resolution (Horowitz and Hill, 2015). Modern drivers support micro-stepping, a technique that divides the original step into 16, 32 and even 256 micro-steps, in order to increase the resolution and accuracy of a motor.

A mirror mount was designed with two 5V 28BYJ-48 stepper motors (fig. 115) (Components101, 2019), where each motor was controlled by a ULN2003 driver (fig. 115) (Welten Holdings Ltd, 2019).

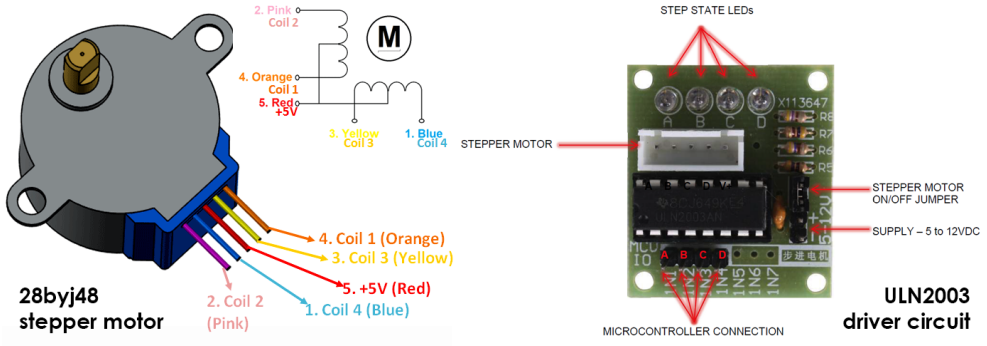

Figure 115: *28BYJ-48 and ULN2003: The 28BYJ-48 stepper motor (Components101, 2019) is shown on the left side of the figure, whereas the ULN2003 driver (Welten Holdings Ltd, 2019) is shown on the right side of the figure.*

The 28BYJ-48 is a small size inexpensive DC (Direct Current) stepper motor with a stride angle of 5.625° per step (Components101, 2019). Therefore, it requires 64 steps to perform one full revolution (360°). Moreover, this stepper motor has a gear ratio[3] of 64 : 1, suggesting that the total number of steps for one full rotation, including gear reduction[4], is 4096 ($(360/5.625) * 64 = 4096$) steps (Rawashdeh, 2017). The 28BYJ-48 is a 4 phase motor, which means that it uses four coils in order to rotate its shaft, and has five input wires, four of which are the extended coils and one wire, usually coloured in red, that powers the motor. The ULN2003 driver is a small sized chip with seven Darlington transistors that control the 28BYJ-48 stepper motor from the Arduino Uno micro-controller (Welten Holdings Ltd, 2019). This driver has four input pins (IN1, IN2, IN3, IN4) that connect to the Arduino Uno's digital pins and four LED lights that indicate which of the coils are enabled (Rawashdeh, 2017).

Figure 116 shows a basic test to determine whether or not a 5V 28BYJ-48 stepper motor could be used to rotate a mirror by 20°. Pre-requisites for the test are: (a) a computer running the Arduino IDE, (b) a mirror of size $16 \times 10 \times 0.30$cm, (c) a base, provided by Edmund Optics (2019b), (d) an Arduino Uno micro-controller, (e) a breadboard, provided with the Arduino Uno, (f) a ULN2003 driver, and (g) a 5V 28BYJ-48 stepper motor. Furthermore, in order to provide the angle to the stepper motor without using the DEMRS simulator, a small program was developed (see appendix C.2) that converts angles into steps, and send the signals directly to the driver of the motor. This test was conducted three times, where in each repetition the rotation of the mirror was recorded using a 360° protractor.

3 In a set of two gears (driver and driven), gear ratio refers to the number of teeth or the diameter of the driver gear in relation to the driven gear (Kreith and Goswami, 2005).

4 In a set of two gears (driver and driven), gear reduction occurs when the driver gear performs more than one revolution for every one revolution of the driven gear (Sandler, 1999).

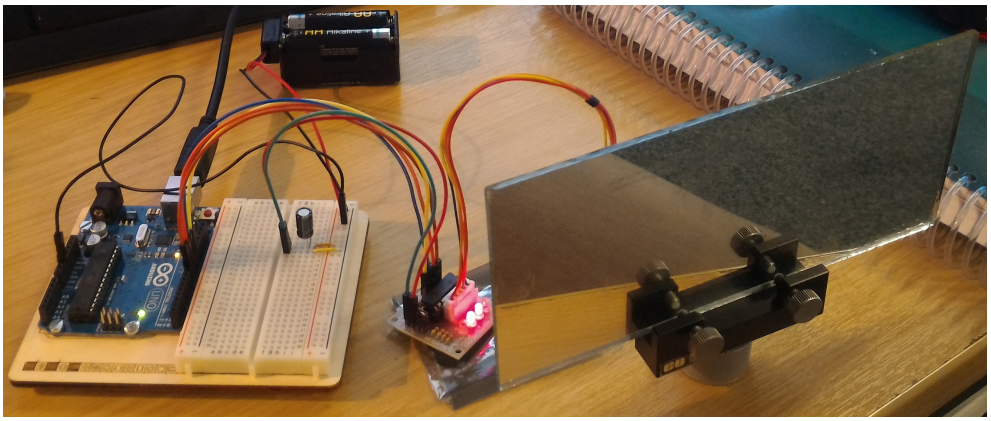

Figure 116: *Testing the rotation of a mirror: The mirror is mounted on a base placed firmly on shaft of the 28BYJ-48 5V stepper motor. The motor is controlled by an ULN2003 driver, whereby two of the four LEDs are turned on when the mirror rotates indicating which coils are enabled. The input pins of the driver are connected into four digital I/O pins on the Arduino Uno, programmed to rotate the mirror by 20°. The driver and motor are powered by an external 6V battery pack, therefore a capacitor was used as precaution to regulate the current.*

The results from this basic test showed that, due to the 5.625° stride angle of the stepper motor and weight of the mirror load, the 28BYJ-48 motor rotated the mirror by an error of $\pm 2 - 3°$. Although this error does not pose a significant risk in the retroversion of strabismus (see subsect. 4.4.5), the precision of the motor was improved by lowering the speed of the motor's rotation, and by implementing half stepping. However, switching from single steps to half steps decreased the torque of the motor, and the shaft could not reach the desired angle (20°). A solution to this problem was to replace the 5V 28BYJ-48 stepper motor with a 12V 28BYJ-48 stepper motor, which greatly improved its output torque during half stepping. Also, the 6V battery pack was replaced by a 12V battery pack in order to supply the new stepper motor with sufficient power and avoid the risk of damaging the motor. An issue that was noted when using the battery pack was that the lifetime of the batteries was drained after several usages, and the torque generated by the 12V 28BYJ-48 stepper motors decreased. To address this issue, a switch mode Bench Top Power Supply was used, which constantly supplied the motors with 13.8V of power. It should be noted that, although these motors operate in 12V, the additional 1.8V supplied by the Bench Top is not threatening the health of the motor.

Similar to a 5V 28BYJ-48 stepper motor, a 12V 28BYJ-48 stepper motor is controlled by five wires. Figure 117 shows two 12V 28BYJ-48 stepper motors connected to the Arduino Uno using: (a) eight wires to connect the microcontroller to the ULN2003 drivers, (b) two wires to supply power to the motors, and (c) two wires to connect to a common ground.

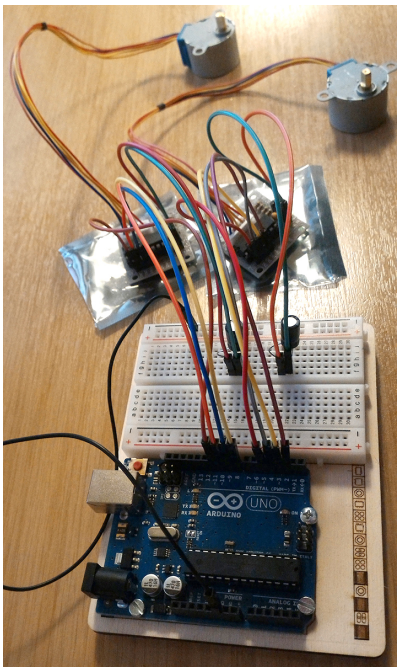

Figure 117: *Connecting two* 12V *28BYJ-48 stepper motors to an Arduino Uno: Two 28BYJ-48 stepper motors connected onto an Arduino Uno micro-controller using two ULN2003 drivers. The left stepper is controlled by the* 9, 10, 11, 12 *digital pins, connected to the* IN1, IN2, IN3, IN4 *inputs of the ULN2003 driver on the left. The right stepper is controlled by the* 2, 3, 4, 5 *digital pins, connected to the* IN1, IN2, IN3, IN4 *inputs of the ULN2003 driver on the right. The black cables are connected to the common ground.*

5.4.2 *The Mirrors*

The DEMRS POC device uses eight high performance cold mirrors, four on each side ($M1_{L/R}, M2_{L/R}, M3_{L/R}, M4_{L/R}$), where $M1_{L/R}$ and $M4_{L/R}$ rotate about their side, and $M2_{L/R}$ and $M3_{L/R}$ rotate about their centre (fig. 104). Each cold mirror is of size $w = 12.70\text{cm}, h = 10.16\text{cm}, d = 0.30\text{cm}$. High performance cold mirrors, manufactured by Edmund Optics (2019a), can transmit $\geqslant 90\%$ of infra-red light and compared to normal mirrors, which reflect $\approx 70\%$ of the visible light, cold mirrors reflect $\geqslant 95\%$ of the visible light. The high reflectivity of these mirrors improves the clarity of a fixation target. Also, cold mirrors allow the use of infra-red eye tracking cameras, which can be placed behind $M1_L$ and $M1_R$ in order to track the position of the eyes. Similar mirrors were used by Ramey *et al.* (2008) to develop a haploscopic viewing apparatus, for diagnostic purposes, using eye tracking cameras to accurately record the position of the normal eye and the deviation of the strabismic eye in three axes of rotation.

5.4.3 *3D Printed Mounts*

Figure 118 illustrates two ways that a mirror can be mounted on a frame so that it can be rotated, about the pivot P. In either case, the motor m_h performs a yaw rotation on the mirror, and motor m_v performs a pitch rotation on the mirror. Motor m_v is attached to a mount rotated by motor m_h so that the mirror can be rotated first horizontally and then vertically, matching the order of rotations applied to a mirror by the DEMRS simulator.

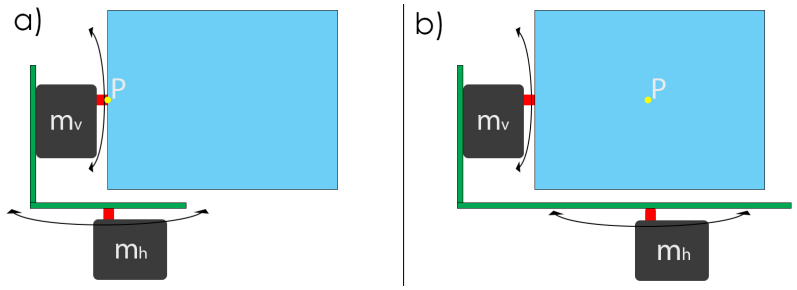

Figure 118: *Abstract mirror rotations: Two types of mirror mounts, whereby two motors (dark grey shapes) are mounted such that a mirror (light blue rectangle) rotates in two dimensions.* m_h *is the motor that rotates the mirror horizontally,* m_v *is the motor that rotates the mirror vertically, and* P *(yellow point) is the pivot of rotation for the mirror. Part (a) shows a mirror that can rotate from its edge, whereas part (b) shows a mirror that rotates from the centre.*

Unfortunately, as discussed in appendix C.1, it is not possible to directly mount a base provided by Edmund Optics (2019b) to a 28BYJ-48 motor, because the shaft of the motor does not fit into the base. Appendix C.3 describes the early attempts of building a mirror mount using 3D printed adapters, L-brackets, rollers, and machine screws, but due to issues related with the weight of a mirror, the mirror could not be securely affixed to the mount causing it to tilt and risk being damaged. Consequently, a set of custom designed mounts were built, using a 3D printer, in order to securely affix a mirror on a pair of 28BYJ-48 motors, with the necessary support to rotate the mirror horizontally and vertically, from its side and centre.

The 3D printer that was used to build the mirror mounts is an Ultimaker 2[5]. Although the Ultimaker 2 is a hobbyist printer, which compared to more advanced 3D printers lacks accuracy of the printed models, the parts that were built using this printer were acceptable for the purpose of building a proof of concept device. Figure 119 illustrates each type of mount, where the individual parts are colour-coded and linked to figure 120.

5 An Ultimaker 2 3D printer uses PLA (Polylactic Acid) filaments, which are biodegradable and bioactive types of thermoplastic (Ultimaker, 2019). Compared to other filaments, such as ABS (Acrylonitrile Butadiene Styrene), PLA is lightweight, stiff and strong, but has low durability, low resistance to impact and heat.

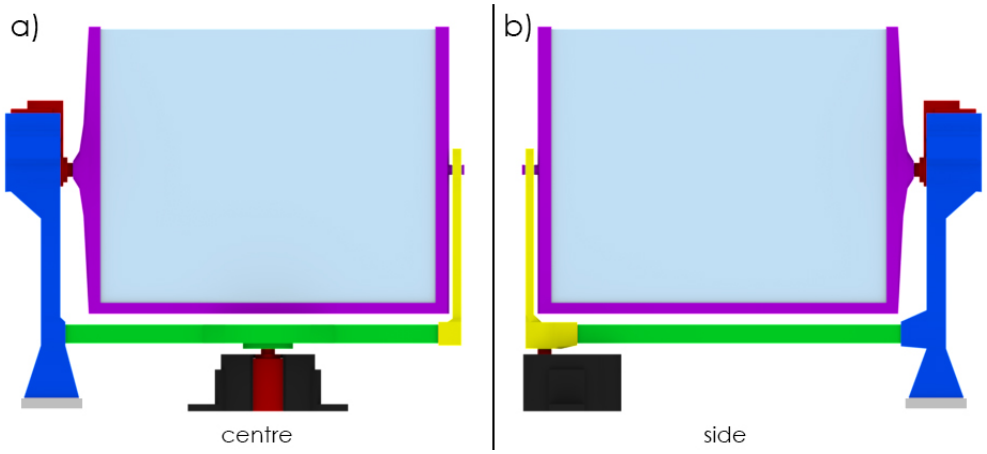

Figure 119: *Mirror mounts: Designs of the mounts that allow a mirror to be rotated from the centre (part a) and side (part b). The stepper motors are coloured in red (Sm_H and Sm_V). The black coloured part, which is called SmH-holder (stepper motor for horizontal rotation), is used to keep the Sm_H firmly in place. The x-axis joint (green) is fitted either onto the shaft of the Sm_H to the support handle (yellow). The yellow part, which is called support handle, fits onto the edge of the x-axis joint and prevents the mirror from tilting. The y-axis joint (blue) is fitted onto the other edge of the x-axis joint and holds the Sm_V (stepper motor for horizontal rotation) firmly in place. At the bottom of the y-axis joint, the bearing case (light grey) holds a small ball bearing that reduces friction. The mirror case (purple) fits onto the shaft of the Sm_V and the support handle. Also, the case allows a mirror (light blue) to slide in.*

Apart from the x-axis joint (green) and support handle (yellow), which are two parts designed differently for when the mirror rotates about its side as opposed to when it rotates about its centre, all other parts have identical designs. When the mirror rotates about its centre, the x-axis joint (green) is printed with a socket at its base that matches the shape of the shaft of the Sm_H, allowing the joint to be mounted firmly onto the motor. However, when the mirror rotates about its side the x-axis joint does not include a socket. Instead, the support handle (yellow) is printed with a similar socket that allows the handle to be mounted firmly onto Sm_H.

Figure 120 shows the individual components of a mirror mount.

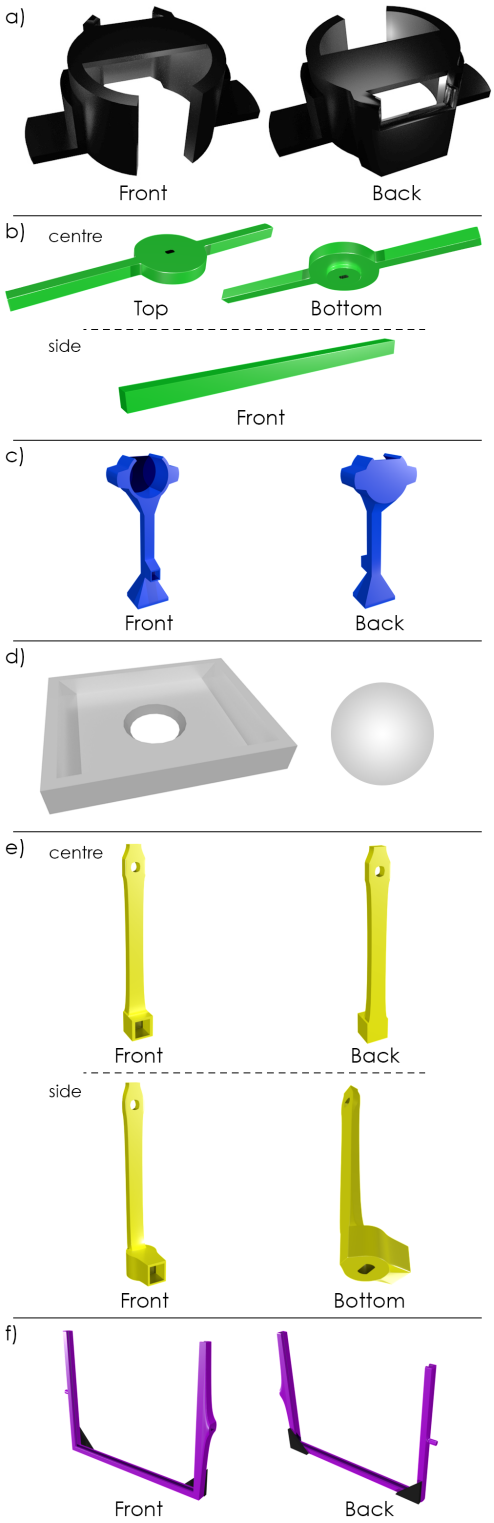

Figure 120: *Individual parts of a mirror mount: The Front / Back labels indicate the views of each part, whereas Centre / Side labels indicate to which type of mirror mount the part belongs to. If no Centre / Side labels are shown, the part can be used in both types of mirror mounts.*

The components of a mirror mount are:

- **SmH-holder:** The SmH-holder (black component, fig. 120a) is designed to affix Sm_H, in order to prevent unintentional movements of the motor while rotating the mirror. The wires of a stepper motor pass through the space at the rear of the SmH-holder. The extrusions on each side of the SmH-holder are used to firmly position the holder onto the base board.

- **X-Axis Joint:** The x-axis joint (green component, fig. 120b) is a relatively thick and rigid bar that connects the support handle (yellow component, fig. 120e) to the y-axis joint (blue component, fig. 120c). The design of the x-axis joint depends on the type of mirror mount, i.e. mount that rotates a mirror about its side or centre.

- **Y-Axis Joint:** The y-axis joint (blue component, fig. 120c) is the sturdiest and heaviest of all mirror components. It is designed to firmly hold the Sm_V in place while the mirror rotates horizontally. The height of the y-axis joint is similar to the height of the mirror, with an additional $5mm$ offset in order to prevent the mirror from colliding with the x-axis joint when performing a pitch rotation.

- **Ball Bearing:** In order to reduce friction between the base board and the y-axis joint, a small ball bearing is centrally fitted under the y-axis joint, and held in place by a bearing case (white component, fig. 120d).

- **Support Handle:** The support handle (fig. 120e) connects to the x-axis joint, and prevents the mirror mount from tilting on one side. Therefore, the support handle is placed opposite to the y-axis joint in order to support and level the mirror.

- **Mirror Case / Frame:** This is the case, or frame, (purple component, fig. 120f) that holds the high performance cold mirror. It is a U-shaped frame, with a socket into which the shaft of Sm_V fits. Also, the mirror case has a small extrusion on one of its vertical sides, which fits into the support handle. The inner surface of the case is grooved so that a mirror can slide in. This groove keeps the mirror in place, and prevents it from accidentally falling out during rotations.

With the exception of the ball bearings, manufactured by E-Meoly (2018), all the above components were printed into scale according to the blueprints in section 5.1. Because the PLA filament shrinks the printed part when cooling down, the scale of each modelled part had to be slightly increased in

Ultimaker Cura[6], in order to compensate for shrinkage. Figure 121 shows the SmH-holder as designed in the blueprint and the resulting 3D printed component of the POC device.

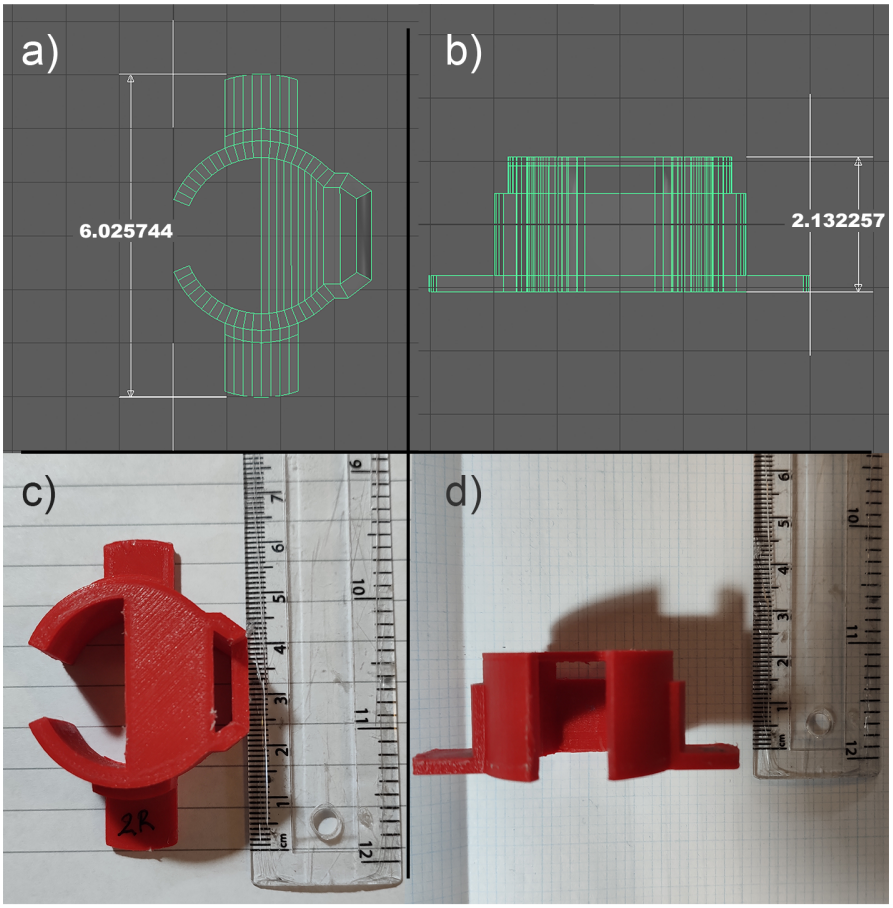

Figure 121: *SmH-holder: (a) and (b) show the top and side views of the SmH-holder design. The length of the holder is measured to be* $\approx 6\text{cm}$ *and the height to be* $\approx 2.1\text{cm}$*. (c) and (d) show the final 3D printed SmH-holder matching the size of the holder in the design.*

TESTING THE MIRROR MOUNTS Eight mirror mounts were fully assembled, i.e. including the drivers, motors and mirrors. The mirror mounts were attached to the decoder-latch board, in order to test whether or not the mirrors could be, horizontally and vertically, rotated by the retroversion angles provided by the Arduino Uno. The tests aim to determine:

1. the stability of the 3D printed mounts, during rotation.
2. the levelling of the mirror, after rotation.
3. if the mirror can be securely rotated.

6 3D printing software provided by Ultimaker.

4. if the motors can cope with the load of the mount and mirror.
5. the restraint of motors, due to potential movements from vibrations.
6. other factors, such as friction, that could impact the accuracy when rotating a mirror.

Pre-requisites for the tests are:

- Computer running the DEMRS simulator.
- Arduino Uno.
- Decoder-latch circuit board.
- Eight fully assembled mirror mounts.

Each mirror mount was tested individually. The mirror mount was placed on a table whose surface was lean and flat, so that the Y-Axis Joint could rotate with reduced friction. Also, the SmH-holder was temporarily glued on the table, so that it could remain firmly in place. A set of test retroversion angles (yaw: 20°, pitch: 45°) were sent from the DEMRS simulator to the Arduino Uno, in order to rotate the mirror mount. Figure 122 shows how one of the mirror mounts was setup for testing. It should be noted that prior to each testing the level of the mirror was measured using a split-level device, and re-measured after the rotation. Furthermore, the angle by which the mirror mount rotated was verified using two 360° protractors.

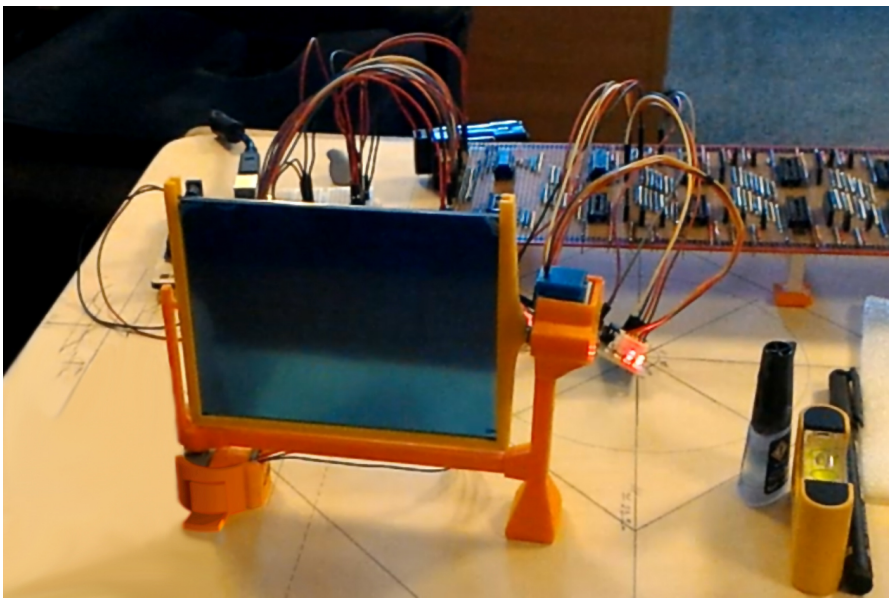

Figure 122: *Testing the assembled component of M_1: This component is used in order to rotate M_{1_L}, from the side.*

A short video demonstrating the rotation of $M1_L$ can be viewed at https://bitbucket.org/cglynos/demrs/src/master/POC_Device/. To aid clarity of the rotation, the protractors were removed.

The tests showed that the mounts:

1. securely rotated the mirror, without risk of damage, as it was tightly constrained by the mirror case.
2. are stable, during rotation, and the mirror remains level, after rotation.
3. successfully rotated the mirror, horizontally and vertically, by the test retroversion angles.
4. are relatively lightweight, therefore the weight of the load does not cause problems with the functionality of the motors.

5.5 BASE BOARD

The purpose of developing a base for the DEMRS POC device is to:

- position the mirrors according to the layout of HV-2.0 such they are level and able to rotate with reduced friction,
- prevent the wires of the stepper motors and decoder-latch circuit board from interfering with the rotation of the mirrors, and
- provide position feedback about the rotation of a mirror, by marking the angles on the surface of the base using a protractor.

The base consists of:

- A wooden drawing board of size $60.0 \times 40.0 \times 0.5$cm. The drawing board is light weight and sturdy, which simplifies the transportation of the POC device and can sustain the weight of the mirrors without bending. The surface of the board is marked with the position and default orientation of each mirror mount (fig. 123).

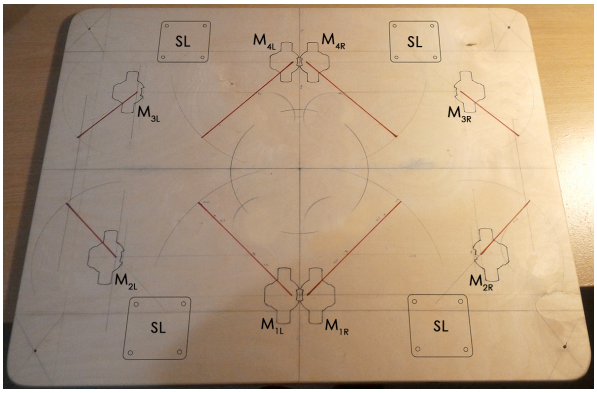

Figure 123: *Wooden board: Drawing board used as the base of the DEMRS POC device. The board includes clear markings of the positions and default orientation of each mirror. The* SL *markings indicate the positions of the four support legs.*

- Four adjustable support legs, used to level the POC device. Additionally, the support legs raise the base so that the decoder-latch circuit board and Arduino Uno can be placed centrally under the base. The wires from the motors, which connect to the decoder-latch circuit board, run through the wooden board via eight 3cm diameter holes.

- A perspex clear acrylic plastic sheet (plexi glass) of size 60.0cm × 60.0cm × 0.2cm. Although a ball bearing is fitted under the y-axis joint (see subsect. 5.4.3), the surface of the wooden board is not completely smooth, and some friction is generated. Therefore, the plexi glass is placed on top of the wooden board in order to minimize fiction between the mirror components and the board, during motion (fig. 124).

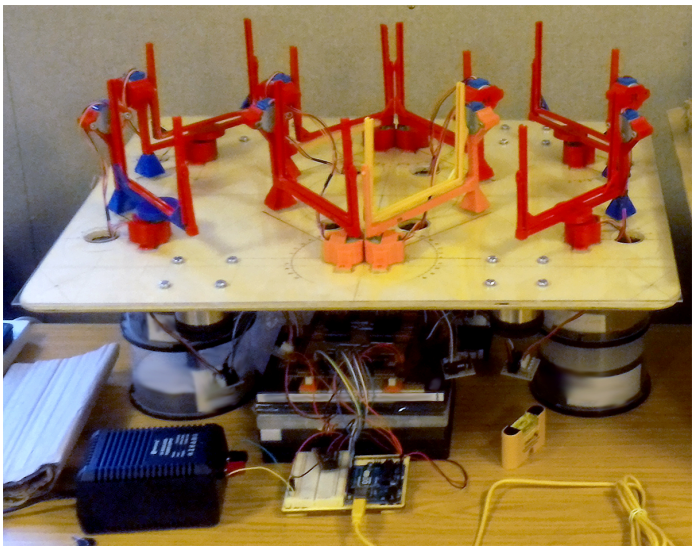

Figure 124: *Plexi glass: Final base of the POC device, including a plexi glass placed between the wooden drawing board and the mirror components.*

TESTING THE BASE BOARD In order to test the effectiveness of the base in the overall device, the DEMRS POC device was programmed to, firstly, rotate each mirror mount horizontally by 10°, and secondly return it to its original position. The 10° angle was marked on the base, and used for position feedback. The test showed that the base levelled the mirrors, and the mirror mounts were able to rotate with reduced friction.

5.6 TESTING THE DEMRS POC DEVICE USING LASERS

A series of tests were designed to determine the efficacy the DEMRS POC device in the retroversion of strabismus, using two laser pointers representing the principal vision vectors of the eyes, and a pin as the fixation target. The objective of this experiment is to use the DEMRS POC device to redirect the emitted light beams, from the lasers, so that they simultaneously converge at the pin. The tests were conducted under laboratory conditions, in a large room with ambient lighting. Pre-requisites for the tests are:

- A red coloured laser to represent the left vision vector, and a green coloured laser to represent the right vision vector.
- Two height adjustable bases for the lasers, allowing them to be rotated.
- A regular-sized pin, used as the fixation target.
- A computer running the DEMRS simulator.
- The DEMRS POC device, placed between the lasers and the pin.

Previously, it was mentioned that latent deviations (phorias), occur only when binocularity is, voluntarily or involuntarily, disrupted (see subsect. 3.3.1). Therefore, until strabismus occurs, normal BSV is present. Although normal BSV does not require retroversion, a DEMRS must retroverse normal BSV, in order to compensate for phorias. Consequently, the DEMRS POC device was tested in the retroversion of:

1. normal BSV, in which both lasers were rotated such that both light points intersected the fixation target.
2. strabismus, namely left exotropia, in which the left laser was rotated outwards, but the right laser was directed towards the fixation target.

The lasers were mounted on the bases, which were firmly placed on a table, 70cm from the wall. Also, the lasers were positioned 6cm apart from each other, which is equivalent to a typical IPD. The fixation target

(pin) was placed on the wall, centrally to the lasers. In each test, the lasers were oriented according to the type of vision. For example, when testing the retroversion of normal BSV, both lasers were horizontally rotated by $\approx$ 2.45° in opposite directions. The DEMRS POC device was placed on the table, $\approx$ 8cm from the lasers. The laptop running the DEMRS simulator was placed near the DEMRS POC device, so that it can be connected with the micro-controller via a USB cable. Furthermore, the DEMRS simulator was configured using the JSON configuration file shown in appendix C.4, which uses the measurements from the blueprints of the POC device. Figure 125 illustrates the setup of the tests, where the lasers are oriented to simulate normal BSV and strabismus, namely left exotropia.

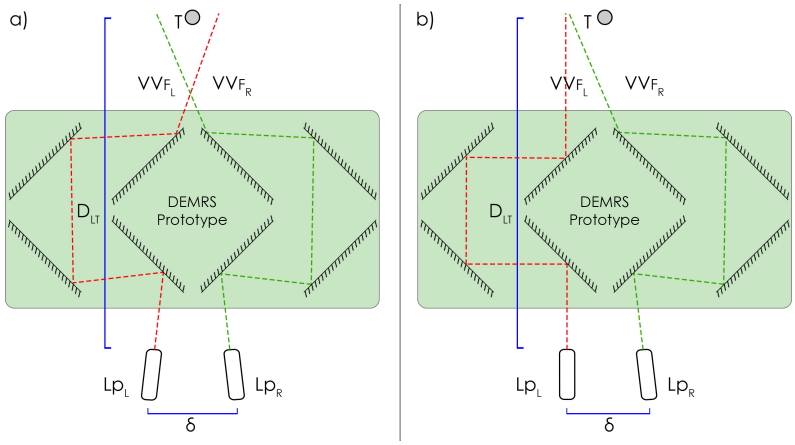

Figure 125: *Evaluation using lasers: Illustrates the setup of the tests, where* $\mathrm{Lp}_{L/R}$ *are the two laser pointers located* $\approx$ 8cm *from the POC device,* δ *is the distance between the lasers,* $\mathrm{VV}_{\mathrm{F}_{L/R}}$ *are the light beams emitted from the lasers that represent both principal vision vectors,* T *is the pin, and* D_{LT} *is the distance from the lasers to the target. (a) shows an example of normal BSV, whereas (b) shows an example of left exotropia.*

5.6.1 *Laser-Based Retroversion of Normal BSV*

In order to test retroversion with normal BSV, both lasers were horizontally rotated by $\approx$ 2.45° in opposite directions, such that their light points could intersect the pin. The command line arguments passed to the DEMRS simulator were:

```
DEMRS_Simulator.exe -ipd 6.0 -dom "both" -trgt 0.0 0.0 70.0
    -sysconfig poc_config.json

where:
-ipd = inter-pupillary distance
```

```
-dom = dominant eye
-trgt = position of fixation target
-sysconfig = system configuration file
```

This test was performed in the following steps:

1. Configure the DEMRS simulator, without calculating retroversion.
2. Observe the position of the laser points projected on the wall, before retroversion.
3. Execute retroversion in the DEMRS simulator, via a keyboard event.
4. Observe the visualization output from the simulator, as reference.
5. Monitor the functionality of the POC device, as the mirror mounts rotate by the calculated retroversion angles.
6. Observe the position of the laser points projected on the wall, after retroversion.
7. Verify that the mirror mounts rotated according to the retroversion angles from the DEMRS simulator.

The results showed that, prior to retroversion, when the system was at its default state the laser points did not converge on the pin (fig. 126). This is because, although the lasers were oriented based on normal BSV, the default orientation of the mirrors caused the laser beams to be reflected away from the fixation target.

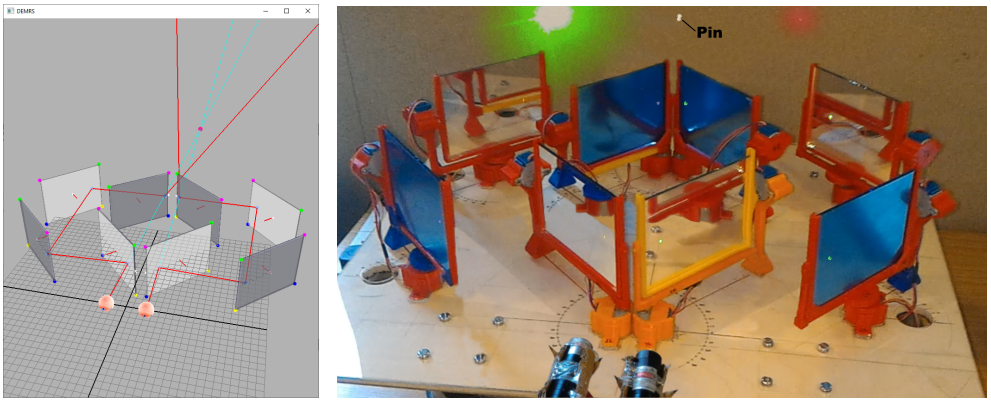

(a) *Visualization* (b) *POC Device*

Figure 126: *Before retroversion: (a) shows the visualization output from the DEMRS simulator as reference. (b) is a picture of the POC device at its default state.*

When retroversion was executed, by the DEMRS simulator, the calculated retroversion angles were transferred from the HCM to the micro-controller

and, next, to the motors, which rotated the mirror mounts. As shown by figure 127, after retroversion, both laser points intersected the pin. The retroversion angles of the mirrors are presented in table 35.

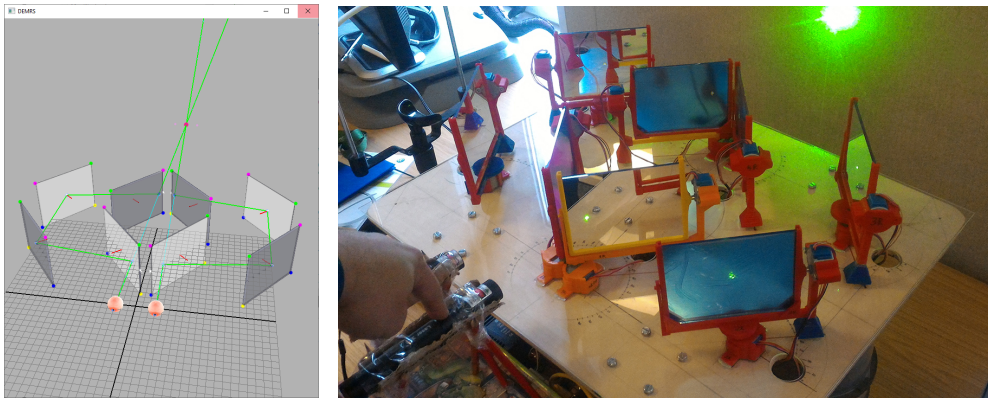

(a) *Visualization* (b) *POC Device*

Figure 127: *After retroversion: (a) the visualization output from the DEMRS simulator as reference. (b) picture of the POC device after the rotation of the mirror mounts. Both laser points overlap, but because the intensity of the green laser is much greater than the red laser, the light point from the red laser is not visible.*

Table 35: *Retroversion angles of the mirrors.*

Parts	Retroversion (°)		
	x (pitch)	y (yaw)	z (roll)
$M1_L$	0.000	4.839	0.000
$M2_L$	0.000	3.612	0.000
$M3_L$	0.000	−5.057	0.000
$M4_L$	0.000	−3.830	0.000
$M1_R$	0.000	−4.839	0.000
$M2_R$	0.000	−3.612	0.000
$M3_R$	0.000	5.057	0.000
$M4_R$	0.000	3.830	0.000

The horizontal (yaw) rotation of the mirrors was verified using the marked angles on the base of the POC device, whereas the vertical (pitch) rotation of the mirrors was verified using a 360° protractor. This test showed that the DEMRS POC device was able to successfully retroverse normal BSV.

5.6.2 *Laser-Based Retroversion of Strabismus*

The type of strabismus simulated in this test was left exotropia with a temporal (outwards) deviation of 8° (≈ 16Δ). In order to test retroversion with a left exotropia, the left laser was horizontally rotated by ≈ 5.55°, simulating the deviating eye, whereas the right laser was horizontally rotated by ≈ 2.45°, simulating the fixating eye. Therefore, only the right laser point could intersect the pin. The command line arguments passed to the DEMRS simulator were:

```
DEMRS_Simulator.exe -ipd 6.0 -dom "right" -strabdev 8.0 0.0
    0.0 -trgt 0.0 0.0 70.0 -sysconfig poc_config.json

where:
-ipd = inter-pupillary distance
-dom = dominant eye
-strabdev = strabismic deviation (pitch, yaw, roll)
-trgt = position of fixation target
-sysconfig = system configuration file
```

This test was performed in the following steps:

1. Configure the DEMRS simulator, without calculating retroversion.
2. Observe the position of the laser points projected on the wall, before retroversion.
3. Execute retroversion in the DEMRS simulator, via a keyboard event.
4. Observe the visualization output from the simulator, as reference.
5. Monitor the functionality of the POC device, as the mirror mounts rotate by the calculated retroversion angles.
6. Observe the position of the laser points projected on the wall, after retroversion.
7. Verify that the mirror mounts rotated according to the retroversion angles from the DEMRS simulator.

The results showed that, prior to retroversion, when the system was at its default state the laser points did not converge on the pin (fig. 128). Although the right laser was oriented based on normal BSV, the default orientation of the mirrors caused the laser beam to be reflected away from the fixation target. Due to strabismus, the left laser deviated outwards and, therefore,

the laser beam could not intersect the pin. However, the default orientation of the mirrors caused the left laser point to be reflected closer to the pin than the right laser point.

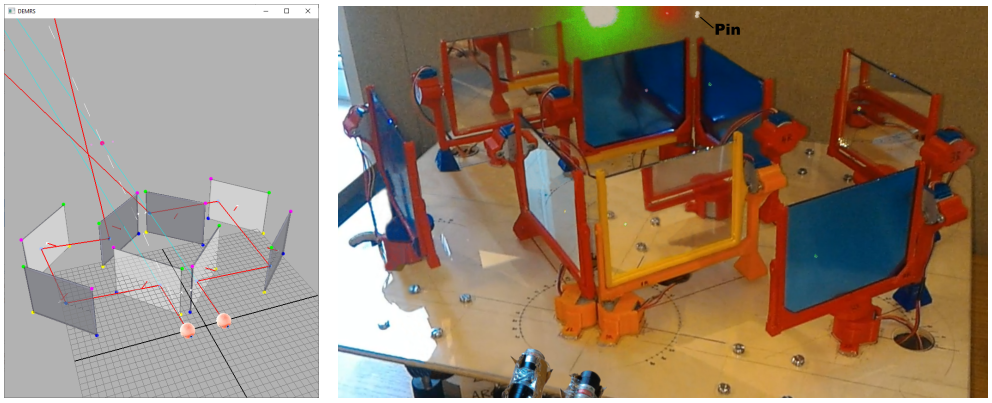

(a) *Visualization* (b) *POC Device*

Figure 128: *Before retroversion: (a) the visualization output from the DEMRS simulator as reference. (b) picture of the POC device at its default state.*

When retroversion was executed, by the DEMRS simulator, the calculated retroversion angles were transferred from the HCM to the micro-controller and, next, to the motors, which rotated the mirror mounts. As shown by figure 129, after retroversion, both laser points converged on the pin. The retroversion angles of the mirrors are presented in table 36.

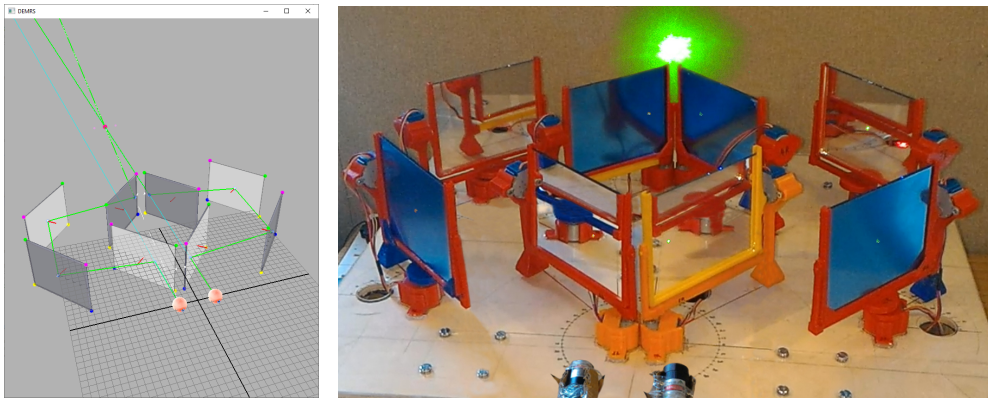

(a) *Visualization* (b) *POC Device*

Figure 129: *After retroversion: (a) the visualization output from the DEMRS simulator as reference. (b) picture of the POC device after the rotation of the mirror mounts. Both laser points overlap, but because the intensity of the green laser is much greater than the red laser, the light point from the red laser is not visible.*

Table 36: *Retroversion angles of the mirrors.*

Parts	Retroversion (°)		
	x (pitch)	y (yaw)	z (roll)
$M1_L$	0.000	0.264	0.000
$M2_L$	0.000	3.037	0.000
$M3_L$	0.000	−5.057	0.000
$M4_L$	0.000	−3.830	0.000
$M1_R$	0.000	−4.839	0.000
$M2_R$	0.000	−3.612	0.000
$M3_R$	0.000	5.057	0.000
$M4_R$	0.000	3.830	0.000

The horizontal (yaw) rotation of the mirrors was verified using the marked angles on the base of the POC device, whereas the vertical (pitch) rotation of the mirrors was verified using a 360° protractor. This test showed that the DEMRS POC device was able to successfully retroverse strabismus.

5.6.3 *A Brief Critique*

The DEMRS POC device met the requirements outlined in section 5.1. Also, the laser tests showed that the components in each cluster functioned correctly, which allowed the POC device to rotate the mirrors according to the retroversion angles from the DEMRS simulator.

Even though the mirror mounts were lightweight, and the surface of the base was smooth, minor inaccuracies occurred during the rotation of the mirrors. This is because the 28BYJ-48 stepper motors are relatively cheap hobbyist devices, where some steps can be missed, or jumped over, during a rotation. Fortunately, such inaccuracies were not frequent, and in most cases the amount of error was within the acceptable margin of error, discussed in subsection 4.4.5. However, if the error in the rotation of a mirror was larger than the accepted margin, the system was reset and the laser test was repeated. Unfortunately, due to the lack of an angle encoder feedback, such inaccuracies could not be corrected during testing.

An alternative to stepper motors, are dynamixels. A dymixel is a programmable high performance actuator, designed for powerful and flexible robotic movements. According to Yoonseok *et al.* (2017), dynamixels "are widely used in robotics because of their various useful functions", including a fully integrated DC servo motor, reduced gearhead, internal controller, motor driver circuitry and daisy-chainable network connection. Future vari-

ants of DRS compliant systems may benefit from the use of dynamixels, as they can reduce the size of the system, and provide encoder feedback for the rotation of each mirror.

During the laser tests it was observed that the green laser produced much higher intensity than the red laser. Consequently, when both lasers overlapped, the light point from the red laser was not visible. Future tests with laser pointers would benefit from a neutral-density (ND) filter, because it can be placed in front of the green laser in order to reduce its intensity. Alternatively, a high power pulse width modulator (PWM) controller can be used, in order to dim the intensity of the green laser.

5.7 SUMMARY

This chapter described the development of a DEMRS proof of concept (POC) device that was based on the design of HV-2.0, because the majority of strabismic deviations are horizontal and vertical. The POC device is divided into four interlinked clusters / groups of components, each of which was described in detail as they are vital to the functionality of the system.

The DEMRS POC device consists of eight high performance cold mirrors whose horizontal and vertical orientations are controlled by sixteen stepper motors. The mirrors and motors are held in place by eight custom designed 3D printed mounts, which are positioned on a base board that allows the mirror mounts to rotate with reduced friction. Once the retroversion angles are calculated, by the retroversion engine, they are received by the HCM, whose purpose is to communicate the simulator with the POC device. The HCM stringifies the angles, and transfers them to an Arduino Uno micro-controller via a USB. The Arduino Uno converts the angles into signals (pulses), and transfers them to the decoder-latch circuit board, which distributes the signals to the corresponding motors of each mirror mount.

This chapter concludes with a series of experiments designed to determine the efficacy of the DEMRS POC device in the retroversion of normal BSV and strabismus, using two laser pointers representing the principal vision vectors of the eyes. These experiments showed that the DEMRS POC device can be tested with human subjects.

6

EVALUATION OF THE DEMRS POC DEVICE

"... ἃ μὴ οἶδα οὐδὲ οἴομαι εἰδέναι"
— Σωκράτης, 470-399 π.Χ.· Πλάτων - Ἀπολογία Σωκράτους[21δ]

"... that which I do not know, I do not think I know"
— Socrates, 470–399 BC; Plato - Apology of Socrates[21d]

This chapter presents the efficacy of the DEMRS POC device, hereafter referred to as DEMRS instance, in the achievement of DRS. The DEMRS instance is evaluated, primarily, in the retroversion of normal BSV and strabismus, and secondly, in the fusibility of the visual stimuli received by both eyes, which determines the grade of binocularity achieved during DRS. The evaluation process, described in this chapter, consists of a number of experiments that were conducted under laboratory conditions. For the purposes of this study, ethical approval was obtained from Bournemouth University Ethics committee in order to enrol a group of human volunteers to take part in the evaluation of the device. In addition to the presentation of the demographic data used in this study, this chapter describes each experiment along with the sequence of interactions between a subject, the DEMRS instance and operator of the DEMRS instance. Finally, this chapter discusses the results of the evaluation experiments, and presents the feedback provided by the subjects who used the DEMRS instance.

6.1 RESEARCH ETHICS

Ethical approval for this study was obtained from Bournemouth University ethics committee (see appendix D.1). For the purpose of evaluating the DEMRS instance, twenty-one[1] volunteer subjects were invited to enrol in the study and take part in a number of experiments, discussed later in this chapter, conducted under laboratory conditions. The laboratory in which the experiments took place, is located at Bournemouth University, and it is a relatively large office room with ambient lighting. It should be highlighted that, in this study, the evaluation of the DEMRS instance does not

1 Due to resource and time constraints, only tweny-one subjects were enrolled in this study.

fall within the scope of clinical evaluation[2]. Additionally, being a proof of concept, the DEMRS instance is not to the standards of a custom medical device that has been manufactured to be used in a clinical setup. Moreover, the National Health Service's (NHS) framework of clinical governance is defined as "a framework through which NHS organizations are accountable for continuously improving the quality of their services and safeguarding high standards of care by creating an environment in which excellence in clinical care will flourish" (Wilson, 1998). Although this study focussed on individuals with strabismus, it was undertaken in a non-clinical University setting by a post-graduate student. The study did not fall under the remit of most of the seven pillars of clinical governance, however 'risk management', 'information management' and 'patient and public involvement' elements were considered during this study.

In order to reduce risk of injuries to the subjects and damages to the DEMRS instance, the following safety measures were implemented: (a) use of a medical head/chin rest, placed at a safe distance from the DEMRS instance, (b) direct control of the DEMRS instance by the subject was restricted, and (c) the examiner was constantly monitoring the progress of each experiment. Data collected from the tests, including subject information, are confidential and securely stored in an external hard drive. Each volunteer/-participant received a participant information sheet (see appendix D.2) that clearly explained the nature of this research and the evaluation process using the DEMRS instance. Furthermore, an informed consent (see appendix D.3) was signed by each participant prior to using the DEMRS instance. Parents or guardians of participants that were under the age of sixteen years were also briefed about the nature of this research before signing a consent form tailored for parents and guardians of young participants.

6.2 DEMOGRAPHIC DATA

A population of 21 volunteers between the age of $8-98$ years (mean 53 years) was enrolled in this study. Participants who were under the age of 16 were considered to be children, whereas participants over the age of 65 were considered to be elderly. The remaining participants within the age range of $16-65$ were considered to be adults. Of these subjects, 9 (42.9%) were males and 12 (57.1%) were females. The IPD of the subjects range between $\approx 5.6\text{cm}$

2 According to Astapenko (2019), clinical evaluation "is a set of ongoing activities that use scientifically sound methods for the assessment and analysis of clinical data to verify the safety, clinical performance and/or effectiveness of the medical device when used as intended by the manufacturer."

and $\approx 6.3\text{cm}$, with mean IPD $\approx 5.95\text{cm}$. On initial review, 11 (52.4%) subjects had normal binocular single vision and 10 (47.6%) subjects had strabismus. The participants with normal BSV were used as control subjects in order to compare the results deriving from the evaluation of the DEMRS instance when used by subjects with strabismus, and also to evaluate the efficacy of the DEMRS instance in the retroversion of normal BSV. Participants with strabismus were selected only if they had been previously diagnosed with strabismus by an ophthalmologist. Table 37 shows the demographic data used in this evaluation.

Table 37: *Demographic data.*

Characteristics	No. Studied	Percent %
Gender		
Male	9	42.9%
Female	12	57.1%
Age range $[7-98]$ (years)		
$\leqslant 52.5$	11	52.4%
> 52.5	10	47.6%
Vision		
BSV	11	52.4%
Strabismus	10	47.6%
Diplopia	3	30.0%
CI	5	50.0%
Exo-tropia	1	10.0%
Hyper-tropia	1	10.0%
Total	**21**	**100%**

A brief medical history was obtained from all subjects in order to further understand their state of health and identify the presence of ocular conditions that could affect the outcome of the experiments, such as myopia, hypermetropia and presbyopia. For example, if a subject had been previously diagnosed with presbyopia, the prescribed corrective lenses or glasses must be worn during testing. However, if a subject was prescribed prismatic glasses in order to manage CI or diplopia, the glasses were not worn during testing with the DEMRS instance. All 21 subjects underwent examination, in accordance with prior training from a strabismologist (see appendix D.4), to verify their visual acuity and type of strabismus.

Of the total 21 participants, 1 (5%) subject had been previously diagnosed with myopia, 1 (5%) subject had been previously diagnosed with hypermetropia, and 5 (25%) subjects had been previously diagnosed with

presbyopia. Participants with existing ocular conditions were asked to wear their prescribed glasses, or corrective lenses, during the evaluation of the DEMRS instance.

6.2.1 *Verifying Normal BSV*

Normal BSV was verified by:

1. Lang's two-pencil test.
2. Anaglyph test.
3. Autostereogram test.

Pre-requisites for the tests are:

- Two pencils of similar colour and length.
- A 3D anaglyph image, and a pair of red and blue colour filter glasses.
- A set of three autostereogram images.

Initially, the subject was asked to sit on a chair and face the examiner, who recorded the IPD. Normal BSV was verified by three tests, in which the first test was divided into two phases. In the first phase, each subject underwent a convergence test using a small object, such as a pencil. In this test, the subject was asked to fixate on a pencil, whilst it was slowly moved in different directions and distances. The subject was asked to report any symptoms that may have occurred during the test, including double vision, dizziness and eye strains. In the second phase, a different pencil, to the one used by the examiner, was given to the subject in order to perform Lang's two-pencil test (see subsect. 3.4.7).

The second test was an anaglyph test (see subsect. 3.4.7). Each subject was asked to view an anaglyph (stereoscopic) image of a leopard using a pair of red and cyan filter glasses, and report whether or not they could perceive the three dimensional illusion, in which the leopard was emerging from the image.

The third test was an autostereogram test (see subsect. 3.4.7). Each subject was asked to view a set of three autostereogram images and describe the shape that was perceived from each image. In this test, the subject was instructed to hold the image at a reading distance but focus on an imaginary target further away. This technique would allow the subject to look "through" the image as both eyes diverge until they are nearly parallel.

Although Frisby Near Stereo-test (FNS) and Frisby Davis Distance (FD2) (see subsect. 3.4.7) can verify binocular vision and stereopsis, such tests have been known to return false positive results because a subject can use familiarity cues in order to pass the test. For example, motion parallax can betray the correct answer of an FNS or FD2 test, thereby allowing a subject without BSV to pass the test. Other stereoscopic vision tests, previously described in subsection 3.4.7, require a clinical setup, use of expensive medical equipment, or are very similar to the anaglyph and autostereogram tests.

All subjects with normal BSV were able to pass the convergence test, Lang's two-pencil test and perceive the illusion form the anaglyph imege, without reporting any symptoms. However, of the 11 subjects with normal BSV, only 4 were able to describe the "hidden" shape of the autostereogram. The remaining 7 subjects were unable to apply the aforementioned technique and, therefore, could not perceive the illusion. Because the medical history of each subject and the verification tests did not indicate the presence of heterophoria, a cover test was not performed for subjects with normal BSV. Additionally, even if a subject with normal BSV had heterophoria, it was not presented during the verification tests and therefore, could not have affected the evaluation experiments of the DEMRS instance.

6.2.2 *Verifying Strabismus*

Strabismus was verified by:

1. Observation, and medical history presented by the subject.
2. Cover-uncover, and alternate-cover test.
3. Reading text from arbitrary distances.
4. Anaglyph test.
5. Partial-occlusion test (see subsect. 3.2.4).

Pre-requisites for the tests are:

- A cover pad, for the cover tests.
- Black-coloured text printed on an A4 white page in 16pt Arial fonts, for the text reading test.
- A 3D anaglyph image, and a pair of red and blue colour filter glasses, for the anaglyph test.

- Black-coloured text printed on a small piece of paper (half of an A4 page), and a picture of a toon shaded object.

Initially, the subject was asked to sit on a chair and face the examiner, who recorded the IPD. Subjects with strabismus were examined through observation, in order to determine any distinguishable deviations. Each subject was asked to provide a brief medical history of the condition including any previous diagnosis performed by an ophthalmologist, which included the strabismic deviation at the time of diagnosis. Also, each subject was asked about the origin of the condition, i.e. congenital or acquired, and whether or not the subject faced symptoms of strabismus on a daily basis, such as double vision.

Next, a cover test (see subsect. 3.4.3) was performed in order to verify the type of strabismus and estimate the angle of deviation. A cover-uncover and alternate-cover test was performed while the subject was asked to fixate initially on a near and then on a far target, at various cardinal directions. Tropia was deduced when the uncovered eye performed a compensatory movement to fixate on the target whilst the opposite eye was covered. Phoria was deduced when a compensatory movement was observed on the covered eye as soon as it was uncovered. Also, in order to determine potential symptoms of blurry or double vision, the target was brought to a near distance from the subject's eyes, from various directions, while both eyes remained uncovered.

In order to determine double vision and crude stereopsis, the final test included reading text and viewing an anaglyph image. Each subject was asked to read a short sentence, printed on an A4 paper using black coloured fonts of size 14, initially from a far distance and then from a near distance. The subject was asked to immediately report any symptoms, including double vision, blurriness and jumping letters. Each subject was asked to repeat the test using a stereoscopic image, instead of reading text, whilst wearing red and blue filtered glasses, and report whether or not they could perceive the illusion.

Of the 10 subjects with strabismus, 7 were cases of congenital strabismus and 3 were cases of acquired strabismus at an older age. The tests verified that: (a) 3 subjects had diplopia, with both eyes opened, (b) 5 subjects had convergence insufficiency (CI), (c) 1 subject had moderate constant exo-tropia on the left eye, and (d) 1 subject had moderate constant hyper-tropia on the right eye. The subjects with exo-tropia and hyper-tropia were tested for Abnormal Retinal Correspondence (ARC) using the partial-occlusion test, described in subsection 3.2.4, which verified the presence of ARC in both subjects. According to their medical history, both subjects with tropias had

undergone one or two corrective surgeries at an early age, which decreased the angle of deviation. Also, due to suppression, neither subject complained about any symptoms of double vision. Although, the subjects with diplopia and CI had undergone vision therapy, they complained about double vision, inability to read clearly, headaches and dizziness.

With regards to the text test and anaglyph test, the 3 subjects with diplopia reported double vision when reading and could not perceive the illusion from the anaglyph image. The 5 subjects with CI were able to read text from a relatively far distance but reported jumpy letters, blurry and double vision when reading text from a near distance. Furthermore, subjects with CI had difficulties perceiving the illusion from the anaglyph image by reporting moving shapes. The subjects with tropia were able to read text clearly and were unable to perceive the illusion from the anaglyph image.

6.3 THE EVALUATION PROCESS

This is a controlled study in which the subjects with normal BSV were considered to be the control group, i.e. the comparator group. In the evaluation of the DEMRS instance all subjects underwent testing, initially without using the DEMRS instance and then using the DEMRS instance (fig. 130).

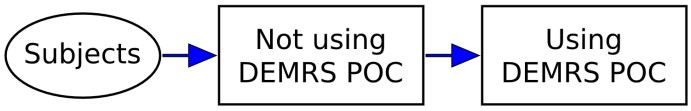

Figure 130: *Controlled study design: An overview of the study design in which all subjects undergo testing, initially without using the DEMRS instance and then using the DEMRS instance.*

The efficacy of the DEMRS instance was evaluated through four experiments: (a) pin test, (b) text test, (c) anaglyph test, and (d) autostereogram test. As explained later in this section, these experiments are designed to use physical objects as fixation targets. Therefore, in order to avoid ambiguities between the physical object used in the experiments and the target defined by the DEMRS simulator, a physical object is hereafter referred to as the physical fixation target, whereas the target defined by the DEMRS simulator is hereafter referred to as the simulated fixation target. Apart from the pin test, the remaining experiments are verified tests used in ophthalmology to diagnose strabismus, normal BSV and stereopsis (see chap. 3). Ideally, in addition to the aforementioned tests, the DEMRS instance would have been tested using other real life three dimensional objects, outside of laboratory conditions. However, due to the fragility of the POC device, which restricted

its movement, the evaluation of the DEMRS instance was conducted in a controlled laboratory environment using simple, low cost, yet valid tests to determine normal BSV and stereopsis. Due to laboratory space limitations, the target was considered to be at a far distance when located $\geqslant 3\text{m}$ from the DEMRS origin.

Appendix D.5 describes the evaluation algorithm of each test, including the sequence of interactions between the subject, DEMRS instance and examiner, who was also the operator of the DEMRS instance.

6.3.1 *Pin Test*

The pin test was designed to determine the fusibility of the visual stimuli, received by both eyes through the DEMRS instance, and if fusible, determine the time required for a subject with strabismus to interpret normal BSV. Unfortunately, this test cannot be used to determine depth perception, because the size and shape of a regular pin-head, which is relatively small and flat, does not allow the perception of the pin as a three dimensional object.

In order to conduct the pin test, under laboratory conditions, the following items were used:

- height adjustable chair
- medical head/chin rest
- regular pin (physical fixation target)
- DEMRS instance

Initially, the subject was asked to sit on a chair and place their head on a medical chin rest, which supported their head and kept it in a fixed position while viewing the pin. The medical chin rest was firmly placed on a desk, located near the wall. A white pin was placed on the wall, which was relatively dark in colour, at a distance of $\approx 40 - 65\text{cm}$ from the subject's eyes. This test was split into two phases where, in the first phase, the subject was asked to view the pin without using the DEMRS instance and, in the second phase, through the DEMRS instance. In each phase, the subject was asked to report the number of pins that were perceived, from a near and far distance, and report potential symptoms that may have occurred during the test, including double vision, blurry vision and confusion. To conduct the second phase of this test, the DEMRS instance was placed on a desk between the subject and pin, thereby allowing the subject to view the pin through the DEMRS instance. The examiner entered the subject's IPD, the position of the physical

fixation target, and estimated strabismic deviation - if any, into the DEMRS simulator in order to calculate retroversion and control the orientation of the mirrors in the DEMRS instance. While the subject viewed the pin, through the DEMRS instance, the examiner used the DEMRS simulator to move the simulated fixation target in various directions, thus causing the DEMRS instance to redirect the subject's fixation on the target defined by the DEMRS simulator, instead of the physical fixation target. Because the pin remained in the same position on the wall, it was possible to determine whether or not the subject could experience physiological diplopia, and if so, estimate the fusional area that allowed the subject to perceive one pin, instead of two. The following questions were asked to the subject during and on completion of the pin test (tab. 38).

Table 38: *Questions asked during and on completion of the pin test.*

"How many pins can you see?"
"Are the pins getting closer of further apart from each other?"
"Did you experience any blurry vision when viewing through the device?"
"Did you experience any confusion or dizziness when viewing through the device?"

Appendix D.5.1 outlines the evaluation algorithm of the pin test, including the sequence of interactions between the subject, DEMRS instance and examiner/operator of the DEMRS instance.

As the pin test was conducted in the lab, all data were collected through in-person interviews. On completion of the test, the subject was asked to provide short feedback about their experience with the DEMRS instance.

The purpose of conducting this test was to determine the effectiveness of the DEMRS instance in achieving DRS, such that a subject with strabismus can perceive one pin binocularly. For example, a subject with diplopia, who perceives two pins, is expected to perceive one pin when using the DEMRS instance. Also, via the DEMRS instance, the pin test can be used to potentially detect a change in the perception of the pin by adult subjects with congenital tropia, who tend to suppress the visual stimuli from the deviating eye. In the pin test, if the visual stimuli, received by both eyes, derive from the same target, the subject is expected to perceive one pin. However, if the visual stimuli do not derive from the same target, the subject is expected to perceive two pins. The pin test is passed when the subject reports the binocular perception of one pin from near and far distances.

6.3.2 *Text Test*

The text test was designed to determine retroversion of strabismus and the fusibility of the visual stimuli, received by both eyes, when reading text through the DEMRS instance. Similar to the pin test, the text test cannot be used to determine depth perception.

In order to conduct the text test, under laboratory conditions, the following items were used:

- height adjustable chair
- medical head/chin rest
- text printed on an A4 page (physical fixation target)
- DEMRS instance

The subject was asked to sit on a chair and place their head on a medical chin rest in order to read the text. In this experiment, the following pangram was printed on white paper (A4 size) with black fonts (14 pt).

"The quick brown fox jumps over the lazy dog."

The physical fixation target, was placed centrally at a reading distance of $\approx 45\text{cm}$ from the subject's eyes. This test was split into two phases where, in the first phase, the subject was asked to read the pangram without using the DEMRS instance and, in the second phase, through the DEMRS instance. In each phase, the subject was asked to report whether or not the text could be read clearly, from a near and relatively far distance of $\approx 1.5\text{m}$, and report potential symptoms that may have occurred during the test, including double vision, blurry vision and confusion. To conduct the second phase of this test, the DEMRS instance was placed on the desk between the subject and text, thereby allowing the subject to read the text through the DEMRS instance. The examiner entered the subject's IPD, the position of the physical fixation target, and estimated strabismic deviation - if any, into the DEMRS simulator in order to calculate retroversion and control the orientation of the mirrors in the DEMRS instance. While the subject read the pangram, through the DEMRS instance, the examiner used the DEMRS simulator to move the simulated fixation target in various directions, thus causing the DEMRS instance to redirect the subject's fixation on the target defined by the DEMRS simulator, instead of the physical fixation target. Because the A4 page with the printed pangram remained in the same position, it was possible to estimate the margins of the fusional area that allowed the subject

to read clearly, by observing when the subject reported that the letters appeared double, or jumpy. The following questions were asked to the subject during and on completion of the text test (tab. 39).

Table 39: *Questions asked during and on completion of the text test.*

"Can you read the sentence clearly?"
"How many times can you see each letter in the sentence?"
"Are the letters doubled or are they blurry?"
"Are the doubled letters getting closer of further apart from each other?"
"Did you experience any blurry vision when viewing through the device?"
"Did you experience any confusion or dizziness when viewing through the device?"

Appendix D.5.2 outlines the evaluation algorithm of the text test, including the sequence of interactions between the subject, DEMRS instance and examiner/operator of the DEMRS instance.

Similar to the pin test, the text test was conducted in the laboratory and, therefore, all data were collected through in-person interviews. On completion of the test, the subject was asked to provide short feedback about their experience with the DEMRS instance.

The purpose of conducting this test was to determine the effectiveness of the DEMRS instance in achieving DRS, such that a subject with diplopia or CI can read text clearly, without reporting symptoms of double vision. For example, a subject with CI, who has difficulties reading text from a near distance, is expected to read the pangram clearly when using the DEMRS instance. The text test is passed when the subject is able to read the pangram.

6.3.3 *Anaglyph Test*

The anaglyph test was designed to determine retroversion of strabismus, crude stereopsis and the fusibility of the visual stimuli, received by both eyes, when viewing the target through the DEMRS instance. Due to the characteristics of an anaglyph image (see subsect. 3.4.7), this test can be used to crudely determine depth perception, as stereoscopic vision must be present in order to perceive the illusion of depth through an anaglyph image using filter glasses.

In order to conduct the anaglyph test, under laboratory conditions, the following items were used:

- height adjustable chair
- medical head/chin rest
- set of two high quality anaglyph images printed on an A4 paper (physical fixation target)
- red/cyan filter 3D glasses
- DEMRS instance

The subject was asked to wear a pair of red/cyan 3D filter glasses, sit on a chair and place their head on a medical chin rest in order to view the anaglyph. In this experiment two anaglyph images were printed on photographic paper (A4 size) at high quality, which retained the clarity of the red and blue superimposed colours. Each anaglyph image depicts an animal. The first image portrays a leopard waking towards the camera, which when viewed stereoscopically the leopard appears to emerge from the image (fig. 131a). The second image portrays an elephant facing the camera, which when viewed stereoscopically the elephant's trunk and ivories appears to emerge from the image (fig. 131b).



(a) *Leopard* (b) *Elephant*

Figure 131: *Anaglyph images: The two anaglyph images used to test successful retroversion of strabismus and crude stereopsis. The use of red/cyan filter glasses is necessary to perceive the 3D illusion from anaglyph images.*

Each anaglyph image was placed at reading distance of $\approx 40 - 65\text{cm}$ from the subject's eyes. This test was split into two phases where, in the first phase, the subject was asked to view each image without using the DEMRS instance and, in the second phase, using the DEMRS instance. In each phase, the subject was asked to report whether or not the 3D illusion was perceived,

describe the 3D illusion, and report potential symptoms that may have occurred during the test, including double vision, blurry vision and confusion. To conduct the second phase of this test, the DEMRS instance was placed on the desk between the subject and anaglyph, thereby allowing the subject to view the image through the DEMRS instance. The examiner entered the subject's IPD, the position of the physical fixation target, and estimated strabismic deviation - if any, into the DEMRS simulator in order to calculate retroversion and control the orientation of the mirrors in the DEMRS instance. While the subject viewed the anaglyph, through the DEMRS instance, the examiner used the DEMRS simulator to move the simulated fixation target in various directions, thus causing the DEMRS instance to redirect the subject's fixation on the target defined by the DEMRS simulator, instead of the physical fixation target. Because each anaglyph remained in the same location, it was possible to estimate the margins of the fusional area that allowed the subject to perceive the illusion stereoscopically, by observing when the subject stopped perceiving the 3D illusion. The following questions were asked to the subject during and on completion of the anaglyph test (tab. 40).

Table 40: *Questions asked during and on completion of the stereoscopic image test.*

"Can you perceive the stereo illusion?"
"Can you see the animal coming towards you?"
"Can you describe what you see?"
"How many animals can you see?"
"Are the animals getting closer of further apart from each other?"
"Was the stereo illusion lost at any point during the test?"
"Did you experience any blurry vision when viewing through the device?"
"Did you experience any confusion or dizziness when viewing through the device?"

Appendix D.5.3 outlines the evaluation algorithm of the anaglyph test, including the sequence of interactions between the subject, DEMRS instance and examiner/operator of the DEMRS instance.

Similar to the previous tests, the anaglyph test was conducted in the laboratory and, therefore, all data were collected through in-person interviews. On completion of the test, the subject was asked to provide short feedback about their experience with the DEMRS instance.

The purpose of conducting this test was to determine the effectiveness of the DEMRS instance in achieving DRS, such that a subject can perceive the illusion from the anaglyph image without reporting symptoms of monocular vision, confusion and double vision. For example, a subject with diplopia, who is unable to perceive the 3D illusion from an anaglyph image, is expected to perceive and describe the illusion when using the DEMRS instance. Also, this test can determine if the subject is able to process the dynamic act of change in the visual stimuli, induced by the DEMRS instance, by changing the position of the simulated fixation target. The anaglyph test is passed when the subject is able to perceive the illusion of depth.

6.3.4 *Autostereogram Test*

The autostereogram test was designed to determine retroversion of normal BSV and strabismus, the presence of stereopsis and perception of depth. Due to the characteristics of an autostereogram image (see subsect. 3.4.7), this test can be used to determine depth perception, without familiarity cues, as normal BSV must be present in order to perceive the illusion (“hidden" shape) through an autostereogram.

In order to conduct the autostereogram test, under laboratory conditions, the following items were used:

- height adjustable chair
- medical head/chin rest
- set of seven autostereogram images (physical fixation target)
- DEMRS instance

The subject was asked to sit on a chair and place their head on a medical chin rest in order to view the autostereogram. In this experiment, seven autostereograms were randomly selected from Magic Eye II (Smith, 1994), ordered in level of difficulty. Figure 132 shows the autostereograms used in this test along with their underlying illusions.

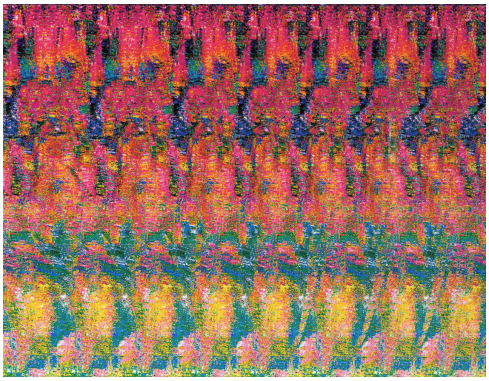

(a) *"Baby Dinosaur" image - easy*

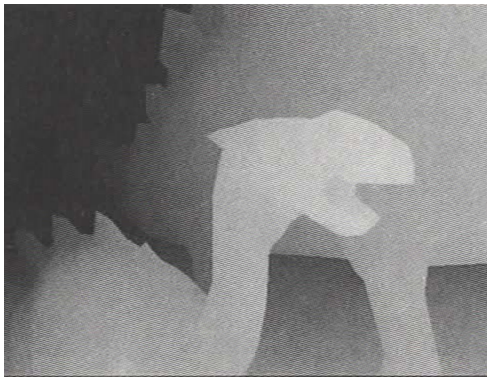

(b) *"Baby Dinosaur" illusion*



(c) *"Andy's Bunny" image - easy*

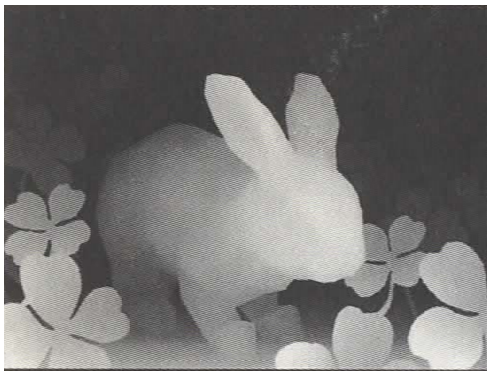

(d) *"Andy's Bunny" illusion*



(e) *"Lost Oasis" image - medium*

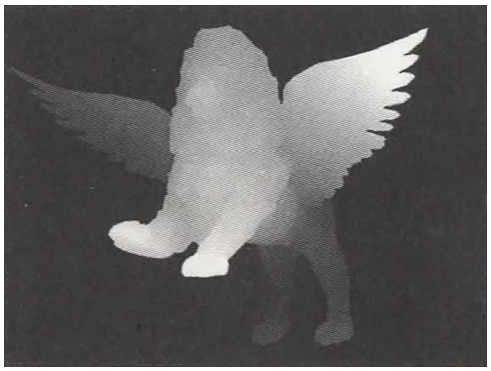

(f) *"Lost Oasis" illusion*



(g) *"Deer" image - medium*

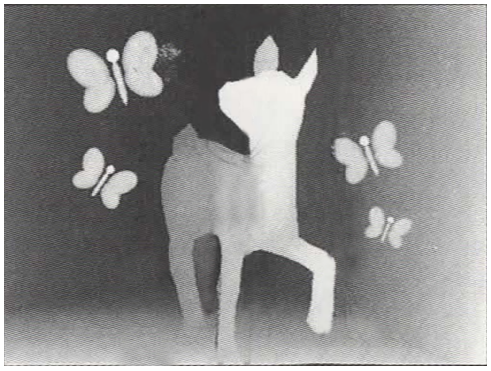

(h) *"Deer" illusion*

Figure 132: *Autostereogram images: (continued on next page)*



(i) *"Walleye" image - medium*

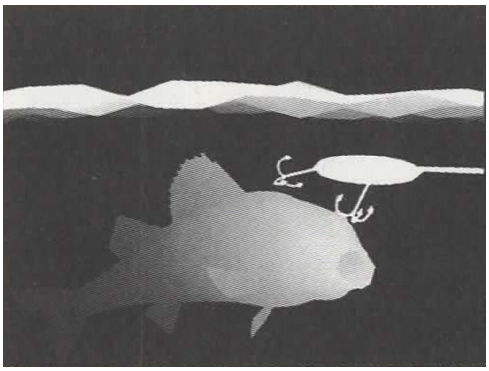

(j) *"Walleye" illusion*



(k) *"Storyland" image - hard*



(l) *"Storyland" illusion*

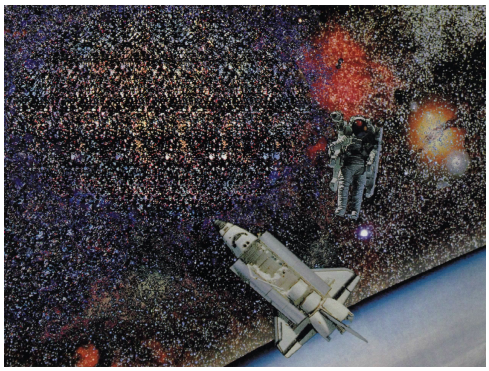

(m) *"The eagle's in flight" image - hard*



(n) *"The eagle's in flight" illusion*

Figure 132: *Autostereogram images: The seven autostereogram images (Magic Eye II (Smith, 1994)) along with their solutions. The technique, described in subsection 3.4.7, must be applied in order to perceive the illusion.*

Of the seven autostereograms, each subject was randomly assigned three autostereograms (easy, medium, hard). Each autostereogram was placed at reading distance of $\approx 40 - 65\text{cm}$ from the subject's eyes. This test was split into two phases where, in the first phase, the subject was asked to view each image without using the DEMRS instance and, in the second phase, using the DEMRS instance. In each phase, the subject was asked to report whether or not the illusion was perceived, from a near and relatively far distance of

$\approx$ 1.5m, and to describe the "hidden" shape. Also, the subject was asked to report potential symptoms that may have occurred during the test, including double vision, blurry vision and confusion. To conduct the second phase of this test, the DEMRS instance was placed on the desk between the subject and autostereogram, thereby allowing the subject to view the image through the DEMRS instance. The examiner entered the subject's IPD, the position of the physical fixation target, and estimated strabismic deviation - if any, into the DEMRS simulator in order to calculate retroversion and control the orientation of the mirrors in the DEMRS instance. While the subject viewed the autostereogram, through the DEMRS instance, the examiner used the DEMRS simulator to move the simulated fixation target in various depths, thus causing the DEMRS instance to redirect the subject's fixation further in or out from the physical fixation target. Because each image remained in the same location, it was possible to estimate the margins of the fusional depth that allowed the subject to perceive the illusion, by observing at which depths the subject stopped perceiving the illusion. In addition to moving the simulated fixation target, the subject was asked to move away from the DEMRS instance for a short period of time ($\approx 1-2\text{mins}$), and then return to viewing through the DEMRS instance, which was left in the retroverted state. The subject was asked to report if the illusion could be perceived once they viewed the autostereogram through the DEMRS instance. The following questions were asked to the subject during and on completion of the autostereogram test (tab. 41).

Table 41: *Questions asked during and on completion of the autostereogram test.*

"Can you clearly see the autostereogram image?"
"Can you make out any illusions?"
"Can you describe the shape that you see?"
"Is the illusion lost?"
"Can you still see the illusion?"
"Did you experience any blurry vision when viewing through the device?"
"Did you experience any confusion or dizziness when viewing through the device?"

Appendix D.5.4 outlines the evaluation algorithm of the autostereogram test, including the sequence of interactions between the subject, DEMRS instance and examiner/operator of the DEMRS instance.

Similar to the previous tests, the autostereogram test was conducted in the laboratory and, therefore, all data were collected through in-person interviews. On completion of the test, the subject was asked to provide short feedback about their experience with the DEMRS instance.

The purpose of conducting this test was to determine the effectiveness of the DEMRS instance in achieving DRS, such that a subject with normal BSV or strabismus can perceive the illusion from an autostereogram. For example, although subjects with normal BSV are able to perceive depth binocularly, they might not be able to perceive the illusion from an autostereogram image because they cannot apply the technique required to perceive the illusion. Using the DEMRS instance, subjects with normal BSV are expected to perceive the illusion and describe the “hidden" shape successfully. Additionally, the autostereogram test can determine if the subject is able to process the dynamic act of change in the visual stimuli, induced by the DEMRS instance, by observing if the subject can perceive the illusion while moving the position of the simulated fixation target. The autostereogram test is passed when the subject is able to successfully perceive and describe the illusion.

6.4 RESULTS

All 21 subjects completed the experiments, described in the previous section. This section analyses the outcome of the experiments, and discusses the effectiveness of the DEMRS instance in achieving retroversion. Also, in order to quantify the total number of completed tests, including repetitions, the following analysis defines a test case as one completed test performed by a subject. For example, if one subject repeats the same experiment twice, the number of test cases is two.

6.4.1 *Pin Test*

The pin test showed that, without the DEMRS instance, all subjects with normal BSV were able to binocularly perceive one pin from near and far distances. Using the DEMRS instance had no effect in their perception of depth, as all subjects continued to perceive one pin from near and far distances. When the examiner moved the simulated fixation target in different directions, all subjects reported two pins. When the examiner reset the position of the simulated fixation target, in order to match the position of the pin, all subjects reported one pin.

Of the 10 subjects with strabismus, without using the DEMRS instance, the 3 subjects with diplopia reported two pins from near and far distances, the 5 subjects with CI reported one pin from a far distance but two pins from a near distance, and the 2 subjects with tropias reported one pin from near and far distances. When the subjects used the DEMRS instance, the 3 subjects with diplopia and the 5 subjects with CI reported one pin from near and far distances. The 2 subjects with tropias continued to report one pin, monocularly. However, the subject with exo-tropia reported perceiving a second blurry pin to the left of the pin.

The pin test comprised of 84 test cases, deriving from 42 tests conducted prior to DRS and 42 tests conducted during DRS. Prior to DRS, 27 of 42 (64.3%) test cases passed the test, whereas during DRS, 38 of 42 (90.5%) test cases passed the test. The results from the pin test are summarized in table 42, which also illustrates two pie charts of the success rate before and during retroversion.

Table 42: *Results from the pin test indicating the number of subjects who passed the test. The two pie charts illustrate the percentage rate of success prior to using the DEMRS instance (left), and while using the DEMRS instance (right).*

	Condition (# Subjects)	Prior to DRS		During DRS	
		near	far	near	far
Pin Test	BSV (11)	11	11	11	11
	Diplopia (3)	0	0	3	3
	CI (5)	0	5	5	5
	Exo-tropia (1)	0	0	0	0
	Hyper-tropia (1)	0	0	0	0

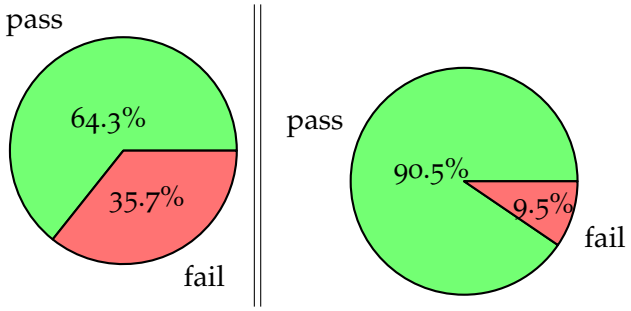

As expected, prior to DRS, subjects with normal BSV were able to pass the pin test without expressing any symptoms of double vision. Repositioning the simulated fixation target outside of their fusional area caused all subjects with normal BSV to experience temporary physiological diplopia, as the DEMRS instance redirected their fixation to the simulated target instead of the physical target. Although the fusional area of each subject was

different, when the simulated target was reset to the position of the physical target all subjects with normal BSV were able to instantly revert back to perceiving one pin. The DEMRS instance had a positive impact on subjects with diplopia and CI who, prior to DRS, expressed symptoms of double vision and dizziness. While using the DEMRS instance these subjects were able to instantly perceive one pin binocularly without having symptoms of double vision. The subjects with diplopia and CI were also able to experience physiological diplopia when the simulated fixation target was moved away from the physical fixation target. Unfortunately, the subjects with tropias could not experience normal BSV, which could be attributed either to suppression and/or lack of accuracy in measuring each subject's deviation, thereby preventing the DEMRS simulator from calculating the correct retroversion angles for the mirrors in the DEMRS instance. Although the tests were repeated, the subjects with tropias were not able to binocularly perceive the physical target. However, both subjects reported that, while using the DEMRS instance, they perceived parts of the surrounding environment that were not perceived prior to DRS. This is attributed to the fact that the brain of each subject received visual stimuli through the DEMRS instance that could not be fused. The subject with exotropia reported a second blurry pin in their perception from near and far distances, which could either be a result of ARC or a relatively accurate estimation of the deviation inputted into the DEMRS simulator that would allow the pin to be perceived by the strabismic eye. The pin test verified that the DEMRS instance: (a) does not have a negative impact on normal vision, (b) can be used to measure Panum's fusional area, and (c) allows subjects with diplopia and CI, but not with tropia, to instantly and binocularly perceive one pin.

6.4.2 *Text Test*

The text test was completed only by the 8 subjects with diplopia and CI who expressed discomfort while reading text. This experiment showed that, without the DEMRS instance, the 3 subjects with diplopia were unable to read the text clearly and reported symptoms of double vision, such as seeing the same character in a word twice. The 5 subjects with CI, were able to read the text from a relatively far distance but complained about jumpy letters, eye strains and double vision from a near distance. When the subjects used the DEMRS instance, all subjects with diplopia and CI were able to clearly read the text, from near and far distances, without expressing symptoms of double vision or confusion.

The text test comprised of 32 test cases, deriving from 16 tests conducted prior to DRS and 16 tests conducted during DRS. Prior to DRS, 5 of 16 (31.3%) test cases passed the test, whereas during DRS, 16 of 16 (100.0%) test cases passed the test. The results from the text test are summarized in table 43, which also illustrates two pie charts of the success rate before and during retroversion.

Table 43: *Results from the text test indicating the number of subjects who passed the test. The two pie charts illustrate the percentage rate of success prior to using the DEMRS instance (left), and while using the DEMRS instance (right).*

Text Test	Condition (# Subjects)	Prior to DRS		During DRS	
		near	far	near	far
	Diplopia (3)	0	0	3	3
	CI (5)	0	5	5	5

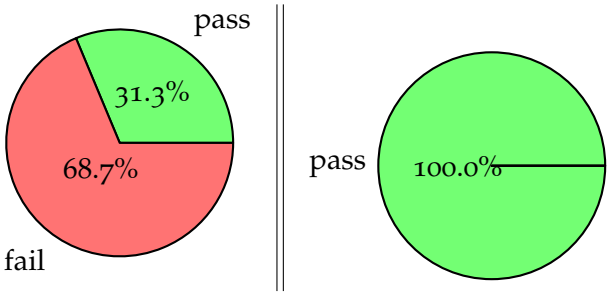

In most cases of strabismus, where double vision is a symptom, the angle of deviation is relatively small, but large enough to exceed Panum's fusional area. Consequently, prior to DRS each subject perceived double words. Unlike subjects with diplopia who constantly perceived double text, subjects with CI complained about moving letters and inability to fixate on a word, causing them eye strains. During DRS, the words were "brought" closer to one another until perceived and read as one, which allowed the subjects to read the text clearly. The text test verified that the DEMRS instance can achieve retroversion at reading distance such that subjects with diplopia and CI are able to clearly read text.

6.4.3 *Anaglyph Test*

The anaglyph test showed that, without the DEMRS instance, all subjects with normal BSV were able to perceive the 3D illusion stereoscopically. Using the DEMRS instance had no effect in their perception of depth, as all subjects continued to perceive the illusion from near and far distances. When the examiner moved the simulated fixation target in different directions, all

subjects reported that the illusion was disturbed and could not perceive the illusion of depth from the image. When the examiner reset the position of the simulated fixation target all subjects perceived the illusion.

Without using the DEMRS instance, the 3 subjects with diplopia reported confusion and were not able to perceive the 3D illusion stereoscopically, from neither far or near distances. Of the 5 subjects with CI, 4 subjects perceived the 3D illusion stereoscopically from a far distance but were unable to perceive the illusion from a near distance. Due to suppression, the 2 subjects with tropias could not perceive the illusion. When the subjects used the DEMRS instance, the 3 subjects with diplopia and 5 subjects with CI were able to perceive the 3D illusion, from near and far distances, without reporting any symptoms. However, the 2 subjects with tropias continued to view the anaglyph monocularly, and therefore could not perceive the illusion.

The anaglyph test comprised of 84 test cases, deriving from 42 tests conducted prior to DRS and 42 tests conducted during DRS. Prior to DRS, 26 of 42 (61.9%) test cases passed the test, whereas during DRS, 38 of 42 (90.5%) test cases passed the test. The results from the anaglyph test are summarized in table 44, which also illustrates two pie charts of the success rate before and during retroversion.

Table 44: *Results from the anaglyph test indicating the number of subjects who passed the test. The two pie charts illustrate the percentage rate of success prior to using the DEMRS instance (left), and while using the DEMRS instance (right).*

	Condition (# Subjects)	Prior to DRS		During DRS	
		near	far	near	far
Anaglyph Test	BSV (11)	11	11	11	11
	Diplopia (3)	0	0	3	3
	CI (5)	0	4	5	5
	Exo-tropia (1)	0	0	0	0
	Hyper-tropia (1)	0	0	0	0

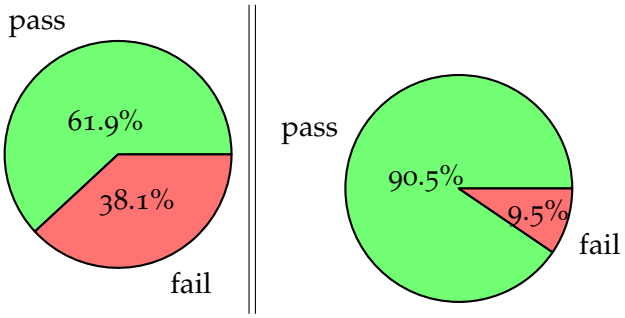

As expected, prior to DRS, subjects with normal BSV were able to pass the anaglyph test without expressing any symptoms of double vision. Repo-

sitioning the simulated fixation target outside of their fusional area caused all subjects with normal BSV to experience temporary physiological diplopia, as the DEMRS instance redirected their fixation to the simulated target instead of the physical target. Consequently, their stereoscopic perception of the anaglyph was disturbed, which prevented them from perceiving the illusion of depth. Although the fusional area of each subject was different, when the simulated target was reset to the position of the physical target all subjects with normal BSV were able to instantly revert back to perceiving the 3D illusion from the image. The DEMRS instance had a positive impact on subjects with diplopia and CI who, prior to DRS, expressed confusion and eye strains as they could not fixate on the anaglyph. While using the DEMRS instance these subjects were able to instantly perceive the 3D illusion stereoscopically without having symptoms of double vision. The subjects with diplopia and CI were also able to experience physiological diplopia when the simulated fixation target was moved away from the physical fixation target, which disturbed their stereoscopic perception. Unfortunately, the subjects with tropias could not experience normal BSV, which similar to the pin test could be attributed either to suppression and/or lack of accuracy in measuring each subject's deviation, thereby preventing the DEMRS simulator from calculating the correct retroversion angles for the mirrors in the DEMRS instance. Although the tests were repeated, the subjects with tropias were not able to binocularly perceive the 3D illusion. The anaglyph test verified that the DEMRS instance can achieve retroversion so that subjects with diplopia and CI can perceive the illusion of depth stereoscopically.

6.4.4 *Autostereogram Test*

The autostereogram test showed that, without the DEMRS instance, only 4 subjects with normal BSV were able to perceive and describe all three illusions, because the remaining 7 subjects were unable to apply the technique required to perceive the illusion from an autostereogram. When the DEMRS instance was used all subjects with normal BSV were able to perceive and describe all illusions. As the examiner moved the simulated fixation target in different depths, all subjects were able to report when the illusion from each autostereogram was lost. When the position of the simulated fixation target was reset, all subjects were able to instantly perceive the illusion. Once a subject reported that they could perceive the illusion they were asked to move away from the DEMRS instance for a short period of time, and then return to viewing through the DEMRS instance, which was left in the retro-

verted state. All subjects reported that the DEMRS instance allowed them to instantly perceive the illusions.

Without using the DEMRS instance, none of the subjects with strabismus were able to perceive and describe any of the illusions from the three autostereograms they were assigned. When these subjects used the DEMRS instance, the 3 subjects with diplopia and 5 subjects with CI were able to perceive and describe all illusions without reporting any symptoms. Unfortunately, the 2 subjects with tropias continued to view the autostereograms monocularly, and therefore could not perceive any of the illusions. However, the subject with exo-tropia reported perceiving a blurry part of the autostereogram, which was not perceived prior to DRS.

Although the autostereogram test was performed only from a reading distance, it comprised of 126 test cases, because each subject repeated the test once for each of the three autostereograms. Therefore, 63 tests conducted prior to DRS and 63 tests conducted during DRS. Prior to DRS, 12 of 63 (19.1%) test cases passed the test, whereas during DRS, 57 of 63 (90.5%) test cases passed the test. The results from the autostereogram test are summarized in table 45, which also illustrates two pie charts of the success rate before and during retroversion.

Table 45: *Results from the autostereogram test indicating the number of subjects who passed the test. The two pie charts illustrate the percentage rate of success prior to using the DEMRS instance (left), and while using the DEMRS instance (right).*

Autostereogram Test	Condition (# Subjects)	Prior to DRS			During DRS		
		easy	mid	hard	easy	mid	hard
	BSV (11)	4	4	4	11	11	11
	Diplopia (3)	0	0	0	3	3	3
	CI (5)	0	0	0	5	5	5
	Exo-tropia (1)	0	0	0	0	0	0
	Hyper-tropia (1)	0	0	0	0	0	0

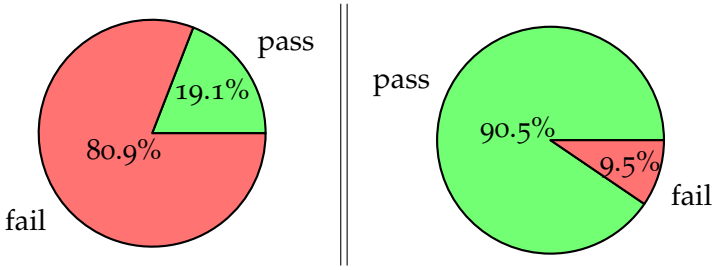

Compared to the previously discussed tests, the autostereogram experiment was relatively hard to pass, even for subjects with normal BSV. This is because a subject must, not only possess binocular and stereoscopic vision

but, also be able to voluntarily control the depth of their fixation in order to perceive the illusion from an autostereogram. Additionally, this test cannot be passed by a subject unless they successfully describe the perceived illusion, whereas in the previous tests a subject may provide false positive or false negative feedback, i.e. claim that the 3D illusion is perceived or that the text is read clearly when it is not, and vice versa.

Due to level of difficulty of this test, prior to DRS, only four subjects with normal BSV were able to apply the technique required to perceive and describe the illusion successfully. It should be noted that, of the four subjects, two had previous experience with viewing autostereograms. The remaining seven subjects with normal BSV could not apply the required technique and, therefore, could not perceive the illusion. Also, due to strabismus, none of the subjects with diplopia, CI, and constant tropias were able to perceive any of the illusions from the autostereograms.

Initially the DEMRS instance achieved retroversion for the original position of the autostereogram so that all subjects could clearly see the autostereogram, without expressing symptoms of double vision. When the examiner used the DEMRS simulator to move the simulated fixation target along the z axis, i.e. further away from the position of the physical fixation target, all subjects experienced a dynamic change in their visual perception. However, only subjects with normal BSV, diplopia, and CI were able to fuse the visual stimuli deriving from the DEMRS instance. The simulated target was moved until the 3D illusion from the autostereogram was finally perceived. Unfortunately, the two subjects with tropias were unable to fuse, and did not perceive the illusion. This could be attributed to suppression, and/or lack of accuracy in measuring each subject's deviation, thereby preventing the DEMRS simulator from calculating the correct retroversion angles for the mirrors in the DEMRS instance. Although the tests were repeated, the subjects with tropias were not able to perceive the 3D illusion. Each subject with normal BSV, diplopia, and CI had a different fusional area, meaning that they reported the illusion perceived at different depths. However, they were able to eventually perceive and describe the illusion. This test had a positive impact on subjects with diplopia and CI because is showed that, through successful retroversion by the DEMRS instance, their stereoscopic vision was restored. Repositioning the simulated fixation target outside of the fusional area of each subject disturbed their stereoscopic perception of the autostereogram, and prevented them from perceiving the illusion. When the simulated target was reset to the position of the physical target all subjects with normal BSV, diplopia, and CI were able to instantly revert back to perceiving the 3D illusion from the autostereogram. In addition to moving

the simulated fixation target, when the examiner asked each subject to move away from the DEMRS instance for a short break, and return to viewing through the DEMRS instance all subjects, apart from the two with constant tropias, were able to instantly perceive the illusion.

The autostereogram test verified that the DEMRS instance can: (a) achieve retroversion of normal BSV, diplopia, and CI, (b) induce a dynamic change in the visual perception of a subject with normal BSV and strabismus, (c) be used to measure the fusional depth of a subject, and (d) assist in the restoration of stereoscopic vision for subjects with diplopia and CI.

6.4.5 *Discussion*

Overall, the evaluation of the DEMRS instance consisted of 326 test cases, where 163 test cases were designed to determine the ability of a subject to pass a test prior to DRS, and 163 test cases were designed to determine the ability of the subject to pass the test during DRS. As illustrated by the pie charts in table 46, prior to DRS, 70 of 163 (42.9%) test cases passed, whereas during DRS, 149 of 163 (91.4%) test cases passed.

Table 46: *Pie charts illustrating the percentage rate of success of the total test cases prior to DRS (left), and during DRS (right).*

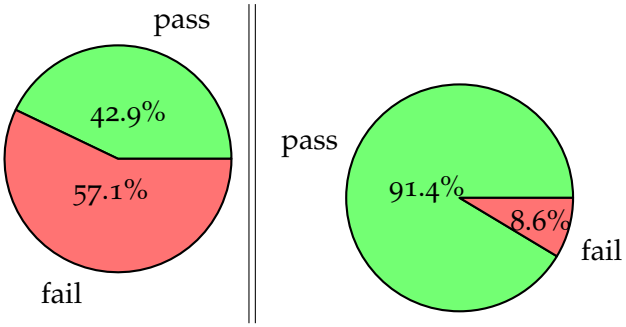

The DEMRS instance achieved retroversion of normal BSV, diplopia and CI. Although normal BSV does not require retroversion, a DRS compliant system must be able to retroverse normal BSV in order to compensate for phorias, i.e. latent deviations that occur only when binocularity is voluntarily or involuntarily disrupted (see subsect. 3.3.1). The experiments showed that, when using the DEMRS instance, these subjects, not only received visual stimuli deriving from the same fixation target but, could instantly fuse both retinal images formed by the normal and strabismic eyes. Therefore, most subjects with strabismus experienced normal BSV and depth perception.

Unfortunately, the two subjects with constant tropias could not experience normal BSV and depth perception. These subjects were adults who,

according to their medical history, suppressed the visual stimuli received by the strabismic eye. Furthermore, the DEMRS instance could not achieve retroversion using the estimated strabismic deviation measured during the preliminary examination of the subjects, as a lack of accuracy in the measurement of strabismus prevented the DEMRS simulator from calculating the correct retroversion angles for the mirrors in the DEMRS instance. Also, because the DEMRS instance did not include a method of tracking the actual position of the eyes, the accommodative deviation of each subject, i.e. the change in strabismic deviation that occurs during the accommodative convergence from a far to a near fixation target, was estimated using the equations from section 2.3, which did not represent the actual accommodative deviation of each subject. Consequently, it was not possible to determine whether the subjects with tropias failed to perceive depth due to suppression, or due to the proof of concept device used in the experiments.

From the perspective of the subjects, the most interesting experiment was the autostereogram test, because it involved a level of difficulty that was challenging. Although the pin, text and anaglyph tests determined the fusibility of a subject during DRS, the involvement of the subject was minimal. However, the autostereogram test required that the subject controlled the depth of their fixation in order to perceive the illusion. Although the voluntary control of fixation was not required by the subject when using the DEMRS instance, the experiment remained interesting to them. A noticeable effect caused by using the DEMRS instance was that, after completing the autostereogram test, the subjects with normal BSV who were previously unable to apply the required technique in order to perceive the illusion, were able to control their fixation such that they could perceive the illusion without using the DEMRS instance.

A few of the feedback given by the subjects when undergoing the evaluation experiments were:

"The letters do not move anymore."
"It takes me straight to 3D."
"It's like the deer is walking out of the picture."

6.5 SUMMARY

This chapter described the evaluation of the DEMRS instance, which comprised of four experiments conducted under laboratory conditions, involving human subjects. Ethical approval was obtained from Bournemouth University ethics committee. Of the twenty-one volunteer subjects that were

invited to enrol in the study, eleven subjects had normal BSV and ten subjects had strabismus. It must be highlighted that the evaluation of the DEMRS instance does not fall under the remit of clinical evaluation, and the DEMRS instance is not to the standards of a custom medical device that has been manufactured to be used in a clinical setup.

The four experiments, namely the pin test, text test, anaglyph test, and autostereogram test, were designed to determine the efficacy of the DEMRS instance in the retroversion of normal BSV and strabismus by testing the fusibility of the visual stimuli received by both eyes, and testing the ability of a subject to perceive depth. The tests showed that the DEMRS instance: (a) does not have a negative impact on normal vision, (b) can be used to measure Panum's fusional area, (c) achieve retroversion of normal BSV, diplopia, and CI, (d) induce a dynamic change in the visual perception of a subject with normal BSV and strabismus, and (e) assist in the restoration of stereoscopic vision for subjects with diplopia and CI.

The evaluation of the DEMRS instance consisted of 326 test cases, where 163 test cases determined the ability of a subject to pass a test prior to DRS, and 163 test cases determined the ability of the subject to pass the test during DRS. The results show an increase of 48.5% in the success rate of the tests, as prior to DRS the success rate was 42.9%, whereas during DRS it was 91.4%. Despite the fact that subjects with constant tropias could not pass the tests, the DEMRS instance achieved retroversion of normal BSV and most types of strabismus considered in this study.

7

DISCUSSION & CONCLUSION

"... τὸ δὲ ζητούμενον ἁλωτόν, ἐκφεύγει δὲ τἀμελούμενον."
— Σοφοκλής, 496-406 π.Χ.

"... what is searched can be found, and lost what is neglected."
— Sophocles, 496-406 BC

This thesis investigates the ophthalmological condition known as strabismus, and explores alternative ways to assist in its diagnosis and treatment. Current methods that are used to diagnose and treat strabismus are limited by the: (a) type of strabismus, (b) age of a subject, (c) variability, size and direction of a deviation, (d) time and day, on which the diagnosis or treatment is conducted, (e) experience of an examiner, or surgeon, and (f) cooperation and motivation of a subject. Unfortunately, the success rate of binocular fusion with the current treatment methods, including surgery, are extremely low. There is no system available capable of compensating strabismus in such a way that the visual stimuli, received by both eyes, dynamically derive from the same fixation target, located in various distances and directions.

The main contribution of this thesis is a novel principle referred to as Dynamic Retroversion of Strabismus (DRS) on which the proposed Dynamic Eye Misalignment Retroversion Systems (DEMRS) are based to assist in the diagnosis and treatment of strabismus. A system is DEMRS, or DRS compliant, when it meets all four criteria of the DRS principle, namely the: (a) simultaneous intersection of both principal vision vectors on the same fixation target, (b) maintenance of normal resultant inter-pupillary distance (IPD), (c) maintenance of normal binocular disparity, and (d) maintenance of normal orientation of the visual stimuli. Furthermore, a DEMRS:

1. Is a non-surgical compensatory method of treating strabismus, as it does not actively change the orientation of a strabismic eye.

2. Achieves retroversion of strabismus for any stable or moving object in the environment, located at various distances and directions.

3. Compensates for all classifications of strabismus, including deviations that arise as a result from an abnormal structure of the skull.

4. Compensates for any variable change in strabismic deviations, and is not restricted by latency, comitancy or frequency of strabismus.

5. Can be used as HBVT and OBVT by various age groups including young children, adults and elderly.

6. Is designed to motivate a subject to undergo and complete therapy, by not using pre-determined fixation targets in office based set-ups, but allowing the subject to perform various personal tasks e.g. watching a film or reading a book.

7. Assists in the diagnosis of strabismus by allowing the dissociation of both eyes to fixate on different targets. Also, it has the potential to gather diagnostic information, such as the orientation of both eyes.

The thesis describes the DEMRS simulator, a custom software application that was developed in order to simulate DRS compliant systems, and presents two designs of DEMRS, one compensating for horizontal and vertical deviations (HV-2.0), and the other for horizontal, vertical and torsional deviations (HVT-2.5). Due to the lesser occurrences of torsional deviations, a proof of concept (POC) device was built based on the design of HV-2.0, so that it can be tested involving human subjects with normal BSV and strabismus. The functionality of the DEMRS POC device, also referred to as DEMRS instance, was verified by conducting two experiments, using two laser pointers to represent the principal vision vectors of the eyes. In the first experiment the DEMRS instance successfully retroverted normal BSV, and in the second experiment the DEMRS instance successfully retroverted a case of left exotropia.

The efficacy of the DEMRS instance was evaluated through four experiments, conducted under laboratory conditions, namely the: (a) pin test, (b) text test, (c) anaglyph test, and (d) autostereogram test. Twenty-one volunteer subjects were invited to enrol in the study, of which eleven subjects had normal BSV, and ten subjects had strabismus. The tests showed that the DEMRS instance achieved retroversion of normal BSV and strabismus, as prior to DRS, the success rate of test cases was 42.9%, whereas during DRS, the success rate of test cases was 91.4%. More precisely, the tests showed that the DEMRS instance: (a) does not have a negative impact on normal vision, (b) can be used to measure Panum's fusional area, (c) achieve retroversion of normal BSV, diplopia, and CI, (d) induce a dynamic change in the visual perception of a subject with normal BSV and strabismus, and (e) assists in the restoration of stereoscopic vision for subjects with diplopia and CI. Although the subject group involved in this study was relatively small, the

results from the evaluation of the DEMRS instance justify further research in the principle of DRS, where a more advanced prototype could be developed in order to conduct experiments involving a larger group of subjects in a clinical setting.

The concept of DRS, along with the designs of DEMRS, was presented to strabismologists who supported the research, and provided valuable feedback with regards to its potential use in ophthalmology. Damanakis (2013) and Hammond (2014) stated that with the current surgical techniques, it is not possible to be accurate when adjusting the orientation of the eyes. However, a DEMRS can "fix these errors" (Hammond, 2014), and open a huge research area towards the actual treatment and understanding of strabismus (Damanakis, 2013). Damanakis (2013) and Hammond (2014) emphasized that a DEMRS can be used as a compensatory treatment pre and post surgery. According to Hammond (2014), "a dynamic act of change in process would be great", as it would complement surgery and act as its supporting agent to the development of binocular vision. Damanakis (2014b) agreed with Hammond (2014) and added that the "system's dynamism is a huge advantage towards the diagnosis of strabismus". Also, Damanakis (2014b) confirmed that such a system can play a significant role in the treatment of strabismus as it has the potential to "train binocular vision in young children", and be used to explore other areas of strabismus that are presented in older ages. In addition to assisting in the diagnosis and treatment of typical cases of strabismus, Damanakis (2014b) mentioned that a DEMRS can be used to treat rare cases of strabismus, such as deviations caused by orbital conditions and vertical disparities, where surgery is not an option. Both, Damanakis (2013) and Hammond (2014) emphasized on the fact that a DEMRS can be of great value to subjects with permanent and persistent diplopia. Hammond (2014) explained that some subjects can selectively switch their suppression on and off, such that they retain binocularity when viewing straight ahead but suppress it when viewing to the side. A DEMRS can "maintain their binocularity while medical staff are treating" (Hammond, 2014) the underlying strabismus. Damanakis (2013) and (Hammond, 2014) stated that compared to office based treatments where motivation is very limited, especially in young ages, a DERMS can motivate children to complete therapy, as they can watch a movie at home. Finally, Damanakis (2013) mentioned that it would be very helpful to the diagnosis of strabismus if a DEMRS could record the position of the eyes, while the subject undergoes therapy at home, so that medical staff can "review the behaviour of the deviation" prior to surgery, as it would assist in the design of a more accurate surgical model.

For consumer use a DEMRS must be a developed as a wearable head mounted device that would allow a subject to perform various personal tasks, e.g. watching films, reading books, playing sports and driving a car. Figure 133 shows a 3D illustration of HVT-2.5 as a head mounted device.

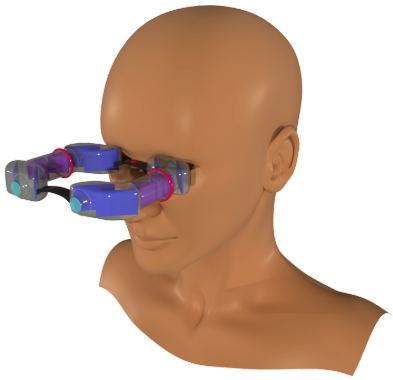

Figure 133: *DEMRS HVT-2.5 as a head mounted wearable device.*

Dynamic Retroversion of Strabismus (DRS) is a novel concept developed to assist in the diagnosis and treatment of strabismus, whereby ophthalmologists and practitioners can use a Dynamic Eye Misalignment Retroversion System (DEMRS) in order to give young children a fighting chance to be treated for strabismus. A chance we did not have.

7.1 FUTURE WORK

This section presents futuristic ideas with the intention to further develop DRS compliant systems in order to improve the capabilities of DEMRS and user experience.

7.1.1 *Improving the GUI of the DEMRS Simulator*

The DEMRS simulator is a project that undergoes amendments on a regular basis, including refactoring the codebase, adding features, and bug fixes. Currently, the simulator is developed such that the user describes the design of a DEMRS through a JSON configuration file passed in as input to the simulator via command line arguments, including other inputs such as the IPD and strabismic deviation. This method is not user friendly, because it requires basic knowledge of scripting/programming and using a terminal (command prompt). Also, the graphical user interface (GUI) of the DEMRS simulator is very limited, and does not allow the user to modify the design while the simulator is running.

Future additions to the simulator include a user friendly GUI where the user would be able to select, move, rotate, and scale each component of the system using an interactive gizmo, i.e. set of handles. Similar gizmos can be found in almost every commercial 3D software package, including Autodesk Maya. Furthermore, the GUI could include a toolbar that would list a set of pre-defined components, ex. mirror, dove prism, delta prism, convex lens, concave lens, from which the user can drag a component into the viewport so that they could design a custom DEMRS without the need to describe it in a JSON configuration file. The software would save and export the design in the form of a JSON configuration file, or another universal scene descriptor (USD) so that it can be loaded back into the simulator. Additionally, the GUI would include a section where the user could set values to the parameters of each component, ex. the refractive index of a lens, and other inputs, such as the IPD and strabismic deviation.

7.1.2 *Field of View Analysis*

The first time the subjects used the DEMRS POC device they reported confusion, as various objects from the surrounding environment were perceived within their peripheral vision. This was because the DEMRS POC device did not have a cover case that could block arbitrary light from entering the system, and did not include convex and concave lenses to constrain the direction of the peripheral visual stimuli. Asking the subjects to focus their attention on the central part of their perception, bypassed this problem. However, it did not allow the subjects to have a wide visual field of the environment, because their peripheral perception was formed with patches from arbitrary parts of the environment. Furthermore, during the evaluation of the DEMRS POC device, the physical fixation target was mostly placed centrally to each subject, i.e. on the mid plane of the face and at eye level. Even when the target was moved to either side, it was not moved by a great distance from the centre. This is because it is not necessary to move the target in extreme directions to determine successful retroversion.

A field of view (FOV) analysis would determine the maximum range of visual field that can be perceived by a subject when using a DEMRS, and the maximum directions that a fixation target can be successfully retroverted by a DEMRS. Similar to wearing prescription glasses, where the range of vision is constrained by the size of the spectacles, the FOV of a DEMRS depends on the size of the system, as retroversion is achieved only when the subject views a fixation target through a DEMRS. The analysis would reveal areas of

improvement so that a DEMRS can be designed to provide the widest visual field possible, and achieve retroversion in extreme directions. For example, in order to expand the FOV of HV-2.0 such that it can compensate for targets in extreme directions, a rail can be added to the design of the system on which $M_{3,4_{L/R}}$ would be mounted so that they can move and rotate during retroversion (fig. 134).

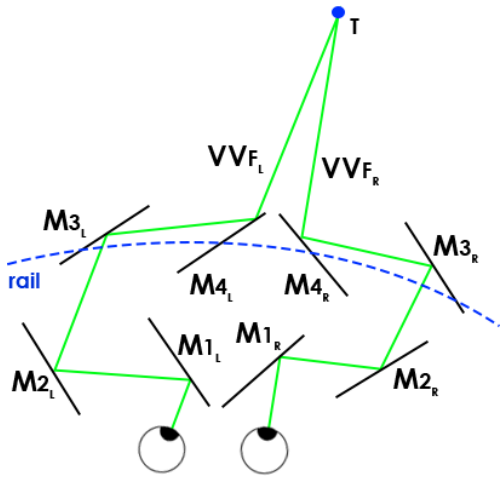

Figure 134: *Hypothetical design of HV-2.0 with a rail: This design includes a rail, illustrated by the blue dashed line, on which mirrors* $M_{3,4_{L/R}}$ *are mounted so that they can move and rotate during retroversion, thereby expanding the FOV of the system.*

7.1.3 *Eye Tracking*

DRS compliant systems are intended to be used during OBVT and HBVT, which suggests that a subject would be able to use a DEMRS at home while performing personal tasks, such as watching a film or reading a book, and outdoors while driving a car or doing sports. In order to compensate for such tasks, a DEMRS requires a method to track the position of both eyes, so that it can continuously achieve retroversion while the subject fixates on various targets. This can be accomplished through eye tracking, which can be used to measure the point of gaze of the normal eye, and the deviation of the strabismic eye. Therefore, eye tracking is critical to the practical viability of a DEMRS.

Eye tracking is the process of tracing the movements and activity of an eye, invasively or non-invasively Al-Rahayfeh and Faezipour (2013). Carter and Luke (2020) define eye tracking as "an experimental method of recording eye motion and gaze location across time and task ... observing the allocation of visual attention". There are four techniques to eye tracking:

1. **Electro oculography (EOG):** This is an invasive method that records "the electric potential differences of the skin surrounding the ocular cavity" (Valenti and Gevers, 2008) in order to monitor eye movements. This technique is based on the standing potential of the eye, which is the difference in the electrical potential between the posterior and anterior segments generated by the RPE (see subsect. 2.1.1) (Yanoff and Duker, 2019). According to Constable *et al.* (2017), the "standing potential of the eye may be assessed using skin electrodes placed near the outer and inner canthi of each eye to record successive horizontal saccadic eye movements". Therefore, the position of the eye is approximated by monitoring small variations in the skin potential around the eye (Chennamma and Yuan, 2013).

2. **Scleral search coils (SSC):** This is the most invasive approach to eye tracking whereby the position of the eye is recorded by a custom designed contact lens that contains small coils of fine wire in the shape of a ring, also referred to as search coils (Ansons and Davis, 2014). The contact lens is tightly fitted "over the sclera of the eye with a slight suction to avoid drift during fast eye movements" (Morimoto and Mimica, 2005). Furthermore, two sets of large field coils are horizontally and vertically placed on opposite sides to the subject's head in order to generate a weak magnetic field that induces small electric currents within the search coils of the lens (Murphy *et al.*, 2001) (Singh, 2012). Klaib *et al.* (2021) explain that the "field induces a voltage in the coil to produce a signal that represents the eye position". They (Klaib *et al.*, 2021) also explain that SSC can be used to determine the torsional orientation of the eye, as an "integrated coil in the contact lens allows detecting the orientation of the coil in a magnetic field".

3. **Infra-red oculography (IOG):** This is a non-invasive eye tracking method based on computer vision[1] and image processing techniques. In non-invasive methods a camera, or another optical/photosensitive device, focuses on the eye and transmits each frame into a software application that processes the image in order to firstly detect the eye, and next estimate the direction of gaze (Al-Rahayfeh and Faezipour, 2013). In IOG, the eye is illuminated by an infra-red (IR) light source in order to brighten the colour of the pupil, in the captured frame, and therefore enhance the contrast between the iris and pupil (Carter and Luke,

1 Computer Vision (CV) is a field of Artificial Intelligence (AI) that enables computers to gain high-level understanding, and derive meaningful information from visual input, such as images or videos.

2020). This is known as a bright pupil effect and it is used to improve the detection of the pupil and, subsequently, the estimation of gaze (Kohlbecher *et al.*, 2008). Furthermore, because infra-red light is part of the invisible light spectrum, the light that is shined into the eye does not distract the subject (Singh, 2012). Klaib *et al.* (2021) explains that in order to "solve the issue of head movement sensitivity, a reference point, which is known as a corneal reflection or glint, is included using an infra-red light source when this technique is applied". According to Morimoto and Mimica (2005), "eye trackers can determine the direction of gaze with a high degree of accuracy by measuring the position of the corneal reflection of an infra-red light relative to the pupil".

4. **Video oculography (VOG):** Similar to IOG, this is a non-invasive eye tracking method based on computer vision and image processing techniques. VOG uses one or more colour (RGB), black and white (BW), or infra-red (IR) cameras to capture the eyes (Clarke *et al.*, 2002) (Wagner *et al.*, 2006). Depending on the method of frame acquisition, i.e. type of camera and illumination method, the pupil can appear brighter or darker than the iris, referred to as bright or dark pupil effect (Chennamma and Yuan, 2013). According to Singh (2012), the steps involved in VOG eye tracking are: (a) frame acquisition, (b) face localization, (c) eye localization, (d) pupil detection, and (e) gaze calculation.

Most invasive methods, including EOG and SSC, require a subject's head to the constrained at primary, or resting, position because the rotation of head can affect the measurements of the eye tracker (Constable *et al.*, 2017) (Murphy *et al.*, 2001). Valenti and Gevers (2008) describe that their eye tracker uses "a high resolution camera combined with a chin rest to limit the allowed head movement". The measurements gathered by an eye tracker are relative to the position of the head (Bérard *et al.*, 2014) (Villanueva *et al.*, 2009). According to Singh (2012), "the methods measuring eye position relative to the head are more accurate, and intended for the study of oculomotor dynamics". Non-invasive techniques rely mainly on pupil detection and gaze estimation algorithms, which according to several authors can operate on interactive rates using commodity hardware, and do not require calibration (Haro *et al.*, 2000) (Clarke *et al.*, 2002) (Wagner *et al.*, 2006) (Kohlbecher *et al.*, 2008) (Villanueva *et al.*, 2009) (Klaib *et al.*, 2021). This section does not discuss such algorithms, because eye tracking is a rapidly evolving field of research in which new algorithms are regularly introduced in order to improve the quality and efficiency of pupil detection and gaze estimation (Zhu and Yang, 2002) (Wang *et al.*, 2005) (Duchowski, 2017).

Chapter 3 mentioned that eye trackers have been previously used in ophthalmology for diagnostic purposes, including haploscopic devices that measure strabismic deviations (Ramey *et al.*, 2008) (Irsch *et al.*, 2008). A DEMRS can incorporate such non-invasive eye tracking systems in order to continuously measure the strabismic deviation, which may vary depending on the type of strabismus, and achieve retroversion for fixation targets in various directions. The type of mirrors used in the designs of DRS compliant systems, previously described in this thesis including the POC device, are high performance cold mirrors that reflect $\geqslant$ 95% of the visible light spectrum and transmit $\geqslant$ 90% of infra-red light. These mirrors would allow two infra-red cameras to be placed behind $M1_{L/R}$ in order to capture the position of the eyes without the distracting the subject. The DEMRS simulator can be extended with computer vision techniques such that it can detect the position of the pupils and calculate the visual direction (principal vision vector) of each eye. Using the vision vectors, the DEMRS simulator can estimate the strabismic deviation and calculate the orientation of the mirrors/prisms in order to achieve retroversion. Also, DEMRS devices can use an accelerometer, or a gyroscope sensor, in order to track the orientation of the head and, therefore, improve eye tracking. Figure 135 shows a potential design of HV-2.0 with two infra-red cameras and an accelerometer.

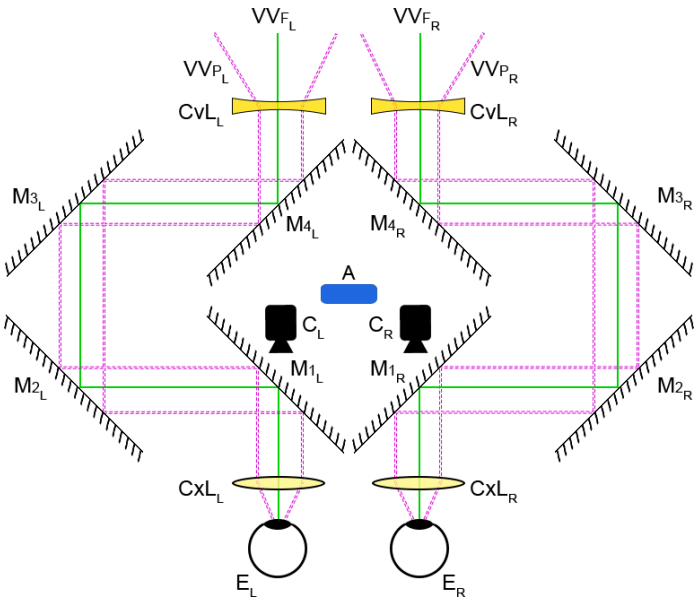

Figure 135: *Extended design of DEMRS HV-2.0: A schematic of the system, where* $C_{L/R}$ *are the two infra-red cameras,* A *is the accelerometer/gyroscope sensor,* $VV_{F_{L/R}}$ *are the left and right principal vision vectors,* $VV_{P_{L/R}}$ *are the peripheral vision vectors,* $CxL_{L/R}$ *and* $CvL_{L/R}$ *are the convex and concave lenses,* $M1_{2,3,4_{L/R}}$ *are the left and right set of mirrors, and* $E_{L/R}$ *are the left and right eyes.*

7.1.4 *Target Deduction*

As previously discussed in subsection 4.3.4, the position of a fixation target can be: (a) set by the DEMRS operator, (b) calculated from the direction of the principal vision vector of the normal eye, and a distance specified by the DEMRS operator, and (c) deduced, or inferred, from the direction of the principal vision vector of the normal eye and the median plane of the subject's face. The first two approaches of defining a fixation target require input from the DEMRS operator, whereas the third approach can estimate the position of the fixation target. The limitation with the third approach is that the fixation target is assumed to be central to the subject's face, which is the reason for using the median plane of the face in order to estimate the position of the fixation target. Figure 136a shows that, because the target T lies on the principal vision vector of the normal eye VV_{F_R} as well as the median-plane (MP), the VV_{F_R} creates an orthogonal triangle $\angle(T, MP, E_R)$. Therefore, the auxiliary vision vector VV_{A_L} of the strabismic eye can be calculated using basic trigonometry, which creates the isosceles triangle $\angle(E_L, T, E_R)$. Unfortunately, without the assumption that T lies on MP, it is not possible to estimate the position of the fixation target using only the visual direction of the normal eye and the IPD. As shown by figure 136b, the normal eye may fixate on one of the potential targets (T_1, T_2, T_3) but the exact target cannot be estimated, because the only known information is the direction of VV_{F_R} and the IPD of the subject. Consequently, a triangle cannot be formed using one angle (VV_{F_R}) and one side (IPD).

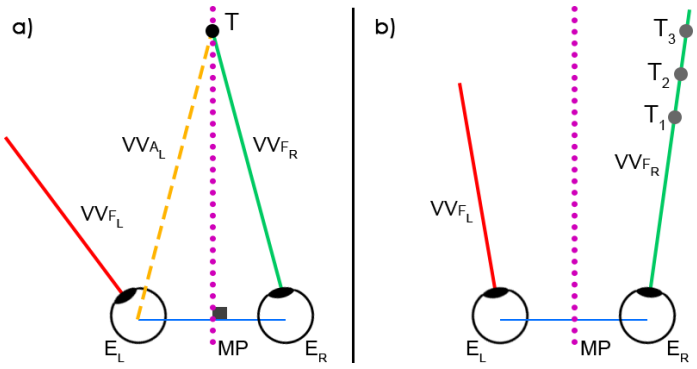

Figure 136: *Target deduction problem: In this figure,* $E_{L/R}$ *are both eyes, the blue line indicates the IPD, the purple dotted line represents the median plane* MP *of the face,* $VV_{F_{L/R}}$ *are the two principal vision vectors,* VV_{A_L} *is the auxiliary vision vector of the strabismic eye, and the black dots are the estimated fixation targets. (a) shows that if* T *is assumed to lie on* MP, VV_{A_L} *can be calculated using basic trigonometry, or by mirroring the direction of* VV_{F_R}. *However, (b) shows that if* T *is not assumed to lie on* MP, VV_{A_L} *cannot be calculated as the only known information are the direction of* VV_{F_R} *and the IPD.*

In theory, the phenomenon of accommodative convergence and AC/A ratio, discussed in section 2.3, can be used to estimate the distance of the fixation target from the normal eye, because for every unit of accommodation there is a relative unit of convergence. For example, when the normal eye fixates on a far target, the accommodative convergence of the deviating eye is 0°. But when the normal eye fixates on a near target, the accommodative convergence of the deviating eye might be 6°. Therefore, due to the relationship between accommodation and convergence, the distance of the fixation target from the normal eye may be estimated using the relative unit of convergence of the deviating eye. A DEMRS would have to be calibrated, per subject, such that the range of accommodative convergence and AC/A ratio, for near and far fixation targets, can be registered and used in order to estimate the distance of the fixation target. Once the distance of the fixation target, from the normal eye, is estimated the auxiliary vision vector of the strabismic eye can be calculated using basic vector algebra.

A method to estimate the position of the fixation target can be used to extend the potential use of a DEMRS, because it would enable the system to operate without the requirement of constraining the target to a particular location, distance from the normal eye, or median plane of the face.

7.1.5 *Detect Alternate Strabismus*

Currently, the DRS compliant systems presented in this thesis are able to achieve retroversion for all types of strabismus, when the fixation target is set by the DEMRS operator. However, a limitation is presented with alternate deviations (see subsect. 3.3.8), where a subject can intensionally or unintentionally decide which eye would assume fixation, i.e. become dominant. Unfortunately, the DEMRS simulator cannot compensate for alternate deviations, when the target is calculated from the direction of the principal vision vector of the normal eye, or deduced using the median plane of the subject's face. This is because the DEMRS simulator calculates retroversion based on the dominant eye, which was set as input by the DEMRS operator during initialization, but does not include a method to determine a change in dominance while the DEMRS is in operation.

To extend the applications of DRS compliant systems, a method could be developed that would determine alternate deviations, so that a DEMRS can be used by subjects who unintentionally alternate their fixation. A common effect of alternate strabismus is that the deviating eye fixates on the target, when assuming dominance, while the normal eye deviates. Therefore,

a simple method of determining alternate strabismus is to check whether the strabismic eye fixates on the target, and if the normal eye has deviated. However, as strabismus is a highly complex polymorphic condition, such a simplistic method would be limited to the: (a) size of a deviation, which might be small enough to determine a change in dominance, (b) direction of a deviation, which might be similar to the direction of the normal eye, (c) frequency, and (d) latency of a deviation, which might complicate the detection of the dominant eye.

7.1.6 *Improving the POC Device*

Unfortunately, due to the inherent limitations of the proof of concept device, including size, mobility, fragility, efficiency, and performance, the DEMRS instance could only be tested under laboratory conditions with supervision. The DEMRS POC device can be improved in the following ways:

1. Attach a pair of concave and convex lenses so that the peripheral stimuli does not cause any confusion to the subjects.
2. Use a hard cover to block arbitrary light from entering the system.
3. Embed two infra-red eye tracking cameras behind $M1_{L/R}$ in order to track the orientation of both eyes. Although estimating the orientation of the eyes, including the strabismic deviation, was sufficient to achieve retroversion of normal BSV, diplopia and CI, a method to track the orientation of both eyes would have been a more efficient way of verifying the strabismic deviation. Additionally, an eye tracking system would enable the DEMRS instance to achieve retroversion even if there is an alteration in the strabismic deviation.
4. Include four delta prisms to test against torsional deviations. Although torsional strabismus is a very rare type of strabismus, it is usually diagnosed in correlation with other types of deviations, such as exotropia (Hammond, 2014).
5. Add an accelerometer in order to improve the accuracy of eye tracking, by detecting the orientation of the eyes relative to the head.
6. Replace the 12V 28BYJ-48 stepper motors with the 5704M-10 high accuracy stepper motor by Lin Engineering, or high accuracy dynamixels. The 5704M-10 motor is small in size, highly accurate by providing a step angle of 0.45° and capable of high torque (Lin Engineering, 2019).

If high accuracy stepper motor are to be used, a position feedback device would also be required in order to check the angle of the mirrors after rotation. Due to the lack of a position feedback device, such as an encoder that detects whether a motor skips pulses, or a torque sensor that measures the load that is being driven by a motor, it was not possible to detect the exact rotation of the mirrors after retroversion. The markings on the base of the DEMRS instance were sufficient to determine if a mirror had rotated by the correct retroversion angle, but it was not possible for the DEMRS instance to correct the rotation error during the retroversion process. Consequently, the DEMRS instance had to be reset and the test repeated, when the mirrors did not rotate as per the retroversion angles calculated by the DEMRS simulator.

7. Aim for a much smaller, but firmer device so that it can be moved and tested in various environments.

A new version of DEMRS is currently being designed that is slightly larger than the size of normal glasses.

APPENDIX A

A.1 AC/A FORMULAE

A.1.1 *Heterophoria Method*

The original equation to calculate the AC/A ratio using this method is:

$$AC/A_{(\Delta/D)} = \delta_{(cm)} + \frac{N_\Delta - F_\Delta}{A_{(D)}} \tag{9}$$

where:

AC/A = accommodative convergence to accommodation

δ = interpupillary distance

N = deviation at near

F = deviation at far

A = accommodation at near

Assuming that, from the centre of the eyes, a near target is located 33cm away and a far target 6m away, the following example (Yanoff and Duker, 2019) shows:

$$\delta = 6cm$$

$$N = 30\Delta$$

$$F = 3\Delta$$

$$A = 3D$$

$$AC/A_{(\Delta/D)} = 6 + \frac{30-3}{3} = 6 + 9 = 15_{(\Delta/D)} \tag{10}$$

The resulting AC/A ratio is considered high indicating an eso-deviation.

A.1.2 *Gradient Method*

The original equation to calculate the AC/A ratio using this method is:

$$AC/A_{(\Delta/D)} = \frac{Q1_{\Delta} - Q0_{\Delta}}{Lp_{(D)}} \tag{11}$$

where:

AC/A = accommodative convergence to accommodation

$Q0$ = the eyes' deviation without using a lens

$Q1$ = the eyes' deviation using a lens

Lp = lens' accommodative power

Assuming that, from the centre of the eyes, a near target is located $33cm$ away and a far target $6m$ away, the following example (Damanakis, 2005) shows:

$$\begin{aligned} Distance &= 6m \\ Q0 &= -10\Delta \\ Q1 &= 5\Delta \\ Lp &= 3D \\ AC/A_{(\Delta/D)} &= \frac{5-(-10)}{3} = 5_{(\Delta/D)} \end{aligned} \tag{12}$$

The resulting AC/A ratio is considered normal.

B

APPENDIX B

B.1 HV-2.0 CONFIGURATION

Listing 2: HV-2.0 Configuration: The JSON configuration, which presents the initial setup of HV-2.0. Because the design of the system is symmetrical, the configuration file sets the values only for one side, which gets mirrored on the other side.

```
{
    "hv20" :
    [
    {
        "symmetrical" : "true",
        "side" : "left"
    },
    {
        "component" : "lens",
        "type" : "convex",
        "translate" : [3.0, 0.0, 2.0]
    },
    {
        "component" : "mirror",
        "id" : 0,
        "pivot" : [6.35, 0.0, 0.0],
        "translate" : [0.51, 0.0, 2.5],
        "rotate" : [0.0, 225.0, 0.0]
    },
    {
        "component" : "mirror",
        "id" : 1,
        "translate" : [17.0, 0.0, 6.99],
        "rotate" : [0.0, 45.0, 0.0]
    },
```

```
        {
                "component" : "mirror",
                "id" : 2,
                "translate" : [17.0, 0.0, 18.01],
                "rotate" : [0.0, 135.0, 0.0]
        },
        {
                "component" : "mirror",
                "id" : 3,
                "pivot" : [-6.35, 0.0, 0.0],
                "translate" : [0.51, 0.0, 22.5],
                "rotate" : [0.0, 315.0, 0.0]
        },
        {
                "component" : "lens",
                "type" : "concave",
                "translate" : [3.0, 0.0, 23.5]
        }
        ]
}
```

B.2 DEMRS FOR HORIZONTAL AND VERTICAL STRABISMUS (VERSION HV-1.0)

HV-1.0 is the first conceptual system designed to retroverse horizontal and vertical strabismus, using a set of mirrors. This system was based on the design of a classic stereoscope (see subsect. 2.5.3), with the only difference that both eyes would be able to simultaneously fixate on the same target, rather than on two different images. HV-1.0 is designed to redirect principal and peripheral vision vectors by orienting a set of mirrors, horizontally about the y-axis (yaw rotation) and vertically about the x-axis (pitch rotation), in order to achieve retroversion. Moreover, this system is not designed to retroverse torsional deviations, because the orientation of the visual stimuli is assumed to be normal.

B.2.1 *Design and Description*

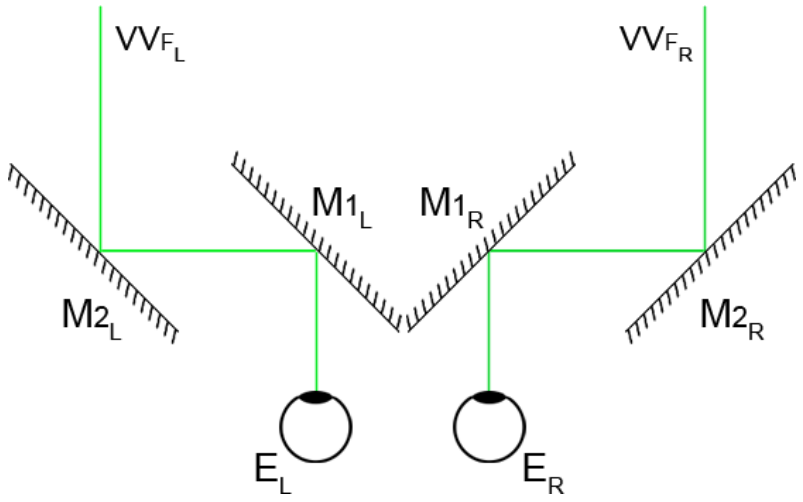

Figure 137: *DEMRS HV-1.0: A schematic of the system, where* $VV_{F_{L/R}}$ *are the left and right principal vision vectors,* $M_{1,2L/R}$ *are the left and right set of mirrors, and* $E_{L/R}$ *represent the left and right eyes.*

The design of HV-1.0 (fig. 137) consists of four mirrors, two on each side ($M_{1_{L/R}}$ and $M_{2_{L/R}}$), for the purpose of redirecting the principal vision vectors ($VV_{F_{L/R}}$) towards the fixation target. Although the creation of HV-1.0 preceded the development of the DEMRS simulator, a potential JSON configuration of HV-1.0 is:

Listing 3: HV-1.0 Configuration: A potential JSON configuration of HV-1.0. Because the design of the system is symmetrical, the configuration file sets the values only for one side, which gets mirrored on the other side.

```
{
    "hv10" :
    [
    {
        "symmetrical" : "true",
        "side" : "left"
    },
    {
        "component" : "mirror",
        "id" : 0,
        "translate" : [3.0, 0.0, 2.5],
        "rotate" : [0.0, 225.0, 0.0]
    },
```

```
        {
                "component" : "mirror",
                "id" : 1,
                "translate" : [17.0, 0.0, 2.5],
                "rotate" : [0.0, 45.0, 0.0]
        }
        ]
}
```

Mirrors $M1_L$ and $M1_R$ are located centrally to the eyes so that the system can provide a larger visual field, when achieving retroversion for: (a) various angles of strabismic deviations, and (b) various directions of a fixation target. Also, the pivots of rotation of $M1_{L/R}$ and $M2_{L/R}$ are central to the mirrors.

The default state of HV-1.0, as shown in figure 137, is based on the assumption that the fixation target is located centrally to both eyes at a distance of $\geqslant 6m$ from the centre of both eyes. This is because at 6m the eyes assume their primary position of gaze (see sect. 2.2). Therefore, by default, each mirror is oriented horizontally about the y-axis (yaw rotation) by 45°. Also, the distance between the points of reflection of VV_{F_L} on $M2_L$ and VV_{F_R} on $M2_R$ is termed resultant pupillary distance.

The sequence in which a vision vector is reflected by the mirrors, as it travels from the eye to a target (T), is as follows:

$$E \rightarrow M_1 \rightarrow M_2 \rightarrow T$$

B.2.2 *Retroversion*

During the development of HV-1.0, the basis of retroversion was that both principal vision vectors must pass through the same fixation target (T). However, when T is located at a distance of $\geqslant 6m$, both vision vectors should be parallel, whereas if T is located at a distance of $< 6m$, both vision vectors should converge on T. Figure 138 illustrates these two cases where HV-1.0 retroverses both vision vectors ($VV_{F_{L/R}}$) when T is at a distance of $\geqslant 6m$ (fig. 138a), and when T is at a distance of $< 6m$ (fig. 138b).

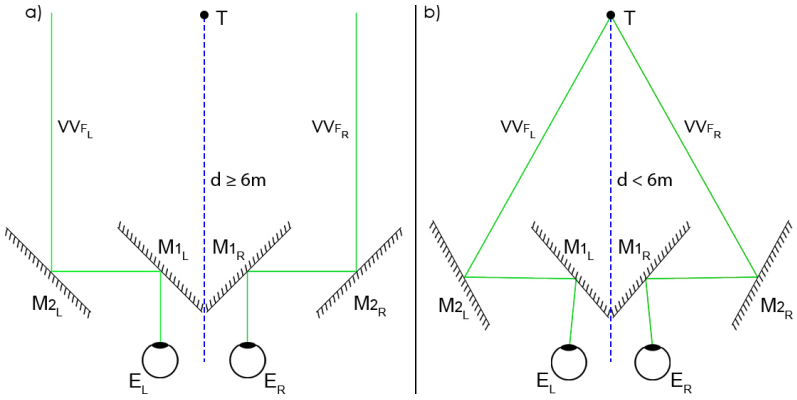

Figure 138: *Retroverse on* T*: An overview of retroversion, where* T *is the fixation target,* $VVF_{L/R}$ *are the left and right principal vision vectors,* $M1,2_{L/R}$ *are the left and right set of mirrors,* $E_{L/R}$ *are the left and right eyes, and* d *represents the distance between the eyes and the fixation target* T*.*

The objective of HV-1.0 is to redirect the vision vector from the strabismic eye, using mirrors, so that it passes through the same fixation target as the vision vector from the normal eye. Figure 139 shows an example of exotropia in which the left eye deviates outwards, viewing a target B, when it is supposed to be fixating on target G. Both G and B are points of a three dimensional environment.

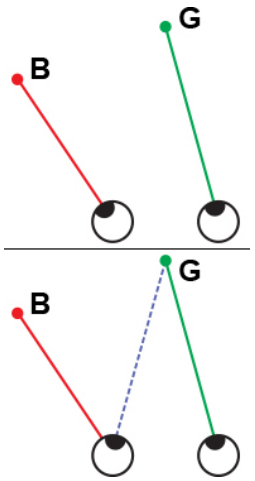

Figure 139: *From* B *to* G*: The upper part of the figure shows an example of strabismus in which the principal vision vector (red line) of a strabismic eye, deviates outwards towards* B*. The principal vision vector (green line) of the dominant eye is directed towards* G*, which is the fixation target. The lower part of this figure illustrates the objective of retroversion, which is to redirect the vision vector of the strabismic eye as if the eye was too fixating on* G*.*

The law of reflection states, that the angle of incidence (θi), which is the angle between an incident ray ($\vec{I_A}$) and the normal vector of a mirror ($\vec{N}$), is equal to the angle of reflection (θr) (fig. 140a). Furthermore, the law of

reflection states that when a mirror rotates by an angle ϕ, the reflected ray will rotate by twice the angle (2ϕ) (fig. 140b).

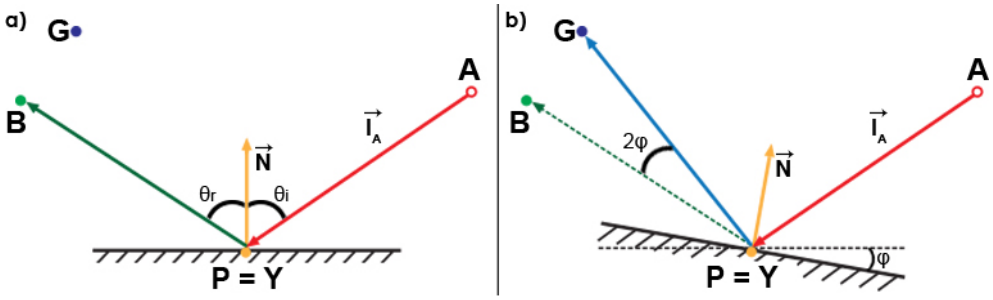

Figure 140: *Law of reflection: The first part of this figure (a) shows a vector $\vec{I_A}$ reflect on a non-oriented mirror, whereas the second part (b) shows the vector $\vec{I_A}$ reflected on a mirror that has been rotated by an angle ϕ. The incidence ray (red line) starts from point A with direction $\vec{I_A}$, the mirror surface is the black horizontal line with P being the pivot of rotation and $\vec{N}$ being the normal vector of the mirror. Y is the point of intersection between the incidence ray and the mirror, θi is the angle of incidence and θr is the angle of reflection.*

The angle ϕ by which a mirror is supposed to rotate in order for the reflected vector to intersect point G, is calculated by equation 13.

$$\psi^\circ = \cos^{-1}\left(\frac{\vec{YB} \odot \vec{YG}}{\left|\vec{YB}\right| \times \left|\vec{YG}\right|}\right), \phi^\circ = \frac{\psi^\circ}{2} \tag{13}$$

where:

$\vec{YB}$ = current reflection vector that intersects point B

$\vec{YG}$ = desired reflection vector that intersects point G

ψ = angle between YB and YG

ϕ = angle of rotation of the mirror

The angle by which each eye is required to rotate, in order to fixate on the target, can be calculated using equation 2 from section 2.3. For example, if a target T is located centrally at a distance of 1m from the centre of the eyes, whose IPD is 6cm, each eye must rotate inwards by $\approx 1.7^\circ$ in order to fixate on the target. To achieve retroversion the orientation of each mirror in HV-1.0 is calculated in an orderly fashion, starting from $M1_{L/R}$ to $M2_{L/R}$. More specifically, the angles of each mirror are calculated such that $VV_{F_{L/R}}$ is, firstly, reflected by $M1_{L/R}$ to the centre of $M2_{L/R}$, and next, by $M2_{L/R}$ to the fixation target. The order by which the mirrors rotate is: $M1_{L/R} \rightarrow M2_{L/R}$. This pattern of calculations can be formed as an algorithm, called chained retroversion, which would sequentially calculate the orientation of the mirrors of HV-1.0 in an orderly fashion.

B.2.3 *Simulations*

The following simulations were designed to evaluate HV-1.0 in the perception of depth by rendering the views from the left and right eyes in order to visualize a single "fused" image. A simple scene was constructed using Autodesk Maya, where a 3D model of a house was used as the fixation target, two 3D modelled spheres represented the eyes, and four planar surfaces with reflective shaders were used as the mirrors (fig. 141). Additionally, the scene includes two cameras, which are placed inside the eyes in order to render the view from each eye, one cyclopean camera, located further behind the mirrors representing the view from a cyclopean eye, and one perspective camera, used to obtain screenshots of HV-1.0 (fig. 141).

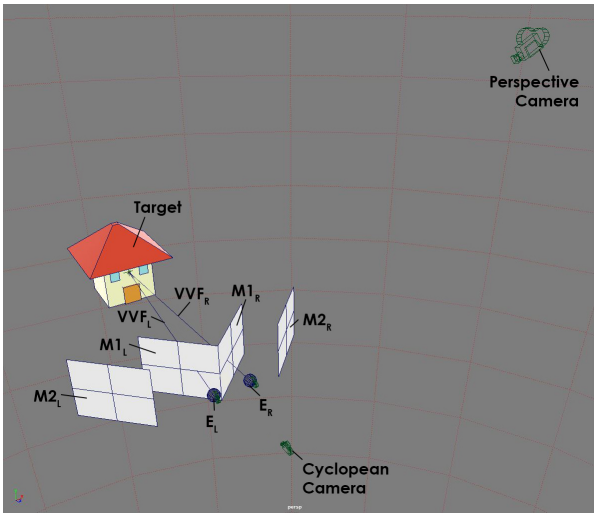

Figure 141: *3D scene: A perspective view of the 3D scene that was used to simulate retroversion. The fixation target is a 3D model of a house, located at a distance of* $\approx 45\text{cm}$ *from the centre of both eyes* ($E_{L/R}$). $M1_{L/R}$ *and* $M2_{L/R}$ *are the four mirrors in the system used to redirect both principal vision vectors. Two cameras are placed inside the eyes, and one cyclopean camera placed further behind the eyes.*

Furthermore, a custom Python application was used to visualize the direction of the retroverted principal vision vectors, using control vertex curves. The program and scene created for the simulations can be accessed at `https://bitbucket.org/cglynos/demrs/src/master/HV_10/`.

Two simulated test were conducted with normal BSV and strabismus. The IPD was set to 6cm and the target was positioned centrally to both eyes (mid-plane of the face) at a distance of 45cm. The first test was performed under the assumption that normal BSV is present. Prior to retroversion, VV_{F_L} and VV_{F_R} were not directed towards the target (fig. 142a). Consequently, the mirrors were rotated so that both $VV_{F_{L/R}}$ could be directed towards the same

target (fig. 142b). Figure 142 includes a rendered image from the cyclopean camera, which shows a monocular view of the target through HV-1.0 (fig. 142c). Additionally, the figure presents two rendered images from the cameras that were placed inside the left and right eyes, in order to show how the target is viewed through HV-1.0 by each eye (fig. 142d, 142e). Although fusion is a highly complex cerebral process (see chap. 2) that cannot be emulated by visualization software, the two rendered views from the eyes were superimposed in order to visualize the "fused" image (fig. 142f).

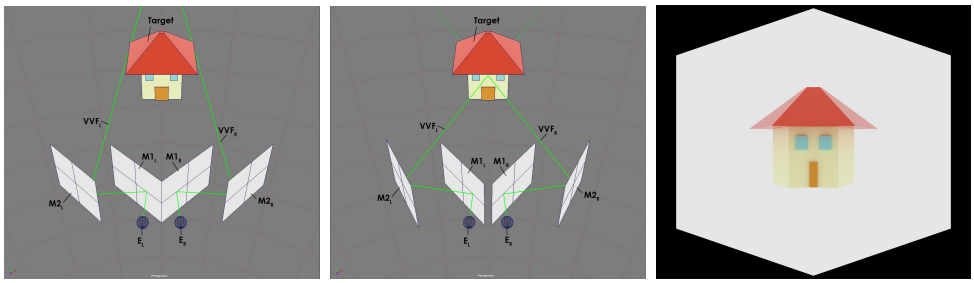

(a) *Default state, where neither* VV_F *intersects the target.* (b) *Retroversion of both* VV_F. (c) *Cyclopean render of the target after retroversion.*

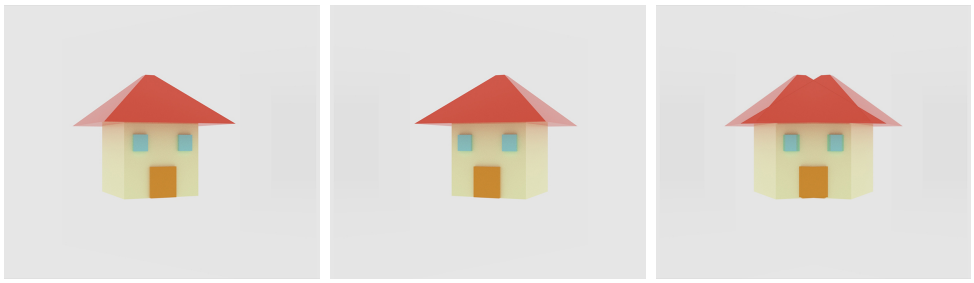

(d) *Render from the left eye.* (e) *Render from the right eye.* (f) *Superimposed renders.*

Figure 142: *DEMRS HV-1.0 with BSV: This figure shows the default and retroverted states of HV-1.0 in the presence of BSV, where* $E_{L/R}$ *are the left and right eyes,* $M1_{L/R}$ *and* $M2_{L/R}$ *are the four mirrors in the system and* $VV_{F_{L/R}}$ *are the two principal vision vectors. When HV-1.0 is at default state, the vision vectors do not intersect the target and the rendered images appear empty. When the mirrors of HV-1.0 are rotated so that both* VV_{F_L} *and* VV_{F_R} *intersect the target, the rendered images show how each eye views the target through the system.*

The second test was performed under the assumption that strabismus is present, namely left exotropia. In this test, the right eye (E_R) assumed dominance and fixated on the target, whereas the left eye deviated outwards by 10° (≈ 20Δ). Figure 143 shows the direction of the vision vectors before and after retroversion. Similar to the previous test, prior to retroversion, VV_{F_L} and VV_{F_R} were not directed towards the target (fig. 143a). Consequently, the mirrors were rotated so that both $VV_{F_{L/R}}$ could be directed towards the same target (fig. 143b). Figure 143c shows the view from the cyclopean camera, whereas figure 143d and figure 143e show the two rendered images

from the cameras that were placed inside the left and right eyes. The “fused" image is shown by figure 142f.

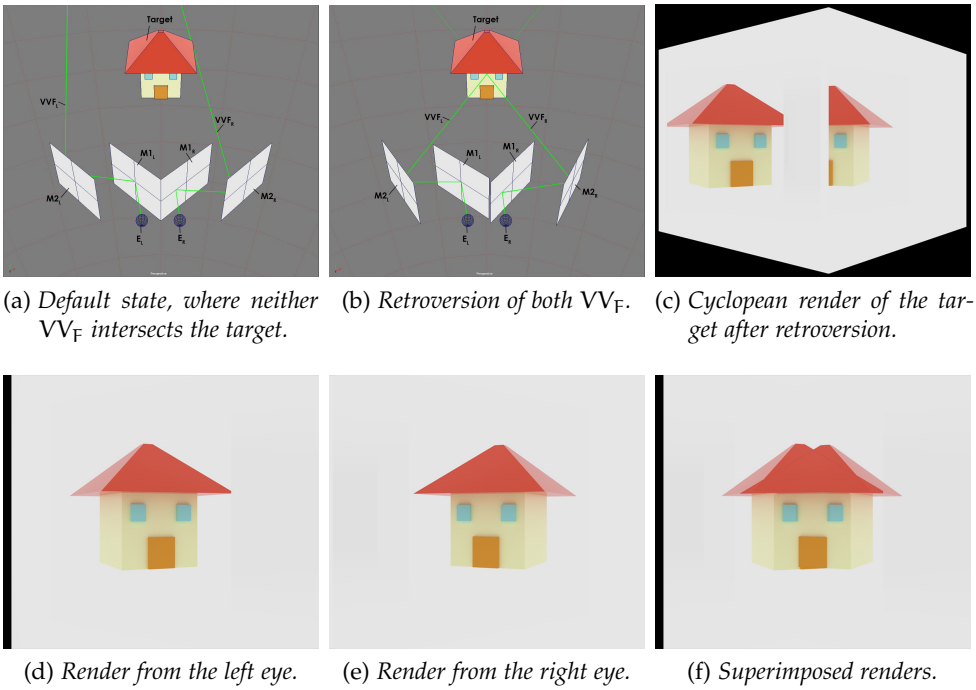

(a) *Default state, where neither* VV_F *intersects the target.*

(b) *Retroversion of both* VV_F.

(c) *Cyclopean render of the target after retroversion.*

(d) *Render from the left eye.*

(e) *Render from the right eye.*

(f) *Superimposed renders.*

Figure 143: *DEMRS HV-1.0 with strabismus: This figure shows the default and retroverted states of HV-1.0 in the presence of exotropia of* $\approx 10°$, *or* $\approx 20\Delta$, *where* $E_{L/R}$ *are the left and right eyes,* $M1_{L/R}$ *and* $M2_{L/R}$ *are the four mirrors in the system and* $VV_{F_{L/R}}$ *are the two principal vision vectors. When HV-1.0 is at default state, the vision vectors do not intersect the target and the rendered images appear empty. When the mirrors of HV-1.0 are rotated so that both* VV_{F_L} *and* VV_{F_R} *intersect the target, the rendered images show how each eye views the target through the system.*

Table 47 shows the retroversion angles of the mirrors in the first and second test.

Table 47: *Retroversion yaw angles of mirrors in HV-1.0.*

Mirrors	Default	BSV	Strabismus
$M1_L$	0.0°	−7.5°	−5.0°
$M2_L$	0.0°	−16.7°	−11.1°
$M1_R$	0.0°	7.5°	7.5°
$M2_R$	0.0°	16.7°	16.7°

Although the cyclopean views between normal BSV and strabismus were different after retroversion, the rendered images from the left and right eyes (cameras), along with the “fused" images, were the same, suggesting that retroversion was successful.

B.2.4 *Evaluation*

A series of physical tests were designed to evaluate the efficacy of HV-1.0 in the perception of depth, with normal BSV and strabismus. These tests would verify whether or not HV-1.0 has adverse effects on subjects with normal BSV, and if subjects with strabismus would be able to receive fusible visual stimuli.

The tests were conducted under laboratory conditions, in a large seminar room with ambient lighting located at Bournemouth University, where several objects could be used as targets. A basic apparatus was assembled based on the design of HV-1.0, which was composed of four mirrors and four bases, provided by Edmund Optics (2019b), that held the mirrors in an upright position. The mirrors were placed on a desk, located near the wall, and rotated according to the default state of HV-1.0, i.e. at a 45° angle. A height adjustable chair was used by the subject in order to level their head with the mirrors, and comfortably view the fixation target through the apparatus, which was placed $\approx 2-5\text{cm}$ from the subject's eyes.

HV-1.0 was evaluated by two tests. In the first test, the fixation target was an autostereogram (fig. 144), depicting three zebras when viewed stereoscopically, placed centrally on the wall at a distance of $\approx 45-50\text{cm}$ from the subject. The subject was asked to describe the illusion.

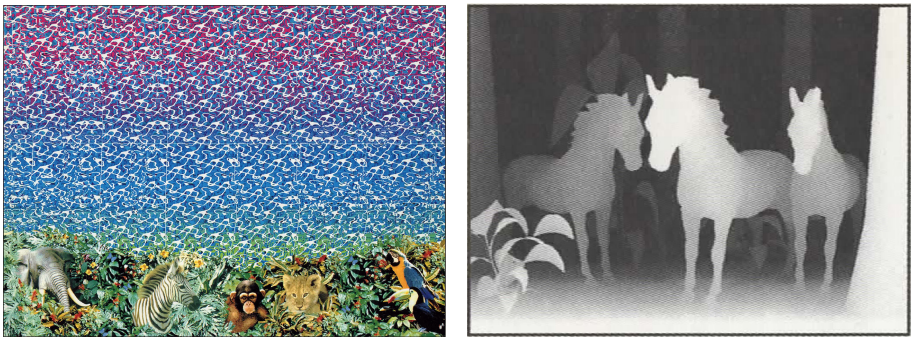

(a) *Original image.* (b) *Illusion of three zebras, when the image is perceived stereoscopically.*

Figure 144: *Autostereogram test: (a) shows the original autostereogram, and (b) shows the illusion perceived when the required technique is applied to view the autostereogram.*

The second test, called far distance test, did not involve a specific fixation target, as the subject was instructed to view any object in the room that was at a relatively far distance ($\approx 3-6\text{m}$), using the apparatus. The subject was asked to report whether or not it was possible to normally perceive the environment.

Five adult volunteers were enrolled in this study, between the age of 22 and 50 years (mean 36 years). The IPD of the subjects range between $\approx$ 5.5cm and $\approx$ 6.0cm, with mean IPD $\approx$ 5.75cm. A brief medical history was obtained from all subjects in order to further understand their state of health and identify the presence of existing ocular conditions that can affect the outcome of the tests, such as myopia, hypermetropia and presbyopia. For example, if a subject had been previously diagnosed with presbyopia, the prescribed corrective lenses or glasses must be worn during testing. Furthermore, the subjects agreed to undergo preliminary examination to verify strabismus. On initial review, 3 (60.0%) subjects had normal BSV, of which 1 wore myopic glasses, and 2 (40.0%) subjects had strabismus. Table 48 lists the demographic data of the subjects who participated in the preliminary evaluation of the HV-1.0 based apparatus.

Table 48: *Demographic data used in the basic evaluation of the DEMRS HV-1.0*

Characteristics	No. Studied	Percent %
Gender		
Male	5	100.0%
Female	0	0.0%
Age range $[22-50]$ (years)		
$\leqslant 36$	3	60.0%
> 36	2	40.0%
Vision		
Normal BSV	3	60.0%
Strabismus	2	40.0%
Exotropia	1	50.0%
CI	1	50.0%
Total	**5**	**100%**

Initially, the IPD of each subject was used in equation 2 (see sect. 2.3) to estimate the orientation of the eyes required to fixate on the target. Subsequently, the mirrors in the apparatus were manually rotated so that the subject could view the fixation target. For the first test, the subject was asked whether or not the autostereogram could be properly viewed, without perceiving the illusion. Next, because of the technique required to perceive the illusion from an autostereogram, the mirrors in HV-1.0 were rotated such that the subject viewed “through" the autostereogram. The subject was asked to report whether or not the illusion was perceived. This step was repeated until the subject was able to describe the illusion. Figure 145 shows a subject undergoing the autostereogram test.



Figure 145: *Convergence test: This figure shows a subject with exotropia using the apparatus. A MacBook (laptop) was used to simulate the test in order to assist in the orientation of the mirrors.*

B.2.5 *Results*

AUTOSTEREOGRAM TEST The autostereogram test showed that, without the HV-1.0 apparatus, 2 out of 3 subjects with normal BSV were able to describe the illusion. The remaining subject with normal BSV was unable to apply the technique required to perceive the illusion. When the HV-1.0 apparatus was used, all 3 subjects were unable to perceive the illusion. Also, the autostereogram test showed that neither subject with strabismus was able to perceive the illusion, regardless of whether or not the HV-1.0 apparatus was used. This suggests that using the HV-1.0 apparatus had no effect in the outcome of this test with strabismus subjects. However, one subject noticed that, whilst using the apparatus, it was possible to view a section of the autostereogram that was not visible before using the apparatus.

All subjects underwent the autostereogram test once. Of the 5 (100%) subjects, the autostereogram test showed that, without the HV-1.0 apparatus, 2 (40%) subjects perceived the illusion, whereas when the HV-1.0 apparatus was used, none (0%) of the subjects perceived the illusion.

FAR DISTANCE TEST The far distance test showed that, without the HV-1.0 apparatus, all 3 subjects with normal BSV were able to view the environment and perceive depth normally. However, when the apparatus was used, all 3 subjects reported symptoms of confusion, eye strains, dizziness, and diplopia. Also, the far distance test showed that, prior to using the HV-1.0 apparatus, the subject with CI was able to normally view the environment, whereas the subject with exotropia was only able to monocularly view the environment. Repeating this test using the HV-1.0 apparatus showed that

the subject with CI reported similar symptoms to the 3 subjects with normal BSV, i.e. confusion, eye strains, dizziness, and diplopia. Although the subject with exotropia continued to use the dominant eye to view the environment through the apparatus, the subject also reported relative confusion.

All subjects underwent the far distance test once. Of the 5 (100%) subjects, the far distance test showed that, without the HV-1.0 apparatus, 4 (80.0%) subjects were able to perceive depth binocularly, whereas when the apparatus was used, none (0.0%) of the subjects could normally view the environment.

B.2.6 *Discussion*

Unfortunately, because HV-1.0 does not satisfy the DRS principle (see sect. 4.1), the basic apparatus: (a) has a negative effect on subjects with normal vision, and (b) prevents normal BSV and depth perception, as the brain did not receive fusible visual stimuli.

HV-1.0 did not retroverse normal BSV and strabismus, due to:

- Estimated orientations of the mirrors. Although the simulation of HV-1.0 was used to calculate the orientation of the mirrors, the rotation of the physical mirrors was matched to the simulation manually using the bases, which introduced errors in the rotations of the mirrors.

- A large resultant IPD, which also created an abnormal binocular disparity. As shown in figure 146a, although both principal vision vectors (VV_{F_L} and VV_{F_R}) converge on target T, the angle $\theta_{L/R}$, which represents the normal binocular disparity from each eye, is considerably smaller than the angle $\phi_{L/R}$, produced by the reflection of $VV_{F_{L/R}}$ onto $M_{2_{L/R}}$. Consequently, the resultant binocular disparity from HV-1.0 exceeds the normal binocular disparity, and therefore fails to satisfy the principle of DRS. The excessive binocular disparity is caused from the distance δ_2 between M_{2_L} and M_{2_R}, which is greater than the pupillary distance δ_1 between both eyes (fig. 146a,b).

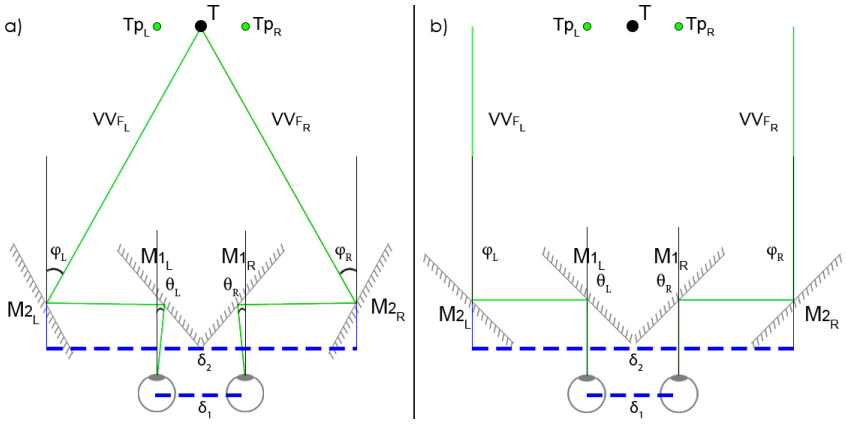

Figure 146: *Problem 1: This figure illustrates the excessive binocular disparity created by the large distance between $M2_L$ and $M2_R$. (a) shows that both principal vision vectors VV_{F_L} and VV_{F_R} converge on target T, whereas (b) shows VV_{F_L} and VV_{F_R} in parallel when T is at far distance. In this figure, δ_1 represents the IPD, δ_2 represents the resultant IPD, $\theta_{L/R}$ is the normal binocular disparity angle, and $\phi_{L/R}$ is the resultant binocular disparity.*

The large distance δ_2, from HV-1.0, is problematic even when the fixation target T is positioned at far distance and both eyes are parallel to each other, which suggests that the binocular disparity angles from the eyes and system are equal. Figure 146b shows that, when T is located at a far distance and both principal vision vectors from the eyes are parallel, the angles $\phi_{L/R}$ and $\theta_{L/R}$ are equal. However, due to the large resultant IPD (δ_2), VV_{F_L} and VV_{F_R} are not able to intersect the parallel targets $Tp_{L/R}$. Consequently, the visual stimuli received by the eyes are not fusible, because they are widely different.

- The inability of $M1_L$ and $M1_R$ to rotate inwards. Due to their central pivot of rotation, $M1_L$ and $M1_R$ could not be rotated inwards by opposite angles, as their sides collided. Figure 147 illustrates an example in which $M1_L$ and $M1_R$ collided when rotated by 15°.

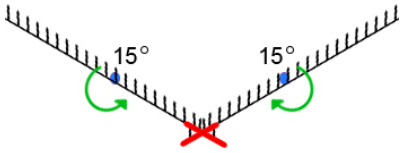

Figure 147: *Problem 3: Illustration of the two central mirrors colliding when rotating inwards.*

Also, rotating a mirror about its centre limits the range of deviations that could be compensated by a DEMRS. For example, a medium sized esotropia, which requires an outwards rotation of $M1_{L/R}$ in order to be reflected onto the centre of $M2_{L/R}$, cannot be compensated by $M1_{L/R}$ if it rotates about the centre. This is because, after the rotation of $M1_{L/R}$,

the principal vision vector of the strabismic eye would not be reflected by the mirror.

- Confusion due to arbitrary peripheral visual stimuli entering the apparatus. An issue that was reported by all subjects, who underwent evaluation using the HV-1.0 apparatus, was that various objects from the environment were perceived in the peripheral field of view, causing confusion. This was due to visual stimuli, coming from various directions, that entered the eye and received by peripheral areas of the retina and fovea. Figure 148 shows that, although both principal vision vectors (VV_{F_L} and VV_{F_R}) intersect the fixation target T, the peripheral vision vectors (VV_{P_L} and VV_{P_R}) escape the system, after being reflected by $M1_{L/R}$, and intersect arbitrary objects in the environment.

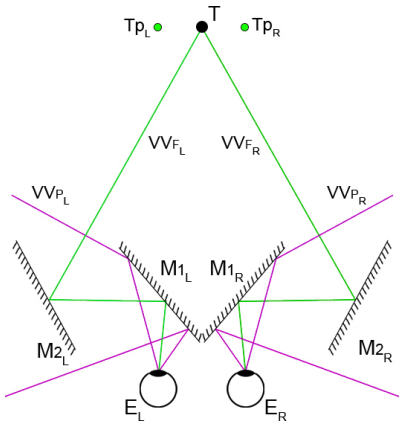

Figure 148: *Problem 2: Illustration of the peripheral vision vectors, VV_{P_L} and VV_{P_R}, that escape the system after being reflected by $M1_{L/R}$. These peripheral vision vectors pass through arbitrary objects in the environment, causing the visual stimuli received by the eyes $E_{L/R}$ to contain arbitrary objects from the environment.*

This issue causes each retinal image to be formed, centrally, by visual stimuli deriving from the target and, peripherally, by visual stimuli deriving from arbitrary objects in the surrounding environment. Consequently, the peripheral parts of the retinal images do not match the environment that exists around the fixation target, causing confusion. During the evaluation HV-1.0 apparatus this problem was relatively easy to bypass, by asking each subject to focus their attention on the central target.

The most significant issues of HV-1.0 that prevented the retroversion of normal BSV and strabismus were the estimated orientations of the mirrors, excessive binocular disparity, large resultant IPD, and collisions between $M1_L$ and $M1_R$.

B.3 PIVOTED MIRROR ROTATION

As shown in figure 149a, the objective is to calculate angle ϕ by which the mirror M is required to rotate, about the pivot of rotation P, in order for the incidence vision vector $\vec{I_A}$ to reflect ($\vec{R_{QG}}$) off of the mirror at point Q and intersect point G.

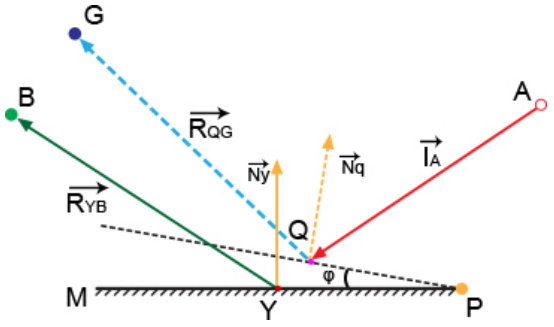

(a) *2D representation of the problem.*

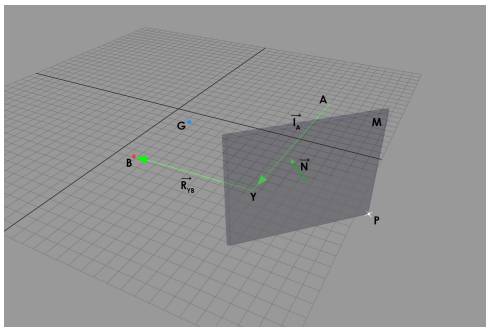

(b) *3D perspective view taken behind* M *showing the known elements of the problem.*

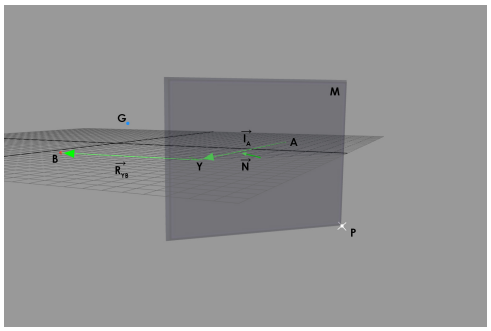

(c) *Lower perspective view showing the elevation of* G *on y-axis, whereas* B *lies on x-z plane.*

Figure 149: *Pivoted rotation problem: The incidence vision vector is defined by point* A *and direction* $\vec{I_A}$. M *is the mirror with normal vector* $\vec{N_y}$ *and pivot of rotation* P. *When* M *has not rotated,* Y *is the point of reflection and* $\vec{R_{YB}}$ *is the reflection vector that intersects point* B. *When* M *is rotated by an angle* ϕ, *which creates the normal* $\vec{N_q}$, $\vec{I_A}$ *is reflected at point* Q *and the reflection vector* $\vec{R_{QG}}$ *intersects point* G. *Parts (b) and (c) are examples of the pivoted mirror rotation problem in 3D, where* G *is elevated and* P *is at the bottom side of* M.

This problem is solved by the following steps:

- **Step 1:** Reverse the direction of the current reflection vector $\vec{R_{YB}}$, which is created when M has not rotated, and consider the reversed vector $\vec{T_{B_1}}$ as tangent to a circle C with centre P. In 3D, C is a sphere. The point of tangency B′, between $\vec{T_{B_1}}$ and P is used to calculate the radius r_p of C, which is the distance between B′ and P (fig. 150).

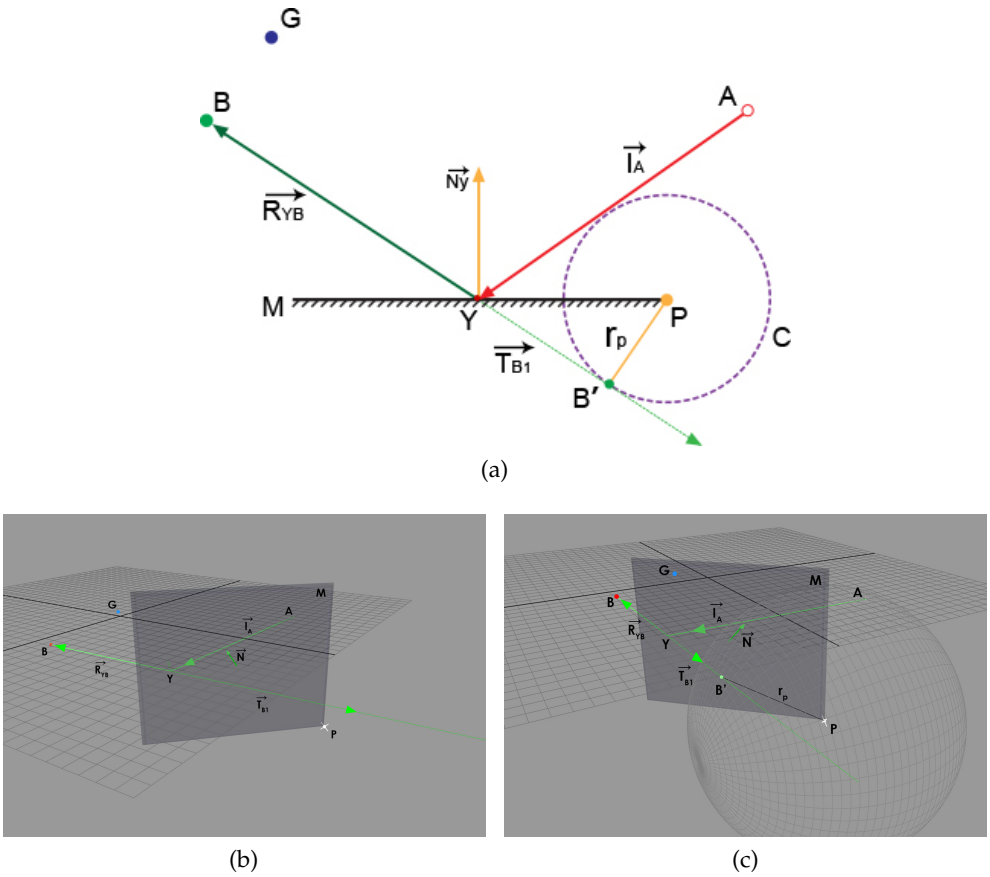

(a)

(b) (c)

Figure 150: *Step 1*

Equations:

$$\vec{T_{B_1}} = -\vec{R_{YB}} \tag{14}$$

$$B' = B + \left[\frac{(P - B) \odot \vec{T_{B_1}}}{\vec{T_{B_1}} \odot \vec{T_{B_1}}} \right] \times \vec{T_{B_1}} \tag{15}$$

$$r_p = d(B', P) \tag{16}$$

where:

$d(...)$ is a function that calculates the euclidean distance transform.

- **Step 2:** Similarly to B, which is a point that gets intersected by $\vec{R_{YB}}$ that is also a tangent to C, G is a point that gets intersected by tangents to C, one of which is a reflection vector of $\vec{I_A}$ when M rotates. As shown in fig. 151a, in 2D, there can only be two tangents ($\vec{T_{G_1}}$ and $\vec{T_{G_2}}$) from G to C. However, in 3D, there are infinite tangents to C that intersect G. Consequently, a point of tangency G′ is found on C, which is used to create a cone with apex G and centre S.

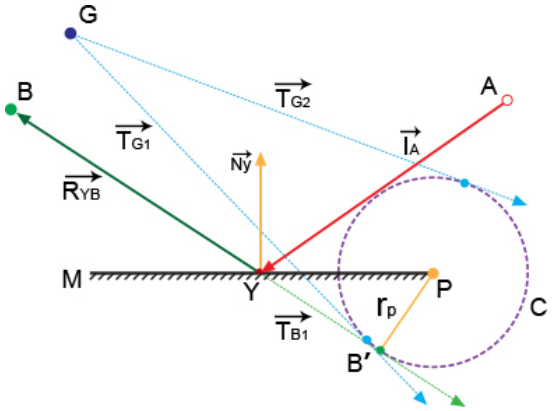

(a)

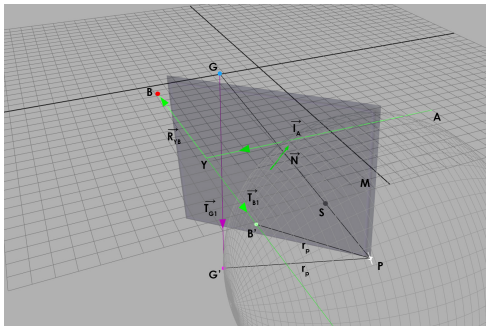

(b)

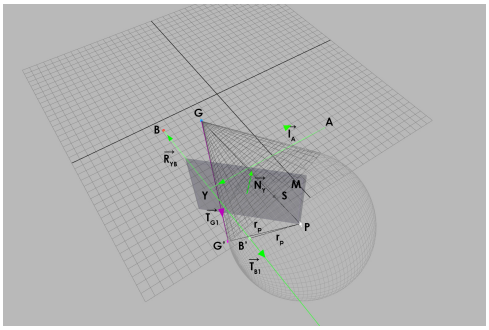

(c)

Figure 151: *Step 2*

Equations:

$$G' = t(P, r_p, G) \tag{17}$$

$$\vec{T_{G_1}} = \|(G' \vec{-} G)\| \tag{18}$$

$$G'' = G + 2 \times d(G, G') \times \vec{T_{G_1}} \tag{19}$$

$$\vec{GP} = \|(P \vec{-} G)\| \tag{20}$$

$$S = G + \left[\frac{(G'' \vec{-} G) \odot \vec{GP}}{\vec{GP} \odot \vec{GP}} \right] \times \vec{GP} \tag{21}$$

where:

$t()$ is a function that calculates a point of tangency from the centre and radius of a sphere, and a point, which the tangent intersects.

- **Step 3:** The intersection between $\vec{I_A}$ and the cone, or $\vec{T_{G_1}}$ and $\vec{T_{G_2}}$ in 2D, provides two points of reflection, q_1 and q_2 (fig. 152). However, only one of these points is the correct point of reflection, whereby the

reflection vector $\vec{R_{QG}}$ intersects G. According to the standard law of reflection, $\theta i = \theta r$, and therefore, the correct point of reflection is determined by comparing the angle of incidence, formed by $\vec{I_A}$ and the normal $\vec{N_{q_{1,2}}}$, with the angle of reflection, formed by $\vec{T_{G_{1,2}}}$ and $\vec{N_{q_{1,2}}}$ (fig. 152). The correct point of reflection is denoted by the letter Q.

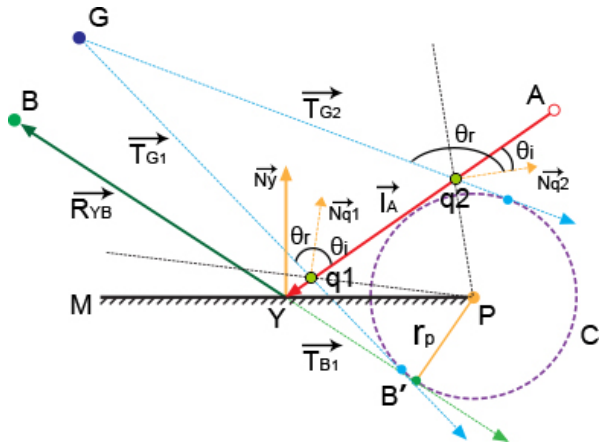

(a)

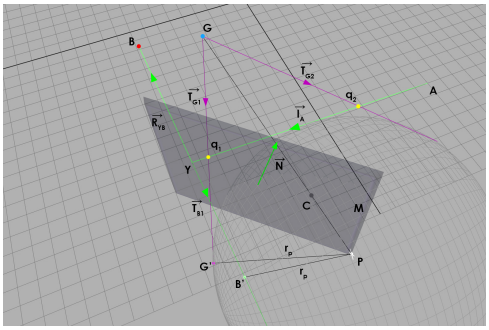

(b)

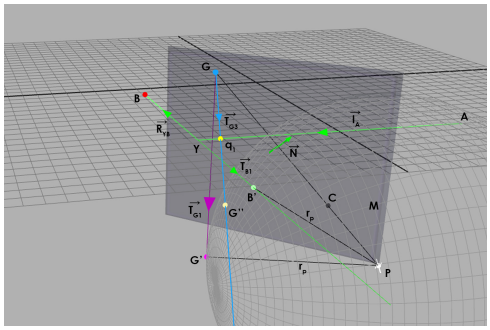

(c)

Figure 152: *Step 3*

Equations:

$$q_1, q_2 = \text{intersect}(A, \vec{I_A}, S, G, d(S, G'')) \tag{22}$$

$$\theta_i = \angle(\vec{I_A}, \vec{N_{q_1}}) \tag{23}$$

$$\theta_r = \angle(\vec{N_{q_1}}, \vec{q_1 G}) \tag{24}$$

$$\begin{cases} Q = q_1, & \text{if } \theta_i = \theta_r \\ Q = q_2, & \text{otherwise} \end{cases} \tag{25}$$

where:

`intersect()` is a function that calculates the point(s) of intersection between a ray and a cone.

- **Step 4:** The angle ϕ of the mirror M is found, either, by calculating the angle $\angle$YPQ, or by calculating the angle between the two normal vectors $\vec{N_Q}$ and $\vec{N_Y}$ (fig. 153).

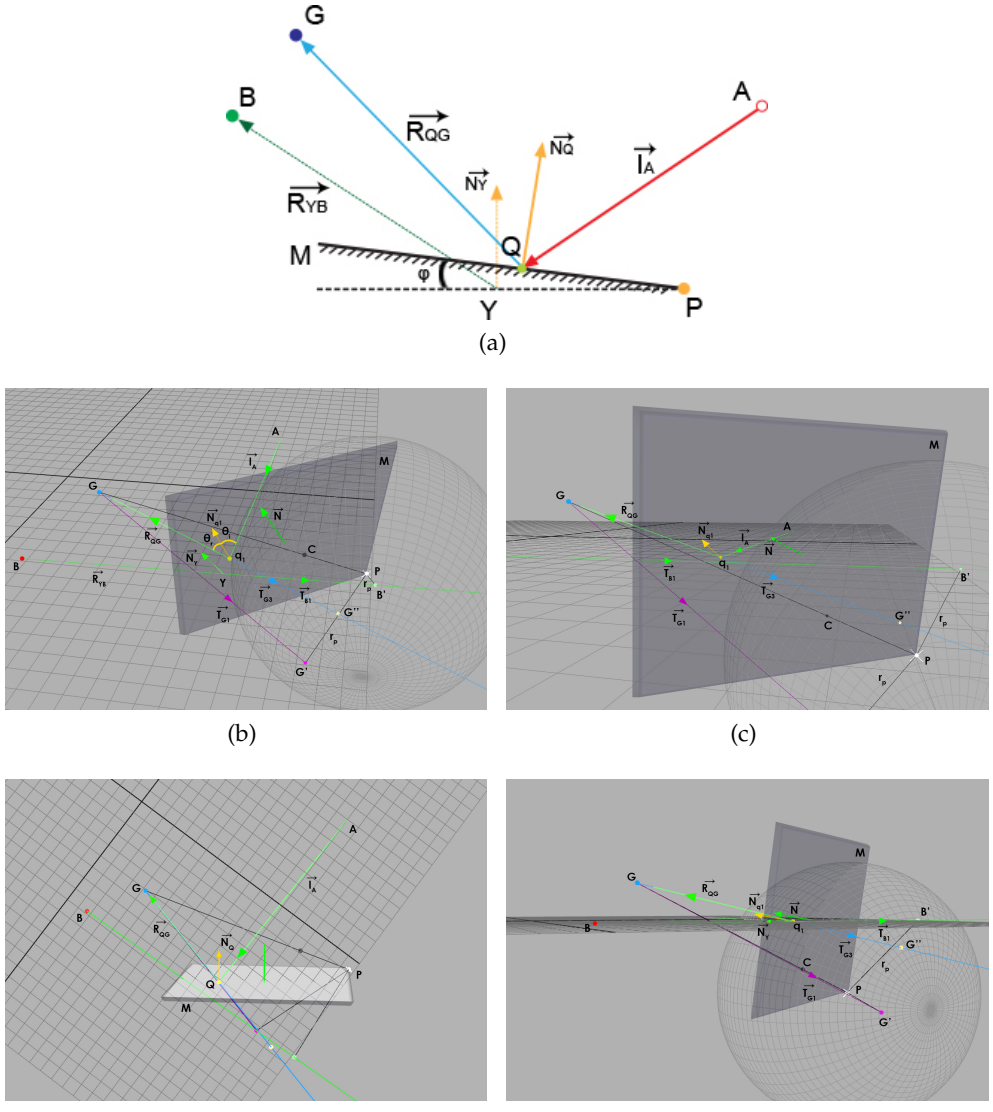

Figure 153: *Step 4*

As shown in figure 153, when the mirror rotates, $\vec{I_A}$ is reflected by M and the resultant reflection vector $\vec{R_{QG}}$ intersects point G.

B.4 HVT-2.5 CONFIGURATION

Listing 4: HVT-2.5 Configuration: The JSON configuration, which presents the initial setup of HVT-2.5. Because the design of the system is symmetrical, the configuration file sets the values only for one side, which gets mirrored on the other side.

```
{
    "hvt25" :
    [
    {
        "symmetrical" : "true",
        "side" : "left"
    },
    {
        "component" : "lens",
        "type" : "convex",
        "translate" : [3.0, 0.0, 2.0]
    },
    {
        "component" : "mirror",
        "id" : 0,
        "pivot" : [6.35, 0.0, 0.0],
        "translate" : [0.51, 0.0, 2.5],
        "rotate" : [0.0, 225.0, 0.0]
    },
    {
        "component" : "mirror",
        "id" : 1,
        "translate" : [17.0, 0.0, 6.99],
        "rotate" : [0.0, 45.0, 0.0]
    },
    {
        "component" : "prism",
        "type" : "delta",
        "id" : 1,
        "translate" : [17.0, 0.0, 13.88]
        "rotate" : [0.0, 0.0, 90.0]
    },
```

```
        {
                "component" : "prism",
                "type" : "delta",
                "id" : 2,
                "translate" : [17.0, 0.0, 18.65]
                "rotate" : [0.0, 0.0, 90.0]
        },
        {
                "component" : "mirror",
                "id" : 2,
                "translate" : [17.0, 0.0, 25.53],
                "rotate" : [0.0, 135.0, 0.0]
        },
        {
                "component" : "mirror",
                "id" : 3,
                "pivot" : [-6.35, 0.0, 0.0],
                "translate" : [0.51, 0.0, 30.02],
                "rotate" : [0.0, 315.0, 0.0]
        },
        {
                "component" : "lens",
                "type" : "concave",
                "translate" : [3.0, 0.0, 31.02]
        }
        ]
}
```

B.5 DEMRS FOR HORIZONTAL, VERTICAL AND TORSIONAL STRABISMUS (VERSION HVT-1.0)

DEMRS HVT-1.0 is a conceptual DRS compliant system designed to retroverse horizontal, vertical and torsional strabismus, using a set of mirrors and rotatory prisms. Similar to HV-2.0, this system is designed to redirect principal and peripheral vision vectors by orienting a set of mirrors, horizontally and vertically, in order to achieve retroversion. The prisms are designed to rotate about $M_{4_{L/R}}$ so that the vision vectors of both eyes can be properly refracted by the prisms, in order to have matching orientations.

B.5.1 *Design and Description*

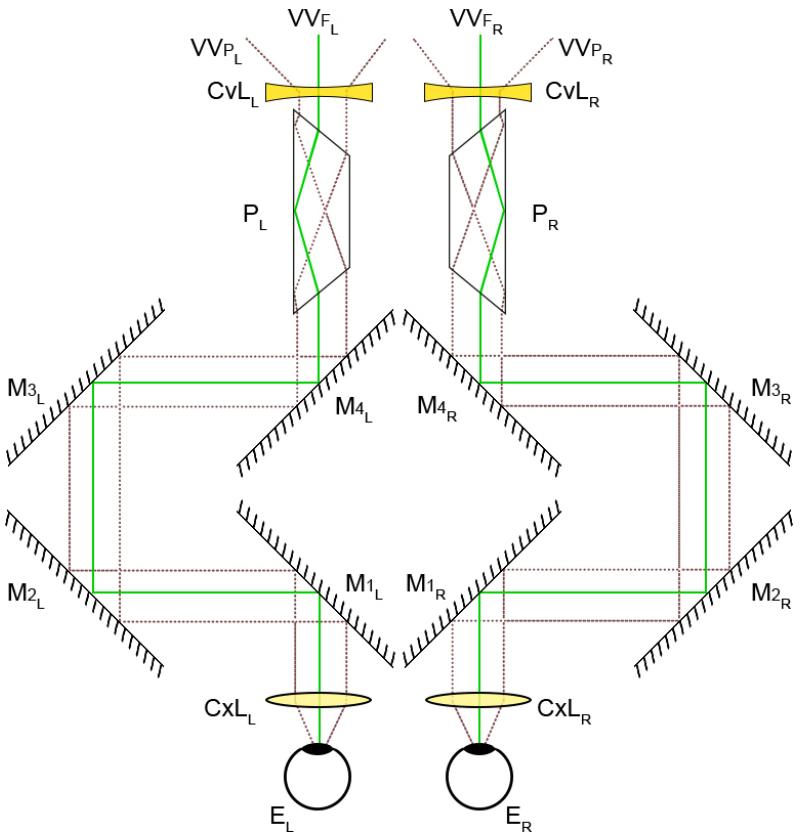

Figure 154: *DEMRS HVT-1.0: A schematic of the system, where* $VV_{F_{L/R}}$ *are the left and right principal vision vectors,* $VV_{P_{L/R}}$ *are the peripheral vision vectors,* $CxL_{L/R}$ *and* $CvL_{L/R}$ *are the convex and concave lenses,* $M_{1,2,3,4_{L/R}}$ *are the left and right set of mirrors,* $E_{L/R}$ *represent the left and right eyes, and* $P_{L/R}$ *are dove prisms.*

The design of HVT-1.0 (fig. 154) consists of eight mirrors, four on each side ($M_{1_{L/R}}$, $M_{2_{L/R}}$, $M_{3_{L/R}}$ and $M_{4_{L/R}}$), for the purpose of redirecting the principal vision vectors ($VV_{F_{L/R}}$) towards the fixation target, whereas the two convex ($CxL_{L/R}$) and two concave ($CvL_{L/R}$) lenses are used to constrain the peripheral vision vectors ($VV_{P_{L/R}}$). Additionally, HVT-1.0 is designed to use two dove prisms, one on each side (P_L, P_R), in order to retroverse torsional deviations. The JSON configuration of HVT-1.0 is:

Listing 5: HVT-1.0 Configuration: The JSON configuration, which presents the initial setup of HVT-1.0. Because the design of the system is symmetrical, the configuration file sets the values only for one side, which gets mirrored on the other side.

```
{
    "hvt10" :
    [
    {
        "symmetrical" : "true",
        "side" : "left"
    },
    {
        "component" : "lens",
        "type" : "convex",
        "translate" : [3.0, 0.0, 2.0]
    },
    {
        "component" : "mirror",
        "id" : 0,
        "pivot" : [6.35, 0.0, 0.0],
        "translate" : [0.51, 0.0, 2.5],
        "rotate" : [0.0, 225.0, 0.0]
    },
    {
        "component" : "mirror",
        "id" : 1,
        "translate" : [17.0, 0.0, 6.99],
        "rotate" : [0.0, 45.0, 0.0]
    },
    {
        "component" : "mirror",
        "id" : 2,
        "translate" : [17.0, 0.0, 18.01],
        "rotate" : [0.0, 135.0, 0.0]
    },
```

```
        {
                "component" : "mirror",
                "id" : 3,
                "pivot" : [-6.35, 0.0, 0.0],
                "translate" : [0.51, 0.0, 22.5],
                "rotate" : [0.0, 315.0, 0.0]
        },
        {
        "component" : "prism",
        "type" : "dove",
        "translate" : [3.0, 0.0, 27.5]
        "rotate" : [0.0, 0.0, 90.0]
        },
        {
                "component" : "lens",
                "type" : "concave",
                "translate" : [3.0, 0.0, 32.5]
        }
        ]
}
```

HVT-1.0 is designed with four mirrors on each side so that $M_{3,4_L}$ and $M_{3,4_R}$ can be used to maintain normal resultant IPD and normal binocular disparity. $M_{1_{L/R}}$ and $M_{4_{L/R}}$ are located centrally to the eyes so that the system can provide a larger visual field, when achieving retroversion for: (a) various angles of strabismic deviations, and (b) various directions of a fixation target. Also, the pivots of rotation of $M_{2_{L/R}}$ and $M_{3_{L/R}}$ remain central to the mirrors, whereas the pivots of rotation of $M_{1_{L/R}}$ and $M_{4_{L/R}}$ are located similar to the mirrors of HV-2.0.

The default state of HVT-1.0, as shown in figure 154, is based on the assumption that the fixation target is located centrally to both eyes at a distance of $\geqslant 6m$ from the DEMRS origin. Therefore, by default, each mirror is oriented horizontally about the y-axis (yaw rotation) by 45°, and each prism is rotated torsionally by 90°.

As previously explained in subsection 4.3.5, a rotatory prism, such as a dove, rotates the transmitted image (refracted visual stimuli) by twice the angle of prism rotation. Therefore, HVT-1.0 was designed with one dove prism, one each side, thereby allowing the transmitted image to be rotated. In this design, the dove prisms are facilitated in front of $M_{4_{L/R}}$ (fig. 154), where the distance between both prisms is equal to the IPD, so that normal

binocular disparity is maintained. Originally, the prisms $P_{L/R}$ were designed to rotate about the LPR on $M4_{L/R}$, so that the principal vision vectors can be properly refracted by the prisms. However, as explained later in this section, this approach was deemed impractical because the LPR is not a standard point on $M4_{L/R}$, but changes depending on the position of the target and strabismic deviation. Therefore, the prisms $P_{L/R}$ were designed to rotate about the centre of $M4_{L/R}$. The sequence in which a vision vector is reflected by the mirrors and refracted by the prisms as it travels from the eye to a target (T), is as follows:

$$E \rightarrow M_1 \rightarrow M_2 \rightarrow M_3 \rightarrow M_4 \rightarrow P \rightarrow T$$

Similar to HV-2.0, the lenses were added to the design of the system in order to constrain the direction of the peripheral vision vectors so that they are not reflected by the mirrors towards arbitrary directions, escaping the system. The design of HVT-1.0 satisfies the following criteria of the DRS principle:

1. The rotation of the mirrors enables the simultaneous intersection of both principal vision vectors on the same fixation target.
2. $M3_{L/R}$ and $M4_{L/R}$ maintain normal resultant IPD.
3. $M4_{L/R}$ maintain normal binocular disparity.

Although the use of dove prisms in HVT-1.0 allows the vision vectors to have matching orientations, the vision vectors are rotated but inverted, because only one prism was used per side. Therefore, HVT-1.0 does not satisfy the fourth criterion of the DRS principle, which is the maintenance of normal orientation of the visual stimuli.

B.5.2 *Retroversion Algorithm*

The retroversion algorithm used in HVT-1.0 is based on the bidirectional retroversion algorithm of HV-2.0 (see subsect. 4.4.2) with modifications that incorporate the rotation of the dove prisms, following the rotation of $M4_{L/R}$. Similar to HV-2.0, in order to maintain normal resultant IPD and normal resultant binocular disparity, it is imperative to determine the last points of reflection (LPR) on $M4_{L/R}$. Consequently, HVT-1.0 uses the auxiliary vision vectors VV_{A_L} and VV_{A_R}, which represent both principal vision vectors under normal BSV, in order to calculate both LPR.

The rotation of $P_{L/R}$ depends on the rotation of $M4_{L/R}$, because the prism is required to rotate about the centre of the mirror after the mirror

has rotated. Therefore, the retroversion algorithm was amended in order to incorporate the rotation of the dove prisms, following the rotation of $M4_{L/R}$. Briefly, after the rotation of $M4_{L/R}$, the prisms are rotated horizontally and vertically about $M4_{L/R}$ so that the principal vision vectors could be centrally refracted by the prisms. Next, the prisms are rotated torsionally by half of the angular difference between the normal eye and the strabismic eye, in order to compensate for the torsional deviation. The bidirectional retroversion algorithm can be split into the following two concurrent tasks:

1. The first task calculates the orientation of $M1_{L/R}$ so that $VV_{F_{L/R}}$ can be reflected by $M1_{L/R}$ to the centre of $M2_{L/R}$. Next, the orientation of $M2_{L/R}$ is calculated so that the reflected $VV_{F_{L/R}}$ can be reflected by $M2_{L/R}$ to the centre of $M3_{L/R}$.
2. The second task uses an inverted $VV_{F_{L/R}}$, noted by $INV_VV_{F_{L/R}}$, that originates from the target and directs to the fovea. In this task the orientation of $M4_{L/R}$ is calculated so that the $INV_VV_{F_{L/R}}$ can be reflected by the LPR, on $M4_{L/R}$, to the centre of $M3_{L/R}$. Next, the orientation of $M3_{L/R}$ is calculated so that the reflected $INV_VV_{F_{L/R}}$ can be reflected by $M3_{L/R}$ to the centre of $M2_{L/R}$. Finally, $P_{L/R}$ performs yaw and pitch about the centre pivot of $M4_{L/R}$, and roll based on the angular difference between the normal eye and the strabismic eye.

The following pseudocode presents the bidirectional retroversion algorithm, modified for HVT-1.0:

Algorithm 3: Bidirectional Retroversion of HVT-1.0

```
Begin
    vv_f ← principal vision vector;
    inv_vv_f ← inverse principal vision vector;
    vv_a ← auxiliary vision vector;
    // ----- Task 1 -----
    for m in [M1, M2] do
        poi = intersection(vv_f, m);
        updated_vv = reflection(vv_f, m);
        next_poi = intersection(updated_vv, m + 1);
        if next_poi not central to m + 1 then
            rotate m so that updated_vv is reflected centrally to
              m + 1;
        end
        update(vv_f);
    end
```

continue on next page...

```
(continue begin)
    // ----- Task 2 -----
    lpr = intersection(vv_a, M_4);
    for m in [M_4, M_3] do
        poi = intersection(inv_vv_f, m);
        updated_vv = reflection(inv_vv_f, m);
        next_poi = intersection(updated_vv, m + 1);
        if next_poi not central to m + 1 then
            rotate m so that updated_vv is reflected centrally to
              m + 1;
        end
        update(inv_vv_f);
    end
    ϕ, θ = get_rotation(M_4);
    ψ = torsion(normal_eye, strabismic_eye)/2;
    rotate(prism, ϕ, θ, ψ);
end
```

The bidirectional algorithm above uses the same method to calculate pivoted rotations as HV-2.0 (see appendix B.3).

B.5.3 *Simulations*

A series of simulations were designed to evaluate the effectiveness of HVT-1.0 in achieving retroversion for near ($\leqslant$ 1m), mid ($\approx$ 3m) and far ($\geqslant$ 6m) fixation targets, at various directions from the DEMRS origin. Because a DRS compliant system must be able to compensate for various types of strabismus, including phorias, HVT-1.0 is tested with normal BSV and strabismus. In the following simulations, the eyes were assigned an IPD of 6cm, whereas the DEMRS simulator was configured based on the JSON configuration file of HVT-1.0. Also, when the fixation target (T) is located at a distance of $<$ 6m from the DEMRS origin, retroversion is successful when both principal vision vectors pass through T. When T is located at a distance $\geqslant$ 6m from the DEMRS origin, retroversion is successful if each principal vision vector passes through the corresponding parallel target Tp_L and Tp_R.

Initially, a simple experiment was conducted to determine whether HVT-1.0 can retroverse normal BSV for a target located centrally at a distance of 8m ($T = \{0, 0, 800\}$). Figure 155 shows screenshots from the DEMRS simulator before and after retroversion. Table 49 presents the retroversion angles of the mirrors and prisms required to achieve retroversion.

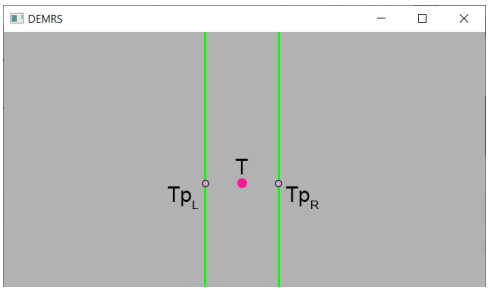

(a) *Target view before retroversion.*

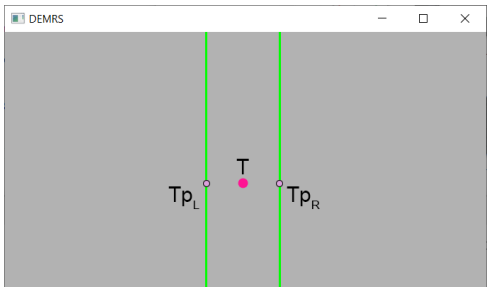

(b) *Target view after retroversion.*

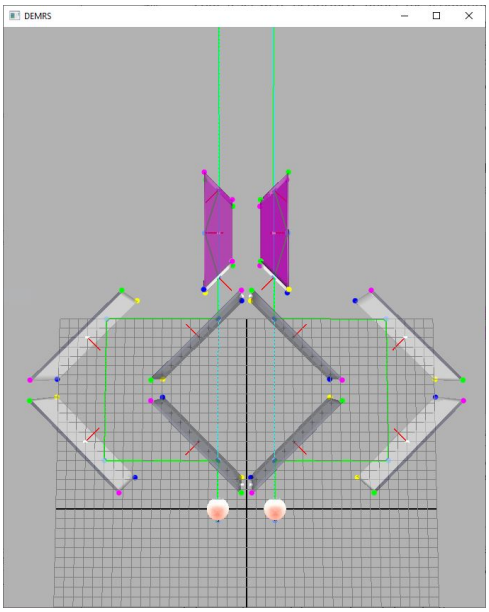

(c) *Before retroversion.*

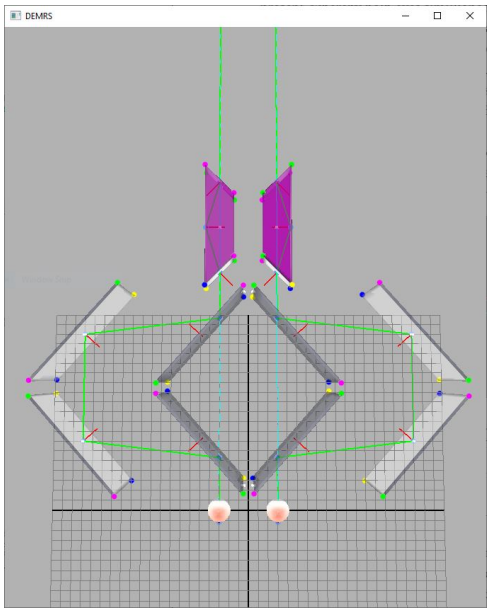

(d) *After retroversion.*

Figure 155: *DEMRS HVT-1.0 retroversion for* $T = \{0, 0, 800\}$*: Simulation tests before (c) and after (d) retroversion of normal BSV, where* $T = \{0, 0, 800\}$*. Because of the far distance of the target from the DEMRS origin, the target is not visible in (c) and (d). Therefore two additional screenshots were taken from a close up view of the target, peripheral and principal vision vectors, before (a) and after (b) retroversion. In this figure, (a) is the extension of (c), and (b) is the extension of (d).*

In the test shown by figure 155 prior to retroversion, both principal vision vectors ($VV_{F_{L/R}}$) were shown in green, which means that they pass through Tp_L and Tp_R even when the mirrors remained at default orientation. Consequently, similar to HV-2.0, no retroversion is required by HVT-1.0 when the target is located centrally at a distance of $\geqslant 6m$. This is because, when both eyes are at rest, the $VV_{F_{L/R}}$ have directions of $< 0, 0, 1 >$, and since T is located centrally at a distance of 8m each parallel target $Tp_{L/R}$ is located straight ahead of each eye $E_{L/R}$, respectively. However, the difference between the non-retroverted and retroverted results of HVT-1.0 is that, prior to retroversion, the $VV_{F_{L/R}}$ were not reflected by the centres of $M_{2_{L/R}}$ and

Table 49: *DEMRS HVT-1.0 retroversion angles for normal BSV, where* $T = \{0, 0, 800\}$.

Components	Retroversion (°)		
	x (pitch)	y (yaw)	z (roll)
$M1_L$	0.000	3.427	0.000
$M2_L$	0.000	3.427	0.000
$M3_L$	0.000	−3.427	0.000
$M4_L$	0.000	−3.427	0.000
P_L	0.000	0.000	0.000
$M1_R$	0.000	−3.427	0.000
$M2_R$	0.000	−3.427	0.000
$M3_R$	0.000	3.427	0.000
$M4_R$	0.000	3.427	0.000
P_R	0.000	0.000	0.000

$M3_{L/R}$, whereas after retroversion, the $VV_{F_{L/R}}$ were reflected by the centres of $M2_{L/R}$ and $M3_{L/R}$. The benefit of $VV_{F_{L/R}}$ being centrally reflected by $M2_{L/R}$ and $M3_{L/R}$ is that the peripheral vision vectors would not escape the system.

Next, HVT-1.0 was tested in retroverting normal BSV for a target located centrally at a distance of 1.5m ($T = \{0, 0, 150\}$). Figure 156 shows screenshots from the DEMRS simulator before and after retroversion. Table 50 presents the retroversion angles of the mirrors and prisms required to achieve retroversion.

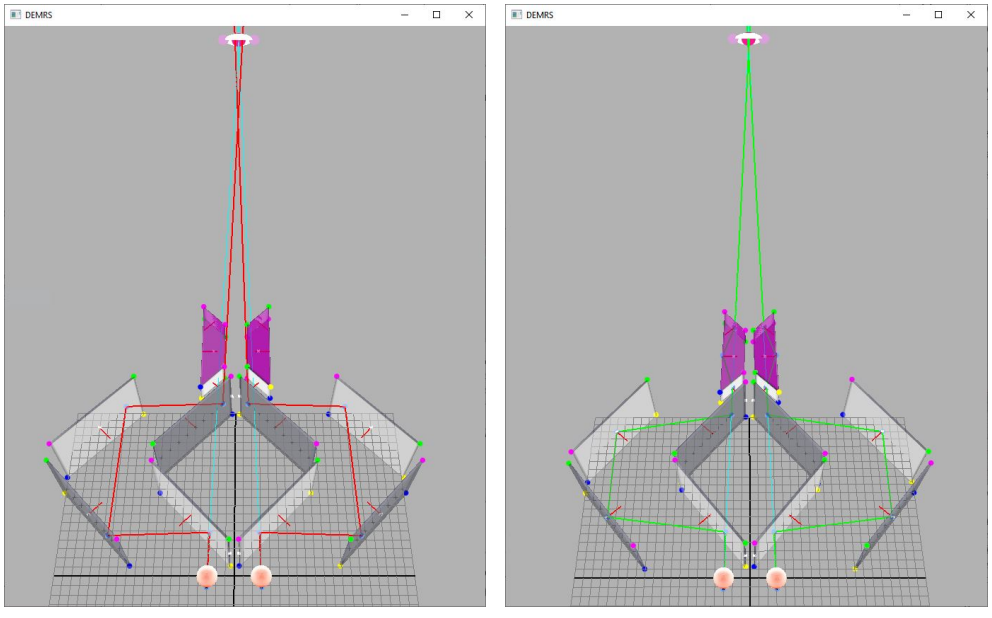

(a) *Before retroversion.* (b) *After retroversion.*

Figure 156: *DEMRS HVT-1.0 retroversion for* $T = \{0, 0, 150\}$*: Simulation tests before (a) and after (b) retroversion of normal BSV, where* $T = \{0, 0, 150\}$.

Table 50: *DEMRS HVT-1.0 retroversion angles for normal BSV, where* $T = \{0, 0, 150\}$.

Components	Retroversion (°)		
	x (pitch)	y (yaw)	z (roll)
$M1_L$	0.000	4.415	0.000
$M2_L$	0.000	3.556	0.000
$M3_L$	0.000	−4.569	0.000
$M4_L$	0.000	−3.710	0.000
P_L	0.000	3.212	0.000
$M1_R$	0.000	−4.415	0.000
$M2_R$	0.000	−3.556	0.000
$M3_R$	0.000	4.569	0.000
$M4_R$	0.000	3.710	0.000
P_R	0.000	−3.212	0.000

In this test the prisms were not required to rotate torsionally (roll), as there is no torsional strabismus. However, the prisms were required to rotate horizontally about $M4_{L/R}$, in order to be placed at the direction of the principal vision vectors after being reflected by $M4_{L/R}$.

The following simulations show the effectiveness of HVT-1.0 in the retroversion of strabismus of various angles. For each deviation, the target moved directions from left to right, and up to down, at various distances. The tests are summarized by table 51.

Table 51: *Summary of strabismus and targets used in the simulations of DEMRS HVT-1.0.*

Strabismus	Deviation (pitch, yaw, roll)	Target (x, y, z)
left exo-hyper-incyclo-tropia	4°, 8°, 10°	0, 0, 100
		0, 0, 700
left exo-incyclo-tropia	0°, 6°, 5°	10, 0, 170
		0, 0, 170
		−10, 0, 170
left eso-excyclo-tropia	0°, 9°, 7°	45, 0, 600
		0, 0, 600
		−45, 0, 600
right hypo-incyclo-tropia	12°, 0°, 8°	25, 0, 200
		0, 0, 200
		−25, 0, 200
left hyper-excyclo-tropia	10°, 0°, 6°	35, 0, 400
		0, 0, 400
		−35, 0, 400

Figures 157, 158, 159, 160 and 161 show screenshots of the results after retroversion. Furthermore, in the following simulations:

- The eyes are illustrated by the two textured 3D models.
- The left principal vision vector is depicted by the green polyline, and the right vision vectors is depicted by the red polyline. The white dashed lines represent the auxiliary vision vectors of each eye, whereas the peripheral vision vectors are displayed as the white thin polylines, parallel to the principal vision vectors. The original principal vision vectors of the eyes are the light blue lines that are not reflected or refracted by the components of the system.
- The mirrors are illustrated by the light grey flat surfaces.
- The dove prisms are illustrated by the purple trapezoidal prismatic meshes located after $M4_{L/R}$.
- The fixation target T is illustrated by a white circle, whereas Tp_L and Tp_R are illustrated by two smaller circles coloured in green and red, respectively.

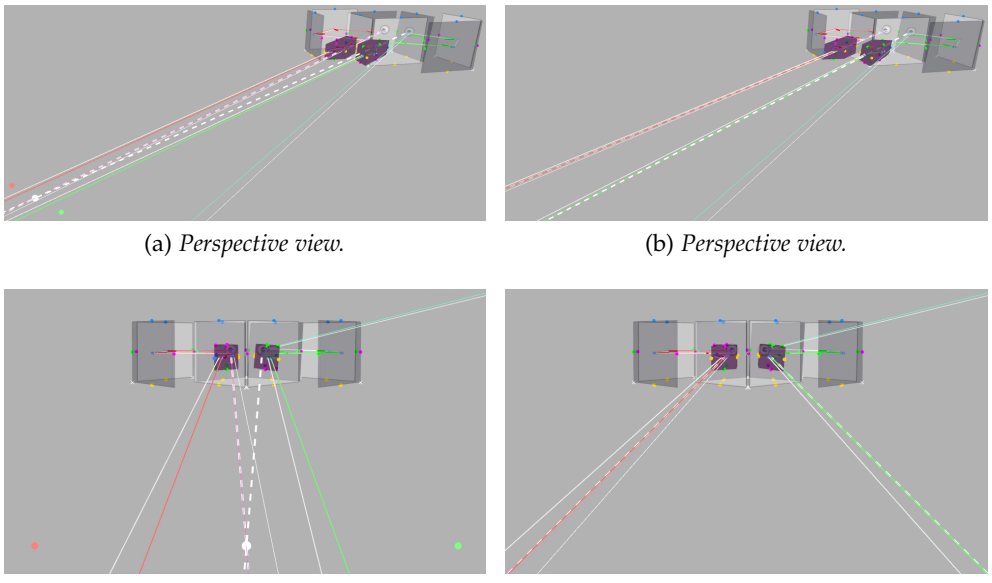

(a) *Perspective view.* (b) *Perspective view.*

(c) *Front view.* (d) *Front view.*

Figure 157: *DEMRS HVT-1.0 retroversion for* $T = \{0, 0, 100\}$*, and* $T = \{0, 0, 700\}$*: Simulation tests showing the attempted retroversion of a left exo-hyper-incyclo-tropia, with horizontal, vertical and torsional deviations of* 8°*,* 4° *and* 10°*. (a) and (c) show the results of the retroversion when* $T = \{0, 0, 100\}$*, whereas (b) and (d) show the results of the retroversion when* $T = \{0, 0, 700\}$*.*

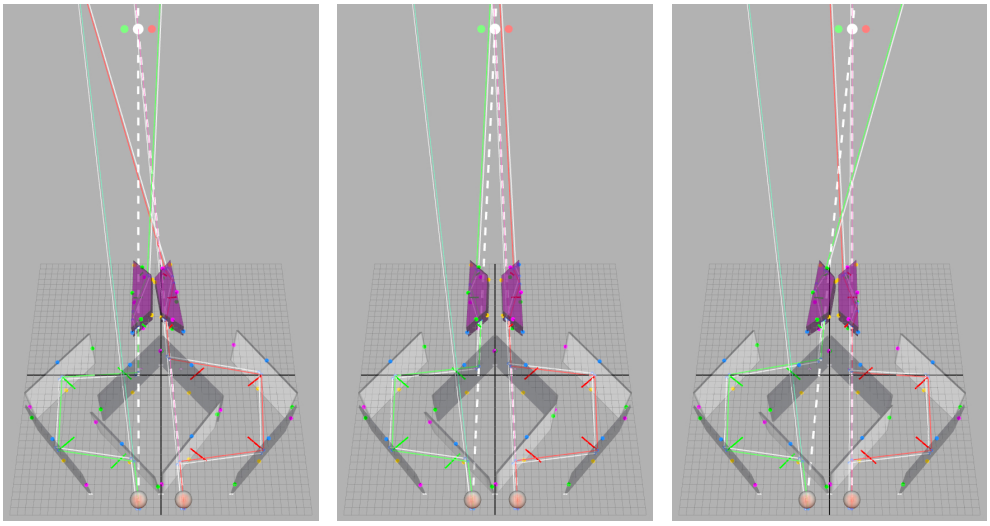

(a) *Target is left.* (b) *Target is central.* (c) *Target is right.*

Figure 158: *DEMRS HVT-1.0 retroversion for* $\mathsf{T} = \{10, 0, 170\}, \{0, 0, 170\}, \{-10, 0, 170\}$*: Simulation tests showing the attempted retroversion of a left exo-incyclo-tropia, with horizontal, and torsional deviations of* 6°*, and* 5°*. (a), (b), and (c) show the results of the retroversion when* T *is left, centre, and right.*

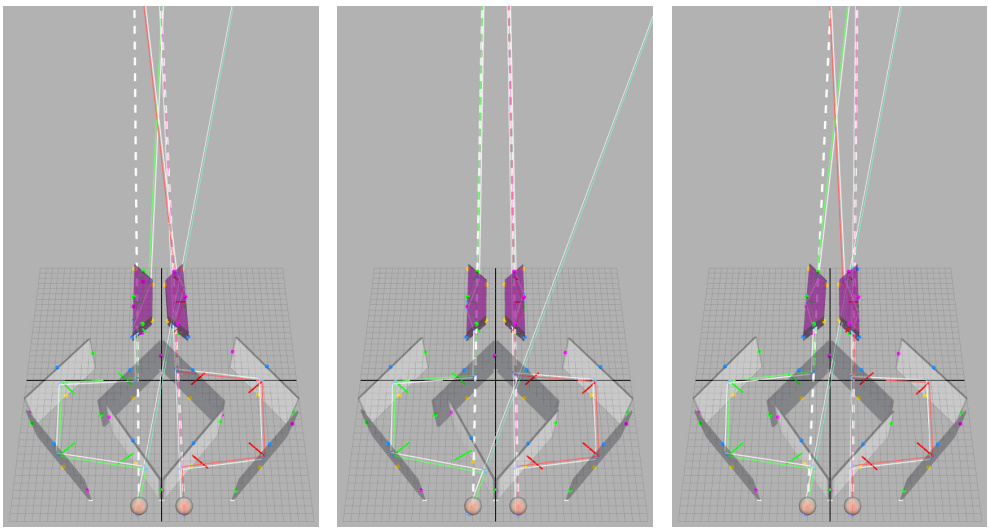

(a) *Target is left.* (b) *Target is central.* (c) *Target is right.*

Figure 159: *DEMRS HVT-1.0 retroversion for* $\mathsf{T} = \{45, 0, 600\}, \{0, 0, 600\}, \{-45, 0, 600\}$*: Simulation tests showing the attempted retroversion of a left eso-excyclo-tropia, with horizontal, and torsional deviations of* 9°*, and* 7°*. (a), (b), and (c) show the results of the retroversion when* T *is left, centre, and right.*

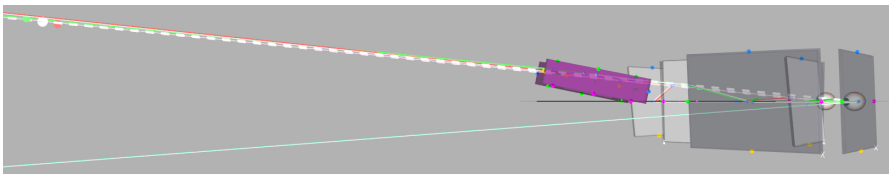

(a) *Target is up.*

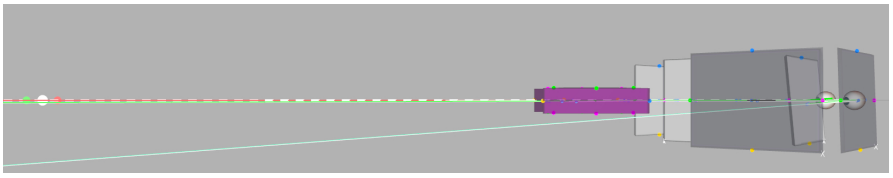

(b) *Target is central.*

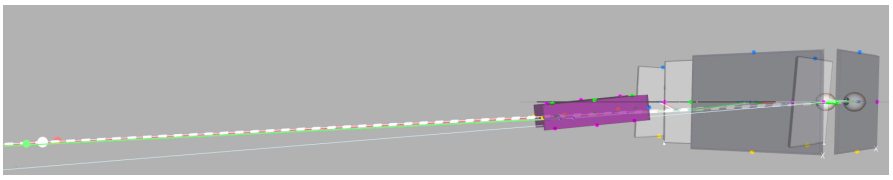

(c) *Target is down.*

Figure 160: *DEMRS HVT-1.0 retroversion for* $\mathsf{T} = \{0, 25, 200\}, \{0, 0, 200\}, \{0, -25, 200\}$*: Simulation tests showing the attempted retroversion of a right hypo-incyclotropia, with vertical, and torsional deviations of* $12°$*, and* $8°$*. (a), (b), and (c) show the results of the retroversion when* T *is up, centre, and down.*

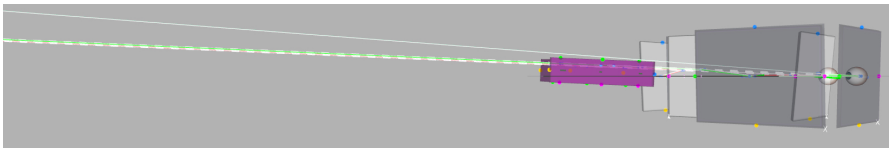

(a) *Target is up.*

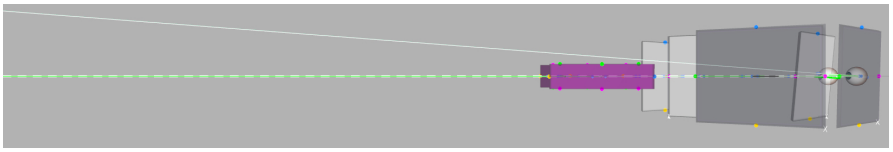

(b) *Target is central.*

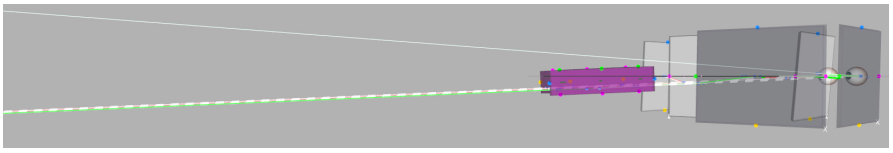

(c) *Target is down.*

Figure 161: *DEMRS HVT-1.0 retroversion for* $\mathsf{T} = \{0, 35, 400\}, \{0, 0, 400\}, \{0, -35, 400\}$*: Simulation tests showing the attempted retroversion of a left hyper-excyclotropia, with vertical, and torsional deviations of* $10°$*, and* $6°$*. (a), (b), and (c) show the results of the retroversion when* T *is up, centre, and down.*

B.5.4 *Discussion*

Unfortunately, the simulations showed that HVT-1.0 could only retroverse normal BSV and strabismus when the target is located centrally at a distance of $\geqslant$ 1m. Although the system was designed to satisfy all the criteria of the DRS principle, the configuration of the prisms prevented HVT-1.0 from dynamically achieving retroversion for non-central targets, or central targets less than 1m away from the DEMRS origin. This was because of the following reasons:

- The vision vectors ($VV_{F_{L/R}}$ and $VV_{P_{L/R}}$) were not properly refracted by the dove prisms. Figure 162 shows that $VV_{F_{L/R}}$ must be refracted centrally by the dove prisms $P_{L/R}$, in order to be rotated and refracted towards the fixation target. Consequently, the pivot of rotation (blue point) of each prism must be the LPR on $M_{4_{L/R}}$. Each prism must be rotated horizontally and vertically about the LPR, in order for the prism to be placed in the direction of $VV_{A_{L/R}}$.

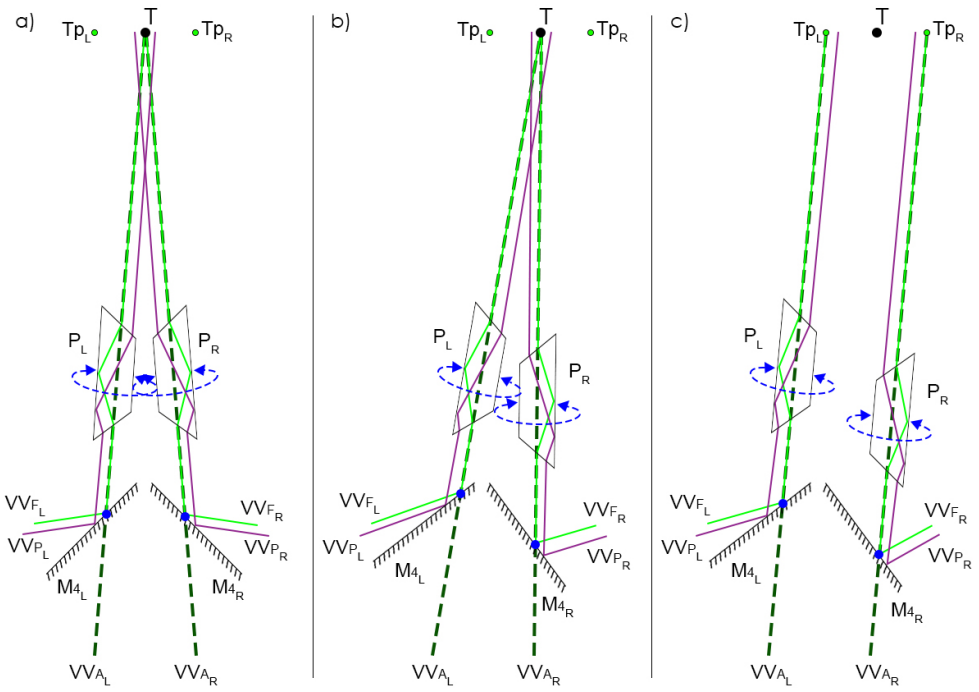

Figure 162: *Pivot of rotation of prisms on* LPR*: Illustrates the ideal configuration of the system in order to retroverse strabismus when: a) the target* T *is central at near distance, b) the target* T *is right at near distance, and c) the target* T *is right at far distance. This figure shows that when each mirror rotates about the* LPR *(blue point) on* $M_{4_{L/R}}$*, both vision vectors pass through the same target.*

However, in HVT-1.0, the pivots of rotation of the prisms are the centres of $M_{4_{L/R}}$. Therefore, when $M_{4_{L/R}}$ rotates, the prisms cannot be

placed in the direction of $VV_{A_{L/R}}$. This is illustrated in figure 163, where the vision vectors do not pass through T because they are not properly refracted by the prisms.

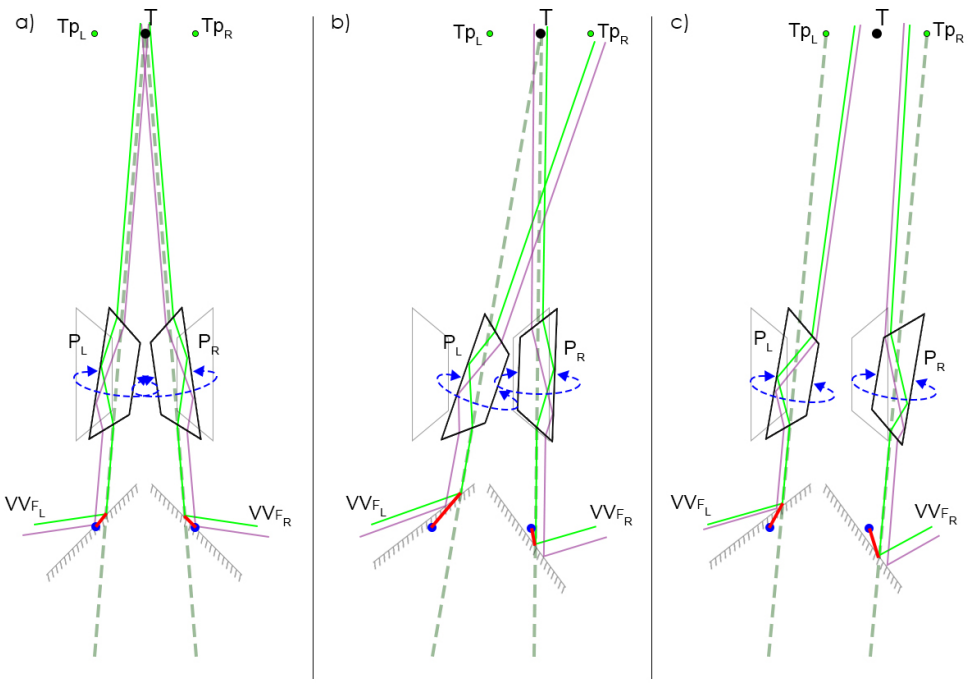

Figure 163: *Pivot of rotation of prisms central to* $M4_{L/R}$*: Illustrates examples of retroversion when the pivots of rotation of the prisms are the centres of* $M4_{L/R}$*. The same targets are used as in the previous figure. When the prisms rotate about* $M4_{L/R}$*, the vision vectors are not centrally refracted by* $P_{L/R}$*, causing* $VVF_{L/R}$ *to deviate.*

- The dove prisms collided when rotated in opposite directions. For targets located less than 6m from the DEMRS origin, the system achieves retroversion by rotating the mirrors in opposite directions such that both vision vectors converge on the fixation target. Consequently, the prisms are also rotated in opposite directions. However, when T is located less than 1m from the DEMRS origin, the prisms collide due to the large angle of opposite rotation. An example is shown by figure 164, where T is located less than 1m from the DEMRS origin.

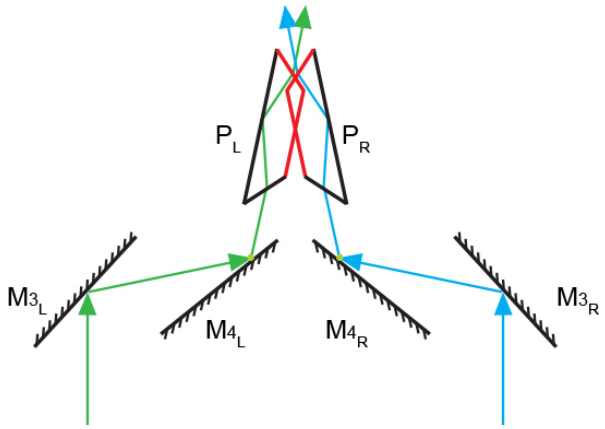

Figure 164: *Collision problem: Illustrates that, even if the pivot of rotation of each prism is located at the last point of reflection on* $M4_{L/R}$*, when both dove prisms* $P_{L/R}$ *converge, i.e. rotate inwards, they collide with each other.*

Unfortunately, this problem would persist even if the prisms were able to rotate about the corresponding LPR.

- The visual stimuli from the prisms are rotated, but also inverted, because only one dove prism was used per side. Consequently the perceived environment would also be inverted, when viewed from an HVT-1.0 based system.

B.6 DEMRS FOR HORIZONTAL, VERTICAL AND TORSIONAL STRABISMUS (VERSION HVT-2.0)

DEMRS HVT-2.0 is a conceptual DRS compliant system designed to retroverse horizontal, vertical and torsional strabismus, using a set of mirrors and rotatory prisms. Similar to HV-2.0, this system is designed to redirect principal and peripheral vision vectors by orienting a set of mirrors, horizontally and vertically, in order to achieve retroversion. Compared to HVT-1.0 in which the dove prisms had to perform pitch, yaw and roll rotations in order to achieve retroversion, the prisms in HVT-2.0 are designed to only rotate torsionally about the z-axis such that the vision vectors of the left and right eyes can have matching orientations.

B.6.1 *Design and Description*

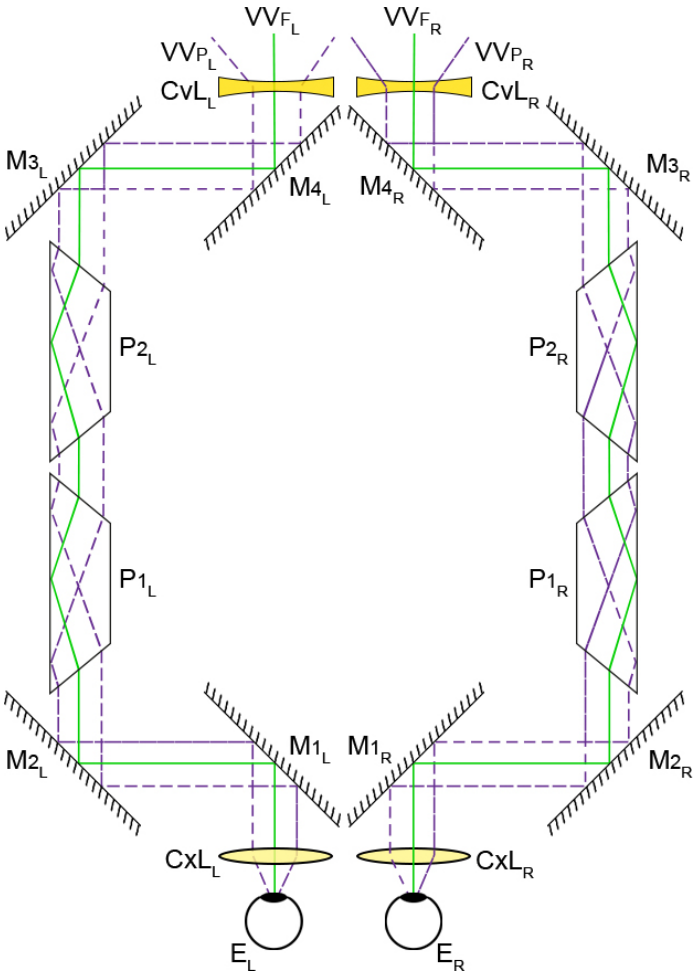

Figure 165: *DEMRS HVT-2.0: A schematic of the system, where* $VV_{F_{L/R}}$ *are the left and right principal vision vectors,* $VV_{P_{L/R}}$ *are the peripheral vision vectors,* $CxL_{L/R}$ *and* $CvL_{L/R}$ *are the convex and concave lenses,* $M_{1,2,3,4_{L/R}}$ *are the left and right set of mirrors,* $E_{L/R}$ *represent the left and right eyes, and* $P_{1,2_{L/R}}$ *are two dove prisms.*

The design of HVT-2.0 (fig. 165) consists of eight mirrors, four on each side ($M_{1_{L/R}}$, $M_{2_{L/R}}$, $M_{3_{L/R}}$ and $M_{4_{L/R}}$), for the purpose of redirecting the principal vision vectors ($VV_{F_{L/R}}$) towards the fixation target, whereas the two convex ($CxL_{L/R}$) and two concave ($CvL_{L/R}$) lenses are used to constrain the peripheral vision vectors ($VV_{P_{L/R}}$). Additionally, HVT-2.0 is designed to use four dove prisms, two on each side ($P_{1_{L/R}}$, $P_{2_{L/R}}$), in order to retroverse torsional deviations. The JSON configuration of HVT-2.0 is:

Listing 6: HVT-2.0 Configuration: The JSON configuration, which presents the initial setup of HVT-2.0. Because the design of the system is symmetrical, the configuration file sets the values only for one side, which gets mirrored on the other side.

```
{
    "hvt20" :
    [
    {
        "symmetrical" : "true",
        "side" : "left"
    },
    {
        "component" : "lens",
        "type" : "convex",
        "translate" : [3.0, 0.0, 2.0]
    },
    {
        "component" : "mirror",
        "id" : 0,
        "pivot" : [6.35, 0.0, 0.0],
        "translate" : [0.51, 0.0, 2.5],
        "rotate" : [0.0, 225.0, 0.0]
    },
    {
        "component" : "mirror",
        "id" : 1,
        "translate" : [17.0, 0.0, 6.99],
        "rotate" : [0.0, 45.0, 0.0]
    },
    {
        "component" : "prism",
        "type" : "dove",
        "id" : 1,
        "translate" : [17.0, 0.0, 18.31]
        "rotate" : [0.0, 0.0, 90.0]
    },
```

```
        {
                "component" : "prism",
                "type" : "dove",
                "id" : 2,
                "translate" : [17.0, 0.0, 31.94]
                "rotate" : [0.0, 0.0, 90.0]
        },
        {
                "component" : "mirror",
                "id" : 2,
                "translate" : [17.0, 0.0, 43.26],
                "rotate" : [0.0, 135.0, 0.0]
        },
        {
                "component" : "mirror",
                "id" : 3,
                "pivot" : [-6.35, 0.0, 0.0],
                "translate" : [0.51, 0.0, 47.75],
                "rotate" : [0.0, 315.0, 0.0]
        },
        {
                "component" : "lens",
                "type" : "concave",
                "translate" : [3.0, 0.0, 48.75]
        }
        ]
}
```

Similar to HVT-1.0 and HV-2.0, this system is designed with four mirrors on each side so that $M_{3,4_L}$ and $M_{3,4_R}$ can be used to maintain normal resultant IPD and normal binocular disparity. $M_{1_{L/R}}$ and $M_{4_{L/R}}$ are located centrally to the eyes so that the system can provide a larger visual field, when achieving retroversion for: (a) various angles of strabismic deviations, and (b) various directions of a fixation target. Also, the pivots of rotation of $M_{2_{L/R}}$ and $M_{3_{L/R}}$ remain central to the mirrors, whereas the pivots of rotation of $M_{1_{L/R}}$ and $M_{4_{L/R}}$ are located similar to the mirrors of HVT-1.0.

The default state of HVT-2.0, as shown in figure 165, is based on the assumption that the fixation target is located centrally to both eyes at a distance of $\geqslant 6m$ from the DEMRS origin. Therefore, by default, each mirror is oriented horizontally about the y-axis (yaw rotation) by 45°.

In order to address the issue of inverted visual stimuli, mentioned in the discussion of HVT-1.0, HVT-2.0 is designed with two dove prisms ($P_{1,2_{L/R}}$), one in front of the other on each side. The second prism ($P_{2_{L/R}}$) is only used to invert the vision vectors that were previously inverted by $P_{1_{L/R}}$. As shown in figure 166, when two dove prisms are consecutively placed one in front of the other the visual stimuli is rotated and inverted by the fist prism but the inversion is corrected by the second prism, thereby allowing the transmitted image to be rotated without undergoing inversion.

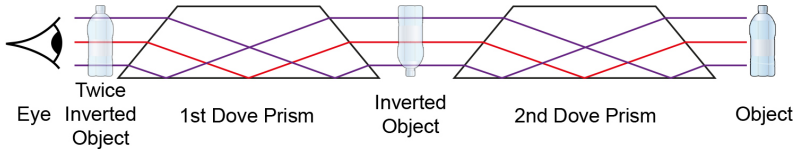

Figure 166: *Consecutive dove prisms: Illustration of two dove prisms placed one in front of the other, where the bottle is inverted by the first prism but re-inverted by the second prism so that it is perceived normally.*

Compared to HVT-1.0, the dove prisms have been placed between $M_{2_{L/R}}$ and $M_{3_{L/R}}$ (fig. 91) so that they only rotate about the z-axis. This is because the bidirectional retroversion algorithm, described in subsection 4.4.2, ensures that the principal vision vectors are centrally reflected by $M_{2_{L/R}}$ and $M_{3_{L/R}}$, thereby directed only along the z-axis. Of the two prisms, $P_{1_{L/R}}$ is designed to rotate by half of the angular difference between the normal eye and the strabismic eye, whereas $P_{2_{L/R}}$ is fixed at a 90° angle. Initially, the vision vectors are reflected by $M_{1_{L/R}}$ to the centre of $M_{2_{L/R}}$ and, next, by $M_{2_{L/R}}$ to the centre of $P_{1_{L/R}}$, which rotates and inverts the vision vectors. Subsequently, the vision vectors are refracted by $P_{2_{L/R}}$, which does not rotate but inverts the rotated vision vectors. Finally, the vision vectors are reflected by $M_{3_{L/R}}$ to the LPR on $M_{4_{L/R}}$. The sequence in which a vision vector is reflected by the mirrors and refracted by the prisms as it travels from the eye to a target (T), is as follows:

$$E \rightarrow M_1 \rightarrow M_2 \rightarrow P_1 \rightarrow P_2 \rightarrow M_3 \rightarrow M_4 \rightarrow T$$

Similar to HV-2.0, the lenses were added to the design of the system in order to constrain the direction of the peripheral vision vectors so that they are not reflected by the mirrors towards arbitrary directions, escaping the system. The design of HVT-2.0 satisfies all the criteria of the DRS principle, as follows:

1. The rotation of the mirrors enables the simultaneous intersection of both principal vision vectors on the same fixation target.

2. $M_{3_{L/R}}$ and $M_{4_{L/R}}$ maintain normal resultant IPD.

3. $M4_{L/R}$ maintain normal binocular disparity.

4. $P1_{L/R}$ and $P2_{L/R}$ maintain normal orientation of the visual stimuli.

B.6.2 *Retroversion Algorithm*

The retroversion algorithm used in HVT-2.0 is based on the bidirectional retroversion algorithm of HV-2.0 (see subsect. 4.4.2) with modifications that incorporate the rotation of dove prisms, following the rotation of $M2_{L/R}$. Similar to HV-2.0, in order to maintain normal resultant IPD and normal resultant binocular disparity, it is imperative to determine the last points of reflection (LPR) on $M4_{L/R}$. Consequently, HVT-2.0 uses the auxiliary vision vectors VV_{A_L} and VV_{A_R}, which represent both principal vision vectors under normal BSV, in order to calculate both LPR.

Because the prisms are configured between $M2_{L/R}$ and $M3_{L/R}$, the orientation of the prisms is not dependant upon the rotation of the mirrors. Of the two prisms, on each side, only the first prism ($P1_{L/R}$), i.e. the one closer to the eyes, is required to rotate torsionally (roll), as the purpose of the second prism ($P2_{L/R}$) is only to invert the vision vectors that were previously inverted by $P1_{L/R}$. Therefore, the bidirectional retroversion algorithm can be split into the following three concurrent tasks:

1. The first task calculates the orientation of $M1_{L/R}$ so that $VV_{F_{L/R}}$ can be reflected by $M1_{L/R}$ to the centre of $M2_{L/R}$. Next, the orientation of $M2_{L/R}$ is calculated so that the reflected $VV_{F_{L/R}}$ can be reflected by $M2_{L/R}$ to the centre of $M3_{L/R}$.

2. The second task calculates the orientation of $P1_{L/R}$ from the angular difference between the normal eye and the strabismic eye.

3. The third task uses an inverted $VV_{F_{L/R}}$, noted by $INV_V V_{F_{L/R}}$, that originates from the target and directs to the fovea. In this task the orientation of $M4_{L/R}$ is calculated so that the $INV_V V_{F_{L/R}}$ can be reflected by the LPR, on $M4_{L/R}$, to the centre of $M3_{L/R}$. Next, the orientation of $M3_{L/R}$ is calculated so that the reflected $INV_V V_{F_{L/R}}$ can be reflected by $M3_{L/R}$ to the centre of $M2_{L/R}$.

The following pseudocode presents the bidirectional retroversion algorithm, modified for HVT-2.0:

Algorithm 4: Bidirectional Retroversion of HVT-2.0

Begin

$vv_f \leftarrow$ principal vision vector;
$inv_vv_f \leftarrow$ inverse principal vision vector;
$vv_a \leftarrow$ auxiliary vision vector;

`// ----- Task 1 -----`

for m *in* $[M_1, M_2]$ **do**
  $poi = intersection(vv_f, m)$;
  $updated_vv = reflection(vv_f, m)$;
  $next_poi = intersection(updated_vv, m+1)$;
  if $next_poi$ *not central to* $m+1$ **then**
    rotate m so that $updated_vv$ is reflected centrally to $m+1$;
  end
  $update(vv_f)$;
end

`// ----- Task 2 -----`

$\psi = torsion(normal_eye, strabismic_eye)/2$;
$rotate(prism, \psi)$;

`// ----- Task 3 -----`

$lpr = intersection(vv_a, M_4)$;

for m *in* $[M_4, M_3]$ **do**
  $poi = intersection(inv_vv_f, m)$;
  $updated_vv = reflection(inv_vv_f, m)$;
  $next_poi = intersection(updated_vv, m+1)$;
  if $next_poi$ *not central to* $m+1$ **then**
    rotate m so that $updated_vv$ is reflected centrally to $m+1$;
  end
  $update(inv_vv_f)$;
end

The bidirectional algorithm above uses the same method to calculate pivoted rotations as HV-2.0 (see appendix B.3).

B.6.3 *Simulations*

A series of simulations were designed to evaluate the effectiveness of HVT-2.0 in achieving retroversion for near ($\leqslant$ 1m), mid ($\approx$ 3m) and far ($\geqslant$ 6m) fixation targets, at various directions from the DEMRS origin. Because a DRS compliant system must be able to compensate for various types of strabismus, including phorias, HVT-2.0 is tested with normal BSV and strabismus. In the following simulations, the eyes were assigned an IPD of 6cm, whereas the DEMRS simulator was configured based on the JSON con-

figuration file of HVT-2.0. Also, when the fixation target (T) is located at a distance of $< 6m$ from the DEMRS origin, retroversion is successful when both principal vision vectors pass through T. When T is located at a distance $\geqslant 6m$ from the DEMRS origin, retroversion is successful if each principal vision vector passes through the corresponding parallel target Tp_L and Tp_R.

Initially, a simple experiment was conducted to determine whether HVT-2.0 can retroverse normal BSV for a target located centrally at a distance of $8m$ ($T = \{0, 0, 800\}$). Figure 167 shows screenshots from the DEMRS simulator before and after retroversion. Table 52 presents the retroversion angles of the mirrors and prisms required to achieve retroversion.

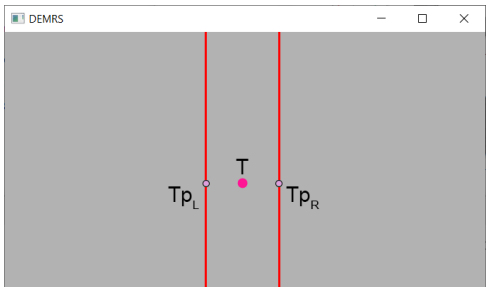

(a) *Target view before retroversion.*

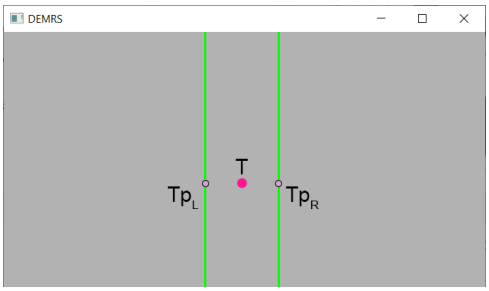

(b) *Target view after retroversion.*

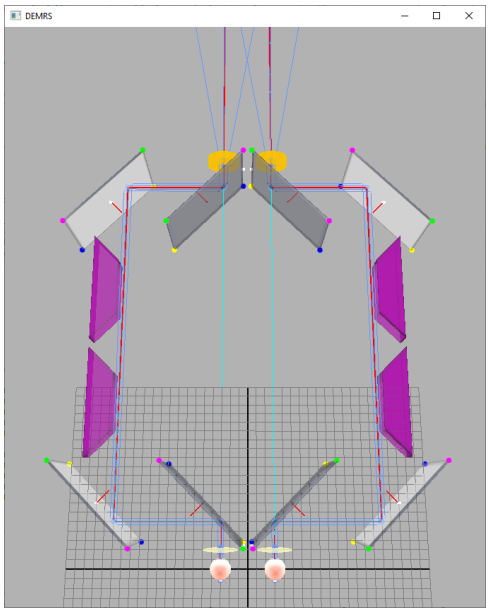

(c) *Before retroversion.*

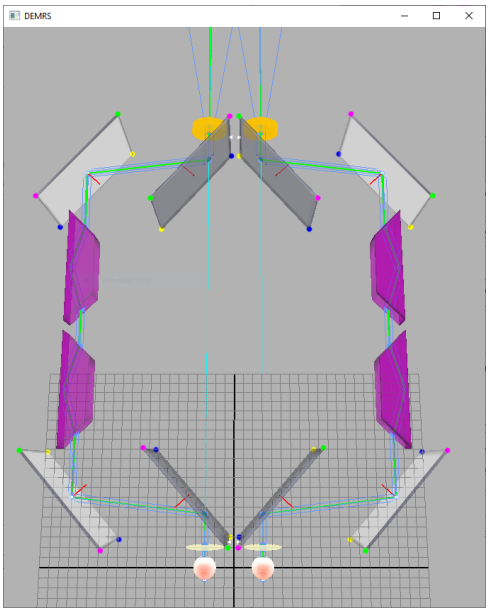

(d) *After retroversion.*

Figure 167: *DEMRS HVT-2.0 retroversion for* $T = \{0, 0, 800\}$*: Simulation tests before (c) and after (d) retroversion of normal BSV, where* $T = \{0, 0, 800\}$*. Because of the far distance of the target from the DEMRS origin, the target is not visible in (c) and (d). Therefore two additional screenshots were taken from a close up view of the target, peripheral and principal vision vectors, where (a) is the extension of (c), and (b) is the extension of (d).*

Table 52: *DEMRS HVT-2.0 retroversion angles for normal BSV, where* $T = \{0, 0, 800\}$.

Components	Retroversion (°)		
	x (pitch)	y (yaw)	z (roll)
$M1_L$	0.000	3.427	0.000
$M2_L$	0.000	3.427	0.000
$P1_L$	0.000	0.000	0.000
$P2_L$	0.000	0.000	0.000
$M3_L$	0.000	−3.427	0.000
$M4_L$	0.000	−3.427	0.000
$M1_R$	0.000	−3.427	0.000
$M2_R$	0.000	−3.427	0.000
$P1_R$	0.000	0.000	0.000
$P2_R$	0.000	0.000	0.000
$M3_R$	0.000	3.427	0.000
$M4_R$	0.000	3.427	0.000

In the test shown by figure 167, prior to retroversion, both principal vision vectors ($VV_{F_{L/R}}$) were shown in red because, although normal BSV is present and both principal vision vectors pass through Tp_L and Tp_R with normal orientation, the DEMRS simulator rejected retroversion because the vision vectors were not refracted by the dove prisms. This is because the principal vision vectors were not centrally reflected by M_2 and M_3, and therefore not centrally refracted by the prisms. After retroversion (fig. 167b), the vision vectors are centrally reflected by M_2 and M_3, and therefore centrally refracted by the dove prisms.

Next, HVT-2.0 was tested in the retroversion of normal BSV for a target that is located centrally at a distance of 1.5m ($T = \{0, 0, 150\}$). Figure 168 shows screenshots from the DEMRS simulator before and after retroversion. Table 53 presents the retroversion angles of the mirrors and prisms required to achieve retroversion.

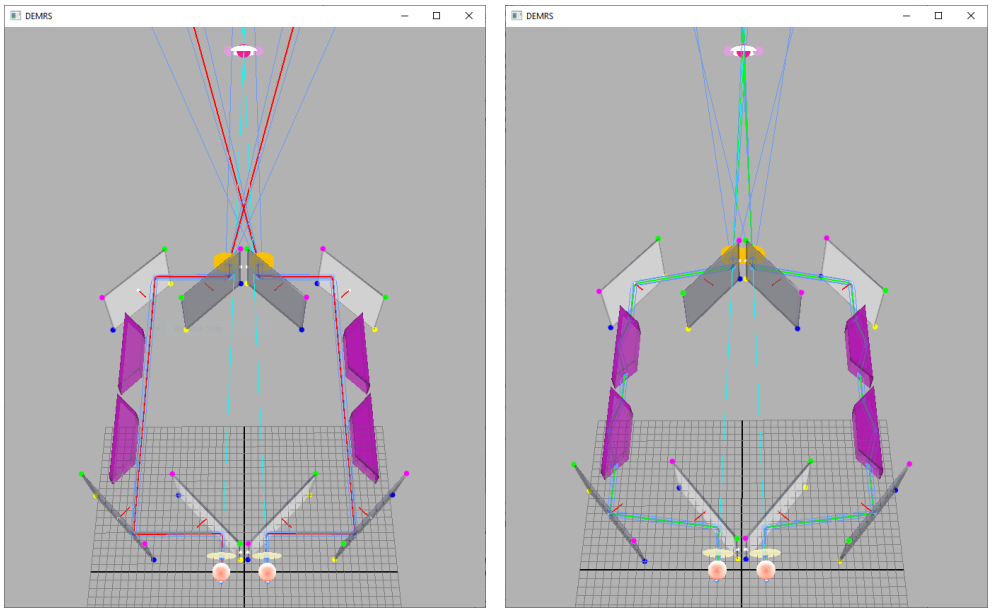

(a) *Before retroversion.* (b) *After retroversion.*

Figure 168: *DEMRS HVT-2.0 retroversion for* $\mathsf{T} = \{0, 0, 150\}$*: Simulation tests before (a) and after (b) retroversion of normal BSV, where* $\mathsf{T} = \{0, 0, 150\}$*.*

Table 53: *DEMRS HVT-2.0 retroversion angles for normal BSV, where* $\mathsf{T} = \{0, 0, 150\}$*.*

Components	Retroversion (°)		
	x (pitch)	y (yaw)	z (roll)
$M1_L$	0.000	4.415	0.000
$M2_L$	0.000	3.556	0.000
$P1_L$	0.000	0.000	0.000
$P2_L$	0.000	0.000	0.000
$M3_L$	0.000	−5.843	0.000
$M4_L$	0.000	−4.984	0.000
$M1_R$	0.000	−4.415	0.000
$M2_R$	0.000	−3.556	0.000
$P1_R$	0.000	0.000	0.000
$P2_R$	0.000	0.000	0.000
$M3_R$	0.000	5.843	0.000
$M4_R$	0.000	4.984	0.000

The following simulations show the effectiveness of HVT-2.0 in the retroversion of strabismus of various angles. For each deviation, the target moved directions from left to right, and up to down, at various distances. The tests are summarized by table 54.

Table 54: *Summary of strabismus and targets used in the simulations of DEMRS HVT-2.0.*

Strabismus	Deviation (pitch, yaw, roll)	Target (x, y, z)
right exo-hypo-incyclo-tropia	$4°, 8°, 15°$	$0, 0, 100$
		$0, 0, 700$
right eso-incyclo-tropia	$0°, 12°, 5°$	$10, 0, 170$
		$0, 0, 170$
		$-10, 0, 170$
right exo-excyclo-tropia	$0°, 9°, 7°$	$45, 0, 600$
		$0, 0, 600$
		$-45, 0, 600$
left hypo-incyclo-tropia	$12°, 0°, 8°$	$25, 0, 200$
		$0, 0, 200$
		$-25, 0, 200$
right hyper-excyclo-tropia	$10°, 0°, 6°$	$35, 0, 400$
		$0, 0, 400$
		$-35, 0, 400$

Figures 169, 170, 171, 172 and 173 show screenshots of the results after retroversion. Furthermore, in the following simulations:

- The eyes are illustrated by the two textured 3D models.
- The left principal vision vector is depicted by the green polyline, and the right vision vectors is depicted by the red polyline. The white dashed lines represent the auxiliary vision vectors of each eye, whereas the peripheral vision vectors are displayed as the white thin polylines, parallel to the principal vision vectors. The original principal vision vectors of the eyes are the light blue lines that are not reflected or refracted by the components of the system.
- The mirrors are illustrated by the light grey flat surfaces.
- The dove prisms are illustrated by the purple trapezoidal prismatic meshes located between $M_{2_{L/R}}$ and $M_{3_{L/R}}$.
- The fixation target T is illustrated by a white circle, whereas Tp_L and Tp_R are illustrated by two smaller circles coloured in green and red, respectively.

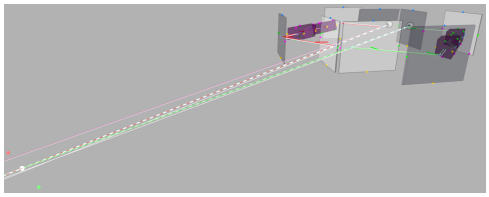

(a) *Perspective view.*

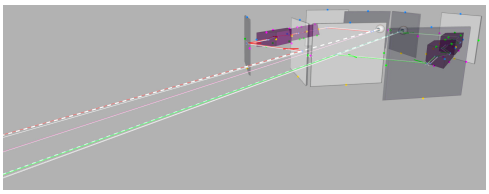

(b) *Perspective view.*

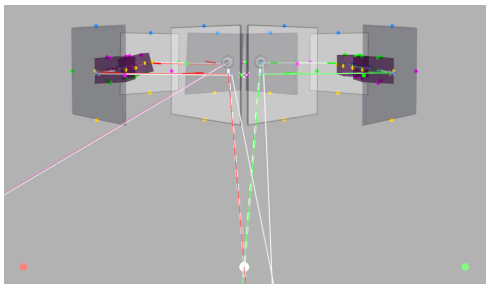

(c) *Front view.*

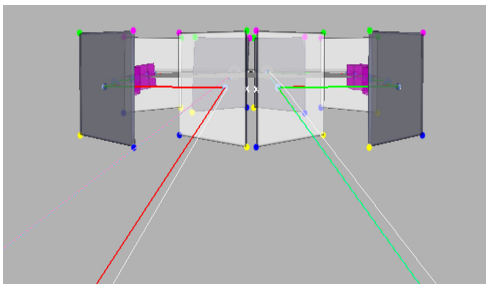

(d) *Front view.*

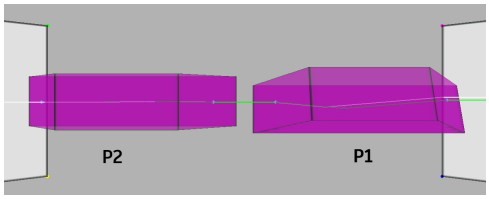

(e) *View of prisms.*

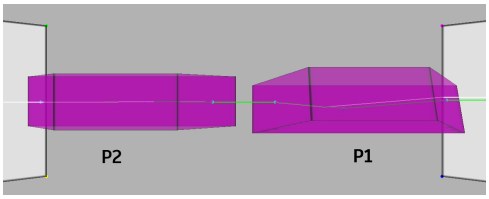

(f) *View of prisms.*

Figure 169: *DEMRS HVT-2.0 retroversion for* $\mathsf{T} = \{0, 0, 100\}$*, and* $\mathsf{T} = \{0, 0, 700\}$*: Simulation tests showing retroversion of a left exo-hypo-incyclo-tropia, with horizontal, vertical and torsional deviations of* $8°$*,* $4°$ *and* $15°$*. (a) and (c) show the results of the retroversion when* $\mathsf{T} = \{0, 0, 100\}$*, whereas (b) and (d) show the results of the retroversion when* $\mathsf{T} = \{0, 0, 700\}$*. (e) and (f) correspond to the tests shown in (a,c) and (b,d) respectively, and show close up views of the prisms emphasizing the torsional rotation of* P_{1_R}*.*

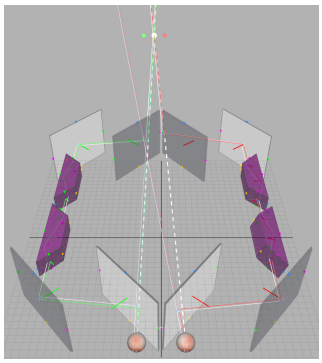

(a) *Target is left.*

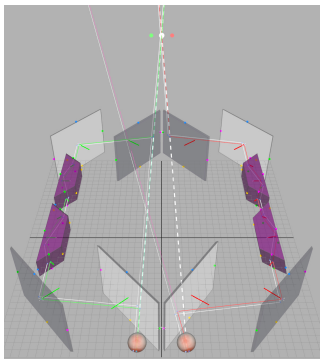

(b) *Target is central.*

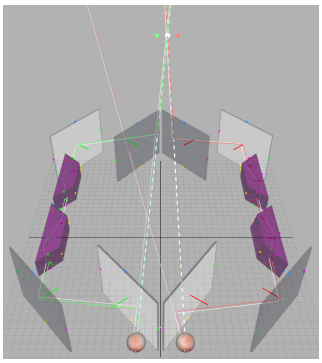

(c) *Target is right.*

Figure 170: *DEMRS HVT-2.0 retroversion for* $\mathsf{T} = \{10, 0, 170\}, \{0, 0, 170\}, \{-10, 0, 170\}$*: Simulation tests showing retroversion of a right eso-incyclo-tropia, with horizontal, and torsional deviations of* $12°$*, and* $5°$*. (a), (b), and (c) show the results of the retroversion when* T *is left, centre, and right.*

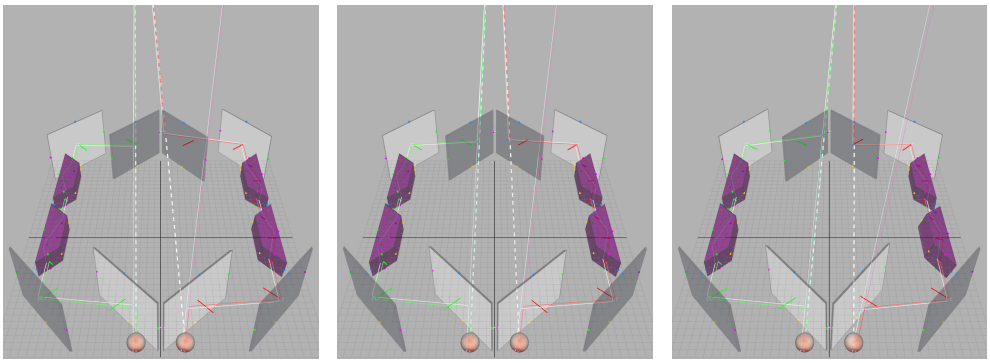

(a) *Target is left.* (b) *Target is central.* (c) *Target is right.*

Figure 171: *DEMRS HVT-2.0 retroversion for* $\mathsf{T} = \{45, 0, 600\}, \{0, 0, 600\}, \{-45, 0, 600\}$*: Simulation tests showing retroversion of a right exo-excyclo-tropia, with horizontal, and torsional deviations of* $9°$*, and* $7°$*. (a), (b), and (c) show the results of the retroversion when* T *is left, centre, and right.*

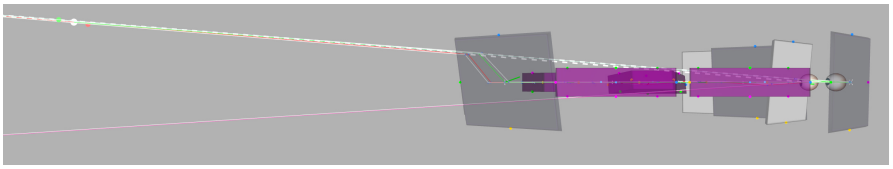

(a) *Target is up.*

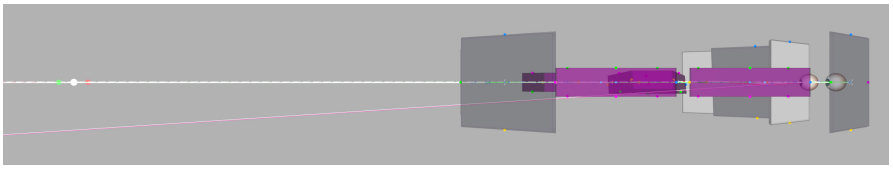

(b) *Target is central.*

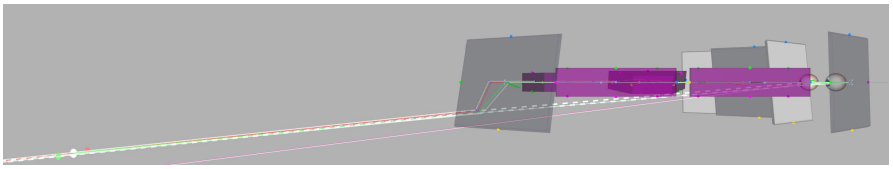

(c) *Target is down.*

Figure 172: *DEMRS HVT-2.0 retroversion for* $\mathsf{T} = \{0, 25, 200\}, \{0, 0, 200\}, \{0, -25, 200\}$*: Simulation tests showing retroversion of a left hypo-incyclo-tropia, with vertical, and torsional deviations of* $12°$*, and* $8°$*. (a), (b), and (c) show the results of the retroversion when* T *is up, centre, and down.*

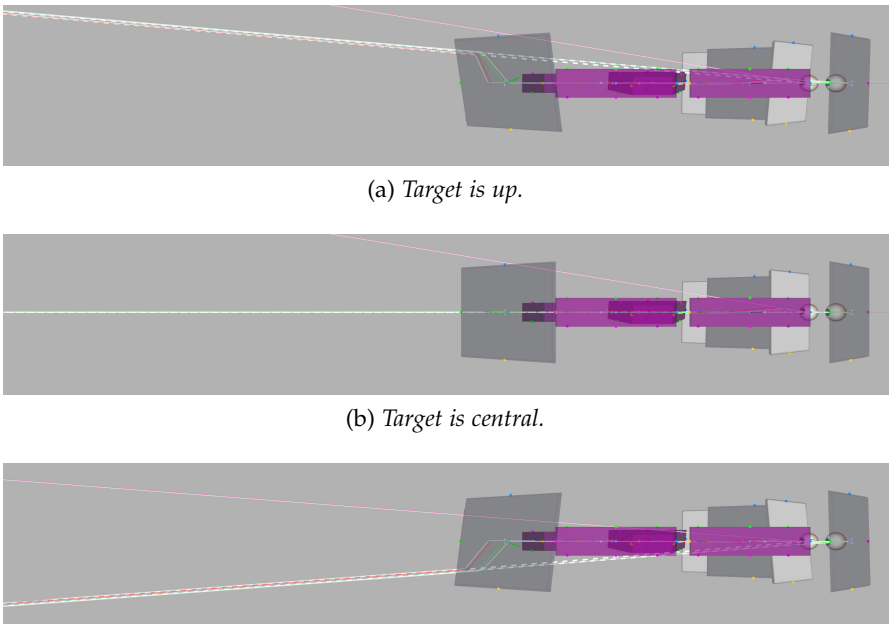

(a) *Target is up.*

(b) *Target is central.*

(c) *Target is down.*

Figure 173: *DEMRS HVT-2.0 retroversion for* $\mathsf{T} = \{0, 35, 400\}, \{0, 0, 400\}, \{0, -35, 400\}$*: Simulation tests showing retroversion of a right hyper-excyclo-tropia, with vertical, and torsional deviations of* $10°$*, and* $6°$*. (a), (b), and (c) show the results of the retroversion when* T *is up, centre, and down.*

B.6.4 *Discussion*

DEMRS HVT-2.0 is a DRS compliant system designed to achieve retroversion of strabismus, including torsional deviations. The additional dove prisms allow the vision vectors to have normal orientation without them being inverted during retroversion. Also, placing the prisms between $M2_{L/R}$ and $M3_{L/R}$ prevented the prisms from colliding with each other, and allowed the vision vectors to be centrally refracted by the prisms, which are only required to roll in order to retroverse torsional deviations. The simulation tests show that the retroversion engine can correctly calculate the rotations of the mirrors and dove prisms, such that the vision vectors pass through the same fixation target with normal orientation. Also, similar to HV-2.0, the retroversion engine takes into consideration mirrors $M3_{L/R}$ and $M4_{L/R}$, which are used to maintain normal binocular disparity and resultant IPD. Moreover, the simulation tests show that HVT-2.0 is able to achieve retroversion for various classifications of strabismus, including deviations that combine torsion with other directions.

A limitation of HVT-2.0 is that the system's size does not allow retroversion of fixation targets that are less than $1m$ away from the DEMRS origin.

APPENDIX C

C.1 SERVO MOTORS IN THE DEMRS POC DEVICE

A servo motor is a type of motor that requires a sensor for position feedback (encoder) in order to control the rotation of the motor's shaft (Toms, 2017) (Kreith and Goswami, 2005). If the motor rotates inaccurately, the feedback sensor sends a signal to the motor, which performs a corrective rotation to compensate for the error (Dedes, 2016).

The mirror mounts of the DEMRS POC device were initially designed to use two SpringRC SM-S4303R servo motors (fig. 174) in order to rotate a mirror horizontally and vertically. Compared to standard servo motors that rotate 180°, a SpringRC SM-S4303R motor is designed to continuously rotate 360° (Pololu, 2019). With a 4.8V power supply, the SpringRC SM-S4303R servo motor generates 43 rotations per minute (rpm) and 3.3kg · cm of torque, which is enough to rotate a small size cold mirror (Pololu, 2019).



Figure 174: *SpringRC SM-S4303R: The white cylindrical part at the top of the motor is the shaft, the black wire is connected to the ground, the red wire is for the power supply and the white wire is the control signal (Pololu, 2019).*

Prior to constructing the mirror mounts, presented in chapter 5, both servo motors were tested by rotating:

1. a paper card, in order to determine the functionality of the motor when the weight of the load is minimal.
2. high performance cold mirror, in order to determine the functionality of the motor when rotating a mirror.

In order to perform these tests, a basic mount was built that allowed the paper card and mirror to be affixed to the motors. The basic mount (fig. 175) consisted of:

- 2 × steel large flat washers M5, 1.2mm
- 2 × zinc plated bolts M3, 5mm
- 1 × cd
- 1 × small piece of card board
- 1 × tac

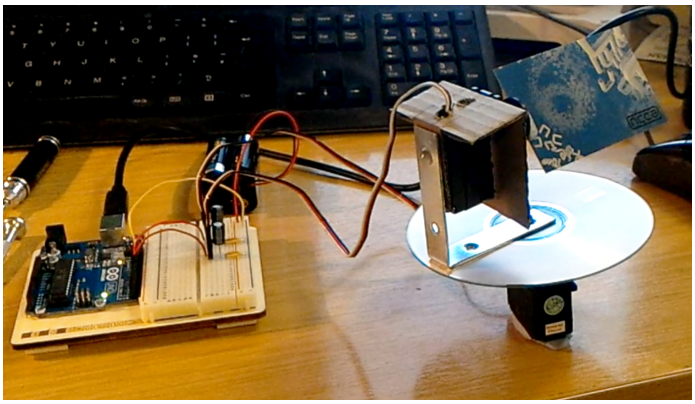

Figure 175: *Testing two SpringRC SM-S4303R servos using a paper card: The base servo performs a yaw rotation of the blue coloured card, whereas the other servo that is mounted on the L bracket, performs a pitch rotation of the card.*

During the first test, an issue that was encountered was that connecting two or more SM-S4303R servo motors to the Arduino Uno decreased the output torque of each servo, which effectively reduced the precision of the motor. This is because an SM-S4303R servo motor draws more current than what the Arduino Uno can provide via its 5V power supply pin. In order to address this issue, a 6V battery pack was used to power the motors (fig. 175) separately to the Arduino Uno micro-controller. Using a battery pack improved the precision of the motor and the output torque, as with a 6V power supply a SpringRC SM-S4303R servo motor produces 54rpm and 5.1kg · cm of torque (Pololu, 2019).

Because a SpringRC SM-S4303R servo motor supports continuous rotation, it cannot be programmed to rotate at a certain angle. Consequently, the only way to stop the motor from rotating is to "cut" the power, once the desired angle has been reached. This angle is determined by the width of the signal, or pulse (pulse-width modulation, PWM), that is received by the motor. For example, a 1.5ms pulse causes a servo motor to rotate its shaft by 90°. However, due to the inertia of the motor and its load, cutting off the power at the desired angle will not rotate the mirror precisely, as the shaft will continue to rotate beyond the desired angle. The problem with inertia also affects the ability of the motor to return to its default position.

Therefore, before conducting the second test with a high performance cold mirror, the two SpringRC SM-S4303R motors in the basic mount were

replaced by two non-continuous Tower Pro MG995 Digi Hi Speed servo motors (fig. 176) (Tower Pro, 2019).



Figure 176: *Tower Pro MG995 Digi Hi Speed servo motor: The metallic cylindrical part at the top of the motor, is the shaft of the motor that rotates. In this motor, the brown wire is connected to the ground, the red wire is for the power supply and the orange (yellow-ish) wire is the control signal.*

Using the Arduino Uno micro-controller, a non-continuous servo motor can be programmed to rotate its shaft by an arbitrary angle, without requiring to "cut off" the power in order to stop the shaft from rotating. The Tower Pro MG995 Digi Hi Speed servo motor also improved the output torque, as this particular motor generates $62\mathrm{rpm}$ and $13.0\mathrm{kg}\cdot\mathrm{cm}$ of torque (Tower Pro, 2019). Unfortunately, due to the angular resolution of this particular servo motor, the rotation of the shaft was not always correct.

In the second test, a high performance cold mirror was used to determine the functionality of both Tower Pro MG995 servo motors when rotating a mirror horizontally and vertically. The mirror was affixed to the motor via a base, provided by Edmund Optics (2019b). Unfortunately, the base includes an M6 machine screw mounting hole, which does not match the shape and size of the motor's shaft. Consequently, the base wiggled and tac filling had to be used in order to secure the base to the motor. This test showed that the basic mirror mount could not sustain the weight of the mirror (fig. 177).



Figure 177: *Basic mount: Tilting under the weight of the cold mirror.*

C.2 ROTATION OF A MIRROR USING AN ARDUINO UNO AND AN 28BYJ48 STEPPER MOTOR

```
// Includes the Stepper class defined in the Arduino API.
#include <Stepper.h>

// Function that converts angles into steps.
double rotate(double angle_)
{
      return (angle_ * (4096.0/360.0));
}

// Creates a new instance of the Stepper class that
// controls a particular stepper motor attached to the
// Arduino board.
// Function arguments:
// steps - the number of steps in one revolution.
// pi1,pi2,pin3,pin4 - pins attached to the motor.
Stepper motor(64, 9,7,8,6);

void setup()
{
      // Sets the motor speed in rotations per minute (rpm).
      motor.setSpeed(500);

      // Turns the motor by a specific number of steps. This
      // function is blocking, which means that it will wait
      // until the motor has finished rotating before it
      // passes control onto the next line of code.
      motor.step(rotate(20.0));

      // Wait for 1 second.
      delay(1000);
}

void loop()
{;}
```

C.3 A MIRROR MOUNT USING ADAPTERS

When a mirror rotates from the side, its pivot of rotation is located at the centre side of the mirror. Therefore, a mount that would allow the mirror to rotate from its side, must respect the location of the pivot of rotation.

Previously, it was mentioned that the mounting hole of a base, provided by Edmund Optics (2019b), is not a match to the shape and size of the shaft of a motor. Therefore, a mirror mount was constructed using custom designed 3D printed adapters, which allowed the base of a mirror to be affixed on a motor. As depicted by figure 178, the mirror mount consists of:

- 2× 3D printed adapters
- 1× MB3240DU glacier bush
- 1× AXK3047 needle thrust roller bearing
- 2× AS3047 needle thrust washers
- 1× 100mm L bracket
- 3× 75mm mending plates
- 3× 40mm pan head slotted machine screws
- 1× metallic base for high performance cold mirrors

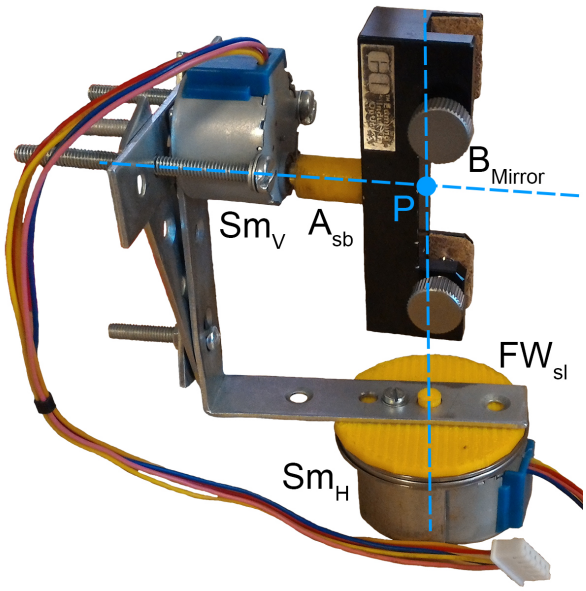

Figure 178: *Mirror mount using adapters: This mount consists of two 28BYJ-48 stepper motors, which are used to rotate the mirror.* B_{Mirror} *is the base of the mirror,* A_{sb} *is the 3D printed adapter that connects the motor with the base,* Sm_V *is the stepper motor responsible for the vertical rotation,* FW_{sl} *is the 3D printed flat wheel that connects the motor with the L bracket, and* Sm_H *is the stepper motor fitted inside the glashier bush responsible for the horizontal rotation. Lastly,* P *indicates the pivot of rotation of this mirror mount.*

The motor responsible for horizontal rotations was placed firmly inside a glashier bush, a mechanical element in the shape of a cylinder that was used in order to prevent the motor from moving unintentionally. Furthermore, the glashier bush was cut such that the shaft of the motor could be positioned at the centre of the bush. Due to the rectangular shape of the shaft of the Sm_H motor, a flat wheel (fig. 179) was designed and built, using a 3D printer, which includes a rectangular shaped hole at its bottom that matches the shape and size of the motors' shaft.

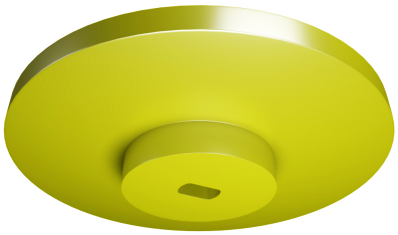

Figure 179: *Flat wheel: This is the design of the flat wheel, which has a rectangular shaped hole at the bottom that matches the shape and size of shaft of the motor.*

On the top side of the flat wheel there is a cylindrical extrusion, which fitted into one of the holes of an L bracket holding the remaining parts of the mirror mount (fig. 178). In order to prevent the L bracket from moving accidentally, a small machine screw was used to lock the L bracket onto the flat wheel. When the flat wheel was fitted on the shaft of the Sm_H motor, it was located higher than the edge of the glashier bush. Therefore, the remaining parts of the mirror mount were lifted entirely by the shaft of the Sm_H motor. This was problematic as the excessive weight could have, not only disturbed the angular resolution of the stepper motor but also, damaged the gears of the motor. In order to address this problem, one needle thrust washer was glued at the bottom of the flat wheel and another at the edge of the glashier bush. Additionally, a thrust roller bearing was placed between the two washers in order to eliminate the friction generated by the contact of the washers during rotation of the motor. The roller bearing and thrust washers assisted in the distribution of the load, as they raised the flat wheel so much that the remaining parts of the mirror mount were not lifted by the motor.

The Sm_V motor, which is responsible for the vertical (pitch) rotations of a mirror, was affixed onto the other side of the L bracket by three 75mm mending plates and three 40mm pan head slotted machine screws (fig. 178). As the shaft of the motor cannot fit into the mounting hole of the base, an adapter screw (fig. 180) was designed and built, using a 3D printer, in which one end has a mounting hole shaped and sized to that of the motors' shaft, and the other end has a mounting hole for an M6 machine screw. Next, the

head of an M6 machine screw was cut so that one side of the screw could be inserted into the adapter, whilst, the other side of the screw could be fitted into the base.

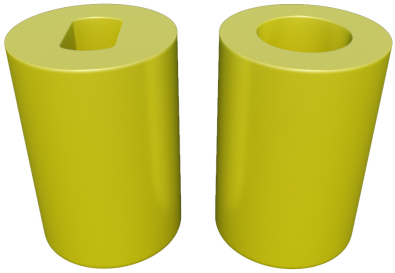

Figure 180: *Illustration of the adapter screw that connects the 28BYJ-48 stepper motor with the metallic base. The figure shows both sides of the same adapter. The left part of the image shows the side of the adapter that fits into the motors' shaft and the right part of the image shows the side connecting to the provided base.*

Unfortunately, it was determined that the mirror mount, described in this section, was unfit for use in the DEMRS POC device due to the following reasons:

1. The weight of the mirror mount, including the mirror and its base, is relatively heavy and makes it difficult for the Sm_H motor to rotate the mirror.

2. The L shaped bracket, which was used to orient the Sm_V motor perpendicularly to Sm_H, was slightly skewed and caused the mirror to tilt.

3. The base of the mirror includes two screws, which are equipped with a plastic tip to avoid scratching the surface of the mirror, intended to affix the mirror. However, when the base is tilted sideways, by 90°, the mirror tends to slide and may get damaged.

4. The size of the mirror mount does not allow two mirrors to be placed near each other, as per the design of HV-2.0 which requires that $M1_{L/R}$ and $M4_{L/R}$ are positioned near one another. Due to the length of the L shaped brackets, if two mirror mounts are placed next to each other, they will collide. Moreover, as shown by figure 181, if the mirror mounts are moved further apart from each other, thereby preventing the L brackets from colliding, the distance between the mirrors would be larger than the average pupillary distance and, therefore, a subject would not be able to see the target through the DEMRS.

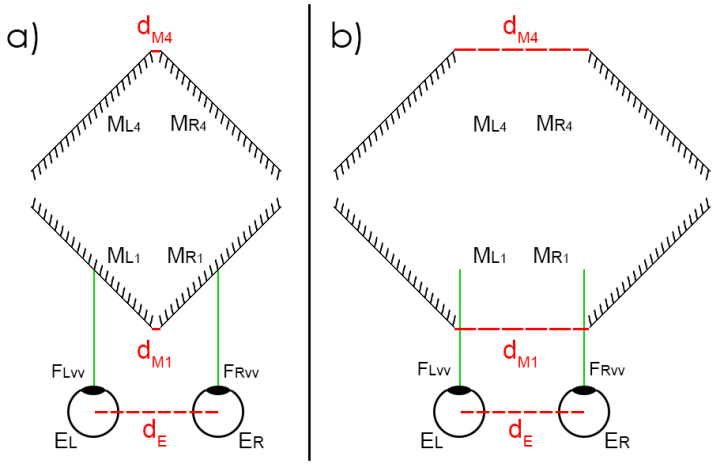

Figure 181: *Problem caused by the size of a mirror mount: Illustration of the problem that would be caused if two mirror mounts are placed further apart from each other. In this figure* E_L *and* E_R *are the left and right eyes with pupillary distance* d_E, d_{M1} *is the distance between the* M_{1_L} *and* M_{1_R}, *and* d_{M4} *is the distance between the* M_{4_L} *and* M_{4_R}.

C.4 DEMRS POC CONFIGURATION

Listing 7: POC Configuration: The JSON configuration, which presents the initial setup of the DEMRS POC. Because the design of the system is symmetrical, the configuration file sets the values only for one side, which gets mirrored on the other side.

```
{
    "poc" :
    [
    {
        "symmetrical" : "true",
        "side" : "left"
    },
    {
        "component" : "mirror",
        "id" : 0,
        "pivot" : [6.35, 0.0, 0.0],
        "translate" : [0.87, 0.0, -15.0],
        "rotate" : [0.0, 225.0, 0.0]
    },
```

```
        {
                "component" : "mirror",
                "id" : 1,
                "translate" : [20.07, 0.0, -10.51],
                "rotate" : [0.0, 45.0, 0.0]
        },
        {
                "component" : "mirror",
                "id" : 2,
                "translate" : [20.07, 0.0, 10.51],
                "rotate" : [0.0, 135.0, 0.0]
        },
        {
                "component" : "mirror",
                "id" : 3,
                "pivot" : [-6.35, 0.0, 0.0],
                "translate" : [0.87, 0.0, 15.0],
                "rotate" : [0.0, 315.0, 0.0]
        }
        ]
}
```

APPENDIX D

D.1 RESEARCH ETHICS CHECKLIST

Research Ethics Checklist

About Your Checklist

Reference Id	13948
Status	Approved
Date Approved	19/07/2019 14:40:28
Date Submitted	30/06/2019 19:26:37

Researcher Details

Name	Constantinos Glynos
Faculty	Faculty of Media & Communication
Status	Postgraduate Research (MRes, MPhil, PhD, DProf, EngD, EdD)
Course	Postgraduate Research - Media
Have you received external funding to support this research project?	No
Please list any persons or institutions that you will be conducting joint research with, both internal to BU as well as external collaborators.	BU

Project Details

Title	A Dynamic Eye Misalignment Retroversion System (DEMRS) for subjects with strabismus
Start Date of Project	16/09/2013
End Date of Project	10/09/2020
Proposed Start Date of Data Collection	01/07/2019
Original Supervisor	Hammadi Nait-Charif
Approver	Research Ethics Panel

Summary - no more than 500 words (including detail on background methodology, sample, outcomes, etc.)

Strabismus is a medical term used to define eye misalignment conditions that prevent both eyes from focusing on the same target simultaneously. Apart from having an aesthetic impact on the subject, strabismus is a disability that prohibits the correct perception of depth. The purpose of going through treatment is to realign the “bad” (strabismic) eye, so that it fixates on the same target as the “good” (dominant) eye.

This research presents a novel system called Dynamic Eye Misalignment Retroversion System (DEMRS), which can dynamically adjust the light rays coming into each eye, such that both eyes are stimulated by the same target, simultaneously. The simulated results have shown that the system is able to re-align both light rays such that they intersect the correct target successfully.

A research prototype of the DERMS was built with the purpose of assessing the efficacy of the system with normal and strabismus subjects. We are looking for 20 participants with strabismus and 20 participants with normal vision to take part in our evaluation. Each evaluation test will take approximately 15 minutes.

The participants who will volunteer to take part in the evaluation, will use the DEMRS prototype to see small objects, read text pages, see various stereoscopic images and see various 3D optical illusion images. During the evaluation test, the participants will be asked to answer a few research related questions with regards to the progress of the evaluation. The evaluation questions are attached to this checklist.

Human Participants

Participants

Describe the number of participants and specify any inclusion/exclusion criteria to used	
We are looking for 20 participants that have a form of strabismus and 20 participants with normal vision to take part in our evaluation. The participants will need to be over the age of 7 years old and will need to have the capacity to consent.	
Are your participants considered vulnerable?	Yes
Please provide details (e.g. children - specify age range, cognitive impairment, prison inmates, etc.)	
Some participants would be young children (minimum age of 7 years) or elders living in a care home (maximum age of 98 years).	
Is a Disclosure and Barring Service (DBS) check Required?	Yes

Recruitment

Please describe how participants will be identified, approached and recruited. Include details of any relationship between researcher(s) and participant(s), e.g. teacher-student	
Most of the subjects are co-workers, friends or family members. Participants at a young age are children of friends and co-workers. Elder participants live in the same care home as my grandmother and I have obtained full permissions from the care home to perform these tests. An individual (employee) within the care home will approach the participants to take part in the research project, therefore avoiding any potential for coercion.	
Do you need a Gatekeeper to access your participants?	Yes
Please provide details, including their roles and any relationship between Gatekeepers and participant(s) (e.g. nursing home manager and residents)	
The care home has been fully briefed about the purpose and rationale of this research and the evaluation process. They have understood the roles and responsibilites, they are aware that the residents are free to withdraw at any time during the evaluation tests and they are not to be forced into taking part against their will.	

Data Collection Activity

Will the research involve the completion of a questionnaire/survey? If yes, don't forget to attach a copy of the questionnaire/survey or sample of questions.	No
Will the research involve interviews and/or focus groups? If yes, don't forget to attach a copy of the interview/focus group questions or sample of questions.	No
Will the research involve the collection of audio materials?	No
Will your research involve the collection of photographic materials which will identify a participant?	No
Will your research involve the collection of video materials?	No
Will the study involve discussions of sensitive topics (e.g. sexual activity, drug use, criminal activity)?	No
Will any drugs, placebos or other substances (e.g. food substances, vitamins) be administered to the participants?	No

Will the study involve invasive, intrusive or potential harmful procedures of any kind?	No
Could your research induce psychological stress or anxiety, cause harm or have negative consequences for the participants or researchers (beyond the risks encountered in normal life)?	No
Will your research involve prolonged or repetitive testing?	No

Consent

Describe the process that you will be using to obtain valid consent. If consent is not to be obtained explain why

Initially, all participants and their guardians (if applicable) will be briefed orally and will have the chance to ask questions about the research topic and the evaluation process. Furthermore, they will be provided with an participant/guardian/child information sheet prior to testing. The participants and their guardians (if applicable) will be required to sign the appropriate concent forms before comensing the evaluation. All participants will have capacity to consent.

If participants are minors or for other reasons are not competent to consent, describe the proposed alternative source of consent

All guardians will be briefed orally and will have the chance to ask questions about the research topic and the evaluation process. They will also be provided with a guardians' information sheet which they will have the opportunity to review before the evaluation. The guardians will also be required to sign the guardians' concent form before comensing the evaluation. All participants will have capacity to consent.

Will it be necessary for participants to take part in your study without their knowledge and consent?	No

Participant Withdrawal

Describe how the participants will be informed of their right to withdraw from the study	During the initial briefing, all participants will be informed about their right to withdraw at any stage during the evaluation process. Furthermore, it is explicitely written in both, the information sheet and the consent form which they will have to sign.
Explain what will be done with the participants' data if they withdraw	If the participant withdraws during the activity, the data will be destroyed instantly. However, due to anonymity, if the participant decides to withdraw from the evaluation test after its' completion, then the data cannot be destroyed.

Participant Compensation

Will participants receive Financial compensation (or course credits) for their participation?	No
Will financial or other inducements (other than reasonable expenses) be offered to participants?	No

Personal Data

Will identifiable personal information be collected, i.e. data which identifies or could enable identification of the research participant?	No

Storage, Access and Disposal of Personal Data

Will any data be stored on the BU's Data Repository "BORDaR"?	No

Risk Assessment

Have you undertaken an appropriate Risk Assessment?	Yes

Attached documents
AgreementConsent_Form_Children.docx - attached on 17/05/2019 13:03:16
AgreementConsent_Form_ParentGuardian.docx - attached on 17/05/2019 13:03:21
AgreementConsent_Form_Participant.docx - attached on 17/05/2019 13:03:25
Evaluation_Questions.docx - attached on 17/05/2019 13:03:29
Information_Sheet__Children.docx - attached on 17/05/2019 13:04:10
Information_Sheet__Parent_Guardian.docx - attached on 17/05/2019 13:04:15
Information_Sheet__Participant.docx - attached on 17/05/2019 13:04:19

D.2 PARTICIPANT INFORMATION SHEETS

Bournemouth University

Participant Information Sheet – Under 16

A Dynamic Eye Misalignment Retroversion System (DEMRS) for people with strabismus

We are asking whether you and your family would like to take part in our research study. Before you decide if you would like to participate, it is important for you to understand why the study is being done and what it is all about. Read the following information carefully with your family.

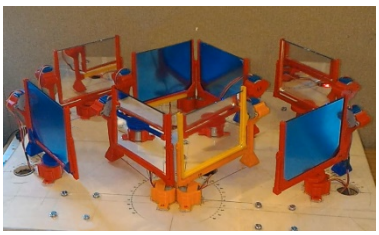

Figure 1: DEMRS Prototype

We will try to tell you as much as possible, but if there is something that doesn't make sense or you have more questions about, feel free to ask us!



"Hi kids! My name is Tom and I was born with strabismus. I am going to discuss this research project with the researcher! So, keep reading…"



"So, what is research?"

"Research is a way for us to discover the answers to questions. We also use research to find new solutions to problems."





"… and what is this research about?"

"This research has to do with our eyes and brain. Normally, when we see a tree, both of our eyes turn, so that each eye will have a view of that tree. This is called binocular vision."





"…"

"Because our eyes are spaced out horizontally on our face, each eye will view the same tree, but from a slightly different angle. Our brain takes these two views from our eyes and creates a single 3D view of the tree."





"…"

"Using our stereoscopic vision, we can tell how far other things are. In other words, we are able to perceive depth."





"Aaahh ok! I get it… But what does any of this have to do with this research?"

"Well, this is the interesting part of the research… Unfortunately, to everyone can perceive depth in the same way."





"??????"

"I can understand your confusion. Well…. When someone's eyes are not properly aligned and do not look at the same object (tree), then the brain receives two widely different views, and cannot create a single 3D view."





"Really???"

"Yes! Some kids cannot perceive depth the same way as kids with normal vision do. They use other ways to estimate depth."





"…"

"This is called Strabismus."





"Are these children ill then?"

"Nope, not at all! They are just different, much like some are short and some are tall."





"So, what is this research about?"

"I'm glad you asked! We have created a special system that can change what children with strabismus can see. We would like to test and see if it works!"





"Hold on… My eyes are exactly like what you have described. Can I use these glasses too?"

"Absolutely! We are looking for such amazing children to take part in our research.

Would you like to take part?"





"Do I have to?"

"Nope, of course not. It's totally up to you! You can even start the test and stop half-way through the test if you want to. There is no pressure at all!"





"But, what if I don't want other kids to know or find out that I took part?"

"No one will ever know, other than you, your family and us. All our test are anonymous."





"So, what will I have to do in these tests?"

"You will use our system to see small objects, read text, see various stereoscopic images and see some 3D illusion images. We will also ask you some questions about what you see?"





"Sure… But, should I be concerned of something going wrong during testing?"

"Absolutely nothing to worry about! The tests and the system are completely safe."





"Ok! I have a couple of more questions if that's alright…"

"Please… feel free to ask anything you like."





"What kind of details do you need from me and why is that important?"

"Good question! Well, you see, sometimes, strabismus cannot be detected by just looking at your eyes. This is why we need to ask you some questions about your eyes and do some small tests before you can use our system."





"…"

"This is for us to make sure that you are viable to take part in our research."





"Will you take pictures or video of me?"

"Nope! No pictures, no videos and no audio recordings."





"Ok… I guess that's all for now. How can I contact you if I have more questions?"

"You and your family are more than welcome to give us a call or email us any time. Your family has all our contact details."





"Ok! Well, thank you for explaining all these things to me."

"No problem! Thank you for considering taking part in this research project."





"Well boys and girls… I think I'll take part in this research!
See you later!"

Bournemouth University

Participant Information Sheet – Parents/Guardians

The title of the research project

A Dynamic Eye Misalignment Retroversion System (DEMRS) for subjects with strabismus

Invitation to take part

Your child is being invited to take part in a research project. Before you decide whether or not you would like your child to take part, it is important for you to understand why the research is being done and what it will involve. Please take time to read the following information carefully and discuss it with others if you wish. Ask us if there is anything that is not clear or if you would like more information. Take time to decide whether or not you wish your child to take part.

What is the purpose of the project?

Strabismus is a medical term used to define eye misalignment conditions that prevent both eyes from focusing on the same target simultaneously. Apart from having an aesthetic impact on the subject, strabismus is a disability that prohibits the correct perception of depth. The purpose of going through treatment is to realign the "bad" (strabismic) eye, so that it fixates on the same target as the "good" (dominant) eye.

This research presents a novel system called Dynamic Eye Misalignment Retroversion System (DEMRS), which can dynamically adjust the light rays coming into each eye, such that both eyes are stimulated by the same target, simultaneously. The simulated results have shown that the system is able to re-align both light rays such that they intersect the correct target successfully.

A research prototype of the DERMS was built with the purpose of assessing the efficacy of the system with normal and strabismus subjects. Each experiment will take approximately 15 minutes.

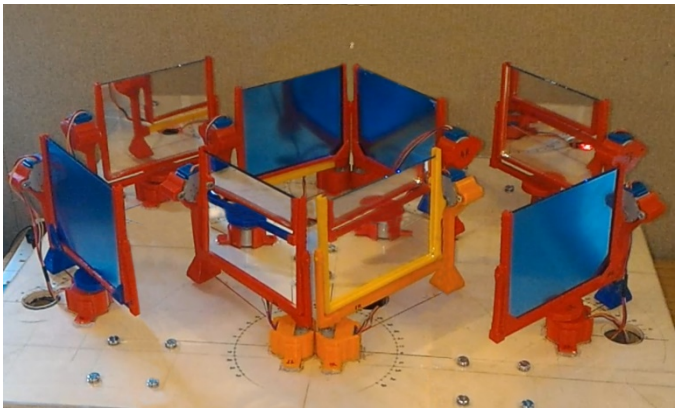

Why has my child I been chosen?

Your child has been chosen because he/she is in the age range of 7 – 16 years old with normal vision or have some form of strabismus. We are looking for 20 participants with strabismus and 20 participants with normal vision to take part in our evaluation.

Does my child have to take part?

It is up to you to decide whether or not your child takes part. If you do decide that your child can take part, you will be given this information sheet to keep and be asked to sign a guardian agreement form. We also ask your child to agree to take part. Your child can withdraw from participation during the evaluation at any time and without giving a reason. If your child decides to withdraw, we will erase any data collected about them from the study. Once the evaluation has finished your child may still be able to withdraw their data up to the point where the data is analysed and incorporated into the research findings or outputs. At this point their data will become anonymous, so their identity cannot be determined, and it may not be possible to identify their data within the anonymous dataset. Withdrawing their data at this point may also adversely affect the validity and integrity of the research.

What would taking part involve?

Your child will undergo evaluation using the DEMRS prototype to see small objects, read text pages, see various stereoscopic images and see various 3D optical illusion images. The experiments will be setup in a room with ambient lighting. Your child will be asked to rest his/her head on a medical chin rest which is going to be placed 40.0 - 65.0 cm away from the target. Your child will then be asked to look through the system and answer a few research related questions while undergoing evaluation. No diagnostic information or tests results will be distributed to you, your child or anyone else at any stage during this research.

What are the advantages and possible disadvantages or risks of taking part?

Whilst there are no immediate benefits for those people participating in the project, it is hoped that the DEMRS will be used to explore new alternative methods of diagnosing and treating strabismus for young children, adults and elders. There are no apparent disadvantages or risks associated with this evaluation.

What type of information will be sought from my child and why is the collection of their information relevant for achieving the research project's objectives?

Your child will be assessed before and after using the DEMRS in the evaluation. If your child has normal vision, then your child will be examined on a convergence test, in which he/she will be asked to follow the tip of a pencil at various directions and distances. If your child suffers from a case of strabismus, your child will be examined by observation for any distinguishable eye misalignment and will be asked to provide some information (brief history) about the origin of his/her strabismus (if known). A simple cover test will then be performed to verify the type of strabismus and the angle of deviation. This information is important to verify if your child is viable to take part in this research.

Will my child be recorded, and how will the recorded media be used?

There will be no video recordings of your child's activities made during this research.

How will my child's information be kept?

All the information we collect about your child during the course of the research will be kept strictly in accordance with current data protection legislation. Research is a task that we perform in the public interest, as part of our core function as a university. Bournemouth University (BU) is a Data Controller of your child's information which means that we are responsible for looking after their information and using it appropriately. BU's Research Participant Privacy Notice sets out more information about how we fulfil our responsibilities as a data controller and about your child's rights as an individual under the data protection legislation. We ask you to read this Notice so that you can fully understand the basis on which we will process their information.

Publication

Your child/legal ward will not be able to be identified in any external reports or publications about the research without your specific consent. Otherwise their information will only be included in these materials in an anonymous form, i.e. they will not be identifiable.

Security and access controls

BU will hold the information we collect about your child/legal ward in hard copy in a secure location and on a BU password protected secure network where held electronically.

Except where it has been anonymised your child's personal information will be accessed and used only by appropriate, authorised individuals and when this is necessary for the purposes of the research or another purpose identified in the Privacy Notice. This may include giving access to BU staff or others responsible for monitoring and/or audit of the study, who need to ensure that the research is complying with applicable regulations

Retention of your child's/legal ward's data

All personal data collected for the purposes of this study will be held for 5 years. Although published research outputs are anonymised, we need to retain underlying data collected for the study in a non-anonymised form for a certain period to enable the research to be audited and/or to enable the research findings to be verified.

Contact for further information

If you have any questions or would like further information with regards to this research evaluation, please contact cglynos@bournemouth.ac.uk or hncharif@bournemouth.ac.uk .

Any concerns about the study should be directed to Constantinos Glynos. If your concerns have not been answered by Constantinos Glynos, you should contact Associate Professor Einar Thorsen, Deputy Dean for Research & Professional Practice, Faculty of Media and Communication, Bournemouth University by email to researchgovernance@bournemouth.ac.uk.

Finally

If you decide that your child can take part, you will be given a copy of the information sheet and a signed parent/guardian consent form to keep.

Thank you for considering taking part in this research project.

Bournemouth University

Participant Information Sheet - Adults

The title of the research project

A Dynamic Eye Misalignment Retroversion System (DEMRS) for subjects with strabismus

Invitation to take part

You are being invited to take part in a research project. Before you decide it is important for you to understand why the research is being done and what it will involve. Please take time to read the following information carefully and discuss it with others if you wish. Ask us if there is anything that is not clear or if you would like more information. Take time to decide whether or not you wish to take part.

What is the purpose of the project?

Strabismus is a medical term used to define eye misalignment conditions that prevent both eyes from focusing on the same target simultaneously. Apart from having an aesthetic impact on the subject, strabismus is a disability that prohibits the correct perception of depth. The purpose of going through treatment is to realign the “bad” (strabismic) eye, so that it fixates on the same target as the “good” (dominant) eye.

This research presents a novel system called Dynamic Eye Misalignment Retroversion System (DEMRS), which can dynamically adjust the light rays coming into each eye, such that both eyes are stimulated by the same target, simultaneously. The simulated results have shown that the system is able to re-align both light rays such that they intersect the correct target successfully.

A research prototype of the DERMS was built with the purpose of assessing the efficacy of the system with normal and strabismus subjects. Each experiment will take approximately 15 minutes.

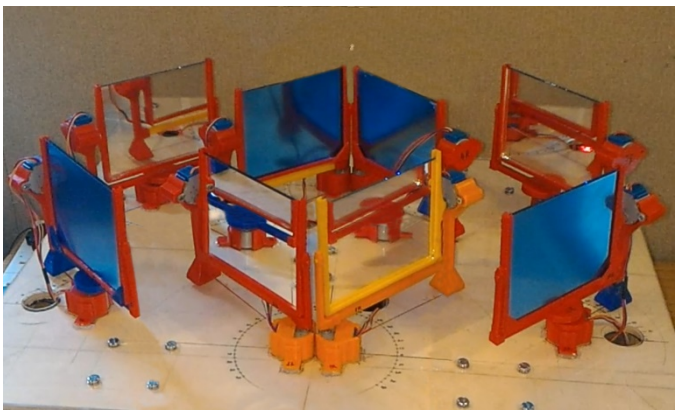

Why have I been chosen?

You have been chosen because you are in the age range of 7 – 90 years old with normal vision or have some form of strabismus. We are looking for 20 participants with strabismus and 20 participants with normal vision to take part in our evaluation.

Do I have to take part?

It is up to you to decide whether or not to take part. If you do decide to take part, you will be given this information sheet to keep and be asked to sign a participant consent form. You can withdraw from participation during the evaluation at any time and without giving a reason. If you decide to withdraw we will erase any data collected about you from the study. Once the evaluation has finished you may still be able to withdraw your data up to the point where the data is analysed and incorporated into the research findings or outputs. At this point your data will become anonymous, so your identity cannot be determined, and it may not be possible to identify your data within the anonymous dataset. Withdrawing your data at this point may also adversely affect the validity and integrity of the research.

What would taking part involve?

You will undergo evaluation using the DEMRS prototype to see small objects, read text pages, see various stereoscopic images and see various 3D optical illusion images. The experiments will be setup in a room with ambient lighting. You will be asked to rest your head on a medical chin rest which is going to be placed 40.0 - 65.0 cm away from the target. You will then be asked to look through the system and answer a few research related questions while undergoing evaluation. No diagnostic information or tests results will be distributed to you or anyone else at any stage during this research.

What are the advantages and possible disadvantages or risks of taking part?

Whilst there are no immediate benefits for those people participating in the project, it is hoped that the DEMRS will be used to explore new alternative methods of diagnosing and treating strabismus for young children, adults and elders. There are no apparent disadvantages or risks associated with this evaluation.

What type of information will be sought from me and why is the collection of this information relevant for achieving the research project's objectives?

You will be assessed before and after using the DEMRS in the evaluation. If you have normal vision, you will be examined on a convergence test, in which you will be asked to follow the tip of a pencil at various directions and distances. If you suffer from a case of strabismus, you will be examined by observation for any distinguishable eye misalignment and will be asked to provide some information (brief history) about the origin of your strabismus (if known). A simple cover test will then be performed to verify the type of strabismus and the angle of deviation. This information is important to verify if you are viable to take part in this research.

Will I be recorded, and how will the recorded media be used?

There will be no video recordings of your activities made during this research.

How will my information be kept?

All the information we collect about you during the course of the research will be kept strictly in accordance with current data protection legislation. Research is a task that we perform in the public interest, as part of our core function as a university. Bournemouth University (BU) is a Data Controller of your information which means that we are responsible for looking after your information and using it appropriately. BU's Research Participant Privacy Notice sets out more information about how we fulfil our responsibilities as a data controller and about your rights as an individual under the data protection legislation. We ask you to read this Notice so that you can fully understand the basis on which we will process your information.

Publication

You will not be able to be identified in any external reports or publications about the research without your specific consent. Otherwise your information will only be included in these materials in an anonymous form, i.e. they will not be identifiable.

Security and access controls

BU will hold the information we collect about you in hard copy in a secure location and on a BU password protected secure network where held electronically.

Except where it has been anonymised your personal information will be accessed and used only by appropriate, authorised individuals and when this is necessary for the purposes of the research or another purpose identified in the Privacy Notice. This may include giving access to BU staff or others responsible for monitoring and/or audit of the study, who need to ensure that the research is complying with applicable regulations.

Retention of your data

All personal data collected for the purposes of this study will be held for 5 years. Although published research outputs are anonymised, we need to retain underlying data collected for the study in a non-anonymised form for a certain period to enable the research to be audited and/or to enable the research findings to be verified.

Contact for further information

If you have any questions or would like further information with regards to this research evaluation, please contact cglynos@bournemouth.ac.uk or hncharif@bournemouth.ac.uk .

Any concerns about the study should be directed to Constantinos Glynos. If your concerns have not been answered by Constantinos Glynos, you should contact Associate Professor Einar Thorsen, Deputy Dean for Research & Professional Practice, Faculty of Media and Communication, Bournemouth University by email to researchgovernance@bournemouth.ac.uk.

Finally

If you decide to take part, you will be given a copy of the information sheet and a signed participant consent form to keep.

Thank you for considering taking part in this research project.

Participant Information Sheet - Elderly

The title of the research project

A Dynamic Eye Misalignment Retroversion System (DEMRS) for subjects with strabismus

Invitation to take part

You are being invited to take part in a research project. Before you decide it is important for you to understand why the research is being done and what it will involve. Please take time to read the following information carefully and discuss it with others if you wish. Ask us if there is anything that is not clear or if you would like more information. Take time to decide whether or not you wish to take part.

What is the purpose of the project?

Strabismus is a medical term used to define eye misalignment conditions that prevent both eyes from focusing on the same target simultaneously. Apart from having an aesthetic impact on the subject, strabismus is a disability that prohibits the correct perception of depth. The purpose of going through treatment is to realign the “bad” (strabismic) eye, so that it fixates on the same target as the “good” (dominant) eye.

This research presents a novel system called Dynamic Eye Misalignment Retroversion System (DEMRS), which can dynamically adjust the light rays coming into each eye, such that both eyes are stimulated by the same target, simultaneously. The simulated results have shown that the system is able to re-align both light rays such that they intersect the correct target successfully.

A research prototype of the DERMS was built with the purpose of assessing the efficacy of the system with normal and strabismus subjects. Each experiment will take approximately 15 minutes.

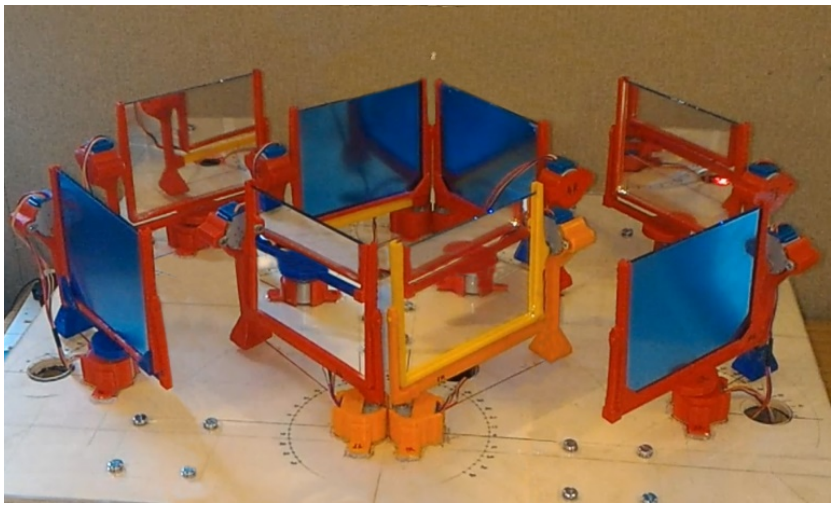

Why have I been chosen?

You have been chosen because you are in the age range of 7 – 90 years old with normal vision or have some form of strabismus. We are looking for 20 participants with strabismus and 20 participants with normal vision to take part in our evaluation.

Do I have to take part?

It is up to you to decide whether or not to take part. If you do decide to take part, you will be given this information sheet to keep and be asked to sign a participant consent form. You can withdraw from participation during the evaluation at any time and without giving a reason. If you decide to withdraw we will erase any data collected about you from the study. Once the evaluation has finished you may still be able to withdraw your data up to the point where the data is analysed and incorporated into the research findings or outputs. At this point your data will become anonymous, so your identity cannot be determined, and it may not be possible to identify your data within the anonymous dataset. Withdrawing your data at this point may also adversely affect the validity and integrity of the research.

What would taking part involve?

You will undergo evaluation using the DEMRS prototype to see small objects, read text pages, see various stereoscopic images and see various 3D optical illusion images. The experiments will be setup in a room with ambient lighting. You will be asked to rest your head on a medical chin rest which is going to be placed 40.0 - 65.0 cm away from the target. You will then be asked to look through the system and answer a few research related questions while undergoing evaluation. No diagnostic information or tests results will be distributed to you or anyone else at any stage during this research.

What are the advantages and possible disadvantages or risks of taking part?

Whilst there are no immediate benefits for those people participating in the project, it is hoped that the DEMRS will be used to explore new alternative methods of diagnosing and treating strabismus for young children, adults and elders. There are no apparent disadvantages or risks associated with this evaluation.

What type of information will be sought from me and why is the collection of this information relevant for achieving the research project's objectives?

You will be assessed before and after using the DEMRS in the evaluation. If you have normal vision, you will be examined on a convergence test, in which you will be asked to follow the tip of a pencil at various directions and distances. If you suffer from a case of strabismus, you will be examined by observation for any distinguishable eye misalignment and will be asked to provide some information (brief history) about the origin of your strabismus (if known). A simple cover test will then be performed to verify the type of strabismus and the angle of deviation. This information is important to verify if you are viable to take part in this research.

Will I be recorded, and how will the recorded media be used?

There will be no video recordings of your activities made during this research.

How will my information be kept?

All the information we collect about you during the course of the research will be kept strictly in accordance with current data protection legislation. Research is a task that we perform in the public interest, as part of our core function as a university. Bournemouth University (BU) is a Data Controller of your information which means that we are responsible for looking after your information and using it appropriately. BU's Research Participant Privacy Notice sets out more information about how we fulfil our responsibilities as a data controller and about your rights as an individual under the data protection legislation. We ask you to read this Notice so that you can fully understand the basis on which we will process your information.

Publication

You will not be able to be identified in any external reports or publications about the research without your specific consent. Otherwise your information will only be included in these materials in an anonymous form, i.e. they will not be identifiable.

Security and access controls

BU will hold the information we collect about you in hard copy in a secure location and on a BU password protected secure network where held electronically.

Except where it has been anonymised your personal information will be accessed and used only by appropriate, authorised individuals and when this is necessary for the purposes of the research or another purpose identified in the Privacy Notice. This may include giving access to BU staff or others responsible

for monitoring and/or audit of the study, who need to ensure that the research is complying with applicable regulations.

Retention of your data

All personal data collected for the purposes of this study will be held for 5 years. Although published research outputs are anonymised, we need to retain underlying data collected for the study in a non-anonymised form for a certain period to enable the research to be audited and/or to enable the research findings to be verified.

Contact for further information

If you have any questions or would like further information with regards to this research evaluation, please contact cglynos@bournemouth.ac.uk or hncharif@bournemouth.ac.uk .

Any concerns about the study should be directed to Constantinos Glynos. If your concerns have not been answered by Constantinos Glynos, you should contact Associate Professor Einar Thorsen, Deputy Dean for Research & Professional Practice, Faculty of Media and Communication, Bournemouth University by email to researchgovernance@bournemouth.ac.uk.

Finally

If you decide to take part, you will be given a copy of the information sheet and a signed participant consent form to keep.

Thank you for considering taking part in this research project.

D.3 PARTICIPANT AGREEMENT FORMS

Bournemouth University

Reference & Version: DEMRS_PAFC v1
Ethics ID: 13948
Date: 14/05/2019

Participant Assent Form – Under 16

Research title: A Dynamic Eye Misalignment Retroversion System (DEMRS) for subjects with strabismus

Name of researcher: *Constantinos Glynos, Demonstrator in Computer Animation, Faculty of Media & Communication, cglynos@bournemouth.ac.uk*

Please tick all boxes if you agree:

- ☐ I am happy to take part in the research.
- ☐ I understand that I do not have to take part in this research, and I can change my mind and stop taking part at any time before the research activities are completed.
- ☐ I understand that my name will not be used in any of the research reports.

_____	_____	_____
Your name	Date (dd/mm/yyyy)	Signature

_____	_____	_____
Name of Researcher	Date (dd/mm/yyyy)	Signature

Thank you!

Participant Agreement Form – Parents/Guardians

Full title of project: *A Dynamic Eye Misalignment Retroversion System (DEMRS) for subjects with strabismus*

Name, position and contact details of researcher: *Constantinos Glynos, Demonstrator in Computer Animation, Faculty of Media & Communication, cglynos@bournemouth.ac.uk*

Name, position and contact details of supervisor: *Hammadi Nait-Charif, Principal Academic in Computer Animation, Faculty of Media & Communication, hncharif@bournemouth.ac.uk*

To be completed prior to data collection activity

Agreement to participate in the study

In this Form we ask you to confirm whether you agree that your Child/Legal Ward can take part in the Study. Your Child/Legal Ward can only agree to participate in the study if you agree with all of the statements in this table and accept that your Child's/Legal Ward's participation will involve the listed activities.

I have read and understood the Participant Information Sheet (DEMRS_PISG v1) and have been given access to the BU Research Participant Privacy Notice which sets out how you will collect and use my Child's/Legal Ward's personal information -(https://www1.bournemouth.ac.uk/about/governance/access-information/data-protection-privacy). I have shared this information with my Child/Legal Ward.
I have had the opportunity to consider the information, ask questions and have had these answered satisfactorily
I understand that my Child's/Legal Ward's participation is voluntary. My Child/Legal Ward can stop participating in research activities at any time without giving a reason and my Child/Legal Ward is free to decline to answer any particular question(s).
I understand that my Child's/Legal Ward's involvement in the research study will include the following:
• my Child's/Legal Ward's words will be quoted in publications, reports, web pages and other research outputs without using their real name.
I understand that, if my Child/Legal Ward withdraws from the study, they will also be able to withdraw their data from further use in the study **except** where my Child's/Legal Ward's data has been anonymised (as they cannot be identified) or it will be harmful to the project to have their data removed.
I understand that my Child/Legal Ward's data may be used in an anonymised form by the research team to support other research projects in the future, including future publications, reports or presentations.

	Initial box to agree
I consent to my Child/Legal Ward taking part in the project on the basis set out above	

I confirm my agreement to my Child/Legal Ward taking part in the project on the basis set out above.

Name of guardian (BLOCK CAPITALS)	Date (dd/mm/yyyy)	Signature
Name of researcher (BLOCK CAPITALS)	Date (dd/mm/yyyy)	Signature

Once a Guardian has signed, **please sign 1 copy** and take 2 photocopies:

- Original kept in the local investigator's file
- 1 copy to be kept by the Parent/Guardian (including a copy of PI Sheet)

Participant Agreement Form - Adults

Full title of project: *A Dynamic Eye Misalignment Retroversion System (DEMRS) for subjects with strabismus*

Name, position and contact details of researcher: *Constantinos Glynos, Demonstrator in Computer Animation, Faculty of Media & Communication, cglynos@bournemouth.ac.uk*

Name, position and contact details of supervisor: *Hammadi Nait-Charif, Principal Academic in Computer Animation, Faculty of Media & Communication, hncharif@bournemouth.ac.uk*

To be completed prior to data collection activity

Agreement to participate in the study

You should only agree to participate in the study if you agree with all of the statements in this table and accept that participating will involve the listed activities.

I have read and understood the Participant Information Sheet (DEMRS_PIS v1) and have been given access to the BU Research Participant Privacy Notice which sets out how we collect and use personal information (https://www1.bournemouth.ac.uk/about/governance/access-information/data-protection-privacy).
I have had the opportunity to consider the information, ask questions and have had these answered satisfactorily
I understand that my participation is voluntary. I can stop participating in research activities at any time without giving a reason and I am free to decline to answer any particular question(s).
I understand that taking part in the research will include the following activity as part of the research:
• my words may- be quoted in publications, reports, web pages and other research outputs without using my real name.
I understand that, if I withdraw from the study, I will also be able to withdraw my data from further use in the study **except** where my data has been anonymised (as I cannot be identified) or it will be harmful to the project to have my data removed.
I understand that my data may be used in an anonymised form by the research team to support other research projects in the future, including future publications, reports or presentations.

	Initial box to agree
I consent to take part in the project on the basis set out above	

I confirm my agreement to take part in the project on the basis set out above.

Name of participant (BLOCK CAPITALS)	Date (dd/mm/yyyy)	Signature
Name of researcher (BLOCK CAPITALS)	Date (dd/mm/yyyy)	Signature

Participant Agreement Form - Elderly

Full title of project: *A Dynamic Eye Misalignment Retroversion System (DEMRS) for subjects with strabismus*

Name, position and contact details of researcher: *Constantinos Glynos, Demonstrator in Computer Animation, Faculty of Media & Communication, cglynos@bournemouth.ac.uk*

Name, position and contact details of supervisor: *Hammadi Nait-Charif, Principal Academic in Computer Animation, Faculty of Media & Communication, hncharif@bournemouth.ac.uk*

To be completed prior to data collection activity

Agreement to participate in the study

You should only agree to participate in the study if you agree with all of the statements in this table and accept that participating will involve the listed activities.

I have read and understood the Participant Information Sheet (DEMRS_PISE v1) and have been given access to the BU Research Participant Privacy Notice which sets out how we collect and use personal information (https://www1.bournemouth.ac.uk/about/governance/access-information/data-protection-privacy).
I have had the opportunity to consider the information, ask questions and have had these answered satisfactorily
I understand that my participation is voluntary. I can stop participating in research activities at any time without giving a reason and I am free to decline to answer any particular question(s).
I understand that taking part in the research will include the following activity as part of the research:
• my words may be quoted in publications, reports, web pages and other research outputs without using my real name.
I understand that, if I withdraw from the study, I will also be able to withdraw my data from further use in the study **except** where my data has been anonymised (as I cannot be identified) or it will be harmful to the project to have my data

removed.
I understand that my data may be used in an anonymised form by the research team to support other research projects in the future, including future publications, reports or presentations.

	Initial box to agree
I consent to take part in the project on the basis set out above	

I confirm my agreement to take part in the project on the basis set out above.

Name of participant (BLOCK CAPITALS)	Date (dd/mm/yyyy)	Signature
Name of researcher (BLOCK CAPITALS)	Date (dd/mm/yyyy)	Signature

Once a Participant has signed, **please sign 1 copy** and take 2 photocopies:

- Original kept in the local investigator's file
- 1 copy to be kept by the participant (including a copy of PI Sheet)

D.4 CERTIFICATE IN BASIC DIAGNOSIS OF STRABISMUS

ALEXANDROS G. DAMANAKIS
Associate Professor of Ophthalmology
University of Athens

119 Vas. Sofias Ave
Athens 11521

Te..: 2106450066
Fax.: 2106465949
al.damanakis@gmail.com

31, 8, 2020

I, Dr. Alexandros Damanakis, Prof. of Ophthalmology at the University of Athens (retired in 2015), acknowledge that, on Monday 29/12/2014 and Tuesday 30/12/2014, I trained Constantinos Glynos to diagnose strabismus to such extent that allows him to perform basic diagnosis of strabismus for the purposes of his PhD research.

ΑΛΕΞΑΝΔΡΟΣ ΔΑΜΑΝΑΚΗΣ
ΑΝ. ΚΑΘΗΓΗΤΗΣ ΟΦΘΑΛΜΟΛΟΓΙΑΣ
ΒΑΣ. ΣΟΦΙΑΣ 119 - ΤΗΛ.: 210 6450066
ΑΦΜ: 016414473 - ΔΟΥ: ΨΥΧΙΚΟΥ
ΑΜΚΑ: 21044802573

D.5 SEQUENCE OF INTERACTIONS DURING THE EVALUATION OF THE DEMRS INSTANCE

This section outlines the evaluation algorithm of each test and provides an example of the entire sequence of interactions between a subject, DEMRS instance and operator (examiner) of the DEMRS instance. Each step was recorded by the examiner and stored confidentially, and anonymously, in an external hard drive.

1. When a potential subject was found the subject was briefly informed about the research study and invited to the lab on a scheduled date and time.

2. When the subject arrived to the lab, the examiner clearly explained the nature of the study along with the tests that the subject would be asked to undergo, as part of the evaluation of the DEMRS instance. The subject received a participant information sheet and was asked to sign an informed consent form. Parents/guardians of participants that were under-age were also briefed about the nature of this study and asked to sign a guardian's consent form.

3. The subject was asked to provide a brief medical history, documented or oral, of the strabismus or any other ocular condition that was present, such as cataract, myopia and presbyopia. If the subject was wearing prescribed glasses or lenses, the subject was asked to wear them during testing.

4. The examiner proceeded in verifying normal BSV (see subsect. 6.2.1) or strabismus (see subsect. 6.2.2). If the subject's visual acuity could not allow the subject to see clearly, due to cataract for instance, the subject was dismissed from the evaluation of the DEMRS instance.

5. The subject was asked to sit on a chair in order for the examiner to measure the subject's pupillary distance. Because the evaluation tests were conducted in sequence, the subject's pupillary distance was only measured during the first test and used throughout the remaining tests.

D.5.1 *Pin Test*

1. The subject was asked to place his/her head on a medical head/chin rest and face the target, i.e. pin on the wall. Initially, the subject was

asked to view the pin without the DEMRS instance, and report the number of pins that were perceived – *"How many pins can you see?"*.

2. Depending on the type of strabismus, if any, the subject was, firstly, moved further away from the pin and, next, closer to the pin. During the transition between viewing the target at near and then at far, if the subject experienced double vision, the subject was asked to report if the pins were getting closer or moving further away from each other – *"Are the pins getting closer of further apart from each other?"*.

3. Next, the pin was placed at various directions on the wall, while the subject remained at the original location. The examiner asked the subject to report the number of pins that were perceived, at each direction – *"How many pins can you see?"*.

4. The DEMRS instance was then placed between the subject and the pin. The examiner, also the operator of the DEMRS instance, reset the device and entered the subject's pupillary distance, target position and estimated angle of the potential strabismus into the software application. The subject interacted with the DEMRS instance by viewing through the device, using the medical head/chin rest, as direct access to the device was not permitted.

5. The examiner/operator of the DEMRS instance executed retroversion via the software application, which caused the DEMRS instance to rotate the mirrors accordingly. The subject was asked to report the number of pins that were perceived – *"How many pins can you see?"*.

6. If the subject was previously able to perceive one pin but reported symptoms of double vision, when using the DEMRS instance, the following issues were considered: (a) the operator may have over-estimated or under-estimated the angle of the strabismic deviation, (b) the operator may have inaccurately measured the distance to the target, and/or (c) the operator may have inaccurately measured the pupillary distance of the subject. Consequently, the examiner/operator of the DEMRS instance adjusted the settings of the DEMRS software application and repeated retroversion. Next, the examiner repeated the previous question to the subject – *"How many pins can you see?"*.

7. The examiner/operator used the software application to change the position of the simulated fixation target, which caused the DEMRS instance to dynamically retroverse both principal vision vectors so that

they would derive from the simulated fixation target. However, the pin on the wall remained in the same position.

8. As the simulated fixation target was moved further in and away from the original position of the target, i.e. the pin, the subject was asked to report how many pins were perceived – *"How many pins can you see?"*, and if the pins were getting closer or moving further away from each other – *"Are the pins getting closer to one another?"*.

9. Next, the pin was placed at various directions on the wall. The examiner/operator adjusted the position of the simulated fixation target to match the position of the pin on the wall, so that the DEMRS instance could retroverse the visual stimuli deriving from the pin. The examiner asked the subject to report the number of pins that were perceived, at each direction – *"How many pins can you see?"*.

10. On completion of the test, the subject was asked to provide short feedback about the overall experience using the DEMRS instance, including if they experienced any symptoms – *"Did you experience any blurry vision when viewing through the device?"*, *"Did you experience any confusion or dizziness when viewing through the device?"* .

D.5.2 *Text Test*

1. The subject was asked to place his/her head on a medical head/chin rest and face the target, i.e. text printed on an A4 page. Initially, the subject was asked to read the text without the DEMRS instance, and report any symptoms of double vision – *"Can you read the sentence clearly?"*.

2. If the subject reported symptoms of double vision, moving or jumpy letters, the examiner asked the subject to report the number of repetitive letters that were perceived – *"How many times can you see each letter in the sentence?"*, and if the letter were double or blurry – *"Are the letters doubled or are they blurry?"*.

3. Depending on the type of strabismus, if any, the subject was, firstly, moved further away from the text and, next, closer to the text. During the transition between viewing the target at near and then at far, if the subject experienced symptoms of double vision, the subject was asked to report if the letters in the text were getting closer or moving further away from each other – *"Are the doubled letters getting closer of further*

apart from each other?", and if the text was becoming clearer or blurrier – *"Can you read the sentence clearly?"*.

4. The DEMRS instance was then placed between the subject and the target. The examiner, also the operator of the DEMRS instance, reset the device and entered the subject's pupillary distance, target position and estimated angle of the potential strabismus into the software application. The subject interacted with the DEMRS instance by viewing through the device, using the medical head/chin rest, as direct access to the device was not permitted.

5. The examiner/operator of the DEMRS instance executed retroversion via the software application, which caused the DEMRS instance to rotate the mirrors accordingly. The subject was asked to read the text and report any symptoms of double vision – *"Can you read the sentence clearly?"*.

6. If the subject was previously able to read the text clearly but reported symptoms of double vision, when using the DEMRS instance, the following issues were considered: (a) the operator may have over-estimated or under-estimated the angle of the strabismic deviation, (b) the operator may have inaccurately measured the distance to the target, and/or (c) the operator may have inaccurately measured the pupillary distance of the subject. Consequently, the examiner/operator of the DEMRS instance adjusted the settings of the DEMRS software application and repeated retroversion. Next, the examiner repeated the previous question to the subject – *"Can you read the sentence clearly?"*.

7. The examiner/operator used the software application to change the position of the simulated fixation target, which caused the DEMRS instance to dynamically retroverse both principal vision vectors so that they would derive from the simulated fixation target. However, the page with the pangram text remained in the same position.

8. As the simulated fixation target was moved further in and away from the original position of the target, the subject was asked to report if the letters in the text were perceived as double – *"How many times can you see each letter in the sentence?"*, and if the letters were getting closer or moving further away from each other – *"Are the doubled letters getting closer to each other?"*.

9. The examiner/operator moved the position of the simulated fixation target at various directions and, at each position, the examiner asked

the subject if the text could be read clearly – *"Can you read the sentence clearly?"*.

10. On completion of the test, the subject was asked to provide short feedback about the overall experience using the DEMRS instance, including if they experienced any symptoms – *"Did you experience any blurry vision when viewing through the device?"*, *"Did you experience any confusion or dizziness when viewing through the device?"* .

D.5.3 *Anaglyph Test*

1. The subject was asked to wear a pair of red/cyan 3D filter glasses, provided by the examiner, and place his/her head on the medical chin rest in order to view the target, i.e. anaglyph image. Initially, the subject was asked to view the anaglyph without the DEMRS instance and report whether or not the 3D illusion could be perceived – *"Can you perceive the stereo illusion?"*, *"Can you see the animal coming towards you?"*. Next, the subject was asked to describe the illusion – *"Can you describe what you see?"*.

2. If the subject reported symptoms of double vision, the examiner asked the subject to report the number of animals that were perceived – *"How many animals can you see?"*.

3. Depending on the type of strabismus, if any, the subject was, firstly, moved further away from the anaglyph and, next, closer to the anaglyph. During the transition between viewing the target at near and then at far, if the subject experienced double vision, the subject was asked to report how many animals were perceived – *"How many animals can you see?"*, and if the animals were getting closer or moving further away from each other – *"Are the animals getting closer to one another?"*

4. Next, the anaglyph image was placed at various directions, while the subject remained at the original location. The examiner asked the subject to report if the illusion was perceived, at each direction – *"Can you perceive the stereo illusion?"*.

5. The DEMRS instance was then placed between the subject and the target. The examiner, also the operator of the DEMRS instance, reset the device and entered the subject's pupillary distance, target position and estimated angle of the potential strabismus into the software application. The subject interacted with the DEMRS instance by viewing

through the device, using the medical head/chin rest, as direct access to the device was not permitted.

6. The examiner/operator of the DEMRS instance executed retroversion via the software application, which caused the DEMRS instance to rotate the mirrors accordingly. The subject was asked to to view the anaglyph through the DEMRS instance and report whether or not the 3D illusion was perceived – *"Can you perceive the stereo illusion?"*, *"Can you see the animal coming towards you?"*. Next, the subject was asked to describe the illusion – *"Can you describe what you see?"*.

7. If the subject was previously able to perceive the illusion but reported symptoms of double vision or lack of depth perception, when using the DEMRS instance, the following issues were considered: (a) the operator may have over-estimated or under-estimated the angle of the strabismic deviation, (b) the operator may have inaccurately measured the distance to the target, and/or (c) the operator may have inaccurately measured the pupillary distance of the subject. Consequently, the examiner/operator of the DEMRS instance adjusted the settings of the DEMRS software application and repeated retroversion. Next, the examiner repeated the previous questions to the subject – *"Can you perceive the stereo illusion?"*, *"Can you see the animal coming towards you?"*, *"Can you describe what you see?"*.

8. The examiner/operator used the software application to change the position of the simulated fixation target, which caused the DEMRS instance to dynamically retroverse both principal vision vectors so that they would derive from the simulated fixation target. However, the anaglyph image remained in the same position.

9. As the simulated fixation target was moved further in and away from the original position of the target, the subject was asked to report how many animals were perceived in the anaglyph image – *"How many animals can you see?"*, and if the animals were getting closer or moving further away from each other – *"Are the animals getting closer of further apart from each other?"*.

10. Next, the anaglyph image was placed at various directions. The examiner/operator adjusted the position of the simulated fixation target to match the position of the anaglyph, so that the DEMRS instance could retroverse the visual stimuli deriving from the image. The subject was asked to view the anaglyph, at each direction, and report whether or

not the 3D illusion could be perceived – *"Can you perceive the stereo illusion?"*, *"Can you see the animal coming towards you?"*.

11. On completion of the test, the subject was asked to provide short feedback about the overall experience using the DEMRS instance, including if they experienced any symptoms – *"Was the stereo illusion lost at any point during the test?"*, *"Did you experience any blurry vision when viewing through the device?"*, *"Did you experience any confusion or dizziness when viewing through the device?"* .

D.5.4 *Autostereogram Test*

1. The subject was asked to sit on a chair and place his/her head on a medical chin rest in order to view the target, i.e. autostereogram image. The examiner explained the technique that would allow the subject to perceive the illusion successfully and instructed the subject on how to perform the test.

2. Initially, the subject was asked to view each image without the DEMRS instance and report whether or not the illusion could be perceived – *"Can you make out any illusions?"*. Next, the subject was asked to describe the illusion ("hidden" shape) – *"Can you describe the shape that you see?"*.

3. If a subject with CI was not able to perceive the illusion, due to symptoms of double vision, the subject was moved further away from the autostereogram and repeated the test.

4. The DEMRS instance was then placed between the subject and the target. The examiner, also the operator of the DEMRS instance, reset the device and entered the subject's pupillary distance, target position and estimated angle of the potential strabismus into the software application. Also, the examiner asked the subject if the image was seen clearly – *"Can you clearly see the autostereogram image?"*. The subject interacted with the DEMRS instance by viewing through the device, using the medical head/chin rest, as direct access to the device prohibited.

5. The examiner/operator of the DEMRS instance executed retroversion via the software application, which caused the DEMRS instance to rotate the mirrors accordingly. The subject was asked to to view the autostereogram through the DEMRS instance and report whether or not the illusion was perceived – *"Can you make out any illusions?"*. Next, the

subject was asked to describe the illusion ("hidden" shape) – *"Can you describe the shape that you see?"*.

6. The examiner/operator used the software application to change the position of the simulated fixation target, which caused the DEMRS instance to dynamically retroverse both principal vision vectors so that they would derive from the simulated fixation target. However, the autostereogram image remained in the same position.

7. As the simulated fixation target was moved further in and away from the original position of the target, the subject was asked to report if the illusion was perceived and, if so, when did the illusion get lost – *"Can you make out any illusions?"*, *"Is the illusion lost?"*.

8. If the subject was previously able to perceive the illusion but couldn't perceive it when using the DEMRS instance, the following issues were considered: (a) the operator may have over-estimated or under-estimated the angle of the strabismic deviation, (b) the operator may have inaccurately measured the distance to the target, and/or (c) the operator may have inaccurately measured the pupillary distance of the subject. Consequently, the examiner/operator of the DEMRS instance adjusted the settings of the DEMRS software application and repeated retroversion. Next, the examiner repeated the previous questions to the subject – *"Can you make out any illusions?"*, *"Can you describe the shape that you see?"*.

9. If the subject was able to successfully perceive the illusion through the DEMRS instance, the subject was asked to move away from the device for a short period of time. Next, the subject was asked to view the autostereogram using the DEMRS instance, which remained in the previously retroverted state that allowed the subject to perceive the illusion. The subject was asked to report whether or not the illusion could still be perceived – *"Can you still see the illusion?"*.

10. Next, the autostereogram was placed at various directions. The examiner/operator adjusted the position of the simulated fixation target to match the position of the autostereogram, so that the DEMRS instance could retroverse the visual stimuli deriving from the image. The examiner asked the subject if the image was seen clearly at every direction – *"Can you clearly see the autostereogram image?"*. The subject was asked to view the autostereogram, at each direction, and report whether or not the illusion was perceived while the examiner/operator used the

software application to reposition the simulated fixation target through the physical location of the autostereogram in order for the DEMRS instance to retroverse the vision vectors as required by the technique to perceive the illusion – *"Can you make out any illusions?"*.

11. On completion of the test, the subject was asked to provide short feedback about the overall experience using the DEMRS instance, including if they experienced any symptoms – *"Did you experience any blurry vision when viewing through the device?"*, *"Did you experience any confusion or dizziness when viewing through the device?"* .

E

APPENDIX Z: A DAY WITH STRABISMUS

Dear reader,

I decided to informally write this short article so that I can share my experience living with strabismus, and potentially provide you with some insights about this condition. I was born with extreme esotropia in the left eye. The deviation was so large that it risked permanent blindness in the left eye, should it remained untreated. I underwent my first surgery at the age of 2, in order to correct the misalignment. Unfortunately, the surgery was not successful, and the deviation turned into extreme exotropia. Around the age of 8 I underwent another corrective surgery, where Dr. Alexandros Damanakis successfully brought my left eye near the primary position of gaze; but not near enough so that I could accomplish binocularity.

As a child I always considered it a fun game to lie about my visual acuity, or perform various tricks with my eyes, during a diagnosis session. My goal was to mislead and confuse the doctor, just so that I could silently laugh at their puzzled facial expressions. Although, sabotaging a diagnosis with such games might have contributed to an unsuccessful surgery, can doctors really blame a young child for trying to entertain himself? Currently, I am diagnosed with constant incomitant moderate exotropia on the left eye (bad eye). Unfortunately, a myth, whereby only two, or three, operations should be performed in strabismus, discouraged my parents from proceeding with another surgery. According to strabismologists, a person can safely undergo as many surgeries as required in order to correct strabismus.

Much like other children with strabismus, I went through vision exercises, eye patching and other therapies. Although, I used such therapeutic exercises as an excuse to get out of doing my homework, eye patching forced me to see with my bad eye. Hint to parents and doctors; we tend to rip off our eye patches the moment we leave the house, so that we don't look like pirates or have to endure other people's curious stare. Also, if we are unable to remove the patch, say for example when our parents have called the school and requested that we are monitored at all times so that we keep the eye patch on, we may come up with fictional stories about how we got into a Holywood-like accident. Anyhow, eye patching was quite effective, because

I learned to intentionally alternate my fixation. In early adulthood I trained myself to align both eyes, imitating normal vision, so that I could pose for a decent picture without relying on compensatory head postures (CHP). I accomplished alignment of both eyes by alternating my vision as fast as possible until I was able to control the orientation of my bad eye while fixating with the good eye. For the curious readers, a video of this alignment can be viewed at https://bitbucket.org/cglynos/demrs/scrapbook/pseudo-normal.mp4. However, being an adult, i.e. not within the critical period, and due to hypermetropia, developed on the left eye as a consequence of strabismus, I cannot achieve normal binocular single vision when I align both eyes.

MY DAY WITH STRABISMUS Begins when I wake up, and prepare for work. I look at the bathroom mirror, and my strabismus is there... Sometimes, while washing up, I throw a bit of extra water in my eye, hoping it corrects the misalignment. As a kid I used to push my eye with my finger, but that method never worked. Oh well; It's just another day, and a reminder for I am still different.

Preparing breakfast is not a challenge. The trick is always to perform tasks with a perspective view of the environment. Due to the lack of depth perception, I rely on various familiarity cues to estimate depth, ex. shadows, textures, relative sizes, etc. In simpler terms, no cues means no depth. For example, it is quite certain that if I pour coffee into a mug, at eye level, I will spill. The cup must be lower than the eyes, so that I can calculate how far the cup is by using the shape of cup's rim. Also, the coffee must be poured from a perspective angle, so that I can measure the distance between the cup and the kettle by contrasting their shapes and relative sizes. It may sound tiresome, but most people with my condition almost never use such cues voluntarily on a daily basis. We rely on the most powerful cue there is; experience. Along with familiarity cues, we perform tasks based on previous experiences, or we try to incorporate similar experiences from the past to new tasks.

I enter my beloved car, and drive off to work. Driving is easy. The perspective of the road, lane markings, other cars, buildings, pedestrians, etc., betray depth very accurately. There is only one thing that can confuse me while driving, and fortunately it is subconsciously ignored. It is called abnormal retinal correspondence (ARC). I first noticed this effect when I was an undergraduate student flying back home for the holidays. When the airplane landed, I leaned my head on the window in order to enjoy the view of the airfield. However, as the airplane drove towards the gate, I was able to perceive objects in the airfield, such as cones and signs, that were not yet

visible to me. The objects became visible only after the airplane passed by them and I could see them with my good eye. I was getting the sensation that I could see through the cabin wall, which gave me a mild panic attack. My right (good) eye was looking straight ahead outside the window, while my left eye deviated outwards. So, how could I perceive an object that was occluded by the cabin wall on the right side of the window? I try to illustrate this effect in figure 182.

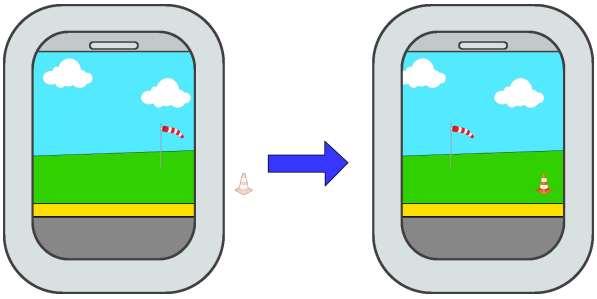

Figure 182: *View from the normal eye: ARC is noticeable in the first picture because the cone is perceived even when it is occluded by the wall of the airplane. As the airplane moves, the cone appears within the visual field of the normal eye.*

Although I didn't know the correct term back then, this is how I noticed ARC for the first time. ARC is noticeable while driving too. There have been several occasions where I have perceived pedestrians waiting to cross the street, but were not visible at the time as they were occluded by the sidebar of the windscreen (see fig. 183).

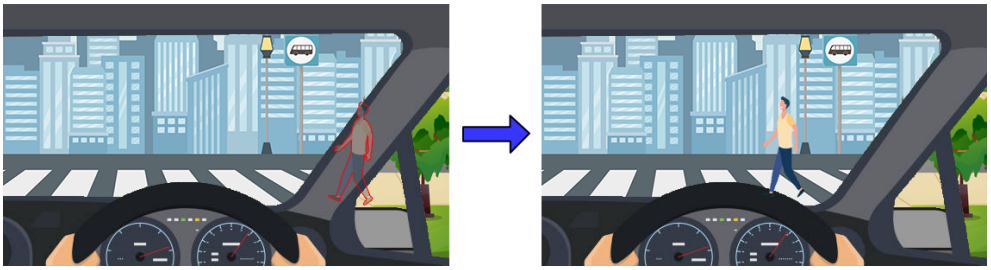

Figure 183: *View from the normal eye: ARC is noticeable in the first picture because the pedestrian is perceived even when they are occluded by the sidebar of the windscreen. The pedestrian becomes visible when crossing the street.*

The way I experience ARC in my daily routine, is how I designed the partial-occlusion test (see subsect. 3.2.4).

I always arrive at work a bit early so that I can find a parking spot near the main entrance. Parking is also very easy for me, as long as I park from a perspective. I remember my driving instructor used to say "You need to align in parallel with the other car, before you reverse, so that you can park properly". That technique never worked for me, because positioning my car parallel to another car reduced my perspective view. Therefore, I

had difficulties estimating the distances between my car, the parking space and the other car. However, when I align the car in a perspective angle, I can estimate depth accurately and park with ease. I look at the rear-view mirror, and my strabismus is still there...

Working for a large-scale institution, or company, means that I get to meet new people almost every day. I am both, excited and a bit hesitant, to meet new people. I greet someone, and wait for the moment their eyes meet mine. That's when their eyes start bouncing from left to right, trying to figure out where I am staring. It is hilarious and stressful at the same time. Hint for everyone who has met a person with strabismus; we know when you realize our eyes are not aligned, and we appreciate your discretion. But please, when you figure it out, don't continue to stare both eyes; just fixate on the one that's looking at you.

Lunch time has arrived, and sometimes one of my colleagues would suggest a game of table tennis. I love sports, but tennis and table tennis are my worst. The sole reason is because I get to play well up until the point my opponent realizes that I miss all high balls. And why is that? You probably guessed it right; there is no perspective and no cues when a small-size ball falls from above. Therefore, it is not possible for me to estimate depth. In tennis, I would see a bright blue sky and a yellow ball, which is so small that its relative size cannot be used to estimate its distance from myself. In table tennis, I would see a beautifully painted white ceiling and a tiny white-ish ball. I try to smile when losing, even though I burn inside. But, my patience is truly tested when my opponent approaches me, with a huge smile, in order to shake my hand and say "good game". Lunch time is over, and I head back to my office.

The benefit of fixating with either eye is that I can work for longer hours without getting tired. My job as a software engineer requires that I spend a considerable amount of time in front of a monitor. It is only natural that, after some time, my eyes would start to hurt. That is no problem for me; I alternate, and fixate with the left while the right takes a nice rest. The only downside is that, due to a hypermetropia in the left eye, I have to focus harder when fixating with my left eye and, therefore, cannot last as long as I would if I were to fixate with my right eye. By the time I get tired of using my left eye, my right eye is rested and ready for more work. I have used this technique several times while writing this thesis.

Time to clock out. After work, I usually go to the gym, play football, or train in muay thai. Unlike other sports, I welcome football and muay-thai any day of the week. Muay-thai is slightly harder, because estimating the distance between myself and my opponent can be problematic when I am

in guard, or blocking. Football is easier because of the perspective provided by the pitch lines, and relative sizes of other players. Also, because the ball is quite large, I can use its relative size to determine the ball's distance from myself. The match is over and we won.

I drive back home, take a shower, have dinner, sit back and relax. Thankfully, the tasks that I perform at home do not require me to use cues, because the layout of the apartment, furniture, and other items, are stored within my experience. Before I turn in, I set the alarm, and turn off my phone. For a split second I see my reflection on the screen of my phone, and my strabismus is still there...

I have dedicated this research to children born with strabismus, because I know what they will probably have to go through if their strabismus remains untreated.

Constantinos M. Glynos

BIBLIOGRAPHY

A.B. Somani R., Hutnik C., F.X. DeSouza J., Tweed D., Nicolle D. and Vilis T., 1998. *"Using a synoptophore to test Listing's law during vergence in normal subjects and strabismic patients"*. *Vision Research*, **38**(22), 3621–3631.

Adler P., 2002. *"Efficacy of treatment for convergence insufficiency using vision therapy"*. *Ophthalmic and Physiological Optics*, **22**(6), 565–571.

Adobe , 2021. *"Blending modes"*. https://helpx.adobe.com/photoshop/using/blending-modes.html. Date Accessed: 03/04/2021.

Agrawal S., 2019. *"Strabismus For every Ophthalmologist"*. Elsevier, 1st edition.

Ahn S. J., Yang H. K. and Hwang J.-M., 2012. *"Binocular Visual Acuity in Intermittent Exotropia: Role of Accommodative Convergence"*. *American Journal of Ophthalmology*, **154**(6), 981 – 986.e3.

Al-Rahayfeh A. and Faezipour M., 2013. *"Eye Tracking and Head Movement Detection: A State-of-Art Survey"*. *IEEE Journal of Translational Engineering in Health and Medicine*, **1**, 2100212 –2100212.

Ancona C., Stoppani M., Odazio V., La Spina C., Corradetti G. and Bandello F., Nov 2014. *"Stereo tests as a screening tool for strabismus: which is the best choice?"*. *Clinical ophthalmology (Auckland, N.Z.)*, **8**, 2221–2227. PMC4235497[pmcid].

Ansons A. M. and Davis H., 2014. *"Diagnosis and Management of Ocular Motility Disorders"*. John Wiley & Sons, Ltd, 4th edition.

Aouchiche K. and Dankner S. R., 1988. *"What's the Difference? Krimsky vs Alternate Cover Testing"*. *American Orthoptic Journal*, **38**(1), 148–150.

Arduino , 2019. *"Arduino Uno Rev3"*. https://store.arduino.cc/arduino-uno-rev3. Date Accessed: 26/04/2019.

Arnoldi K. A., 1999. *"Convergence Excess: Characteristics and Treatment"*. *American Orthoptic Journal*, **49**(1), 37–47.

Astapenko E. M., 2019. *"Clinical Evaluation"*. http://www.imdrf.org/docs/imdrf/final/technical/imdrf-tech-191010-mdce-n56.pdf. IMDRF MDCE WG/N56FINAL:2019 (formerly GHTF/SG5/N2R8:2007).

Awadein A., Sharma M., Bazemore M. G., Saeed H. A. and Guyton D. L., 2008. *"Adjustable suture strabismus surgery in infants and children"*. *Journal of American Association for Pediatric Ophthalmology and Strabismus*, **12**(6), 585–590.

Aziz S., Cleary M., Stewart H. K. and Weir C. R., 2006. *"Are Orthoptic Exercises an Effective Treatment for Convergence and Fusion Deficiencies?"*. *Strabismus*, **14**(4), 183–189.

Babinsky E., Sreenivasan V. and Candy T. R., Jan 2015. *"Near heterophoria in early childhood"*. *Investigative ophthalmology & visual science*, **56**(2), 1406–1415. PMC4340430[pmcid].

Bailey I. and Lovie J., November 1976. *"New design principles for visual acuity letter charts"*. *American journal of optometry and physiological optics*, **53**(11), 740—745.

Baker D. H., Meese T. S. and Hess R. F., 2008. *"Contrast masking in strabismic amblyopia: Attenuation, noise, interocular suppression and binocular summation"*. *Vision Research*, **48**(15), 1625 – 1640.

Barlow H. B., Blakemore C. and Pettigrew J. D., Jan 1967. *"The neural mechanism of binocular depth discrimination"*. *The Journal of Physiology*, **193**(2), 327–342.

Barry R. J. and Denniston A. K., 2017. *"yoke muscles"*.

Bateman J. B. and Isenberg S. J. 2013. 1 – 19. *"Chapter 139 - Strabismus*. In Rimoin D., Pyeritz R. and Korf B., editors, *Emery and Rimoin's Principles and Practice of Medical Genetics*, Academic Press.

Beauchamp G. R., Black B. C., Coats D. K., Enzenauer R. W., Hutchinson A. K., Saunders R. A., Simon J. W., Stager D. R., Stager D. R., Wilson M., Zobal-Ratner J. and Felius J., 2003. *"The management of strabismus in adults—I. clinical characteristics and treatment"*. *Journal of American Association for Pediatric Ophthalmology and Strabismus*, **7**(4), 233 – 240.

Benjamin W. J. and Borish I. M., 2006. *"Borish's Clinical Refraction"*. Butterworth-Heinemann, 2nd edition.

Bérard P., Bradley D., Nitti M., Beeler T. and Gross M., nov 2014. *"High-Quality Capture of Eyes"*. *ACM Trans. Graph.*, **33**(6).

Berryman A., Rasavage K., Politzer T. and Gerber D., 2020. *"Oculomotor Treatment in Traumatic Brain Injury Rehabilitation: A Randomized Controlled*

Pilot Trial". *The American journal of occupational therapy: official publication of the American Occupational Therapy Association*, **74**(1), 740118505op1–740118505op7. 32078510[pmid].

Bielschowsky A., 08 1934. *"Divergence Excess"*. *Archives of Ophthalmology*, **12** (2), 157–166.

Billson F., 2003. *"Strabismus: Fundamentals of Clinical Opthalmology"*. Fundamentals of Clinical Opthalmology. Wiley.

Bohr I. and Read J. C. A., 12 2013. *"Stereoacuity with Frisby and Revised FD2 Stereo Tests"*. *PLOS ONE*, **8**(12), 1–12.

Bowers B., 2001. *"Sir Charles Wheatstone FRS, 1802-1875"*. Institution of Engineering and Technology, 2nd edition.

Brodsky M. C., 09 1999. *"Dissociated Vertical Divergence: A Righting Reflex Gone Wrong"*. *Archives of Ophthalmology*, **117**(9), 1216–1222.

Brodsky M. C., 2007. *"Dissociated horizontal deviation: clinical spectrum, pathogenesis, evolutionary underpinnings, diagnosis, treatment, and potential role in the development of infantile esotropia"*. *Transactions of the American Ophthalmological Society*, **105**, 272–293. 18427617[pmid].

Brodsky M. C., 2016. *"Pediatric Neuro-Ophthalmology"*. Springer-Verlag, 3rd edition.

Brodsky M. C. and Fray K. J., Dec 2007. *"Dissociated Horizontal Deviation After Surgery for Infantile Esotropia: Clinical Characteristics and Proposed Pathophysiologic Mechanisms"*. *Archives of Ophthalmology*, **125**(12), 1683–1692.

Brodsky M. C., Gräf M. H. and Kommerell G., Aug 2005. *"The Reversed Fixation Test: A Diagnostic Test for Dissociated Horizontal Deviation"*. *Archives of Ophthalmology*, **123**(8), 1083–1087.

Brodsky M. C. and Tusa R. J., 02 2004. *"Latent Nystagmus: Vestibular Nystagmus With a Twist"*. *Archives of Ophthalmology*, **122**(2), 202–209.

Brown S., Weih L., Mukesh N., McCarty C. and Taylor H., 2001. *"Assessment of adult stereopsis using the Lang 1 Stereotest: a pilot study"*. *Binocular vision & strabismus quarterly*, **16**(2), 91—98.

Bui Quoc E. and Milleret C., 09 2014. *"Origins of strabismus and loss of binocular vision. Frontiers in integrative neuroscience*, **8**, 71.

Campos E., 1995. *"Amblyopia - Major Review"*. *Survey of Ophthalmology*, **40** (1), 23 – 39.

Campos E. C., 1986. *"Sensory and sensori-motor adaptations in strabismus: Their role in space perception"*. *Acta Psychologica*, **63**(3), 281 – 295.

Capo H., Roth E., Johnson T., Munoz M. and Siatkowski R. M., 1996. *"Vertical Strabismus after Cataract Surgery"*. *Ophthalmology*, **103**(6), 918–921.

Carruthers J., 09 1995. *"The treatment of congenital nystagmus with Botox"*. *Journal of pediatric ophthalmology and strabismus*, **32**, 306–308.

Carter B. T. and Luke S. G., 2020. *"Best practices in eye tracking research"*. *International Journal of Psychophysiology*, **155**, 49–62.

Carvelho T., Allison R. S., Irving E. L. and Herriot C., 2008. *"Computer gaming for vision therapy"*. *Virtual Rehabilitation*, 198–204.

Charman W. N., 2008. *"The eye in focus: accommodation and presbyopia"*. *Clinical and Experimental Optometry*, **91**(3), 207–225.

Chen A. H. and Aziz A., Jan 2003. *"Heterophoria in young adults with emmetropia and myopia"*. *The Malaysian journal of medical sciences : MJMS*, **10**(1), 90–94. PMC3557116[pmcid].

Chennamma H. R. and Yuan X., 2013. *"A Survey on Eye-Gaze Tracking Techniques"*. *ArXiv*, **abs/1312.6410**.

Christiansen S. P., Antunes-Foschini R. S. and McLoon L. K., Nov 2010. *"Effects of recession versus tenotomy surgery without recession in adult rabbit extraocular muscle"*. *Investigative ophthalmology & visual science*, **51**(11), 5646–5656. 20538996[pmid].

Clarke A. H., Ditterich J., Drüen K., Schönfeld U. and Steineke C., Nov 2002. *"Using high frame rate CMOS sensors for three-dimensional eye tracking"*. *Behavior Research Methods, Instruments, & Computers*, **34**(4), 549–560.

Clarkson J. 2008. 165 – 198. *"HUMAN CAPABILITY AND PRODUCT DESIGN"*. In Schifferstein H. N. and Hekkert P., editors, *Product Experience*, Elsevier.

Components101 , 2019. *"28BYJ-48 Stepper Motor Pinout Wiring, Specifications, Uses Guide & Datasheet"*. https://components101.com/motors/28byj-48-stepper-motor. Date Accessed: 19/05/2019.

Constable P. A., Bach M., Frishman L. J., Jeffrey B. G. and Robson A. G., Feb 2017. *"ISCEV Standard for clinical electro-oculography (2017 update)"*. *Documenta ophthalmologica. Advances in ophthalmology*, **134**(1), 1–9. 28111038o[pmid].

contributors W., 2021. *"Autostereogram — Wikipedia, The Free Encyclopedia"*. https://en.wikipedia.org/w/index.php?title=Autostereogram&oldid=999732112. Date Accessed: 19/02/2021.

Cooper J., Ciuffreda K. J. and Kruger P. B., 1982. *"Stimulus and response AC/A ratios in intermittent exotropia of the divergence-excess type"*. *British Journal of Ophthalmology*, **66**(6), 398–404.

Cooper J. and Record C. D., Jan 1986. *"Suppression and retinal correspondence in intermittent exotropia"*. *British Journal of Ophthalmology*, **70**(9), 673–676.

Cooper J., 1988. *"Review of Computerized Orthoptics with Specific Regard to Convergence Insufficiency"*. *Optometry and Vision Science*, **65**(6), 455–463.

Cooper J. and Jamal N., April 2012. *"Convergence insufficiency - a major review"*. *Optometry (St. Louis, Mo.)*, **83**(4), 137–158.

Cooper J. S., 2007. *"Computerized Vision Therapy for Home and Office Treatment of Accommodative & Vergence Disorders, & Amblyopia"*. *Journal of Behavioral Optometry*, **18**(4), 88–93.

Cooper J. S. and Duckman R., 1978. *"Convergence insufficiency: incidence, diagnosis, and treatment"*. *Journal of the American Optometric Association*, **49**(6), 673–680.

Coussens T. and Ellis F. J., 2015. *"Considerations on the etiology of congenital Brown syndrome"*. *Current Opinion in Ophthalmology*, **26**(5).

Covington B. P. and Al Khalili Y., 2020. *"Neuroanatomy, Nucleus Lateral Geniculate"*. *StatPearls*.

Crawford L. J. and Griffiths H., 2015. *"The repeatability of the Sbisa bar for testing density of suppression"*. *The British and Irish orthoptic journal*, **12**, 35–40.

Damanakis A., 2013. *"Binocular vision and strabismus"*. Personal Interview with Prof. A. Damanakis (M.D.), 31 December 2013.

Damanakis A., 2014a. *"Methods for Testing and Diagnosing Strabismus"*. Personal Interview with Prof. A. Damanakis (M.D.), 26 December 2014.

Damanakis A., 2014b. *"Methods to estimate the target of a strabismus patient"*. Personal Interview with Prof. A. Damanakis (M.D.), 27 December 2014.

Damanakis A. G., 2005. *"Στραβισμοί και οφθαλμοκίνητες διαταραχές [Strabismus and oculomotor disturbances]"*. Medical Books Litsas, 2nd edition.

Damanakis A. G., 2011. *"Διάθλαση [Refraction]"*. Medical Books P.CH. Paschalidis.

Danchaivijitr C. and Kennard C., 2004. *"Diplopia and eye movement disorders"*. *Journal of Neurology, Neurosurgery & Psychiatry*, **75**(suppl 4), iv24–iv31.

Daum K. M., 1984. *"Divergence Excess: Characteristics and Results of Treatment with Orthoptics"*. *Ophthalmic and Physiological Optics*, **4**(1), 15–24.

De Bock F., Braun V. and Renz-Polster H., 2017. *"Deformational plagiocephaly in normal infants: a systematic review of causes and hypotheses"*. *Archives of Disease in Childhood*, **102**(6), 535–542.

de la Malla C., Buiteman S., Otters W., Smeets J. B. J. and Brenner E., 07 2016. *"How various aspects of motion parallax influence distance judgments, even when we think we are standing still"*. *Journal of Vision*, **16**(9), 8–8.

de Lahunta A. and Glass E. 2009. 319 – 347. *"Chapter 12 - Vestibular System: Special Proprioception"*. In de Lahunta A. and Glass E., editors, *Veterinary Neuroanatomy and Clinical Neurology (Third Edition)*, W.B. Saunders.

Dedes V., 2016. *"Controlled rotations using servo motors"*. Personal Interview with V. Dedes, 26 August 2016.

Deepa B., Valarmathi A. and Benita S., 2019. *"Assessment of stereo acuity levels using random dot stereo acuity chart in college students"*. *Journal of Family Medicine and Primary Care*, **8**(12), 3850–3853.

Dictionary C. E., 2021. *"Definition of retroversion"*. https://www.dictionary.com/browse/retroversion. Date Accessed: 03/05/2021.

Dolman P., 1919. *"The Maddox Rod Screen Test"*. *Transactions of the American Ophthalmological Society*, **17**, 235–249. 16692471[pmid].

Dorhman S. S., Mar 2015. *"Bruckner Testing"*. https://www.eyedolatryblog.com/2015/03/bruckner-testing.html. Date Accessed: 13/02/2021.

Duane A., 02 1932. *"DIPLOPIA AND OTHER DISORDERS OF BINOCULAR PROJECTION"*. *Archives of Ophthalmology*, **7**(2), 187–210.

Duchowski A. T., 2017. *"Serious gaze"*. In *2017 9th International Conference on Virtual Worlds and Games for Serious Applications (VS-Games)*, 276–283.

E-Meoly , 2018. *"Mini Nylon Ball Transfer Bearing Unit Table Conveyor Roller Ball"*. https://www.amazon.co.uk/gp/product/B06XHH3PSS/ref=ppx_yo_dt_b_asin_title_o01_s00?ie=UTF8&psc=1. Date Accessed: 04/07/2018.

Economides J. R., Adams D. L. and Horton J. C., 2012. *"Perception via the Deviated Eye in Strabismus"*. *Journal of Neuroscience*, **32**(30), 10286–10295.

Economides J. R., Adams D. L. and Horton J. C., 2014. *"Eye Choice for Acquisition of Targets in Alternating Strabismus"*. *Journal of Neuroscience*, **34**(44), 14578–14588.

Economides J. R., Adams D. L. and Horton J. C., Jan 2016. *"Variability of Ocular Deviation in Strabismus"*. *JAMA ophthalmology*, **134**(1), 63–69. PMC4713272[pmcid].

Edmund Optics , 2019a. *"45° AOI, 101x127mm, Cold Mirror: Edmund Optics"*. https://www.edmundoptics.co.uk/p/45deg-aoi-101-x-127mm-cold-mirror/19164/. Date Accessed: 18/05/2019.

Edmund Optics , 2019b. *"Fixed Filter Mounts: Edmund Optics"*. https://www.edmundoptics.com/f/fixed-filter-mounts/11776/. Date Accessed: 21/05/2019.

Edmund Optics , 2021a. *"Uncoated Double-Concave (DCV) Lenses"*. https://www.edmundoptics.co.uk/f/uncoated-double-concave-dcv-lenses/12020/. Date Accessed: 03/05/2021.

Edmund Optics , 2021b. *"Uncoated Double-Convex (DCX) Lenses"*. https://www.edmundoptics.co.uk/f/uncoated-double-convex-dcx-lenses/12004/. Date Accessed: 03/05/2021.

Engle E. C., Mar 2006. *"The Genetic Basis of Complex Strabismus"*. *Pediatric Research*, **59**(3), 343–348.

Erkelens C. J. and van Ee R., 2002. *"The role of the cyclopean eye in vision: sometimes inappropriate, always irrelevant"*. *Vision Research*, **42**(9), 1157 – 1163.

Erkkilä H., Lindberg L. and Kallio A.-K., 1996. *"Strabismus in children with cerebral palsy"*. *Acta Ophthalmologica Scandinavica*, **74**(6), 636–638.

Eskridge J. B., Wick B. and Perrigin D., September 1988. *"The Hirschberg test: a double-masked clinical evaluation"*. *American journal of optometry and physiological optics*, **65**(9), 745–750.

Esposito Veneruso P., Bruzzese D. and Magli A., 09 2018. *"Long-term development of refractive error in refractive, nonrefractive and partially accommodative esotropia"*. *PLOS ONE*, **13**(9), 1–13.

Evans B. J. W., 2007. *"Monovision: a review"*. *Ophthalmic and Physiological Optics*, **27**(5), 417–439.

Fawcett S. L., Stager D. R. and Felius J., 2004. *"Factors influencing stereoacuity outcomes in adults with acquired strabismus"*. *American Journal of Ophthalmology*, **138**(6), 931 – 935.

Frank J. W., France T. D. and Harrington J., 1981. *"The Worth Four Dot Test: Is it Really "Worthless"?"*. *American Orthoptic Journal*, **31**(1), 68–71.

Frantz K., Cotter S. and Wick B., October 1992. *"Re-evaluation of the four prism diopter base-out test"*. *Optometry and vision science : official publication of the American Academy of Optometry*, **69**(10), 777—786.

Fray K. J., 2017. *"Fusional Amplitudes: Developing Testing Standards"*. *Strabismus*, **25**(3), 145–155. PMID: 28759298.

Friedman D., Repka M., Katz J., Giordano L., Ibironke J., Hawse P. and Tielsch J., 11 2009. *"Prevalence of Amblyopia and Strabismus in White and African American Children Aged 6 through 71 Months. The Baltimore Pediatric Eye Disease Study"*. *Ophthalmology*, **116**(11), 2128–2134.e2.

Furman J. 2014. 687. *"Optokinetic Nystagmus"*. In Aminoff M. J. and Daroff R. B., editors, *Encyclopedia of the Neurological Sciences (Second Edition)*, Academic Press.

Garnham L. and Sloper J. J., 2006. *"Effect of age on adult stereoacuity as measured by different types of stereotest"*. *British Journal of Ophthalmology*, **90**(1), 91–95.

Gawęcki M., Jan 2020. *"Adjustable Versus Nonadjustable Sutures in Strabismus Surgery - Who Benefits the Most?"*. *Journal of clinical medicine*, **9**(2), 292. 31973012[pmid].

Georgievski Z., 1995. *"Synoptophore versus prism and cover test measurements in strabismus.: A question of instrument convergence?"*. *Strabismus*, **3**(2), 71–77.

Georgievski Z., Sleep M. and Koklanis K., 2007. *"Simulated torsional disparity disrupts horizontal fusion and stereopsis"*. *Journal of American Association for Pediatric Ophthalmology and Strabismus*, **11**(2), 120 – 124.

Giannikakis S., 2008. *"Eye anatomy and structure"*. Personal Interview with S. Giannikakis (M.D.), 18 December 2008.

Giaschi D., Narasimhan S., Solski A., Harrison E. and Wilcox L. M., 2013. *"On the typical development of stereopsis: Fine and coarse processing"*. *Vision Research*, **89**, 65–71.

Glynos C. M., Aina O. O. and Nait-Charif H., Oct 2016. *"Dynamic Eye Misalignment Retroversion System (DEMRS)"*. In *2016 IEEE Applied Imagery Pattern Recognition Workshop (AIPR)*, Washington DC, USA. 1–7.

Glynos C. M., Aina O. O. and Nait-Charif H., Nov 2019. *"Dynamic Eye Misalignment Retroversion System (DEMRS)"*. *Medical Systems (Submitted)*.

Glynos C. M., Glynos M. C., Aina O. O. and Nait-Charif H., 2019. *"Assessing the Efficacy of the Dynamic Eye Misalignment Retroversion System (DEMRS) Prototype with Normal and Strabismus Subjects"*. In *Proceedings of the 2019 4th International Conference on Biomedical Imaging, Signal Processing*, ICBSP '19, New York, NY, USA. Association for Computing Machinery, 39–46.

Godts D., Trau R. and Tassignon M.-J., 2006. *"Effect of refractive surgery on binocular vision and ocular alignment in patients with manifest or intermittent strabismus"*. *British Journal of Ophthalmology*, **90**(11), 1410–1413.

Goldchmit M., Felberg S. and Souza-Dias C., 2003. *"Unilateral anterior transposition of the inferior oblique muscle for correction of hypertropia in primary position"*. *Journal of American Association for Pediatric Ophthalmology and Strabismus*, **7**(4), 241 – 243.

Goldrich S., January 1980. *"Optometric therapy of divergence excess strabismus"*. *American journal of optometry and physiological optics*, **57**(1), 7—14.

Goodman L. K., Black J. M., Phillips G., Hess R. F. and Thompson B., 2011. *"Excitatory binocular interactions in two cases of alternating strabismus"*. *Journal of American Association for Pediatric Ophthalmology and Strabismus*, **15**(4), 345 – 349.

Grosvenor T., March 1978. *"Etiology of astigmatism"*. *American journal of optometry and physiological optics*, **55**(3), 214—218.

Guo D.-d., Wu J.-f., Hu Y.-y., Sun W., Lv T.-l., Jiang W.-j., Wu H., Wang X.-r., Jonas J. B. and Bi H.-s., 07 2016. *"Stereoacuity and Related Factors: The Shandong Children Eye Study"*. *PLOS ONE*, **11**(7), 1–13.

Haines D. E. and Mihailoff G. A., 2018. *"Fundamental Neuroscience for Basic and Clinical Applications"*. Elsevier.

Hainline L., Riddell P., Grose-Fifer J. and Abramov I., 1992. *"Development of accommodation and convergence in infancy"*. *Behavioural Brain Research*, **49** (1), 33 – 50. Normal and Abnormal Visual Development in Infants and Children.

Hammond C., 2014. *"The potential use and threats of a Dynamic Eye Misalignment Retroversion System in Strabismus"*. Personal Interview with Prof. C. Hammond (M.D.), 20 March 2014.

Hansard M. and Horaud R., 2010. *"Cyclorotation Models for Eyes and Cameras"*. *IEEE Transactions on Systems, Man, and Cybernetics, Part B (Cybernetics)*, **40** (1), 151–161.

Hansen A. K., 09 1954. *"AFTER-IMAGE TRANSFER TEST IN ANOMALOUS RETINAL CORRESPONDENCE"*. *A.M.A. Archives of Ophthalmology*, **52**(3), 369–374.

Haro A., Essa I. and Flickner M., 2000. *"A Non-Invasive Computer Vision System for Reliable Eye Tracking"*. In *CHI '00 Extended Abstracts on Human Factors in Computing Systems*, CHI EA '00, New York, NY, USA. Association for Computing Machinery, 167–168.

Haslwanter T., 1995. *"Mathematics of three-dimensional eye rotations"*. *Vision Research*, **35**(12), 1727–1739.

Hatt S. R., Wang X. and Holmes J. M., Nov 2015. *"Interventions for dissociated vertical deviation"*. *The Cochrane database of systematic reviews*, **11**(11), CD010868–CD010868. 26587695[pmid].

Havertape S., Cruz O. and Chu F., 11 2001. *"Sensory strabismus - Eso or Exo?"*. *Journal of pediatric ophthalmology and strabismus*, **38**, 327–30; quiz 354.

Helveston E. M., 1973. *"Cyclic Strabismus"*. *American Orthoptic Journal*, **23**(1), 48–51.

Helveston E. M., Mar 2010. *"Understanding, detecting, and managing strabismus"*. *Community eye health*, **23**(72), 12–14.

Hendrickson A. 2009. 327 – 334. *"Fovea: Primate"*. In Squire L. R., editor, *Encyclopedia of Neuroscience*, Academic Press.

Hepworth L., Rowe F., Walker M., Rockliffe J., Noonan C., Howard C. and Currie J., 2015. *"Post-stroke visual impairment: a systematic literature review of types and recovery of visual conditions"*. *Ophthalmology Research: An International Journal*, **5**.

Hibbard P. B., Haines A. E. and Hornsey R. L., 2017. *"Magnitude, precision, and realism of depth perception in stereoscopic vision"*. *Cognitive research: principles and implications*, **2**(1), 1–11.

Hiles D. A., Davies G. T. and Costenbader F. D., 10 1968. *"Long-Term Observations on Unoperated Intermittent Exotropia"*. *Archives of Ophthalmology*, **80** (4), 436–442.

Hochberg J., 1964. *"Depth Perception Loss with Local Monocular Suppression: A Problem in the Explanation of Stereopsis"*. *Science*, **145**(3638), 1334–1336.

Holmes J. M., Leske D. A., Hatt S. R., Brodsky M. C. and Mohney B. G., 2011. *"Stability of near stereoacuity in childhood intermittent exotropia"*. *Journal of American Association for Pediatric Ophthalmology and Strabismus*, **15**(5), 462 – 467.

Holmes J. M., Leske D. A. and Hohberger G. G., 2008. *"Defining Real Change in Prism-Cover Test Measurements"*. *American Journal of Ophthalmology*, **145** (2), 381–385.

Hore J., Watts S. and Vilis T., 1992. *"Constraints on arm position when pointing in three dimensions: Donders' law and the Fick gimbal strategy"*. *Journal of Neurophysiology*, **68**(2), 374–383. PMID: 1527564.

Horowitz P. and Hill W., 2015. *"The art of electronics"*. Cambridge University Press, 3rd edition.

Houston C. A., Cleary M., Dutton G. N. and McFadzean R. M., 1998. *"Clinical characteristics of microtropia—is microtropia a fixed phenomenon?"*. *British Journal of Ophthalmology*, **82**(3), 219–224.

Hrynchak P. K., Herriot C. and Irving E. L., 2010. *"Comparison of alternate cover test reliability at near in non-strabismus between experienced and novice examiners"*. *Ophthalmic and Physiological Optics*, **30**(3), 304–309.

Hubel D. H., 1998. *"Eye, brain, and vision"*. Scientific American Library.

Hughes H. C. and Townsend J. T., 1998. *"Varieties of Binocular Interaction in Human Vision"*. *Psychological Science*, **9**(1), 53–60.

Huynh S. C., Ojaimi E., Robaei D., Rose K. and Mitchell P., 2005. *"Accuracy of the Lang II Stereotest in Screening for Binocular Disorders in 6-year-old Children"*. *American Journal of Ophthalmology*, **140**(6), 1130–1132.

Ibironke J. O., 2011. *"Microtropia: clinical findings and management for the primary eye care practitioner"*. *Optometry - Journal of the American Optometric Association*, **82**(11), 657 – 661.

Irsch K., Ramey N. A., Kurz A., Guyton D. L. and Ying H. S., 2008. *"Video-Based Head Movement Compensation for Novel Haploscopic Eye-Tracking Apparatus"*. *Investigative Ophthalmology & Visual Science*, **50**(3), 1152–1157.

Irsch K., 2015. *"Optical issues in measuring strabismus"*. *Middle East African Journal of Ophthalmology*, **22**(3), 265–270.

Issaho D. C., Wang S. X. and Weakley Jr. D. R., 12 2017. *"Intermittent exotropia surgery: results in different age groups"*. *Arquivos Brasileiros de Oftalmologia*, **80**(6), 355–358.

J. S., Nov 2017. *"A Stepwise Approach to Vision Therapy in Nystagmus with Strabismus"*. *Optometry & Visual Performance*, **5**(5), 192–196.

Jacobson D. M., 09 2000. *"Divergence Insufficiency Revisited: Natural History of Idiopathic Cases and Neurologic Associations"*. *Archives of Ophthalmology*, **118** (9), 1237–1241.

Jivraj I. and Patel V., Feb 2015. *"Treatment of Ocular Motor Palsies"*. *Current Treatment Options in Neurology*, **17**(3), 11.

Jones G. R., Lee D., Holliman N. S. and Ezra D., 2001. *"Controlling perceived depth in stereoscopic images"*. In Bolas M. T., Woods A. J., Bolas M. T., Merritt J. O. and Benton S. A., editors, *Stereoscopic Displays and Virtual Reality Systems VIII*, volume 4297. International Society for Optics and Photonics, SPIE, 42 – 53.

Julesz B., 1964. *"Binocular Depth Perception without Familiarity Cues: Random-dot stereo images with controlled spatial and temporal properties clarify problems in stereopsis"*. *Science*, **145**(3630), 356–362.

Kabbani H. and Raghuveer T. S., Jun 2004. *"Craniosynostosis"*. *American family physician*, **69**(12), 2863–70.

Kalevar A., Ong Tone S. and Flanders M., 2015. *"Duane syndrome: Clinical features and surgical management"*. *Canadian Journal of Ophthalmology*, **50**(4), 310 – 313.

Kang S. L., Shaikh A. G. and Ghasia F. F., May 2018. *"Vergence and Strabismus in Neurodegenerative Disorders"*. *Frontiers in neurology*, **9**, 299–299. PMC5964131[pmcid].

Kapoor N., Ciuffreda K. J. and Han Y., 2004. *"Oculomotor rehabilitation in acquired brain injury: A case series"*. *Archives of Physical Medicine and Rehabilitation*, **85**(10), 1667–1678.

Karthiga I., 2020. *"Extraocular movements"*. *Kerala Journal of Ophthalmology*, **32**(2), 209–212.

Kim I. G., Park J. M. and Lee S. J., Jun 2012a. *"Factors associated with the direction of ocular deviation in sensory horizontal strabismus and unilateral organic ocular problems"*. *Korean journal of ophthalmology : KJO*, **26**(3), 199–202. PMC3364432[pmcid].

Kim S. and Kim S., 01 2008. *"Normal Distance Stereoacuity by Age Assessed by the Frisby Davis Distance Stereotest"*. *Journal of The Korean Ophthalmological Society*, **49**.

Kim W. K., Kang S. Y., Rhiu S., Chung S. A. and Lee J. B., Feb 2012b. *"The analysis of AC/A ratio in nonrefractive accommodative esotropia treated with bifocal glasses"*. *Korean journal of ophthalmology : KJO*, **26**(1), 39–44. PMC3268167[pmcid].

Kimmel R., 2002. *"3D Shape Reconstruction from Autostereograms and Stereo"*. *Journal of Visual Communication and Image Representation*, **13**(1), 324–333.

Kimonis V., Gold J.-A., Hoffman T. L., Panchal J. and Boyadjiev S. A., 2007. *"Genetics of Craniosynostosis"*. *Seminars in Pediatric Neurology*, **14**(3), 150 – 161. Advances in Clinical Genetics (Part II).

Kiyak Yilmaz A., Kose S., Guven Yilmaz S. and Uretmen O., 2015. *"The impact of prism adaptation test on surgical outcomes in patients with primary exotropia"*. *Clinical and Experimental Optometry*, **98**(3), 224–227.

Klaib A. F., Alsrehin N. O., Melhem W. Y., Bashtawi H. O. and Magableh A. A., 2021. *"Eye tracking algorithms, techniques, tools, and applications with an emphasis on machine learning and Internet of Things technologies"*. *Expert Systems with Applications*, **166**, 114037.

Kniestedt C. and Stamper R. L., June 2003. *"Visual acuity and its measurement"*. *Ophthalmology clinics of North America*, **16**(2), 155—70, v.

Kohlbecher S., Bardinst S., Bartl K., Schneider E., Poitschke T. and Ablassmeier M., 2008. *"Calibration-Free Eye Tracking by Reconstruction of the Pupil Ellipse in 3D Space"*. ETRA '08, New York, NY, USA. Association for Computing Machinery, 135–138.

Kohmoto H., Inoue K. and Wakakura M., Dec 2010. *"Divergence insufficiency associated with high myopia"*. *Clinical ophthalmology (Auckland, N.Z.)*, **5**, 11–16. PMC3032998[pmcid].

Kolb H., Fernandez E. and Nelson R., 05 2020. *"Webvision: the organization of the vertebrate retina"*. Webvision.

Kowal L. and Georgievski Z., 1996. *"Evaluating Torsion with the Torsionometer, Synoptophore, Double Maddox Rod Test and Maddox Wing: A Reliability Study"*.

Kraft S. P., O'Donoghue E. P. and Roarty J. D., 1992. *"Improvement of Compensatory Head Postures after Strabismus Surgery"*. *Ophthalmology*, **99**(8), 1301 – 1308.

Kreith F. and Goswami Y. D., 2005. *"The CRC Handbook of Mechanical Engineering"*. CRC Press, 2nd edition.

Kushner B. J., 11 2002. *"Intractable Diplopia After Strabismus Surgery in Adults"*. *Archives of Ophthalmology*, **120**(11), 1498–1504.

Kushner B. J., 12 2010. *"Incomitant Strabismus: Does Extraocular Muscle Form Denote Function?"*. *Archives of Ophthalmology*, **128**(12), 1604–1609.

Lambert S. R. and Lyons C. J., 2017. *"Taylor and Hoyt's Pediatric Ophthalmology and Strabismus"*. Elsevier, 5th edition.

Lambooij M., Fortuin M., Ijsselsteijn W., Evans B. and Heynderickx I., 2010. *"Measuring visual fatigue and visual discomfort associated with 3-D displays"*. *Journal of the Society for Information Display*, **18**(11), 931–943.

Lang J., Aug 1966. *"Evaluation in small angle strabismus or microtropia"*. In A. A., editor, *International Strabismus Symposium - An Evaluation of the Present Status of Orthopedics, Pleoptics and Related Diagnostic Treatment Regimes*, Giessen, Germany. 219–222.

Laughlin J., Luerssen T. G., Dias M. S., the Committee on Practice and Medicine A., 2011. *"Prevention and Management of Positional Skull Deformities in Infants"*. *Pediatrics*, **128**(6), 1236–1241.

Lavrich J. B., 2010. *"Convergence insufficiency and its current treatment"*. *Current Opinion in Ophthalmology*, **21**(5), 356–360.

Lee J., October 1996. *"Paralytic and incomitant strabismus"*. *Current opinion in ophthalmology*, **7**(5), 19—23.

Lembo A., Serafino M., Strologo M. D., Saunders R. A., Trivedi R. H., Villani E. and Nucci P., Feb 2019. *"Accommodative esotropia: the state of the art"*. *International Ophthalmology*, **39**(2), 497–505.

Lim Z., Seenyen L. and Quah B. L., 2011. *"Characteristics of divergence excess type intermittent exotropia in Asian children"*. *Journal of American Association for Pediatric Ophthalmology and Strabismus*, **15**(5), 468 – 472.

Lin Engineering , 2019. *"5704M-10 Stepper Motor: NEMA 23:* 0.45°*"*. https://www.linengineering.com/products/stepper-motors/5704-series/5704m-10/#fndtn-standard_motor. Date Accessed: 30/05/2019.

Lipton E. L., 1970. *"A Study of the Psychological Effects of Strabismus"*. *The Psychoanalytic Study of the Child*, **25**(1), 146–174.

Lueder G. T., 2011. *"Pediatric Practice Ophthalmology"*. McGraw-Hill Education, 1st edition.

Lueder G. T., 2015. *"Orbital Causes of Incomitant Strabismus"*. *Middle East African journal of ophthalmology*, **22**(3), 286–291. PMC4502170[pmcid].

MacKinnon S., Oystreck D. T., Andrews C., Chan W.-M., Hunter D. G. and Engle E. C., 2014. *"Diagnostic Distinctions and Genetic Analysis of Patients Diagnosed with Moebius Syndrome"*. *Ophthalmology*, **121**(7), 1461 – 1468.

Malacara-Hernandez D. and Malacara-Hernandez Z., 2017. *"Handbook of optical design"*. CRC Press, 3rd edition.

Matsuo T., Yabuki A., Hasebe K., Shira Y. H., Imai S. and Ohtsuki H., Dec 2010. *"Postural Stability Changes during the Prism Adaptation Test in Patients with Intermittent and Constant Exotropia"*. *Investigative Ophthalmology & Visual Science*, **51**(12), 6341–6347.

Maurer D. and McKee S. P., 2018. *"Classification and diversity of amblyopia"*. *Visual Neuroscience*, **35**, E012. E012.

Mazur V., Si. and Boichuk I., 2018. *"Changes in the characteristics of superficial electromyography potentials recorded from the horizontal extraocular muscles in children with non-alternating nonaccommodative comitant strabismus after electrical stimulation treatment"*. *Oftalmologicheskii zhurnal*, **74**, 74–79.

McKee S. P., 1983. *"The spatial requirements for fine stereoacuity"*. *Vision Research*, **23**(2), 191–198.

McKee S. P., Verghese P., Ma-Wyatt A. and Petrov Y., Dec 2007. *"The wallpaper illusion explained"*. *Journal of Vision*, **7**(14), 10–10.

MediSense , Mar 2018. *"Maddox Wing Test"*. https://www.smelltest.eu/en/product/maddox-wing-test/. Date Accessed: 13/02/2021.

Metz H. S., 1983. *"Saccadic velocity measurements in strabismus"*. *Transactions of the American Ophthalmological Society*, **81**, 630–692. 6676980[pmid].

Metz H., 1976. *"Forced duction, active force generation, and saccadic velocity tests"*. *International ophthalmology clinics*, **16**(3), 47—73.

Michaelides M. and Moore A. T., 2004. *"The genetics of strabismus"*. *Journal of Medical Genetics*, **41**(9), 641–646.

Miller J. M., Hall H. L., Greivenkamp J. E. and Guyton D. L., Apr 1995. *"Quantification of the Brückner test for strabismus"*. *Investigative Ophthalmology & Visual Science*, **36**(5), 897–905.

Mohamad Fadzil N., Mohammed Z., Mohamad Shahimin M. and Saliman N. H., Nov 2019. *"Reading Performance and Compensatory Head Posture in Infantile Nystagmus after Null Zone Training"*. *International journal of environmental research and public health*, **16**(23), 4728. 31783492[pmid].

Mohney B. G., Cotter S. A., Chandler D. L., Holmes J. M., Wallace D. K., Yamada T., Petersen D. B., Kraker R. T., Morse C. L., Melia B. M. and Wu R., 2019. *"Three-Year Observation of Children 3 to 10 Years of Age with Untreated Intermittent Exotropia"*. *Ophthalmology*, **126**(9), 1249 – 1260.

Mojon D. S., 2009. *"A New Stereotest for Strabismologists: The Covered two Pencil Test"*. *European Journal of Ophthalmology*, **19**(4), 530–534. PMID: 19551665.

Momeni Moghaddam H., Kundart J., Azimi A. and Hassanyani F., 01 2015. *"The Effectiveness of Home-based Pencil Push-up Therapy Versus Office-based Therapy for the Treatment of Symptomatic Convergence Insufficiency in Young Adults"*. *Middle East African journal of ophthalmology*, **22**, 97–102.

MOONS , 2021. *"MS23HAAL4500"*. https://www.moonsindustries.com/p/nema-23-high-precision-hybrid-stepper-motors/ms23haal4500-000004611110015322. Date Accessed: 23/08/2021.

Morimoto C. H. and Mimica M. R., 2005. *"Eye gaze tracking techniques for interactive applications"*. *Computer Vision and Image Understanding*, **98**(1), 4–24. Special Issue on Eye Detection and Tracking.

Morris B., Smith V., Elphick J. and Laws D. E., Feb 2009. *"Compensatory head posture and neck problems: is there an association? A cohort study of nystagmus patients"*. *Eye*, **23**(2), 279–283.

Morris R. J. and Luff A. J., 1992. *"Adjustable sutures in squint surgery"*. *British Journal of Ophthalmology*, **76**(9), 560–562.

Mulvihill A., MacCann A., Flitcroft I. and O'Keefe M., 2000. *"Outcome in refractive accommodative esotropia"*. *British Journal of Ophthalmology*, **84**(7), 746–749.

Murphy P. J., Duncan A. L., Glennie A. J. and Knox P. C., 2001. *"The effect of scleral search coil lens wear on the eye"*. *British Journal of Ophthalmology*, **85**(3), 332–335.

Murray A. D. N., 2015. *"An Approach to Some Aspects of Strabismus from Ocular and Orbital Trauma"*. *Middle East African journal of ophthalmology*, **22**(3), 312–319. 26180469[pmid].

Murty M. V. R. K., 1973. *"A comparison of two image rotating prisms"*. *Proceedings of the Indian National Science Academy - Part A: Physical Sciences*, **39**(4), 292–297.

Nehad T., Salem T. and Elmohamady M. N., Feb 2018. *"Combined Office-based Vergence Therapy and Home Therapy System for Convergence Insufficiency in Egyptian Children"*. *The open ophthalmology journal*, **12**, 12–18. 29541278[pmid].

Nelson L. B., 2019. *"Pediatric Ophthalmology (Color Atlas & Synopsis of Clinical Ophthalmology)"*. Lippincott Williams and Wilkins, 2nd edition.

Nelson L. B. and Olitsky S. E., 2014. *"Harley's Pediatric Ophthalmology"*. Lippincott Williams and Wilkins, 6th edition.

Nihalani B. R. and Hunter D. G., Oct 2011. *"Adjustable suture strabismus surgery"*. *Eye (London, England)*, **25**(10), 1262–1276.

Nongpiur M. and Sharma P., 2010. *"Horizontal lang two-pencil test as a screening test for stereopsis and binocularity"*. *Indian Journal of Ophthalmology*, **58** (4), 287–290.

Noorden G. K. v. and Campos E. C., 2002. *"Binocular vision and ocular motility theory and management of strabismus"*. Mosby, 6th edition.

Nuzzi G. and Cantù C., 2003. *"Spatial Perception in Normal and Strabismic Subjects: Role of Stereopsis and Monocular Clues"*. *European Journal of Ophthalmology*, **13**(6), 507–514. PMID: 12948307.

Oei T. H., Verhagen W. I. M. and Horsten G. P. M., 1983. *"Forced Duction Test in Clinical Practice"*. *Ophthalmologica*, **186**(2), 87–90.

Ohtsuki H., Hasebe S., Kono R., Yamane T., Fujiwara H. and Shiraga F., 2001. *"Prism adaptation response is useful for predicting surgical outcome in selected types of intermittent exotropia"*. *American Journal of Ophthalmology*, **131**(1), 117–122.

Olitsky S. E., Sudesh S., Graziano A., Hamblen J., Brooks S. E. and Shaha S. H., 1999. *"The negative psychosocial impact of strabismus in adults"*. *Journal of American Association for Pediatric Ophthalmology and Strabismus*, **3**(4), 209 – 211.

Olivan Gonzalvo G., 10 2018. *"Frequency of Strabismus in Children Adopted from Russia, Ukraine and Kazakhstan: Relationships with Perinatal History and Medical Diagnosis"*. *Clinics in Pediatrics, Remedy Publications LLC*, **1**, 1006.

Onua A., 08 2019. *"Risk Factors of Strabismus in Children in a Southern Nigerian Tertiary Hospital"*. *World Journal of Ophthalmology & Vision Research*, **2**.

Optician , Dec 2017. *"Commonly Used Stereotests"*. https://www.opticianonline.net/cet-archive/4723. Date Accessed: 19/02/2021.

Ortony A., 01 1971. *"A system for stereo viewing"*. *The Computer Journal*, **14** (2), 140–144.

Osborne D. C., Greenhalgh K. M., Evans M. J. E. and Self J. E., Dec 2018. *"Atropine Penalization Versus Occlusion Therapies for Unilateral Amblyopia after the Critical Period of Visual Development: A Systematic Review"*. *Ophthalmology and therapy*, **7**(2), 323–332. PMC6258585[pmcid].

Oya Y., Yagasaki T., Maeda M., Tsukui M. and Ichikawa K., 2009. *"Effects of vertical offsets of the horizontal rectus muscles in V-pattern exotropia without oblique dysfunction"*. *Journal of AAPOS : the official publication of the American Association for Pediatric Ophthalmology and Strabismus*, **13**(6), 575–577.

Oystreck D. T. and Lyons C. J., Jul 2012. *"Comitant strabismus: Perspectives, present and future"*. *Saudi journal of ophthalmology : official journal of the Saudi Ophthalmological Society*, **26**(3), 265–270. PMC3729504[pmcid].

Padgett M. and Paul Lesso J., 02 1999. *"Dove prisms and polarized light"*. *Journal of Modern Optics*, **46**, 175–179.

Parker A. 2009. 411 – 417. *"Stereoscopic Vision"*. In Squire L. R., editor, *Encyclopedia of Neuroscience*, Academic Press.

Parker A. J., May 2019. *"Stereopsis and Depth Perception"*. *Oxford Research Encyclopedia of Neuroscience*.

Parks M. M., 1969. *"The monofixation syndrome"*. *Transactions of the American Ophthalmological Society*, **67**, 609–657. 5381308[pmid].

Phillips N., Massey K., Arefin M. S. and Swan J. E., March 2019. *"Design, Assembly, Calibration, and Measurement of an Augmented Reality Haploscope"*. In *2019 IEEE Conference on Virtual Reality and 3D User Interfaces (VR)*, 1770–1774.

Pickwell L. D., May 1980. *"A model for sensory adaptations of the visual system in squint"*. *The British journal of ophthalmology*, **64**(5), 345–348. PMC1043693[pmcid].

Pickwell L., February 1979. *"Prevalence and management of divergence excess"*. *American journal of optometry and physiological optics*, **56**(2), 78—81.

Piña-Garza J. E. 2013. 295 – 312. *"Chapter 15 - Disorders of Ocular Motility"*. In Piña-Garza J. E., editor, *Fenichel's Clinical Pediatric Neurology (Seventh Edition)*, W.B. Saunders.

Pointer J. S., 2005. *"An enhancement to the Maddox Wing test for the reliable measurement of horizontal heterophoria"*. *Ophthalmic and Physiological Optics*, **25**(5), 446–451.

Pololu , 2019. *"SpringRC SM-S4303R Continuous Rotation Servo"*. https://www.pololu.com/product/1248. Date Accessed: 19/05/2019.

Porter A., 1979. *"A simple method of detecting abnormal retinal correspondence"*. *British Journal of Ophthalmology*, **63**(5), 353–354.

Prasad S. and Volpe N. J., 2010. *"Paralytic Strabismus: Third, Fourth, and Sixth Nerve Palsy"*. *Neurologic Clinics*, **28**(3), 803 – 833. Neuro-Ophthalmology.

Pratt-Johnson J. A. and Tillson G., 1984. *"Suppression in strabismus-an update"*. *British Journal of Ophthalmology*, **68**(3), 174–178.

Pritchard C. and Jr. G. S. E., 2007. *"Manifest Strabismus Following Pseudostrabismus Diagnosis"*. *American Orthoptic Journal*, **57**(1), 111–117.

Pugesgaard T., Krogh E., Nyholm M. and Nordström I., 1987. *"Predictive value of Lang two-pencil test, TNO stereotest, and Bagolini glasses. Orthoptic examination of an adult group"*. *Acta Ophthalmologica*, **65**(4), 487–490.

Qin D., Takamatsu M. and Nakashima Y., Jan 2004. *"Measurement for the Panum's Fusional Area in Retinal Fovea Using a Three-Dimention Display Device"*. *Journal of Light & Visual Environment*, **28**(3), 126.

Qin D., Takamatsu M. and Nakashima Y., Jan 2006. *"Disparity Limit for Binocular Fusion in Fovea"*. *Optical Review*, **13**(1), 34–38.

Ramey N. A., Ying H. S., Irsch K., Müllenbroich M. C., Vaswani R. and Guyton D. L., 2008. *"A novel haploscopic viewing apparatus with a three-axis eye tracker"*. *Journal of American Association for Pediatric Ophthalmology and Strabismus*, **12**(5), 498–503.

Rashad M. A., 2012. *"Pharmacological enhancement of treatment for amblyopia"*. *Clinical ophthalmology (Auckland, N.Z.)*, **6**, 409–416. 22536029[pmid].

Rawashdeh M., Oct 2017. *"BYJ48 Stepper Motor"*. https://www.instructables.com/id/BYJ48-Stepper-Motor/. Date Accessed: 19/05/2019.

Read J. C. A., Begum S. F., McDonald A. and Trowbridge J., 2013. *"The Binocular Advantage in Visuomotor Tasks Involving Tools"*. *i-Perception*, **4**(2), 101–110. PMID: 23755355.

Rechichi C., Mojà G. D. and Aragona P., 2017. *"Video Game Vision Syndrome: A New Clinical Picture in Children?"*. *Journal of pediatric ophthalmology and strabismus*, **54**(6), 346–355.

Remington L. A., 2012. *"Clinical Anatomy and Physiology of the Visual System"*. Butterworth-Heinemann Elsevier, 3rd edition.

Richard J. M. and Parks M. M., 1983. *"Intermittent Exotropia: Surgical Results in Different Age Groups"*. *Ophthalmology*, **90**(10), 1172 – 1177.

Richards W., 1970. *"Stereopsis and stereoblindness"*. *Experimental Brain Research*, **10**(4), 380–388.

Roper-Hall G., 2004. *"The "Worth" of the Worth Four Dot Test"*. *American Orthoptic Journal*, **54**(1), 112–119.

Roper-Hall G., 2006. *"The Hess Screen Test"*. *American Orthoptic Journal*, **56** (1), 166–174.

Rowe F. J., 2012. *"Clinical Orthoptics"*. John Wiley & Sons, Ltd, 3rd edition.

Rutstein P. R., Cogen S. M., Cotter A. S., Daum M. K., Mozlin L. R. and Ryan M. J., 2011. *"Care of the Patient with Strabismus: Esotropia and Exotropia"*. American Optometric Association.

Rutstein R. P., 2008. *"Update on accommodative esotropia"*. *Optometry - Journal of the American Optometric Association*, **79**(8), 422 – 431.

Salmon J., 2019. *"Kanski's Clinical Ophthalmology: A Systematic Approach"*. Elsevier Health Sciences, 9th edition.

Sandler B.-Z., 1999. *"Robotics - Designing the Mechanisms for Automated Machinery"*. Academic Press, 2nd edition.

Scheiman M., Mitchell G. L., Cotter S., Cooper J., Kulp M., Rouse M., Borsting E., London R. and Wensveen J., Jan 2005. *"A Randomized Clinical Trial of Treatments for Convergence Insufficiency in Children"*. *Archives of Ophthalmology*, **123**(1), 14–24.

Schlossman A. and Shier J. M., 1955. *"Criteria for the Management of Alternating Strabismus*"*. *American Journal of Ophthalmology*, **39**(3), 351 – 358.

Schultinga L., Burggraaf F., Polling J. R. and Gutter M., 2013. *"Bagolini Glasses: Do They Affect The Horizontal Prism Fusion Amplitude?"*. *Strabismus*, **21**(2), 127–130.

Schutte S., Polling J. R., van der Helm F. C. T. and Simonsz H. J., Oct 2008. *"Human error in strabismus surgery: quantification with a sensitivity analysis"*. *Graefe's Archive for Clinical and Experimental Ophthalmology*, **247**(3), 399–409.

Scott A. B., 1981. *"Botulinum toxin injection of eye muscles to correct strabismus"*. *Transactions of the American Ophthalmological Society*, **79**, 734–770.

Sefi-Yurdakul N. and Tuğcu B., 2016. *"Development of Strabismus in Children Initially Diagnosed with Pseudostrabismus"*. *Strabismus*, **24**(2), 70–73. PMID: 27220260.

Sekeroğlu H. T., Sanac A. S., Arslan U. and Sener E. C., 2013. *"Superior oblique surgery: when and how?"*. *Clinical ophthalmology (Auckland, N.Z.)*, **7**, 1571–1574. 23946644[pmid].

Sengpiel F., Jirmann K.-U., Vorobyov V. and Eysel U. T., 01 2006. *"Strabismic Suppression Is Mediated by Inhibitory Interactions in the Primary Visual Cortex"*. *Cerebral Cortex*, **16**(12), 1750–1758.

Serra A. and Leigh R. J., 2002. *"Diagnostic value of nystagmus: spontaneous and induced ocular oscillations"*. *Journal of Neurology, Neurosurgery & Psychiatry*, **73**(6), 615–618.

SGS Thomson , 1993. *"OCTAL D-TYPE LATCH WITH 3 STATE OUTPUT HCT563 INVERTING - HCT573 NON INVERTING"*. https://www.rapidonline.com/st-m74hct573b1r-octal-tri-state-trans-latch-83-0034. SGS Thomson datasheet at https://www.alldatasheet.com/datasheet-pdf/pdf/131128/STMICROELECTRONICS/M74HCT573B1R.html.

Sharma P., Gaur N., Phuljhele S. and Saxena R., Mar 2017. *"What's new for us in strabismus?"*. *Indian journal of ophthalmology*, **65**(3), 184–190.

Shen E., Porco T. and Rutar T., 01 2013. *"Errors in Strabismus Surgery"*. *JAMA Ophthalmology*, **131**(1), 75–79.

Shumway C. L., Motlagh M. and Wade M., Jun 2019. *"Anatomy, Head and Neck, Eye Extraocular Muscles"*. *StatPearls [Internet]*.

Singh H., 09 2012. *"Human Eye Tracking and Related Issues: A Review"*. *International Journal of Scientific and Research Publications*, **2**, 1–9.

Singman E. L., Matta N. S. and Silbert D. I., 2014. *"Convergence Insufficiency Associated with Migraine: A Case Series"*. *American Orthoptic Journal*, **64**(1), 112–116.

Sireteanu R., 1982. *"Binocular vision in strabismic humans with alternating fixation"*. *Vision Research*, **22**(8), 889 – 896.

Sloan M. C., 2010. *"Aristotle's Nicomachean Ethics as the Original Locus for the Septem Circumstantiae"*. *Classical Philology*, **105**(3), 236–251.

Smith C., 1994. *"Magic Eye II: Now You See It..."*. Andrews McMeel Publishing, 2nd edition.

Snell R. S. and Lemp M. A., 2013. *"Clinical Anatomy of the Eye"*. Wiley-Blackwell, 2nd edition.

Sparrrow J. R., Hicks D. and Hamel C. P., 2010. *"The Retinal Pigment Epithelium in Health and Disease"*. *Current Molecular Medicine*, **10**(9), 802–823.

Speeg-Schatz C., Burgun P. and Gottenkiene S., 2017. *"To what Extent May Botulinum Toxin Type A Injections be an Alternative Choice to Surgery in Infantile Esotropia?"*. *European Journal of Ophthalmology*, **27**(3), 285–288. PMID: 28362053.

Standring S., 2008. *"Gray's anatomy: the anatomical basis of clinical practice"*. Churchill Livingstone Elsevier, 40th edition.

Stidwill D. and Fletcher R., 2010. *"Normal Binocular Vision: Theory, Investigation and Practical Aspects"*. John Wiley & Sons, Ltd.

Sung J. Y., Yang H. K. and Hwang J.-M., Mar 2020. *"Comparison of surgery versus observation for small angle intermittent exotropia"*. *Scientific Reports*, **10** (1), 4631.

Swift D., 1972. *"Image rotation devices - a comparative survey"*. *Optics & Laser Technology*, **4**(4), 175–188.

Texas Instruments , 1988. *"Texas Instruments SN74LS138N 3 Line to 8 Line Dec Multi"*. https://www.ti.com/store/ti/en/p/product/?p=SN74LS138N. Motorola datasheet at https://www.alldatasheet.com/datasheet-pdf/pdf/5654/MOTOROLA/SN74LS138N.html.

Thomas A., 2000. *"Divergence insufficiency"*. *Journal of American Association for Pediatric Ophthalmology and Strabismus*, **4**(6), 359 – 361.

Thomas S. and Guha S., 2010. *"Large-Angle Strabismus: Can a Single Surgical Procedure Achieve a Successful Outcome?"*. *Strabismus*, **18**(4), 129–136.

Thorisdottir R. L., Sundgren J., Sheikh R., Blohme J., Hammar B., Kjellström S. and Malmsjö M., 2018. *"Comparison of a new digital KM screen test with conventional Hess and Lees screen tests in the mapping of ocular deviations"*. *Journal of American Association for Pediatric Ophthalmology and Strabismus*, **22**(4), 277–280.e6.

Thorlabs , 2021. *"Unmounted Dove Prisms"*. https://www.thorlabs.com/newgrouppage9.cfm?objectgroup_id=146. Date Accessed: 13/09/2021.

Timms C., 2006. *"The Lees Screen Test"*. *American Orthoptic Journal*, **56**(1), 180–183.

Tomaç S., Şener E. C. and Sanaç A. Ş., 2002. *"Clinical and Sensorial Characteristics of Microtropia"*. *Japanese Journal of Ophthalmology*, **46**(1), 52 – 58.

Toms G., 2017. *"Circuit design and mechatronics"*. Personal Interview with G. Toms, 15 March 2017.

Tower Pro , 2019. *"MG995"*. https://www.towerpro.com.tw/product/mg995/. Date Accessed: 19/05/2019.

Traboulsi E. and Utz V., 2016. *"Practical Management of Pediatric Ocular Disorders and Strabismus"*. Springer-Verlag, 1st edition.

Tychsen L., 2005. *"Can Ophthalmologists Repair the Brain in Infantile Esotropia? Early Surgery, Stereopsis, Monofixation Syndrome, and the Legacy of Marshall Parks"*. *Journal of American Association for Pediatric Ophthalmology and Strabismus*, **9**(6), 510 – 521.

Tyler C. W. and Clarke M. B., 1990. *"The Autostereogram"*. In Merritt J. O. and Fisher S. S., editors, *Stereoscopic Displays and Applications*, volume 1256. International Society for Optics and Photonics, SPIE, 182 – 197.

Ultimaker , 2019. *"Safety data sheet PLA"*. UM180816 datasheet, ver. 4.002, Jan. 2019.

Valenti R. and Gevers T., 2008. *"Accurate eye center location and tracking using isophote curvature"*. In *2008 IEEE Conference on Computer Vision and Pattern Recognition*, 1–8.

Van Cott H. P. and Kinkade R. G., 1972. *"Human Engineering Guide to Equipment Design (Revised Edition)"*. American Institutes for Research.

van Dam L. C. J. and van Ee R., Oct 2006. *"Retinal image shifts, but not eye movements per se, cause alternations in awareness during binocular rivalry"*. *Journal of Vision*, **6**(11), 3–3.

van Leeuwen A. F., Collewijn H., de Faber J.-T. H. and van der Steen J., 2001. *"Saccadic binocular coordination in alternating exotropia"*. *Vision Research*, **41** (25), 3425 – 3435.

Villanueva A., Cabeza R., Porta S., Böhme M., Droege D. and Mulvey F., 2009. *"Report on New Approaches to Eye Tracking. Summary of new algorithms."*. In *IST-2003-511598 (NoE) COGAIN Communication by Gaze Interaction*, 1–19.

Vincent S. J. and Read S. A., 2014. *"Progressive adult antimetropia"*. *Clinical and Experimental Optometry*, **97**(4), 375–378.

Vishwanath D. and Hibbard P. B., 2013. *"Seeing in 3D With Just One Eye: Stereopsis Without Binocular Vision"*. *Psychological Science*, **24**(9), 1673–1685.

Vivian A. J., Lyons C. J. and Burke J., 2002. *"Controversy in the management of convergence excess esotropia"*. *British Journal of Ophthalmology*, **86**(8), 923–929.

von Noorden G. K. and Avilla C. W., 1990. *"Accommodative Convergence in Hypermetropia"*. *American Journal of Ophthalmology*, **110**(3), 287 – 292.

von Noorden G. K. and Avilla C. W., 1986. *"Nonaccommodative Convergence Excess"*. *American Journal of Ophthalmology*, **101**(1), 70 – 73.

Voss P., 2013. *"Sensitive and critical periods in visual sensory deprivation"*. *Frontiers in Psychology*, **4**, 664.

Wagner P., Bartl K., Günthner W., Schneider E., Brandt T. and Ulbrich H., 2006. *"A Pivotable Head Mounted Camera System That is Aligned by Three-dimensional Eye Movements"*. In *Proceedings of the 2006 Symposium on Eye Tracking Research & Applications*, ETRA '06, New York, NY, USA. ACM, 117–124.

Walraven J., 1975. *"TNO test for stereoscopic vision"*. https://museum.aco.org.au/archive/3424-tno-test-for-stereoscopic-vision. Date Accessed: 10/02/2021.

Walsh L. A., LaRoche G. and Tremblay F., 2000. *"The use of binocular visual acuity in the assessment of intermittent exotropia"*. *Journal of American Association for Pediatric Ophthalmology and Strabismus*, **4**(3), 154–157.

Wang J.-G., Sung E. and Venkateswarlu R., 2005. *"Estimating the eye gaze from one eye"*. *Computer Vision and Image Understanding*, **98**(1), 83–103. Special Issue on Eye Detection and Tracking.

Wang J., Hatt S. R., O'Connor A. R., Drover J. R., Adams R., Birch E. E. and Holmes J. M., 2010. *"Final Version of the Distance Randot Stereotest:*

Normative data, reliability, and validity". *Journal of American Association for Pediatric Ophthalmology and Strabismus*, **14**(2), 142–146.

Watts P., Nayak H., Lim M. K., Ashcroft A., Al Madfai H. and Palmer H., 2011. *"Validity and ease of use of a computerized Hess chart"*. *Journal of American Association for Pediatric Ophthalmology and Strabismus*, **15**(5), 451–454.

Weinstock V. M., Weinstock D. J. and Kraft S. P., Feb 1998. *"Screening for childhood strabismus by primary care physicians"*. *Canadian family physician Medecin de famille canadien*, **44**, 337–343. PMC2277602[pmcid].

Welten Holdings Ltd , 2019. *"4 Phase ULN2003 Stepper Motor Driver PCB"*. http://www.electronicoscaldas.com/datasheet/ULN2003A-PCB.pdf. Date Accessed: 19/05/2019.

Westheimer G., 02 1979. *"Scaling of Visual Acuity Measurements"*. *Archives of Ophthalmology*, **97**(2), 327–330.

Westheimer G., 2014. *"The law of equal innervation of both eyes: Thomas Reid preceded Hering by a century. An historical note"*. *Vision Research*, **101**, 32 – 33.

Westheimer G. and McKee S. P., Jul 1975. *"Visual acuity in the presence of retinal-image motion"*. *J. Opt. Soc. Am.*, **65**(7), 847–850.

Williams F., Beneish R., Polomeno R. C. and Little J. M., 1984. *"Congenital Exotropia"*. *American Orthoptic Journal*, **34**(1), 92–94.

Wilson E. M., Saunders R. and Rupal T., 2009. *"Pediatric Ophthalmology: Current Thought and A Practical Guide"*. Springer-Verlag, 1st edition.

Wilson J., 1998. *"Clinical Governance"*. *British Journal of Nursing*, **7**(16), 987–988. PMID: 9830912.

Wong A. M., 2004. *"Listing's law: clinical significance and implications for neural control"*. *Survey of Ophthalmology*, **49**(6), 563 – 575.

Wong A. M., Lueder G. T., Burkhalter A. and Tychsen L., 2000. *"Anomalous retinal correspondence: Neuroanatomic mechanism in strabismic monkeys and clinical findings in strabismic children"*. *Journal of American Association for Pediatric Ophthalmology and Strabismus*, **4**(3), 168 – 174.

Woo S.-J., Seo J.-M. and Hwang J.-M., Aug 2005. *"Clinical characteristics of cyclodeviation"*. *Eye*, **19**(8), 873–878.

Wright K. W., Spiegel P. H. and L. T., 2006. *"Handbook of Pediatric Strabismus and Amblyopia"*. Elsevier.

Wybar K., Mar 1974. *"Relevance of the AC-A ratio"*. *The British journal of ophthalmology*, **58**(3), 248–254.

Xu T. T., Bothun C. E., Hendricks T. M., Mansukhani S. A., Bothun E. D., Hodge D. O. and Mohney B. G., 2020. *"Pseudostrabismus in the First Year of Life and the Subsequent Diagnosis of Strabismus"*. *American Journal of Ophthalmology*, **218**, 242 – 246.

Yanoff M. and Duker J. S., 2019. *"Ophthalmology"*. Elsevier, 5th edition.

Yehezkel O., Belkin M. and Wygnanski-Jaffe T., 2020. *"Automated Diagnosis and Measurement of Strabismus in Children"*. *American Journal of Ophthalmology*, **213**, 226 – 234.

Yekta A., Pickwell L. and Jenkins T., 1989. *"Binocular vision, age and symptoms"*. *Ophthalmic and Physiological Optics*, **9**(2), 115–120.

Yoder P. J. and Vukobratovich D., 2015. *"Opto-mechanical systems design: design and analysis of opto-mechanical assemblies"*, volume 1. CRC Press, 4th edition.

Yoo H. S., Park E., Rhiu S., Chang H.-J., Kim K., Yoo J., Heo J. H. and Nam H. S., May 2017. *"A computerized red glass test for quantifying diplopia"*. *BMC Ophthalmology*, **17**(1), 71.

Yoonseok P., Hancheol C., Leon J. and Darby L., 12 2017. *"ROS Robot Programming"*. ROBOTIS.

Zakher M., Simon J. W. and Zobal-Ratner J., 2019. *"Acquired, Comitant, Non-Accommodative Esotropia (ANAET): Evaluation, Treatment, and Prognosis"*. *Journal of Binocular Vision and Ocular Motility*, **69**(1), 24–25. PMID: 30806582.

Zhao L. and Wu H., 2019. *"The difference in stereoacuity testing: contour-based and random dot-based graphs at far and near distances"*. *Annals of Translational Medicine*, **7**(9).

Zheng Y., Fu H., Li R., Lo W.-L., Chi Z., Feng D. D., Song Z. and Wen D., 2019. *"Intelligent Evaluation of Strabismus in Videos Based on an Automated Cover Test"*. *Applied Sciences*, **9**(4).

Zhu J. and Yang J., 2002. *"Subpixel eye gaze tracking"*. In *Proceedings of Fifth IEEE International Conference on Automatic Face Gesture Recognition*, 131–136.

Zivotofsky A. Z. and Schrader S. R., 2004. *"Temporal Influences on Retinal Correspondence: Ocular Motor Findings in Paradoxical Spatial Projection"*. *Optometry and Vision Science*, **81**(9).